Chemical concepts for the induced degradation of EVH1, GRB2, and YAP1

Inaugural-Dissertation

zur

Erlangung des Doktorgrades

der Mathematisch-Naturwissenschaftlichen Fakultät

der Universität zu Köln

Vorgelegt von

Felix Blüm

aus Dormagen

Köln, Februar 2026

Kurzzusammenfassung

Frühere Studien haben gezeigt, dass von ProMs (Prolin-basierte konformationell definierte Dipeptid-Module) abgeleitete Ena/VASP EVH1-Binder die Chemotaxis in Xenograft-Zebrafischmodellen hemmen können. Ihre begrenzte Bindungsaffinität und die hohen zellulären Konzentrationen, die benötigt werden, schränken jedoch die Eignung für therapeutische Anwendungen ein. Um diese Limitationen zu überwinden, untersucht diese Arbeit den Einbau von EVH1-Bindern in PROTACs (proteolysis targeting chimeras), die über einen katalytischen Wirkmechanismus agieren. Dazu wurden auf Grundlage des aktuellen Wissensstands geeignete EVH1-Binder ausgewählt. Unter Berücksichtigung des Bindungsmodus wurden optimierte Linker und Strategien für ihre Anbindung entwickelt, um moderne E3-rekrutierende Einheiten zu installieren. Eine Bibliothek von 28 EVH1-adressierenden PROTACs wurde synthetisiert, aufgereinigt und charakterisiert. Die Bindungsaffinitäten zu EVH1 wurden mittels Biolayer-Interferometrie gemessen. Erste zelluläre Ergebnisse deuten auf einen Abbau des Zielproteins sowie eine Hemmung der Chemotaxis hin. Darüber hinaus untersuchte diese Arbeit die Verwendung von ProMs zur gezielten Bindung an die SH3- und WW-Domänen von GRB2 und YAP1, wodurch die Gruppe der adressierbaren, Prolin-reichen Motivbindungsdomänen erweitert wurde. Biolayer-Interferometrie-Methoden wurden unter Verwendung der in dieser Arbeit hergestellten, biotinylierten Peptiden etabliert. Native Bindungspeptide für beide Zielproteine wurden mit ProM-Einheiten substituiert, verkürzt und auf ihre Bindungsaffinitäten untersucht. Insgesamt wurden im Rahmen dieser Arbeit 36 Peptide synthetisiert und charakterisiert. Diese Ergebnisse bilden die Grundlage für die weitere Entwicklung von niedermolekularen GRB2- und YAP1-bindern.

Abstract

Previous studies demonstrated that ProM (proline-based conformationally restricted dipeptide modules) based Ena/VASP EVH1 binders can inhibit chemotaxis in xenograft zebrafish models. However, their limited binding affinities and the requirement for high cellular concentrations restrict their suitability for therapeutic applications. To address these limitations, this work explores the integration of EVH1 binders into the emerging class of PROTACs (proteolysis-targeting chimeras), which act through a catalytic mode of action. Therefore, suitable EVH1 binders were selected based on the current state of knowledge. Taking the binding mode into account, optimized linkers and strategies for their attachment were developed for the installation of state-of-the-art E3 recruiters. A library of 28 EVH1-directed degraders was synthesized, purified, and characterized. Binding affinities to EVH1 were measured by biolayer interferometry. Initial cellular results indicate target degradation and inhibition of chemotaxis. Furthermore, this work explored the use of ProMs to target the SH3 and WW domains of GRB2 and YAP1, thereby expanding the range of addressable proline-rich motif binding domains. Biolayer interferometry assays were established using biotinylated tracer peptides generated in this work. Native binding peptides for both targets were substituted with ProM units, truncated, and investigated for their binding affinities. In total, 36 peptides were synthesized and characterized within this work, forming the foundation for further development of small molecule binders for GRB2 and YAP1.

Table of Content

1 Introduction

Proteins are fundamental building blocks of organisms and are involved in almost all biological processes including scaffolding, biochemical catalysis, signaling, and regulation of gene expression. Due to their fundamental role in cellular function, proteins not only sustain normal physiology, but also drive pathological processes when dysregulated.[1]

Scientific progress over the past century has expanded our understanding of biological processes, enabling the development of therapies capable of correcting physiological balance. Numerous modern therapeutics operate by inhibiting proteins, thereby selectively blocking their biological activity.[2] Nevertheless, a significant number of proteins are considered undruggable as they lack well defined binding pockets or possess large, featureless surfaces that are difficult to target with conventional small molecules.[3]

Remarkably, the human body possesses highly sophisticated quality-control mechanisms that continuously monitor the cellular proteome to identify and eliminate proteins that are misfolded, damaged, mutated, or produced in excessive amounts. A key component of this regulatory network is the ubiquitin-proteasome system (UPS). The groundbreaking elucidation of this system's function was acknowledged with the *Nobel* prize in chemistry in 2004.[4]

Modern biochemical research is exploring strategies to hijack the cell's intrinsic quality control to selectively target disease associated proteins to restore homeostasis. Such strategies bear the potential to drug the undruggable and therefore significantly expand therapeutic options.[5]

2 State of Knowledge

2.1 Ubiquitin-Proteasome System

Protein quality control is a fundamental process that maintains cellular function. Misfolded, mutated, or otherwise obsolete proteins are efficiently degraded by the ubiquitin-proteasome system (UPS) in eukaryotic cells.[6-7] When protein quality control fails, misfolded or aggregation-prone proteins accumulate, leading to proteinopathies such as *Alzheimer's*, *Parkinson's*, or *Huntington's* disease.[8-9]

2.1.1 Ubiquitin

Ubiquitin (Ub) is a highly conserved modifier protein involved in various biological pathways such as proteasomal degradation.[6] It is the eponymous member of the ubiquitin protein family, whose members share a common fold but differ in sequence. Ubiquitin exhibits exceptionally high interspecies conservation, showing 96% sequence identity between human and yeast, underlining its strong functional constraint.[10] Ubiquitin-like proteins adopt a globular shape and possess a *C*-terminal diglycine motif that enables formation of an *iso*peptide bond with lysine side chains of proteins. In certain cases, *N*-terminal ubiquitination has also been described.[11-12] Ubiquitin has seven lysine residues exposed on its surface and an unmodified *N*-terminus, providing eight addressable sites for ubiquitination (Figure 1).

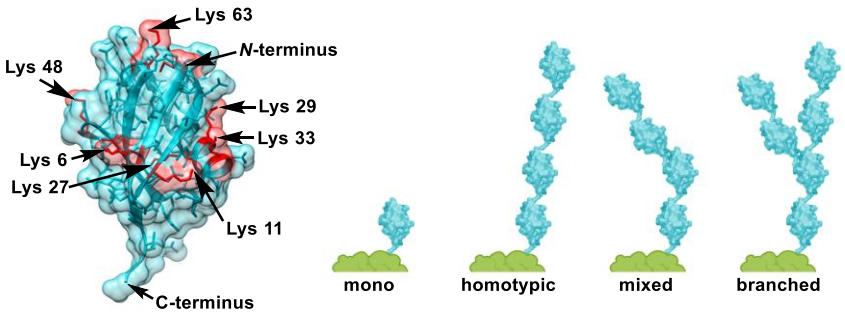

Figure 1: Left: X-ray structure of Ubiquitin (PDB[13]: 1UBQ). Possible ubiquitination sites (red) with arrow heads pointing onto the respective nitrogen. **Right:** Representation of possible ubiquitination (cyan) patterns on a substrate protein (green).[14]

Multiple ubiquitin moieties can be attached to a single ubiquitin, resulting in branched polyubiquitin chains. Moreover, ubiquitin chains themselves can be further modified including acetylation and phosphorylation, thereby further expanding the variety of distinct downstream signals.[15] Lys48-linked polyubiquitin chains are the most common type of linkage, often accounting for more than half of the ubiquitin chain

linkages (Figure 1). They serve as the canonical signal for the recruitment of proteins to the proteasome for degradation.[6, 16]

A tetra-ubiquitin chain is often reported to be the minimal motif for efficient proteasomal targeting, although in certain examples monoubiquitination is sufficient to trigger substrate proteolysis.[17-18] Commonly, proteins are found to be ubiquitinated at multiple sites before degradation.[19] Proteasomal degradation generally requires not only a ubiquitin tag, but also an unstructured region, which is either already exhibited in the native folding or generated by a protein unfoldase.[20]

2.1.2 26S Proteasome

The 26S proteasome is an approximately 2.5 MDa, ATP-dependent proteolytic complex that mediates the selective degradation of ubiquitinated proteins in eukaryotic cells.[7, 21] It is composed of two major subcomplexes: The 20S proteolytic core particle (CP) and the 19S regulatory particle (RP).[22]

The CP is a barrel-shaped complex composed of four stacked heptameric rings. The two inner β-rings create a central cavity in which substrate proteolysis takes place.[23] Among the seven β-subunits, β1, β2, and β5 contribute caspase-like, trypsin-like, and chymotrypsin-like activities, respectively.[24] The dimeric β-ring pair is flanked by two terminal α-rings that serve as gatekeepers, modulating substrate access to the proteolytic chamber. These α-rings also provide the interaction surface for the docking of the 19S RP (Figure 2).[25-26]

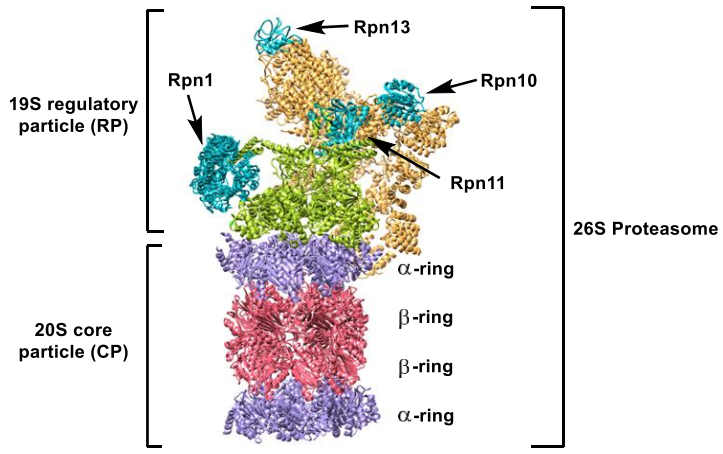

Figure 2: Cryo-EM structure of the yeast 26S proteasome (PDB[27]: 3JCP). α-, β- and ATPase rings are shown in purple, pink, and green, respectively. Catalytically inactive scaffolding subunits are shown in orange, ubiquitin receptors Rpn1, Rpn10, and Rpn13 as well as deubiquitinase Rpn11 are shown in cyan.

The RP is organized into two major substructures, termed base and lid. The base is formed by a hexameric ATPase ring positioned on top of an α-ring of the CP. ATP hydrolysis is the engine that drives large conformational changes, leading to relocalization of the substrate into the proteolytic chamber.[28-30] The lid consists of eight catalytically inactive subunits that provide a scaffolding structure for three ubiquitin receptors (Rpn1, Rpn10, and Rpn13) and a substrate deubiquitinase (Rpn11) that cleaves off the ubiquitin tag after target engagement (Figure 3).[31]

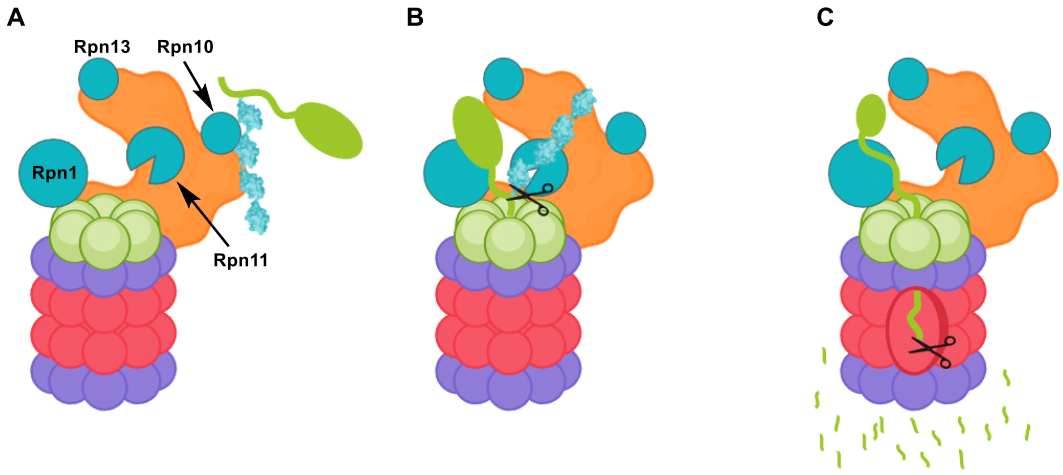

Figure 3: Stages of ubiquitin-mediated degradation. **A:** The ubiquitin motif is recognized by a ubiquitin-interacting moiety. **B:** Interaction of an unfolded protein region with the ATPase hexamer is induced and deubiquitinase Rpn11 cleaves the ubiquitin-substrate *iso*peptide bond. **C:** The peptide chain is proteolyzed by the core particle.[7]

Binding of a ubiquitin-tagged protein induces a conformational change of the RP from its resting state into the processing state. The conformational change leads to an interaction of an unstructured region of the substrate with the ATPase ring.[32] The ATPase unit mechanically pushes the target through the α-ring gate into the proteolytic chamber, while cleavage of the *iso*peptide bond between the substrate and the ubiquitin tag by the Rpn11 subunit is induced (Figure 3).[33-34]

Glycine and alanine rich sequences within the peptide chain can cause ‘slipping’ of the ATPase motor and thereby leading to incomplete degradation.[35] Remarkably, the substrate protein can be processed from *N* to *C* or *C* to *N* terminus.[36] After proteolytic cleavage, peptide fragments 2-10 amino acids in length leave through the other end of the CP.[37]

In addition, another 19S RP can associate with the opposite α-ring of the CP, yielding the double-capped 30S proteasome complex.[38] It is functionally equivalent to the 26S proteasome, but is able to process two substrate chains simultaneously.[33] The exact

mechanism by which peptides leave the CP of the 30S proteasome remains unclear. Nevertheless, diffusion through pores within the CP has been proposed.[39]

2.1.3 The E1-E2-E3 machinery

Proteins are ubiquitinated through an enzymatic cascade comprising three main classes of enzymes: E1 ubiquitin-activating enzymes, E2 ubiquitin-conjugating enzymes, and E3 ubiquitin ligases.[40]

In humans, ubiquitin is activated by one of the two ubiquitin-activating enzymes UBA1 or UBA6, which are members of a family of eight E1 enzymes.[41-42] The remaining six E1 enzymes UBA2, UBA3, UBA4, UBA5, UBA7, and ATG7 do not activate ubiquitin, but the ubiquitin-like proteins SUMO, NEDD8, URM1, UFM1, ISG15, and ATG8/ATG12, respectively.[43-48] The activation process is outlined in Scheme 1.

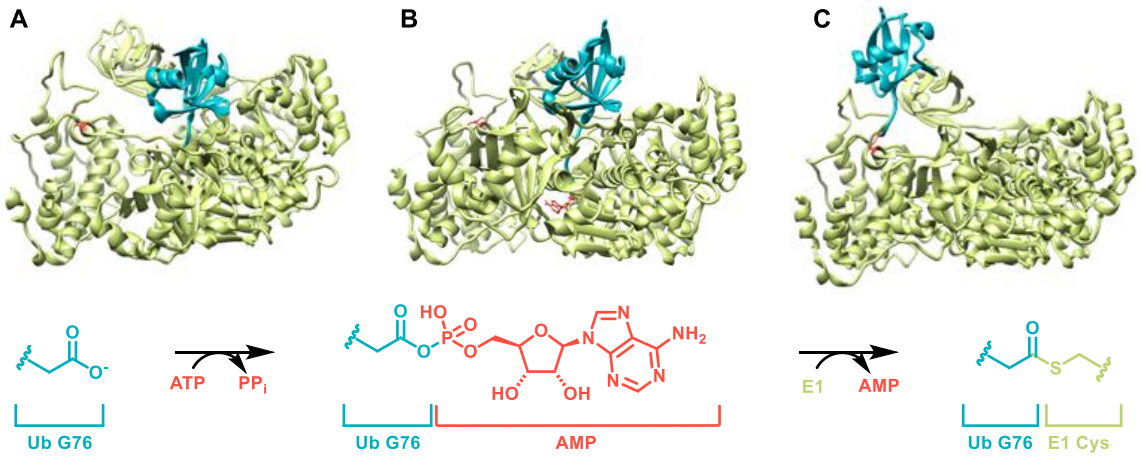

Scheme 1: X-ray structures of yeasts E1-Ubiquitin complex (expressed in E. coli). **A:** ubiquitin unbound (PDB[49]: 3CMM). **B:** ubiquitin adenylated (PDB[50]: 4NNJ). **C:** ubiquitin thioester (PDB[50]: 4NNJ). Ubiquitin and E1 are shown in cyan and green, reactive amino acids and ATP derived units are shown in red. The ubiquitin *C*-terminal binding mode for each stage is shown beneath.

Initially, ubiquitin interacts noncovalently with the E1 (Scheme 1A). Subsequently, E1 recruits an ATP molecule in proximity to the *C*-terminal glycine of ubiquitin, and the carboxylate is adenylated under the elimination of pyrophosphate (Scheme 1B).[51-52] The catalytic cysteine of E1 attacks the adenylated ubiquitin, substituting the AMP and generating the ubiquitin-E1 thioester intermediate (Scheme 1C).[41] Notably, a second molecule of ubiquitin can already be adenylated at this stage.[50]

Thioester formation and interaction with the E2 enzyme promotes a conformational change of the E1-Ub complex, which enables interaction with an E2 ubiquitin conjugating enzyme.[50] From two ubiquitin E1 enzymes, the pathway broadens to

roughly 40 E2 ubiquitin-conjugating enzymes, reflecting a substantial diversification of ubiquitin functions and specificities.[53] The transfer of Ub from E1 to E2 is depicted in Scheme 2A.

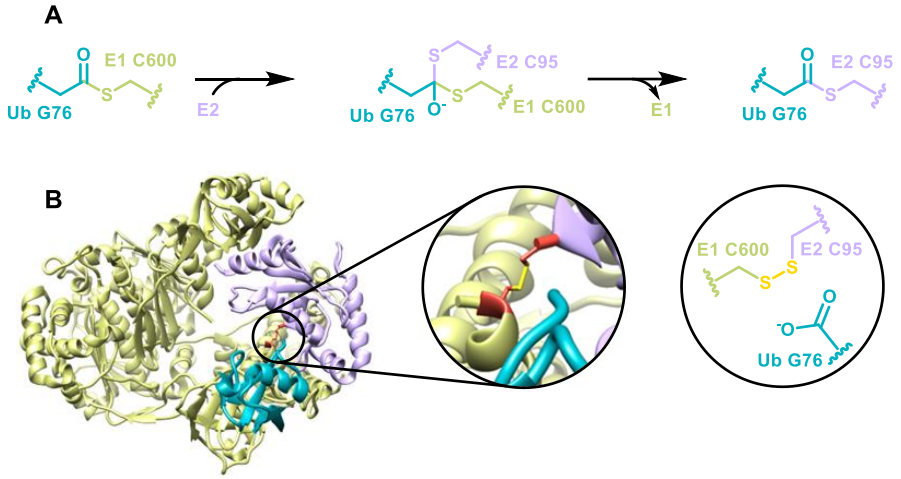

Scheme 2: A: Predicted mechanism for the transfer of ubiquitin from E1 to E2. **B:** X-ray structure PDB[54]: 7K5J) of a trimeric complex of yeast E1 (UBA1), E2 (Cdc34), and ubiquitin, expressed in E. coli, stabilized by a disulfide bond between the catalytic cysteines of E1 and E2.

Formation of an E2-E1-Ub adduct positions the E2 catalytic cysteine near the E1-Ub thioester bond, enabling nucleophilic attack of the E2 active-site cysteine onto the E1-Ub thioester bond, followed by the elimination of the E1 cysteine residue (Scheme 2A).[51] Evidence for this mechanism is provided by a trimeric crystal structure of E1 (UBA1), E2 (Cdc34), and ubiquitin. A disulfide bond induced between E1 and E2 stabilizes the complex while providing proof of proximity between the three reactive amino acids as shown in Scheme 2B.[54] The activated E2-Ub conjugate is not suitable for crystallization,[55] but the partial overlap between the E1 and E3 binding interfaces on E2 implies the presence of free E2-Ub conjugate (Figure 4).[56-57]

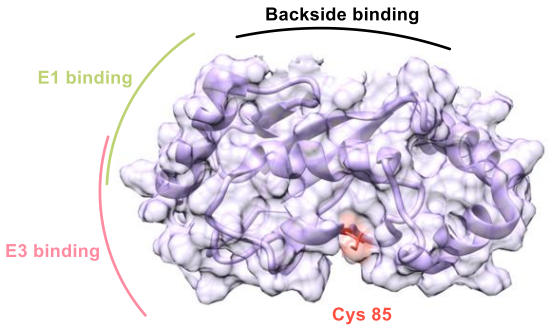

Figure 4: Solution NMR structure (PDB[58]: 2FUH) of human E2 (UbcH5C) expressed in E. coli. The reactive cysteine is shown in red, E3, E1 and backside binding sites are shown in pink, green and black, respectively.

The E2 catalytic cysteine is in a cavity of the protein structure flanked by conserved loops, which provides a geometrically constrained surrounding for binding of the ubiquitin *C*-terminus (Figure 4).[58-59]

Diversity expands further at the level of E3 ligases: The human genome encodes 600-1000 E3 ligases, depending on classification criteria.[60-61] E3 ubiquitin ligases can be clustered into four major families – RING, HECT, RBR, and U-box ligases.[62] A well-investigated example of a RING E3 ligase complex (VHL-EloBC-Cul2-Rbx1) is shown in Figure 5.

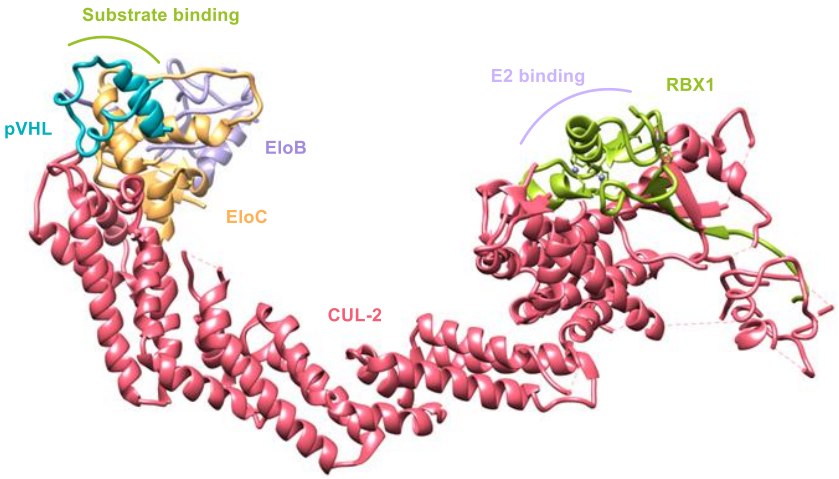

Figure 5: X-ray structure (PDB[63]: 5N4W) of a human E3 complex (pVHL-EloBC-Cul2-Rbx1) expressed in E. coli with color-coded subunits.

The main scaffold is a CUL2-based RING ligase that provides two docking interfaces for additional subunits. At one terminus, it associates with the RING protein RBX1, which recruits the E2 enzyme. At the opposite terminus, it engages the pVHL substrate-recognition module *via* the adaptor proteins EloB and EloC.[64]

The E3 ligase positions a substrate lysine residue near the E2-ubiquitin thioester, enabling the ε-amino group of the lysine to initiate a nucleophilic attack on the thioester bond. This attack results in formation of the final *iso*peptide bond between ubiquitin and the substrate lysine (Scheme 3A).[65]

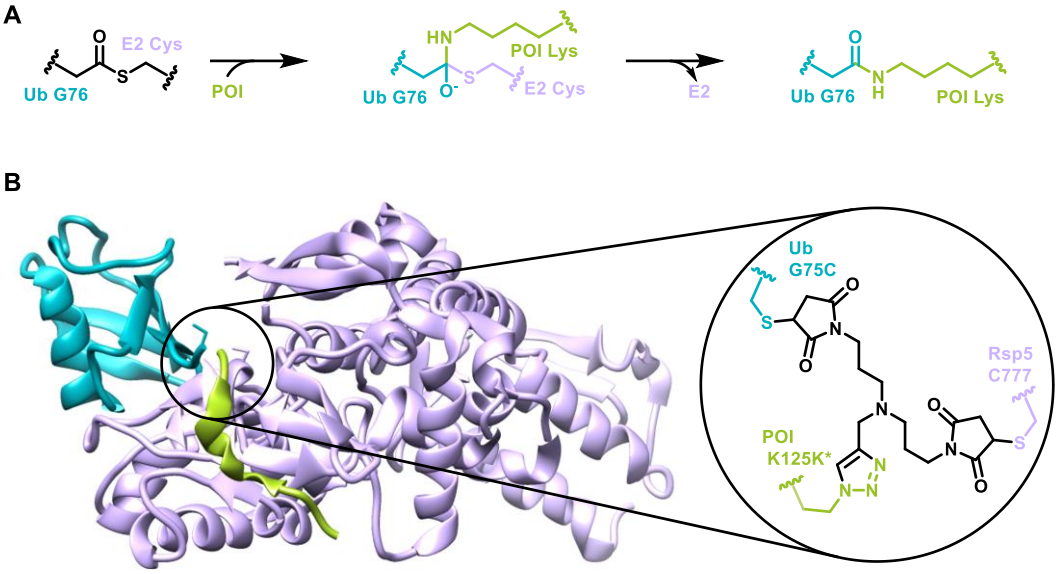

Scheme 3: A: Proposed mechanism for the nucleophilic attack of a lysine side chain of a protein of interest (POI) to the E2-ubiquitin thioester and subsequent elimination of the E2 cysteine.[66] **B:** X-ray structure (PDB[67]: 4LCD) of yeasts non-RING E3 (Rsp5), unnatural modified Ub, and unnatural modified POI (Sna3) in violet, cyan, and green, respectively. The linker is not resolved in the X-ray structure.

In contrast to RING and U-box E3 ligases, HECT-type and RBR-type E3 ligases form a ubiquitin thioester themselves, followed by transfer of ubiquitin onto a target lysine in the same manner.[68] Evidence for this mechanism is provided by proof of proximity between the three reactive residues by covalent trapping as shown in Scheme 3B.[67]

The sequence of interactions in the ubiquitin-proteasome system including the E1-E2-E3 enzyme cascade outlined above are summarized in Scheme 4, which schematically traces the ubiquitin through the pathway.

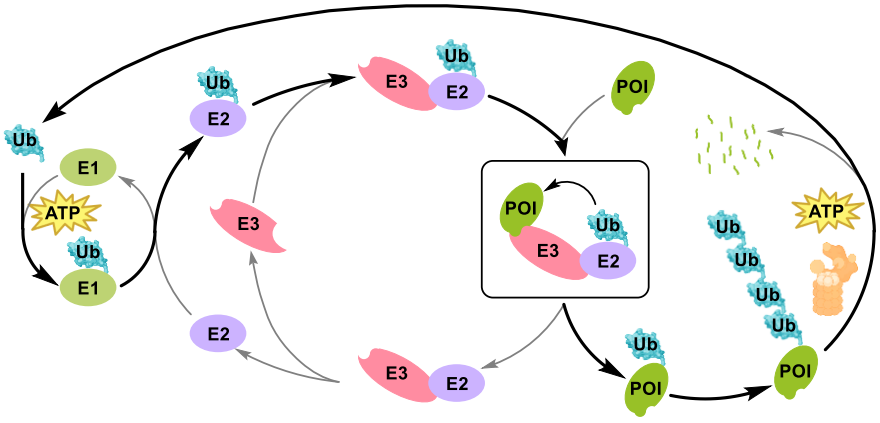

Scheme 4: Schematic overview of the ubiquitin-proteasome system and the E1-E2-E3 machinery. The ubiquitin path is indicated by black arrows while other paths are shown with grey arrows.

Ubiquitin is first activated by an E1 enzyme in an ATP-dependent manner. The activated ubiquitin is then transferred to an E2 enzyme within an E1-E2 complex. Subsequent dissociation of the E1-E2 complex permits assembly of an E2-E3 complex

that mediates substrate ubiquitination. The E3 ligase induces proximity to a substrate protein of interest (POI) which triggers the transfer of ubiquitin under the formation of an *iso*peptide bond. After ubiquitin transfer, the complex dissociates allowing E2 and E3 proteins to reenter the catalytic cycle. The monoubiquitinated substrate can undergo multiple cycles of ubiquitination, forming a polyubiquitin tag, which can be recognized by the proteasome. In an ATP-dependent process, the ubiquitin tag is released from the substrate, and the protein is degraded into peptide fragments.

2.2 Proteolysis Targeting Chimeras

An innovative therapeutic approach manipulates the natural ubiquitin-proteasome system to trigger proteolysis of neo substrates.[69] It was first described by *Crews* and *Deshaies* in 2001.[70]

2.2.1 Mechanism, Principles, and Advantages

Proteolysis targeting chimeras (PROTACs) are heterobifunctional molecules consisting of three compartments: A target-binding ligand (warhead), an E3 ligase binding ligand (recruiter), and a linker that connects these two ligands.[71] PROTACs bind to the E3 ligase and the target protein simultaneously, inducing proximity that can result in ubiquitination and proteasomal degradation of the neo target (Scheme 5).

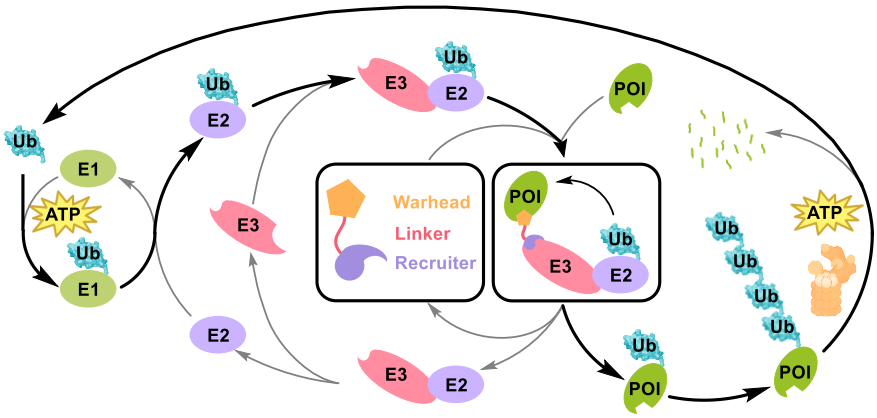

Scheme 5: Schematic overview of the mechanism of action of PROTACs.

Notably, PROTACs act in a catalytic manner and, therefore, only substoichiometric amounts are required to induce target degradation.[72] PROTACs follow an event-driven pharmacology while protein inhibitors follow an occupancy-driven pharmacology. Consequently, inhibitors need to reach higher cellular concentrations to inhibit protein function (Scheme 6A).[72-73]

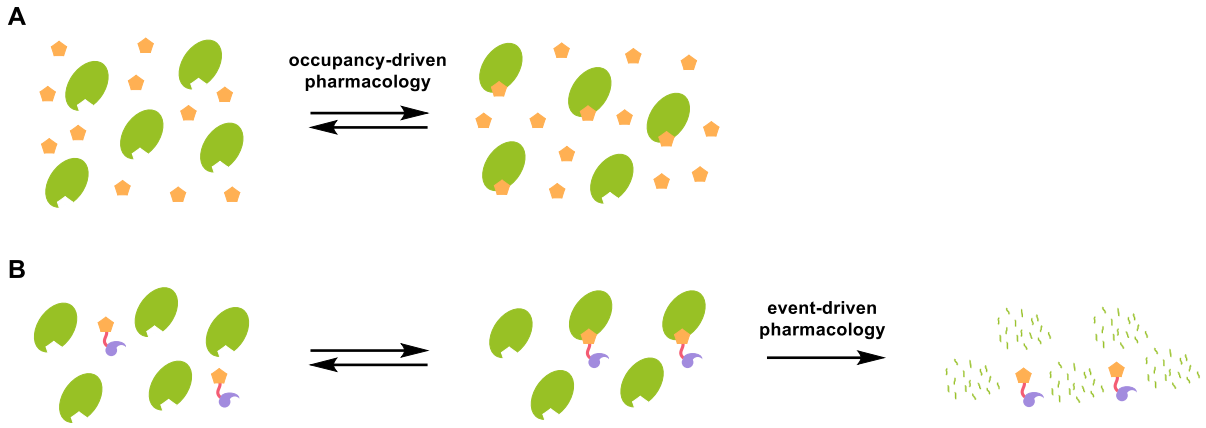

Scheme 6: A: Protein inhibition with small molecule inhibitors. **B:** PROTACs following an event-driven mechanism.

In contrast to protein inhibitors, PROTAC warheads do not need to bind a majority of the target protein. After initially induced proximity, the resulting protein-protein interactions (PPIs) can stabilize the complex.[74] Constructive PPIs lead to a ternary complex with a binding affinity higher than the sum of the two binary affinities (Figure 6A).[74]

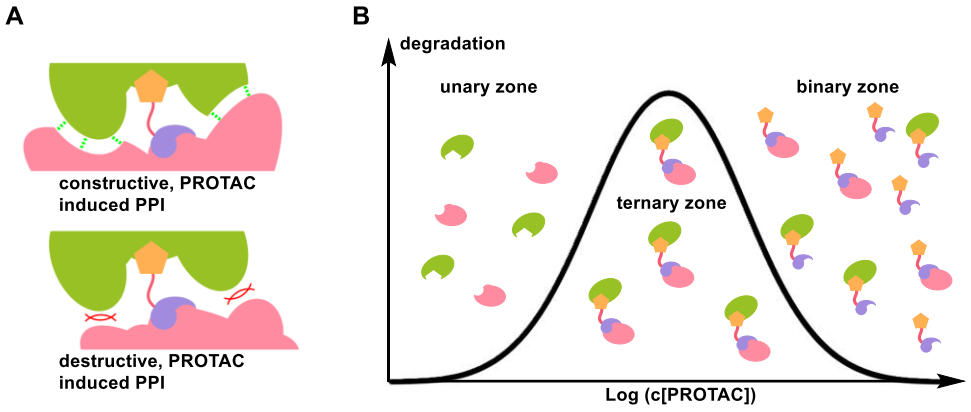

Figure 6: A: Constructive (top) and destructive (bottom) protein-protein interaction induced by a PROTAC. **B:** concentration-dependent loss of efficiency due to the high-dose hook effect.

Therefore, PROTACs can exhibit comparatively low binding affinity towards the isolated target protein. Further, PROTACs do not necessarily need to inhibit function but can bind any accessible epitope on the target protein.[75] Consequently, PROTACs offer the potential to target proteins previously considered undruggable.[76] However, a high concentration of PROTAC can lead to binary saturation of both proteins (Figure 6B).[77-78] Especially destructive ternary complexes are prone to this loss of degradation efficiency, which is called high-dose hook effect.[71]

Further, PROTACs can offer enhanced selectivity compared to their isolated warhead. Although the isolated warhead might bind to multiple proteins, PROTACs frequently induce selective degradation of only a subset, or even a single protein, which does not necessarily coincide with the highest-affinity binding partner.[79] Selectivity arises from a combination of favorable PPIs within the ternary complex, the presence of accessibility of lysine residues for ubiquitination, and the architecture of the PROTAC.[79-80]

2.2.2 Chemical structure and design of PROTACs

One of the three compartments that make up each PROTAC, the recruiter, binds to an E3 ubiquitin ligase. Although more than 600 E3 ligase complexes are known, only in a few cases is it known how they can be targeted with small molecules.[81] Within this limited set, *Cereblon* (CRBN) and *von Hippel-Lindau* (VHL) are the predominantly utilized E3 ligases, accounting for approximately 53% and 41% of the reported PROTACs, respectively.[82] One contributing factor is their early prominence, as both attracted the interest of the pharmaceutical industry at an early stage. Further E3-recruiting motifs occasionally addressed such as IAP and MDM2 are reviewed by *Xie* and coworkers.[83]

Shortly after the approval of thalidomide (**1**) as the sleeping drug *Contergan* in 1957, it was found to cause birth defects in more than 10,000 cases, and its approval was withdrawn in 1961.[84] The underlying mechanism remained unclear until 2010, when it was discovered that thalidomide (**1**) binds the CRBN subunit of the CRBN-DDB1-CUL2-RBX1 E3 ligase complex.[85] Binding of thalidomide (**1**) to CRBN reprograms the E3 ligase to ubiquitinate SALL4, leading to its proteasomal degradation, which was proven to be the cause of the birth defects (Figure 7).[86]

An E3-binding motif that promotes target degradation in the absence of an attached warhead is referred to as a molecular glue. The distinction between glues and PROTACs is not strictly defined; however, glues are generally smaller, use a single binding motif to bind both the target and the E3 ligase, and do not have a discrete linker unit.[87-88]

While (R)-thalidomide (**(R)-1**) was considered the therapeutically relevant enantiomer, the (S)-enantiomer (**(S)-1**) shows a six to ten times higher binding affinity to CRBN. While binding is only moderately dependent on the stereo information, the NH motif is

crucial; *N*-methylation inhibits the binding to CRBN (**2**).[89-91] Notably, the exclusive therapeutic use of (R)-thalidomide (**(R)-1**) would not have provided a safety advantage, as the compound undergoes racemization under physiological conditions.[84] Thalidomide is still in clinical use today for different indications, particularly for the treatment of erythema nodosum leprosum in patients with leprosy.[92]

An X-ray structure of the thalidomide-CRBN complex shows a surface-exposed side of the aryl ring suitable for further attachments (Figure 7B).[93] Introduction of an amine leads to pomalidomide (**3**) and substitution of a carbonyl with a methylene unit to lenalidomide (**4**). Both are blockbuster therapeutics for the treatment of multiple myeloma.[94] Both molecules induce degradation of IKZF1/IKZF3 as their main therapeutic targets.[94]

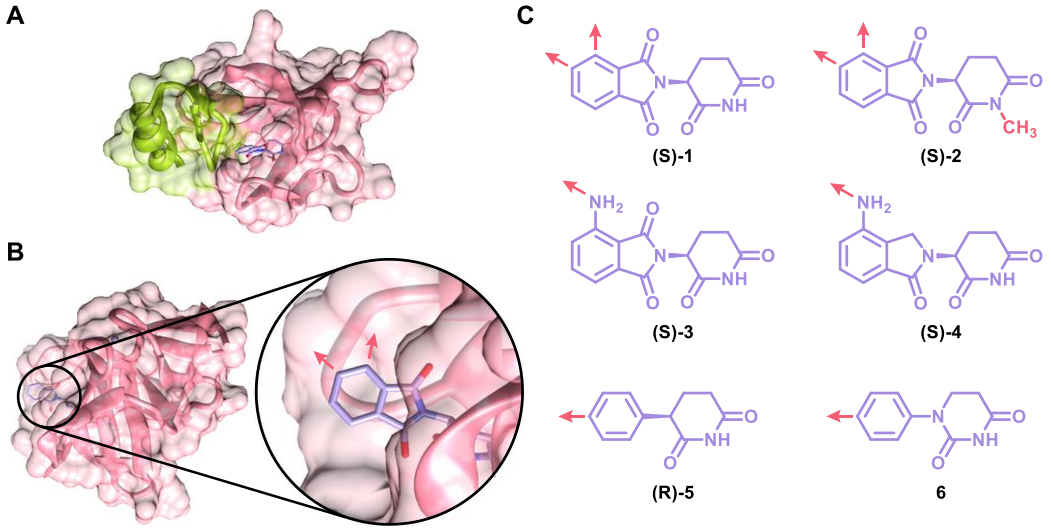

Figure 7: A: X-ray structure (PDB[93]: 7BQU) of a trimeric complex of human CRBN and SALL4 (expressed in E. coli) induced by (S)-thalidomide (**(S)-1**). **B:** X-ray structure (PDB[95]: 4V2Y) of a dimeric complex of CRBN (expressed in *Magnetospirillum gryphiswaldense* MSR-1) and (S)-thalidomide (**(S)-1**) showing its surface-exposed aryl ring. **C:** Thalidomide derivatives: (S)-thalidomide (**(S)-1**) and its respective nonbinding control **(S)-2**. (S)-Pomalidomide (**(S)-3**) and (S)-Lenalidomide (**(S)-4**). Other CRBN binding motifs (R)-phenyl glutarimide (**(R)-5**) and phenyl dihydrouracil **6**. Common exit vectors for the attachment of functionalization are indicated as arrows.

Removal of one carbonyl from pomalidomide (**3**) to lenalidomide (**4**) did not reduce the binding affinity.[96] Furthermore, the physiological stability is enhanced, rendering the molecule less prone to hydrolysis, and a reduction in the number of imide and amide bonds favorably impacts its physicochemical properties.[97] More stable and drug-like CRBN recruiters with (R)-phenyl glutarimide (PG) **(R)-5** and phenyl dihydrouracil (PD) **6** core motifs were developed.[98-99] Importantly, PROTACs based on PG and PD show higher binding affinities for CRBN compared to (S)-thalidomide (**(S)-1**)).[91, 98-100] The *von Hippel-Lindau* target recognition subunit of the pVHL-EloBC-Cul2-Rbx1 E3 ligase

complex (see also Figure 5) derives its name from a polycystic disease originally described by *Eugen von Hippel* and *Arvid Lindau*. It is caused by a rare genetic mutation of the gene that encodes for the pVHL protein.[101]

Hypoxia-inducible factor-1α (HIF1α) was identified as a key regulator that promotes the production of red blood cells under hypoxic conditions (Scheme 7A).[101]

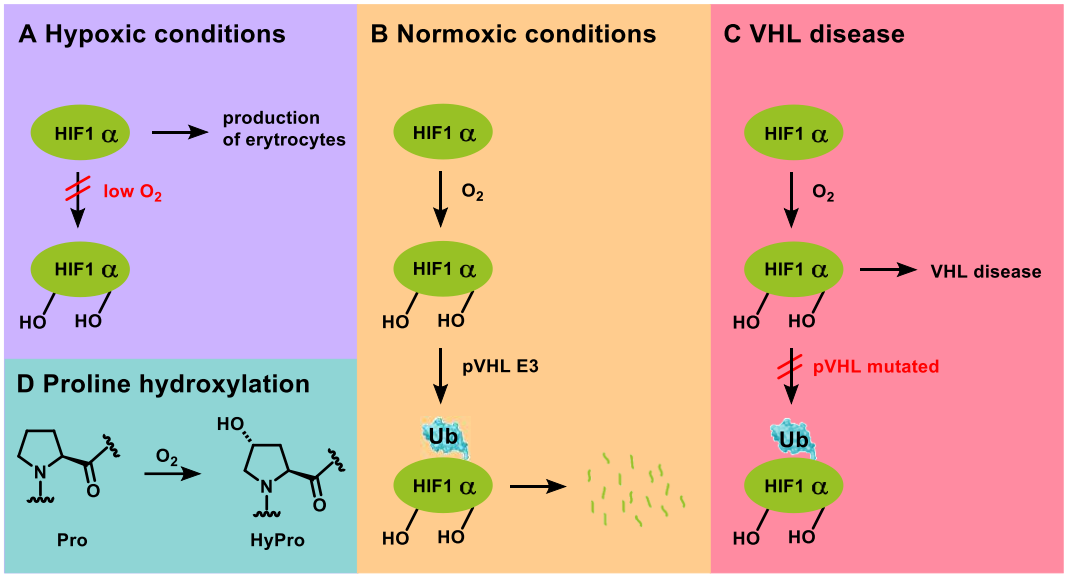

Scheme 7: Schematic representation of HIF1α pathway and signaling under different physiological conditions. **A:** Signaling for erythrocyte production under hypoxic conditions. **B:** HIF1α degradation under normoxic conditions. **C:** Accumulation of hydroxylated HIF1α due to VHL disease. **D:** Hydroxylation position of HIF1α prolines for VHL recognition.[101-103]

Under normoxic conditions, cellular concentrations of HIF1α are low due to hydroxylation of specific proline residues (Scheme 7D).[102] This posttranslational modification is recognized by the VHL-based E3 complex, leading to ubiquitination and subsequent degradation (Scheme 7B).[102] Under VHL disease conditions, mutations in pVHL hinder recognition of HIF1α, which leads to accumulation of hydroxylated HIF1α (Scheme 7C). This allows for its dimerization with HIF1β, causing transcription of various genes leading to the disease phenotype.[102-103]

Studies of the VHL disease, including an X-ray structure of the *C*-terminal oxygen-dependent degradation domain (CODD) of HIF1α bound to VHL (Figure 8A), provided the conceptual foundation for the development of VHL-recruiting ligands. Initially, the CODD-derived epitope peptide **7** was employed for VHL recruitment.[104] To improve the pharmacological properties of the recruiter, the labs of *Crews* and *Cuilli* developed the first smallmolecule VHL binder **8** with single digit micromolar affinity (Figure 8B).[105-106] Further optimization led to peptoid **9**, which binds VHL with a

nanomolar binding affinity, while the epimer **epi-9** was shown to be a suitable non-binding negative control. (Figure 8D).[105-106] The development of small molecule VHL binders and their application in PROTACs was reviewed in detail by *Cuilli* and coworker.[107]

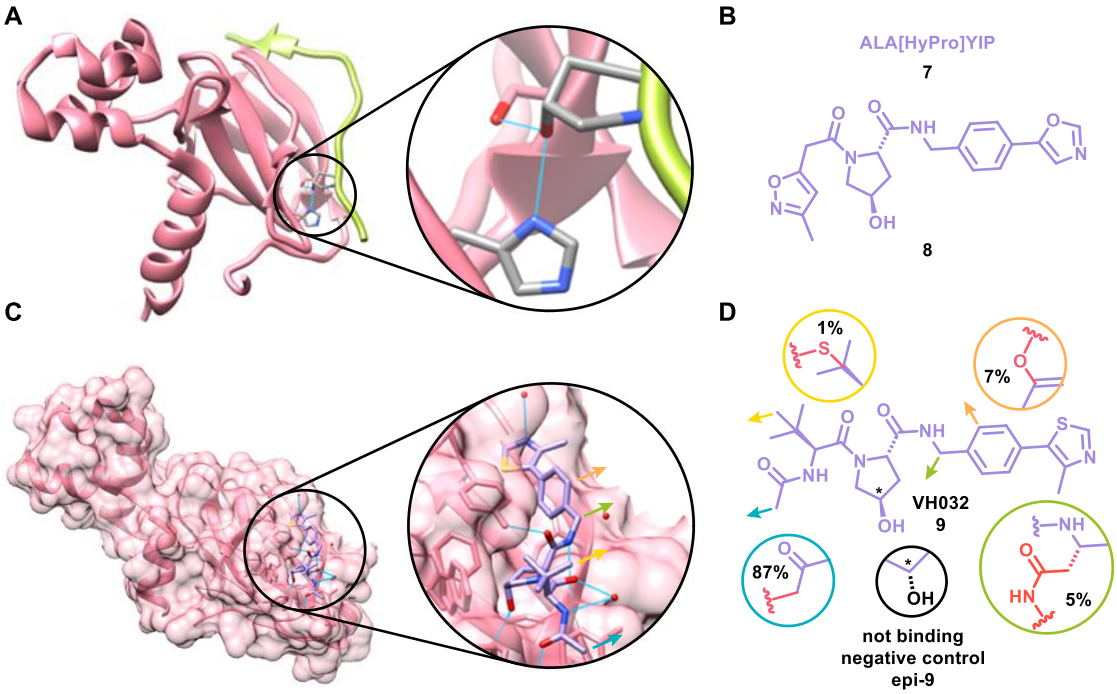

Figure 8: A: X-ray structure (PDB[108]: 1LM8) of human pVHL (expressed in E. coli) in complex with the *C*-terminal oxygen-dependent degradation motif (CODD) of HIF1α. **B:** CODD epitope peptide **7** sequence derived from HIF1α, which was initially employed as a VHL recruiter, and early small molecule VHL binder **8**. **C:** X-ray structure (PDB[106]: 4W9H) of human pVHL (expressed in E. coli) in complex with VH032 (**9**). Surface-exposed sites for the attachment of linkers are indicated by arrows. **D:** VHL binder VH032 (**9**) Commonly employed linker attachment sites are indicated by arrows. Structural modifications for the attachment of linkers and percentage abundance of each linker attachment strategy are shown in color-coded circles respective to the exit vectors.[109] Epimerization of the hydroxyproline stereocenter gives the nonbinding epimer ***epi*-9**, which is commonly used as a nonbinding negative control.

An X-ray structure of VH032 (**9**) bound to VHL reveals surface-exposed binding sites suitable for linker attachment (Figure 8C).[106] Most common linker attachment strategies for VH032 (**9**), the respective chemical modifications, and the percentage of literature-known PROTACs that employ these linker attachment strategies are shown in Figure 8D. Notably, VH032 derivatives are most commonly functionalized *via* an amide linkage between a linker's carboxy group and the N-terminal amine, which replaces the original acetamide moiety of VH032 (**9**).[109]

The linker is a critical compartment that significantly affects PROTAC's performance. It can determine not only the efficiency but also the selectivity of target protein degradation.[110] Each combination of E3 ligase recruiter and target warhead requires

individual linker optimization, as the PPI interface differs in each case.[75] The *de novo* design of PROTACs remains challenging, even with modern computer-aided approaches, as ternary complex formation is difficult to predict. Therefore, linker structures are often optimized empirically through iterative SAR screening.[75]

Although there is no generally standardized procedure for optimizing PROTAC linkers, published examples offer some guiding principles that can be used for efficient linker design and refinement.[75] Linkers consist of a linear motif that is covalently bound to ligands at both ends. For PROTAC design, it is crucial that the linker is connected to a solvent-exposed region of each ligand to avoid disruption of the ligand-protein interaction.[111] Common binding sites for the conjugation of linkers to E3 recruiters have already been outlined above. Ideally, the binding mode of warhead and target protein is known through X-ray or cryo EM structures to enable rational design.

In addition, the nature of the linkage also requires careful consideration. For efficient screening, linkers ideally contain two orthogonal reactive functionalities, one at each terminus, enabling selective and late-stage conjugation of warhead and recruiter. In practice, the available functionalities of the ligands largely determine the type of linkage that can be employed.

The elongating linker motif can be highly variable. Nonetheless, analysis of published PROTACs shows that ethylene glycol, alkyl, and extended glycol-based linkers predominate, accounting for approximately 54%, 31%, and 14% abundance in reported examples, respectively (Figure 9A).[75, 112]

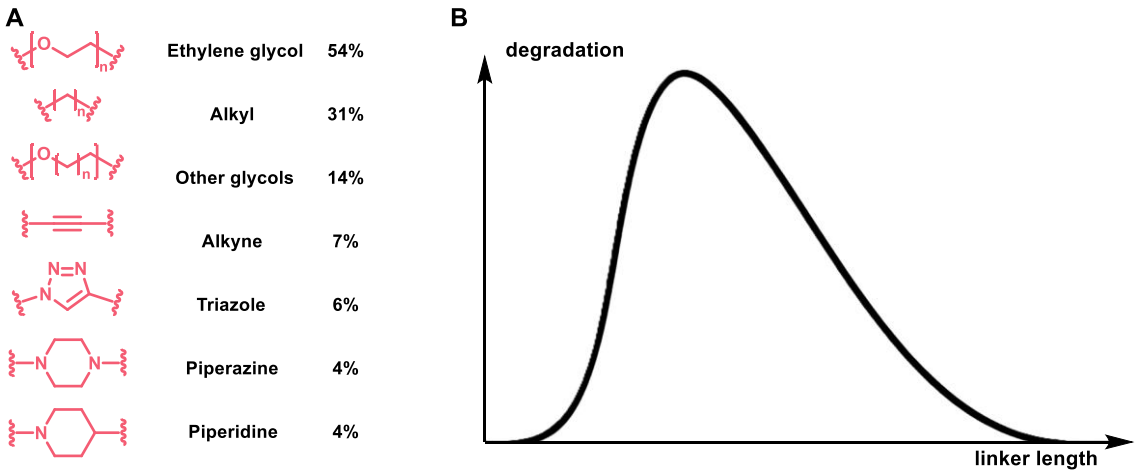

Figure 9: A: Most common motifs found in PROTAC linkers.[75, 112] **B:** Dependence of ternary complex formation on linker length.

These linker motifs offer several advantageous properties, including broad commercial availability, straightforward synthetic accessibility, compatibility with robust chemical transformations, and easy adjustment of the linker length. Together, these features make them particularly well suited for early-stage design.[75, 111] Most PROTACs incorporate combinations of these linker elements to fine-tune overall linker architecture and length.[75]

The relationship between linker length and degradation efficiency is outlined in Figure 9B. If the linker is too short, no ternary complex can be formed even though the PROTAC can bind both proteins individually. This is caused by steric collision between the proteins during formation of a ternary complex. Elongation of the linker leads to a sharp rise in degradation efficiency, indicating a state in which the linker is still under conformational constraint, yet already capable of supporting formation of a productive ternary complex. At an optimal linker length, degradation reaches its maximum, which is accompanied by highly efficient formation of a ternary complex. In this range, a distinct and productive ternary complex architecture is induced.[110]

When the linker is extended beyond its optimal length, degradation efficiency gradually declines, in contrast to the steep improvement as the optimum is approached. This occurs as the PROTAC can still bind to both proteins and promote their proximity, but the increased conformational freedom allows for a larger ensemble of geometries, many of which do not lead to target ubiquitination. Further elongation reduces proximity and thus degradation efficacy. Therefore, during early-stage linker optimization, it is reasonable to begin with relatively long linkers and subsequently refine the design by stepwise shortening.[110]

Once linker attachment points and approximate length have been established, more advanced optimization can focus on parameters such as bioavailability, physiological stability, and lipophilicity. This often involves increasing linker rigidity by constraining it into the conformation preferentially adopted within a productive ternary complex.[113] Commonly used rigidifying elements include alkyne-, piperazine-, and piperidine- motifs, which account for approximately 7%, 4%, and 4% of reported cases, respectively.[75, 112] Aromatic units are also frequently incorporated to enhance linker rigidity; however, they are often not reflected in statistical analysis due to their structural diversity (Figure 9A).

In a majority of PROTACs, recruiter and linker motifs are conserved, whereas the warhead exhibits the highest structural diversity, with 360 distinct examples currently reported in PROTAC-DB 2.0.[114]

A widely used warhead is JQ1 targeting BRD4, a bromodomain and extra-terminal (BET) family protein that reads histone acetylation and coordinates transcription, especially transcription elongation by RNA polymerase II.[115] In cancer, BRD4 is frequently overexpressed and drives oncogenic transcription programs, including super-enhancer-driven expression of MYC and other oncogenes in hematologic and solid tumors.[115] BRD4 has been shown to be degradable by a variety of different PROTACs. Therefore, BRD4 is a common benchmark for PROTAC research towards other objectives than new targets e.g. studies addressing new E3 ligases or delivery strategies.[116] Some examples of PROTACs targeting BRD4 by a JQ1 warhead are shown in Figure 10.

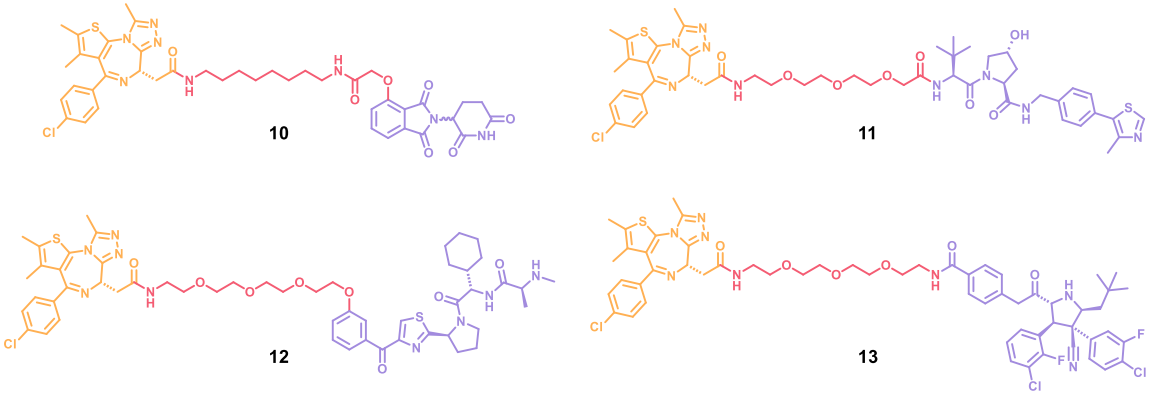

Figure 10: JQ1-based PROTACs **10**[117], **11**[118], **12**[119], and **13**[120] recruiting the E3 ligases CRBN, VHL, cIAP1, and MDM2, respectively. JQ1 warhead, linkers, and recruiters in orange, red and purple, respectively.

While some targets appear to be permissive to a broad range of E3 ligases, others display pronounced E3 ligase selectivity. Therefore, it is advisable to explore multiple E3 ligases when establishing a new warhead. Some examples of clinically advanced PROTACs are shown in Figure 11.

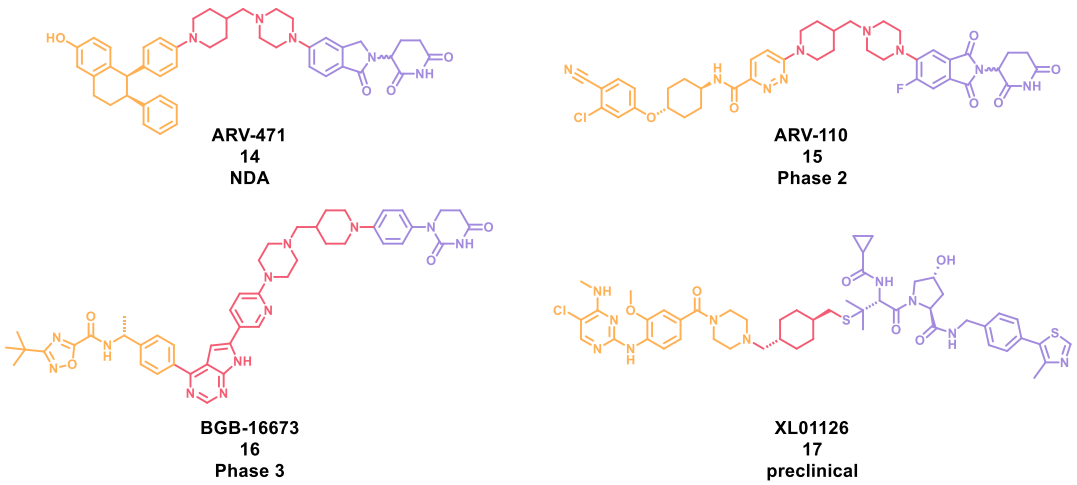

Figure 11: Examples of optimized PROTACs (**14**[121], **15**[122], **16**[123], and **17**[124]) for clinical investigation. Current investigation status is given beneath each compound.

In contrast to the examples shown in Figure 10, all contain rigidified linkers employing the structures discussed above. Notably, all these examples are orally bioavailable. Among the most advanced PROTACs in clinical development is the estrogen receptor degrader ARV-471[121] (**14**), being evaluated for ER-positive/HER2- negative breast cancer. Following positive phase 3 trial results, *Arvinas* and *Pfizer* have submitted a new drug application to the FDA, positioning PROTAC **14** as a promising candidate to become the first FDA-approved PROTAC therapeutic (Figure 11).[121]

Another clinically advanced example from *Arvinas* is the androgen receptor degrader ARV-110[122] (**15)**, which is being evaluated in clinical phase 2 studies for the treatment of AR-positive prostate cancer. Notably, ARV-110 is under investigation not only in patients harboring wild-type androgen receptors, but also in those carrying clinically relevant AR mutations that confer resistance to conventional anti-androgen therapies.[122]

BGB-16673[123] (**16**), a *Burton*'s tyrosine kinase degrader developed by *BeiGene*, is currently undergoing phase 3 clinical evaluation for the treatment of B-cell non-*Hodgkin* lymphomas. Whereas the PROTACs **14** and **15** recruit CRBN *via* thalidomide-derived ligands, PROTAC **16** utilizes a higher-affinity PG-derived CRBN-recruiter, offering improved stability and binding characteristics.

A PROTAC with particularly favorable pharmacological characteristics is XL01126[124] (**17**) currently in preclinical development for the treatment of *Parkinson*'s disease. Notably, it targets the brain-localized leucine-rich repeat kinase 2 (LRRK2), and

XL01126 (**17**) has been reported to cross the blood-brain barrier, a key prerequisite for central nervous system activity.

With the PROTAC modality now firmly established in academic research and pharmaceutical industry, several recruiters advanced to clinical evaluation. Current efforts increasingly shift towards broadening the spectrum of tractable targets. PROTACs are highly attractive for proteins that resist conventional small molecule inhibition, for example when ligands bind in a non-competitive, allosteric fashion or engage the active site too weakly to achieve durable inhibition.[125]

2.3 Proline-rich motif binding domains and how to address them

Proline-rich motifs (PRMs) and their recognition are particularly important in signal transduction, cytoskeletal organization, and regulation of immune system function.[126] These interactions are characteristically low in affinity while exhibiting a large interaction surface.[127] Six examples of PRM recognizing domains bound to their respective substrate are presented in Figure 12.

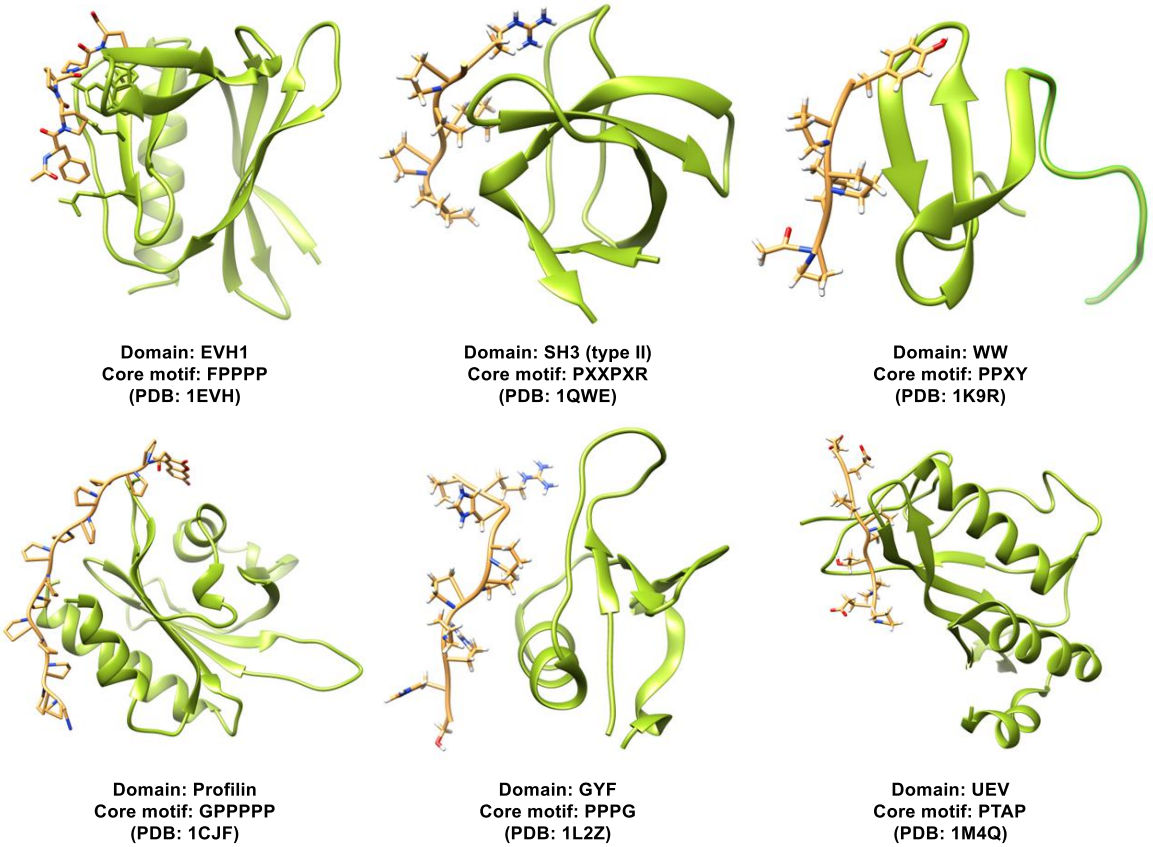

Figure 12: Structures of PRM recognizing domains (green) with a PPII helical interaction partner (orange) and their core binding motifs beneath: EVH1[128] (PDB[129]: 1EVH), SH3[130] (PDB[131]: 1QWE), WW[132] (PDB[133]: 1K9R), profilin[134] (PDB[134]: 1CJF), GYF[135] (PDB[136]: 1L2Z), UEV[137] (PDB[138]: 1M4Q).

Proteins containing PRM binding domains are of high interest as potential drug targets as they are deeply embedded in cellular signaling networks.[139] They play central roles in diverse signaling cascades, and pharmacological rewiring of these PRM-mediated interactions can modulate downstream responses or restore physiological homeostasis in disease settings.[139]

2.3.1 Ena/VASP homology proteins

The Ena/VASP proteins family is a highly conserved protein family, whose members include mammalian Enabling protein (Mena), vasodilator-stimulated phosphoprotein (VASP), and Ena/VASP-like protein (EVL).[140-141] Ena/VASP proteins participate in multiple processes that regulate cell shape and migration by promoting the elongation of actin filaments in structures such as filopodia and lamellipodia.[142-143] The overall domain organization of Ena/VASP family members and their schematic function is depicted in Figure 13.

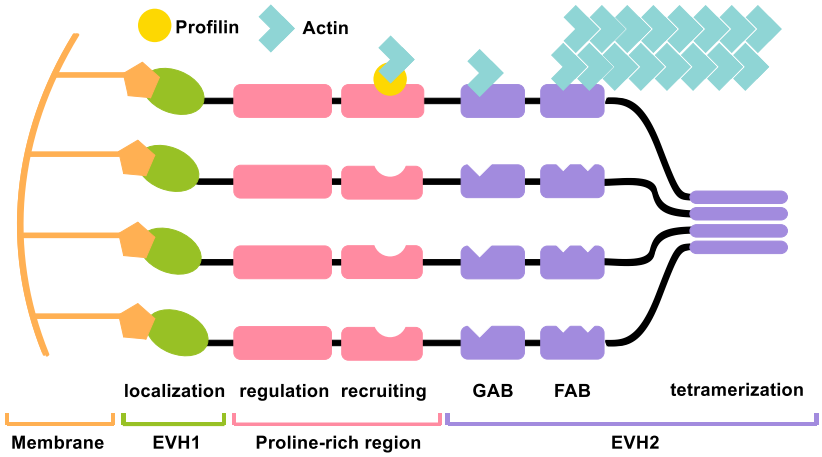

Figure 13: General structure of Ena/VASP protein family members and their schematic mode of action.

Ena/VASP family members contain an *N*-terminal EVH1 domain that binds proline-rich FPPPP-containing motifs in scaffold proteins, such as Zyxin, LPP, and ActA.[144] This interaction is essential for targeting Ena/VASP proteins to focal adhesions and other actin-rich sites, thereby mediating their subcellular localization.[145]

Next to the *N*-terminal EVH1 domain, a proline-rich regulatory region binds to several interaction partners bearing SH3 or WW domains, further emphasizing the functional relevance of this class of low-affinity protein-protein interactions.[146] Further, *Gupton* and coworkers showed that the activity of VASP can be regulated by multiple, non-degradative monoubiquitinations induced by TRIM9 E3 ligase, proving that VASP can be ubiquitinated in several positions. Notably, no ubiquitination of Ena and Mena were observed. Furthermore, netrin-dependent deubiquitination can lead to a recovery of function.[147-149]

The *C*-terminal part of the proline-rich region contains three GPPPPP motifs, which form the core binding motif of profilin.[145] By engaging profilin, which is complexed with G-actin, this region effectively recruits G-actin monomers. G-actin is subsequently

transferred to the G-actin-binding (GAB) region within the *C*-terminal EVH2 domain, where monomeric actin is incorporated into the growing F-actin filament associated with the F-actin-binding (FAB) region of the EVH2 domain.[150] At the *C*-terminus, the EVH2 domain contains a coiled-coil tetramerization unit (Figure 13).[146]

Since Ena/VASP proteins regulate actin filament elongation and are overexpressed in several types of cancer including breast, colorectal, and pancreatic cancer, they represent promising oncogenic targets.[151] Blocking the EVH1 domain is expected to delocalize the protein, thereby disrupting actin filament elongation and thus potentially inhibiting the cell migration, which is a crucial step in the metastatic cascade.[151] A long standing collaboration between *Schmalz* and *Kühne*, which led to the founding of the spin-off *Prosion GmbH*, investigated targeting the EVH1 domain using rigidified structural mimetics. Key findings and the fundamental concept are shown in Figure 14.[152-153]

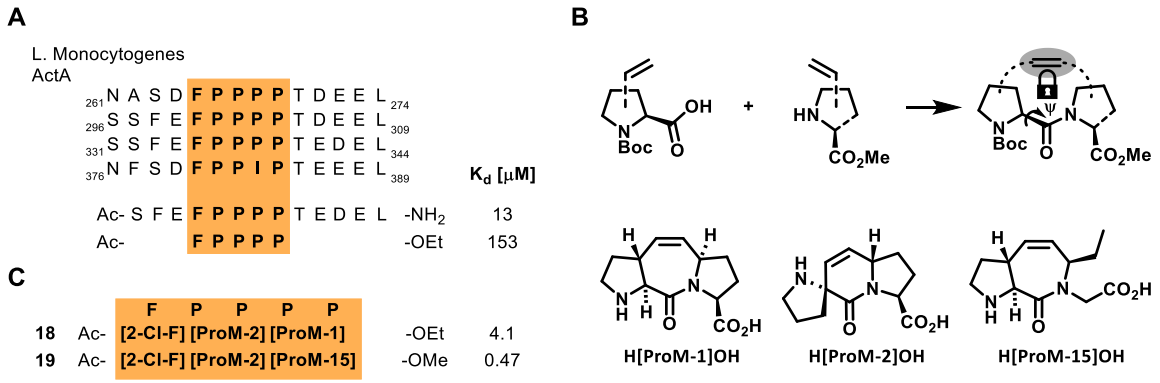

Figure 14: A: EVH1 binding sequences of its interaction partner ActA, derived peptide sequences, and dissociation constants (K_d).[152] Pentapeptidic core motif is shown in orange. **B:** Conceptual overview of proline-derived modules (ProM) and structures of some successfully incorporated ProMs. **C:** ProM-derived, peptoidic EVH1 binders and their dissociation constants.[152]

To specifically target the EVH1 binding site, its natural ligand ActA was chosen as a starting point for the development of small molecule binders. ActA comprises four EVH1-binding motifs that share a conserved pentapeptidic core, flanked by characteristic amino acid sequences that modulate affinity and specificity. A tridecapeptide derived from ActA demonstrated a dissociation constant of 13 μM for the EVH1 domain of Mena, but when truncated to the pentapeptidic core motif, binding significantly decreases to 153 μM (Figure 14A).[152] A possible explanation is the loss of PPII helical secondary structure,[154] which led to the idea that conformational restriction could regain binding affinity.[155-156] The ProM concept originally required two vinylated proline building blocks that were connected by an amide bond. Subsequent

ring closing metathesis disables rotation of the Ψ bond, thereby preserving the secondary structure.[153, 156]

Subsequent increase of the scope of vinylated modules and synthetic procedures[153, 155-161] led to a variety of ProMs. Examples include further modifications such as variation of the ring sizes and ring openings,[162-165] substitution and functionalization of the backbone,[166-167] and *C*-terminal decarboxylation[168] were investigated. Three relevant examples, [ProM-1], [ProM-2], and [ProM-15] are shown in Figure 14B.

Besides rigidification of the pentapeptide, spot on solid phase peptide synthesis based screening revealed a significant increase in binding affinity by chlorination of the *ortho* position of the phenylalanine residue.[169] When the modifications were combined (**18**), significantly higher binding affinities were obtained compared to the pentapeptidic core motif. Substitution of [ProM-1] with the ring opened unit [ProM-15] yielded the first nanomolar binder **19** (Figure 14C).[152, 169] The compound demonstrated significant antimetastatic activity in xenograft zebrafish models.[152]

2.3.2 Growth factor receptor-bound protein 2

The growth factor receptor-bound protein 2 (GRB2) is a small adapter protein found in the cytosol. It consists of a central SH2 domain flanked by two PRM-binding SH3 domains (Figure 15 top).[170-171]

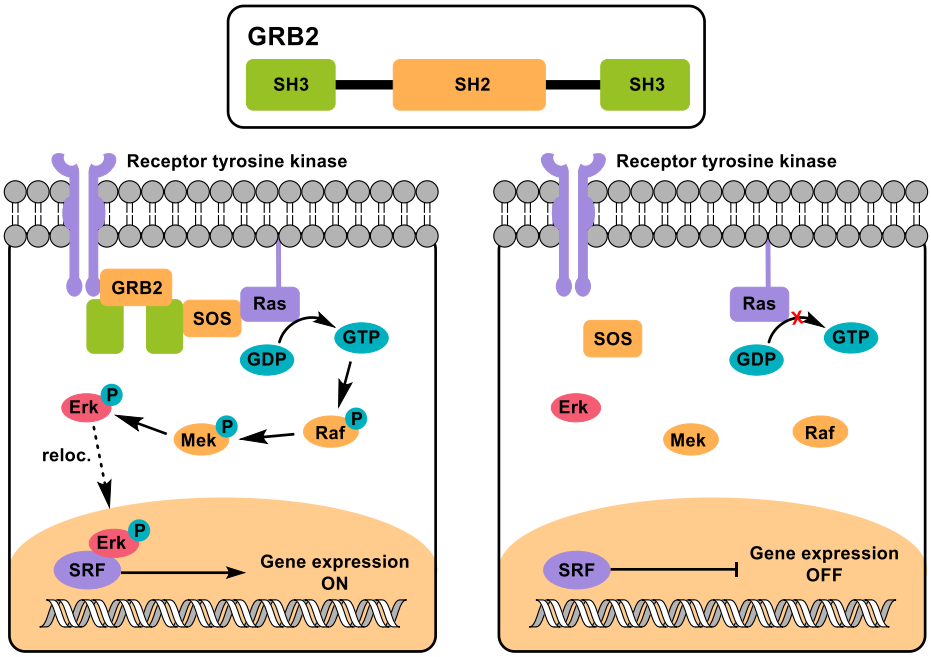

Figure 15: Top: Domain organization of GRB2. **Bottom left:** Activation of the Ras phosphorylation cascade induced by GRB2 leading to increased gene expression. **Bottom right:** Inactive state in the absence of GRB2.

The central SH2 domain binds to a receptor tyrosine kinase located at the membrane,[172] while the SH3 domains bind PRMs of substrates leading to downstream regulations. Recruitment of SOS to Ras leads to activation of Ras-GTP production, which recruits and activates Raf.[173] Raf phosphorylates Mek1/2. Mek1/2 phosphorylates and therefore activates Erk for relocalization towards the nucleus, which leads to the activation of transcription factors and modulates gene expression (Figure 15 bottom, left).[174-175] These gene expressions control cellular functions such as proliferation, differentiation, and survival.[176] Modulation of translation could be a promising therapeutic approach. Therefore, inhibition of the GRB2-SOS interaction or degradation of GRB2 could potentially interrupt the signaling cascade (Figure 15 bottom, right).

2.3.3 Yes-associated protein 1

The Yes-associated protein 1 (YAP1) and its paralog TAZ are transcriptional co-activators that function as the main downstream effector of the Hippo pathway (Figure 16).[177]

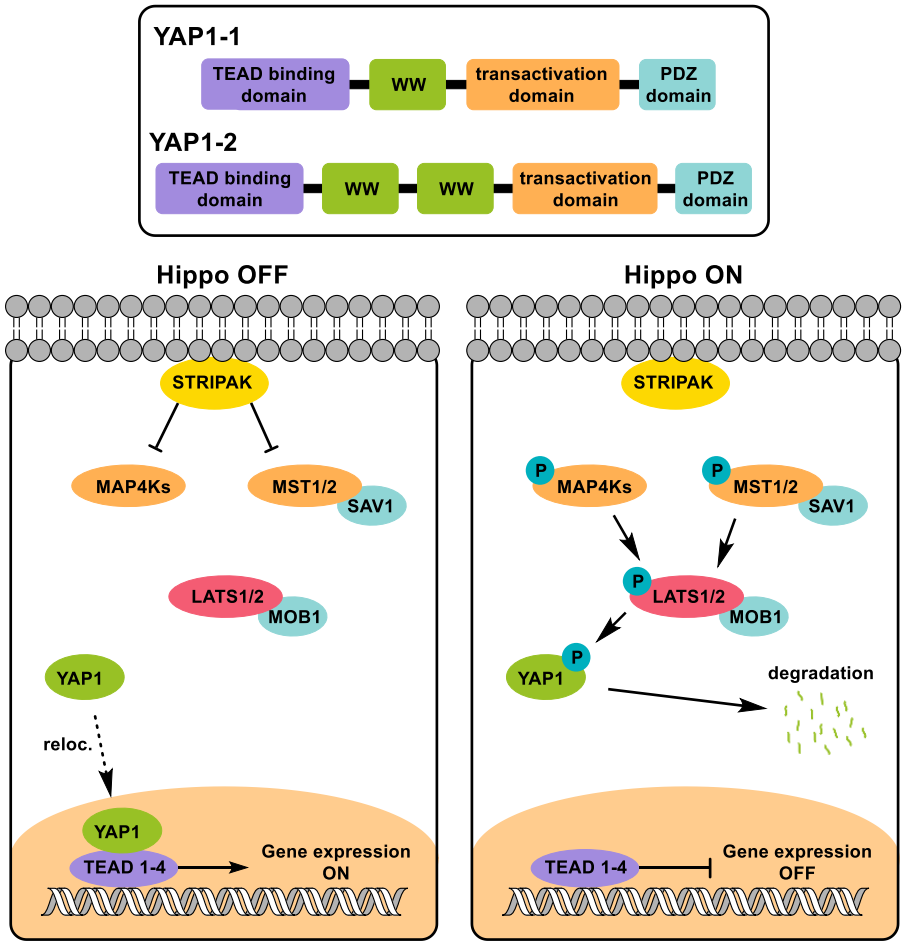

Figure 16: Top: Domain organization of the YAP1 isoforms 1 and 2. **Bottom:** Hippo pathway protein interactions. **Left:** Hippo pathway off. **Right:** Hippo pathway on.

Two isoforms of YAP1 with either one or two PRM binding WW domains in the central region of the protein are known.[178] The interaction partner of the WW domain(s) is a PRM exhibited on the surface of the LATS protein.[179] *N*-terminal of the WW domain is a TEAD binding region. *C*-terminal of the WW domain(s) a transactivation domain controls the expression of several genes when YAP is bound to TEAD.[180] The most *C*-terminal domain interacts with PDZ-domain scaffold proteins and is involved in intracellular relocalization (Figure 16).[181] The cellular concentration and localization of YAP1 is controlled by the Hippo pathway.[177] When the Hippo pathway is off, stratin-interacting phosphatase and kinase (STRIPAK) inhibits the phosphorylation of MAP4Ks and MST1/2. Under these conditions, YAP1 relocalizes to the nucleus, binds

TEAD1-4, and induces the expression of a variety of genes (Figure 16 left).[180, 182] When the Hippo pathway is on, MAP4Ks and MST1/2 phosphorylate LATS1/2, which then binds to the WW domain of YAP1. The phosphorylation inhibits relocalization to the nucleus while simultaneously signaling for YAP1 degradation (Figure 16 right).[179, 183]

The Hippo pathway controls several biological processes involved in cell proliferation[184], organ size regulation[185], and immune functions.[186] Control of this pathway is thus of high therapeutic interest, and as it is the principal effector of TEAD1-4, YAP1 is a promising target. Inhibition of the YAP-LATS interaction could block the phosphorylation of YAP, thereby increasing relocalization to the nucleus and upregulating gene expression. In order to reduce YAP1-induced gene expression, degradation of YAP1 was already investigated. Two strategies for the induced degradation of YAP1 are known in literature.[187-188] In 2024, *Li* and coworkers reported the first small molecule YAP degrader **20** (Figure 17).[187]

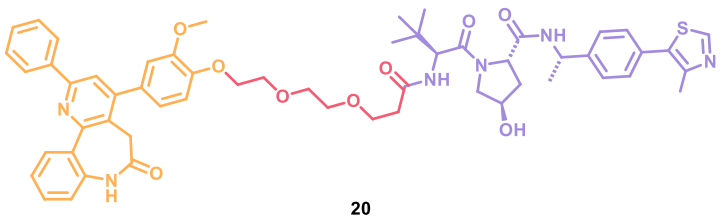

20

Figure 17: Published TEAD degrader **20** reported to efficiently degrade YAP1. Warhead, linker, and recruiter compartments are shown in orange, red, and purple, respectively.

The warhead of degrader **20** binds the TEAD interaction site of YAP, while VHL is addressed by the recruiter to induce ubiquitination. A screening of different warhead attachment sides and linkers, as well as YAP degradation and tumor growth inhibition in mice are described within the work.[187] Another strategy was reported by *Zhou et al*. in 2025.[188] Nanobodies with nanomolar binding affinities to YAP were developed by three generations of phage display. These binders were incorporated into fusion proteins comprised of these nanobodies and an E3 ligase. Within this study, inhibition of cancer cell migration *in vitro* and *in vivo* was reported.[188]

3 Aim of the Project

The ProM-derived EVH1 binders have demonstrated chemotaxis inhibition in xenograft zebrafish models.[152] However, their limited binding affinities and the requirement for high cellular concentrations restrict their suitability for therapeutic applications. In contrast, PROTACs operate under an event-driven mechanism, and their catalytic mode of action enables effective protein degradation at lower cellular concentrations. Furthermore, PROTACs can sustain high degradation efficacy with ligands of moderate affinity due to proximity-induced constructive interactions within the ternary complex.[79] Consequently, the aim of this project was to incorporate ProM-derived EVH1 binders into PROTACs.

A suitable EVH1 binder should be selected based on the current state of knowledge.[152] Based on its binding mode, an appropriate linker attachment site should be identified. Taking into account the existing literature, linkers for the installation of state-of-the-art E3 recruiters are to be developed. Various linker compositions and lengths were to be investigated. The developed EVH1 degraders had to be synthesized, purified, and characterized. Binding affinities to EVH1, target degradation, and chemotaxis inhibition were to be investigated in collaboration with *Prosion GmbH*.

The second aim of the project was to investigate the use of ProMs to target the SH3 and WW domains of GRB2 and YAP1 in collaboration with *Prosion GmbH*. Initially, peptidic binders described in literature should be synthesized and evaluated. The binding affinities should be measured by biolayer interferometry (BLI), which requires the development of biotinylated tracer peptides. Once the assay has been successfully established, ProM-substituted peptides were to be synthesized, evaluated, and systematically truncated. The resulting affinity profiles will serve as the foundation of subsequent optimization and development of low-molecular weight inhibitors.

4 Results and Discussion

4.1 Design, Synthesis, and Evaluation of Ena/VASP homology proteins targeting PROTACs

4.1.1 Design of Ena/VASP homology proteins targeting PROTACs

At the beginning of the design process for an Ena/VASP targeting PROTAC, an EVH1 binder had to be chosen to begin with. Therefore, binding affinity, synthetic accessibility, and knowledge about the binding mode were considered. As already described in Figure 13, the EVH1 binder **19** exhibited one of the highest binding affinities among the published binders. It could be synthesized reliably and in large quantities.[189] Lastly, the binding mode of the corresponding acid **21** is known by X-ray structure (Figure 18).

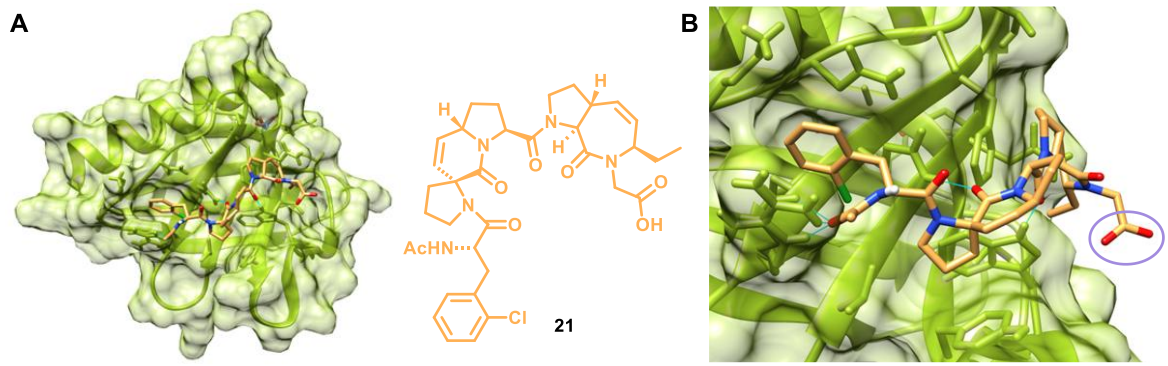

Figure 18: A: X-ray structure (PDB[152]:6RCF) of EVH1 in complex with binder **21**. **B:** Different view of the same structure, highlighting the exposed *C*-terminus of binder **21**.

With binder **21** as a potential warhead in mind, a suitable region for the linker attachment was required. Therefore, solvent exposure and chemical addressability were considered. As shown in Figure 18B, the *C*-terminus of binder **21** is not involved in binding EVH1. It is exposed to the solvent and could therefore be suitable for linker attachment. The acid function provides a chemical handle that is addressable for linker attachments without modification of the binder. Therefore, the *C*-terminus was chosen for the linker attachment. With the *C*-terminal acid of the binder as the reactive handle in mind, the next question was how to attach a linker. Partially unpublished results by *Prosion GmbH* have shed light on several optimizations and *C*-terminal modifications (Figure 19).[189]

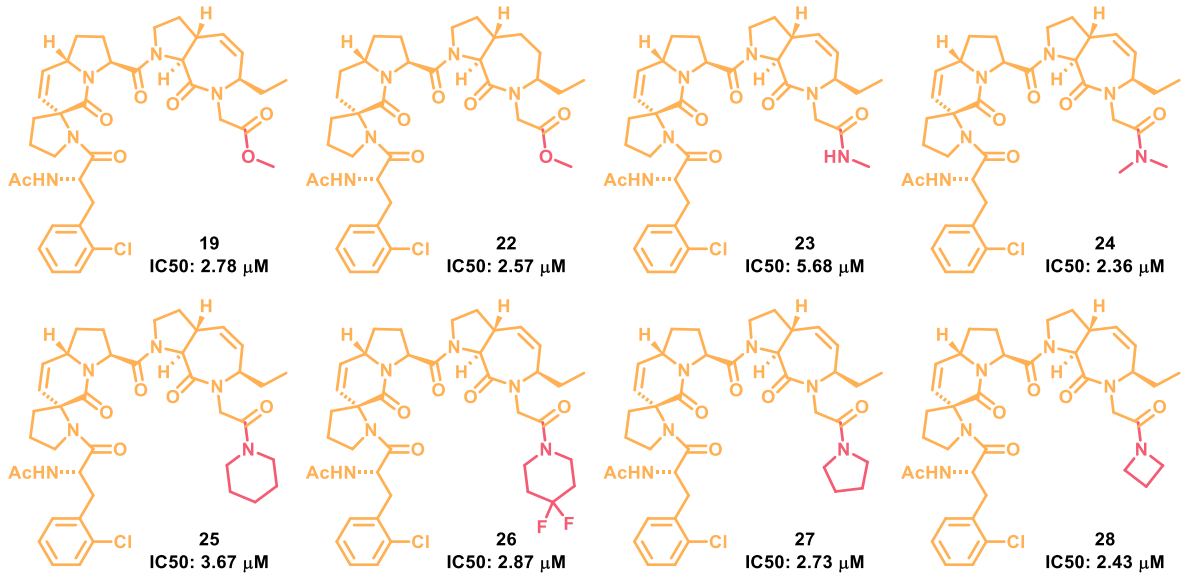

Figure 19: Structure and IC50 values for the binding to EnaH-EVH1 for different inhibitors mainly varying in their *C*-terminal modification.[189]

Comparison of binders **19** and **22** showed that the backbone double bonds can be reduced to the saturated ProM-scaffold without loss of binding affinity, while increasing stability by preventing allylic migration of the double bond. However, esters are known to be prone to hydrolysis under physiological conditions and were therefore not considered.[190] The amide analogue **23** was found to have a slightly lower binding affinity, but a higher physiological lifetime was expected and therefore this strategy was considered. Formal N-methylation of binder **23** leads to binder **24** which was shown to bind EVH1 similarly strong as binder **22**. However, asymmetrically substituted amides from secondary amines exhibit a *cis-trans* isomerism when the partial double bond character of the amide bond is considered. A possible way to prevent *cis-trans* isomers is by symmetry. Therefore, cyclic amides can be employed as shown with binders **25-28**. Further, derivative **26** indicated that functionalization of the 4-position of piperidine capping is tolerated (Figure 19). While *cis-trans* isomerism can be prevented by cyclic amides, monosubstitution of the ring leads to axial isomers along the C-N amide bond when the partial double bond character is considered (Figure 20B).

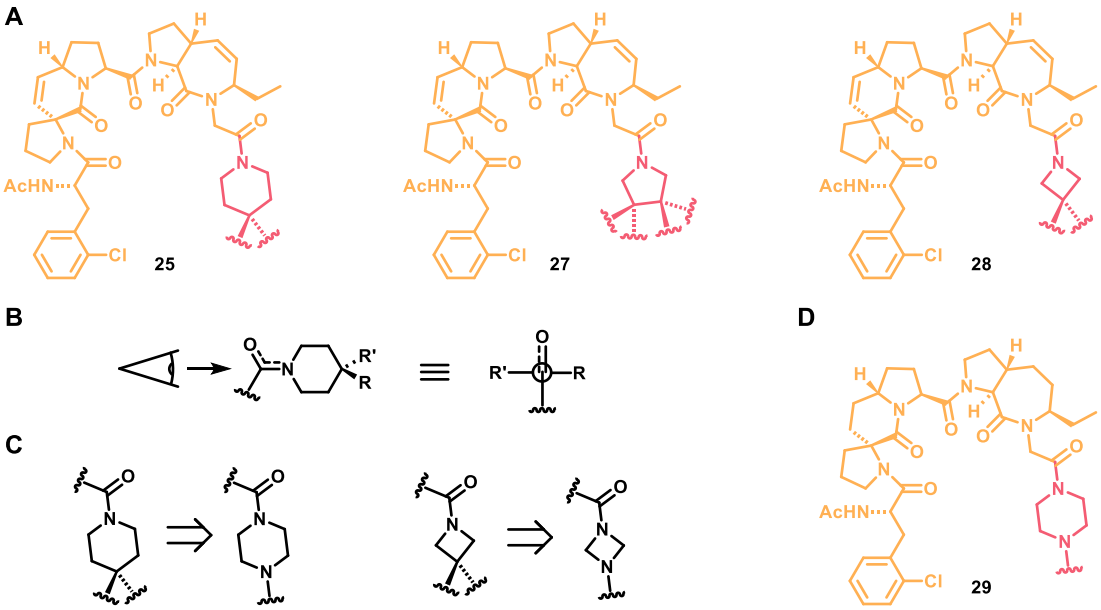

Figure 20: A: Structures of binders **25**, **27**, and **28** with indicated exit vectors for linker attachment. **B:** representation of the axial isomers resulting from the partial double bond character of the amide bond. **C:** Envisioned amine substitution for the linker design. **D:** Envisioned design for the warhead attachment and the first linker compartment **29**.

Notably, rings with odd ring sizes such as in binder **27** were not considered as additional *cis-trans* isomers would be formed (Figure 20A).To reduce the number of possible isomers, installation of cyclic diamines such as piperazine or 1,3-diazetidine were considered (Figure 20C). As derivative **26** demonstrated that the 4-position of the six-membered ring tolerates substitution and as it could be easily addressed, it was envisioned to functionalize the warhead with a piperazine derived linker as shown in Figure 20D. The linker attachment strategy for the recruiter had to be carefully considered as well. Different literature-known attachment strategies have been outlined in Figure 7. The envisioned linker-recruiter strategies are shown in Figure 21.

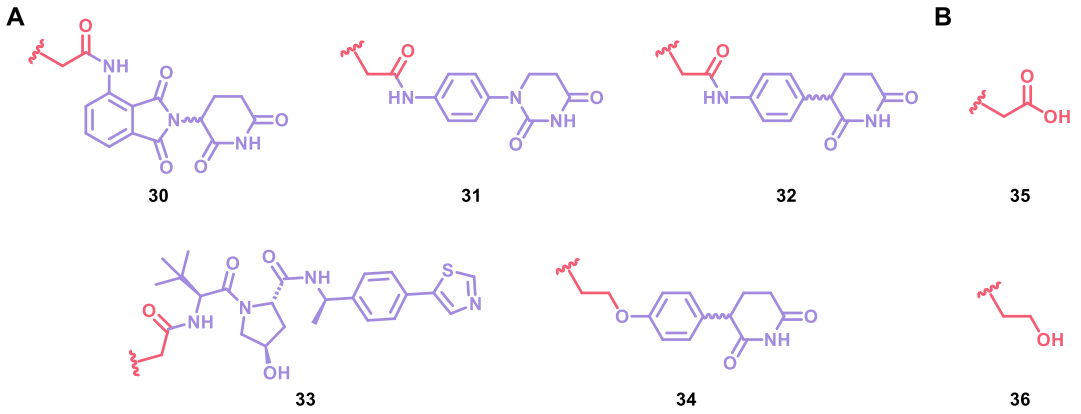

Figure 21: A: Structures of different E3 ligase recruiters with the envisioned linker strategy (**30**-**34**). B: Synthetic equivalents **35** and **36**.

As described in Figures 7 and 8, pomalidomide and VHL recruiters are commonly addressed *via* their amines and were therefore envisioned to be addressed by amide coupling with an acid linker moiety (substructures **30** and **33**; Figure 21A). Therefore, both E3 ligase recruiters could be addressed with the same set of linkers, which was considered beneficial. Also, PG and PD derived recruiters could be addressed by the same linker. Therefore, *para*-amide attachment was envisioned (substructures **31** and **32**; Figure 21A). Finally, attachment of a PG recruiter *via* an ether linkage was envisioned to optimize for low molecular weight and topological polar surface area (TPSA), as well as reduced number of heteroatoms, and amide bonds (substructure **34**; Figure 21A). The respective linker equivalents **35** and **36** are shown in Figure 21B.

Finally, with both linker attachments defined, the interconnection between the two compartments was the last missing part of the design. The envisioned linker subunits are shown in Figure 22.

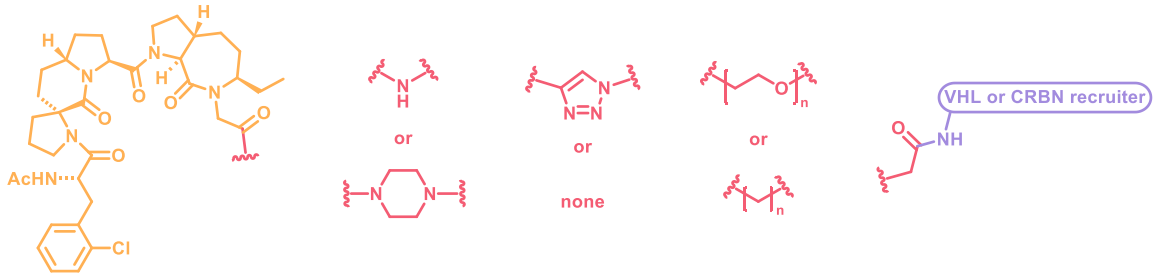

Figure 22: Linker strategy envisioned for the design of PROTACs.

As highlighted in Figure 9, the length of the linker can have a crucial influence on degradation efficacy. Therefore, units of variable length shall be incorporated to screen this parameter. Alkyl- and ethylene glycol linkers are predominantly employed in early stage PROTAC development, which were also envisioned for this project. To ensure successful late-stage assembly, a triazole moiety was envisioned to be installed by click chemistry. Due to synthetic accessibility, alkyne and azide moieties were planned to be attached to the warhead and the recruiter side, respectively (Figure 22).

4.1.2 Synthesis of EVH1-binding Warhead

The synthesis of linker **37**, warhead **38**, and warhead-linker construct **39** are shown in Scheme 8. The linker **37** was obtained from Boc-protected piperazine (**40**) and propargyl bromide (**41**) *via* nucleophilic substitution, following the procedure reported by *Kapic et al*.[191] Acidic deprotection of intermediate **42** yielded the desired linker **37** (Scheme 8).

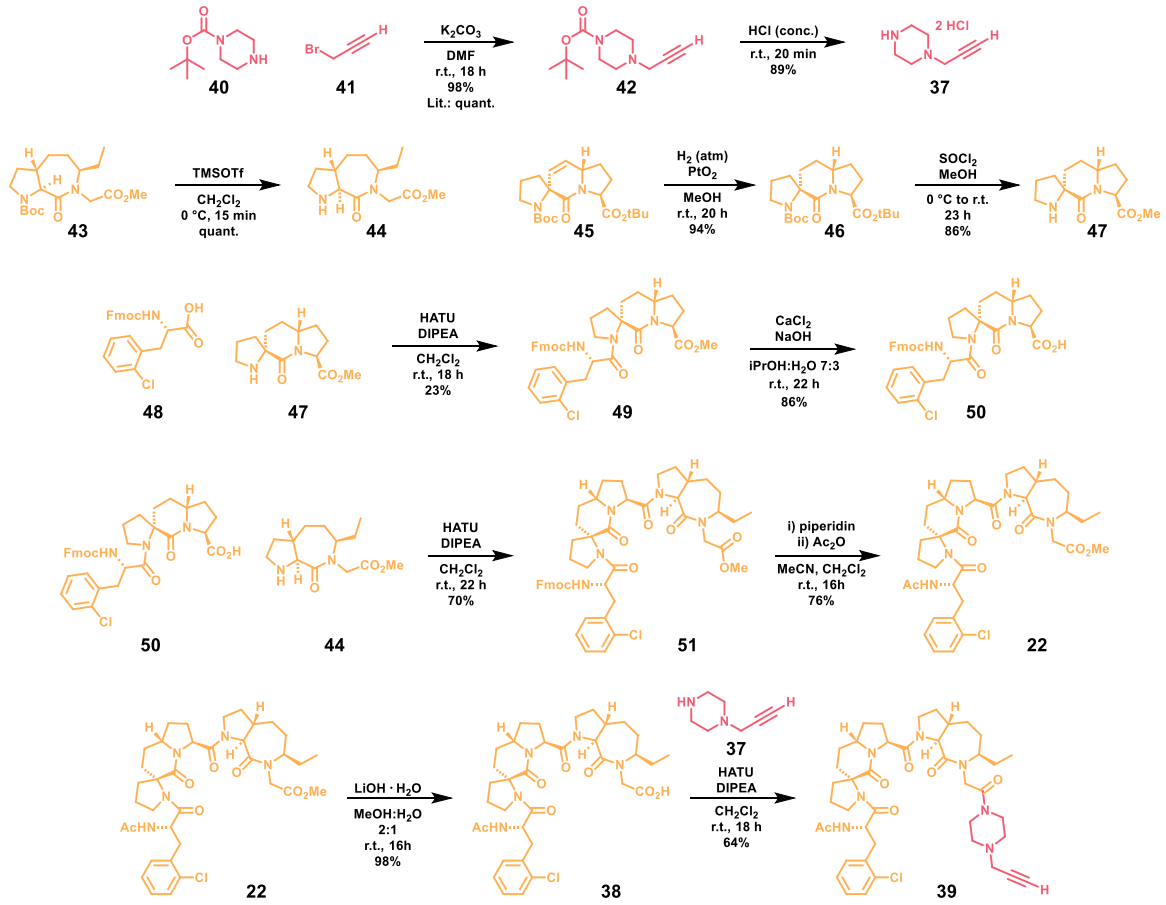

Scheme 8: Synthesis of linker **37**, warhead **38**, and warhead-linker conjugate **39**. Linker and warhead compartments are shown in red and orange, respectively.

ProM building blocks **43** and **45**, as well as some later intermediates were synthesized and provided by *Prosion GmbH* according to published procedures.[153, 192-193] The building blocks were further modified for warhead assembly using the same procedures applied to the corresponding non-hydrogenated analogues.[153] ProM building block **43** was deprotected employing TMSOTf to yield intermediate **44**. Building block **45** was hydrogenated to yield intermediate **46**. Boc deprotection and transesterification were achieved by treatment with $SOCl_2$ yielding building block **47**. Amide coupling with 2-chlorophenylalanine **48** gave the desired tripeptoid **49**. The methyl ester **49** was hydrolyzed to receive the tripeptoid **50**. Building block **50** was

coupled with amine **44** to receive pentapeptoid **51**. Fmoc deprotection and *N*-terminal acetylation were achieved in one step giving binder **22**. The methyl ester was hydrolyzed to receive warhead **38**. Warhead-linker conjugate **39** was synthesized by an amide coupling of warhead **38** and linker **37** (Scheme 8).

4.1.3 Synthesis of CRBN-recruiting PROTACs

After successful synthesis of warhead-linker conjugate **39**, azide functionalized linker-recruiter conjugates shall be synthesized and coupled to the warhead. Incorporation of the commercially available pomalidomide (**3**) is shown in Scheme 9.

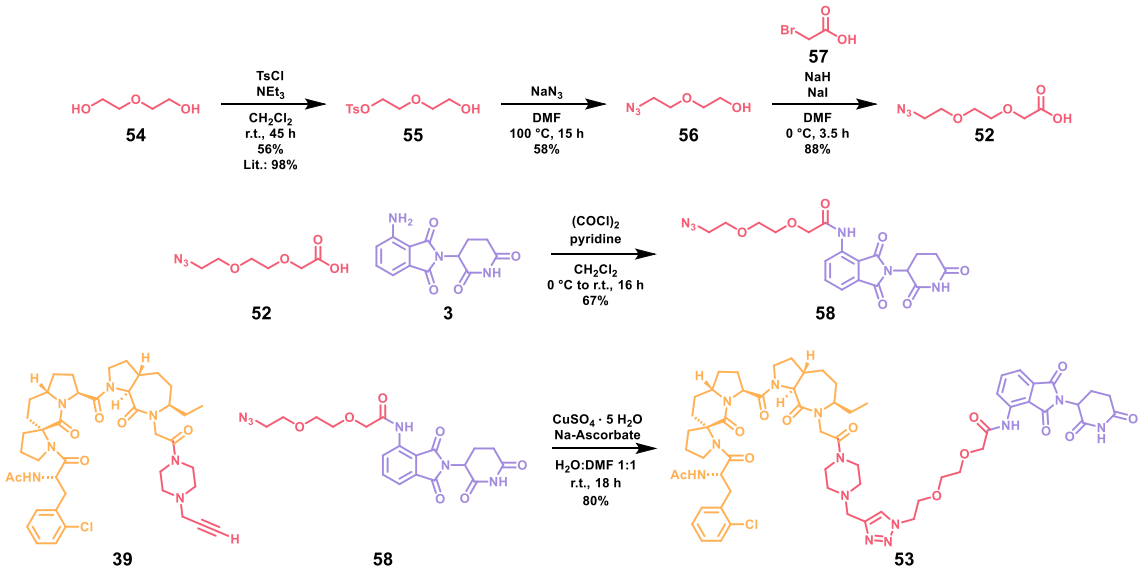

Scheme 9: Synthesis of linker **52** and CRBN-recruiting PROTAC **53**. Warhead, linker, and recruiter compartments are shown in orange, red, and purple, respectively.

To synthesize the PEG-derived azide-acid linker **52**, diethylene glycol (**54**) was monotosylated according to a procedure by *Zhang* and coworkers to yield intermediate **55**.[194] The tosyl group was substituted with sodium azide to receive building block **56**. Synthesis of linker **52** was achieved by nucleophilic substitution on the α-position of bromoacetic acid (**57**) with linker intermediate **56**. Linker **52** was coupled with pomalidomide (**3**). As described in literature, the electron deficient amine of pomalidomide (**3**) requires activation of acid **52** *via* formation of the acid chloride.[195] The resulting linker-recruiter construct **58** was then connected to the warhead-linker construct **39** according to a procedure by *Prante* and coworkers, resulting in the formation of PROTAC **53** (Scheme 9).[196] As the synthesis of PROTAC **53** was successful, the PG derived recruiter was incorporated employing the same linker strategy (Scheme 10).

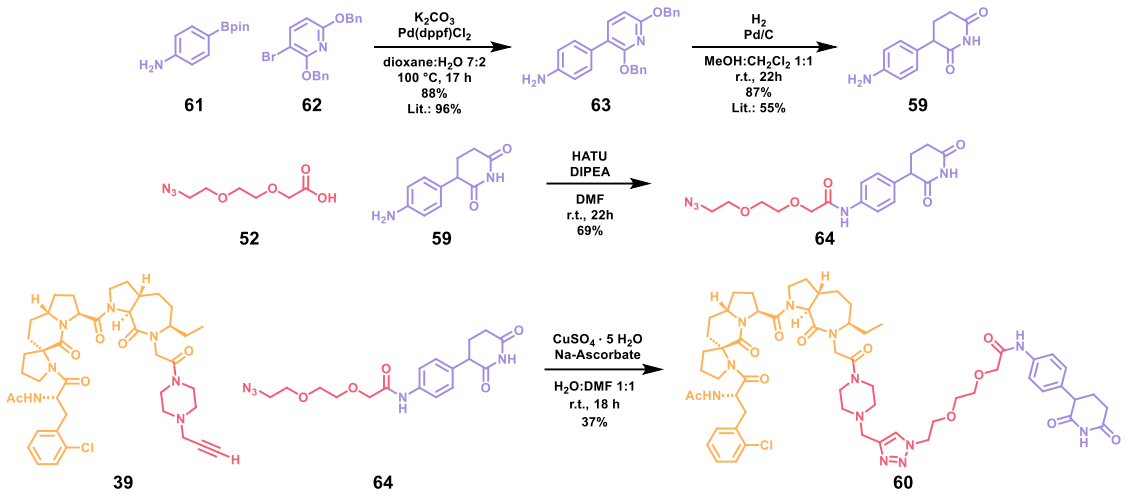

Scheme 10: Synthesis of CRBN binding recruiter **59** and CRBN-recruiting PROTAC **60**. Warhead, linker, and recruiter compartments are shown in orange, red, and purple, respectively.

CRBN recruiter **59** was synthesized according to *Lei et al*.[197] Therefore, boronic acid ester **61** and protected glutarimide **62** were coupled under *Suzuki* conditions. The resulting intermediate **63** was deprotected by hydrogenation to achieve recruiter **59**. Linker **52** and recruiter **59** were coupled yielding linker-recruiter construct **64**. The linker-recruiter construct was connected with the warhead-linker construct **39** employing click chemistry, resulting in the formation of PROTAC **60** (Scheme 10). In the same manner, the PD recruiter shall be incorporated into a PROTAC (Scheme 11).

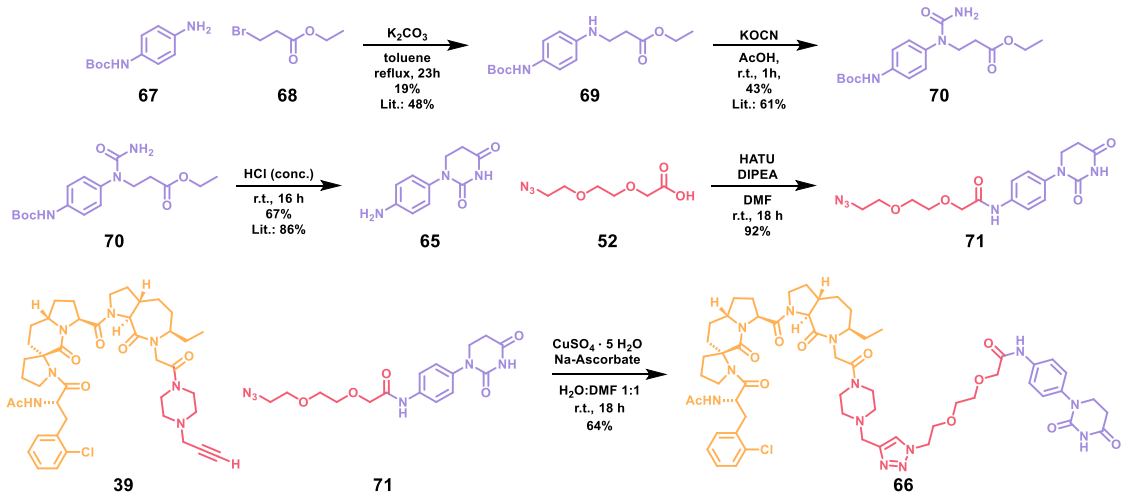

Scheme 11: Synthesis of CRBN binding recruiter **65** and CRBN-recruiting PROTAC **66**. Recruiter, linker, and Warhead compartments are shown in purple, red, and orange, respectively.

The phenyl dihydrouracil recruiter **65** was prepared as described by *Norris et al*.[198] Mono protected diamine **67** was coupled with bromide **68** through nucleophilic substitution to receive building block **69**. Subsequent treatment with potassium isocyanate introduced the urea moiety, yielding building block **70**. Treatment with HCl

cleaved the Boc-protection group and simultaneously promoted dihydrouracil ring formation leading to recruiter **65** (Scheme 11). Linker **52** was coupled with recruiter **65** giving linker-recruiter construct **71**. The resulting linker-recruiter construct **71** was then connected to the warhead-linker construct **39** employing click chemistry, resulting in the formation of PROTAC **66** (Scheme 11). To decrease the heteroatom count, a linker strategy omitting the triazole moiety and incorporating an ether moiety between linker and recruiter was envisioned. The first synthetic attempt is outlined in Scheme 12.

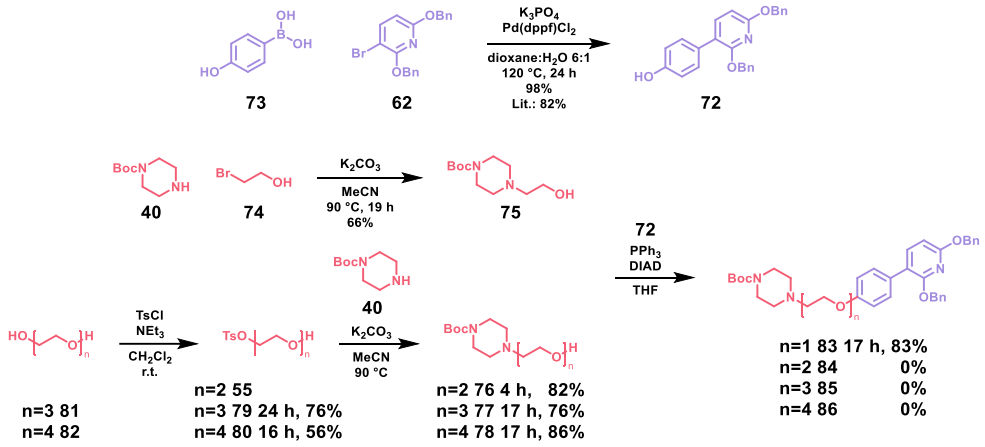

Scheme 12: Synthesis of CRBN binding recruiter **72** and synthetic attempt for linker attachment. Recruiter and linker compartments are shown in purple and red, respectively.

The protected phenyl glutarimide **72** was synthesized by *Suzuki* coupling of boronic acid **73** and aryl bromide **62** according to *Nishiguchi et al*.[199] Linker **75** was synthesized from Boc-protected piperazine (**40**) and bromoethanol (**74**). Derivatives **76**-**78** were synthesized starting from the tosylated ethylene glycols **55**, **79**, and **80**, respectively. Tosylated ethylene glycols **79** and **80** were obtained from ethylene glycols **81** and **82** according to the same procedure employed for the synthesis of the monotosylated ethylene glycol **55** (Scheme 9).[194] To address the linker-recruiter conjugates **83**-**86**, *Mitsunobu* coupling of the protected recruiter **72** with the respective linkers were envisioned. However, only the shortest linker-recruiter construct **83** was successfully synthesized while no product was obtained for the reactions towards derivatives **84**-**86**. Notably, the formation of triphenyl phosphine oxide was observed in each case. A possible mechanistic explanation is shown in Scheme 13.

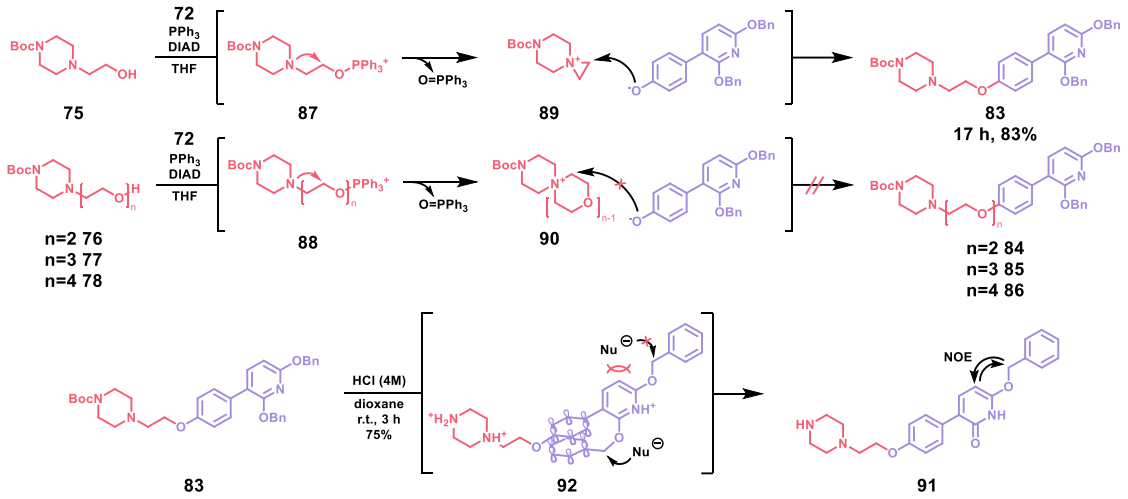

Scheme 13: Predicted mechanism explaining the observed selectivity for the coupling of linkers to **72** and deprotection of **83**. Linker and recruiter compartments are shown in red and purple, respectively.

One explanation could be that after the initial activation of the alcohols **75-78** (Scheme 13), the nucleophilic attack occurred intramolecular by the amine (**87** and **88**), leading to the respective ammonium salts **89** and **90** (Scheme 13). Among these, the aziridinium cation **89** could have reacted under the formation of product **83** driven by strain release while the ammonium salts **90** were not reactive.

In the subsequent step, intermediate **83** was subjected to acidic deprotection. Product analysis further revealed highly selective cleavage of one of the benzyl groups. Unexpectedly, NOE experiments revealed that the *ortho* position was deprotected (Product **91**; Scheme 13). *Para* selective debenzylation was described in literature for a similar system, notably without indication that selectivity was investigated.[200] A possible explanation could be a π-π-interaction between the phenyl linker and the *ortho* benzyl group, leading to a *cis* orientation of the C-O bond and therefore steric exposure of the CH_2 group (Intermediate **92**; Scheme 13).

In a second attempt, Cbz was employed instead of the Boc-protection group to globally deprotect the linker-recruiter construct in a single step (Scheme 14).

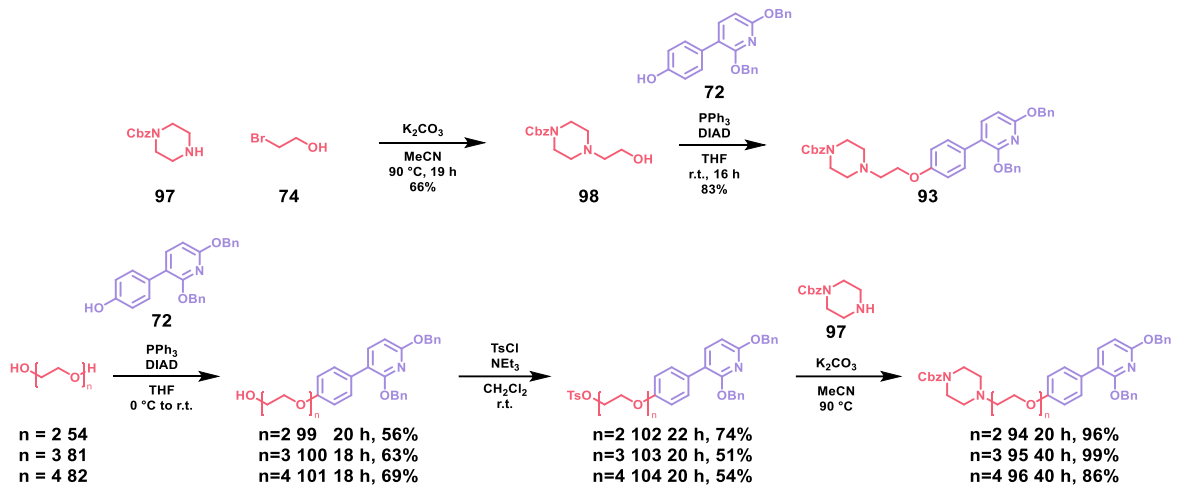

Scheme 14: Synthesis of **93-96** according to an alternative synthetic route. Linker and recruiter compartments are shown in red and purple, respectively.

Therefore, the protected linker-recruiter conjugate **93** was synthesized from piperazine **97**, bromoethanol (**74**), and recruiter **72** following the same strategy already successful for conjugate **83** (Scheme 13 and 14). Further, the protected recruiter **72** was successfully coupled under *Mitsunobu* conditions with ethylene glycols **54**, **81**, and **82**. The resulting conjugates **99-101** were tosylated to receive intermediates **102-104**, respectively. Nucleophilic substitution with the protected piperazine **97** gave the envisioned conjugates **94-96** (Scheme 14). The obtained linker-recruiter conjugates **94-96** were deprotected and incorporated into PROTACs as described in Scheme 15.

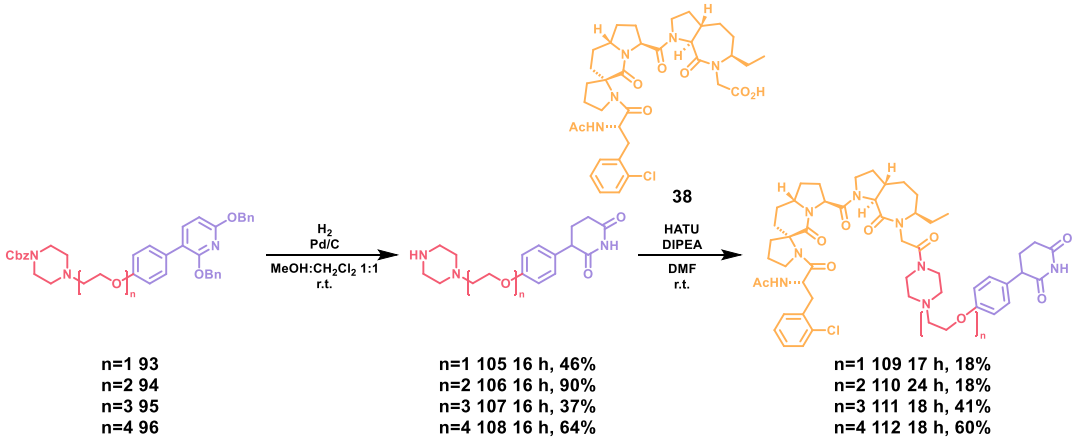

Scheme 15: Synthesis of CRBN-recruiting PROTACs **109-112**. Warhead, linker, and recruiter compartments are shown in orange, red, and purple, respectively.

The protected linker-recruiter conjugates **93-96** were deprotected by hydrogenation to afford the linker-recruiter conjugates **105-108**, respectively (Scheme 15). The obtained linker-recruiter conjugates were coupled to warhead **38** to receive the PROTACs **109-112** (Scheme 15).

4.1.4 Synthesis of VHL-recruiting PROTACs

Different VHL-recruiting PROTACs were envisioned to be tested for the degradation of Ena/VASP proteins. As a reference, the VHL recruiter **113** was acetylated to receive control compound **114** according to a procedure by *Zhao et al*.[201] as shown in Scheme 16.

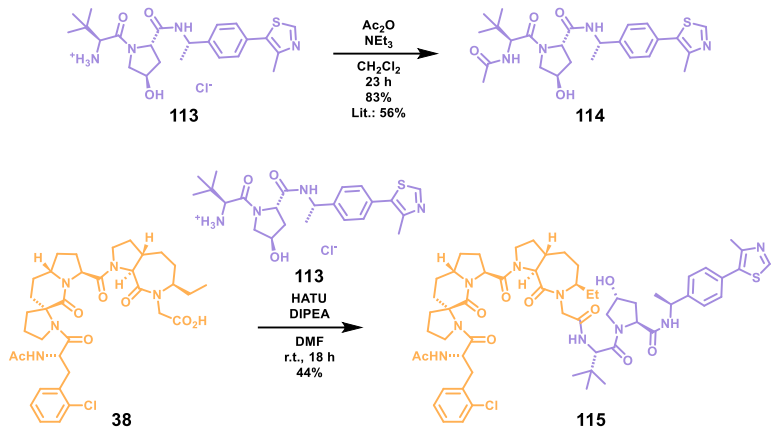

Scheme 16: Acetylation of VHL recruiter **114** and synthesis of VHL-recruiting glue-like compound **115**. Warhead and recruiter compartments are shown in orange and purple, respectively.

Further, direct amide coupling between recruiter **113** and warhead **38** gave the linker-free PROTAC **115** (Scheme 16). Different PEG-derived acid-azide linkers were incorporated as shown in Scheme 17.

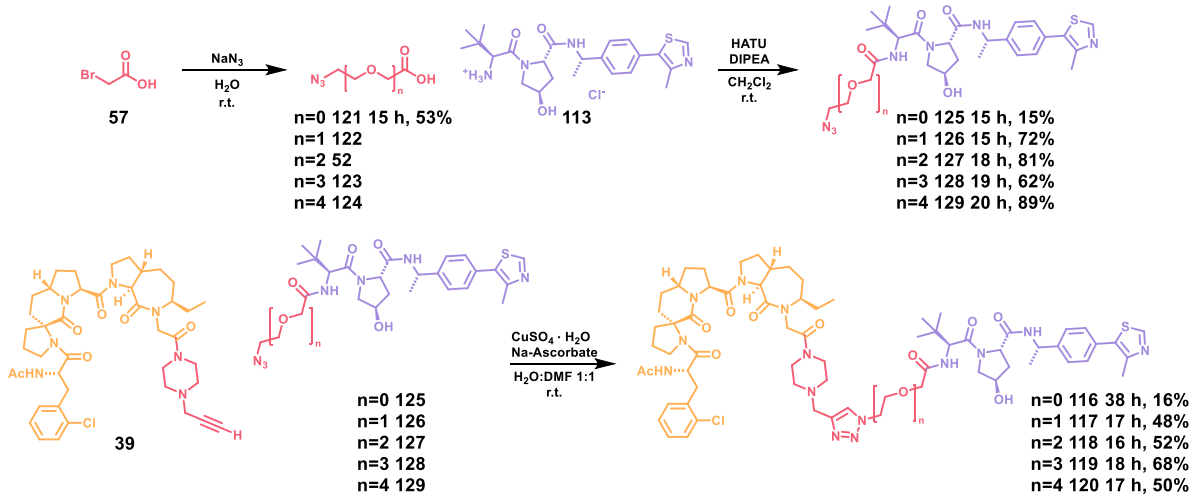

Scheme 17: Synthesis of VHL-recruiting PROTACs **116-120**. Warhead, linker, and recruiter compartments are shown in orange, red, and purple, respectively.

Therefore, bromoacetic acid (**57**) was reacted with sodium azide to receive linker **121**. The synthesis of linker **52** is described in Scheme 9. Linkers **122-124** were bought from commercial sources. HATU coupling with recruiter **113** gave the linker-recruiter conjugates **125-129** (Scheme 17). Warhead-linker conjugate **39** was reacted with

linker-recruiter conjugates **125-129** to receive the PROTACs **116-120**, respectively (Scheme 17).

Prosion GmbH supplied two further warhead-linker conjugates **130** and **131** with varying warheads, which were further incorporated into PROTACs (Scheme 18).

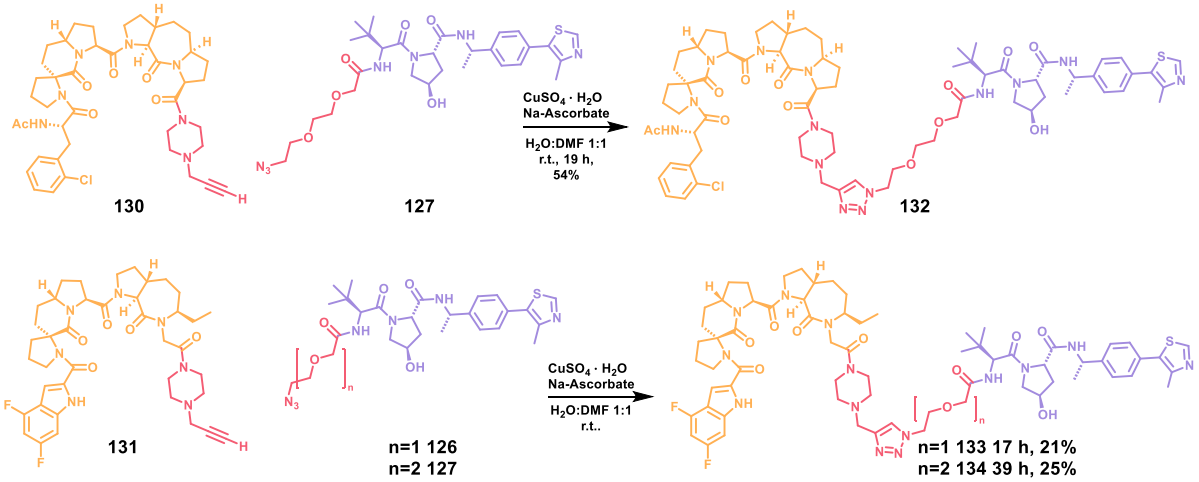

Scheme 18: Synthesis of VHL-recruiting PROTACs **132-134**. Warhead, linker, and recruiter compartments are shown in orange, red, and purple, respectively.

Both warhead-linker conjugates were reacted with linker-recruiter conjugate **127** to yield the respective PROTACs **132** and **134**. Warhead **130** was further coupled with linker-recruiter conjugate **126** to yield PROTAC **133** (Scheme 18).

To yield a VHL non-recruiting negative control, the hydroxyproline-epimerized non-binding recruiter **135** was synthesized (Scheme 19).

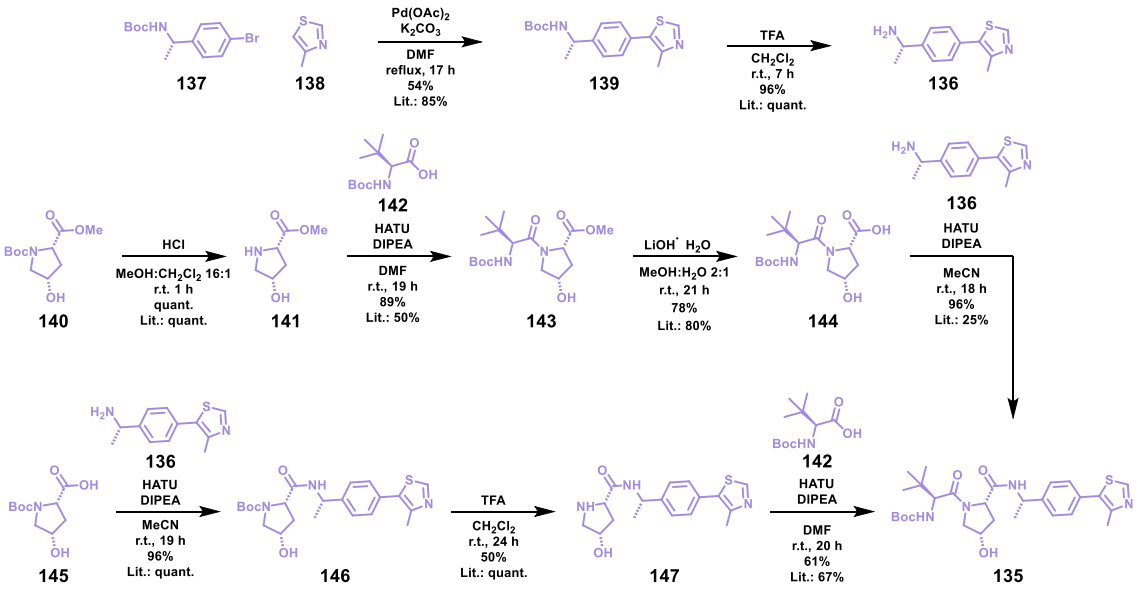

Scheme 19: Synthesis of Boc-protected, VHL non-binding negative control **135** *via* two synthetic routes.

C-terminal amine **136** was synthesized as described by *He et al*.[202] Therefore, aryl bromide **137** and heterocycle **138** were coupled under *Suzuki* conditions to yield intermediate **139**, followed by acidic deprotection. The recruiter was assembled following two different, literature-known synthetic strategies.

According to a synthetic strategy by *Shah et al*.[203] hydroxyproline **140** was *N*-terminally deprotected under acid conditions to yield **141**. Following the synthetic strategy by *He et al*.[202] *tert*-leucine **142** was introduced by HATU coupling to receive dipeptide **143**. *C*-terminal hydrolysis yielded acid **144**, which was HATU coupled to the previously synthesized amine **136** to yield the Boc-protected non-binding recruiter **135** (Scheme 19).

According to the strategy by *Desantis et al*.[204] hydroxyproline derivative **145** was coupled with amine building block **136** to yield intermediate **146**. *N*-terminal deprotection gave amine **147**. HATU coupling with *tert*-leucine **142** gave the desired intermediate **135** (Scheme 19).

Further, the synthesis of negative controls ***epi*-114** and ***epi*-118** based on construct **135** is shown in Scheme 20.

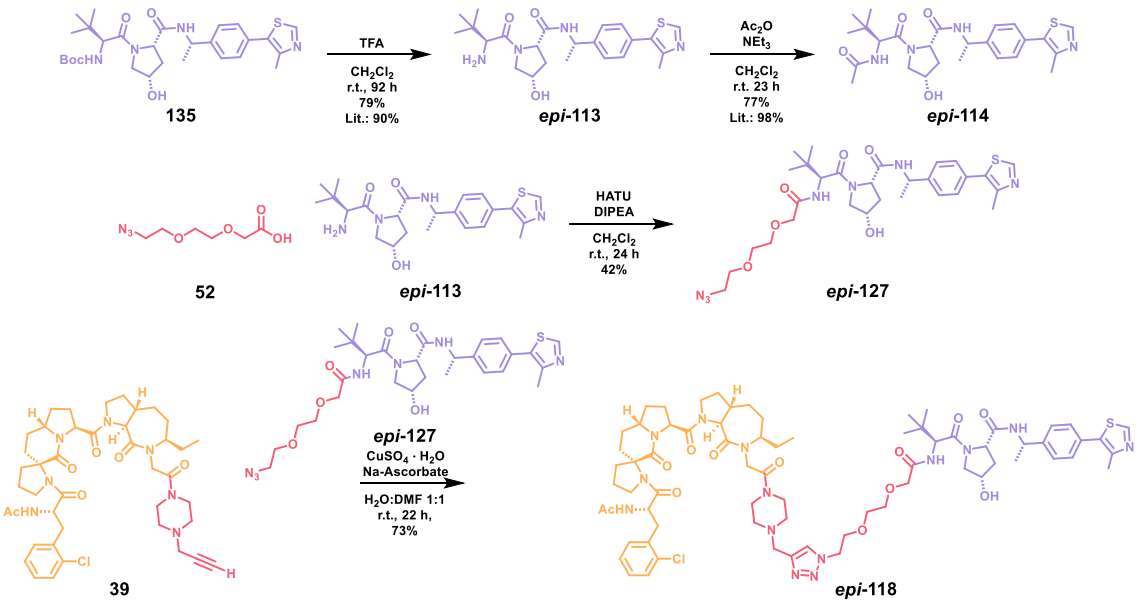

Scheme 20: Deprotection and acetylation of VHL non-binding negative control ***epi*-114**, synthesis of VHL non-binding control PROTAC ***epi*-118**. Warhead, linker, and recruiter compartments are shown in orange, red, and purple, respectively.

The non-binding recruiter **135** was deprotected yielding amine ***epi*-113**. Acetylation gave the non-binding equivalent of VHL binder **114** (Scheme 20). As a negative control for the parent PROTAC **118** (Scheme 17), the non-binding recruiter ***epi*-113** was

coupled to linker **52** yielding conjugate ***epi*-127**. Click reaction with warhead-linker conjugate **39** gave the negative control PROTAC ***epi*-118** (Scheme 20).

To substitute the PEG motifs with alkyl motifs, the linkers **148-151** were envisioned (Scheme 21).

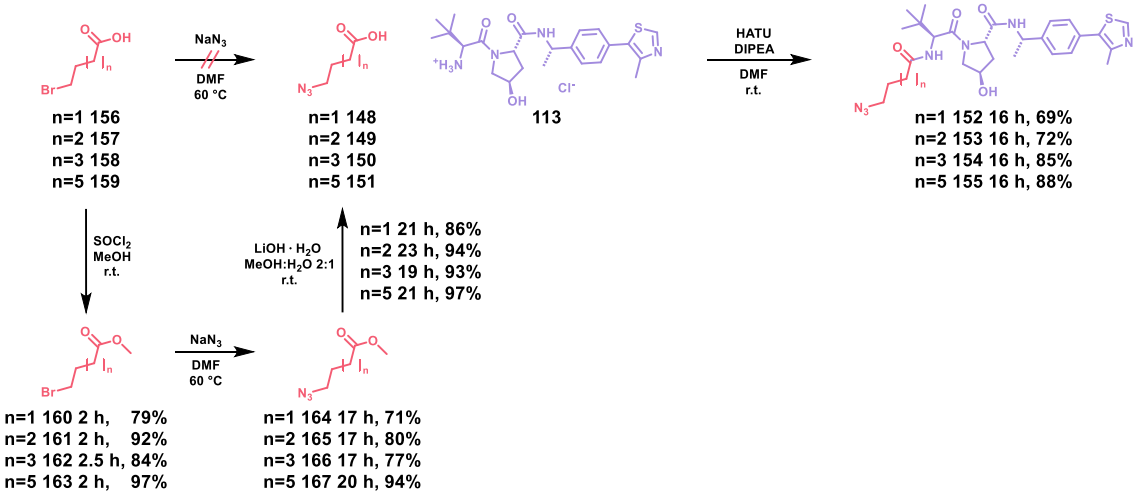

Scheme 21: Synthesis of linker-recruiter conjugates **152-155**. Linker and recruiter compartments are shown in red and purple, respectively.

Nucleophilic substitution of the respective bromides **156-159** with sodium azide (5 equivalents) did not lead to the formation of the envisioned products. Therefore, the carboxylic acids were methylated to receive esters **160-163**, which were then successfully substituted with sodium azide to receive intermediates **164-167**, respectively. Methyl esters **164-167** were hydrolyzed yielding the envisioned linkers **148-151**, which were coupled with recruiter **113** to receive the linker-recruiter conjugates **152-155**, respectively (Scheme 21). The obtained linker-recruiter conjugates **152-155** were coupled with warhead-linker conjugate **39** to yield the PROTACs **168-171**, respectively (Scheme 22).

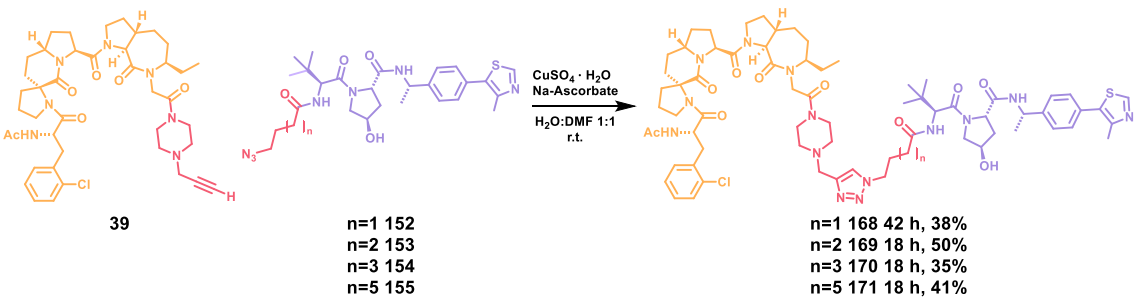

Scheme 22: Synthesis of VHL-recruiting PROTACs **168-171**. Warhead, linker, and recruiter compartments are shown in orange, red, and purple, respectively.

To further increase the linker scope, PROTACs with PEG or alkyl-derived amino-acid linkers were envisioned. The synthesis of the PEG amino-acid linked PROTACs **172-174** is shown in Scheme 23.

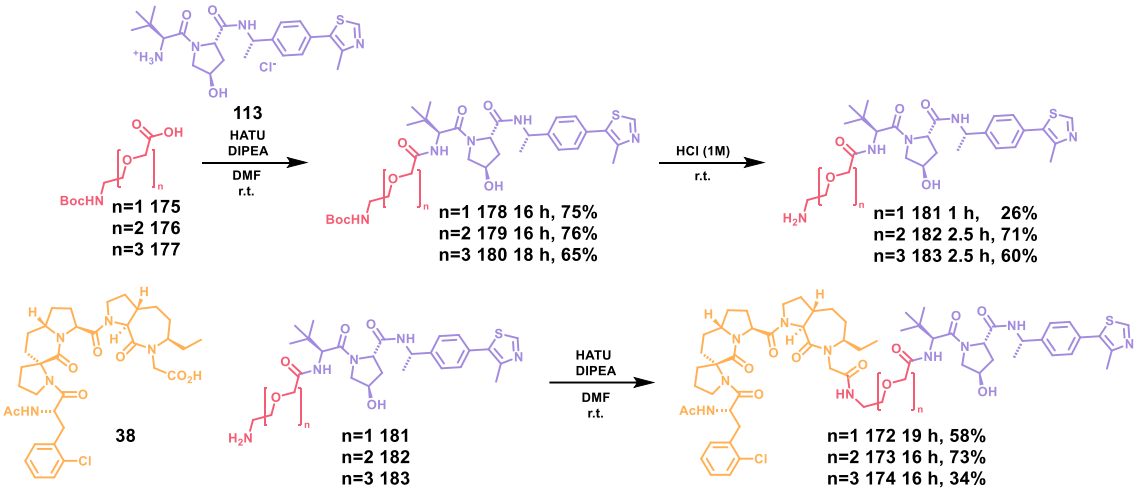

Scheme 23: Synthesis of VHL-recruiting PROTACs **172-174**. Warhead, linker, and recruiter compartments are shown in orange, red, and purple, respectively.

The PEG-derived linkers **175-177** were coupled to recruiter **113** yielding conjugates **178-180**, which were deprotected under acidic conditions yielding linker-recruiter conjugates **181-183**, respectively (Scheme 23). Warhead **38** was coupled with linker-recruiter conjugates **181-183** to receive the PROTACs **172-174**, respectively (Scheme 23). Further, a set of PROTACs with amino-acid linkers was envisioned. The synthetic route towards PROTACs **184-187** is shown in Scheme 24.

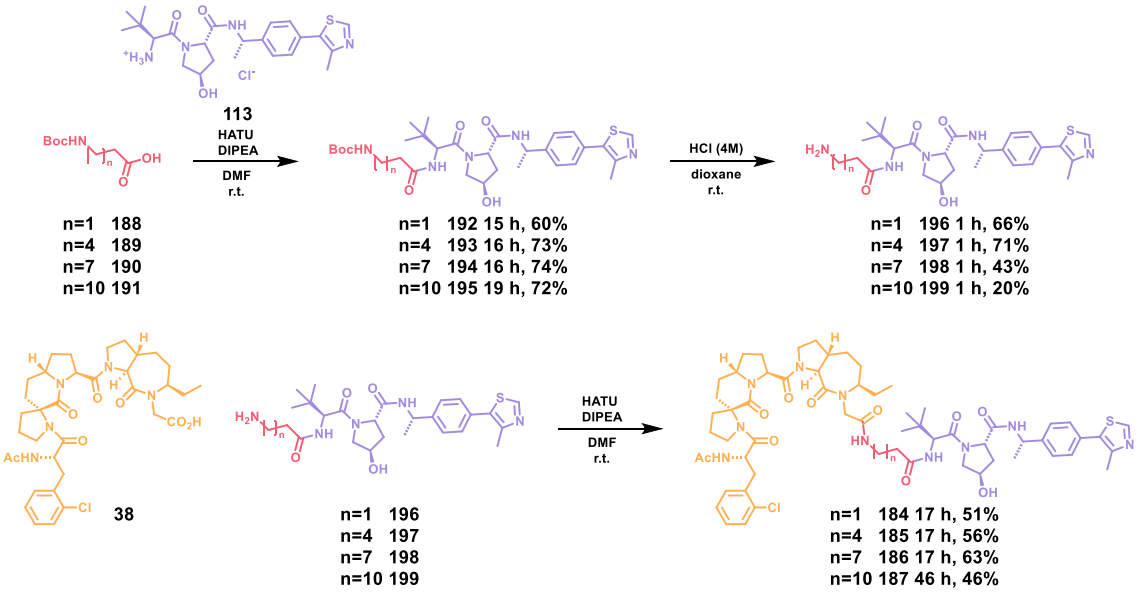

Scheme 24: Synthesis of VHL-recruiting PROTACs **184-187**. Warhead, linker, and recruiter compartments are shown in orange, red, and purple, respectively.

Therefore, the commercially available amino acid linkers **188-191** were coupled to recruiter **113** yielding conjugates **192-195**. These intermediates were deprotected under acidic conditions yielding conjugates **196-199**, respectively. Warhead **38** was coupled with linker-recruiter conjugates **196-199** to yield the PROTACs **184-187**, respectively (Scheme 24).

4.1.5 Evaluation of Ena/VASP homology proteins targeting PROTACs

The PROTAC candidates generated in this work are categorized into nine structural groups, as depicted in Figure 23.

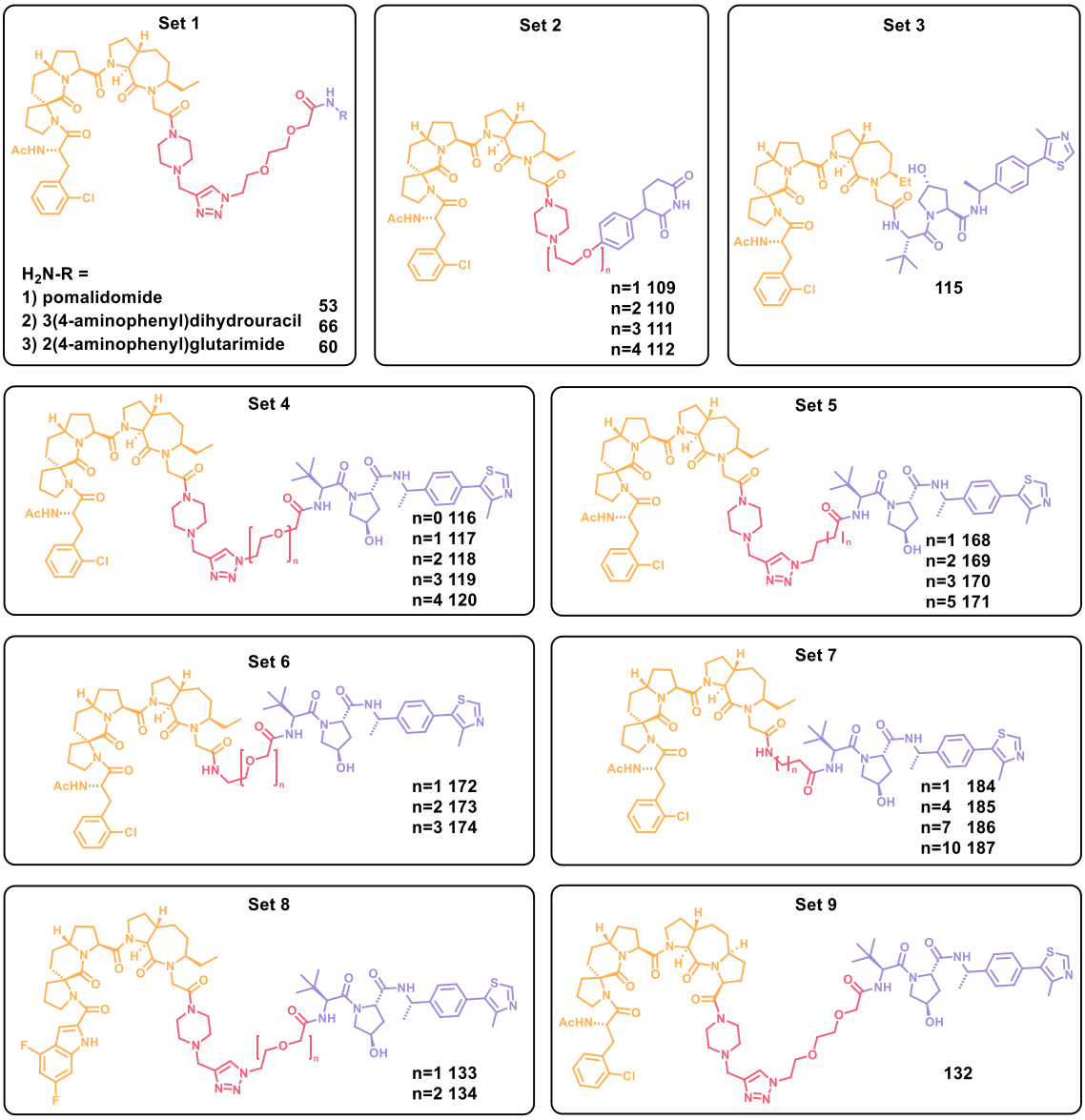

Figure 23: Depiction of PROTAC candidates synthesized during the project, categorized into nine sets based on structural similarity. Warhead, linker, and recruiter compartments are shown in orange, red, and purple, respectively.

Set 1 comprises three PROTACs, **53**, **66**, and **60**, which differ in their CRBN-recruiting units. **Set 2**, including PROTACs **109**-**112**, utilizes a PG based CRBN recruiter and varies in linker length. It was optimized for its drug like properties. **Set 3** consists of a single PROTAC (**115**), which recruits VHL and lacks a linker. **Set 4** contains PROTACs **116**-**120**, characterized by a piperazine motif linked *via* PEG chains of different lengths to a VHL recruiter. **Set 5** includes PROTACs **168**-**171**, which incorporate the same piperazine motif but employ alkyl linkers of different lengths. **Set 6** consists of PROTACs **172**-**174**, all sharing a PEG-derived amino acid linker of varying lengths bridging the warhead and the VHL recruiter. **Set 7** comprises PROTACs **184**-**187**, which feature alkyl-derived amino acid linkers of variable lengths connected to a VHL recruiter. **Set 8** features a different warhead with two different linker variants investigated for PROTACs **133** and **134**, both targeting VHL. **Set 9** includes PROTAC **132**, distinguished by a modified warhead (Figure 23). For comparative analysis of selected parameters, each synthesized PROTAC was assigned a representative identifier. The first digit corresponds to the respective set, while the second digit specifies the number of repetition units within the set. The numbering for **set 1** is illustrated in Figure 23; for sets containing only one PROTAC, no second number was assigned.

A key parameter examined in this work was the linker length. For quantitative comparison, the linker length was defined as the number of atoms in the shortest continuous chain connecting the first atom of the warhead to the first atom of the recruiter. The resulting linker lengths for all PROTACs are illustrated in Figure 24.

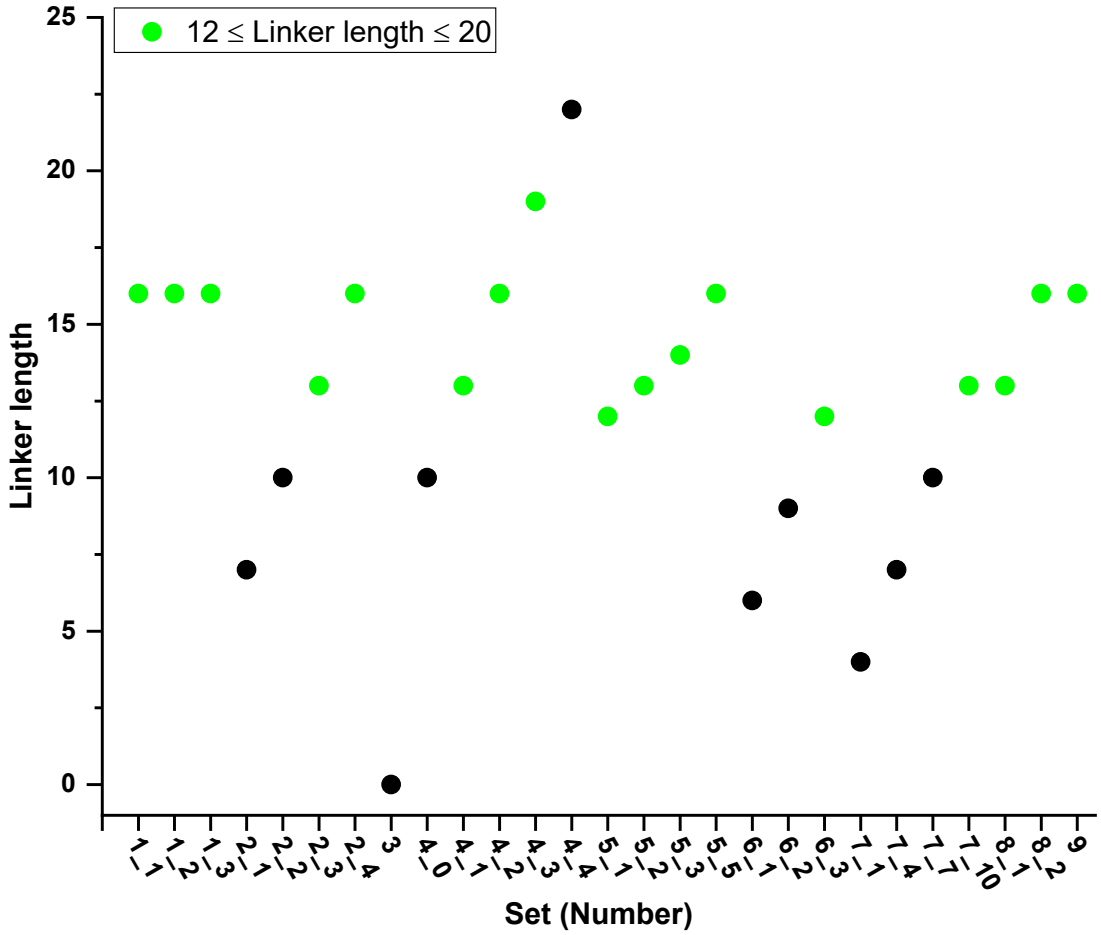

Figure 24: Length of the linker, defined as the number of atoms in the shortest continuous chain connecting the first atom of the warhead to the first atom of the recruiter for the PROTACs obtained during the project. Data points within the range reported as the commonly addressed scope of PROTAC linkers are shown in green.[75]

Unlike the other examples, **set 3** does not contain a linker connecting the warhead and the recruiting moiety. Across the series, linker lengths range spanning from 4 to 22 atoms were examined. Most of the synthesized PROTACs are within the typical linker length of 12-20 atoms frequently reported in literature.[75]

The distribution coefficient between water and octanol (cLogP) is frequently employed in drug discovery as a measure of compound lipophilicity. For this project, cLogP values were kindly provided by the *Swiss Institute of Bioinformatics*. It should be noted that the underlying algorithms were trained on small molecules and may not accurately reflect the physicochemical behavior of PROTACs. The calculated values are shown in Figure 25.

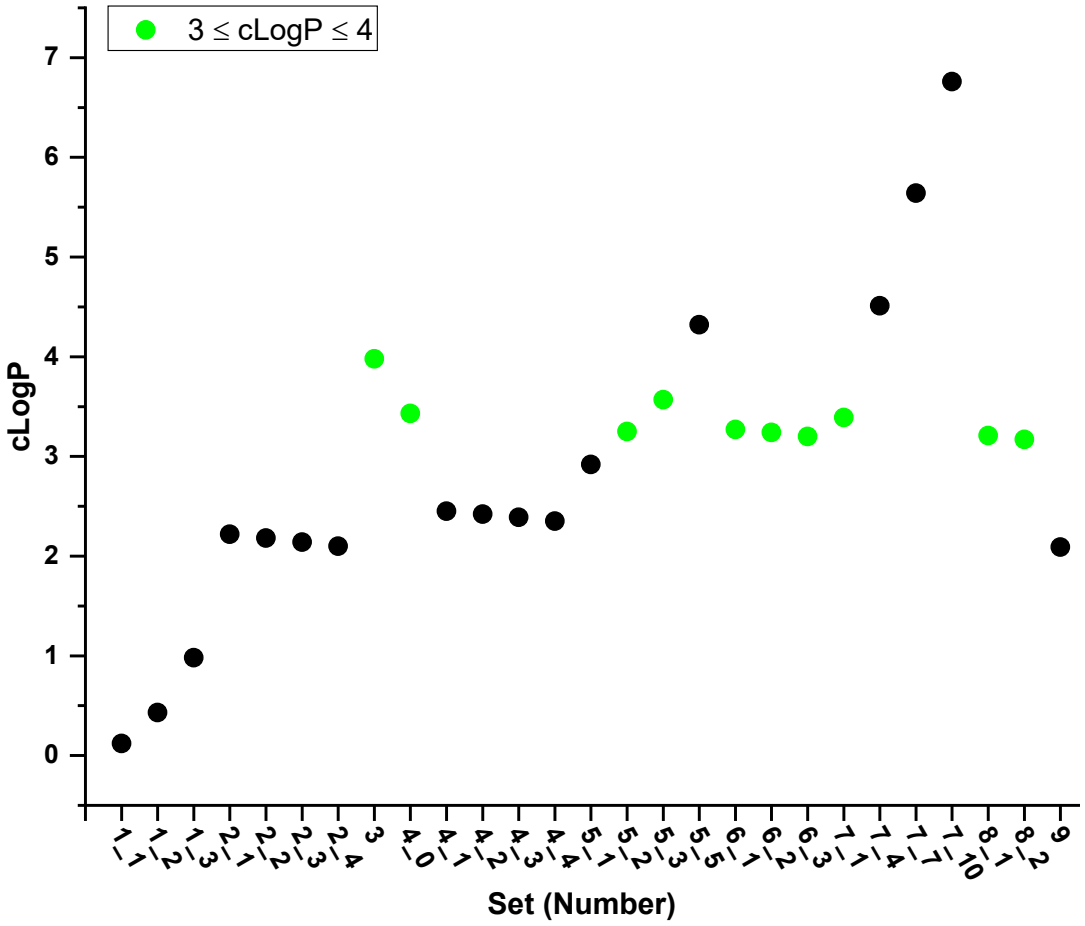

Figure 25: Depiction of the cLogP values for the PROTACs synthesized during the project. Data points within the optimal range of 3-4 reported in literature, are highlighted in green.[205]

The cLogP values obtained in this study cover a wide range from approximately 0 to 7. According to literature, an optimal cLogP range for PROTACs is between 3 and 4.[205] A substantial portion of the compounds obtained during this work is within this optimal range, while the majority lies between 2 and 5.

Another parameter frequently considered in drug development is the topological polar surface area (TPSA). The calculated TPSA values for the synthesized PROTACs are presented in Figure 26.

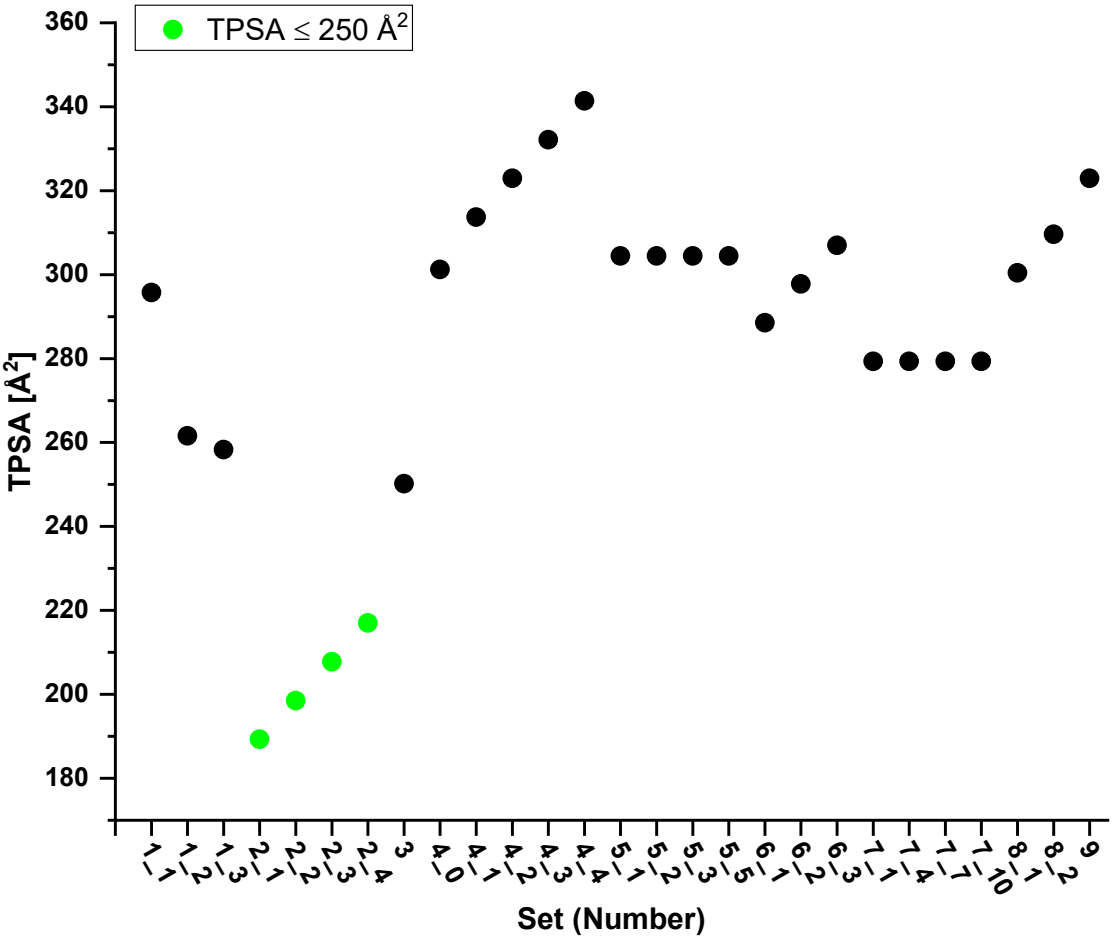

Figure 26: Depiction of the calculated TPSA values for the PROTACs synthesized during the project. Data points within the common range of clinical PROTACs are shown in green.[205]

The PROTACs synthesized in this study had TPSAs between 190 and 340 Å^2. As outlined by the *Veber* rules, a TPSA below 140 Å^2 is typically associated with oral bioavailability.[206] However, TPSA values as high as 238 Å^2 have been reported for orally available PROTACs in clinical trials.[205] A possible explanation is that PROTACs, being large and flexible molecules, can adopt folded conformations that enable intramolecular interactions that effectively reduce their exposed polar surface area. Consequently, the experimentally determined polar surface area (EPSA) is often substantially lower than the corresponding calculated TPSA values. For the warhead explored in this work, a TPSA below 250 Å^2 was only achieved when CRBN recruiters were employed. PROTAC **115** (**Set 3**), pairing the warhead with a VHL recruiter, results in a TPSA of around 250 Å^2 even without any linker.

The last calculated parameter considered in this work is the molecular weight (Figure 27).

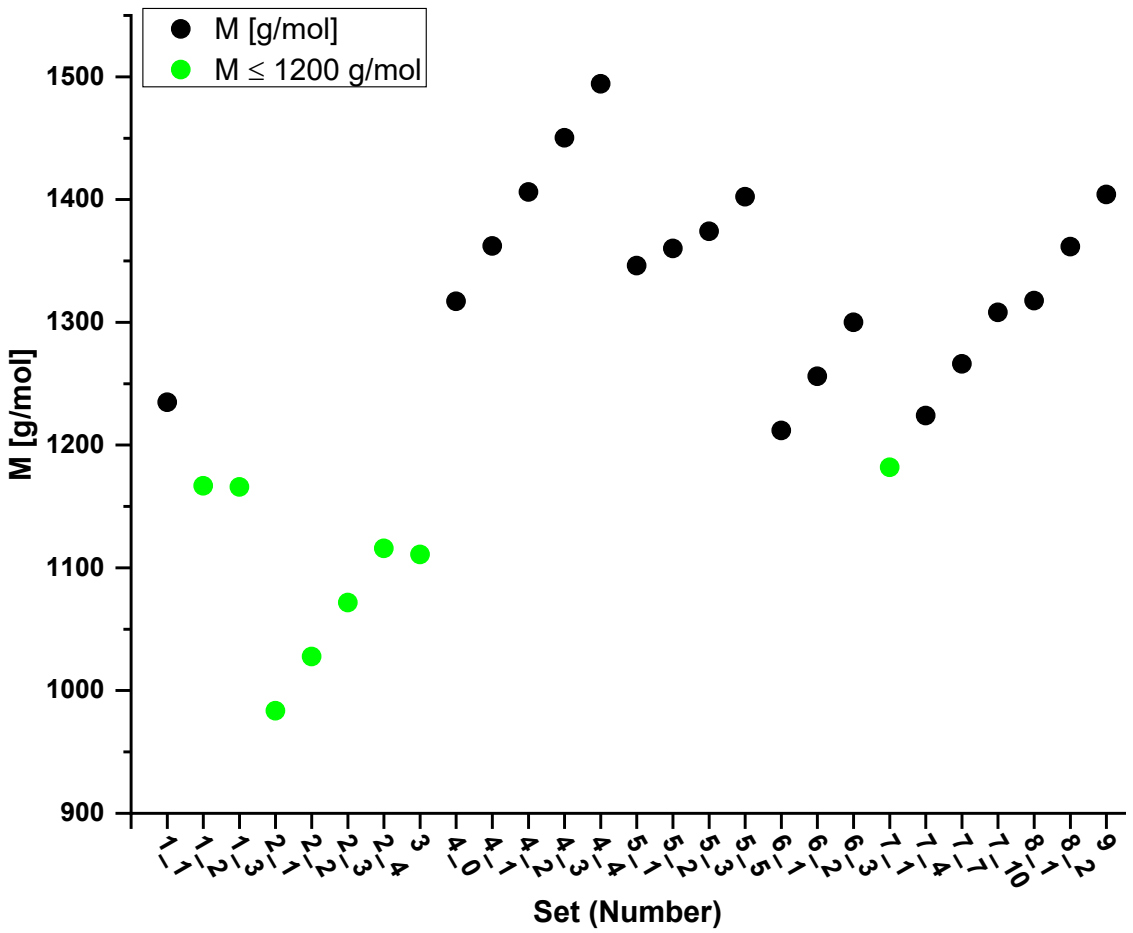

Figure 27: Molecular weights of the PROTACs obtained in this project. Data points falling within the literature-reported range for clinical PROTACs are highlighted in green.[207]

The PROTACs synthesized in this work exhibited molecular weights ranging from 1000 to 1500 g/mol. Although molecular weights below 500 g/mol are generally considered optimal for small molecules,[208] PROTACs typically exceed this threshold, with values between 700 and 1200 g/mol commonly reported.[207] Notably, molecular weights below 1200 g/mol were found almost exclusively among the CRBN-recruiting compounds in **set 1** and **set 2** (Figure 27).

A summary indicating whether each PROTAC meets the criteria defined above is presented in Figure 28.

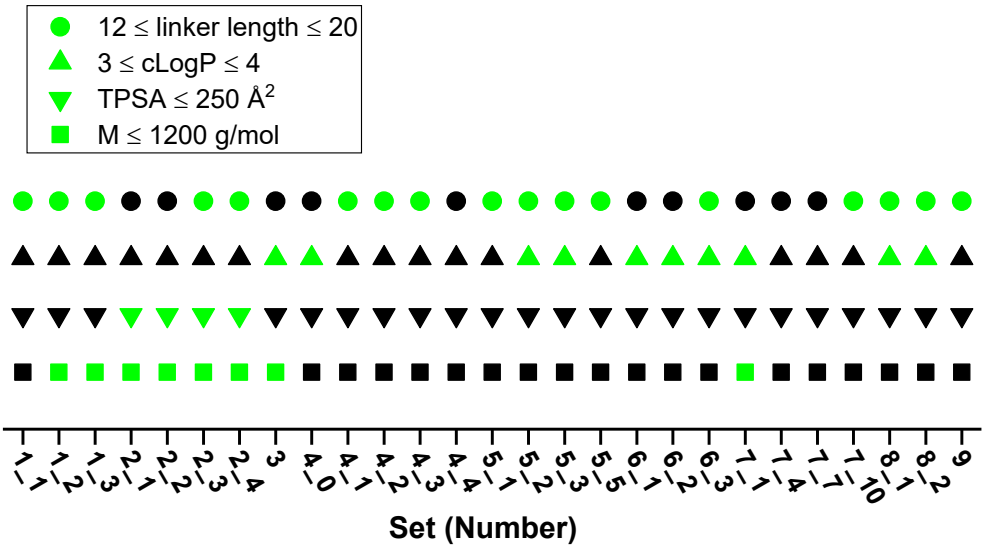

Figure 28: Summary of the parameters calculated for the PROTACs obtained during the project. Data points fulfilling the literature reported criteria are depicted in green, otherwise in black.[75, 205, 207]

Although none of the PROTACs met all four established criteria, the study revealed promising candidates that align closely with key design principles. Notably, the VHL-recruiting **sets 3-9** could not meet the TPSA and molecular weight requirements, as warhead and recruiter without a linker were already at the upper limit for both parameters (**Set 3**). Only **set 2**, which was specifically designed with an emphasis on drug-like properties, satisfied the TPSA criteria. Within this set, **2_3** and **2_4** emerged as the most promising candidates for further investigation, fulfilling three out of the four criteria (Figure 28).[75, 205, 207]

The PROTACs were shipped to *Prosion GmbH* for biophysical and biological evaluation. Due to limited capacity, IC50 values were determined for 10 out of the 28 compounds. The corresponding structures and IC50 values are presented in Figure 29.

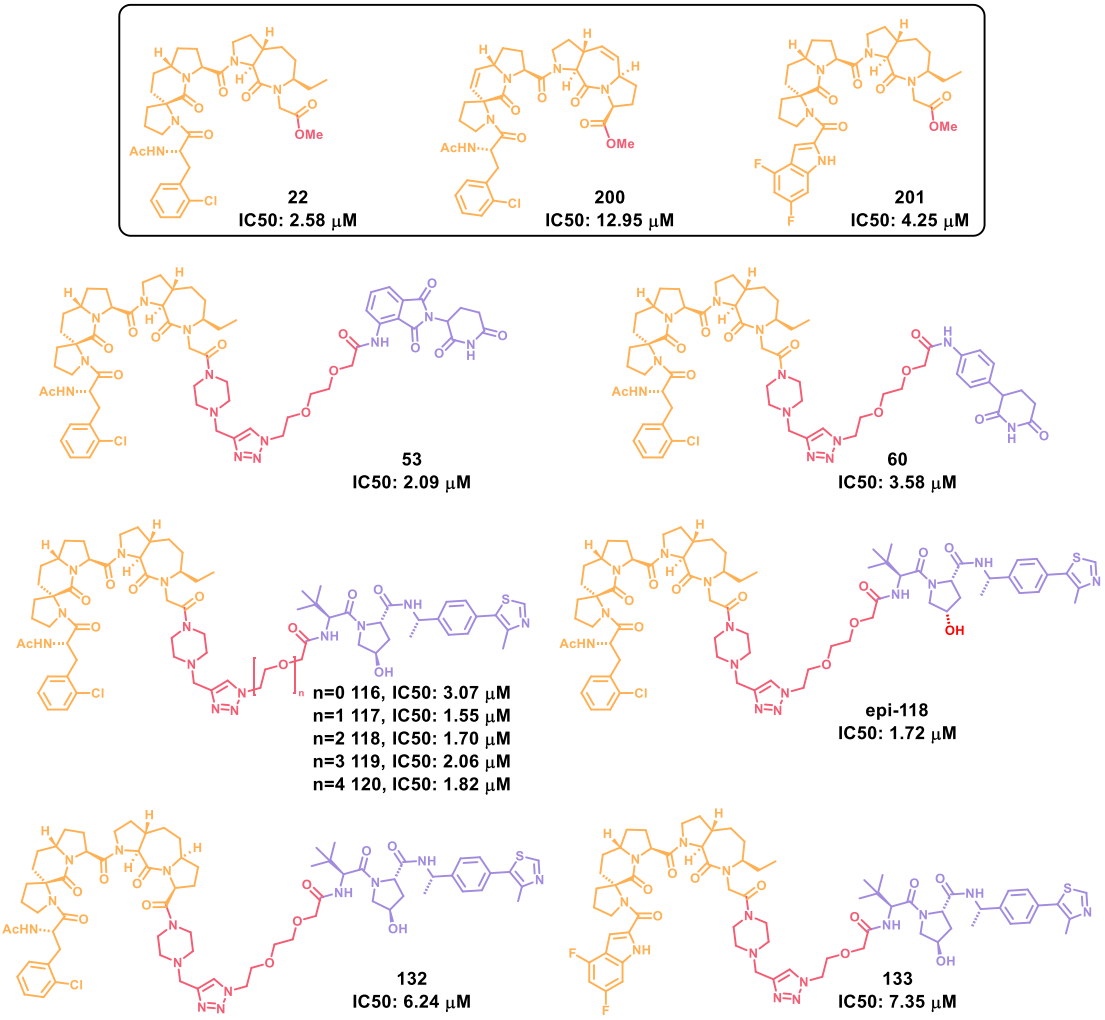

Figure 29: Structures and IC50 values of selected binders and PROTACs.[189]

The IC50 values of the investigated PROTACs lie in the same range as those of the parent binders **22**, **200**, and **201**, demonstrating that the linker attachment strategy is tolerated and does not compromise EVH1 binding.

To investigate cellular activity, target degradation was assessed in a dose-dependent manner. In a preliminary experiment, cells were seeded in medium containing the indicated concentrations of PROTAC **118** and incubated for 24 h. The cells were lysed and normalized in concentration. The resulting western blot for PROTAC **118** is shown in Figure 30A. Inhibition of chemotaxis was assessed using an Incucyte-based assay, previously established at *Prosion GmbH*. In this double-layered setup, separated by a *Matrigel* membrane and filled with compound-containing medium, cells were seeded into the upper chamber, while a chemoattractant was added to the lower chamber (Figure 30B).

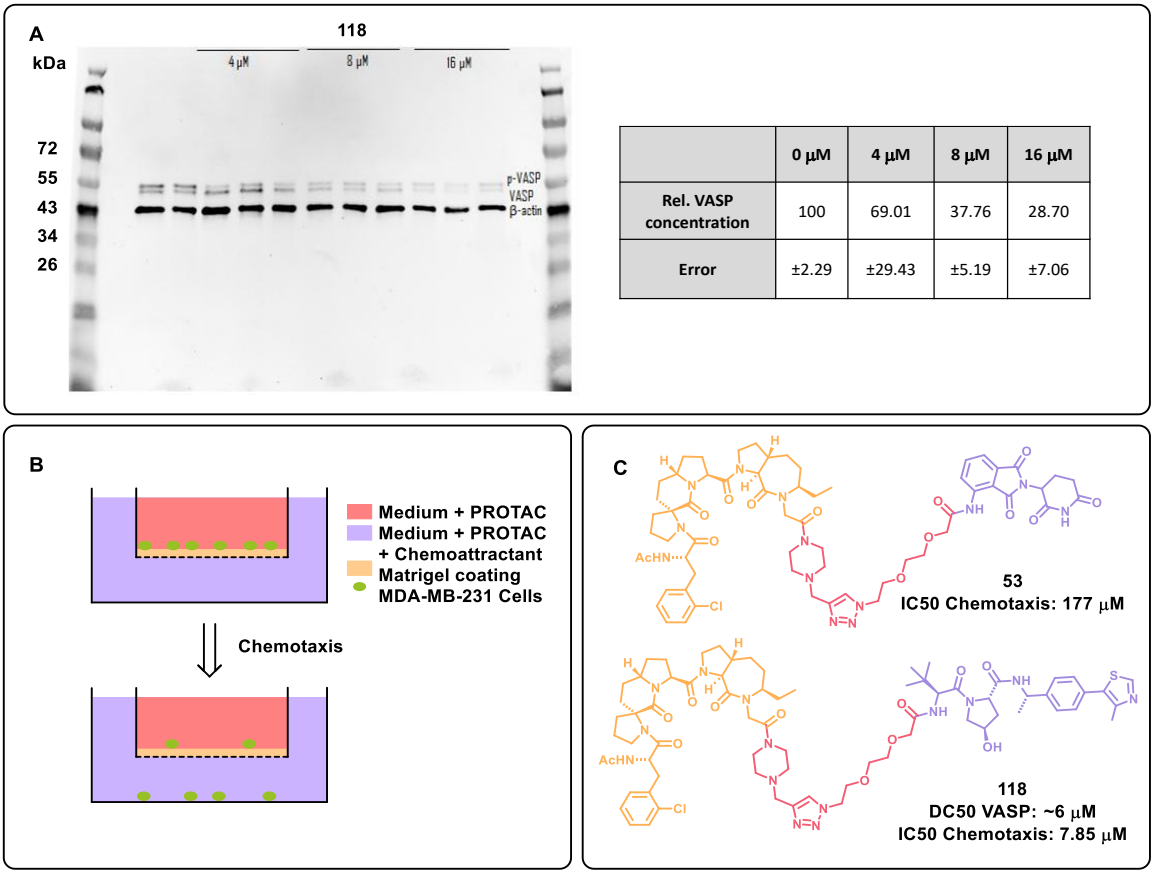

	0 µM	4 µM	8 µM	16 µM
Rel. VASP concentration	100	69.01	37.76	28.70
Error	±2.29	±29.43	±5.19	±7.06

Figure 30: *In vivo* investigation of PROTACs **53** and **118**. **A:** Results of the VASP degradation assay. MDA-MB-231 cells were treated with the indicated concentrations of PROTAC **118** overnight in triplicates. VASP degradation is summarized in the table. **B:** Schematic setup of the chemotaxis inhibition assay. **C:** Structure of PROTACs **53**, and **118** with an approximate degradation constant based on **A** and calculated IC50 values for chemotaxis inhibition by PROTAC **118**.

Although the blot shown in Figure 30A appears to indicate VASP degradation, the experiment could not be reproduced due to incomplete documentation of the experimental conditions. Later replication attempts did not confirm the observed degradation. Two PROTACs, **53** and **118** (Figure 30C), were further evaluated using the chemotaxis inhibition assay. For PROTAC **53** an IC50 value for the chemotaxis inhibition of 177 µM was determined, whereas PROTAC **118** exhibited a significantly lower IC50 value of 7.85 µM. Consequently, PROTAC **118** demonstrated significant cellular activity in two independent assays. Due to limited resources at *Prosion GmbH*, further compounds were not tested.

4.2 Synthesis and evaluation of ProM substituted peptides

To develop ProM-derived small molecule binders targeting GRB2 and YAP1, literature-known binding peptides for these targets were identified, synthesized and evaluated as a starting point for further development. Therefore, biolayer interferometry (BLI) was envisioned to measure target binding as it does not require fluorescent labeling of protein or peptide. The distinct steps of a BLI measurement are depicted in Figure 31.

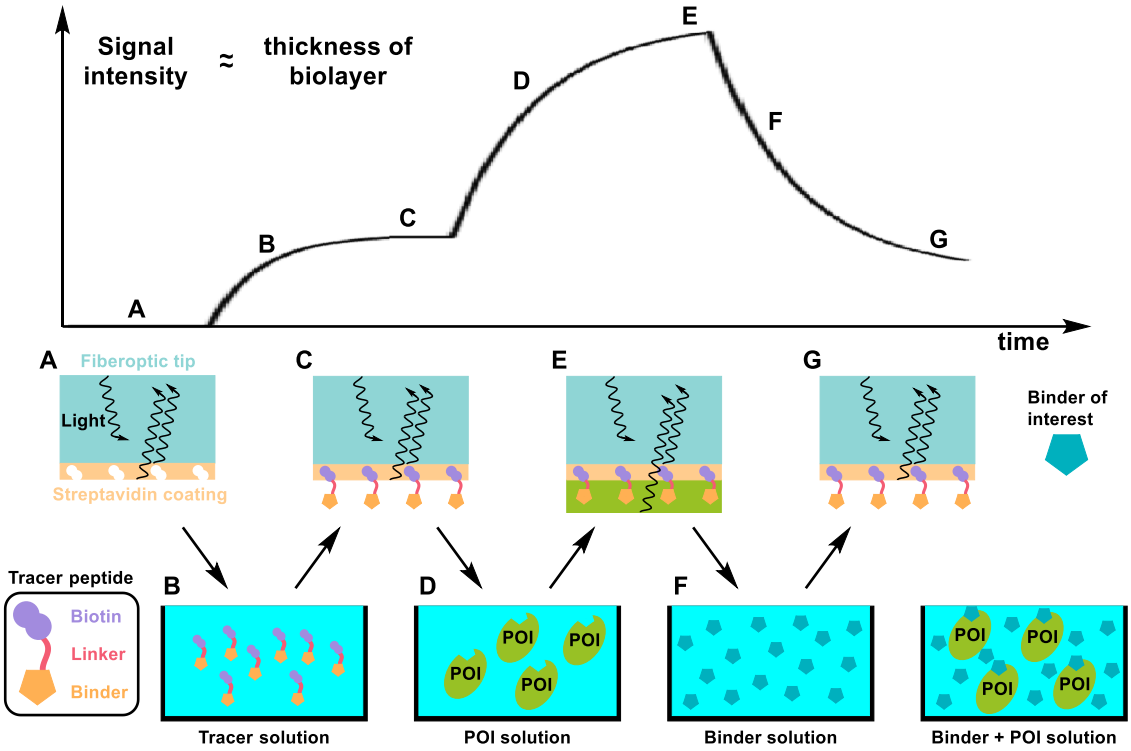

Figure 31: A: Equilibrated tip covered with immobilized streptavidin. **B:** The tip is incubated in a tracer peptide solution leading to a small increase in biolayer thickness. **C:** After an equilibrium is reached, the tip is functionalized with the tracer peptide. **D:** The tip is dipped in a solution of the protein of interest which increases the thickness of the biolayer. **E:** An equilibrium is reached and the tip is loaded with the POI. **F:** The tip is then dipped into a solution of the binder of interest competing with the tracer peptide. Binding to the POI leads to dissociation from the tip which can be quantified. **G:** Depicts a case of full dissociation of the POI representing a high concentration and affinity of the binder.

Accordingly, biotin-labeled tracer peptides were designed, synthesized and evaluated. Therefore, the shift in phase due to the thickening of the biolayer while loading the protein of interest (Figure 31C to E) can be quantified. The signal is not directly proportional to the thickness of the biolayer and therefore defined as a unitless signal intensity. Different concentrations of the tracer solution can be employed. To compare different tracer peptides, a tracer score is defined as signal intensity per concentration [mg/mL] of the tracer peptide in solution. BLI measurements were carried out by *Prosion GmbH*.

4.2.1 GRB2 binding sequences

To address the GRB2 SH3 domains, three literature-known peptide sequences[209-211] were chosen to be converted into tracer peptides. Therefore, *N*-terminal elongation with 6-amino-hexanoic acid (Ahx) and biotin gave tracer peptides **202**-**204** (Table 1).

Table 1: List of biotinylated peptides synthesized and investigated as GRB2 tracers. Biotin, linker, and binding sequence in purple, red, and orange respectively.

No.	Sequence	Purity	Tracer score GRB2 cSH3 / GRB2 nSH3
202	Biotin-[Ahx]-IQPPPVNRNLKPDRK -COOH	>99%	44.4 / n.b.
203	Biotin-[Ahx]-PPPPLPPRRRR -NH_2	>99%	n.b. / 14.5
204	Biotin-[Ahx]-PKNMTPYRSPPPYVPP-NH_2	99%	n.b. / n.b.

When peptide **202** was tested for BLI measurement, sufficient binding of the GRB2 cSH3 domain was detected, while no binding to GRB2 nSH3 was observed. Peptide **203** sufficiently bound the GRB2 nSH3 domain while no binding of the GRB2 cSH3 domain was detected. The tracer peptide **204** neither bound the cSH3 nor the nSH3 domain. Therefore, peptides **202** and **203** were used as tracer peptides for GRB2 cSH3 and nSH3, respectively. GRB2 binding peptides synthesized for the development of a suitable binder are listed in Table 2.

Table 2: List of peptides synthesized and evaluated for the development of ProM substituted and truncated GRB2 binding sequences. Binding sequences, substitutions, and deletions are shown in orange, blue, and red, respectively.

No.	Sequence	Purity	IC50 GRB2 [µM] cSH3 (rel. **202**)/ nSH3 (rel. **203**)
205	Ac- P P P P L P P RRRR-NH_2	98%	9.71 / 35.6
206	Ac- P P P P L[dH-1]RRRR-NH_2	99%	13.4 / 79.2
207	Ac- P P [dH-1]L P P RRRR-NH_2	>99%	5.91 / 31.7
208	Ac- P [dH-1] P L P P RRRR-NH_2	99%	17.1 / 97.5
209	Ac-[dH-1] P P L P P RRRR-NH_2	>99%	6.75 / 33.5
210	Ac- P P [dH-1]L[dH-1]RRRR-NH_2	99%	14.6 / 74.2
211	Ac- P [dH-1] P L[dH-1]RRRR-NH_2	99%	46.1 / 152
212	Ac-[dH-1] P P L[dH-1]RRRR-NH_2	>99%	16.9 / 83.2
213	Ac-[dH-1][dH-1]L P P RRRR-NH_2	99%	8.24 / 29.3
214	Ac-[dH-1][dH-1]L[dH-1]RRRR-NH_2	>99%	16.5 / 63.6
215	Ac- P P [dH-1]V P P RRRR-NH_2	94%	11.5 / 34.9
216	Ac- P P [dH-1]L P P R~~RRR~~-NH_2	>99%	23.8 / 155
217	Ac- P P [dH-1]L P P ~~RRRR~~-NH_2	98%	n.b. / n.b.
218	Ac- ~~P~~ ~~P~~ [dH-1]L P P RRRR-NH_2	98%	7.34 / 33.6
219	Ac- ~~P~~ ~~P~~ [dH-1]L P P R~~RRR~~-NH_2	98%	29.3 / n.b.
220	Ac- ~~P~~ ~~P~~ [dH-1]L[dH-1]R~~RRR~~-NH_2	>99%	124 / n.b.
221	Ac- ~~P~~ ~~P~~ [dH-1]V[dH-1]R~~RRR~~-NH_2	>99%	74.9 / n.b.

Initially, the literature-known peptide **205** was synthesized. Notably, significant binding affinity towards the GRB2 cSH3 domain was observed, while the biotinylated version **203** showed no detectable binding, indicating steric hindrance of the *N*-terminus when in complex with GRB2 cSH3 (Table 1). To investigate substitution with the diproline mimetic [dH-1] (**222**), all combinations of proline pairs were substituted with [dH-1] (**222**) as shown in Table 2 (peptides **206**-**214**). While no increase in binding affinity towards GRB2 cSH3 was detected, improved binding affinities to the nSH3 domain were observed for peptides **207**, **209**, and **213**. Substitution of the leucine of peptide **207** with valine[130] gave peptide **215**, which led to a slight decrease in binding affinity.

Next, truncation of the peptide was investigated. Starting from peptide **207**, either three (**216**) or four (**217**) *C*-terminal arginines were truncated. For peptide **217**, no binding was detected. Deletion of three arginines decreased binding affinities. However, as a tetra arginine motif is not suitable for a small molecule drug development, this loss in binding affinity must be considered. As one arginine residue on the *C*-terminus is required, truncation is limited to retaining a single *C*-terminal arginine (Table 2). Truncation of the two *N*-terminal prolines (**218**) was tolerated without significant loss of binding affinity (compare peptide **207**). A combination of both truncations (peptide **219**) led to a loss of GRB2 nSH3 binding, but the cSH3 affinity was still in the range of peptide **216**. Further modification of peptide **219** by introducing a second diproline mimetic [dH-1] (**222**) gave peptide **220**, causing a loss of binding affinity. Interestingly, leucine to valine modification (peptide **221**) increased binding affinity in this case (Table 2).

These ProM substitution and truncation studies formed the foundation for further optimization studies carried out at *Prosion GmbH* directed to the development of small molecule GRB2 binder. *Prosion GmbH* contributed by synthesis of [dH-1] (**222**), protein expression and isolation, and BLI measurements.

4.2.2 YAP1 binding sequences

To investigate binding of YAP1 WW targeting sequences, a suitable tracer peptide was required. The literature-known YAP1 WW binding sequence DQWPPPYPRH was explored for biotin attachment (Table 3).[212]

Table 3: List of biotinylated peptides synthesized and investigated as YAP1 tracers. Biotin, linker, and binding sequence in purple, red, and orange respectively.

No.	Sequence	Purity	Tracer score YAP1 WW
223	Biotin-DQWPPPYPRH-NH_2	99%	2.9
224	Biotin-[Ahx]SGS DQWPPPYPRH-NH_2	>99%	5.2
225	Biotin-[Ahx]SGSG DQWPPPYPRH-NH_2	>99%	4.2
226	Biotin-[Ahx]SGSGS DQWPPPYPRH-NH_2	>99%	3.3
227	Biotin-[PEG4] DQWPPPYPRH-NH_2	>99%	4.2
228	Biotin-[PEG5] DQWPPPYPRH-NH_2	>99%	2.6
229	Ac-DQWPPPYPRHK(Biotin)-NH_2	>99%	9.8
230	Ac-DQWPPPYPRHK([PEG4]Biotin)-NH_2	>99%	11.7
231	Ac-DQWPPPYPRHK([PEG8]Biotin)-NH_2	>99%	10.0

In the initial, synthetically simple approach biotin was coupled to the *N*-terminus of the peptide giving **223**, which showed a relatively small tracer score. A possible reason could be steric hindrance between the protein and the streptavidin tip. Therefore, different linkers were investigated. The *N*-terminus was elongated with alternating serine and glycines, followed by a 6-amino-hexanoic acid (Ahx) linker for biotin attachment (peptides **224**-**226**). These modifications only slightly increased binding. Two different PEG linkers were introduced between the *N*-terminus and biotin (peptides **227** and **228**). However, no significant increase in tracer score was observed in any of these cases (Table 3).

Alternatively, attachment of biotin towards the *C*-terminus was envisioned. Therefore, an orthogonal protected lysine was added to the *C*-terminus. After successful synthesis of the main peptide chain, the lysine was deprotected. Biotin was either directly attached (peptide **229**) or bridged by a PEG linker (peptides **230** and **231**) forming an *iso*peptide bond with the ε-amine of the side chain. *C*-terminal attachment resulted in significantly higher tracer scores in a suitable range for BLI measurement. As measurements had already started, tracer **229** was used for measurement of all YAP1 binding sequences (Table 3).

Peptide sequences synthesized and investigated for the development of small molecule YAP1 WW binders are shown in Table 4.

Table 4: List of peptides synthesized and evaluated for the development of ProM substituted and truncated binding sequences for the YAP1 WW domain. Binding sequences and substitutions are shown in orange and blue, respectively.

No.	Sequence	Purity	IC50 YAP1 WW [μM] (rel. **229**)
232	Ac- DQWPPPYPRH -NH_2	>99%	60.5
233	Amine-DQWPPPYPRH -COOH	>99%	44.8
234	Ac- L P P P P YRHR-NH_2	91%	27.0
235	Ac- L[ProM-1] P P YRHR-NH_2	>99%	10.9
236	Ac- L P [ProM-1] P YRHR-NH_2	>99%	8.3
237	Ac- L P P [ProM-1]YRHR-NH_2	>99%	5.4
238	Ac- L [dH-1] [dH-1] YRHR-NH_2	99%	9.8

Initially, the literature-known peptide sequence already employed for tracer peptides was synthesized, once *N*-terminal acetylated and *C*-terminal amidated (peptide **232**) and once with uncapped termini (peptide **233**). Further, the literature-known YAP1 WW binding motif **234** was synthesized.[213] A higher binding affinity was observed for peptide **234**, which was therefore used as a lead structure for further development. To investigate substitution with the diproline mimetic [ProM-1] (**239**), all proline pairs were substituted with [ProM-1] (**239**) once, as shown in Table 4 (Peptides **235**-**237**). Further, both pairs of prolines were once substituted with [dH-1] (**222**). Notably, each substitution led to an increase in binding affinity (Table 4).

Prosion GmbH contributed by the synthesis of [ProM-1] (**239**) and [dH-1] (**222**), protein expression and isolation, and BLI measurements. These ProM substitution studies formed the foundation for further truncation and optimization studies carried out at *Prosion GmbH* directed to the development of a small molecule YAP1 WW binder.

5 Summary and Outlook

In this study, three EVH1 binding motifs were explored as warheads for PROTACs. Suitable strategies for linker functionalization were developed and applied to incorporate state-of-the-art E3 recruiters. The CRBN-recruiting PROTACs generated during this work are illustrated in Figure 32.

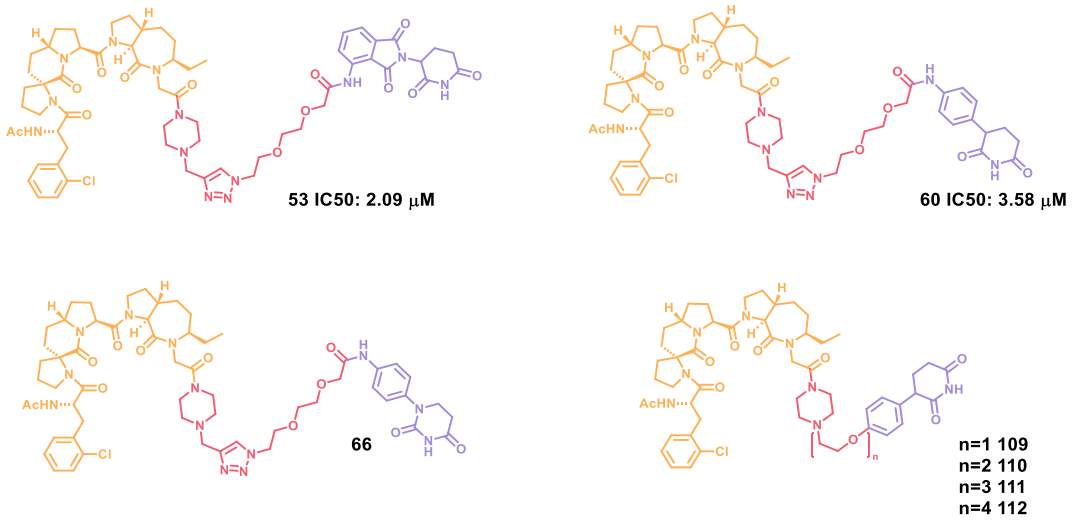

Figure 32: CRBN-recruiting PROTACs synthesized in this study. IC50 values for EVH1 binding are shown, where available, below the corresponding structure. Warhead, linker, and recruiter compartments are shown in orange, red, and purple, respectively.

To investigate the influence of the E3 ligase recruiter, three CRBN-recruiting ligands were examined within an identical warhead-linker framework (PROTACs **53**, **60**, and **66**). The EVH1 binding affinities of PROTACs **53** and **60** were found to be in the same range as that of the parent inhibitors **22** (IC50 = 2.57 μM) and **25** (IC50 = 3.67 μM), demonstrating that the chosen linker architecture retains EVH1 engagement. In addition, a series of CRBN-recruiting PROTACs (**109-112**) was synthesized with optimized molecular weight and TPSA values. These compounds lack the triazole motif, and the linker is connected to the recruiter by an ether instead of an amide. Further, the number of PEG units was varied. Notably, this series exhibits the lowest molecular weights and TPSA values among the PROTACs obtained during this study, making them promising candidates for further evaluation.

In addition to the CRBN-directed constructs, the VHL E3 ligase was addressed for targeted degradation. The corresponding compounds are depicted in Figure 33.

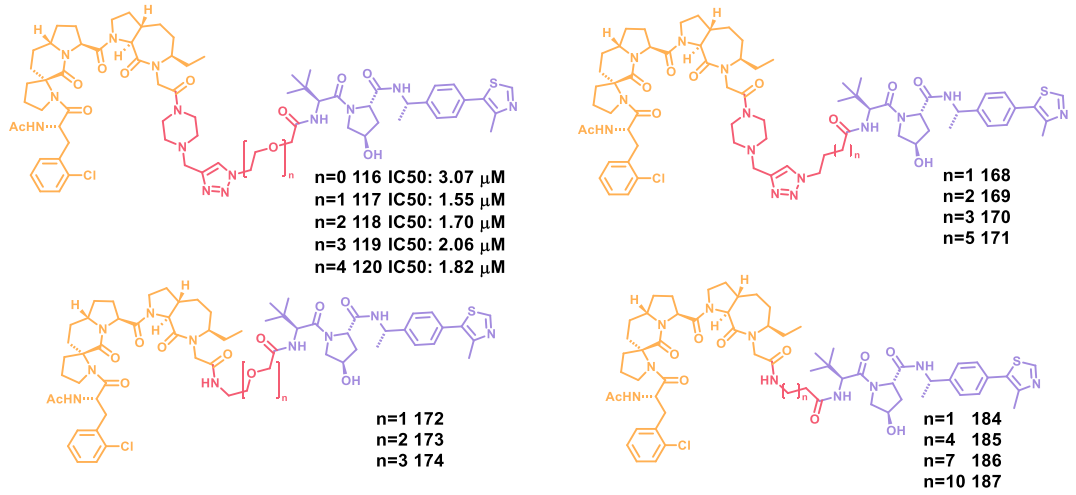

Figure 33: Sets of VHL-recruiting PROTACs synthesized during this study. The IC50 values for EVH1 binding are displayed, where available, below the respective structure. Warhead, linker, and recruiter compartments are shown in orange, red, and purple, respectively.

Diverse linker designs were investigated, utilizing either triazole-based linkers (Figure 33 top) or simpler amino acid linkers (Figure 33 bottom), derived from PEG (Figure 33 left) or alkyl (Figure 33 right) scaffolds. The length of the variable linker segment was systematically modulated within each series. Notably, PROTAC **118** showed preliminary *in cellulo* activity in both, a target degradation assay and a chemotaxis inhibition assay. Owing to incomplete experimental documentation by *Prosion GmbH*, reproduction of the results was not possible, and subsequent efforts did not yield the same outcomes. Other variations for VHL-related PROTACs obtained during the project are shown in Figure 34.

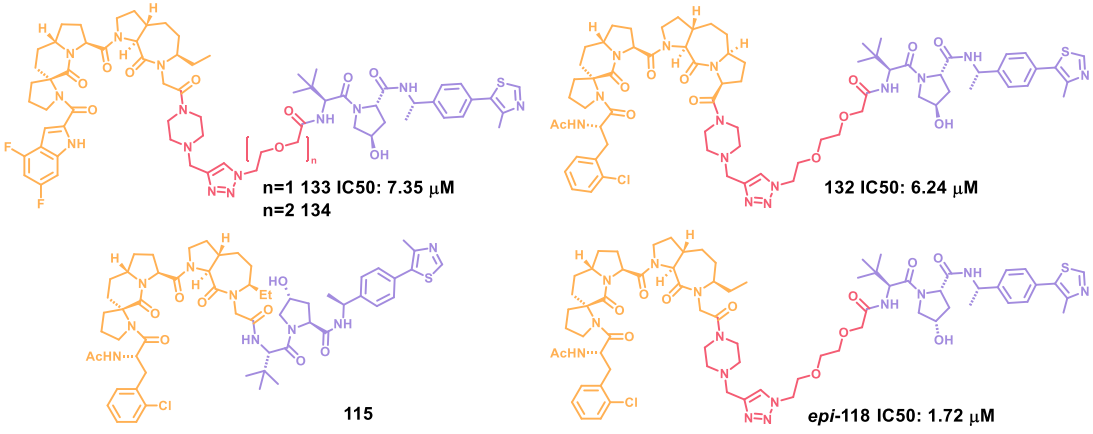

Figure 34: Additional VHL-related PROTACs incorporating alternative warheads (**132-134**), the linker-free degrader **115**, and the negative control ***epi*-118** are shown. Determined IC50 values for EVH1 binding are displayed, where available, below the corresponding structures. Warhead, linker, and recruiter compartments are shown in orange, red, and purple, respectively.

To further broaden the scope, two additional warheads provided by *Prosion GmbH* were incorporated into PROTACs **132-134**. Notably, PROTACs **132** and **133** exhibited EVH1-binding affinities comparable to their parent ligands, further validating the applied linker attachment strategy.

In total, 28 PROTACs were designed, synthesized, and characterized during this project. A selected subset of these compounds was investigated by *Prosion GmbH* for their target binding affinity, and two compounds were evaluated *in cellulo*, indicating activity for one of these compounds. Further investigation of the remaining PROTACs synthesized in this work would be the next step for the development.

Further, *Prosion GmbH* demonstrated that *C*-terminal truncation of the binder is tolerated, as illustrated in Figure 35A. Based on these findings, a new set, PROTACs **241-243**, with optimized physicochemical properties could be envisioned (Figure 35B).

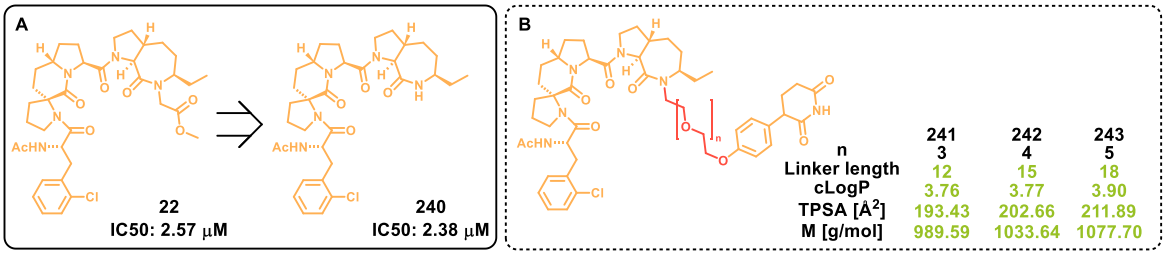

Figure 35: A: *C*-terminal truncation of binder **22** led to binder **240** investigated by *Prosion GmbH*.[189] **B:** Set of newly designed Ena/VASP PROTACs optimized for their physicochemical properties.

For the newly designed set presented in Figure 35B, all four physicochemical parameters for each compound were calculated to be within the range of clinically evaluated PROTACs reported in the literature.[75, 205, 207]

During the synthesis of conjugates **83**-**86**, an unexpected selectivity was observed for the *Mitsunobu* reaction. The proposed mechanism is depicted in Scheme 25.

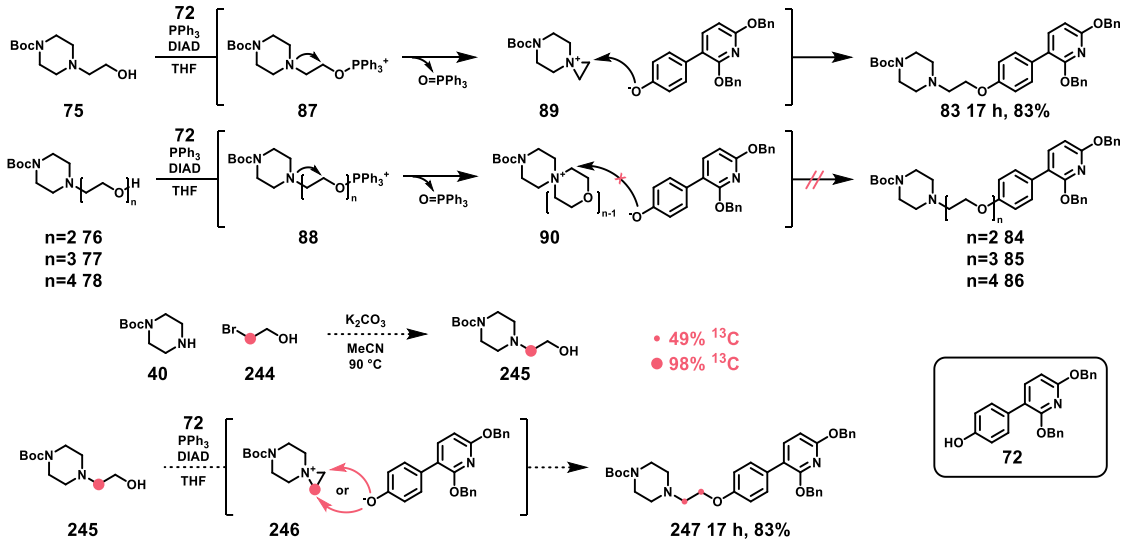

Scheme 25: Selectivity observed for the *Mitsunobu* coupling of protected recruiter **72** with intermediates **75**-**78** and the hypothesized mechanism (top). Isotope labeling experiment suggested for mechanistic proof (bottom).

To confirm the formation of the proposed aziridinium intermediate **89**, incorporation of ^{13}C-labeled bromoethanol (**244**) could be employed. The resulting labeled linker **245** would be subjected to the same reaction conditions. Formation of an aziridinium ion **246** should lead to equal distribution of the ^{13}C-label between the two methylene groups of the C2 fragment of **247**.

During the acidic deprotection of linker-recruiter conjugate **83**, another unexpected selectivity was observed (Scheme 26).

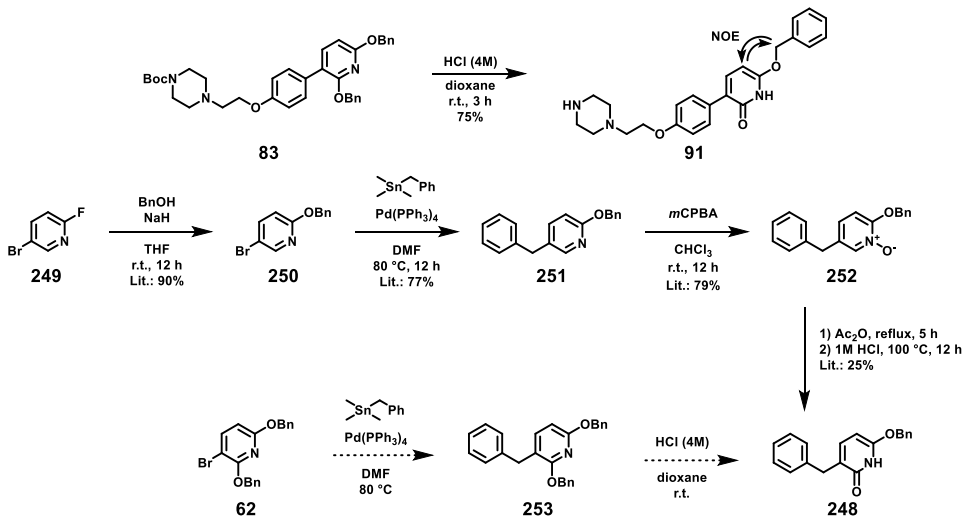

Scheme 26: Selectivity of the debenzylation observed during the acidic treatment of intermediate **83** (top). Literature-known synthesis of inhibitor **248** and a possible alternative strategy (bottom). [214]

Besides Boc deprotection, cleavage of one benzyl group was detected. Unexpectedly, NOE experiments revealed selective deprotection at the *ortho* position, whereas *para*-selective deprotection was described in literature for a similar example, notably without a proof of regioselectivity.[200] The observed selectivity is of potential synthetic relevance. *Kozikowski* and coworkers conducted a study evaluating a series of 2-pyridone derivatives as inhibitors of bacterial enoyl-ACP reductase (EAR).[214] EAR plays a central role in bacterial fatty acid synthesis. It constitutes an attractive target for the development of novel antibacterial agents. The synthesis of the highest affinity derivative **248** identified in the screening is presented in Scheme 26. Initially, a benzyl ether was introduced by nucleophilic substitution towards fluoropyridine **249**. The resulting intermediate **250** was coupled under *Stille* conditions resulting in the formation of building block **251**. Oxidation gave pyridine-*N*-oxide **252**. Treatment with acetic anhydride and hydrochloric acid lead to the formation of the desired product **248**.

A more straightforward synthetic route could involve accessing intermediate **253** from building block **62** *via* the same *Stille* coupling applied in the synthesis of building block **250**. The resulting benzyl-substituted intermediate **253** may show the same selectivity in acidic debenzylation observed for compound **83** (Scheme 26), which would lead to the desired product **248**.

In collaboration with *Prosion GmbH*, biotinylated tracer peptides targeting GRB2 SH3 and YAP1 WW domains were designed, synthesized, and purified. Based on these peptides, *Prosion GmbH* established BLI assays for quantitative binding analysis. For both targets, ProM-substituted and truncated binder sequences were designed, synthesized, and evaluated for their binding affinity to establish a foundation for the development of improved small molecule binders. In total, 36 peptides were synthesized, purified and characterized. Since the resulting peptides still exhibit relatively low binding affinities, further exploration of alternative ProM building blocks for substitution could be beneficial.

6 Experimental Section

6.1 General experimental Information

Reactions under inert conditions

If indicated by the use of *Schlenk* equipment: Reactions were performed under an argon atmosphere with Linde® Argon 4.6 (99.996%, <1 ppm H_2O, <1 ppm O_2) using *Schlenk* technique. The glass equipment was heated under vacuum with a propane-butane torch and flushed with argon before usage. Solids were transferred under an argon counter flow. Liquids were added through a septum using syringes prior flashed with argon.

Solvents and reagents

All chemicals were bought from *ABCR*, *Acros Organics*, *BLD Pharm*, *Carbolution*, *Fisher Scientific*, *Merck*, *Sigma Aldrich*, and *TCI*, or provided by *Prosion GmbH*. Unless otherwise noted, all chemicals were used without prior purification. If not stated otherwise, all salt solutions were aqueous and saturated.

Chromatography

For thin layer chromatography (TLC), silica gel 60 F_{254} aluminum sheets, with a thickness of 0.25 mm by *Merck* were used. Substances were detected under UV-light (λ = 254 and 365 nm) or by potassium permanganate stain (2.50 g $KMnO_4$, 16.7 g K_2CO_3, 0.21 g NaOH, 500 mL H_2O).

For normal phase column chromatography (NP), silica (0.035-0.070 µm, 60 Å) by *Acros Organics* was used. The mixing ratios of the solvents are noted in fractions of volume.

For reverse-phase column chromatography (RP), CHROMABOND ® 3 mL cartridges, 200 mg C_{18} ec. Were used. The mixing ratios of the solvents are noted in fractions of volume.

For preparative high-performance liquid chromatography (prep HPLC) the following modules were used: *Elite LaChrom*, *Hitachi* (Chiyoda, Japan); Autosampler *L2200*, Pump *L-2130*, Diode Array Detector *L-2455* and Fraction Collector *FoxyR1*, *Teledyne*

ISCO (Lincoln, Nebraska, USA) column: VP 250/16 NUCLEODUR 1005 C18ec, *Macherey Nagel* (Lincoln, Nebraska, USA).

High-performance liquid chromatography (HPLC) analysis were performed on a *Knauer* HPLC system (*AZURA* series) equipped with an UV-detector (*UVD 2.1L*) and a pump (*P6.1L*). Detection was performed at λ = 215 nm. Separation was carried out on a *Waters XSelect CSG C18* column at 30 °C. The mobile phase consisted of water (A) and acetonitrile (B). The following gradient was applied: Starting at 95:5 (A:B) to 10:90 (A:B) over 15 min. This gradient was held for 10 min, followed by re-equilibration to the initial conditions within 5 min.

For liquid chromatography mass spectrometry (LCMS), the following modules were used: LC: *Hewlett-Packard* series 1100 (*Agilent*) MS: LTQ-XL, *Thermo Scientific* (Waltham, Massachusetts, USA), columns: *AerisTM* 3.6 µm *PEPTIDE XB-C18* 100 Å, *Phenomenex* (Aschaffenburg, Germany) EC 125/4.6 *NUCLEODUR* 100-5 C18ec, *Macherey-Nagel* (Düren, Germany).

Fourier-transform-infrared-spectroscopy (FT-IR):

IR spectra were recorded employing an *UATR Two Instrument* from *Perkin Elmer* at room temperature. The wave numbers ν are reported in cm^{-1}. The intensities are defined as w = weak, m = medium, s = strong and br = broad.

High-resolution mass spectroscopy (HR-MS)

HR-MS was recorded employing a *THERMO Scientific LTQ Orbitrap XL* using the electrospray ionization method (ESI). For the spray voltage a value of 3.4 kV was applied. The capillary voltage and the tube lens voltage had a value of 3.0 V.

Nuclear magnetic resonance spectroscopy (NMR)

NMR spectra were recorded on *DPX 300* (300 MHz), *Avance 400* (400 MHz), Avance NEO 400 (400 MHz), *Avance III* (500 MHz) and *Avance II+* (600 MHz) spectrometers by *Bruker*. All experiments were recorded at room temperature. The spectra were referenced to TMS or the residual non-deuterated solvent signal. Chemical shifts are reported in parts per million (ppm) and the coupling constants *J* are given in hertz (Hz). The multiplicities are given by s (singlet), d (doublet), t (triplet), q (quartet), quin (quintet) and m (multiplet). The assignment is based on 2D spectra (HSQC, HMBC, and COSY).

Lyophilization

Samples for lyophilization were dissolved in the indicated solvent mixtures and frozen in liquid nitrogen. An Alpha 2-4 LD plus lyophilizer from *Christ* was used to freeze-dry the sample.

Biolayer interferometry (BLI)

Compound binding to protein domains was evaluated using biolayer interferometry (BLI) on an Octet R2 system from *Sartorius* with super-streptavidin biosensors.

For YAP1-WW1 measurements, the biotinylated tracer peptide **229** was employed, with binding measurements performed at a protein concentration of 22.5 µg/mL. Test compounds were serially diluted 1:3 from 180 µM over eight steps. All assays were performed at 23 °C in PBS, 2mM TCEP, 0.5% DMSO, 0.1% Tween 20, pH 7.4.

For GRB2-nSH3 measurements, the biotinylated tracer peptide **203** was employed, with binding measurements performed at a protein concentration of 40 µg/mL in PBS, 250mM NaCl, 2mM TCEP, 0.5% DMSO, 0.1% Tween 20, pH 7.4.

For GRB2-cSH3 measurements, the biotinylated tracer peptide **202** was employed, with binding measurements performed at a protein concentration of 7 µg/mL in PBS, 2mM TCEP, 0.5% DMSO, 0.1% Tween 20, pH 7.4. Test compounds were serially diluted 1:3 from 180 µM over eight steps.

The following protocol was used: Baseline equilibration, association phase, and sensor regeneration in SDS-containing buffer. Double referencing was applied using biosensors without immobilized tracer peptide and sample wells without protein. Data were acquired using *Octet Analysis Studio Software* with reference sensor subtraction and baseline correction. IC_{50} values were determined using the fitting tool of *CDD Vault*.

Centrifuges

The following centrifuge models were used for this work: *Heraeus Pico 17*, *Thermo Scientific* (Waltham, Massachusetts, USA); *Heraeus Multifuge X1R*, *Thermo Scientific* (Waltham, Massachusetts, USA); *Centrifuge 5147 R*, *Eppendorf* (Hamburg, Germany); *Centrifuge 5417 C*, *Eppendorf* (Hamburg, Germany); *MIKRO 22 R*, *Hettich* (Tuttlingen, Germany).

6.2 Synthesis of PROTACs

6.2.1 Synthesis towards Warhead conjugate 39

6.2.1.1 Synthesis of 42

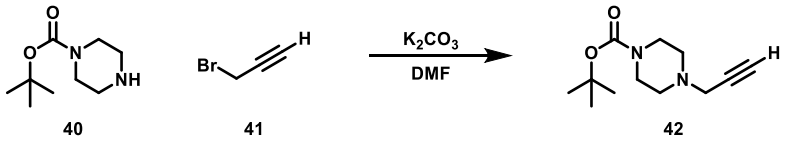

40 41 42

According to a modified procedure by *Kapic et al*.[191]: In a 100 mL round bottom flask, 5.14 g (27.6 mmol; 2.00 eq.) of piperazine **40** were dissolved in 30 mL of DMF. Next, 5.72 g (41.4 mmol; 3.00 eq.) of K_2CO_3 were added. The resulting thick suspension was diluted with another 30 mL of DMF before 1.50 mL (9.2M in toluene; 13.8 mmol; 1.00 eq.) of alkyne **41** were added. The reaction mixture was stirred at room temperature until full conversion of alkyne **41** was observed by TLC after 18 h. The reaction mixture was diluted with 200 mL of H_2O and the aqueous phase was extracted with 200 mL of EtOAc three times. The combined organic layers were washed with 200 mL $NaHCO_3$ solution and 200 mL of NaCl solution two times. The organic phase was dried over $MgSO_4$, filtered, and the solvent was removed under reduced pressure. The crude product was purified by column chromatography (SiO_2, *c*Hex/EtOAc 2:1) to obtain 3.06 g (13.6 mmol; 98%; 95 wt%) of the desired product **42** as a pale-yellow oil.

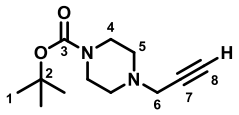

M ($C_{12}H_{20}N_2O_2$):	224.30 g/mol.
Yield:	3.06 g (13.6 mmol; 98%; 95 wt%, Lit.: quant.).
R_f:	(SiO_2, *c*Hex/EtOAc 1:1) = 0.39.
^{1}H NMR:	(500 MHz, $CDCl_3$) δ [ppm] = 3.47 (t, ^3J = 4.86 Hz, 4H, H4), 3.32 (d, ^4J = 2.4 Hz, 2H, H6), 2.52 (t, ^3J = 4.86 Hz, 4H, H5), 2.26 (t, ^4J = 2.45 Hz, 1H, H8), 1.46 (s, 9H, H1).
^{13}C NMR:	(125 MHz, $CDCl_3$) δ [ppm] = 154.8 (C3); 79.9 (C2); 78.5 (C7); 73.6 (C8); 51.8 (C5); 47.1 (C6); 43.0 (C4); 28.6 (C1). Note: C4 was detected in the HSQC.

6.2.1.2 Synthesis of 37

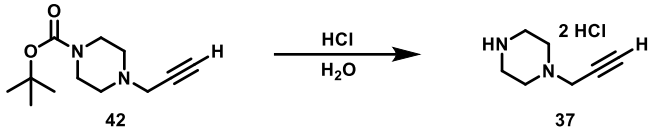

This experiment was carried out by *Rafael Claßen*. In a 10 mL round bottom flask, 323 mg (1.44 mmol; 1.00 eq.) of the Boc-protected piperazine **42** were dissolved in 0.60 mL of HCl (conc.). The mixture was stirred for 20 min at room temperature resulting in a clear solution. The reaction mixture was poured into 5 mL of acetone at 0 °C. The resulting precipitate was filtered off, washed with cold acetone two times, and dried under reduced pressure to obtain 253 mg (1.28 mmol; 89%) of the desired product **37** as a colorless solid.

M ($C_7H_{14}N_2Cl_2$):	197.10 g/mol.
Yield:	253 mg (1.28 mmol; 89%).
R_f:	(SiO_2, CH_2Cl_2/MeOH/NEt_3 100:5:1) = 0.13.
^{1}H NMR:	(500 MHz, D_2O) δ [ppm] = 4.06 (d, ^4J = 2.56 Hz, 2H, H3), 3.59 (s, 8H, H1, H2), 3.13 (t, ^4J = 2.52 Hz, 1H, H5).
^{13}C NMR:	(125 MHz, D_2O) δ [ppm] = 80.1 (C5); 71.8 (C4); 47.8 (C2); 46.1 (C3); 41.3 (C1).

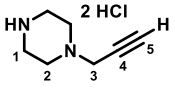

6.2.1.3 Synthesis of 46

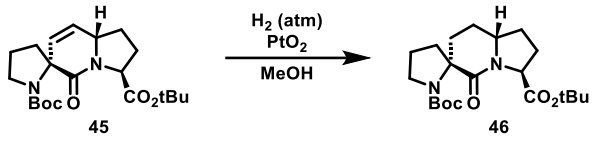

According to a modified procedure by *Albat*[189]: In a 25 mL *Schlenk* flask, 300 mg (767 μmol; 1.00 eq.) of Boc[ProM-2]O*t*Bu (**45**) were dissolved in 5.6 mL of MeOH. To the solution, 17.6 mg (76.7 μmol; 10 mol%) of PtO_2 were added and a balloon filled with hydrogen gas was attached to the flask. The mixture was vigorously stirred while purged with hydrogen gas. After 20 h, the mixture was filtered once through a silica pad and once through a syringe filter. The solvent was removed under reduced pressure to obtain 306 mg (721 μmol; 94%; 93 wt%) of the desired product Boc[dH-2]O*t*Bu (**46**) as a colorless solid.

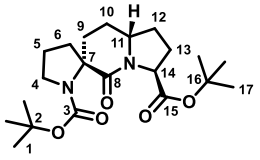

M ($C_{21}H_{34}N_2O_5$):	394.51 g/mol.
Yield:	306 mg (721 μmol; 94%; 93 wt%).
R_f:	(SiO_2, *c*Hex/EtOAc 1:1) = 0.43.
^{1}H NMR:	(300 MHz, $CDCl_3$) δ [ppm] = 4.54-4.43 (m, 1H, H14), 3.68-3.40 (m, 3H, H11, H4), 2.48-2.28 (m, 3H, H6a, H9a, H13a), 2.18-2.07 (m, 1H, H12a), 2.00-1.71 (m, 7H, H5, H6b, H9b, H10, H13b),1.67-1.57 (m, 1H, H12b), 1.50-1.39 (m, 18H, H1, H17).

6.2.1.4 Synthesis of 47

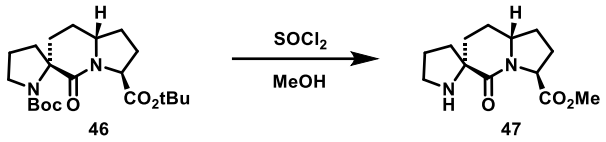

According to a modified procedure by *Albat*[189]: In a 25 mL round bottom flask, 285 mg (721 μmol; 1.00 eq.) of Boc[dH-2]O*t*Bu (**46**) were dissolved in 7.3 mL of MeOH. The mixture was cooled to 0 °C and 300 μL (4.21 mmol; 5.80 eq.) of $SOCl_2$ were added dropwise. The mixture was allowed to slowly warm to room temperature and after 23 h, full conversion of Boc[dH-2]O*t*Bu (**46**) was observed by TLC. The solvent was removed under reduced pressure, 20 mL of $NaHCO_3$ solution were added, and the mixture was extracted six times with 100 mL of CH_2Cl_2. The combined organic layers were dried over $MgSO_4$, filtered, and the solvent was removed under reduced pressure to obtain 157 mg (622 μmol; 86%) of the desired product H[dH-2]OMe (**47**) as a colorless solid.

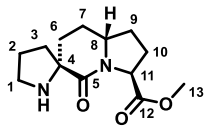

M ($C_{13}H_{20}N_2O_3$): 252.31 g/mol.

Yield: 157 mg (622 μmol; 86%).

R_f: (SiO_2, *c*Hex/EtOAc/MeOH 3:3:1) = 0.11.

^{1}H NMR: (300 MHz, $CDCl_3$) δ [ppm] = 4.52 (t, ^3J = 8.5 Hz, 1H, H11), 3.75-3.68 (m, 4H, H8, H13), 3.17 (ddd, ^2J = 10.7 Hz, ^3J = 6.2 Hz, ^3J = 4.9 Hz, 1H, H1a), 2.85 (dt, ^2J = 14.3 Hz, ^3J = 7.1 Hz, H1b), 2.39-2.32 (m, 1H, H10a), 2.27 (ddd, ^2J = 12.6 Hz, ^3J = 9.1 Hz, ^3J = 6.2 Hz, 1H, H3a), 2.16-2.12 (m, 1H, H9a), 2.03-1.74 (m, 7H, H1b, H2, H6, H7a, H10b), 1.63-1.50 (m, 3H, H3b, H7b, H9b), 1.46 (s, 1H, N*H*).

6.2.1.5 Synthesis of 49

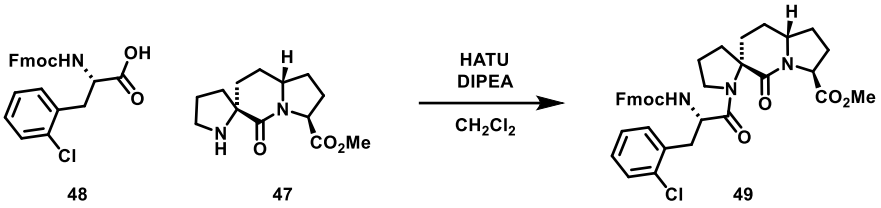

48 47 49

According to a modified procedure by *Albat*[189]: In a 50 mL *Schlenk* tube, 305 mg (723 μmol; 1.20 eq.) of phenylalanine **48** were dissolved in 12 mL of CH_2Cl_2, followed by 355 mg (934 μmol; 1.55 eq.) of HATU and 158 μL (905 μmol; 1.50 eq.) of DIPEA. In a 25 mL *Schlenk* tube, 152 mg (603 μmol; 1.00 eq.) of H[dH-2]OMe (**47**) were dissolved in 12 mL of CH_2Cl_2, followed by 127 μL (723 μmol; 1.20 eq.) of DIPEA. After 1 h at room temperature, the mixture was added to the solution of phenylalanine **48**. After 18 h at room temperature, full conversion of H[dH-2]OMe (**47**)was observed by TLC and the solvent was removed under reduced pressure. The crude product was purified by column chromatography (SiO_2, *c*Hex/EtOAc/MeOH 40:40:1 to 25:25:1) to obtain 132 mg (167 μmol; 23%; 83 wt%) of the desired product **49** as a colorless solid.

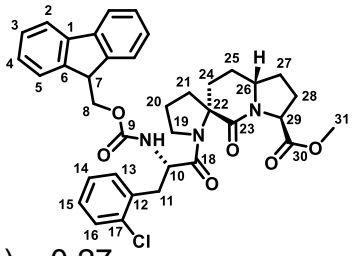

M ($C_{37}H_{38}N_3O_6Cl$): 656.18 g/mol.

Yield: 132 mg (167 μmol; 23%).

R_f: (SiO_2, *c*Hex/EtOAc/MeOH 25:25:1) = 0.27.

^{1}H NMR: (500 MHz, $CDCl_3$) δ [ppm] = 7.74 (d, ^3J = 7.5 Hz, 2H, H2), 7.49 (t, ^3J = 7.4 Hz, 2H, H5), 7.38 (t, ^3J = 7.7 Hz, 2H, H3), 7.33 (d, ^3J = 8.2 Hz, 1H, H16), 7.30-7.27 (m, 2H, H4), 7.24 (d, ^3J = 7.6 Hz, 1H, H13), 7.14-7.05 (m, 2H, H14, H15), 5.58 (d, ^3J = 9.2 Hz, 1H, N*H*), 4.88 (td, ^3J = 10.2 Hz, ^4J = 3.7 Hz, 1H, H10), 4.67 (t, ^3J = 8.7 Hz 1H, H3), 4.22-4.17 (m, 1H, H8a), 4.05-3.99 (m, 2H, H8b, H7), 3.94-3.83 (m, 2H, H19), 3.74-3.68 (m, 4H, H26, H31), 3.40 (dd, ^2J = 14.3 Hz, ^4J = 3.9 Hz, 1H, H11a), 2.83 (dd, ^2J = 13.8 Hz, ^3J = 11.5 Hz, 1H, H11b), 2.43-2.33 (m, 3H, H21a, H24a, H25a), 2.20-2.09 (m, 3H, H20a, H25b, H27a), 2.03-1.91 (m, 4H, H20b, H21b; H24b, H28a), 1.88-1.80 (m, 1H, H28b), 1-74-1.66 (m, 1H, H27b).

6.2.1.6 Synthesis of 50

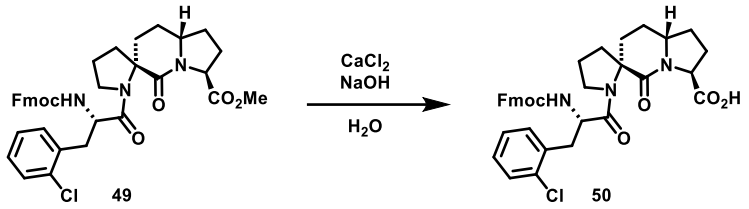

According to a modified procedure by *Albat*[189]: A headspace vial, 110 mg (168 μmol; 1.00 eq.) of tripeptoid **49** were dissolved in 4.2 mL of *i*PrOH and 1.8 mL of H_2O. Next, 528 mg (4.76 mmol; 28.3 eq.) of $CaCl_2$ and 7.8 mg (0.2 mmol; 1.2 eq.) of NaOH were added and the mixture was stirred at room temperature for 22 h. Full conversion of tripeptoid **49** was observed by TLC and the solution was acidified to pH 1 with HCl (1M). The solvent was removed under reduced pressure; the crude product was dissolved in 5 mL of H_2O and acidified with 0.5 mL of HCl (1M). The aqueous phase was extracted six times with CH_2Cl_2, and the combined organic layers were dried over $MgSO_4$ and filtered. The solution was concentrated, filtered through a syringe filter, and the solvent was removed under reduced pressure. The residue was lyophilized from H_2O/MeCN to obtain 93 mg (145 μmol; 86%) of the desired product **50** as a colorless lyophilizate.

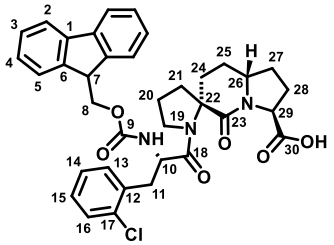

M ($C_{36}H_{36}N_3O_6Cl$): 642.15 g/mol.

Yield: 93 mg (145 μmol; 86%).

R_f: (SiO_2, *c*Hex/EtOAc/MeOH/AcOH 50:50:5:1) = 0.10.

^{1}H NMR: (500 MHz, $CDCl_3$) δ [ppm] = 7.74 (d, ^3J = 7.5 Hz, 2H, H2), 7.50 (t, ^3J = 6.2 Hz, 2H, H5), 7.40-7.34 (3H, H3, H13/H16), 7.30-7.24 (m, 2H, H4), 7.19-7.12 (3H, H14, H15, H13/H16), 5.57 (d, ^3J = 8.3 Hz, 1H, N*H*), 4.85 (td, ^3J = 9.2 Hz, ^3J = 4.5 Hz, 1H, H10), 4.72 (t, ^3J = 9.0 Hz, 1H, H29), 4.27-4.21 (m, 1H, H8a), 4.11-4.00 (m, 2H, H7, H8b), 3.91-3.87 (m, 1H, H19a), 3.69-3.60 (m, 2H, H19b, H26), 3.29 (dd, ^2J = 13.3 Hz, ^3J = 4.4 Hz, 1H, H11a), 2.90 (dd, ^2J = 13.6 Hz, ^3J = 5.6 Hz, 1H, H11b), 2.34-2.29 (m, 4H, H21a, H24a, H25/H28), 2.18-1.90 (m, 7H, H21b, H24b, H25/H28), 1.83 (td, ^3J = 12.5 Hz, ^4J = 5.0 Hz, 1H, H27a), 1.75-1.67 (m, 1H, H27b).

6.2.1.7 Synthesis of 44

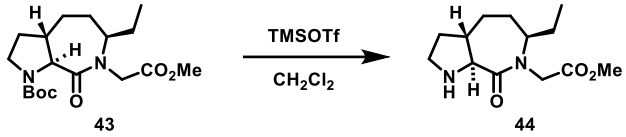

According to a modified procedure by *Albat*[189]: In a 25 mL *Schlenk* flask, 504 mg (1.43 mmol; 1.00 eq.) of Boc[dH-15]OMe (**43**) were dissolved in 8 mL of CH_2Cl_2. The mixture was cooled to 0 °C and 366 µL of TMSOTf (2.10 mmol; 1.50 eq.) were added dropwise. After 15 min, full conversion of Boc[dH-15]OMe (**43**) was observed by TLC. Then, 2 mL of $NaHCO_3$ solution were added, the layers were separated and the aqueous phase was extracted five times with 100 mL of CH_2Cl_2. The combined organic layers were dried over $MgSO_4$, filtered and the solvent was removed under reduced (max. 100 mbar at 40 °C) pressure to obtain 462 mg (1.42 mmol; quant., 79 wt%) of the desired product **44** as an orange oil.

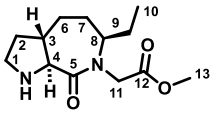

M ($C_{13}H_{22}N_2O_3$): 254.33 g/mol.

Yield: 462 mg (1.42 mmol; quant., 79 wt%).

R_f: (SiO_2, CH_2Cl_2/MeOH 10:1) = 0.18.

^{1}H NMR: (500 MHz, $CDCl_3$) δ [ppm] = 6.45 (s, 1H, N*H*), 4.49 (d, ^3J = 10.7 Hz, 1H, H4), 4.37 (d, ^2J = 17.5 Hz, 1H, H11a), 3.89 (d, ^2J = 17.5 Hz, 1H, H11b), 3.74 (s, 3H, H13), 3.65 (q, J = 8.3 Hz, 1H, H8), 3.49 (t, ^3J = 9.6 Hz, 1H, H2a), 3.24 (td, ^3J = 11.3 Hz, ^3J = 7.2 Hz, 1H, H2b), 2.21-2.12 (m, 3H, H1a, H3, H7a), 1.89-1.59 (m, 5H, H1b, H6, H9a, 7b), 1.53 (dq, ^3J = 7.6 Hz, ^3J = 7.6 Hz, 1H, H9b), 0.99 (t, ^3J = 7.3 Hz, 3H,H10).

^{13}C NMR: (125 MHz, $CDCl_3$) δ [ppm] = 172.1 (C5); 170.2 (C12); 64.1 (C4); 60.1 (C8); 52.5 (C13); 45.9 (C2); 43.9 (C11); 42.7 C3); 33.5 (C1); 32.3 (C7); 30.8 (C6); 26.7 (C9); 11.7 (C10).

6.2.1.8 Synthesis of 51

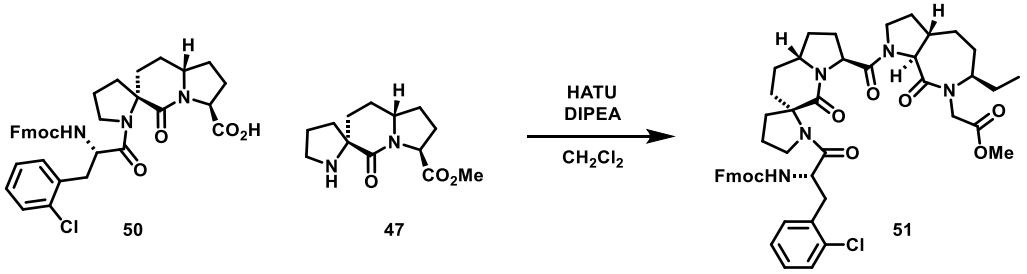

According to a modified procedure by *Albat*[189]: In a 50 mL *Schlenk* tube, 211 mg (232 μmol; 1.20 eq.) of tripeptoid **50** were dissolved in 4.9 mL of CH_2Cl_2. To the mixture, 160 mg (422 μmol; 1.50 eq.) of HATU and 65 μL (370 μmol; 1.3 eq.) of DIPEA were added. In a 25 mL *Schlenk* tube, 80 mg (280 μmol; 1.0 eq., 88 wt%) of H[dH-15]OMe (**47**) were dissolved in 4.9 mL of CH_2Cl_2 and 65 μL (370 μmol; 1.3 eq.) of DIPEA. After 30 min, the mixture was added to the solution of tripeptide **50**. After 22 h, full conversion of H[dH-15]OMe (**47**) was detected by TLC. The solution was filtered through a celite pad and solvent was removed under reduced pressure. The crude product was purified by column chromatography (SiO_2, *c*Hex/EtOAc/MeOH 6:6:1 to 4:4:1) to obtain 177 mg (192 μmol; 70%; 96 wt%) of the desired product **51** as a colorless solid.

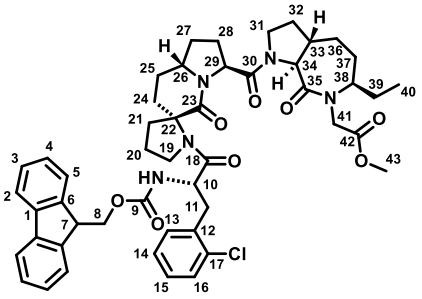

M ($C_{49}H_{56}N_5O_8Cl$): 878.46 g/mol.

Yield: 177 mg (192 μmol; 70%, 96 wt%).

R_f: (SiO_2, *c*Hex/EtOAc/MeOH 3:3:1) = 0.37.

^{1}H NMR: (500 MHz, $CDCl_3$) δ [ppm] = 7.73 (d, ^3J = 7.7 Hz, 2H, H2), 7.49 (t, ^3J = 6.7 Hz, 2H, H5), 7.38 (t, ^3J = 7.0 Hz, 2H, H3), 7.33 (d, ^3J = 7.6 Hz, 1H, H13/H16), 7.30-7.24 (m, 3H, H13/H16, H4), 7.12 (td, ^3J = 7.6 Hz, ^4J = 1.3 Hz, 1H, H14/H15), 7.07 (t, ^3J = 7.3 Hz H14/H15), 5.62 (d, ^3J = 8.6 Hz, 1H, N*H*), 4.95 (t, ^3J = 8.3 Hz, H29), 4.89 (td, ^3J = 10.1 Hz, ^4J = 3.5 Hz 1H, H10), 4.74 (d, ^3J = 10.3 Hz,

1H, H38), 4.60 (d, ^{2}J = 18.1 Hz, 1H, H41a), 4.21-3.99 (m, 4H, H7, H8, H31a), 3.93-3.82 (m, 2H, H19), 3.80-3.66 (m, 6H, H26, H41b, H43), 3.48-3.40 (m, 2H, H11a, H36a/H37a), 2.90-2.81 (m, 1H, H11b), 2.42-2.34 (m, 3H, H21a, H24a, H28a), 2.34-2.23 (m, 11H, H20, H21b, H25, H27, H31b, H33, H34, H36b/H37b), 1.71-1.45 (m, 6H, H24b, H32b, H36/H37, H39), 0.95 (t, ^{3}J = 7.1 Hz, 3H, H40).

^{13}C NMR: (125 MHz, $CDCl_3$) δ [ppm] = 172.5 (C35); 171.1 (C30); 170.4 (C42); 169.9 (C18 or C23); 169.6 (C18 or C23); 155.7 (C9); 143.9 (C6); 141.3 (C1); 134.6 (C12, C17); 132.4, 129.6, 128.5, 126.8, (C13, C14, C15, C16); 127.7, 127.1, 125.4, 125.3, 120.0, (C2, C3, C4, C5) 67.0 (C8); 65.7 (C22); 62.9 (C38); 59.2 (C26); 58.1 (C29); 52.5 (C10); 52.2 (C43); 48.7 (C19); 47.1 (C31); 46.9 (C7); 43.2 (C41); 41.5 (C33); 41.3 (C21); 36.7 (C11, C24); 36.5 (C34); 33.4 (C27); 33.3 (C36 or C37); 33.2 (C36 or C37); 31.0 (C32); 28.4 (C25); 27.8 (C28); 27.1 (C39); 24.1 (C20); 12.0 (C40).

HR-MS (ESI):

Ion	Calc. mass [u]	Exp. mass [u]	Δ [ppm]
$[M+Na]^+$	900.37096	900.37063	-0.37

6.2.1.9 Synthesis of 22

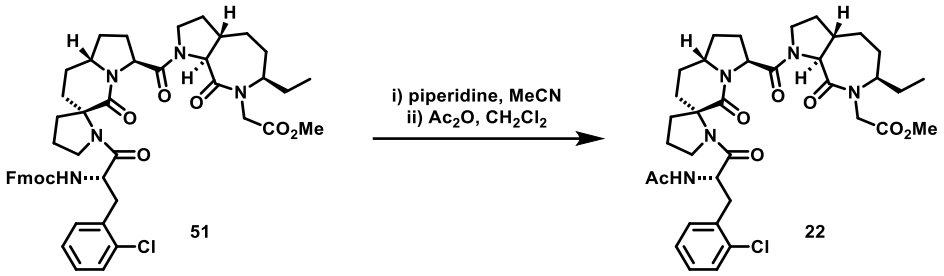

According to a modified procedure by *Albat*[189]: In a 50 mL round bottom flask,177 mg (192 μmol; 1.00 eq., 96 wt%) of the pentapeptoid **51** were dissolved in 12 mL of MeCN and 3.00 mL (30.2 mmol; 157 eq.) of piperidine and stirred at room temperature for 3 h. Full conversion of pentapeptoid **51** was observed by TLC and the solvent was removed under reduced pressure. The residue was dissolved in 10 mL of CH_2Cl_2 and 95 μL of Ac_2O (1.0 mmol; 5.2 eq.) were added. After stirring at room temperature for 16 h, full conversion was observed by TLC and the absence of free amines was proven by ninhydrin staining. The solvent was removed under reduced pressure, and the crude product was purified by column chromatography (SiO_2, *c*Hex/EtOAc/MeOH 2:2:1) to obtain 102 mg (146 μmol; 76%) of the desired product **22** as a colorless solid.

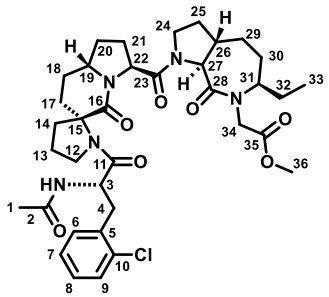

M ($C_{36}H_{48}N_5O_7Cl$): 698.26 g/mol.

Yield: 102 mg (146 μmol; 76%).

R_f: (SiO_2, *c*Hex/EtOAc/MeOH 2:2:1) = 0.22.

^{1}H NMR: (500 MHz, $CDCl_3$) δ [ppm] = 7.34-7.32 (m, 1H, H9), 7.23-7.21 (m, 1H, H6), 7.17-7.15 (2H, H7, H8), 6.18 (d, ^3J = 8.2 Hz, 1H, N*H*), 5.11 (td, ^3J = 9.7 Hz, ^3J = 3.5 Hz, 1H, H3), 4.94 (t, ^3J = 8.6 Hz, 1H, H22), 4.74 (d, ^3J = 10.6 Hz, 1H, H31), 4.62 (d, ^2J = 17.3 Hz, 1H, H34a), 4.06 (t, ^3J = 9.6 Hz, 1H, H34b), 3.96-3.91 (m, 1H, H12a), 3.84-3.73 (m, 3H, H12b, H19, H27), 3.70 (s, 3H, H36), 3.66 (d, 1H, H24a), 3.47-3.43 (m, 1H, H24b), 3.35 (dd, ^2J = 13.9 Hz, ^3J = 10.1 Hz, 1H, H4a), 2.85 (dd, ^2J = 14.1,

^{3}J = 10.5 Hz, 1H, H4b), 2.41-2.32 (m, 3H, H14a, H17a, H21a), 2.30-2.23 (m, 1H, H26), 2.21-1.84 (m, 11H, H13, H14b, H17b, H18, H20a, H21b, H25a, H29), 1.81 (s, 3H, H1), 1.69-1.60 (m, 4H, H20b H25b, H30a, H32a), 1.53-1.43 (m, 2H, 30b, H32b), 0.95 (t, ^{3}J = 7.6 Hz, 3H, H33).

^{13}C NMR: (125 MHz, $CDCl_3$) δ [ppm] = 172.7 (C28); 171.0 (C23); 170.4 (C35); 169.9, 169.6 (C11 and C16); 169.5 (C2); 134.7, 134.6 (C5, C10); 132.1 (C6); 129.6, 128.5, 126.8 (C7, C8, C9); 65.6 (C15); 62.9 (C27); 59.2 (C19); 59.1 (C26); 58.0 (C22); 52.2 (C36); 50.9 (C3); 48.7 (C12); 46.9 (C24); 43.2 (C34); 41.5 (C14); 41.3 (C31); 36.4 (C17); 36.1 (C4); 33.4 (C20); 33.4 (C29 or 30); 33.2 (C29 or 30); 31.0 (C25); 28.5 (C18); 27.8 (C21); 27.2 (C32); 24.0 (C13); 23.2 (C1); 12.0 (C33).

HR-MS (ESI):

Ion	Calc. mass [u]	Exp. mass [u]	Δ [ppm]
$[M+Na]^+$	720.31345	720.31259	-1.20

6.2.1.10 Synthesis of 38

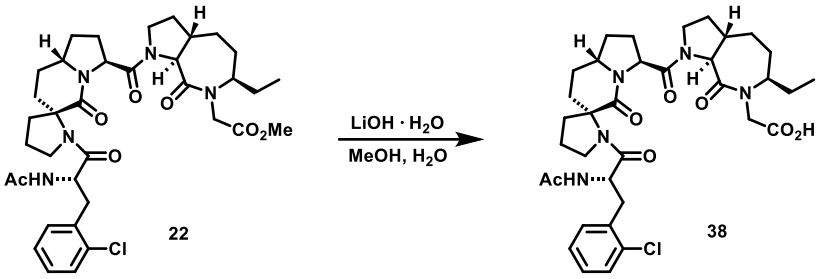

According to a modified procedure by *Albat*[189]: In a 5 mL reaction vessel, 500 mg (716 μmol; 1.00 eq.) of binder **22** were dissolved in 2 mL of MeOH and 1 mL of H_2O. Next, 90 mg (3.7 mmol; 5.5 eq.) of LiOH hydrate were added. The mixture was stirred at room temperature until full conversion of binder **22** was observed by TLC after 16 h. The mixture was washed with 20 mL of M*t*BE, the aqueous phase was acidified to pH 1 with HCl (conc.) and extracted five times with 100 mL of CH_2Cl_2. The combined organic layers were dried over $MgSO_4$, filtered, and the solvent was removed under reduced pressure. The product was dissolved in H_2O/MeOH and lyophilized to obtain 479 mg (700 μmol; 98%) of the desired product **38** as a colorless lyophilizate.

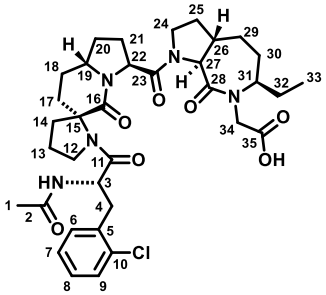

M ($C_{35}H_{46}N_5O_7Cl$): 684.23 g/mol.

Yield: 479 mg (700 μmol; 98%).

R_f: (SiO_2, *c*Hex/EtOAc/MeOH 2:2:1) = 0.04.

^{1}H NMR: (500 MHz, $CDCl_3$) δ [ppm] = 7.35-7.31 (m, 1H, H9), 7.23-7.21 (m, 1H, H6), 7.18-7.13 (2H, H7, H8), 6.35 (d, ^3J = 8.2 Hz, 1H, N*H*), 5.10 (td, ^3J = 9.8 Hz, ^3J = 3.7 Hz, 1H, H3), 4.89 (t, ^3J = 8.5 Hz, 1H, H22), 4.74 (d, ^3J = 10.5 Hz, 1H, H31), 4.50 (d, ^2J = 17.8 Hz, 1H, H34a), 4.09 (t, ^3J = 8.8 Hz, 1H, H34b), 3.96-3.92 (m, 1H, H12a), 3.81-3.70 (m, 4H, H12b, H19, H27, H24a), 3.48-3.42 (m, 1H, H24b), 3.32 (dd, ^2J = 14.6 Hz, ^3J = 10.4 Hz, 1H, H4a), 2.85 (dd, ^2J = 14.2, ^3J = 10.4 Hz, 1H, H4b), 2.41-2.32 (m, 3H, H14a, H17a, H21a), 2.25-2.21 (m, 1H, H26), 2.12-1.85 (m, 11H, H13, H14b, H17b, H18, H21b, H20a, H25a, H29),

1.80 (s, 3H, H1), 1.75-1.59 (m, 4H, H20b, H25b, H30a, H32a), 1.53-1.44 (m, 2H, 30b, H32b), 0.95 (t, ^{3}J = 7.2 Hz, 3H, H33).

^{13}C NMR: (125 MHz, $CDCl_3$) δ [ppm] = 172.7 (C28); 171.9 (C35); 171.0 (C23); 170.1, 169.8, 169.6 (C2, C11, C16); 134.7, 134.6 (C5, C10); 132.1 (C6); 129.6, 128.5, 126.8, (C7, C8, C9); 65.6 (C15); 63.1 (C27); 59.4 (C19); 59.3 (C26); 58.2 (C22); 50.8 (C3); 48.7 (C12); 47.1 (C24); 43.7 (C34); 41.4 (C14); 41.3 (C31); 36.5 (C17); 36.0 (C4); 33.4 (C20); 33.3 (C29 or C30); 33.1 (C29 or C30); 31.0 (C25); 28.4 (C18); 27.8 (C21); 27.1 (C32); 24.1 (C13); 23.1 (C1); 12.0 (C33).

HR-MS (ESI):

Ion	Calc. mass [u]	Exp. mass [u]	Δ [ppm]
$[M+H]^+$	684.31585	684.31669	+1.22
$[M+Na]^+$	706.29780	706.29800	+0.28

LC-MS (ESI):

t_r [min]		12.74-13.46
Ion	Calc. mass [u]	Exp. mass [u]
$[M+H]^+$	684.32	684.47

6.2.1.11 Synthesis of 39

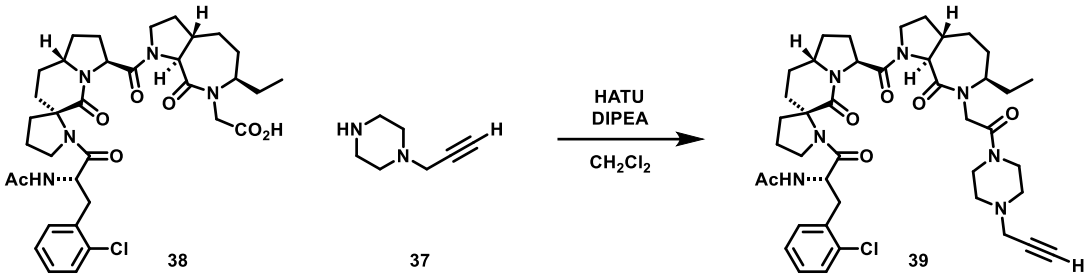

In a 5 mL *Schlenk* tube, 90 mg (130 μmol; 1.0 eq.) of warhead **38** were dissolved in 1 mL of CH_2Cl_2. Next, 65 mg (170 μmol; 1.3 eq.) of HATU were added followed by 25 μL (140 μmol; 1.1 eq.) of DIPEA. In a 2 mL *Schlenk* tube, 23 mg (180 μmol; 1.4 eq.) of linker **37** were dissolved in 1 mL of CH_2Cl_2. After 30 min, the mixture was added to the solution of warhead **38**. After 18 h, full conversion of warhead **38** was observed by TLC and the solvent was removed under reduced pressure. The crude product was purified by column chromatography (dryload, SiO_2, EtOAc/MeOH/NEt_3 20:2:1). The product was dissolved in H_2O/MeCN and lyophilized to obtain 71 mg (84 μmol; 64%; 94 wt%) of the desired product **39** as a colorless lyophilizate.

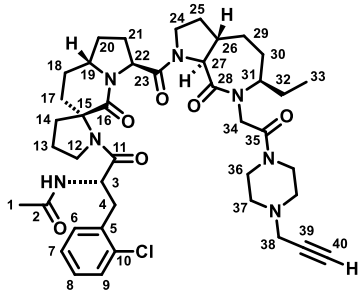

M ($C_{42}H_{56}N_7O_6Cl$): 790.40 g/mol.

Yield: 71 mg (84 μmol; 64%; 94 wt%).

R_f: (SiO_2, EtOAc/MeOH/NEt_3 20:2:1) = 0.13.

^{1}H NMR: (500 MHz, $CDCl_3$) δ [ppm] = 7.34-7.31 (m, 1H, H9), 7.23-7.21 (m, 1H, H6), 7.18-7.14 (m, 2H, H7, H8), 6.15 (d, ^3J = 8.8 Hz, 1H, N*H*), 5.13-5.09 (m, 1H, H3), 4.94 (t, ^3J = 8.4 Hz, 1H, H22), 4.83 (d, ^2J = 16.6 Hz, 1H, H34a), 4.74 (d, ^3J = 10.0 Hz, 1H, H27), 4.05 (t, ^3J = 8.7 Hz, 1H, H24a), 3.95-3.91 (m, 1H, H12a), 3.83-3.72 (m, 3H, H12b, H19, H26), 3.66-3.57 (m, 3H, H34b, H37a), 3.53-3.41 (m, 3H, H24b, H37b), 3.37-2.75 (m, 4H, H4, H38), 2.62-2.49 (m, 4H, H36), 2.41-2.32 (m, 4H, H14a, H17a, H21a, H31), 2.26 (t, ^4J = 2.4 Hz, 1H, H40), 2.10-1.84 (m, 11H, H13,

H14b, H17b, H18, H20a, H21b, H25a, H29), 1.80 (s, 3H, H1), 1.67-1.61 (4H, H20b, H25b, H30a, H32a), 1.52-1.42 (m, 2H, H30b, H32b), 0.95 (t, ^{3}J = 7.2 Hz, 3H, H33).

^{13}C NMR: (125 MHz, $CDCl_3$) δ [ppm] = 172.6 (C28); 170.3 (C23); 169.8, 169.6, 169.4 (C2, C11, C16); 167.4 (C35); 134.7, 134.7 (C5, C10); 132.1 (C6); 129.6, 128.5, 126.8 (C7, C8, C9); 78.3 (C39); 73.8 (C40); 65.6 (C15); 63.1 (C27); 59.2 (C19); 59.1 (C26); 58.0 (C22); 51.8 (C36a); 51.5 (C37); 50.8 (C3); 48.7 (C12); 47.0 (C24); 46.0 (C38); 43.0 (C34); 42.0 (C36b); 41.6 (C14); 41.1 (C31); 36.4 (C17); 36.1 (C4); 33.4 (C20); 33.4 (C29, C30); 30.5 (C25); 28.5 (C18); 27.8 (C21); 27.1 (C32); 24.0 (C13); 23.2 (C1); 12.0 (C33).

HR-MS (ESI):

Ion	Calc. mass [u]	Exp. mass [u]	Δ [ppm]
$[M+H]^+$	790.40534	790.40621	+1.11
$[M+Na]^+$	812.38728	812.38758	+0.37

6.2.2 Synthesis towards PROTACs 53, 60, and 66

6.2.2.1 Synthesis of 55

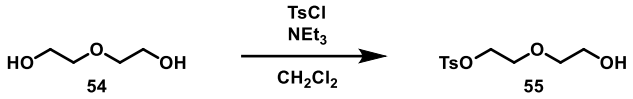

According to a modified procedure by *Li et al*.[194]: In a 500 mL three neck flask, 31.8 g (300 mmol; 7.00 eq.) of diethylene glycol (**54**) were dissolved in 90 mL of CH_2Cl_2 and 6.25 mL (42.8 mmol; 1.00 eq.) of NEt_3. In a 250 mL dropping funnel, 8.20 g (47.1 mmol; 1.10 eq.) of TsCl were dissolved in 140 mL of CH_2Cl_2. The TsCl solution was added to the reaction within 5 min. The mixture was stirred at room temperature until major conversion of the TsCl was observed by TLC after 45 h. Into the reaction mixture, 50 mL of HCl (1M) and 60 mL of NaCl solution were added, and the mixture was vigorously stirred for 30 min. The layers were separated, and the aqueous phase was extracted with 5 mL of CH_2Cl_2 two times. The combined organic layers were dried over $MgSO_4$, filtered, and the solvent was removed under reduced pressure. The crude product was purified by column chromatography (SiO_2, *c*Hex/EtOAc 3:1 to 1:1) to obtain 6.43 g (4.95 mmol; 58%) of the desired product **55** as a colorless oil.

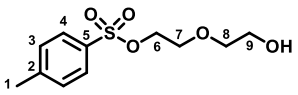

M ($C_{11}H_{16}O_5S$): 260.30 g/mol.

Yield: 6.43 g (4.95 mmol; 58%; Lit.[194]: 98%).

R_f: (SiO_2, *c*Hex/EtOAc 1:1) = 0.19.

^{1}H NMR: (400 MHz, $CDCl_3$) δ [ppm] = 7.81 (d, ^3J = 8.5 Hz, 2H, H4), 7.35 (d, ^3J = 8.0 Hz, 2H, H3), 4.20 (t, J = 4.7 Hz, 2H, H6), 3.71-3.66 (m, 4H, H7, H9), 3.55-3.52 (m, 2H, H8), 2.45 (s, 3H, H1), 1.91 (s, 1H, O*H*).

^{13}C NMR: (100 MHz, $CDCl_3$) δ [ppm] = 145.1 (C2); 133.1 (C5); 130.0 (C3); 128.1 (C4); 72.6 (C8); 69.3 (C6); 68.7 (C7); 61.9 (C9); 21.8 (C1).

LC-MS (ESI):

t_r [min]		12.23-12.57
Ion	Calc. mass [u]	Exp. mass [u]
$[M+H]^+$	261.31	261.12

6.2.2.2 Synthesis of 56

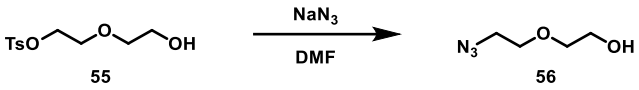

According to a modified procedure by *Simonin et al*.[215]: In a 250 mL round bottom flask, 5.20 g (20.0 mmol; 1.00 eq.) of monotosylated diethylene glycol (**55**) were dissolved in 50 mL of DMF, followed by 1.95 g (30.0 mmol; 1.50 eq.) of NaN_3. The mixture was stirred at 100 °C until full conversion of monotosylated diethylene glycol (**55**) was observed by TLC after 15 h. At room temperature, 300 mL H_2O were added and the aqueous phase was extracted five times with 100 mL of EA. The combined organic layers were washed with 300 mL of H_2O and 200 mL of NaCl solution, dried over $MgSO_4$, filtered, and the solvent was removed under reduced pressure. The crude product was purified by column chromatography (SiO_2, *c*Hex/EtOAc 2:1 to 1:1) to obtain 1.52 g (11.6 mmol; 58%) of the desired product **56** as a pale-yellow oil.

M ($C_4H_9N_3O_2$):	131.135 g/mol. 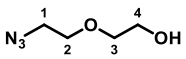
Yield:	1.52 g (11.6 mmol; 58%).
R_f:	(SiO_2, *c*Hex/EtOAc 1:1) = 0.30.
^{1}H NMR:	(500 MHz, $CDCl_3$) δ [ppm] = 3.77 (t, ^3J = 4.6 Hz, 2H, H4), 3.71 (t, ^3J = 4.8 Hz, 2H, H2), 3.62 (t, ^3J = 4.5 Hz, 2H, H3), 3.42 (t, ^3J = 4.8 Hz, 2H, H1).
^{13}C NMR:	(125 MHz, $CDCl_3$) δ [ppm] = 72.5 (C3); 70.2 (C2); 61.9 (C4); 50.9 (C1).

6.2.2.3 Synthesis of 52

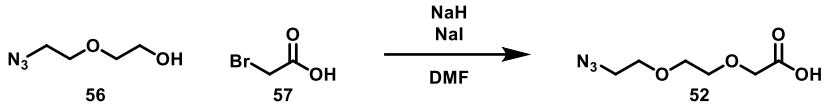

According to a modified procedure by *Heller et al*.[216]: In a 25 mL *Schlenk* flask, 405 mg (3.09 mmol; 1.00 eq.) of azide **56** were dissolved in 11.2 mL of DMF. Next, 516 mg (3.71 mmol; 1.20 eq.) of bromoacetic acid (**57**) were added, followed by 10 mg (60 μmol; 2 mol%) of NaI. The mixture was cooled to 0°C and 371 mg (9.27 mmol; 3.00 eq., 60 wt% in mineral oil) of NaH were added. The mixture was stirred at 0°C until full conversion of azide **56** was observed by TLC after 3.5 h. The mixture was poured into 50 g of crushed ice and the mixture was allowed to melt. The aqueous phase was then washed with 50 mL of EtOAc, acidified to pH 2 with HCl (1M), and extracted with EtOAc three times. The combined organic layers were dried over $MgSO_4$, filtered, and the solvent was removed under reduced pressure. The crude product was purified by column chromatography (SiO_2, *c*Hex/EtOAc/AcOH 25:25:1) to obtain 514 mg (2.17 mmol; 88%) of the desired product **52** as a colorless oil.

M ($C_6H_{11}N_3O_4$):	189.17 g/mol.
Yield:	514 mg (2.17 mmol; 88%).
R_f:	(SiO_2, *c*Hex/EtOAc/AcOH 25:25:1) = 0.16.
^{1}H NMR:	(500 MHz, $CDCl_3$) δ [ppm] = 8.40 (s, 1H, O*H*), 4.21 (s, 2H, H5), 3.79-3.77 (m, 2H, H4), 3.73-3.69 (m, 4H, H2, H3), 3.42 (t, *J* = 5.0 Hz, 2H, H1).
^{13}C NMR:	(125 MHz, $CDCl_3$) δ [ppm] = 173.9 (C6); 71.4 (C4); 70.6 (C3); 70.2 (C2); 68.6 (C5); 50.7 (C1).

6.2.2.4 Synthesis of 58

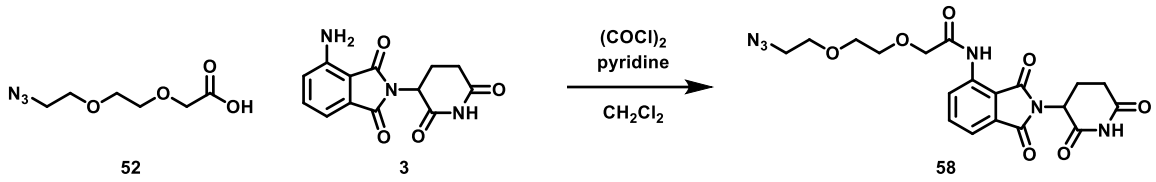

According to a modified procedure by *Kawamata et al*.[217]: In a 10 mL *Schlenk* tube, 189 mg (1.00 mmol; 1.10 eq.) of linker **52** were dissolved in 5 mL of CH_2Cl_2 and 0.05 mL of DMF. The mixture was cooled to 0 °C and 86 μL (1.0 mmol; 1.1 eq.) of $(COCl)_2$ were added dropwise and the mixture was stirred for 1 h at 0 °C. Next, 246 mg (0.91 mmol; 1.00 eq.) of recruiter **3** and 322 μL (4.00 mmol; 4.40 eq.) of pyridine were added. The mixture was stirred for 16 h while warming to room temperature. The mixture was poured into 10 mL of NaCl solution and extracted with 30 mL of CH_2Cl_2 three times. The combined organic layers were dried over $MgSO_4$, filtered, and the solvent was removed under reduced pressure. The crude product was purified by column chromatography (dryload, SiO_2, *c*Hex/EtOAc 2:1 to 1:2) to obtain 297 mg (668 μmol; 67%) of the desired product **58** as a pale-yellow solid.

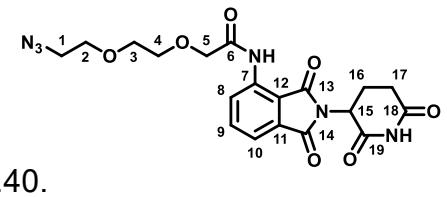

M ($C_{19}H_{20}N_6O_7$): 444.40 g/mol.

Yield: 297 mg (668 μmol; 67%).

R_f: (SiO_2, *c*Hex/EtOAc 1:2) = 0.40.

^{1}H NMR: (500 MHz, $CDCl_3$) δ [ppm] = 10.46 (s, 1H, N*H*), 8.87 (d, ^3J = 8.5 Hz, 1H, H8), 8.34 (s, 1H, N*H*), 7.73 (dd, ^3J = 7.9 Hz, ^3J = 7.9 Hz, 1H, H9), 7.58 (d, ^3J = 7.2 Hz, 1H, H10), 4.97 (dd, ^3J = 12.2 Hz, ^3J = 5.2 Hz, 1H, H15), 4.22 (s, 2H, H5), 3.86-3.81 (m, 4H, H3, H4), 3.73 (t, J = 5.2 Hz, 2H, H2), 3.39 (t, ^3J = 5.1 Hz, 2H, H1), 2.94-2.90 (m, 1H, H17a), 2.87-2.72 (m, 2H, H17b, H16a), 2.19-2.13 (m, 1H, H16b).

^{13}C NMR: (125 MHz, $CDCl_3$) δ [ppm] = 171.0 (C18); 169.4 (C6); 168.6 (C13); 168.0 (C19); 166.9 (C14); 136.9 (C11); 136.5 (C9); 131.5 (C15); 125.4 (C8); 119.0 (C10); 116.3 (C12); 71.7 (C4); 71.2 (C5); 70.7 (C3); 70.3 (C2); 50.8 (C1); 49.4 (C15); 31.5 (C17); 22.8 (C16).

HR-MS (ESI):

Ion	Calc. mass [u]	Exp. mass [u]	Δ [ppm]
$[M+H]^+$	445.14662	445.14715	+1.19
$[M+Na]^+$	467.12837	467.12900	+0.93

6.2.2.5 Synthesis of 53

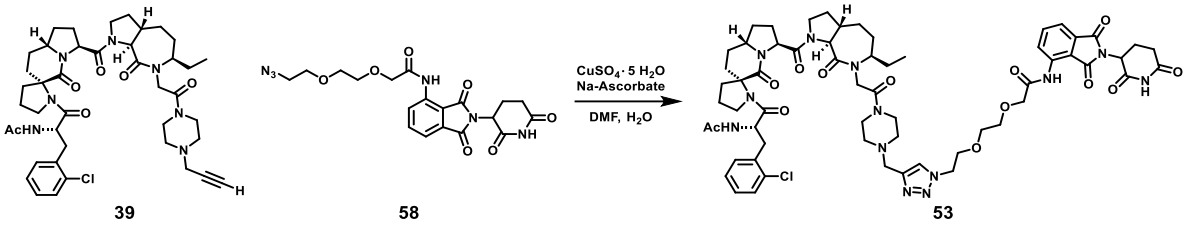

39 58 53

According to a modified procedure by *Banerjee et al*.[196]: In a headspace vial, 20 mg (25 μmol; 1.0 eq.) of warhead-linker conjugate **39** and 17 mg (38 μmol; 1.5 eq.) of conjugate **58** were dissolved in 2 mL of DMF. Next, 1 mL of an aqueous solution (3mM; 3 μmol; 10 mol%) of $CuSO_4$ and 1 mL of an aqueous solution (6mM; 6 μmol; 20 mol%) of sodium ascorbate were added, and the mixture was stirred at room temperature for 18 h. Full conversion of warhead-linker conjugate **39** was observed by TLC and the solvent was removed under reduced pressure. The crude product was purified by column chromatography (dryload, 7 g ultra-pure silica, EtOAc/MeOH/NEt_3 1:0:0 to 20:4:1). The product was dissolved in CH_2Cl_2, filtered through a syringe filter, and the solvent was removed under reduced pressure. The product was dissolved in MeCN/H_2O and lyophilized to obtain 25 mg (20 μmol; 80%) of the desired product **53** as a pale-yellow lyophilizate.

M ($C_{61}H_{76}N_{13}O_{13}Cl$):	1234.81 g/mol.			
Yield:	25 mg (20 μmol; 80%).			
R_f:	(SiO_2, EtOAc/MeOH/NEt_3 20:4:1) = 0.18.			
HR-MS (ESI):	Ion	Calc. mass [u]	Exp. mass [u]	Δ [ppm]
	$[M+H]^+$	1234.54469	1234.54550	+0.66
	$[M+Na]^+$	1256.52663	1256.52641	-0.17
HPLC:	t_r [min]		6.82-7.33	
	Purity [%]		94	

6.2.2.6 Synthesis of 63

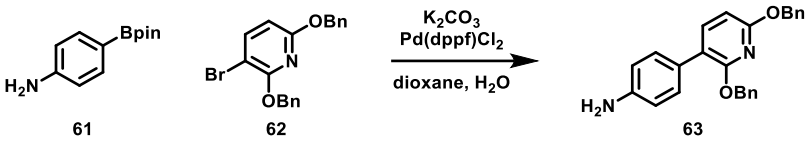

According to a modified procedure by *Lei et al*.[197]: In a 100 mL *Schlenk* flask, 1.07 g (4.91 mmol; 1.00 eq.) of building block **61**, 2.00 g (5.40 mmol; 1.10 eq.) of aryl bromide **62**, 2.03 g (14.7 mmol; 3.00 eq.) of K_2CO_3, and 0.37 g (0.49 mmol; 10 mol%) of $Pd(dppf)Cl_2$ were dissolved in 31.5 mL of dioxane and 9.5 mL of H_2O. The mixture was stirred at 100 °C until full conversion of building block **61** was observed by TLC after 17 h. After cooling to room temperature, the mixture was extracted with 30 mL of EtOAc three times and the combined organic layers were washed with 50 mL of NaCl solution, dried over $MgSO_4$, filtered, and the solvent was removed under reduced pressure. The crude product was purified by column chromatography (SiO_2, dryload, *c*Hex/EtOAc 3.1 to 2:1) to obtain 1.65 g (4.31 mmol; 88%) of the desired product **63** as an orange oil.

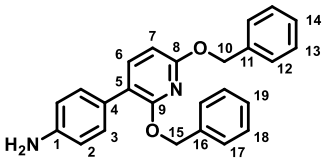

M ($C_{25}H_{22}N_2O_2$):	382.46 g/mol.
Yield:	1.65 g (4.31 mmol; 88%; Lit.[197]: 96%).
R_f:	(SiO_2, *c*Hex/EtOAc 2:1) = 0.44.
^{1}H NMR:	(500 MHz, $CDCl_3$) δ [ppm] = 7.56 (d, ^3J = 8.2 Hz, 1H, H6), 7.56 – 7.27 (m, 13H, H2, H3, H12, H13, H14, H17, H18), 6.71 (d, ^3J = 8.5 Hz, 1H, H19), 6.44 (d, ^3J = 8.0 Hz, 1H, H7), 5.41 (s, 2H, H15), 5.34 (s, 2H, H10), 3.67 (s, 2H, NH_2)
^{13}C NMR:	(125 MHz, $CDCl_3$) δ [ppm] = 160.8 (C9); 158.3 (C8); 145.1 (C1); 141.4 (C6); 138.2 (C16); 137.8 (C11); 130.1; 128.6, 128.4, 127.9, 127.5, 127.3 (C2, C3, C12, C13, C14, C17, C18, C19); 116.3 (C4); 115.1 (C5); 102.4 (C7); 67.9 (C15); 67.6 (C10).

6.2.2.7 Synthesis of 59

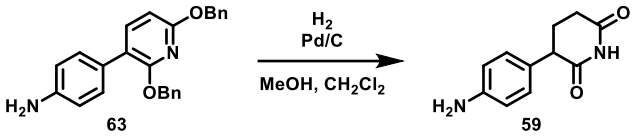

According to a modified procedure by *Lei et al*.[197]: In a 100 mL *Schlenk* flask, 1.60 g (4.18 mmol; 1.00 eq.) of recruiter **63** were dissolved in 27 mL of MeOH and 27 mL of CH_2Cl_2. To the solution, 320 mg (20 wt%) Pd/C were added, the flask was purged with hydrogen gas, and the mixture was stirred until full conversion of recruiter **63** was observed by TLC after 22 h. The mixture was filtered through a pad of silica and the solvent was removed under reduced pressure. The crude product was recrystallized from MeOH/ CH_2Cl_2 to obtain 742 mg (3.63 mmol; 87%) of the desired product **59** as a colorless solid.

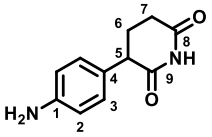

M ($C_{11}H_{12}N_2O_2$):	204.23 g/mol.
Yield:	742 mg (3.63 mmol; 87%; Lit.[197]: 55%).
R_f:	(SiO_2, CH_2Cl_2/MeOH/NEt_3 100:5:1) = 0.30.
^{1}H NMR:	(500 MHz, DMSO-d_6) δ [ppm] = 10.72 (s, 1H, N*H*), 6.84 (d, ^3J = 8.1 Hz, 2H, H3), 6.51 (d, ^3J = 8.2 Hz, 2H, H2), 4.97 (s, 2H, NH_2), 3.61 (dd, ^3J = 10.4 Hz, ^3J = 5.4 Hz, 1H, H5), 2.59 (ddd, ^2J = 17.1 Hz, ^3J = 10.8 Hz, ^3J = 5.4 Hz, 1H, H7a), 2.43 (dt, ^2J = 17.4 Hz, ^3J = 4.8 Hz, 1H, H7b), 2.10-1.95 (m, 2H, H6).
^{13}C NMR:	(125 MHz, DMSO-d_6) δ [ppm] = 174.8 (C9); 173.5 (C8), 147.5 (C1); 128.8 (C3); 125.8 (C4); 113.8 (C2), 46.4 (C5), 31.0 (C7), 26.1 (C6).

6.2.2.8 Synthesis of 64

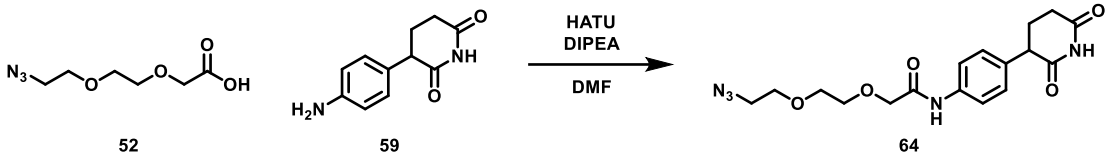

52 59 64

This experiment was carried out by *Rafael Claßen*. In a 50 mL *Schlenk* flask, 144 mg (0.76 mmol; 1.20 eq.) of linker **52** were dissolved in 12 mL of DMF and 0.15 mL (0.86 mmol; 1.35 eq.) of DIPEA. Next, 360 mg (0.96 mmol; 1.50 eq.) of HATU were added, and the mixture was stirred at room temperature. In a 25 mL *Schlenk* flask, 130 mg (0.64 mmol; 1.00 eq.) of recruiter **59** were dissolved in 12 mL of DMF and 0.15 mL (0.86 mmol; 1.35 eq.) of DIPEA. After 30 min, the mixture was added to the solution of linker **52**, and the mixture was stirred at room temperature until full conversion of recruiter **59** was observed by TLC after 22 h. The solvent was removed under reduced pressure, and the crude product was purified by column chromatography (SiO_2, dryload, *c*Hex/EtOAc 3:1 to 1:1) to obtain 166 mg (442 μmol; 69%) of the desired product **64** as a pale-yellow solid.

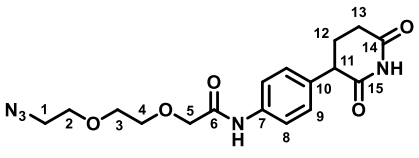

M ($C_{17}H_{21}N_5O_5$): 375.38 g/mol.

Yield: 166 mg (442 μmol; 69%).

R_f: (SiO_2, *c*Hex/EtOAc 1:2) = 0.09.

^{1}H NMR: (500 MHz, $CDCl_3$) δ [ppm] = 8.59 (s, 1H, N*H*), 7.96 (s, 1H, N*H*), 7.61 (d, ^3J = 8.5 Hz, 2H, H8), 7.19 (d, ^3J = 8.5 Hz, 1H, H9), 4.13 (s, 2H, H5), 3.80-3.73 (m, 7H, H2, H3, H4, H11), 3.44 (t, ^3J = 4.8 Hz, 2H, H1), 2.76-2.61 (m, 2H, H13), 2.32-2.19 (m, 2H, H12).

^{13}C NMR: (125 MHz, $CDCl_3$) δ [ppm] = 173.1 (C15); 172.2 (C14); 168.1 (C6); 137.0 (C7); 133.1 (C10); 128.8 (C9); 120.6 (C8); 71.2, 71.2, 70.7, 70.3 (C2, C3, C4, C5); 50.7 (C1); 47.6 (C11); 31.0 (C13); 26.5 (C12).

HR-MS (ESI):

Ion	Calc. mass [u]	Exp. mass [u]	Δ [ppm]
$[M+H]^+$	376.16154	376.16190	+0.94
$[M+Na]^+$	398.14349	398.14372	+0.59

6.2.2.9 Synthesis of 60

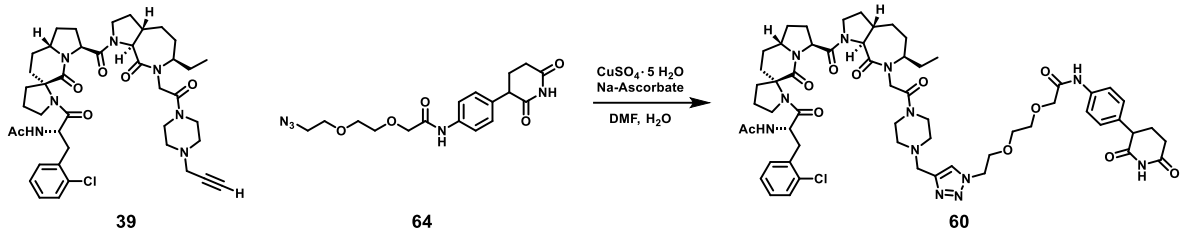

39 64 60

According to a modified procedure by *Banerjee et al*.[196]: In a headspace vial, 23 mg (30 μmol; 1.0 eq.) of warhead-linker conjugate **39** and 17 mg (44 μmol; 1.5 eq.) of linker-recruiter conjugate **64** were dissolved in 2 mL of DMF. Next, 1 mL of an aqueous solution (3mM; 3 μmol; 10 mol%) of $CuSO_4$ and 1 mL of an aqueous solution (6mM; 6 μmol; 20 mol%) of sodium ascorbate were added. The mixture was stirred at room temperature until full conversion of **39** was observed by TLC after 17 h. The solvent was removed under reduced pressure, and the crude product was purified by column chromatography (SiO_2, dryload, EtOAc/MeOH/NEt_3 1:0:0 to 20:4:1). The residue was dissolved in CH_2Cl_2 and filtered through a syringe filter and the solvent was removed under reduced pressure. The residue was purified by reverse phase column chromatography (MeCN/H_2O 2:8 to 7:3) and lyophilized to obtain 13 mg (11 μmol; 37%) of the desired product **60** as a colorless lyophilizate.

M ($C_{59}H_{77}N_{12}O_{11}Cl$):	1165.79 g/mol.			
Yield:	13 mg (11 μmol; 37%).			
R_f:	(SiO_2, EtOAc/MeOH/NEt_3 20:4:1) = 0.06.			
HR-MS (ESI):	Ion	Calc. mass [u]	Exp. mass [u]	Δ [ppm]
	$[M+H]^+$	1165.55960	1165.55875	-0.73
	$[M+Na]^+$	1187.54155	1187.53893	-2.21
HPLC:	t_r [min]		10.67-10.92	
	Purity [%]		96	

6.2.2.10 Synthesis of 69

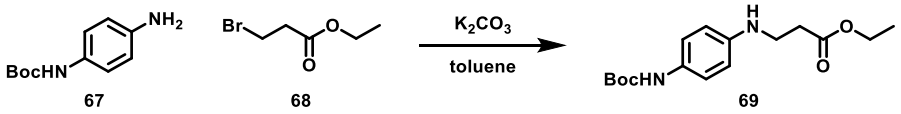

67 68 69

This experiment was carried out by *Rafael Claßen*. According to a modified procedure by *Norris et al*.[198]: In a 250 mL round bottom flask, 5.22 g (28.8 mmol; 2.00 eq.) of building block **67**, 3.00 g (14.4 mmol; 1.00 eq.) of ester **68**, and 1.99 g (14.4 mmol; 1.00 eq.) of K_2CO_3 were suspended in 55 mL of toluene. The mixture was heated to reflux until full conversion of building block **67** was observed by TLC After 23 h. The solvent was removed under reduced pressure and the crude product was purified by column chromatography (SiO_2, *c*Hex/EtOAc 3:1 to 1:2) to obtain 860 mg (2.79 mmol; 19%) of the desired product **69** as a brown solid.

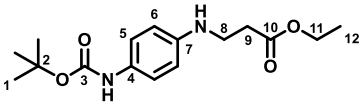

M ($C_{16}H_{24}N_2O_4$):	308.38 g/mol.
Yield:	860 mg (2.79 mmol; 19%; Lit.[198]: 48%).
R_f:	(SiO_2, *c*Hex/EtOAc 1:1) = 0.75.
^{1}H NMR:	(500 MHz, $CDCl_3$) δ [ppm] = 7.16 (d, ^3J = 7.2 Hz, 2H, H5), 6.58 (d, ^3J = 8.8 Hz, 2H, H6), 6.23 (s, 1H, N, ^3J = 7.1 Hz, 2H, H9), 3.98 (s, 1H, N*H*), 3.41 (t, ^3J = 6.3 Hz, 2H, H8), 2.59 (t, ^3J = 6.3 Hz, 2H, H11), 1.50 (s, 9H, H1), 1.26 (t, ^3J = 7.1 Hz, 3H, H12).
^{13}C NMR:	(125 MHz, $CDCl_3$) δ [ppm] = 172.5 (C10), 143.9 (C3), 128.9 (C7), 121.1 (C5), 113.8 (C6), 80.0 (C2), 60.8 (C11), 40.2 (C8), 34.0 (C9), 28.5 (C1), 14.1 (C12). Note: C12, C7, C5, C4, C3, and C2 were detected by HSQC.

6.2.2.11 Synthesis of 70

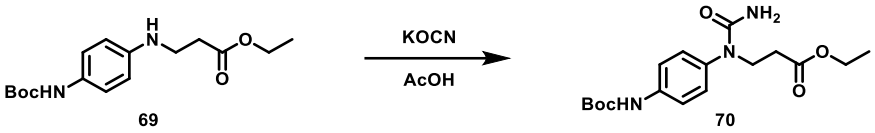

This experiment was carried out by *Rafael Claßen*. According to a modified procedure by *Norris et al*.[198]: In a 10 mL round bottom flask, 404 mg (1.31 mmol; 1.00 eq.) of intermediate **69** and 117 mg (1.44 mmol; 1.10 eq.) of KOCN were dissolved in 2 mL of AcOH. The mixture was stirred at room temperature until full conversion of intermediate **69** was observed by TLC after 1 h. The solvent was removed under reduced pressure, the residue was washed with 8 mL of MeCN three times, and the product was dried under reduced pressure to obtain 227 mg (557 μmol; 43%) of the desired product **70** as a colorless solid.

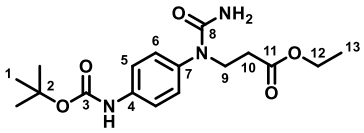

M ($C_{17}H_{25}N_3O_5$): 351.40 g/mol.

Yield: 227 mg (557 μmol; 43%; 86 wt%, Lit.[198]: 61%).

R_f: (SiO_2, *c*Hex/EtOAc 1:2) = 0.30.

^{1}H NMR: (500 MHz, $CDCl_3$) δ [ppm] = 7.43 (d, ^3J = 8.5 Hz, 2H, H6), 7.19 (d, ^3J = 8.7 Hz, 2H, H5), 6.67 (s, 1H, N*H*), 4.90 (s, 2H, NH_2), 4.06 (q, ^3J = 7.2 Hz, 2H, H12), 3.94 (t, ^3J = 7.2 Hz, 2H, H9), 2.56 (t, ^3J = 7.2 Hz, 2H, H10), 1.53 (s, 9H, H1), 1.21 (t, ^3J = 7.1 Hz, 3H, H13).

^{13}C NMR: (125 MHz, $CDCl_3$) δ [ppm] = 171.8 (C11); 158.7 (C8); 138.5 (C7); 135.9 (C4); 129.2 (C5); 120.0 (C6); 81.1 (C2); 60.7 (C12); 45.6 (C9); 33.7 (C10); 28.4 (C1); 14.3 (C13).
Note: C2 was detected in the HSQC, C3 was not detected.

6.2.2.12 Synthesis of 65

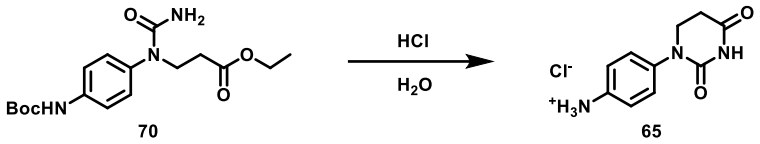

70 65

This experiment was carried out by *Rafael Claßen*. According to a modified procedure by *Norris et al*.[198]: In a 25 mL round bottom flask, 560 mg (1.61 mmol; 1.00 eq.) of intermediate **70** were suspended in 4 mL of HCl (conc.) and the mixture was stirred at room temperature until full conversion of intermediate **70** was observed by TLC after 16 h. The solvent was removed under reduced pressure; the residue was washed with MeCN and dried under reduced pressure to obtain 260 mg (1.07 mmol; 67%) of the desired product **65** as a pink solid.

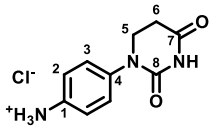

M ($C_{10}H_{12}N_3O_2Cl$):	241.67 g/mol.
Yield:	260 mg (1.07 mmol; 67%; Lit.[198]: 86%).
R_f:	(SiO_2, *c*Hex/EtOAc 1:1) = 0.0.
^{1}H NMR:	(500 MHz, DMSO-d_6) δ [ppm] = 10.43 (s, 1H, N*H*), 10.17 (s, 1H, NH_3^+), 7.42 (d, ^3J = 8.8 Hz, 2H, H2), 7.36 (d, ^3J = 8.8 Hz, 2H, H3), 3.79 (t, ^3J = 6.5 Hz, 2H, H5), 3.74 (s, 2H, NH_3^+), 2.71 (t, ^3J = 6.7 Hz, 2H, H6).
^{13}C NMR:	(125 MHz, DMSO-d_6) δ [ppm] = 170.6 (C7); 152.2 (C8); 141.1 (C4); 130.0 (C1); 126.4 (C2); 123.0 (C3); 44.4 (C5); 31.0 (C6).

6.2.2.13 Synthesis of 71

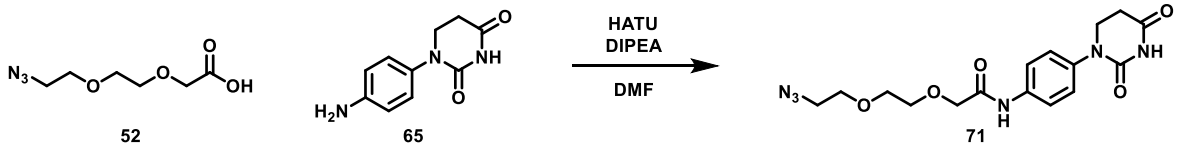

52 65 71

This experiment was carried out by *Rafael Claßen*. In a 50 mL *Schlenk* flask, 88 mg (0.47 mmol; 1.2 eq.) of linker **52** were dissolved in 8 mL of DMF and 90 μL (0.53 mmol; 1.3 eq.) of DIPEA. Next, 222 mg (0.59 mmol; 1.50 eq.) of HATU were added, and the mixture was stirred at room temperature. In a 25 mL *Schlenk* flask, 80 mg (0.39 mmol; 1.0 eq.) of recruiter **65** were dissolved in 8 mL of DMF and 160 μL (0.92 mmol; 2.35 eq.) of DIPEA. After 30 min, the mixture was added to the solution of linker **52**, and the mixture was stirred at room temperature until full conversion of recruiter **65** was observed by TLC after 18 h. The solvent was removed under reduced pressure, and the crude product was purified by column chromatography (SiO_2, dryload, *c*Hex/EtOAc 5:1 to 1:2) to obtain 135 mg (360 μmol; 92%) of the desired product **71** as a colorless solid.

M ($C_{16}H_{20}N_6O_5$): 376.37 g/mol.

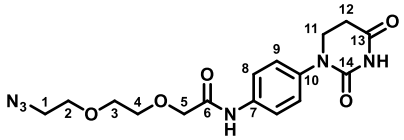

Yield: 135 mg (360 μmol; 92%).

R_f: (SiO_2, *c*Hex/EtOAc/MeOH, 3:3:1) = 0.31.

^{1}H NMR: (500 MHz, $CDCl_3$) δ [ppm] = 10.34 (s, 1H, N*H*), 9.67 (s, 1H, N*H*), 7.64 (d, ^3J = 8.8 Hz, 2H, H8), 7.27 (d, ^3J = 8.8 Hz, 2H, H9), 4.10 (s, 2H, H5), 3.75 (t, ^3J = 6.7 Hz, 2H, H11), 3.70-3.64 (m, 6H, H2, H3, H4), 3.42 (t, ^3J = 4.9 Hz, 2H, H1), 2.70 (t, ^3J = 6.7 Hz, 2H, H12).

^{13}C NMR: (125 MHz, $CDCl_3$) δ [ppm] = 170.6 (C13); 168.2 (C6); 152.2 (C14); 137.4, 136.0 (C7, C10); 125.6 (C9); 119.8 (C8); 70.3, 70.2, 69.4, 69.2 (C2, C3, C4, C5); 49.9 (C1); 45.7 (C11); 31.0 (C12).

HR-MS (ESI):

Ion	Calc. mass [u]	Exp. mass [u]	Δ [ppm]
$[M+H]^+$	377.15679	377.15713	+0.90
$[M+Na]^+$	399.13874	399.13897	+0.57

6.2.2.14 Synthesis of 66

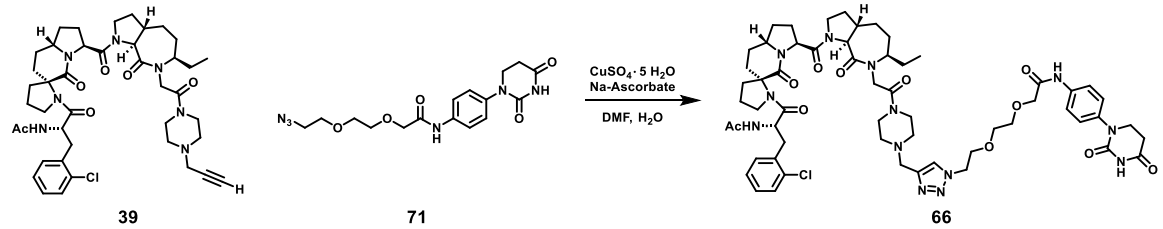

39 71 66

According to a modified procedure by *Banerjee et al*.[196]: In a headspace vial, 22 mg (29 μmol; 1.0 eq.) of warhead-linker conjugate **39** and 17 mg (44 μmol; 1.5 eq.) of the linker-recruiter conjugate **71** were dissolved in 2 mL of DMF. Next, 1 mL of an aqueous solution (3mM; 3 μmol; 10 mol%) of $CuSO_4$ and 1 mL of an aqueous solution (6mM; 6 μmol; 20 mol%) of sodium ascorbate were added. The mixture was stirred at room temperature until full conversion of warhead-linker conjugate **39** was observed by TLC after 19 h. The solvent was removed under reduced pressure and the crude product was purified by column chromatography (SiO_2, dryload, EtOAc/MeOH/NEt_3 1:0:0 to 20:4:1). The solvent was removed under reduced pressure, the residue was dissolved in CH_2Cl_2, filtered through a syringe filter and the solvent was removed under reduced pressure. The residue was then purified by reverse phase column chromatography (MeCN/H_2O 2:8 to 7:3) and lyophilized to obtain 22 mg (19 μmol; 64%) of the desired product **66** as a colorless lyophilizate.

M ($C_{58}H_{76}N_{13}O_{11}Cl$):	1166.78 g/mol.			
Yield:	22 mg (19 μmol; 64%).			
R_f:	(SiO_2, EtOAc/MeOH/NEt_3, 20:4:1) = 0.03.			
HR-MS (ESI):	Ion	Calc. mass [u]	Exp. mass [u]	Δ [ppm]
	$[M+H]^+$	1166.55485	1166.55622	+1.17
	$[M+Na]^+$	1188.53680	1188.53634	-0.39
LC-MS (ESI):	t_r [min]		9.62-10.06	
	Ion	Calc. mass [u]	Exp. mass [u]	Purity [%]
	$[M+H]^+$	1166.55	1166.79	94

6.2.3 Synthesis towards PROTACs 109-112

6.2.3.1 Synthesis of 72

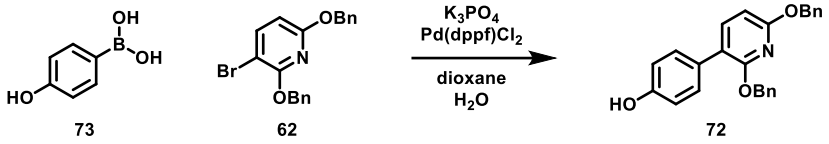

This experiment was carried out by *Alexander Klingert*. According to a modified procedure by *Nishiguchi et al*.[199]: In a 100 mL *Schlenk* flask, 3.51 g (25.5 mmol; 2.00 eq.) of boronic acid **73**, 4.72 g (12.7 mmol; 1.00 eq.) of aryl bromide **62**, 5.80 g (27.4 mmol; 2.15 eq.) of K_3PO_4, and 0.84 g (1.02 mmol; 8 mol%) of $Pd(dppf)Cl_2$ were dissolved in a degassed mixture of 30 mL of dioxane and 5 mL of H_2O and heated to 120 °C. Full conversion was observed by TLC after 24 h and the mixture was filtered through a celite pad. The mixture was washed with 50 mL of NaCl solution, dried over Na_2SO_4, filtered, and the solvent was removed under reduced pressure. The crude mixture was purified by column chromatography (SiO_2, *c*Hex/EtOAc 10:1 to 5:1) to obtain 4.80 g (12.1 mmol; 98%; 95 wt%) of the desired product **72** as a colorless solid.

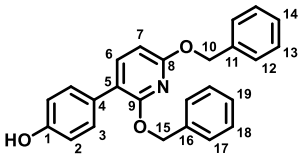

M ($C_{25}H_{21}NO_3$):	383.45 g/mol.
Yield:	4.80 g (12.1 mmol; 98%; 95 wt%, Lit.[199]: 82%).
R_f:	(SiO_2, *c*Hex/EtOAc 5:1) = 0.22.
^{1}H NMR:	(400 MHz, $CDCl_3$) δ [ppm] = 7.56 (d, ^3J = 8.8 Hz, 1H, H6), 7.45-7.22 (m, 12H, H3, H12, H13, H14, H17, H18, H19), 6.86-6.83 (m, 2H, H2), 6.45 (d, ^3J = 8.1 Hz, 1H, H7), 5.41 (s, 2H, H10/H15), 5.35 (s, 2H, H10/H15), 4.79 (s, 1H, O*H*).
^{13}C NMR:	(100 MHz, $CDCl_3$) δ [ppm] = 161.1 (C9); 158.3 (C8); 154.5 (C1); 141.6 (C6); 138.1, 137.7 (C11, C16); 130.4 (C3); 129.8, 128.6, 128.5, 127.9, 127.9, 127.6, 127.3 (C2, C12, C13, C14, C17, C18, C19); 129.6 (C4); 120.9 (C7); 115.8 (C5); 68.0, 67.7 (C10 and C15).

FT-IR: (ATR) ῡ [cm^{-1}] = 3249 (m), 3091 (w), 3061 (w), 3031 (w), 2933 (w), 2879 (w), 2712 (w), 2534 (w), 2451 (w), 2351 (w), 2339 (w), 2323 (w), 2287 (w), 2198 (w), 2178 (w), 2168 (w), 2116 (w), 2077 (w), 2051 (w), 1995 (w), 1980 (w), 1960 (w), 1933 (w), 1892 (w), 1823 (w), 1767 (w), 1715 (w), 1662 (w), 1596 (s), 1574 (m), 1515 (m), 1498 (m), 1470 (m), 1455 (m), 1446 (s), 1401 (m), 1383 (m), 1355 (s), 1307 (s), 1287 (m), 1239 (s), 1228 (s), 1204 (s), 1175 (s), 1115 (m), 1106 (m), 1080 (m), 1046 (m), 1029 (m), 1003 (s), 997 (s), 957 (m), 911 (m), 887 (m), 841 (m), 826 (s), 811 (m), 765 (m), 747 (s), 739 (s), 719 (m), 696 (s), 647 (m), 627 (m), 620 (m), 603 (s), 595 (s), 557 (m), 539 (s), 532 (s), 504 (m).

6.2.3.2 Synthesis of 98

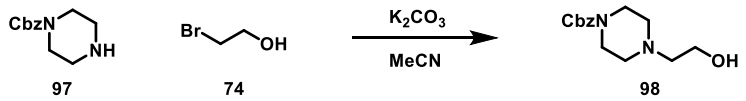

97 74 98

This experiment was carried out by *Alexander Klingert*. According to a modified procedure by *Brown et al*.[218]: In a 50 mL round bottom flask, 1.50 g (6.81 mmol; 1.00 eq.) of piperazine **97** and 2.80 g (20.4 mmol; 3.00 eq.) of K_2CO_3 were dissolved in 20 mL of MeCN. Next, 1.28 g (10.2 mmol; 1.50 eq.) of bromoethanol (**74**) were added and the mixture was heated to 90 °C until full conversion of piperazine **97** was observed by TLC after 19 h. The mixture was filtered, and the solvent was removed under reduced pressure and the crude product was purified by column chromatography (SiO_2, EtOAc/MeOH 9:1) to obtain 1.29 g (4.53 mmol; 66%; 93 wt%) of the desired product **98** as a yellow oil.

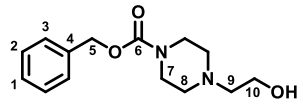

M ($C_{14}H_{20}N_2O_3$): 264.32 g/mol.

Yield: 1.29 g (4.53 mmol; 66%; 93 wt%).

R_f: (SiO_2, EtOAc/MeOH 9:1) = 0.30.

^{1}H NMR: (400 MHz, $CDCl_3$) δ [ppm] = 7.37-7.29 (m, 5H, H1, H2, H3), 5.14 (s, 2H, H5), 3.63 (t, ^3J = 5.4 Hz, 2H, H10), 3.53 (t, ^3J = 5.0 Hz, 4H, H7), 2.56 (t, ^3J = 5.4 Hz, 2H, H9), 2.48 (s, 4H, H8).

^{13}C NMR: (100 MHz, $CDCl_3$) δ [ppm] = 155.3 (C6); 136.8 (C4); 128.7, 128.1 (C2, C3); 128.2 (C1); 67.3 (C5), 59.5 (C9), 57.9 (C10), 52.8 (C8), 44.0 (C7).

FT-IR: (ATR) $\bar{\upsilon}$ [cm^{-1}] = 3425 (w), 3090 (w), 3065 (w), 3033 (w), 2942 (w), 2868 (w), 2814 (w), 2343 (w), 2216 (w), 2084 (w), 1951 (w), 1871 (w), 1697 (s), 1608 (w), 1587 (w), 1525 (w), 1498 (w), 1455 (m), 1428 (s), 1362 (m), 1334 (w), 1303 (m), 1288 (m), 1234 (s), 1125 (s), 1076 (m), 1053 (m), 1026 (m), 1002 (m), 969 (m), 940 (w), 921 (w), 873 (w), 793 (w), 762 (m), 754 (m), 735 (m), 697 (s), 641 (w), 604 (m), 580 (m), 556 (m).

LC-MS (ESI):

t_r [min]		6.82-7.65
Ion	Calc. mass [u]	Exp. mass [u]
$[M+H]^+$	265.32	265.18

6.2.3.3 Synthesis of 93

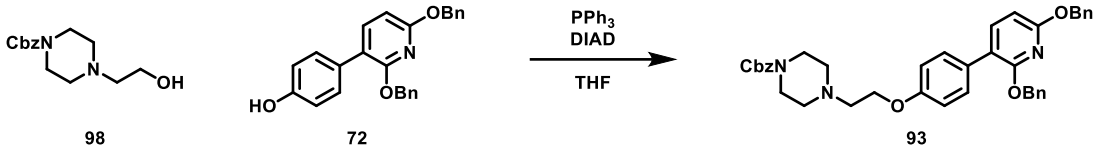

This experiment was carried out by *Alexander Klingert*. According to a modified procedure by *Roy et al*.[219]: In a 25 mL *Schlenk* flask, 180 mg (0.48 mmol; 1.00 eq.) of recruiter **72**, 200 mg (760 μmol; 1.60 eq.) of linker **98**, and 180 mg (0.71 mmol; 1.50 eq.) of triphenylphosphine were dissolved in 6.5 mL of THF. The mixture was cooled to 0 °C and 0.15 mL (0.76 mmol; 1.60 eq.) of DIAD were added. The mixture was stirred at room temperature until full conversion of recruiter **72** was observed by TLC after 16 h. The solvent was removed under reduced pressure. The crude mixture was purified by column chromatography (SiO_2, *c*Hex/EtOAc 9:1 to 1:1) to obtain 0.25 g (0.40 mmol; 83%) of the desired product **93** as a colorless oil.

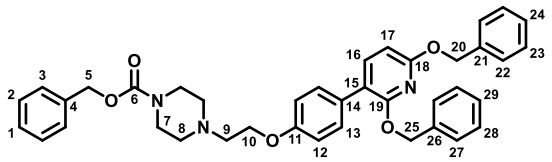

M ($C_{39}H_{39}N_3O_5$): 629.76 g/mol.

Yield: 0.25 g (0.40 mmol; 83%).

R_f: (SiO_2, *c*Hex/EtOAc 1:1) = 0.23.

^{1}H NMR: (400 MHz, $CDCl_3$) δ [ppm] = 7.57 (d, ^3J = 8.1 Hz, 1H, H16), 7.48 (d, ^3J = 8.6 Hz, 2H, H13), 7.43-7.27 (m, 15H, H1, H2, H3, H22, H23, H24, H27, H28, H29), 6.92 (d, ^3J = 8.9 Hz, 2H, H12), 6.46 (d, ^3J = 8.1 Hz, 1H, H17), 5.42 (s, 2H, H20/H25), 5.35 (s, 2H, H20/H25), 5.14 (s, 2H, H5), 4.13 (t, ^3J = 5.6 Hz, 2H, H10), 3.55 (t, ^3J = 4.9 Hz, 4H, H7), 2.84 (t, ^3J = 8.8 Hz, 2H, H9), 2.56 (s, 4H, H8).

^{13}C NMR: (100 MHz, $CDCl_3$) δ [ppm] = 161.1, 158.3 (C18, C19); 157.7 (C11); 155.4 (C6); 141.6 (C16); 138.1, 137.8 (C21, C26); 136.9 (C4); 130.2 (C13); 129.6 (C14); 129.6, 128.6, 128.6, 128.5, 128.2, 128.1, 127.9, 127.6, 127.4 (C1, C2, C3, C21, C22, C23, C24, C27, C28, C29); 115.8 (C15); 114.4 (C12); 102.5 (C17); 68.0, 67.7 (C20, C25); 67.3 (C5); 66.0 (C10); 60.5, 57.4 (C9); 53.4 (C8); 43.9 (C7).

FT-IR: (ATR) ῡ [cm^{-1}] = 3427 (w), 3066 (w), 3032 (w), 2959 (w), 2928 (m), 2873 (w), 2860 (w), 2388 (w), 2080 (w), 1944 (w), 1719 (s), 1598 (w), 1582 (w), 1516 (w), 1505 (w), 1460 (m), 1408 (w), 1380 (w), 1357 (w), 1338 (w), 1303 (w), 1266 (s), 1247 (s), 1173 (w), 1115 (s), 1101 (s), 1051 (w), 1019 (m), 979 (w), 959 (w), 909 (w), 874 (w), 835 (w), 810 (w), 795 (w), 767 (w), 729 (s), 696 (w), 647 (w), 632 (w), 599 (w).

HR-MS (ESI):

Ion	Calc. mass [u]	Exp. mass [u]	Δ [ppm]
$[M+H]^+$	630.29625	630.29636	+0.19
$[M+Na]^+$	652.27819	652.27841	+0.33

6.2.3.4 Synthesis of 105

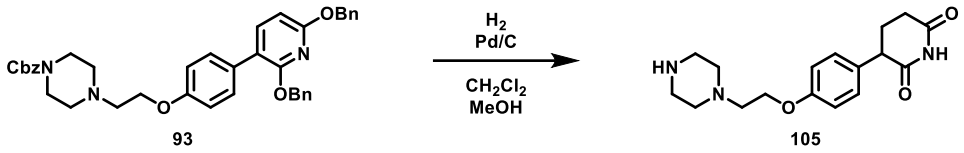

According to a modified procedure by *Lei et al*.[220]: In a 25 mL *Schlenk* flask, 160 mg (237 μmol; 1.00 eq.) of linker-recruiter conjugate **93** were dissolved in 2 mL of MeOH and 2 mL of CH_2Cl_2. Next, 33 mg (20 wt%) of Pd/C were added and the flask was purged with hydrogen gas. After 16 h, full conversion of **93** was observed by TLC and the solvent was removed under reduced pressure. The crude mixture was purified by column chromatography (dryload, SiO_2, EtOAc/MeOH/NEt_3 1:0:0 to 20:4:1). The crude product was dissolved in CH_2Cl_2, filtered through a syringe filter. The solvent was removed under reduced pressure to obtain 35 mg (110 μmol; 46%) of the desired product **105** as a yellow oil.

M ($C_{17}H_{23}N_3O_3$): 317.39 g/mol.

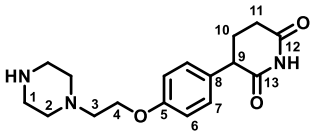

Yield: 35 mg (0.11 mmol; 46%).

R_f: (SiO_2, EtOAc /MeOH/NEt_3 20:4:1) = 0.07.

^{1}H NMR: (400 MHz, $CDCl_3$) δ [ppm] = 7.13 (d, ^3J = 8.8 Hz, 2H, H7), 6.91 (d, ^3J = 8.8 Hz, 2H, H6), 4.10 (t, ^3J = 5.5 Hz, 2H, H4), 3.73 (dd, ^3J = 9.7 Hz, ^3J = 5.3 Hz, 1H, H9), 3.08 (t, ^3J = 4.7 Hz, 4H, H1), 2.85 (t, ^3J = 10.5 Hz, 2H, H3), 2.77-2.71 (m, 4H, H2), 2.68-2.57 (m, 2H, H11), 2.31-2.15 (m, 2H, H10).

^{13}C NMR: (100 MHz, $CDCl_3$) δ [ppm] = 173.7 (C13); 172.6 (C12); 158.2 (C5); 129.6 (C8); 129.3 (C7); 115.1 (C6); 66.0 (C4); 57.3 (C3); 52.4 (C2); 47.3 (C9); 44.5 (C1); 31.1 (C11); 26.5 (C10).

FT-IR: (ATR) $\bar{\upsilon}$ [cm^{-1}] = 3429 (w), 3067 (w), 2943 (w), 2828 (w), 2251 (w), 2126 (w), 1997 (w), 1704 (w), 1679 (w), 1612 (w), 1582 (w), 1513 (w), 1461 (w), 1441 (w), 1357 (w), 1323 (w), 1299 (w), 1235 (w), 1190 (w), 1117 (w), 1052 (s), 1024 (s), 1005 (s), 821 (m), 759 (m), 723 (w), 697 (w), 683 (w), 623 (m), 614 (m), 594 (m), 542 (m).

HR-MS (ESI):

Ion	Calc. mass [u]	Exp. mass [u]	Δ [ppm]
$[M+H]^+$	318.18122	318.18162	+1.26

6.2.3.5 Synthesis of 109

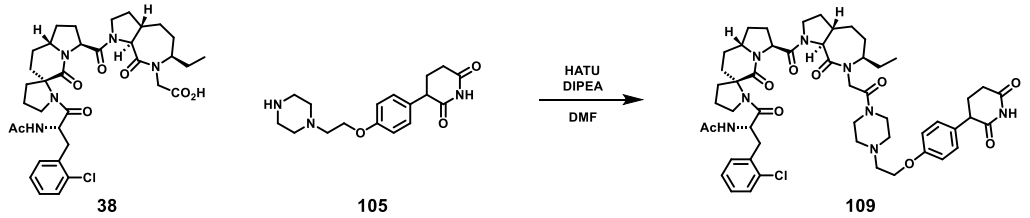

38 105 109

In a 25 mL *Schlenk* flask, 30 mg (44 μmol; 1.0 eq.) of warhead **38**, 22 mg (57 μmol; 1.3 eq.) of HATU and 19 μL (110 μmol; 2.5 eq.) of DIPEA were added in 1.8 mL of DMF. In a 10 mL *Schlenk* flask, 14 mg (44 μmol; 1.0 eq.) of linker-recruiter conjugate **105** were dissolved in 1.8 mL of DMF. After 30 min, the mixture was added to the solution of warhead **38**, and the mixture was stirred at room temperature until full conversion of warhead **38** was observed by TLC after 17 h. The solvent was removed under reduced pressure and the crude product was purified by column chromatography (dryload, SiO_2, EtOAc/MeOH/NEt_3 1:0:0 to 20:4:1). The residue was dissolved in CH_2Cl_2, filtered through a syringe filter, and the solvent was removed under reduced pressure. The residue was purified by reverse phase column chromatography (MeCN/H_2O 2:8 to 7:3) and lyophilized to obtain 8.0 mg (8.1 μmol; 18%) of the desired product **109** as a colorless lyophilizate.

M ($C_{52}H_{67}N_8O_9Cl$):	983.60 g/mol.			
Yield:	8.0 mg (8.1 μmol; 18%).			
R_f:	(SiO_2, EtOAc/MeOH/NEt_3 20:4:1) = 0.21.			
HR-MS (ESI):	Ion	Calc. mass [u]	Exp. mass [u]	Δ [ppm]
	$[M+H]^+$	983.47923	983.48017	+0.95
	$[M+Na]^+$	1005.46117	1005.46054	-0.63
HPLC:	t_r [min]		8.11-8.37	
	Purity [%]		92	

6.2.3.6 Synthesis of 99

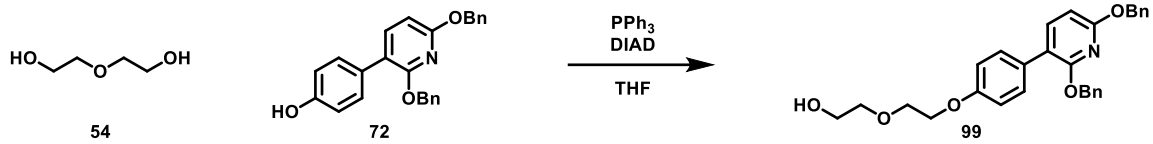

This experiment was carried out by *Alexander Klingert*. According to a modified procedure by *Roy et al*.[219]: In a 25 mL *Schlenk* flask, 400 mg (1.04 mmol; 1.00 eq.) of recruiter **72**, 770 mg (7.28 mmol; 7.00 eq.) of diethylene glycol (**54**), and 410 mg (1.56 mmol; 1.50 eq.) of triphenylphosphine were dissolved in 8.5 mL of THF. The mixture was cooled to 0 °C and 330 µL (1.67 mmol; 1.50 eq.) of DIAD were added. The mixture was stirred at room temperature until full conversion of recruiter **72** was observed by TLC after 20 h. The solvent was removed under reduced pressure and the residue was purified by column chromatography (SiO_2, *c*Hex/EtOAc 3:1 to 1:1) to obtain 0.28 g (0.58 mmol; 56%; 98 wt%) of the desired product **99** as a pale-yellow solid.

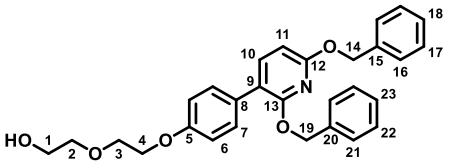

M ($C_{29}H_{29}NO_5$): 471.55 g/mol.

Yield: 0.28 g (0.58 mmol; 56%; 98 wt%).

R_f: (SiO_2, *c*Hex/EtOAc 1:1) = 0.26.

^{1}H NMR: (400 MHz, $CDCl_3$) δ [ppm] = 7.57 (d, ^3J = 8.1 Hz, 1H, H10), 7.49 (d, ^3J = 8.8 Hz, 2H, H7), 7.44-7.27 (m, 10H, H16, H17, H18, H21, H22, H23), 6.95 (d, ^3J = 8.7 Hz, 2H, H6), 6.46 (d, ^3J = 8.0 Hz, 1H, H11), 5.42 (s, 2H, H14), 5.36 (s, 2H, H19), 4.19-4.16 (m, 2H, H4), 3.89 (t, ^3J = 4.7 Hz, 2H, H3), 3.80-3.74 (m, 2H, H1), 3.70-3.68 (m, 2H, H2).

^{13}C NMR: (100 MHz, $CDCl_3$) δ [ppm] = 161.1 (C13); 158.4 (C12); 157.7 (C5); 141.6 (C10); 138.4 (C15); 137.8 (C20); 130.2 (C7); 129.6 (C8); 129.7, 128.6, 128.5, 127.9, 127.6, 127.4 (C16, C17, C18, C21, C22, C23); 115.7 (C9); 114.4 (C6); 102.5 (C11); 72.4 (C2); 69.9 (C3); 68.0 (C14); 67.7 (C19); 67.6 (C4); 62.0 (C1).

FT-IR: (ATR) ū [cm^{-1}] = 3353 (w), 3111 (w), 3091 (w), 3063 (w), 3034 (w), 2963 (w), 2933 (w), 2892 (w), 2719 (w), 2527 (w), 2324 (w), 2163 (w), 2141 (w), 2115 (w), 2063 (w), 1958 (w), 1920 (w), 1892 (w), 1816 (w), 1741 (w), 1594 (s), 1582 (m), 1568 (m), 1515 (m), 1498 (w), 1485 (w), 1470 (m), 1446 (s), 1424 (m), 1398 (m), 1377 (w), 1351 (s), 1305 (s), 1284 (s), 1243 (s), 1224 (s), 1216 (s), 1180 (m), 1136 (s), 1124 (s), 1109 (s), 1083 (m), 1055 (s), 1046 (s), 1027 (s), 1017 (m), 1002 (s), 941 (m), 929 (m), 889 (m), 839 (s), 820 (s), 814 (s), 767 (m), 754 (m), 734 (s), 696 (s), 630 (s), 616 (s), 594 (s), 562 (m), 537 (m), 502 (m).

HR-MS (ESI):

Ion	Calc. mass [u]	Exp. mass [u]	Δ [ppm]
$[M+H]^+$	472.21184	472.21229	+0.93
$[M+Na]^+$	494.19379	494.19349	-0.62

6.2.3.7 Synthesis of 102

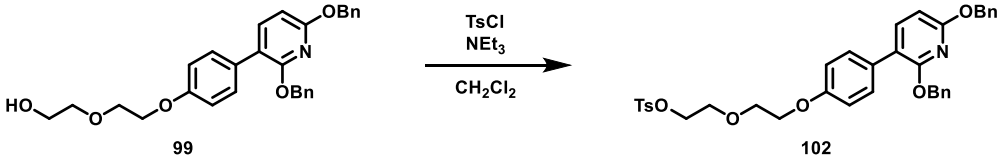

This experiment was carried out by *Alexander Klingert*. According to a modified procedure by *Li et al*.[194]: In a 10 mL round bottom flask, 274 mg (580 μmol; 1.00 eq.) of linker-recruiter conjugate **99**, 80 μL (0.64 mmol; 1.1 eq.) of NEt_3, and 330 mg (1.74 mmol; 3.00 eq.) of TsCl were added to 3 mL of CH_2Cl_2. The mixture was stirred at room temperature until full conversion of linker-recruiter conjugate **99** was observed by TLC after 22 h. The reaction mixture was diluted with 20 mL of CH_2Cl_2 and 0.2 mL of HCl (1M) were added. The layers were separated, and the aqueous phase was extracted with 20 mL of CH_2Cl_2 two times. The combined organic layers were dried over $MgSO_4$, filtered, and the solvent was removed under reduced pressure. The crude mixture was purified by column chromatography (SiO_2, *c*Hex/EtOAc 1:1) to obtain 257 mg (430 μmol; 74%; 95 wt%) of the desired product **102** as a colorless oil.

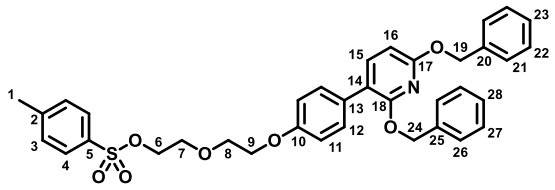

M ($C_{36}H_{35}NO_7S$): 625.74 g/mol.

Yield: 257 mg (430 μmol; 74%; 95 wt%).

R_f: (SiO_2, *c*Hex/EtOAc 3:1) = 0.32.

^{1}H NMR: (400 MHz, $CDCl_3$) δ [ppm] = 7.79 (d, ^3J = 8.3 Hz, 2H, H4), 7.57 (d, ^3J = 8.0 Hz, 1H, H15), 7.48 (d, ^3J = 8.8 Hz, 2H, H12), 7.44-7.42 (m, 2H, H3), 7.38-7.27 (m, 10H, H21, H22, H23, H26, H27, H28), 6.90 (d, ^3J = 8.8 Hz, 2H, H11), 6.46 (d, ^3J = 8.0 Hz, 1H, H16), 5.42 (s, 2H, H19), 5.36 (s, 2H, H24), 4.21-4.18 (m, 2H, H6), 4.07-4.05 (m, 2H, H9), 3.80-3.75 (m, 4H, H7, H8), 2.38 (s, 3H, H1).

^{13}C NMR: (100 MHz, $CDCl_3$) δ [ppm] = 161.1 (C18); 158.4 (C17); 157.7 (C10); 144.9 (C2); 141.6 (C15); 138.1 (C25); 137.8 (C20); 130.2 (C12); 129.9 (C3); 129.7 (C13); 129.6 (C5); 128.1 (C4); 128.6, 128.5, 127.9, 127.6, 127.4 (C21, C22, C23, C26, C27, C28); 115.8 (C14); 114.4 (C11); 102.5 (C16); 70.1 (C7/C8); 69.4 (C6); 69.0 (C7/C8); 68.0 (C24); 67.7 (C19); 67.5 (C9); 21.7 (C1).

FT-IR: (ATR) ῡ [cm^{-1}] = 3656 (w), 3089 (w), 3064 (w), 3032 (w), 2927 (w), 2878 (w), 2587 (w), 2525 (w), 2328 (w), 2075 (w), 1920 (w), 1884 (w), 1809 (w), 1739 (w), 1596 (m), 1583 (m), 1569 (w), 1516 (w), 1496 (w), 1470 (m), 1447 (s), 1425 (w), 1399 (m), 1354 (s), 1306 (m), 1291 (m), 1244 (s), 1220 (m), 1189 (m), 1174 (s), 1137 (m), 1108 (m), 1097 (m), 1064 (m), 1047 (m), 1011 (s), 1001 (s), 914 (s), 836 (m), 811 (s), 769 (m), 756 (s), 735 (s), 695 (s), 662 (s), 629 (m), 596 (w), 582 (m), 553 (s), 510 (m).

HR-MS (ESI):

Ion	Calc. mass [u]	Exp. mass [u]	Δ [ppm]
$[M+H]^+$	626.22069	626.22075	+0.08
$[M+Na]^+$	648.20264	648.20250	-0.23

6.2.3.8 Synthesis of 94

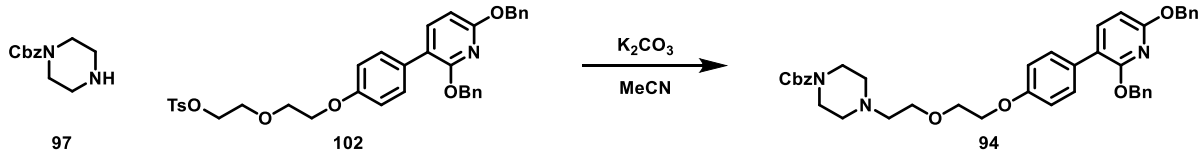

According to a modified procedure by *Brown et al*.[218]: In a 50 mL round bottom flask, 124 mg (563 μmol; 1.60 eq.) of piperazine **97**, 239 mg (355 μmol; 1.00 eq.) of tosylate **102**, and 155 mg (1.12 mmol; 3.20 eq.) of K_2CO_3 were dissolved in 6.2 mL of MeCN. The mixture was heated to 90 °C until full conversion of tosylate **102** was observed by TLC after 20 h. After cooling to room temperature, 20 mL of EtOAc and 4 mL of H_2O were added. The layers were separated, and the aqueous phase was extracted with 20 mL of EtOAc two times. The combined organic layers were washed with NaCl solution, dried over $MgSO_4$, filtered, and the solvent was removed under reduced pressure to obtain 272 mg (341 μmol; 96%, 84 wt%) of the desired product **94** as a yellow oil.

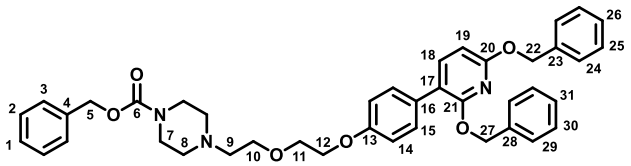

M ($C_{41}H_{43}N_3O_6$): 673.81 g/mol.

Yield: 272 mg (341 μmol; 96%, 84 wt%).

R_f: (SiO_2, *c*Hex/EtOAc 1:1) = 0.08.

^{1}H NMR: (400 MHz, $CDCl_3$) δ [ppm] = 7.56 (d, ^3J = 8.0 Hz, 1H, H18), 7.46 (d, ^3J = 8.8 Hz, 2H, H15), 7.44-7.28 (m, 15H, H1, H2, H3, H24, H25, H26, H29, H30, H31), 6.92 (d, ^3J = 8.7 Hz, 2H, H14), 6.45 (d, ^3J = 8.1 Hz, 1H, H19), 5.41 (s, 2H, H22), 5.35 (s, 2H, H27), 5.12 (s, 2H, H5), 4.16-4.09 (m, 2H, H12), 3.83 (t, ^3J = 4.8 Hz, 2H, H11), 3.71 (s, 2H, H10), 3.53 (s, 4H, H8), 2.64 (s, 2H, H9), 2.49 (s, 4H, H7).

^{13}C NMR: (100 MHz, $CDCl_3$) δ [ppm] = 161.1 (C21); 158.4 (C20); 157.8 (C13); 155.4 (C6); 141.6 (C18); 138.1 (C23); 137.8 (C28); 136.9 (C4); 130.2 (C15); 129.4 (C16); 128.6, 128.5, 128.1, 128.0, 128.0, 127.9, 127.7, 127.5, 127.3 (C1, C2, C3, C24, C25, C26, C29, C30, C31); 115.8 (C17); 114.4 (C14); 102.5 (C19); 69.7 (C11); 69.2 (C9 or C10); 68.0

(C27); 67.7 (C12); 67.6 (C22); 67.2 (C5); 58.0 (C9 or C10); 53.4 (C7); 43.9 (C8).

FT-IR: (ATR) ῡ [cm^{-1}] = 3656 (w), 3089 (w), 3064 (w), 3032 (w), 2927 (w), 2878 (w), 2587 (w), 2525 (w), 2328 (w), 2075 (w), 1920 (w), 1884 (w), 1809 (w), 1739 (s), 1596 (m), 1583 (m), 1569 (w), 1516 (w), 1496 (w), 1470 (m), 1447 (s), 1425 (m), 1399 (m), 1354 (m), 1306 (m), 1291 (m), 1244 (s), 1220 (m), 1189 (m), 1174 (s), 1137 (m), 1108 (m), 1097 (m), 1064 (s), 1047 (w), 1011 (w), 1001 (m), 914 (m), 836 (m), 811 (m), 769 (s), 756 (m), 735 (w), 695 (w), 662 (w), 629 (w), 596 (m), 582 (m), 553 (w), 510 (s).

HR-MS (ESI):

Ion	Calc. mass [u]	Exp. mass [u]	Δ [ppm]
$[M+H]^+$	674.32246	674.32211	-0.53
$[M+Na]^+$	696.30440	696.30323	-1.70

6.2.3.9 Synthesis of 106

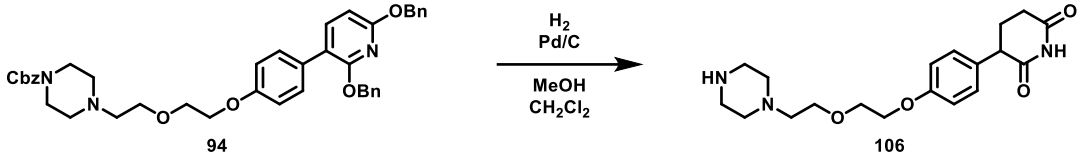

According to a modified procedure by *Lei et al*.[220]: In a 25 mL *Schlenk* flask, 24 mg (36 μmol; 1.0 eq.) of the linker-recruiter conjugate **94** were dissolved in 1 mL of MeOH and 1 mL of CH_2Cl_2. Next, 24 mg (100 wt%) of Pd/C were added and the flask was purged with hydrogen gas. After 16 h, the mixture was centrifuged, decanted, and the solvent was removed under reduced pressure to obtain 12 mg (33 μmol; 90%) of the desired product **106** as a yellow oil.

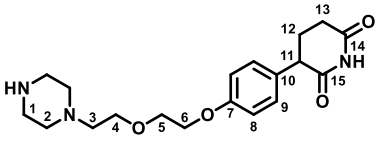

M ($C_{19}H_{27}N_3O_4$):	361.44 g/mol.			
Yield:	12 mg (33 μmol; 90%).			
HR-MS (ESI):	Ion	Calc. mass [u]	Exp. mass [u]	Δ [ppm]
	$[M+H]^+$	362.20743	362.20772	+0.80
LC-MS (ESI):	t_r [min]		2.77-3.09	
	Ion	Calc. mass [u]	Exp. mass [u]	
	$[M+H]^+$	362.21	362.28	

The product was used without further characterization.

6.2.3.10 Synthesis of 110

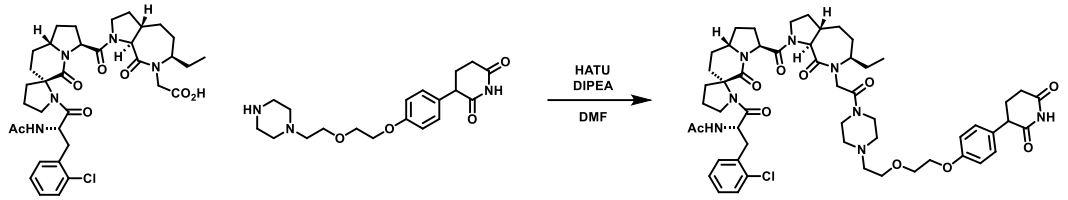

38 106 110

In a 10 mL *Schlenk* flask, 23 mg (33 μmol; 1.0 eq.) of warhead **38**, 16 mg (43 μmol; 1.3 eq.) of HATU and 10.1 μL (116 μmol; 1.75 eq.) of DIPEA were added in 0.6 mL of DMF. In a 10 mL *Schlenk* flask, 12 mg (33 μmol; 1.0 eq.) of linker-recruiter conjugate **106** were dissolved in 0.6 mL of DMF and 10.1 μL (116 μmol; 1.75 eq.) of DIPEA. After 30 min, the mixture was added to the solution of warhead **38** and the mixture was stirred at room temperature until full conversion of warhead **38** was observed by LC-MS after 24 h. The crude reaction mixture was purified by preparative HPLC and lyophilized. The residue was purified by reverse phase column chromatography ($MeCN/H_2O$ 2:8 to 7:3) and lyophilized to obtain 6.0 mg (5.8 μmol; 18%) of the desired product **110** as a colorless lyophilizate.

M ($C_{54}H_{71}N_8O_{10}Cl$):	1027.66 g/mol.			
Yield:	6.0 mg (5.8 μmol; 18%).			
R_f:	(SiO_2, EtOAc/MeOH/NEt_3 20:4:1) = 0.18.			
HR-MS (ESI):	Ion	Calc. mass [u]	Exp. mass [u]	Δ [ppm]
	$[M+H]^+$	1027.50544	1027.50512	-0.32
	$[M+Na]^+$	1049.48739	1049.48488	-2.39
LC-MS (ESI):	t_r [min]		8.19-8.57, 10.23-11.79	
	Ion	Calc. mass [u]	Exp. mass [u]	
	$[M+H]^+$	1027.50	1027.78	

6.2.3.11 Synthesis of 100

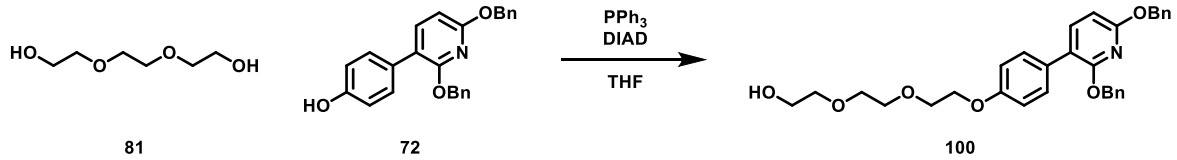

81 72 100

According to a modified procedure by *Roy et al*.[219]: In a 25 mL *Schlenk* flask, 400 mg (1.04 mmol; 1.00 eq.) of recruiter **72**, 1.09 g (7.28 mmol; 7.00 eq.) of triethylene glycol (**81**), and 410 mg (1.56 mmol; 1.50 eq.) of triphenylphosphine were dissolved in 8.5 mL of THF. The mixture was cooled to 0 °C and 330 μL (1.67 mmol; 1.50 eq.) of DIAD were added. The mixture was stirred at room temperature until full conversion of recruiter **72** was observed by TLC after 18 h. The solvent was removed under reduced pressure and the crude mixture was purified by column chromatography (SiO_2, *c*Hex/EtOAc 1:1) to obtain 340 mg (650 μmol; 63%; 55 wt%) of the desired product **100** as a pale-yellow solid.

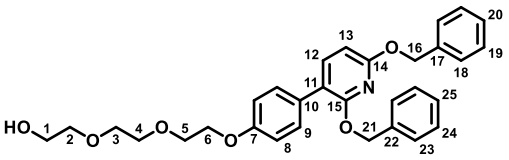

M ($C_{31}H_{33}NO_6$): 515.606 g/mol.

Yield: 0.34 g (0.65 mmol; 63%; 55 wt%).

R_f: (SiO_2, EtOAc) = 0.31.

^{1}H NMR: (400 MHz, $CDCl_3$) δ [ppm] = 7.57-7.56 (m, 1H, H12), 7.45-7.43 (m, 2H, H9), 6.94 (d, ^3J = 8.8 Hz, 2H, H8), 6.45 (d, ^3J = 8.1 Hz, 1H, H13), 5.42 (s, 2H, H21), 5.35 (s, 2H, H16), 4.17 (t, ^3J = 4.8 Hz, 2H, H6), 3.88 (t, ^3J = 4.8 Hz, 2H, H5), 3.76-3.69 (m, 6H, H1, H3, H4), 3.63-3.61 (m, 2H, H2).

^{13}C NMR: (100 MHz, $CDCl_3$) δ [ppm] = 161.1 (C15); 158.3 (C14); 157.8 (C7); 141.6 (C12); 138.1 (C17); 137.8 (C22); 130.2 (C9); 129.6 (C10); 128.7, 128.6, 128.5, 127.9, 127.5, 127.3 (C18, C19, C20, C23, C24, C25); 115.8 (C11); 114.5 (C8); 102.5 (C13); 72.6 (C2); 71.0, 70.6, 69.9 (C3, C4, C5); 68.0 (C16); 67.7 (C21); 67.5 (C6); 61.9 (C1).

6.2.3.12 Synthesis of 103

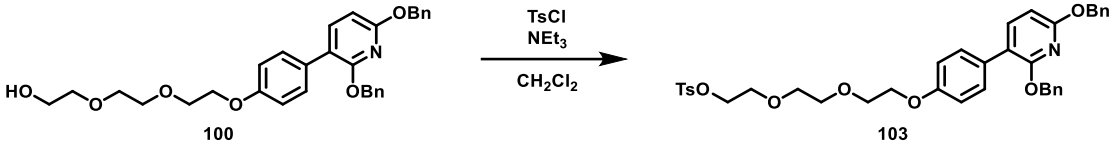

According to a modified procedure by *Li et al*.[194]: In a 10 mL round bottom flask, 318 mg (620 μmol; 1.00 eq.) of linker-recruiter conjugate **100**, 118 μL (680 μmol; 1.10 eq.) of NEt_3, and 350 mg (1.85 mmol; 3.00 eq.) of TsCl were added to 3.2 mL of CH_2Cl_2. The mixture was stirred at room temperature until full conversion of linker-recruiter conjugate **100** was observed by TLC after 20 h. The reaction mixture was diluted with 20 mL of CH_2Cl_2 and 2 mL of HCl (1M) were added. The layers were separated, and the aqueous phase was extracted with 20 mL of CH_2Cl_2 two times. The combined organic layers were dried over $MgSO_4$, filtered, and the solvent was removed under reduced pressure. The crude mixture was purified by column chromatography (SiO_2, *c*Hex/EtOAc 3:1 to 2:1) to obtain 210 mg (313 μmol; 51%) of the desired product **103** as a pale-yellow oil.

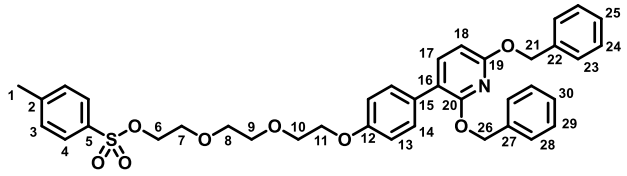

M ($C_{38}H_{39}NO_8S$): 669.79 g/mol.

Yield: 210 mg (313 μmol; 51%).

R_f: (SiO_2, *c*Hex/EtOAc 1:1) = 0.69.

^{1}H NMR: (400 MHz, $CDCl_3$) δ [ppm] = 7.82 (d, ^3J = 8.4 Hz, 2H, H4), 7.59 (d, ^3J = 8.2 Hz, 1H, H17), 7.50 (d, ^3J = 8.9 Hz, 2H, H14), 7.47-7.44 (m, 2H, H3), 7.41-7.30 (m, 10H, H23, H24, H25, H28, H29, H30), 6.95 (d, ^3J = 8.9 Hz, 2H, H11), 6.58 (d, ^3J = 8.1 Hz, 1H, H18), 5.44 (s, 2H, H21), 5.38 (s, 2H, H26), 4.20-4.12 (m, 4H, H6-H11), 3.86 (t, ^3J = 4.8 Hz, 2H, H6-H11), 3.73-3.68 (m, 4H, H6-H11), 3.65-3.63 (m, 2H, H6-H11), 2.44 (s, 3H, H1).

^{13}C NMR: (100 MHz, $CDCl_3$) δ [ppm] = 160.9 (C20); 158.2 (C19); 157.7 (C12); 144.7 (C2); 141.6 (C17); 138.0 (C22); 137.7 (C27); 130.2 (C14); 129.9 (C3); 129.7 (C15); 129.6 (C5); 128.6, 128.5, 128.1, 127.9, 127.5, 127.3 (C23, C24, C25,

C28, C29, C30); 115.6 (C16); 114.4 (C13), 102.5 (C18), 71.0, 70.9, 70.0, 69.4, 68.9 (C6, C7, C8, C9, C10, C11), 68.0 (C26), 67.7 (C21); 21.7 (C1)

Note: C20, C19, C12, C12, C22, C27, C15, C5, C16, and C1 were detected in the HSQC.

6.2.3.13 Synthesis of 95

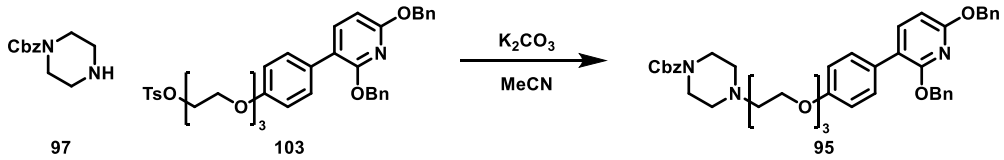

According to a modified procedure by *Brown et al*.[218]: In a 50 mL round bottom flask, 97 mg (440 μmol; 1.4 eq.) of piperazine **97**, 210 mg (313 μmol; 1.00 eq.) of tosylate **103**, and 120 mg (868 μmol; 2.80 eq.) of K_2CO_3 were dissolved in 5.4 mL of MeCN. The mixture was heated to 90 °C until full conversion of tosylate **103** was observed after 40 h by TLC. After cooling to room temperature, 20 mL of EtOAc and 4 mL of H_2O were added. The layers were separated, and the aqueous phase was extracted with 20 mL of EtOAc two times. The combined organic layers were dried over $MgSO_4$, filtered, and the solvent was removed under reduced pressure to obtain 264 mg (312 μmol; 99%; 85 wt%) of the desired product **95** as a yellow oil.

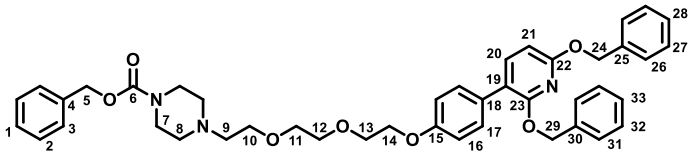

M ($C_{43}H_{47}N_3O_7$): 717.86 g/mol.

Yield: 264 mg (312 μmol; 99%; 85 wt%).

R_f: (SiO_2, *c*Hex/EtOAc 1:1) = 0.65.

^{1}H NMR: (400 MHz, $CDCl_3$) δ [ppm] = 7.56 (d, ^3J = 8.0 Hz, 1H, H20), 7.47 (d, ^3J = 8.9 Hz, 2H, H17), 7.43-7.29 (m, 15H, H1, H2, H3, H26, H27, H28, H31, H32, H33), 6.93 (d, ^3J = 8.9 Hz, 2H, H16), 6.45 (d, ^3J = 8.0 Hz, 1H, H21), 5.41 (s, 2H, H24), 5.35 (s, 2H, H29), 5.12 (s, 3H, H5), 4.15 (t, ^3J = 4.9 Hz, 2H, H14), 3.86 (t, ^3J = 4.9 Hz, 2H, H13), 3.74-3.71 (m, 2H,

H10), 3.53-3.48 (m, 6H, H8, H11/H12), 2.85 (s, 2H, H11/H12), 2.60 (t, ^3J = 5.3 Hz, 2H, H9), 2.47 (s, 4H, H7).

^{13}C NMR: (100 MHz, $CDCl_3$) δ [ppm] = 161.1 (C23); 158.3 (C22); 157.8 (C15); 155.4 (C6); 141.6 (C20); 138.1 (C25); 137.8 (C30); 136.9 (C4); 130.2 (C17); 129.6 (C18); 128.6, 128.5, 128.2, 128.1, 128.0, 128.0, 127.9, 127.5, 127.3 (C1, C2, C3, C26, C27, C28, C31, C32, C33); 115.8 (C19); 114.4 (C16); 102.5 (C21); 71.0, 70.6, 69.9, 69.0, 67.7, 67.3, 57.9 C9-C14); 68.0 (C29); 67.6 (C24); 67.2 (C5); 53.4 (C7); 43.9 (C8).

6.2.3.14 Synthesis of 107

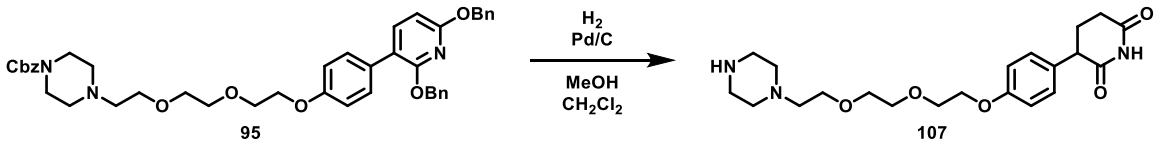

According to a modified procedure by *Lei et al*.[220]: In a 25 mL *Schlenk* flask, 264 mg (368 μmol; 1.00 eq.) of linker-recruiter conjugate **95** were dissolved in 3 mL of MeOH and 3 mL of CH_2Cl_2. Next, 53 mg (20 wt%) of Pd/C were added and the flask was purged with hydrogen gas. After 16 h, full conversion of linker-recruiter conjugate **95** was observed by TLC. The mixture was centrifuged, decanted, and the solvent was removed under reduced pressure. The crude product was purified by column chromatography (dryload, SiO_2, EtOAc/MeOH/NEt_3 1:0:0 to 20:4:1) to obtain 56 mg (140 μmol; 37%) of the desired product **107** as a yellow oil.

M ($C_{21}H_{31}N_3O_5$): 405.495 g/mol.

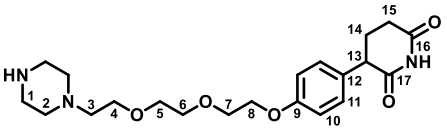

Yield: 56 mg (140 μmol; 37%).

R_f: (SiO_2, EtOAc/MeOH/NEt_3 20:4:1) = 0.05.

HR-MS (ESI):	Ion	Calc. mass [u]	Exp. mass [u]	Δ [ppm]
	$[M+H]^+$	406.23365	406.23385	+0.50
	$[M+Na]^+$	428.21559	428.21564	+0.11

The product was used without further characterization.

6.2.3.15 Synthesis of 111

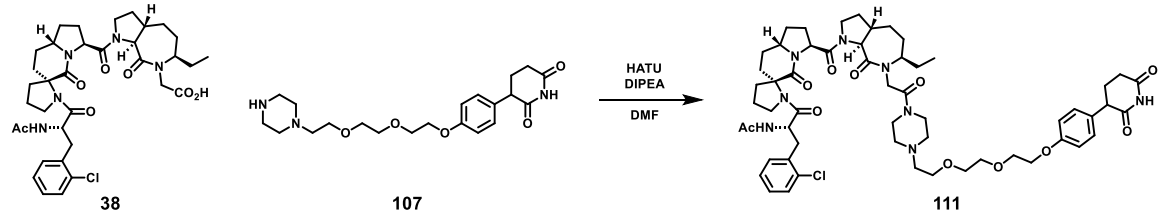

38 107 111

In a 10 mL *Schlenk* flask, 76 mg (112 μmol; 1.0 eq.) of warhead **38**, 55 mg (0.15 mmol; 1.3 eq.) of HATU and 34 μL (0.2 mmol; 1.7 eq.) of DIPEA were added in 2.5 mL of DMF. In a 10 mL *Schlenk* flask, 50 mg (0.12 mmol; 1.1 eq.) of linker-recruiter conjugate **107** and 34 μL (0.2 mmol; 1.7 eq.) of DIPEA were added in 2.5 mL of DMF. After 30 min, the mixture was added to the solution of warhead **38** and the mixture was stirred at room temperature until full conversion of warhead **38** was observed by TLC after 18 h and the solvent was removed under reduced pressure. The crude product was purified by column chromatography (dryload, SiO_2, EtOAc/MeOH/NEt_3 1:0:0 to 20:4:1). The residue was dissolved in CH_2Cl_2, filtered through a syringe filter, and the solvent was removed under reduced pressure. The residue was purified by reverse phase column chromatography (MeCN/H_2O 2:8 to 8:2) and lyophilized to obtain 49 mg (46 μmol; 41%) of the desired product **111** as a colorless lyophilizate.

M ($C_{56}H_{75}N_8O_{11}Cl$):	1070.71 g/mol.			
Yield:	49 mg (46 μmol; 41%).			
R_f:	(SiO_2, EtOAc/MeOH/NEt_3 20:4:1) = 0.16.			
HR-MS (ESI):	Ion	Calc. mass [u]	Exp. mass [u]	Δ [ppm]
	$[M+H]^+$	1071.53166	1071.53228	+0.58
	$[M+Na]^+$	1093.51360	1093.51265	-0.87
HPLC:	t_r [min]		9.04-9.27	
	Purity [%]		95	

6.2.3.16 Synthesis of 101

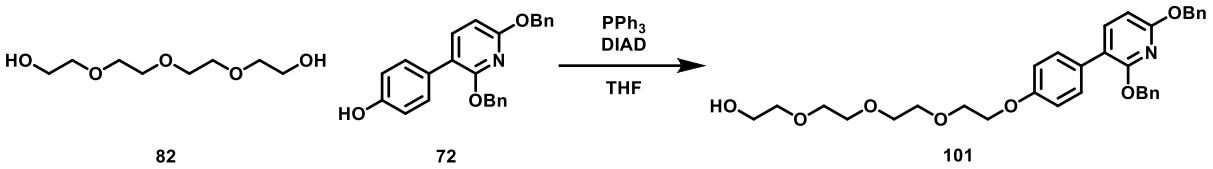

82 72 101

According to a modified procedure by *Roy et al*.[219]: In a 25 mL *Schlenk* flask, 400 mg (1.04 mmol; 1.00 eq.) of recruiter **72**, 1.41 g (7.28 mmol; 7.00 eq.) of tetraethylene glycol (**82)**, and 410 mg (1.56 mmol; 1.50 eq.) of triphenylphosphine were dissolved in 8.5 mL of THF. The mixture was cooled to 0 °C and 330 μL (1.67 mmol; 1.50 eq.) of DIAD were added. The mixture was stirred at room temperature until full conversion of recruiter **72** was observed by TLC after 18 h and the solvent was removed under reduced pressure. The crude mixture was purified by column chromatography (SiO_2, *c*Hex/EtOAc 1:2 to 0:1) to obtain 401 mg (720 μmol; 69%; 75 wt%) of the desired product **101** as a pale-yellow solid.

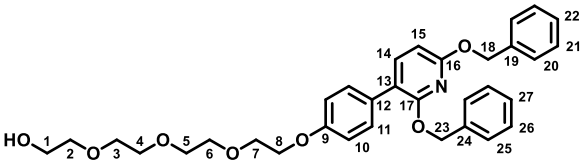

M ($C_{33}H_{37}NO_7$): 559.66 g/mol.

Yield: 401 mg (0.72 mmol; 69%; 75 wt%).

R_f: (SiO_2, EtOAc) = 0.18.

^{1}H NMR: (400 MHz, $CDCl_3$) δ [ppm] = 7.58-7.56 (m, 1H, H14), 7.42-7.38 (m, 2H, H11), 6.94 (d, ^3J = 8.8 Hz, 2H, H10), 6.45 (d, ^3J = 8.1 Hz, 1H, H13), 5.42 (s, 2H, H23), 5.35 (s, 2H, H18), 4.17 (t, ^3J = 4.8 Hz, 2H, H8), 3.87 (t, ^3J = 4.8 Hz, 2H, H7), 3.76-3.67 (m, 10H, H1, H3, H4, H5, H6), 3.62-3.59 (m, 2H, H2).

^{13}C NMR: (100 MHz, $CDCl_3$) δ [ppm] = 161.1 (C17); 158.4 (C16); 157.8 (C9); 141.6 (C14); 138.1 (C19); 137.8 (C24); 130.2 (C11); 129.5 (C12); 128.6, 128.6, 128.5, 127.9, 127.5, 127.3 (C20, C21, C22, C25, C26, C27); 115.8 (C13); 114.5 (C10); 102.5 (C15); 72.6 (C2); 71.0, 70.8, 70.8, 70.5, 69.9 (C3, C4, C5, C6, C7); 68.0 (C18); 67.7 (C23); 67.6 (C8); 61.9 (C1).

6.2.3.17 Synthesis of 104

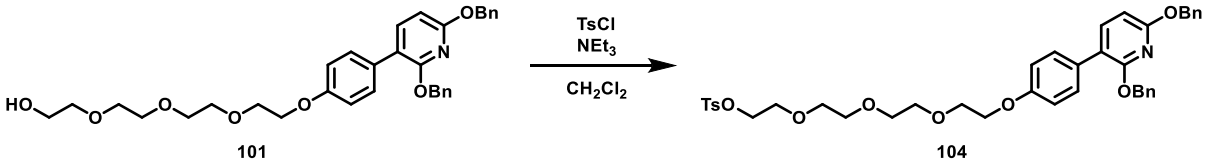

101 104

According to a modified procedure by *Li et al*.[194]: In a 10 mL round bottom flask, 141 mg (252 μmol; 1.00 eq.) of linker-recruiter conjugate **101**, 48 μL (0.28 mmol; 1.1 eq.) of NEt_3, and 144 mg (756 μmol; 3.00 eq.) of TsCl were added to 1.3 mL of CH_2Cl_2. The mixture was stirred at room temperature until full conversion of linker-recruiter conjugate **101** was observed by TLC after 20 h. The reaction mixture was diluted with 10 mL of CH_2Cl_2 and 2 mL of HCl (1M) were added. The layers were separated, and the aqueous phase was extracted with 10 mL of CH_2Cl_2 two times. The combined organic layers were dried over $MgSO_4$, filtered, and the solvent was removed under reduced pressure. The crude mixture was purified by column chromatography (SiO_2, *c*Hex/EtOAc 3:1 to 1:1) and the solvent CH_2Cl_2 was removed under reduced pressure to obtain 98 mg (140 μmol; 54%) of the desired product **104** as a pale-yellow oil.

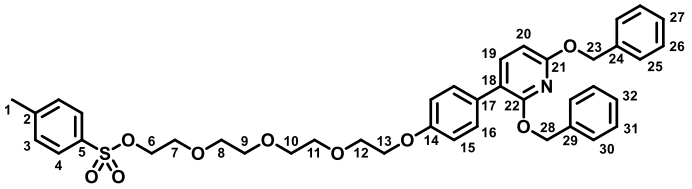

M ($C_{40}H_{43}NO_9S$): 713.84 g/mol.

Yield: 98 mg (140 μmol; 54%).

R_f: (SiO_2, *c*Hex/EtOAc 1:1) = 0.50.

^{1}H NMR: (400 MHz, $CDCl_3$) δ [ppm] = 7.81 (d, ^3J = 8.3 Hz, 2H, H4), 7.59 (d, ^3J = 8.1 Hz, 1H, H19), 7.50 (d, ^3J = 8.9 Hz, 2H, H16), 7.45 (d, ^3J = 7.6 Hz, 2H, H3), 7.41-7.30 (m, 10H, H25, H26, H27, H30, H31, H32), 6.95 (d, ^3J = 8.8 Hz, 2H, H15), 6.48 (d, ^3J = 8.1 Hz, 1H, H20), 5.44 (s, 2H, H23), 5.38 (s, 2H, H28), 4.17 (t, ^3J = 4.7 Hz, 4H, H6-13), 3.88 (t, ^3J = 4.9 Hz, 2H, H6-13), 3.75-3.66 (m, 6H, H6-13), 3.64-3.59 (m, 4H, H6-13), 2.45 (s, 3H, H1).

^{13}C NMR: (100 MHz, $CDCl_3$) δ [ppm] = 161.1 (C22); 158.3 (C21); 157.8 (C14); 144.6 (C2); 141.6 (C19); 138.1 (C29); 137.8 (C24); 130.2 (C16); 130.0 (C3); 128.6, 128.5, 128.1, 127.9, 127.5, 127.4 (C25 C26, C27, C30, C31, C32); 115.3 (C18), 114.4 (C15), 102.5 (C20), 71.0, 70.9, 70.8, 70.7, 70.4, 69.9, 69.4, 68.8, 67.6 (C6-13), 68.0 (C28), 67.7 (C23), 21.7 (C1).

Note: C22, C21, C2, C3, and C1 were detected in the HSQC, C17 and C9 were not detected.

6.2.3.18 Synthesis of 96

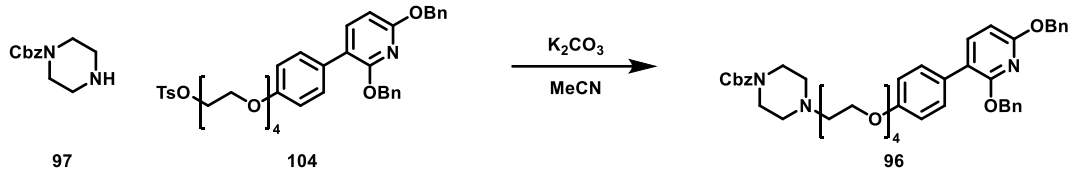

97 104 96

According to a modified procedure by *Brown et al*.[218]: In a 50 mL round bottom flask, 42 mg (0.19 mmol; 1.4 eq.) of piperazine **97**, 210 mg (137 μmol; 1.00 eq.) of tosylate **104**, and 52 mg (0.38 mmol; 2.0 eq.) of K_2CO_3 were dissolved in 2.4 mL of MeCN. The mixture was heated to 90 °C until full conversion of tosylate **104** was observed after 40 h by TLC. After cooling to room temperature, 20 mL of EtOAc and 4 mL of H_2O were added. The layers were separated, and the aqueous phase was extracted with 20 mL of EtOAc two times. The combined organic layers were dried over $MgSO_4$, filtered, and the solvent was removed under reduced pressure to obtain 125 mg (164 μmol; 86%) of the desired product **96** as a yellow oil.

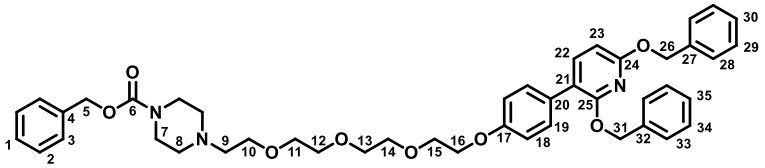

M ($C_{45}H_{51}N_3O_8$): 761.92 g/mol.

Yield: 125 mg (164 μmol; 86%).

R_f: (SiO_2, *c*Hex/EtOAc 1:1) = 0.50.

^{1}H NMR: (400 MHz, $CDCl_3$) δ [ppm] = 7.56 (d, ^3J = 8.1 Hz, 1H, H22), 7.48 (d, ^3J = 8.7 Hz, 2H, H19), 7.38-7.28 (m, 15H, H1, H2, H3, H28, H29, H30, H33, H34, H35), 6.93 (d, ^3J = 8.9 Hz, 2H, H18), 6.45 (d, ^3J = 8.1 Hz, 1H, H23), 5.42 (s, 2H, H26), 5.35 (s, 2H, H31), 5.12 (s, 2H, H5), 4.15 (t, ^3J = 4.8 Hz, 2H, H16), 3.86 (t, ^3J = 4.8 Hz, 2H, H15), 3.74-3.72 (m, 2H, H10), 3.69-3.64 (m, 4H, 2x H11/H12/H13/H14), 3.53-3.48 (m, 6H, H8, H11/H12/H13/H14), 2.85 (s, 2H, H11/H12/H13/H14), 2.60 (t, ^3J = 5.3 Hz, 2H, H9), 2.47 (s, 4H, H7).

^{13}C NMR: (100 MHz, $CDCl_3$) δ [ppm] = 160.8 (C25); 158.2 (C24); 157.8 (C17); 155.2 (C6); 141.6 (C22), 138.2 (C27), 137.8 (C32), 136.9 (C4), 130.2 (C19), 129.5 (C20); 128.6, 128.5, 128.1, 128.0, 127.9, 127.5, 127.3 (C1, C2, C3, C28, C29, C30, C33, C34, C35); 115.8 (C21); 114.5 (C18); 102.5 (C23); 71.0, 70.8, 70.6, 69.9, 69.0, 67.6, 67.3,(C9-C16); 68.0 (C31), 67.7 (C26), 67.2 (C5); 53.4 (C7); 45.9 (C10).
Note: C25, C24, C6, C27 were detected in the HSQC.

6.2.3.19 Synthesis of 108

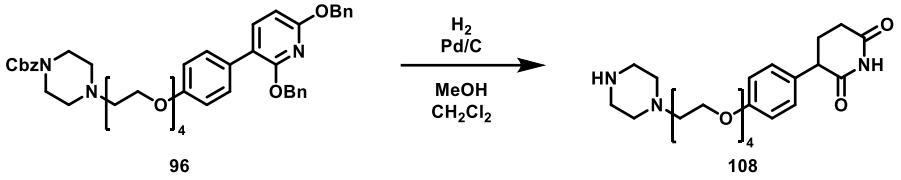

According to a modified procedure by *Lei et al*.[220]: In a 25 mL *Schlenk* flask, 125 mg (278 μmol; 1.00 eq.) of linker-recruiter conjugate **96** were dissolved in 2 mL of MeOH and 2 mL of CH_2Cl_2. Next, 25 mg (20 wt%) of Pd/C were added and the flask was purged with hydrogen gas. After 16 h, full conversion of linker-recruiter conjugate **96** was observed by TLC. The mixture was centrifuged, decanted, and the solvent was removed under reduced pressure. The crude product was purified by column chromatography (dryload, SiO_2, EtOAc/MeOH/NEt_3 1:0:0 to 20:4:1). The residue was dissolved in CH_2Cl_2, filtered through a syringe filter, and the solvent was removed under reduced pressure to obtain 47 mg (0.10 mmol; 64%) of the desired product **108** as a yellow oil.

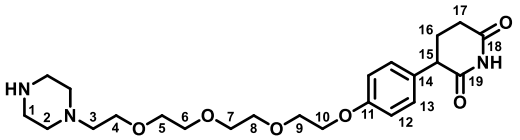

M ($C_{23}H_{35}N_3O_6$):	449.55 g/mol.			
Yield:	47 mg (0.10 mmol; 64%).			
R_f:	(SiO_2, EtOAc/MeOH/NEt_3 20:4:1) = 0.09.			
HR-MS (ESI):	Ion	Calc. mass [u]	Exp. mass [u]	Δ [ppm]
	$[M+H]^+$	450.25986	450.26020	+0.75
	$[M+Na]^+$	472.24181	472.24185	+0.10
	t_r [min]		5.23-7.81	
LC-MS (ESI):				
	Ion	Calc. mass [u]	Exp. mass [u]	
	$[M+H]^+$	450.26	450.36	

The product was used without further characterization.

6.2.3.20 Synthesis of 112

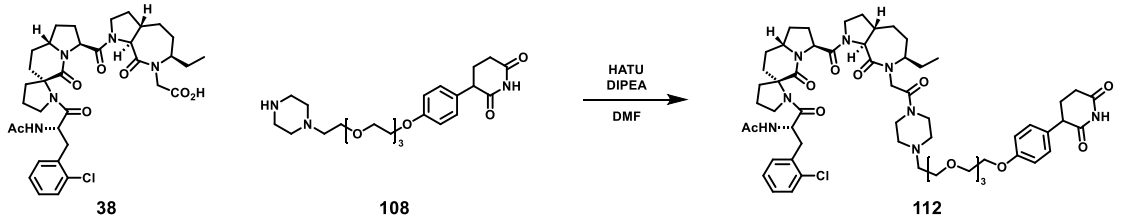

38 108 112

In a 10 mL *Schlenk* flask, 62 mg (91 μmol; 1.0 eq.) of warhead **38**, 45 mg (0.12 mmol; 1.3 eq.) of HATU and 27 μL (0.16 mmol; 1.7 eq.) of DIPEA were added in 2 mL of DMF. In a 10 mL *Schlenk* flask, 45 mg (0.10 mmol; 1.1 eq.) of linker-recruiter conjugate **108** and 27 μL (0.16 mmol; 1.7 eq.) of DIPEA were added in 2 mL of DMF. After 30 min, the mixture was added to the solution of warhead **38** and the mixture was stirred at room temperature until full conversion of warhead **38** was observed by TLC after 18 h. The solvent was removed under reduced pressure and the crude product was purified by column chromatography (dryload, SiO_2, EtOAc/MeOH/NEt_3 1:0:0 to 20:4:1). The residue was dissolved in CH_2Cl_2, filtered through a syringe filter, and the solvent was removed under reduced pressure. The residue was purified by reverse phase column chromatography (MeCN/H_2O 2:8 to 8:2) and lyophilized to obtain 61 mg (55 μmol; 60%) of the desired product **112** as a colorless lyophilizate.

M ($C_{58}H_{79}N_8O_{12}Cl$):	1115.76 g/mol.			
Yield:	61 mg (55 μmol; 60%).			
R_f:	(SiO_2, EtOAc/MeOH/NEt_3 20:4:1) = 0.10.			
HR-MS (ESI):	Ion	Calc. mass [u]	Exp. mass [u]	Δ [ppm]
	$[M+H]^+$	1115.55787	1115.55858	+0.63
	$[M+Na]^+$	1137.53982	1137.53907	-0.66
HPLC:	t_r [min]		8.31-8.83	
	Purity [%]		89	

6.2.4 Synthesis towards PROTACs 114-120 and 132-134

6.2.4.1 Synthesis of 114

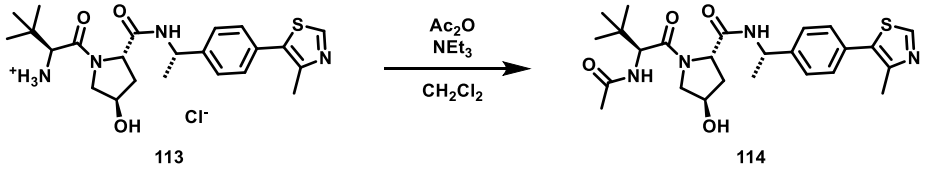

113 114

According to a modified procedure by *Zhao et al*.[201]: In a 10 mL *Schlenk* flask, 80 mg (0.17 mmol; 1.0 eq.) of recruiter **113** and 58 µL (0.42 mmol; 2.5 eq.) of NEt_3 were dissolved in 4 mL of CH_2Cl_2 and 24 µL (0.25 mmol; 1.5 eq.) of Ac_2O were added. The mixture was stirred at room temperature until full conversion of recruiter **113** was observed by TLC after 23 h. The crude reaction mixture was purified by column chromatography (CH_2Cl_2/MeOH/NEt_3 1:0:0 to 100:5:1). The residue was then purified by reverse phase column chromatography (MeCN/H_2O 2:8 to 8:2) and lyophilized to obtain 64 mg (0.13 mmol; 83%) of the desired product **114** as a colorless lyophilizate.

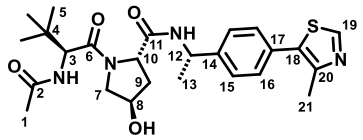

M ($C_{25}H_{34}N_4O_4S$): 486.63 g/mol.

Yield: 64 mg (0.13 mmol; 83%; Lit.[201]: 56%).

R_f: (SiO_2, CH_2Cl_2/MeOH/NEt_3 100:5:1) = 0.17.

^{1}H NMR: (500 MHz, $CDCl_3$) δ [ppm] = 8.68 (s, 1H, H19), 7.44-7.36 (m, 5H, H15, H16, N*H*), 6.19 (d, ^3J = 9.0 Hz, 1H, N*H*), 5.41 (d, ^3J = 9.6 Hz, 1H, O*H*), 5.09 (quin, ^3J = 7.3 Hz, 1H, H12), 4.72 (t, ^3J = 8.9 Hz, 1H, H10), 4.55 (d, ^3J = 9.2 Hz, 1H, H3), 4.52 (s, 1H, H8), 4.09 (d, ^3J = 11.5 Hz, 1H, H7a), 3.60 (dd, ^3J = 11.0 Hz, ^3J = 4.2 Hz, 1H, H7b), 2.53 (s, 3H, H21), 2.56-2.50 (m, 1H, H9a), 2.09-2.04 (m, 1H, H9b), 2.00 (s, 3H, H1), 1.48 (d, ^3J = 6.9 Hz, 3H, H13), 1.05 (s, 9H, H5).

^{13}C NMR: (125 MHz, $CDCl_3$) δ [ppm] = 172.2 (C6); 170.9 (C2); 169.7 (C11); 150.5 (C19); 148.7 (C20); 143.2 (C14); 131.7 (C18); 131.1 (C17); 129.7 (C16); 126.6 (C15); 70.2 (C8); 58.6 (C10); 57.9 (C3); 56.8 (C7); 49.0 (C12); 35.3 (C9); 35.1 (C4); 26.6 (C5); 23.2 (C1); 22.4 (C13); 16.2 (C21).

HR-MS (ESI):	Ion	Calc. mass [u]	Exp. mass [u]	Δ [ppm]
	$[M+H]^+$	487.23735	487.23731	-0.09
	$[M+Na]^+$	509.21930	509.21857	-1.43
LC-MS (ESI):	t_r [min]		11.25-11.71	
	Ion	Calc. mass [u]	Exp. mass [u]	Purity [%]
	$[M+H]^+$	487.24	487.18	96

6.2.4.2 Synthesis of 115

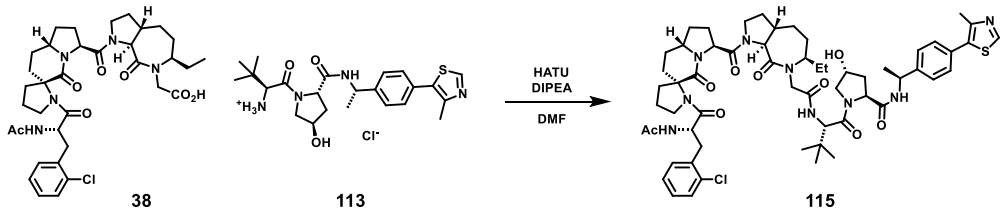

According to a modified procedure by *Banerjee et al*.[196]: In a 10 mL *Schlenk* flask, 25 mg (36 μmol; 1.0 eq.) of warhead **38**, 12 mg (40 μmol; 1.1 eq.) of HATU and 8.0 μL (91 μmol; 1.2 eq.) of DIPEA were added in 0.8 mL of DMF. In a 10 mL *Schlenk* flask, 18 mg (38 μmol; 1.0 eq.) of recruiter **113** and 8.0 μL (91 μmol; 1.2 eq.) of DIPEA were added in 0.8 mL of DMF. After 30 min, the mixture was added to the solution of warhead **38** and the mixture was stirred at room temperature until full conversion of warhead **38** was observed by TLC after 18 h and the solvent was removed under reduced pressure. The crude product was purified by column chromatography (dryload, SiO_2, EtOAc/MeOH/NEt_3 1:0:0 to 20:4:1). The residue was dissolved in CH_2Cl_2, filtered through a syringe filter, and the solvent was removed under reduced pressure. The residue was then purified by reverse phase column chromatography (MeCN/H_2O 2:8 to 8:2) and lyophilized to obtain 18 mg (46 μmol; 44%) of the desired product **111** as a colorless lyophilizate.

M ($C_{58}H_{76}N_9O_9SCl$):	1110.81 g/mol.			
Yield:	18 mg (16 μmol; 44%).			
R_f:	(SiO_2, EtOAc/MeOH/NEt_3 20:4:1) = 0.28.			
HR-MS (ESI):	Ion	Calc. mass [u]	Exp. mass [u]	Δ [ppm]
	$[M+H]^+$	1110.52480	1110.52637	+1.42
	$[M+Na]^+$	1132.50674	1132.50587	-0.77
LC-MS (ESI):	t_r [min]		13.44-14.77	
	Ion	Calc. mass [u]	Exp. mass [u]	Purity [%]
	$[M+H]^+$	1110.53	1110.57	98

6.2.4.3 Synthesis of 121

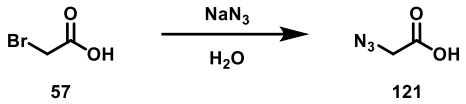

57 121

According to a modified procedure by *Xiao et al*.[221]: In a 250 mL round bottom flask, 13.9 g (100 mmol; 1.00 eq.) of bromoacetic acid (**57**) were dissolved in 160 mL of H_2O. Next, 13.0 g (200 mmol; 2.0 eq.) of NaN_3 were added in small portions and the mixture was stirred for 15 h at room temperature. The mixture was acidified with HCl (1M) to pH 2 and the mixture was extracted with 100 mL of EtOAc three times. The combined organic layers were dried over $MgSO_4$, filtered, and the solvent was removed under reduced pressure to obtain 5.29 g (52.2 mmol; 53%; 89 wt%) of the desired product **121** as a pale-yellow oil.

M ($C_2H_3N_3O_2$):	101.06 g/mol.	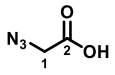
Yield:	5.29 g (52.2 mmol; 53%; 89 wt%).	
^{1}H NMR:	(500 MHz, $CDCl_3$) δ [ppm] = 10.34 (s, 1H, O*H*), 3.98 (s, 2H, H1).	

6.2.4.4 Synthesis of 125

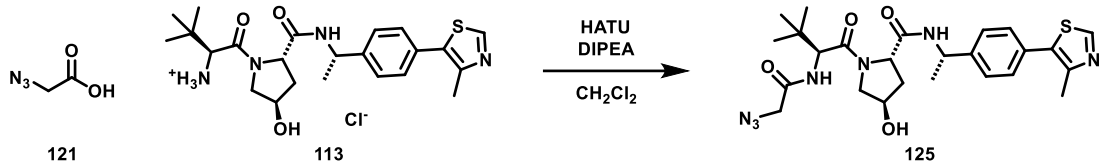

121 113 125

In a 50 mL *Schlenk* flask, 60 mg (0.60 mmol; 1.2 eq.) of linker **121**, 285 mg (750 μmol; 1.50 eq.) of HATU, and 235 μL (1.35 mmol; 2.70 eq.) of DIPEA were added in 18 mL of CH_2Cl_2. After 30 min at room temperature, 222 mg (500 μmol; 1.00 eq.) of recruiter **113** were added. The mixture was stirred at room temperature until full conversion as observed by TLC after 15 h and the solvent was removed under reduced pressure. The crude product was purified by column chromatography (dryload, SiO_2, *c*Hex/EtOAc/MeOH 25:25:1 to 20:20:1) to obtain 40 mg (75.8 μmol; 15%) of the desired product **125** as a colorless solid.

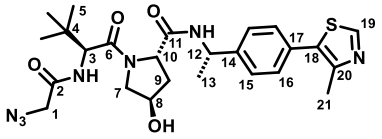

M ($C_{25}H_{33}N_7O_4S$): 527.644 g/mol.

Yield: 40 mg (76 μmol; 15%).

R_f: (SiO_2, *c*Hex/EtOAc/MeOH 25:25:1) = 0.19.

^{1}H NMR: (600 MHz, $CDCl_3$) δ [ppm] = 8.69 (s, 1H, H19), 7.42-7.39 (m, 3H, H16, N*H*), 7.36 (d, ^3J = 8.3 Hz, 2H, H15), 6.81 (d, ^3J = 8.7 Hz, 1H, N*H*), 5.42 (s, 1H, H8), 5.09 (quin, ^3J = 7.3 Hz, 1H, H12), 4.77 (t, ^3J = 8.1 Hz, 1H, H10), 4.44 (d, ^3J = 8.6 Hz, 1H, H3), 4.29 (d, ^3J = 12.2 Hz, 1H, H7a), 4.05 (d, ^3J = 16.4 Hz, 1H, H1a), 3.88 (d, ^3J = 16.4 Hz, 1H, H1b), 3.71 (dd, ^3J = 12.2 Hz, ^3J = 4.2 Hz, 1H, H7b), 2.88-2.84 (m, 1H, H9a), 2.53 (s, 3H, H21), 2.23-2.18 (m, 1H, H9b), 1.48 (d, ^3J = 6.9 Hz, 3H, H13), 1.06 (s, 9H, H5).

^{13}C NMR: (150 MHz, $CDCl_3$) δ [ppm] = 171.7 (C6); 168.7 (C2); 167.0 (C11); 150.5 (C19); 148.7 (C20); 142.9 (C14); 131.6 (C18); 131.2 (C17); 129.7 (C16); 126.6 (C15); 74.4 (C8); 58.3 (C10); 57.7 (C3); 54.0 (C7); 52.6 (C1a); 50.5 (C1b); 49.2 (C12); 35.0 (C4); 31.8 (C9); 26.6 (C5); 22.3 (C13); 16.2 (C21).

HR-MS (ESI):

Ion	Calc. mass [u]	Exp. mass [u]	Δ [ppm]

$[M+H]^+$	528.23875	528.23919	+0.82
$[M+Na]^+$	550.22069	550.22098	+0.51

6.2.4.5 Synthesis of 116

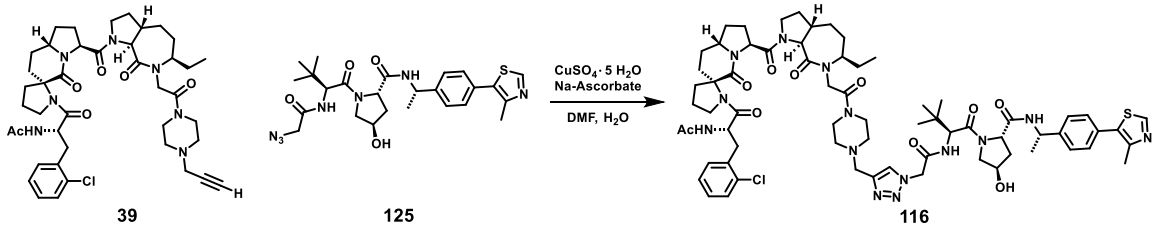

According to a modified procedure by *Banerjee et al*.[196]: In a headspace vial, 23 mg (29 μmol; 1.0 eq.) of warhead-linker conjugate **39** and 15 mg (28 μmol; 1.0 eq.) of linker-recruiter conjugate **125** were dissolved in 3 mL of DMF. Next, 1 mL of an aqueous solution (3mM; 3 μmol; 10 mol%) of $CuSO_4$ and 1 mL of an aqueous solution (6mM; 6 μmol; 20 mol%) of sodium ascorbate were added and the mixture was stirred at room temperature for 38 h. Full conversion of warhead-linker conjugate **39** was observed by TLC and the solvent was removed under reduced pressure. The crude product was purified by column chromatography (dryload, 7 g ultra-pure silica, EtOAc/MeOH/NEt_3 1:0:0 to 20:4:1). The product was dissolved in CH_2Cl_2, filtered through a syringe filter, and the solvent was removed under reduced pressure. The residue was purified by reverse phase column chromatography (MeCN/H_2O 2:8 to 8:2) and lyophilized to obtain 6.0 mg (4.5 μmol; 16%) of the desired product **116** as a pale-yellow lyophilizate.

M ($C_{67}H_{89}N_{14}O_{10}SCl$):	1316.05 g/mol.			
Yield:	6.0 mg (4.5 μmol; 16%).			
R_f:	(SiO_2, EtOAc/MeOH/NEt_3 20:4:1) = 0.12.			
HR-MS (ESI):	Ion	Calc. mass [u]	Exp. mass [u]	Δ [ppm]
	$[M+H]^+$	1317.63681	1317.64368	+5.21
	$[M+Na]^+$	1339.61875	1339.62329	+3.39
HPLC:	t_r [min]		13.01-13.44	
	Purity [%]		90	

6.2.4.6 Synthesis of 126

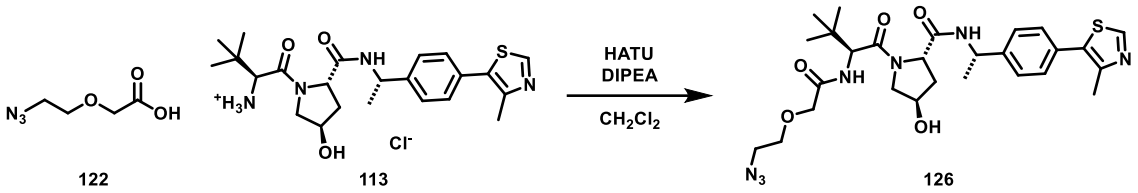

In a 10 mL *Schlenk* flask, 87 mg (0.60 mmol; 1.2 eq.) of linker **122**, 285 mg (750 μmol; 1.50 eq.) of HATU, and 235 μL (1.35 mmol; 2.70 eq.) of DIPEA were added in 9 mL of CH_2Cl_2. In a 50 mL *Schlenk* flask, 241 mg (500 μmol; 1.00 eq.) of recruiter **113** and 117 μL (0.68 mmol; 1.35 eq.) of DIPEA were added in 9 mL of CH_2Cl_2. After 30 min, the mixture was added to the solution of linker **122**. The mixture was stirred at room temperature until full conversion was observed by TLC after 15 h and the solvent was removed under reduced pressure. The crude product was purified by column chromatography (dryload, SiO_2, EtOAc/MeOH 20:1 to 10:1) to obtain 206 mg (360 μmol; 72%) of the desired product **126** as a colorless oil.

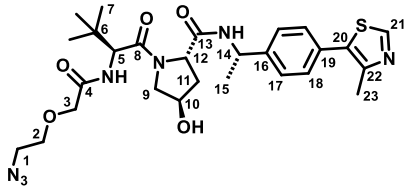

M ($C_{27}H_{37}N_7O_5S$): 571.70 g/mol.

Yield: 206 mg (360 μmol; 72%).

R_f: (SiO_2, EtOAc/MeOH 10:1) = 0.18.

^{1}H NMR: (500 MHz, $CDCl_3$) δ [ppm] = 8.69 (s, 1H, H21), 7.50 (d, ^3J = 7.9 Hz, 1H, N*H*), 7.41 (d, ^3J = 8.2 Hz, 2H, H18), 7.37 (d, ^3J = 8.2 Hz, 2H, H17), 7.24 (d, ^3J = 8.2 Hz, 1H, N*H*), 5.08 (q, ^3J = 7.3 Hz, 1H, H14), 4.77 (t, ^3J = 7.7 Hz, 1H, H12), 4.52-4.51 (m, 2H, H5, H10), 4.13 (d, ^3J = 11.5 Hz, 1H, H9a), 4.06 (d, ^3J = 15.5 Hz, 1H, H3a), 3.99 (d, ^3J = 15.5 Hz, 1H, H3b), 3.74-3.67 (m, 2H, H2), 3.61 (dd, ^3J = 11.3 Hz, ^3J = 3.7 Hz, 1H, H9b), 3.54-3.50 (m, 1H, H1a), 3.47-3.43 (m, 1H, H1b), 2.59 (ddd, ^3J = 13.4 Hz, ^3J = 7.2 Hz, ^3J = 4.9 Hz, 1H, H11a), 2.53 (s, 3H, H23), 2.07-2.03 (m, 1H, H11b), 1.48 (d, ^3J = 6.9 Hz, 3H, H15), 1.08 (s, 9H, H7).

^{13}C NMR: (125 MHz, $CDCl_3$) δ [ppm] = 171.9 (C8); 170.0 (C4); 169.6 (C13); 150.5 (C21); 148.7 (C22); 143.3 (C16); 131.8 (C20); 131.0 (C19); 129.7 (C18); 126.6 (C17); 70.7, 70.4 (C2, C3); 70.3 (C10); 58.3 (C12); 57.6 (C5); 56.7 (C9); 50.9 (C1); 49.1 (C14); 35.3 (C11); 34.9 (C6); 26.6 (C7); 22.4 (C15); 16.2 (C23).

HR-MS (ESI):

Ion	Calc. mass [u]	Exp. mass [u]	Δ [ppm]
$[M+H]^+$	572.26496	572.26444	-0.91
$[M+Na]^+$	594.24691	594.24621	-1.17

6.2.4.7 Synthesis of 117

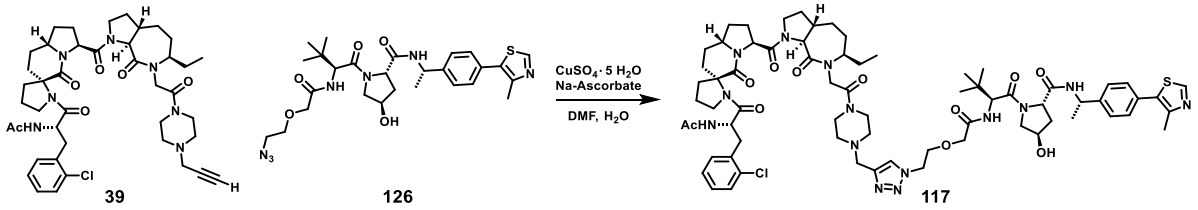

According to a modified procedure by *Banerjee et al*.[196]: In a headspace vial, 23 mg (29 μmol; 1.0 eq.) of warhead-linker conjugate **39** and 25 mg (44 μmol; 1.5 eq.) of linker-recruiter conjugate **126** were dissolved in 2 mL of DMF. Next, 1 mL of an aqueous solution (3mM; 3 μmol; 10 mol%) of $CuSO_4$ and 1 mL of an aqueous solution (6mM; 6 μmol; 20 mol%) of sodium ascorbate were added and the mixture was stirred at room temperature for 17 h. Full conversion of warhead-linker conjugate **39** was observed by TLC and the solvent was removed under reduced pressure. The crude product was purified by column chromatography (dryload, 6 g ultra-pure silica, EtOAc/MeOH/NEt_3 1:0:0 to 20:4:1). The product was dissolved in CH_2Cl_2, filtered through a syringe filter, and the solvent was removed under reduced pressure. The residue was purified by reverse phase column chromatography (MeCN/H_2O 2:8 to 8:2) and lyophilized to obtain 19 mg (14 μmol; 48%) of the desired product **117** as a colorless lyophilizate.

M ($C_{69}H_{93}N_{14}O_{11}SCl$):	1362.10 g/mol.			
Yield:	19 mg (14 μmol; 48%).			
R_f:	(SiO_2, EtOAc/MeOH/NEt_3 20:4:1) = 0.05.			
HR-MS (ESI):	Ion	Calc. mass [u]	Exp. mass [u]	Δ [ppm]
	$[M+H]^+$	1361.66303	1361.66882	+4.25
	$[M+Na]^+$	1383.64497	1383.64807	+2.24
HPLC:	t_r [min]		11.87-12.06	
	Purity [%]		98	

6.2.4.8 Synthesis of 133

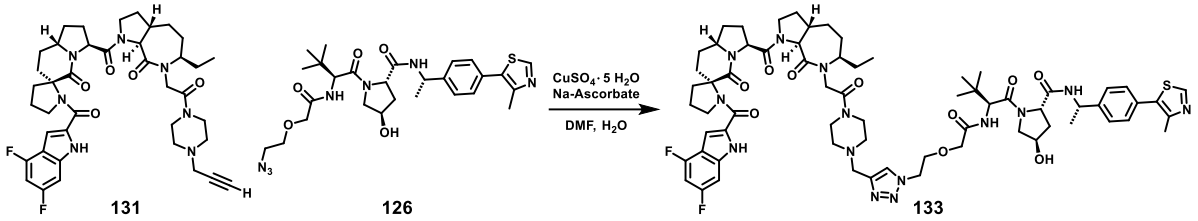

According to a modified procedure by *Banerjee et al*.[196]: In a headspace vial, 22 mg (29 μmol; 1.0 eq.) of warhead-linker conjugate **131** and 25 mg (44 μmol; 1.5 eq.) of linker-recruiter conjugate **126** were dissolved in 2 mL of DMF. Next, 1 mL of an aqueous solution (3mM; 3 μmol; 10 mol%) of $CuSO_4$ and 1 mL of an aqueous solution (6mM; 6 μmol; 20 mol%) of sodium ascorbate were added and the mixture was stirred at room temperature for 17 h. Full conversion of warhead-linker conjugate **131** was observed by TLC and the solvent was removed under reduced pressure. The crude product was purified by column chromatography (dryload, 6 g ultra-pure silica, EtOAc/MeOH/NEt_3 1:0:0 to 20:4:1). The product was dissolved in CH_2Cl_2, filtered through a syringe filter, and the solvent was removed under reduced pressure. The residue was purified by reverse phase column chromatography (MeCN/H_2O 4:6) and lyophilized to obtain 8.0 mg (6.1 μmol; 21%) of the desired product **133** as a colorless lyophilizate.

M ($C_{67}H_{86}N_{14}O_{10}F_2S$):	1317.57 g/mol.			
Yield:	8.0 mg (6.1 μmol; 21%).			
R_f:	(SiO_2, EtOAc/MeOH/NEt_3 20:4:1) = 0.05.			
HR-MS (ESI):	Ion	Calc. mass [u]	Exp. mass [u]	Δ [ppm]
	$[M+H]^+$	1317.64129	1317.64340	+1.60
	$[M+Na]^+$	1339.62323	1339.62354	+0.23
HPLC:	t_r [min]		9.82-10.23	
	Purity [%]		84	

6.2.4.9 Synthesis of 127

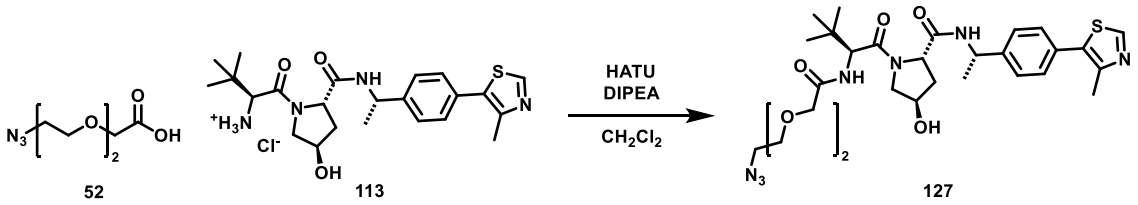

In a 25 mL *Schlenk* flask, 113 mg (600 μmol; 1.20 eq.) of linker **52**, 285 mg (750 μmol; 1.50 eq.) of HATU, and 118 μL (0.68 mmol; 1.35 eq.) of DIPEA were added in 9 mL of CH_2Cl_2. In a 50 mL *Schlenk* flask, 241 mg (500 μmol; 1.00 eq.) of recruiter **113** and 117 μL (0.68 mmol; 1.35 eq.) of DIPEA were added in 9 mL of CH_2Cl_2. After 30 min, the mixture was added to the solution of linker **52**. The mixture was stirred at room temperature until full conversion was observed by TLC after 18 h and the solvent was removed under reduced pressure. The crude product was purified by column chromatography (dryload, SiO_2, EtOAc/MeOH 20:1 to 10:1). The residue was dissolved in CH_2Cl_2, filtered through a syringe filter and the solvent was removed under reduced pressure. The residue was dissolved in MeCN/H_2O and lyophilized to obtain 248 mg (403 μmol; 81%) of the desired product **127** as a colorless lyophilizate.

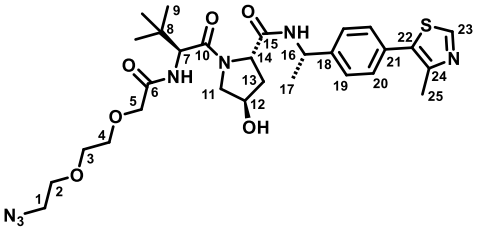

M ($C_{29}H_{41}N_7O_6S$): 615.750 g/mol.

Yield: 248 mg (403 μmol; 81%).

R_f: (SiO_2, EtOAc/MeOH 10:1) = 0.19.

^{1}H NMR: (500 MHz, $CDCl_3$) δ [ppm] = 8.68 (s, 1H, H23), 7.49 (d, ^3J = 7.9 Hz, 1H, N*H*), 7.41 (d, ^3J = 8.2 Hz, 2H, H20), 7.37 (d, ^3J = 8.2 Hz, 2H, H19), 7.24 (d, ^3J = 8.2 Hz, 1H, N*H*), 5.08 (q, ^3J = 7.3 Hz, 1H, H16), 4.77 (t, ^3J = 7.7 Hz, 1H, H14), 4.54-4.52 (m, 2H, H7, H12), 4.11-4.08 (m, 1H, H11a), 4.06 (d, ^3J = 15.5 Hz, 1H, H5a), 4.00 (d, ^3J = 15.5 Hz, 1H, H5b), 3.72-3.66 (m, 6H, H2, H3, H4), 3.62 (dd, ^3J = 11.3 Hz, ^3J = 3.7 Hz, 1H, H11b), 3.46-3.38 (m, 2H, H1), 2.56-2.51 (m, 1H, H13a), 2.53 (s, 3H, H25), 2.08-2.03 (m, 1H, H13b), 1.48 (d, ^3J = 6.9 Hz, 3H, H17), 1.07 (s, 9H, H9).

^{13}C NMR: (125 MHz, $CDCl_3$) δ [ppm] = 171.7 (C10); 170.6 (C6); 169.8 (C15); 150.5 (C23); 148.6 (C24); 143.3 (C18); 131.7 (C22); 131.0 (C21); 129.7 (C20); 126.6 (C19); 71.2, 70.5, 70.5 (C2, C3, C4, C5); 70.2 (C12); 58.5 (C14); 57.4 (C7); 56.7 (C11); 50.7 (C1); 49.0 (C16); 35.5 (C13); 35.1 (C8); 26.6 (C9); 22.4 (C17); 16.2 (C25).

HR-MS (ESI):

Ion	Calc. mass [u]	Exp. mass [u]	Δ [ppm]
$[M+H]^+$	616.29118	616.29125	+0.11
$[M+Na]^+$	638.27312	638.27245	-1.06

6.2.4.10 Synthesis of 118

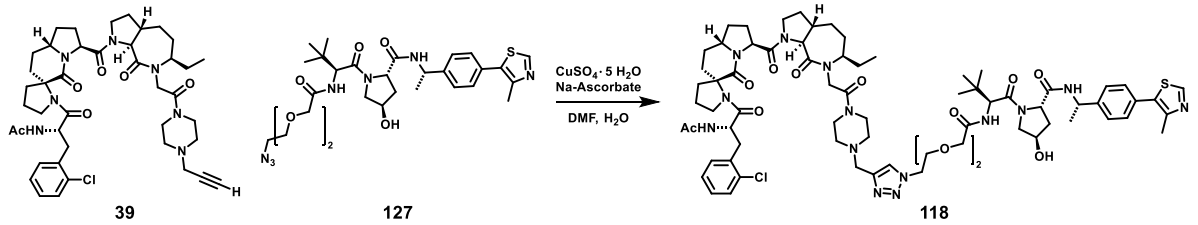

39 127 118

According to a modified procedure by *Banerjee et al*.[196]: In a headspace vial, 46 mg (58 μmol; 1.0 eq.) of warhead-linker conjugate **39** and 54 mg (88 μmol; 1.5 eq.) of linker-recruiter conjugate **127** were dissolved in 4 mL DMF. Next, 2 mL of an aqueous solution (3mM; 6 μmol; 10 mol%) of $CuSO_4$ and 2 mL of an aqueous solution (6mM; 12 μmol; 20 mol%) of sodium ascorbate were added. The mixture was stirred at room temperature for 16 h. Full conversion of warhead-linker conjugate **39** was observed by TLC and the solvent was removed under reduced pressure. The crude product was purified by column chromatography (dryload, 13 g ultra-pure silica, EtOAc/MeOH/NEt_3 1:0:0 to 20:4:1). The product was dissolved in CH_2Cl_2, filtered through a syringe filter, and the solvent was removed under reduced pressure. The residue was purified by reverse phase column chromatography (MeCN/H_2O 4:6) and lyophilized to obtain 43 mg (31 μmol; 52%) of the desired product **118** as a colorless lyophilizate.

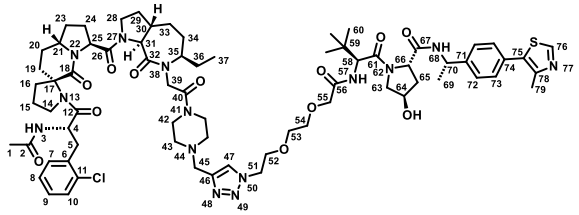

M ($C_{71}H_{97}N_{14}O_{12}SCl$): 1406.15 g/mol.

Yield: 43 mg (31 μmol; 52%).

R_f: (SiO_2, EtOAc/MeOH/NEt_3 20:4:1) = 0.07.

^{1}H NMR: (500 MHz, DMSO-d_6/D_2O 9:1) δ [ppm] = 8.98 (s, 1H, H76), 8.84 (s, 1H, H57), 8.50 (d, ^3J = 7.4 Hz, 1H, H68), 8.21 (d, ^3J = 8.7 Hz, 1H, H3), 8.02 (s, 1H, H47), 7.48-7.45 (m, 2H, H73), 7.42-7.37 (m, 4H, H7, H10, H72), 7.29-7.24 (m, 2H, H8, H9), 5.33 (d, ^3J = 2.5 Hz, 1H, O*H*), 4.91 (q, ^3J = 6.8 Hz, 1H, H70), 4.83 (dd, ^3J = 10.6 Hz, ^3J = 3.7 Hz, 1H, H4), 4.73 (t, ^3J = 8.4 Hz, 1H, H25), 4.61 (d, ^3J = 9.5 Hz, 1H, H31), 4.58-4.56 (m, 3H, H51, H58), 4.47 (t, ^3J = 8.3 Hz, 1H, H66), 4.33-4.27 (m, 2H, H39a, H64), 4.00-3.96 (m, 3H,

H28a, H55), 3.93-3.86 (m, 3H, H39b, H52), 3.80-3.71 (m, 3H, H14, H35), 3.65-3.55 (m, 9H, H21, H45, H53, H54, H63), 3.49-3.38 (m, 4H, H42), 3.31-3.21 (m, 1H, H28b), 3.10 (dd, ^{2}J = 14.3 Hz, ^{3}J = 3.6 Hz, 1H, H5a), 2.74 (dd, ^{2}J = 14.1 Hz, ^{3}J = 10.7 Hz, 1H, H5b), 2.51-2.29 (m, 8H, H24a, H43, H79), 2.21-2.16 (m, 1H, H19a), 2.15-2.07 (m, 3H, H16a, H23a, H29a), 2.07-2.03 (m, 1H, H30), 2.03-1.99 (m, 2H, H33), 1.95-1.75 (m, 11H, H15, H16b, H19b, H20, H24b, H29b, H34a, H65), 1.73 (s, 3H, H1), 1.63-1.50 (m, 3H, H23b, H34b, H36a), 1.43-1.33 (m, 1H, H36b), 1.37 (s, 3H, H69), 0.96 (s, 9H, H60), 0.91 (t, ^{3}J = 7.1 Hz, 3H, H37).

^{13}C NMR: (125 MHz, DMSO-d_6/D_2O 9:1) δ [ppm] = 173.52 (C32); 172.51 (C67); 172.43 (C61); 171.31 (C56); 171.14 (C2); 171.02 (C12); 170.78 (C26); 170.76 (C18); 169.25 (C40); 153.54 (C76); 149.61 (C78); 146.45 (C46); 136.94 (C6); 135.09 (C11); 134.02 (C7); 133.11 (C75); 131.57 (C74), 130.92 (C71); 130.82 (C10); 130.76 (C72); 130.37 (C9); 128.75 (C8); 128.26 (C73); 126.46 (C47); 72.32 (C54); 71.42 (C55); 71.32 (C53); 70.78 (C52); 70.61 (C64); 66.62 (C17); 64.20 (C31); 60.57 (C21); 60.54 (C66); 60.19 (C35); 59.39 (C25); 58.40 (C63); 57.70 (C58); 53.96 (C45); 53.62 (C43); 51.72 (C4); 51.23 (C51); 49.82 (C14); 49.65 (C70); 48.43 (C28); 45.84 (C42a); 44.82 (C39); 43.16 (C42b); 42.37 (C30); 42.34 (C16); 39.42 (C65); 37.72 (C59); 37.50 (C19); 36.45 (C5); 34.63 (C33); 34.61 (C23); 34.10 (C29); 32.02 (C34); 29.56 (C20); 28.96 (C24); 28.08 (C60); 27.81 (C36); 25.19 (C15); 24.15 (C69); 23.97 (C1), 17.76 (C79); 13.56 (C37).

^{15}N NMR: (61 MHz, $CDCl_3$) δ [ppm] = 244.0 (N50); 131.6 (N68); 126.5 (N27); 119.7 (N3); 113.6 (N57); 90.4 (N38); 68.8 (N77).

HR-MS (ESI):	Ion	Calc. mass [u]	Exp. mass [u]	Δ [ppm]
	$[M+H]^+$	1405.68924	1405.69015	+0.65
	$[M+Na]^+$	1427.67118	1427.66986	-0.93
HPLC:	t_r [min]		7.63-7.91	
	Purity [%]		>99	

6.2.4.11 Synthesis of 132

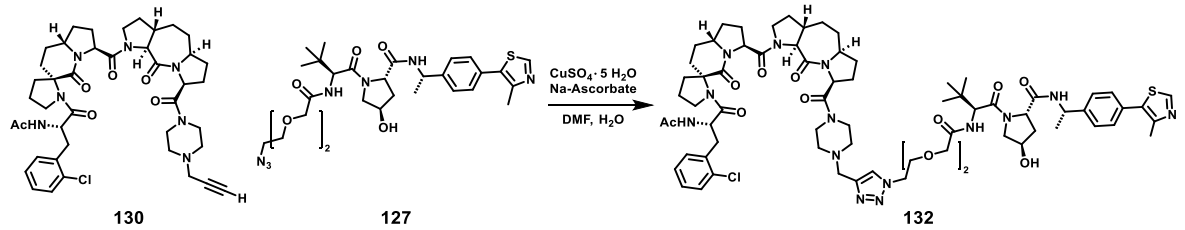

130 127 132

According to a modified procedure by *Banerjee et al*.[196]: In a headspace vial, 23 mg (29 μmol; 1.0 eq.) of warhead-linker conjugate **130** and 27 mg (44 μmol; 1.5 eq.) of linker-recruiter conjugate **127** were dissolved in 2 mL of DMF. Next, 1 mL of an aqueous solution (3mM; 3 μmol; 10 mol%) of $CuSO_4$ and 1 mL of an aqueous solution (6mM; 6 μmol; 20 mol%) of sodium ascorbate were added and the mixture was stirred at room temperature for 19 h. Full conversion of warhead-linker conjugate **130** was observed by TLC and the solvent was removed under reduced pressure. The crude product was purified by column chromatography (dryload, 6 g ultra-pure silica, EtOAc/MeOH/NEt_3 1:0:0 to 20:4:1). The product was dissolved in CH_2Cl_2, filtered through a syringe filter, and the solvent was removed under reduced pressure. The residue was purified by reverse phase column chromatography (MeCN/H_2O 4:6) to obtain 22 mg (16 μmol; 54%) of the desired product **132** as a colorless lyophilizate.

M ($C_{71}H_{95}N_{14}O_{12}SCl$): 1404.137 g/mol.

Yield: 22 mg (16 μmol; 54%).

R_f: (SiO_2, EtOAc/MeOH/NEt_3 20:4:1) = 0.05.

HR-MS (ESI):	Ion	Calc. mass [u]	Exp. mass [u]	Δ [ppm]
	$[M+H]^+$	1403.67359	1403.67236	-0.87
	$[M+Na]^+$	1425.65553	1425.65157	-2.78
HPLC:	t_r [min]		11.94-12.20	

	Purity [%]	99

6.2.4.12 Synthesis of 134

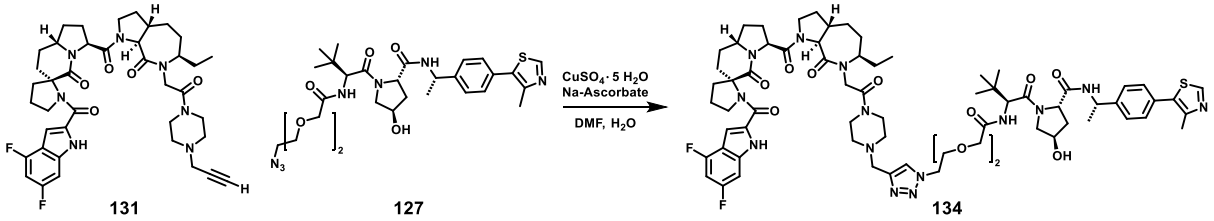

According to a modified procedure by *Banerjee et al*.[196]: In a headspace vial, 22 mg (29 μmol; 1.0 eq.) of warhead-linker conjugate **131** and 27 mg (44 μmol; 1.5 eq.) of linker-recruiter conjugate **127** were dissolved in 2 mL of DMF. Next, 1 mL of an aqueous solution (3mM; 3 μmol; 10 mol%) of $CuSO_4$ and 1 mL of an aqueous solution (6mM; 6 μmol; 20 mol%) of sodium ascorbate were added, and the mixture was stirred at room temperature for 39 h. Full conversion of warhead-linker conjugate **131** was observed by TLC and the solvent was removed under reduced pressure. The crude product was purified by column chromatography (dryload, 7 g ultra-pure silica, EtOAc/MeOH/NEt_3 1:0:0 to 20:4:1). The product was dissolved in CH_2Cl_2, filtered through a syringe filter, and the solvent was removed under reduced pressure. The residue was purified by reverse phase column chromatography (MeCN/H_2O 4:6) and lyophilized to obtain 10 mg (7.3 μmol; 25%) of the desired product **134** as a colorless lyophilizate.

M ($C_{69}H_{90}N_{14}O_{11}F_2S$):	1361.62 g/mol.			
Yield:	10 mg (7.3 μmol; 25%).			
R_f:	(SiO_2, EtOAc/MeOH/NEt_3 20:4:1) = 0.06.			
HR-MS (ESI):	Ion	Calc. mass [u]	Exp. mass [u]	Δ [ppm]
	$[M+H]^+$	1361.66750	1361.66608	-1.04
	$[M+Na]^+$	1383.64945	1383.64528	-3.01
HPLC:	t_r [min]		13.64-13.96	
	Purity [%]		>99	

6.2.4.13 Synthesis of 128

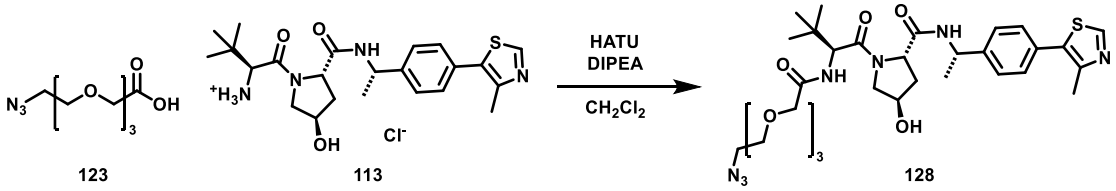

In a 25 mL *Schlenk* flask, 140 mg (600 μmol; 1.20 eq.) of linker **123**, 285 mg (750 μmol; 1.50 eq.) of HATU, and 236 μL (1.35 mmol; 2.70 eq.) of DIPEA were added in 9 mL of CH_2Cl_2. In a 50 mL *Schlenk* flask, 241 mg (500 μmol; 1.00 eq.) of recruiter **113** and 117 μL (680 μmol; 1.35 eq.) of DIPEA were added in 9 mL of CH_2Cl_2. After 30 min, the mixture was added to the solution of linker **123**. The mixture was stirred at room temperature until full conversion was observed by TLC and the solvent was removed under reduced pressure after 19 h. The crude product was purified by column chromatography (dryload, SiO_2, EtOAc/MeOH 20:1 to 10:1). The residue was dissolved in CH_2Cl_2, filtered through a syringe filter and the solvent was removed under reduced pressure. The residue was dissolved in MeCN/H_2O and lyophilized to obtain 205 mg (311 μmol; 62%) of the desired product **128** as a colorless lyophilizate.

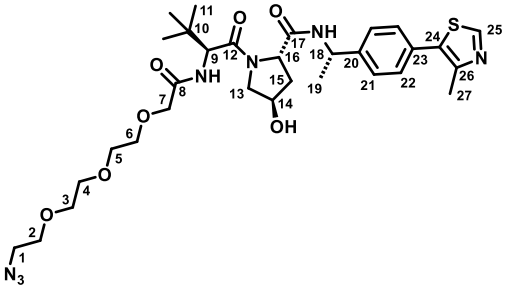

M ($C_{31}H_{45}N_7O_7S$): 659.80 g/mol.

Yield: 205 mg (311 μmol; 62%).

R_f: (SiO_2, EtOAc/MeOH 10:1) = 0.21.

^{1}H NMR: (600 MHz, $CDCl_3$) δ [ppm] = 8.68 (s, 1H, H25), 7.48 (d, ^3J = 8.0 Hz, 1H, N*H*), 7.41 (d, ^3J = 8.3 Hz, 2H, H22), 7.37 (d, ^3J = 8.3 Hz, 2H, H21), 7.31 (d, ^3J = 8.3 Hz, 1H, N*H*), 5.08 (q, ^3J = 7.0 Hz, 1H, H18), 4.76 (t, ^3J = 7.6 Hz, 1H, H16), 4.53-4.51 (m, 2H, H9, H14), 4.13 (d, ^3J = 11.2 Hz, 1H, H13a), 4.05 (d, ^3J = 15.8 Hz, 1H, H7a), 4.00 (d, ^3J = 15.8 Hz, 1H, H7b), 3.70-3.66 (m, 10H, H2, H3, H4, H5, H6), 3.61 (dd, ^3J = 14.4 Hz, ^4J = 3.9 Hz, 1H, H13b), 3.38

(t, ^3J = 5.0 Hz, 2H, H1), 2.60-2.56 (m, 1H, H15a), 2.53 (s, 3H, H27), 2.07-2.04 (m, 1H, H15b), 1.48 (d, ^3J = 6.8 Hz, 3H, H19), 1.08 (s, 9H, H11).

^{13}C NMR: (150 MHz, $CDCl_3$) δ [ppm] = 171.9 (C12); 170.8 (C8); 169.7 (C17); 150.5 (C25); 148.7 (C26); 143.3 (C20); 131.7 (C24); 131.1 (C23); 129.7 (C22); 126.6 (C21); 71.3, 70.9, 70.9, 70.7, 70.5, 70.3 (C2, C3, C4, C5, C6, C7); 70.2 (C14); 58.3 (C16); 57.4 (C9); 56.7 (C13); 50.8 (C1); 49.0 (C18); 35.4 (C15); 35.0 (C10); 26.6 (C11); 22.4 (C19); 16.2 (C27).

HR-MS (ESI):

Ion	Calc. mass [u]	Exp. mass [u]	Δ [ppm]
$[M+H]^+$	660.31739	660.31744	+0.07
$[M+Na]^+$	682.29934	682.29866	-0.99

6.2.4.14 Synthesis of 119

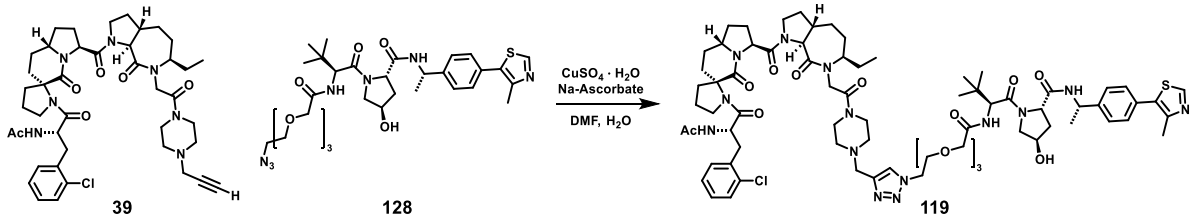

According to a modified procedure by *Banerjee et al*.[196]: In a headspace vial, 23 mg (29 μmol; 1.0 eq.) of warhead-linker conjugate **39** and 29 mg (44 μmol; 1.5 eq.) of linker-recruiter conjugate **128** were dissolved in 2 mL DMF. Next, 1 mL of an aqueous solution (3mM; 3 μmol; 10 mol%) of $CuSO_4$ and 1 mL of an aqueous solution (6mM; 6 μmol; 20 mol%) of sodium ascorbate were added, and the mixture was stirred at room temperature for 18 h. Full conversion of warhead-linker conjugate **39** was observed by TLC and the solvent was removed under reduced pressure. The crude product was purified by column chromatography (dryload, 7 g ultra-pure silica, EtOAc/MeOH/NEt_3 1:0:0 to 20:4:1). The product was dissolved in CH_2Cl_2, filtered through a syringe filter, and the solvent was removed under reduced pressure. The residue was purified by reverse phase column chromatography (MeCN/H_2O 4:6) and lyophilized to obtain 29 mg (20.0 μmol; 68%) of the desired product **119** as a colorless lyophilizate.

M ($C_{73}H_{101}N_{14}O_{13}SCl$):	1450.21 g/mol.			
Yield:	29 mg (20 μmol; 68%).			
R_f:	(SiO_2, EtOAc/MeOH/NEt_3 20:4:1) = 0.07.			
HR-MS (ESI):	Ion	Calc. mass [u]	Exp. mass [u]	Δ [ppm]
	$[M+H]^+$	1449.71545	1449.72034	+3.37
	$[M+Na]^+$	1471.69740	1471.69971	+0.55
HPLC:	t_r [min]		11.88-12.11	
	Purity [%]		93	

6.2.4.15 Synthesis of 129

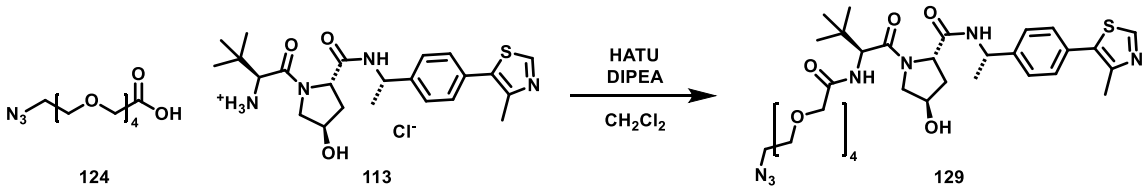

In a 25 mL *Schlenk* flask, 166 mg (600 μmol; 1.20 eq.) of linker **124**, 285 mg (750 μmol; 1.50 eq.) of HATU, and 118 μL (680 μmol; 1.35 eq.) of DIPEA were added in 9 mL of CH_2Cl_2. In a 50 mL *Schlenk* flask, 222 mg (500 μmol; 1.00 eq.) of recruiter **113** and 117 μL (680 μmol; 1.35 eq.) of DIPEA were added in 9 mL of CH_2Cl_2. After 30 min, the mixture was added to the solution of linker **124**. The mixture was stirred at room temperature until full conversion of recruiter **113** was observed by TLC after 20 h and the solvent was removed under reduced pressure. The crude product was purified by column chromatography (dryload, SiO_2, EtOAc/MeOH 20:1 to 10:1) to obtain 313 mg (445 μmol; 89%) of the desired product **129** as a colorless oil.

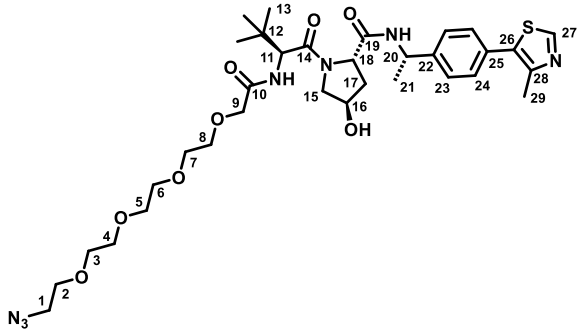

M ($C_{33}H_{49}N_7O_8S$): 703.86 g/mol.

Yield: 313 mg (445 μmol; 89%).

R_f: (SiO_2, *c*Hex/EtOAc/MeOH 3:3:1) = 0.29.

^{1}H NMR: (500 MHz, $CDCl_3$) δ [ppm] = 8.68 (s, 1H, H27), 7.48 (d, ^3J = 7.8 Hz, 1H, N*H*), 7.41 (d, ^3J = 8.1 Hz, 2H, H24), 7.37 (d, ^3J = 8.1 Hz, 2H, H23), 7.32 (d, ^3J = 8.3 Hz, 1H, N*H*), 5.08 (q, ^3J = 7.2 Hz, 1H, H20), 4.76 (t, ^3J = 7.7 Hz, 1H, H18), 4.53-4.51 (m, 2H, H11, H16), 4.13 (d, ^3J = 11.2 Hz, 1H, H15a), 4.05 (d, ^3J = 15.8 Hz, 1H, H9a), 4.00 (d, ^3J = 15.8 Hz, 1H, H9b), 3.70-3.65 (m, 14H, H2, H3, H4, H5, H6, H7, H8), 3.60 (dd, ^3J = 14.4 Hz, ^4J = 3.9 Hz, 1H, H15b), 3.38 (t, ^3J = 5.0 Hz, 2H, H1), 2.60-2.55 (m, 1H, H17a), 2.53 (s, 3H, H29), 2.08-2.03 (m, 1H, H17b), 1.48 (d, ^3J = 6. Hz, 3H, H21), 1.07 (s, 9H, H13).

^{13}C NMR: (125 MHz, $CDCl_3$) δ [ppm] = 171.9 (C14); 170.8 (C10); 169.7 (C19); 150.4 (C27); 148.7 (C28); 143.3 (C22); 131.7 (C26); 131.1 (C25); 129.7 (C24); 126.6 (C23); 71.3, 70.8, 70.8, 70.6, 70.5, 70.2, (C2, C3, C4, C5, C6, C7, C8, C9); 70.2 (C16); 58.4 (C18); 57.4 (C11); 56.7 (C15); 50.8 (C1); 49.0 (C20); 35.4 (C17); 35.0 (C12); 26.6 (C13); 22.4 (C21); 16.2 (C29).

HR-MS (ESI):

Ion	Calc. mass [u]	Exp. mass [u]	Δ [ppm]
$[M+H]^+$	704.34361	704.34414	+0.76
$[M+Na]^+$	726.32555	726.32546	-0.13

6.2.4.16 Synthesis of 120

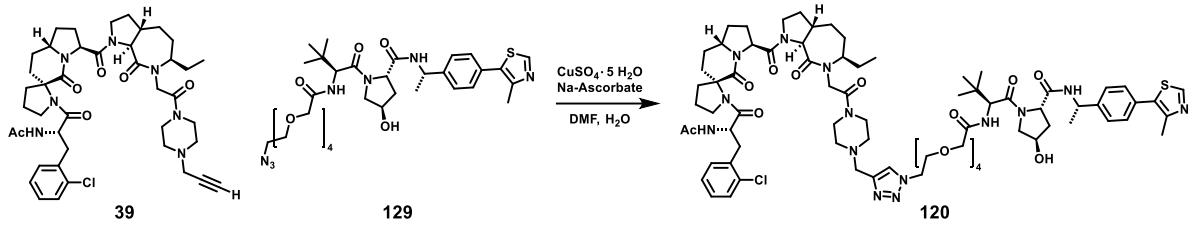

According to a modified procedure by *Banerjee et al*.[196]: In a headspace vial, 23 mg (29 μmol; 1.0 eq.) of warhead-linker conjugate **39** and 31 mg (44 μmol; 1.5 eq.) of linker-recruiter **129** were dissolved in 2 mL DMF. Next, 1 mL of an aqueous solution (3mM; 3 μmol; 10 mol%) of $CuSO_4$ and 1 mL of an aqueous solution (6mM; 6 μmol; 20 mol%) of sodium ascorbate were added, and the mixture was stirred at room temperature for 17 h. Full conversion of warhead-linker conjugate **39** was observed by TLC and the solvent was removed under reduced pressure. The crude product was purified by column chromatography (dryload, 7 g ultra-pure silica, EtOAc/MeOH/NEt_3 1:0:0 to 20:4:1). The product was dissolved in CH_2Cl_2, filtered through a syringe filter, and the solvent was removed under reduced pressure. The residue was purified by reverse phase column chromatography (MeCN/H_2O 4:6) and lyophilized to obtain 22 mg (15 μmol; 50%) of the desired product **120** as a colorless lyophilizate.

M ($C_{75}H_{105}N_{14}O_{14}SCl$):	1494.26 g/mol.			
Yield:	22 mg (15 μmol; 50%).			
R_f:	(SiO_2, EtOAc/MeOH/NEt_3 20:4:1) = 0.05.			
HR-MS (ESI):	Ion	Calc. mass [u]	Exp. mass [u]	Δ [ppm]
	$[M+H]^+$	1493.74167	1493.75122	+6.39
	$[M+Na]^+$	1515.72361	1515.72937	+3.80
HPLC:	t_r [min]		11.98-12.27	
	Purity [%]		81	

6.2.5 Synthesis towards control compounds *epi*-114 and *epi*-118

6.2.5.1 Synthesis of 139

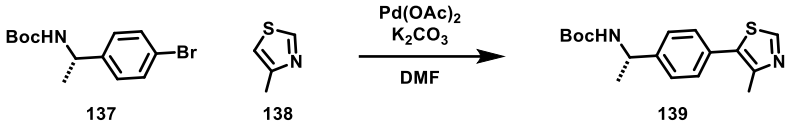

According to a modified procedure by *He et al*.[202]: In a 250 mL *Schlenk* flask, 7.50 g (25.0 mmol; 1.00 eq.) of aryl bromide **137**, 3.45 g (25.0 mmol; 1.00 eq.) of K_2CO_3 and 60 mg (0.25 mmol; 1 mol%) of $Pd(OAc)_2$ were dissolved in 75 mL of DMF. Next, 5.00 g (50.0 mmol; 2.00 eq.) of heterocycle **138** were added and the mixture was heated to reflux until full conversion of aryl bromide **137** was observed by TLC after 17 h. At room temperature, 20 mL of H_2O and 200 mL of EtOAc were added. The aqueous phase was extracted with 100 mL of EtOAc four times. The combined organic layers were combined and washed with 100 mL of NaCl solution. The solution was dried over Na_2SO_4, filtered, and the solvent was removed under reduced pressure. The crude product was purified by column chromatography (SiO_2, *c*Hex/EtOAc 5:1 to 3:1) to obtain 4.34 g (13.6 mmol; 54%) of the desired product **139** as a pale-yellow oil.

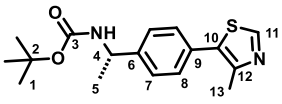

M ($C_{17}H_{22}N_2O_2S$): 318.43 g/mol.

Yield: 4.34 g (13.6 mmol; 54%; Lit.[202]: 85%).

R_f: (SiO_2, *c*Hex/EtOAc 3:1) = 0.25.

^{1}H NMR: (500 MHz, $CDCl_3$) δ [ppm] = 8.67 (s, 1H, H11), 7.41 (d, ^3J = 8.2 Hz, 2H, H8), 7.36 (d, ^3J = 8.2 Hz, 2H, H7), 4.84-4.66 (m, 2H, H4, N*H*), 2.54 (s, 3H, H13), 1.48 (d, ^3J = 6.2 Hz, 3H, H5), 1.44 (s, 9H, H1).

^{13}C NMR: (125 MHz, $CDCl_3$) δ [ppm] = 155.2 (C3); 150.3 (C11); 148.6 (C12); 144.1 (C6); 131.8 (C10); 130.9 (C9); 129.6 (C8); 126.3 (C7); 79.7 (C2); 50.0 (C4); 28.5 (C1); 22.8 (C5); 16.3 (C13).

6.2.5.2 Synthesis of 136

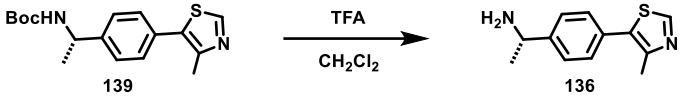

According to a modified procedure by *He et al*.[202]: In a round bottom flask, 4.34 g (13.6 mmol; 1.00 eq.) of the Boc-protected amine **139** were dissolved in 30 mL of CH_2Cl_2. To the solution, 7.4 mL of TFA were added and the mixture was stirred at room temperature for 7 h. Next, 30 mL of H_2O and 50 mL of CH_2Cl_2 were added and $NaHCO_3$ was added until no more gas formation was detected. The aqueous phase was extracted with 100 mL of CH_2Cl_2 five times and the combined organic layers were dried over Na_2SO_4, filtered, and the solvent was removed under reduced pressure to obtain 2.86 g (13.1 mmol; 96%) of the desired product **136** as a pale-yellow oil.

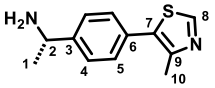

M ($C_{12}H_{14}N_2S$):	218.32 g/mol.
Yield:	2.86 g (13.1 mmol; 96%; Lit.[202]: quant.).
R_f:	(SiO_2, *c*Hex/EtOAc 10:1) = 0.00.
^{1}H NMR:	(500 MHz, $CDCl_3$) d [ppm] = 8.67 (s, 1H, H8), 7.41 (s, 4H, H4, H5), 4.18 (q, ^3J = 6.6 Hz, 1H, H2), 2.54 (s, 3H, H10), 1.89 (s, 2H, NH_2); 1.43 (d, ^3J = 6.7 Hz, 3H, H1).
^{13}C NMR:	(125 MHz, $CDCl_3$) d [ppm] = 150.3 (C8); 148.5 (C9); 147.4 (C3); 131.9 (C7); 130.6 (C6); 129.6 (C5); 126.3 (C4); 51.2 (C2); 25.6 (C1); 16.2 (C10).

6.2.5.3 Synthesis of 141

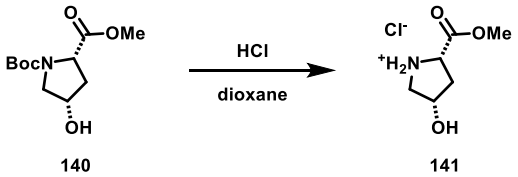

140 141

According to a modified procedure by *Shah et al*.[203]: In a 250 mL round bottom flask, 3.00 g (12.2 mmol; 1.00 eq.) of hydroxyproline **140** was dissolved in 3 mL of CH_2Cl_2 and 49 mL of MeOH. Next, 12 mL of a solution of HCl (4M in dioxane) was added and the mixture was stirred at room temperature for 1 h. The solvent was removed under reduced pressure to obtain 2.36 g (12.2 mmol; quant.; 96 wt%) of the desired product **141** as a colorless solid.

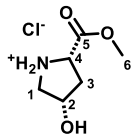

M ($C_6H_{12}NO_3Cl$):	181.05 g/mol.
Yield:	2.36 g (12.2 mmol; quant.; 96 wt%; Lit.[203]: quant.).
R_f:	(SiO_2, *c*Hex/EtOAc 1:1) = 0.00.
^{1}H NMR:	(500 MHz, DMSO-d_6) δ [ppm] = 9.73 (s, 2H, NH_2^+), 5.45 (s, 1H, O*H*), 4.49 (dd, ^3J = 9.8 Hz, ^3J = 3.7 Hz, 1H, H4), 4.38-4.35 (m, 1H, H2), 3.75 (s, 3H, H6), 3.21 (dd, ^3J = 11.8 Hz, ^3J = 3.9 Hz, 1H, H1a), 3.15 (d, ^3J = 11.7 Hz, 1H, H1b), 2.31 (ddd, ^3J = 13.8 Hz, ^3J = 10.0 Hz, ^3J = 4.6 Hz, 1H, H3a), 2.14 (dquin. , ^3J = 13.6 Hz, ^3J = 1.6 Hz, 1H, H3b).
^{13}C NMR:	(125 MHz, DMSO-d_6) δ [ppm] = 169.6 (C5); 68.1 (C2); 57.4 (C4); 53.0 (C6); 53.0 (C1), 37.0 (C3).

6.2.5.4 Synthesis of 143

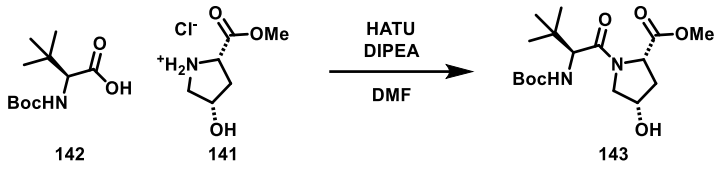

According to a modified procedure by *He et al*.[202]: In a 50 mL *Schlenk* flask, 2.33 g (10.1 mmol; 1.00 eq.) of acid **142**, 1.83 g (12.6 mmol; 1.25 eq.) of amine **141**, 4.01 g (10.6 mmol; 1.05 eq.) of HATU and 6.1 mL (38 mmol; 3.8 eq.) of DIPEA were added in 19 mL of DMF. The mixture was stirred at room temperature until full conversion of **142** was observed by TLC after 19 h. To the mixture, 75 mL of H_2O were added, and the mixture was extracted with 200 mL of EtOAc four times. The combined organic layers were washed with 5% citric acid, $NaHCO_3$ solution and NaCl solution, dried over $MgSO_4$, filtered, and the solvent was removed under reduced pressure to obtain 3.20 g (8.93 mmol; 89%; 97 wt%) of the desired product **143** as a colorless oil.

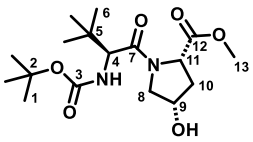

M ($C_{17}H_{30}N_2O_6$): 358.43 g/mol.

Yield: 3.20 g (8.93 mmol; 89%; 97 wt%; Lit.[202]: 50%).

R_f: (SiO_2, *c*Hex/EtOAc 1:1) = 0.46.

^{1}H NMR: (500 MHz, $CDCl_3$) δ [ppm] = 5.22 (d, ^3J = 9.6 Hz, 1H, N*H*), 4.61 (dd, ^3J = 9.7 Hz, ^3J = 2.4 Hz, 1H, H11), 4.48-4.44 (m, 1H, H9); 4.25 (d, ^3J = 9.7 Hz, 1H, H4), 3.92 (dd, ^3J = 11.1 Hz, ^3J = 4.6 Hz, 1H, H8a), 3.84 (d, ^3J = 3.7 Hz, 1H, H8b), 3.78 (s, 3H, H13), 3.36 (d, ^3J = 8.7 Hz, 1H, O*H*), 2.34 (ddd, ^3J = 14.2 Hz, ^3J = 9.8 Hz, ^3J = 4.6 Hz, 1H, H10a), 2.11 (d, ^3J = 3.7 Hz, 1H, H10b), 1.42 (s, 9H, H1), 1.05 (s, 9H, H6).

^{13}C NMR: (125 MHz, $CDCl_3$) δ [ppm] = 174.6 (C12); 171.6 (C7); 155.9 (C3); 79.8 (C2); 71.2 (C9); 58.4 (C4); 57.7 (C11); 56.7 (C8); 52.9 (C13); 36.9 (C10); 35.7 (C5); 28.5 (C1); 26.4 (C6).

6.2.5.5 Synthesis of 144

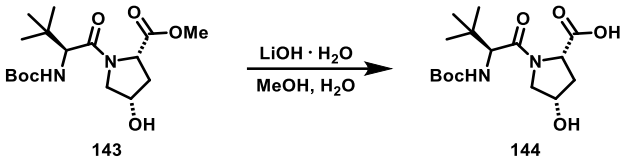

143 144

According to a modified procedure by *He et al*.[202]: In a 50 mL round bottom flask, 848 mg (2.36 mmol; 1.00 eq.) of dipeptide **143** were dissolved in 9 mL of MeOH and 4.5 mL of H_2O. To the mixture, 129 mg (3.07 mmol; 1.30 eq.) of LiOH hydrate were added. The mixture was stirred at room temperature until full conversion of dipeptide **143** was observed by TLC after 21 h. The solvent was removed under reduced pressure, and the residue was dissolved in 20 mL of H_2O. The aqueous solution was washed with 20 mL of M*t*BE, acidified with HCl (1M) to pH 1, and extracted with 100 mL of CH_2Cl_2 five times. The combined organic layers were dried over $MgSO_4$, filtered, and the solvent was removed under reduced pressure. The residue was dissolved in MeCN/H_2O and lyophilized to obtain 638 mg (1.85 mmol; 78%) of the desired product **144** as a colorless lyophilizate.

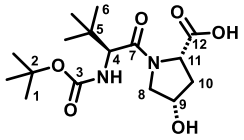

M ($C_{16}H_{28}N_2O_6$): 344.41 g/mol.

Yield: 638 mg (1.85 mmol; 78%; Lit.[202]: 80%).

R_f: (SiO_2, *c*Hex/EtOAc 1:1) = 0.07.

^{1}H NMR: (500 MHz, $CDCl_3$) δ [ppm] = 5.28 (d, ^3J = 9.4 Hz, 1H, N*H*), 4.71 (d, ^3J = 9.0 Hz, 1H, H11), 4.51 (s, 1H, H9), 4.26 (d, ^3J = 9.7 Hz, 1H, H4), 3.93 (dd, ^3J = 11.0 Hz, ^3J = 3.5 Hz, 1H, H8a), 3.81 (d, ^3J = 11.0 Hz, 1H, H8b), 2.42 (d, ^3J = 13.8 Hz, 1H, H10a), 2.31-2.26 (m, 1H, H10b), 1.43 (s, 9H, H1), 1.04 (s, 9H, H6).

^{13}C NMR: (125 MHz, $CDCl_3$) δ [ppm] = 173.7 (C12); 172.3 (C7); 155.9 (C3); 80.2 (C2); 71.0 (C9); 58.8 (C4); 58.6 (C11); 57.3 (C8); 35.8 (C10); 35.5 (C5); 28.5 (C1); 26.4 (C6).

LC-MS (ESI):

t_r [min]		12.33-13.60
Ion	Calc. mass [u]	Exp. mass [u]
$[M+H]^+$	345.202	345.15

6.2.5.6 Synthesis of 135 variant A

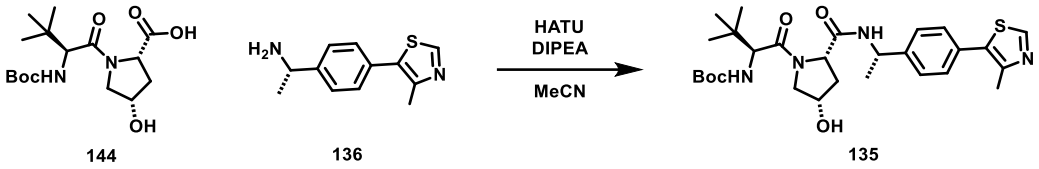

According to a modified procedure by *Desantis et al*.[204]: In a 50 mL Schlenk flask, 1.62 g (4.70 mmol; 1.00 eq.) of acid **144**, 1.02 g (4.70 mmol; 1.00 eq.) of amine **136**, 1.97 g (5.17 mmol; 1.10 eq.) of HATU, and 2.05 mL (11.8 mmol; 2.50 eq.) of DIPEA were added in 26 mL of MeCN. The mixture was stirred at room temperature until full conversion of amine **136** was observed by TLC after 18 h and the solvent was removed under reduced pressure. The crude product was purified by column chromatography (SiO_2, *c*Hex/EtOAc 1:2 to 0:1). The residue was dissolved in MeCN/H_2O lyophilized to obtain 2.46 g (4.51 mmol; 96%) of the desired product **135** as a colorless lyophilizate.

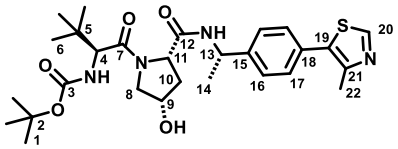

M ($C_{28}H_{40}N_4O_5S$): 544.71 g/mol.

Yield: 2.46 g (4.51 mmol; 96%; Lit.[204]: 25%).

R_f: (SiO_2, *c*Hex/EtOAc 1:2) = 0.12.

^{1}H NMR: (500 MHz, $CDCl_3$) δ [ppm] = 8.68 (s, 1H, H20); 7.64 (d, ^3J = 7.6 Hz, 1H, N*H*), 7.43 (d, ^3J = 7.8 Hz, 2H, H17), 7.37 (d, ^3J = 8.3 Hz, 2H, H16), 5.41 (d, ^3J = 9.2 Hz, 1H, N*H*), 5.17 (d, ^3J = 9.2 Hz, 1H, O*H*); 5.08 (t, ^3J = 7.0 Hz, 1H, H13), 4.79 (d, ^3J = 8.6 Hz, 1H, H11), 4.50-4.44 (m, 1H, H9); 4.24 (d, ^3J = 9.7 Hz, 1H, H4), 3.91 (dd, ^3J = 11.0 Hz, ^3J = 3.9 Hz, 1H, H8a), 3.80 (d, ^3J = 11.0 Hz, 1H, H8b), 2.54 (s, 3H, H22), 2.38 (d, ^3J = 14.0 Hz, 1H, H10a), 2.21-2.12 (m, 1H, H10b), 1.50 (d, ^3J = 6.8 Hz, 3H, H14), 1.43 (s, 9H, H1), 1.05 (s, 9H, H6).

^{13}C NMR: (125 MHz, $CDCl_3$) δ [ppm] = 173.2 (C7); 171.6 (C12); 155.8 (C3); 150.0 (C20); 148.8 (C21); 142.4 (C15); 131.6 (C19); 131.4 (C18); 129.9 (C17); 126.6 (C16); 80.0 (C2); 71.2 (C9); 60.0 (C11); 58.9 (C8), 58.6 (C4); 49.5 (C13);

35.5 (C5); 34.6 (C10); 28.5 (C1); 26.5 (C6); 22.1 (C14); 16.3 (C22).
Note: C20 was assigned by HSQC.

6.2.5.7 Synthesis of 146

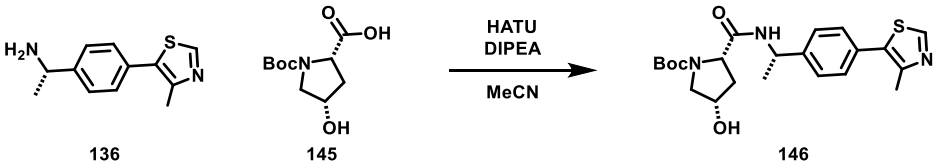

According to a modified procedure by *Desantis et al*.[204]: In a 25 mL *Schlenk* flask, 469 mg (2.03 mmol; 1.05 eq.) of acid **145**, 422 mg (1.93 mmol; 1.00 eq.) of amine **136**, 833 mg (2.19 mmol; 1.10 eq.) of HATU, and 765 µL (4.39 mmol; 2.20 eq.) of DIPEA were added in 10 mL of MeCN. The mixture was stirred at room temperature until full conversion of amine **136** was observed by TLC after 19 h. The solvent was removed under reduced pressure, and the residue was purified by column chromatography (SiO_2, *c*Hex/EtOAc/MeOH 25:25:1 to 10:10:1) to obtain 803 mg (1.86 mmol; 96%; 97 wt%) of the desired product **146** as a colorless oil.

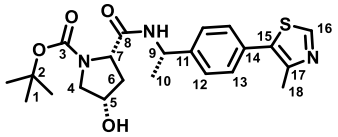

M ($C_{22}H_{29}N_3O_4S$): 431.55 g/mol.

Yield: 803 mg (1.86 mmol; 96%; 97 wt%; Lit.[204]: quant.).

R_f: (SiO_2, *c*Hex/EtOAc/MeOH 25:25:1) = 0.08.

^{1}H NMR: (500 MHz, $CDCl_3$) d [ppm] = 8.70 (s, 1H, H16), 7.67 (d, ^3J = 7.1 Hz, 1H, N*H*), 7.42 (d, ^3J = 8.3 Hz, 2H, H13), 7.38 (d, ^3J = 8.3 Hz, 2H, H12), 5.15 (s, 1H, O*H*), 5.07 (quin, ^3J = 8.3 Hz, 1H, H9), 4.44 (d, ^3J = 8.8 Hz, 1H, H7), 4.38 (s, 1H, H5), 3.64-3.43 (m, 2H, H4), 2.53 (s, 3H, H18), 2.37-2.09 (m, 2H, H6), 1.53-1.37 (m, 12H, H1, H10).

^{13}C NMR: (125 MHz, $CDCl_3$) d [ppm] = 172.6 (C8); 156.1 (C3); 150.6 (C16); 148.5 (C17); 143.0 (C11); 131.8 (C15); 131.0 (C14); 129.7 (C13); 126.6 (C12); 81.0 (C2); 70.9 (C5); 59.8 (C7); 57.2 (C4); 49.4 (C9); 35.5 (C6); 28.5 (C1); 22.0 (C10); 16.1 (C18).

6.2.5.8 Synthesis of 147

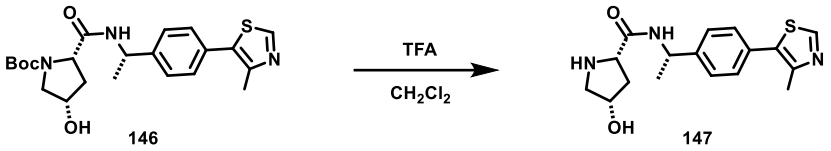

According to a modified procedure by *Desantis et al*.[204]: In a 25 mL round bottom flask, 800 mg (1.92 mmol, 1.00 eq.) of the Boc-protected amine **146** were dissolved in 4 mL of CH_2Cl_2 and 1 mL of TFA was added to the mixture. After 24 h, full conversion of the Boc-protected amine **146** was observed by TLC and the solvent was removed under reduced pressure. Next, 30 mL of H_2O and 50 mL of CH_2Cl_2 were added and $NaHCO_3$ was added until no more gas formation was detected. The aqueous phase was extracted with 100 mL of CH_2Cl_2 five times and the combined organic layers were dried over $MgSO_4$, filtered, and the solvent was removed under reduced pressure to obtain 320 mg (966 μmol; 50%) of the desired product **147** as a pale-yellow oil.

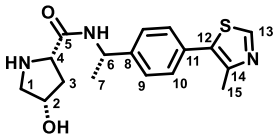

M ($C_{17}H_{21}N_3O_2S$): 331.43 g/mol.

Yield: 320 mg (966 μmol; 50%; Lit.[204]: quant.).

R_f: (SiO_2, EtOAc/MeOH/NEt_3 20:4:1) = 0.22.

^{1}H NMR: (500 MHz, $CDCl_3$) d [ppm] = 8.68 (s, 1H, H13), 7.77 (d, ^3J = 8.4 Hz, 1H, N*H*), 7.42 (d, ^3J = 8.3 Hz, 2H, H10), 7.38 (d, ^3J = 8.3 Hz, 2H, H9), 5.13 (quin, ^3J = 7.4 Hz, 1H, H6), 4.41 (sept, ^3J = 8.3 Hz, 1H, H2), 3.80 (dd, ^3J = 9.9 Hz, ^3J = 3.4 Hz, 1H, H4), 3.16 (dd, ^2J = 11.0 Hz, ^3J = 4.2 Hz, 1H, H1a), 3.06 (dt, ^2J = 11.0 Hz, ^3J = 1.6 Hz, 1H, H1b), 2.53 (s, 3H, H15), 2.31 (ddd, ^2J = 13.9 Hz, ^3J = 9.6 Hz, ^3J = 4.7 Hz, 1H, H3a), 2.14 (dquin, ^2J = 13.8 Hz, ^3J = 1.7 Hz, 1H, H3b), 1.52 (d, ^3J = 6.9 Hz, 3H, H7).

^{13}C NMR: (125 MHz, $CDCl_3$) d [ppm] = 174.3 (C5); 150.3 (C13); 148.2 (C14); 143.3 (C8); 131.7 (C12); 131.0 (C11); 129.7 (C10); 126.7 (C9); 72.2 (C2); 59.7 (C4); 55.2 (C1); 48.1 (C6); 40.0 (C3); 21.9 (C7); 16.2 (C15).

6.2.5.9 Synthesis of 135 variant B

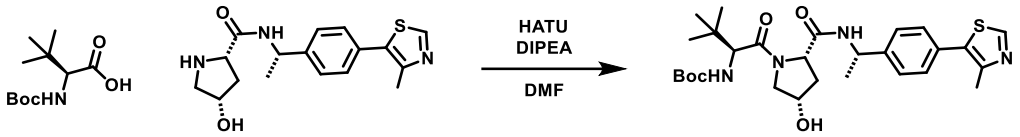

According to a modified procedure by *Desantis et al*.[204]: In a 10 mL *Schlenk* flask, 259 mg (1.12 mmol; 1.20 eq.) of acid **142**, 498 mg (1.31 mmol; 1.40 eq.) of HATU, and 203 μL (1.17 mmol; 1.25 eq.) of DIPEA were added in 2.5 mL of DMF. In a 10 mL *Schlenk* flask, 310 mg (935 μmol; 1.00 eq.) of amine **147** and 203 μL (1.17 mmol; 1.25 eq.) of DIPEA were added in 2.5 mL of DMF. After 30 min, the mixture was added to the solution of acid **142**. The mixture was stirred at room temperature until full conversion of amine **147** was observed by TLC after 20 h and the solvent was removed under reduced pressure. The crude product was purified by column chromatography (dryload, SiO_2, *c*Hex/EtOAc 1:2) and the solvent was evaporated. The residue was dissolved in CH_2Cl_2, filtered through a syringe filter, and the solvent was removed under reduced pressure to obtain 309 mg (567 μmol; 61%) of the desired product **135** as a pale-yellow oil.

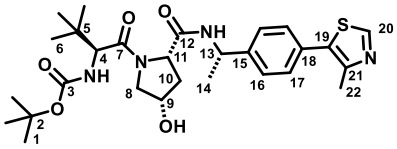

M ($C_{28}H_{40}N_4O_5S$): 544.71 g/mol.

Yield: 309 mg (567 μmol; 61%; Lit.[204]: 67%).

R_f: (SiO_2, *c*Hex/EtOAc 1:2) = 0.12.

^{1}H NMR: (500 MHz, $CDCl_3$) δ [ppm] = 8.68 (s, 1H, H20); 7.64 (d, ^3J = 7.6 Hz, 1H, N*H*), 7.43 (d, ^3J = 7.8 Hz, 2H, H17), 7.37 (d, ^3J = 8.3 Hz, 2H, H16), 5.41 (d, ^3J = 9.2 Hz, 1H, N*H*), 5.17 (d, ^3J = 9.2 Hz, 1H, O*H*); 5.08 (t, ^3J = 7.0 Hz, 1H, H13), 4.79 (d, ^3J = 8.6 Hz, 1H, H11), 4.50-4.44 (m, 1H, H9); 4.24 (d, ^3J = 9.7 Hz, 1H, H4), 3.91 (dd, ^3J = 11.0 Hz, ^3J = 3.9 Hz, 1H, H8a), 3.80 (d, ^3J = 11.0 Hz, 1H, H8b), 2.54 (s, 3H, H22), 2.38 (d, ^3J = 14.0 Hz, 1H, H10a), 2.21-2.12 (m, 1H, H10b), 1.50 (d, ^3J = 6.8 Hz, 3H, H14), 1.43 (s, 9H, H1), 1.05 (s, 9H, H6).

^{13}C NMR: (125 MHz, $CDCl_3$) δ [ppm] = 173.2 (C7); 171.6 (C12); 155.8 (C3); 150.0 (C20); 148.8 (C21); 142.4 (C15); 131.6 (C19); 131.4 (C18); 129.9 (C17); 126.6 (C16); 80.0 (C2); 71.2 (C9); 60.0 (C11); 58.9 (C8), 58.6 (C4); 49.5 (C13); 35.5 (C5); 34.6 (C10); 28.5 (C1); 26.5 (C6); 22.1 (C14); 16.3 (C22).
Note: C20 was assigned by HSQC.

LC-MS (ESI):

t_r [min]		18.22-18.50
Ion	Calc. mass [u]	Exp. mass [u]
$[M+H]^+$	545.28	545.27

6.2.5.10 Synthesis of *epi*-113

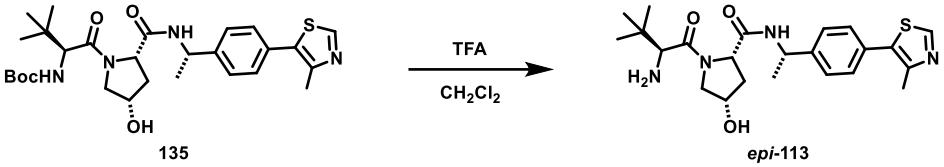

According to a modified procedure by *He et al*.[202]: In a 10 mL round bottom flask, 303 mg (556 μmol; 1.00 eq.) of the Boc-protected amine **135** were dissolved in 1 mL of CH_2Cl_2 and 250 μL of TFA were added. After 92 h, full conversion of the Boc-protected amine **135** was observed by TLC and the solvent was removed under reduced pressure. The residue was dissolved in 20 mL of CH_2Cl_2 and 20 mL of $NaHCO_3$ and the aqueous phase was extracted with 100 mL of CH_2Cl_2 five times. The combined organic layers were dried over Na_2SO_4, filtered, and the solvent was removed under reduced pressure to obtain 197 mg (443 μmol; 79%; 99 wt%) of the desired product ***epi*-113** as a colorless foam.

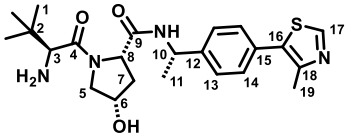

M ($C_{23}H_{32}N_4O_3S$): 444.59 g/mol.

Yield: 197 mg (443 μmol; 79%; 99 wt%; Lit.[202]: 90%).

R_f: (SiO_2, *c*Hex/EtOAc 1:2) = 0.11.

^{1}H NMR: (500 MHz, $CDCl_3$) δ [ppm] = 8.68 (s, 1H, H17), 7.8 (d, ^3J = 7.5 Hz, 1H, N*H*), 7.43 (d, ^3J = 8.2 Hz, 2H, H14), 7.38 (d, ^3J = 9.2 Hz, 2H, H13), 5.08 (quin, ^3J = 7.2 Hz, 1H, H10), 4.81 (d, ^3J = 8.9 Hz, 1H, H8), 4.47 (t, ^3J = 4.3 Hz, 1H, H6), 3.79-3.71 (m, 2H, H5), 3.31 (s, 1H, H3), 2.54 (s, 3H, H19), 2.38 (d, ^3J = 14.3 Hz, 1H, H7a), 2.11 (ddd, ^2J = 14.0 Hz, ^3J = 8.9 Hz, ^3J = 4.9 Hz, 1H, H7b), 1.50 (d, ^3J = 7.0 Hz, 3H, H11), 1.04 (s, 9H, H1).

^{13}C NMR: (125 MHz, $CDCl_3$) δ [ppm] = 175.3 (C4); 171.7 (C9); 150.5 (C17); 148.7 (C18); 142.5 (C12); 131.6 (C16); 131.3 (C15); 129.6 (C14); 126.6 (C13); 71.1 (C6); 60.5 (C3); 59.9 (C8); 58.5 (C5); 49.4 (C10); 38.7 (C7); 35.8 (C2); 26.2 (C1); 22.0 (C11); 16.2 (C19).

6.2.5.11 Synthesis of *epi*-114

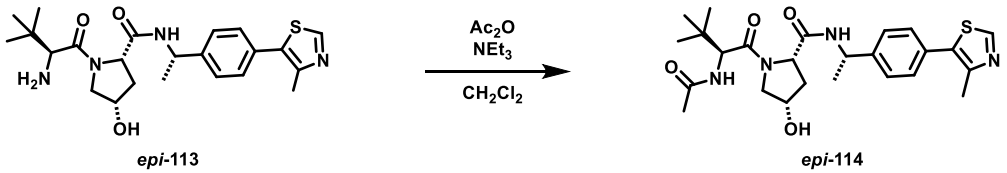

epi-113 *epi*-114

According to a modified procedure by *Zhao et al*.[201]: In a 10 mL *Schlenk* flask, 80 mg (0.17 mmol; 1.0 eq.) of amine ***epi*-113** and 58 μL (0.42 mmol; 2.5 eq.) of NEt_3 were dissolved in 4 mL of CH_2Cl_2 and 24 μL (0.25 mmol; 1.5 eq.) of Ac_2O were added. The mixture was stirred at room temperature until full conversion of amine ***epi*-113** was observed by TLC after 23 h. The crude reaction mixture was purified by column chromatography (CH_2Cl_2/MeOH/NEt_3 1:0:0 to 100:5:1). The residue was then purified by reverse phase column chromatography (MeCN/H_2O 2:8 to 7:3) and lyophilized to obtain 62 mg (0.13 mmol; 77%) of the desired product ***epi*-114** as a colorless lyophilizate.

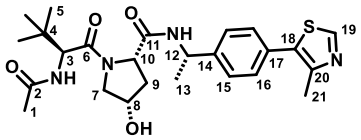

M ($C_{25}H_{34}N_4O_4S$): 486.63 g/mol.

Yield: 62 mg (0.13 mmol; 77%; Lit.[201]: 98%).

R_f: (SiO_2, CH_2Cl_2/MeOH 10:1) = 0.43.

^{1}H NMR: (500 MHz, $CDCl_3$) δ [ppm] = 8.69 (s, 1H, H19), 7.56 (d, ^3J = 8.1 Hz, 1H, N*H*), 7.43 (d, ^3J = 8.2 Hz, 2H, H16), 7.37 (d, ^3J = 8.2 Hz, 2H, H15), 6.08 (d, ^3J = 9.0 Hz, 1H, N*H*), 5.41 (d, ^3J = 9.3 Hz, 1H, O*H*), 5.09 (quin, ^3J = 7.3 Hz, 1H, H12), 4.74 (d, ^3J = 8.9 Hz, 1H, H10), 4.58 (d, ^3J = 9.4 Hz, 1H, H3), 4.48 (dt, ^3J = 9.5 Hz , ^3J = 4.5 Hz, 1H, H8), 3.94 (dd, ^3J = 11.0 Hz, ^3J = 4.2 Hz, 1H, H7a), 3.83 (d, ^3J = 11.1 Hz, 1H, H7b), 2.54 (s, 3H, H21), 2.36 (d, ^3J = 13.7 Hz, 1H, H9a), 2.14 (ddd, ^3J = 14.3 Hz, ^3J = 9.2 Hz, ^3J = 4.2 Hz, 1H, H9b), 2.02 (s, 3H, H1), 1.50 (d, ^3J = 6.9 Hz, 3H, H13), 1.06 (s, 9H, H5).

^{13}C NMR: (125 MHz, $CDCl_3$) δ [ppm] = 172.7 (C6); 171.5 (C2); 170.2 (C11); 150.5 (C19); 148.8 (C20); 142.4 (C14); 131.5 (C18); 131.4 (C17); 129.8 (C16); 126.6 (C15); 71.1 (C8); 60.1 (C10); 58.9 (C3); 57.2 (C7); 49.4 (C12); 35.3 (C9); 34.8 (C4); 26.5 (C5); 23.4 (C1); 22.1 (C13); 16.2 (C21).

HR-MS (ESI):

Ion	Calc. mass [u]	Exp. mass [u]	Δ [ppm]
$[M+H]^+$	487.23735	487.23728	-0.14
$[M+Na]^+$	509.21930	509.21863	-1.31

LC-MS (ESI):

t_r [min]		11.63-12.19	
Ion	Calc. mass [u]	Exp. mass [u]	Purity [%]
$[M+H]^+$	487.24	487.19	91

6.2.5.12 Synthesis of *epi*-127

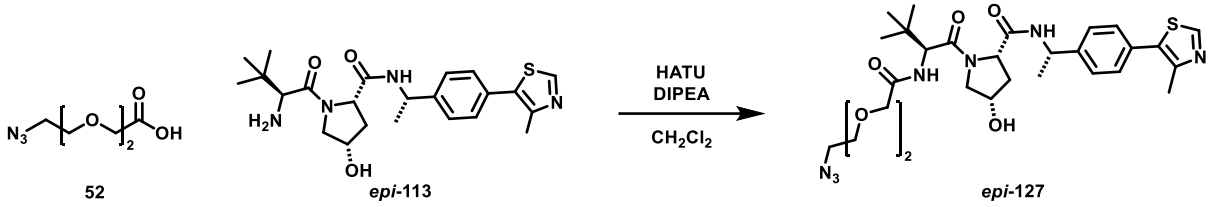

52 *epi*-113 *epi*-127

In a 5 mL *Schlenk* flask, 31 mg (0.16 mmol; 1.2 eq.) of linker **52**, 77 mg (0.20 mmol; 1.5 eq.) of HATU, and 32 μL (0.18 mmol; 1.3 eq.) of DIPEA were added in 2.4 mL of CH_2Cl_2. In a flame dried 10 mL *Schlenk* flask, 60 mg (0.14 mmol; 1.0 eq.) of amine ***epi*-113** and 32 μL (0.18 mmol; 1.3 eq.) of DIPEA were added in 2.4 mL of CH_2Cl_2. After 30 min, the mixture was added to the solution of linker **52** and the mixture was stirred at room temperature until full conversion of amine ***epi*-113** was observed by TLC after 24 h. The solvent was removed under reduced pressure, and the residue was purified by column chromatography (SiO_2, dryload, EtOAc/MeOH 10:1). The residue was dissolved in CH_2Cl_2, filtered through a syringe filter, and the solvent was removed under reduced pressure. The residue was dissolved in MeCN/H_2O and lyophilized to obtain 35 mg (57 μmol; 42%) of the desired product ***epi*-127** as a colorless lyophilizate.

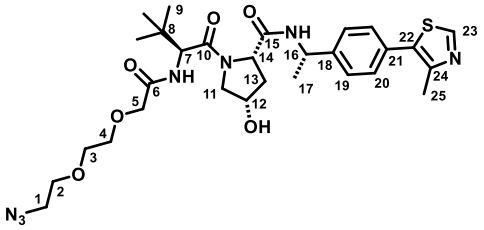

M ($C_{29}H_{41}N_7O_6S$): 615.75 g/mol.

Yield: 35 mg (57 μmol; 42%).

R_f: (SiO_2, EtOAc/MeOH 10:1) = 0.22.

^{1}H NMR: (500 MHz, $CDCl_3$) δ [ppm] = 8.69 (s, 1H, H23), 7.60 (d, ^3J = 7.9 Hz, 1H, N*H*), 7.43 (d, ^3J = 8.4 Hz, 2H, H20), 7.37 (d, ^3J = 8.4 Hz, 2H, H19), 7.24 (d, ^3J = 9.0 Hz, 1H, N*H*), 5.42 (d, ^3J = 7.3 Hz, 1H, O*H*), 5.09 (quin, ^3J = 7.2 Hz, 1H, H16), 4.77 (d, ^3J = 9.2 Hz, 1H, H14), 4.61 (d, ^3J = 9.0 Hz, 1H, H7), 4.47 (dt, ^3J = 9.2 Hz , ^3J = 4.1 Hz , 1H, H12), 4.07 (d, ^3J = 15.5 Hz, 1H, H5a), 4.00 (d, ^3J = 15.5 Hz, 1H, H5b), 3.94 (dd, ^3J = 10.9 Hz, ^3J = 4.2 Hz, 1H, H11a), 3.82 (d, ^3J = 11.0 Hz, 1H, H11b), 3.73-3.68 (m, 6H, H2, H3, H4), 3.48-3.00 (m, 2H, H1), 2.54 (s, 3H, H25), 2.37 (t,

^3J = 14.3 Hz, 1H, H13a), 2.12 (ddd, ^3J = 10.9 Hz, ^3J = 9.1 Hz, ^3J = 5.0 Hz, 1H, H13b), 1.51 (d, ^3J = 6.9 Hz, 3H, H17), 1.07 (s, 9H, H9).

^{13}C NMR: (125 MHz, $CDCl_3$) δ [ppm] = 172.1 (C10); 171.6 (C6); 169.8 (C15); 150.2 (C23); 148.8 (C24); 142.5 (C18); 131.6 (C22); 131.4 (C21); 129.8 (C20); 126.6 (C19); 71.3, 70.6, 70.6, 70.3 (C2, C3, C4, C5); 71.2 (C12); 60.0 (C14); 58.9 (C7); 56.6 (C11); 50.7 (C1); 49.9 (C16); 35.4 (C13); 34.7 (C8); 26.5 (C9); 22.0 (C17); 16.3 (C25).

HR-MS (ESI):

Ion	Calc. mass [u]	Exp. mass [u]	Δ [ppm]
$[M+H]^+$	616.29118	616.29161	+1.02
$[M+Na]^+$	638.27312	638.27318	+0.09

6.2.5.13 Synthesis of *epi*-118

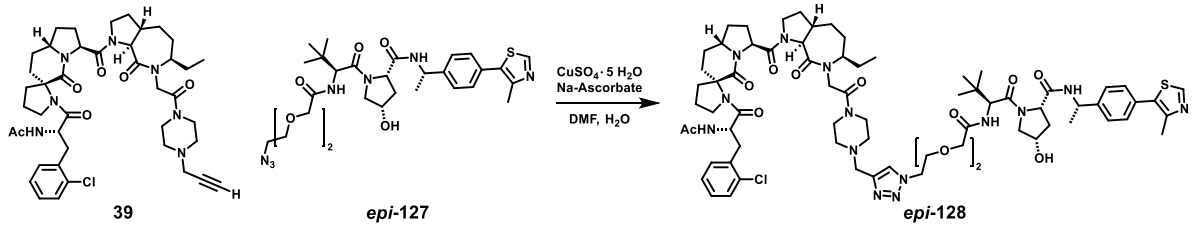

According to a modified procedure by *Banerjee et al*.[196]: In a headspace vial, 23 mg (29 μmol; 1.0 eq.) of warhead-linker conjugate **39** and 27 mg (44 μmol; 1.5 eq.) of linker-recruiter conjugate ***epi*-127** were dissolved in 2 mL of DMF. Next, 1 mL of an aqueous solution (3mM; 3 μmol; 10 mol%) of $CuSO_4$ and 1 mL of an aqueous solution (6mM; 6 μmol; 20 mol%) of sodium ascorbate were added, and the mixture was stirred at room temperature for 22 h. Full conversion of warhead-linker conjugate **39** was observed by TLC and the solvent was removed under reduced pressure. The crude product was purified by column chromatography (dryload, 7 g ultra-pure silica, EtOAc/MeOH/NEt_3 1:0:0 to 20:4:1). The product was dissolved in CH_2Cl_2, filtered through a syringe filter, and the solvent was removed under reduced pressure. The residue was purified by reverse phase column chromatography (MeCN/H_2O 4:6) and lyophilized to obtain 30 mg (21 μmol; 73%) of the desired product ***epi*-118** as a colorless lyophilizate.

M ($C_{71}H_{97}N_{14}O_{12}SCl$):	1406.15 g/mol.			
Yield:	30 mg (21 μmol; 73%).			
R_f:	(SiO_2, EtOAc/MeOH/NEt_3 20:4:1) = 0.06.			
HR-MS (ESI):	Ion	Calc. mass [u]	Exp. mass [u]	Δ [ppm]
	$[M+H]^+$	1405.68924	1405.68788	-0.97
	$[M+Na]^+$	1427.67118	1427.66734	-2.69
LC-MS (ESI):	t_r [min]		11.09-11.60, 12.69-13.26	
	Ion	Calc. mass [u]	Exp. mass [u]	Purity [%]
	$[M+H]^+$	1405.69	1405.97	>99

6.2.6 Synthesis towards PROTACs 168-171

6.2.6.1 Synthesis of 160

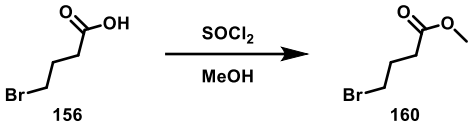

This experiment was carried out by *Alexander Klingert*. According to a modified procedure by *Albat*[193]:3.00 g (18.0 mmol; 1.00 eq.) of acid **156** were dissolved in 60 mL of MeOH and 1.98 mL (26.9 mmol; 1.50 eq.) of $SOCl_2$ were added. The mixture was stirred at room temperature until full conversion of acid **156** was observed by TLC after 2 h. The solvent was removed under reduced pressure and the residue was purified by column chromatography (SiO_2, *c*Hex/EtOAc 10:1). The solvent was removed under reduced pressure to obtain 2.56 g (14.1 mmol; 79%) of the desired product **160** as a pale-yellow oil.

M ($C_5H_9O_2Br$):	181.03 g/mol.
Yield:	2.56 g (14.1 mmol; 79%).
R_f:	(SiO_2, *c*Hex/EtOAc 10:1) = 0.53.
^{1}H NMR:	(300 MHz, $CDCl_3$) δ [ppm] = 3.69 (s, 3H, H5), 3.47 (t, ^3J = 6.3 Hz, 2H, H1), 2.52 (t, ^3J = 7.7 Hz, 2H, H3), 2.18 (quin, ^3J = 6.8 Hz, 2H, H2).

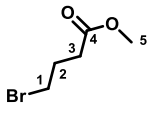

6.2.6.2 Synthesis of 164

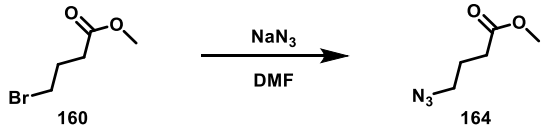

This experiment was carried out by *Alexander Klingert*. According to a modified procedure by *Simonin et al*.[215]: In a 50 mL round bottom flask, 2.56 g (14.1 mmol; 1.00 eq.) of ester **160** were dissolved in 7.6 mL of DMF, 3.68 g (56.6 mmol; 4.00 eq.) of NaN_3 were added, and the mixture was stirred at 60 °C for 17 h. After cooling to room temperature, 10 mL of H_2O were added, and the mixture was extracted with 20 mL of Et_2O three times. The combined organic layers were washed with 20 mL of H_2O three times, followed by 20 mL of NaCl solution. The mixture was dried over $MgSO_4$, filtered, and the solvent was removed under reduced pressure to obtain 1.44 g (10.1 mmol; 71%) of the desired product **164** as a pale-yellow oil.

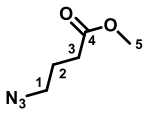

M ($C_5H_9N_3O_2$):	143.15 g/mol.
Yield:	1.44 g (10.1 mmol; 71%).
R_f:	(SiO_2, *c*Hex/EtOAc 10:1) = 0.39.
^{1}H NMR:	(300 MHz, $CDCl_3$) δ [ppm] = 3.69 (s, 3H, H5); 3.36 (t, ^3J = 6.5 Hz, 2H, H1), 2.42 (t, ^3J = 7.5 Hz, 2H, H3), 1.92 (quin, ^3J = 7.0 Hz, 2H, H2).

6.2.6.3 Synthesis of 148

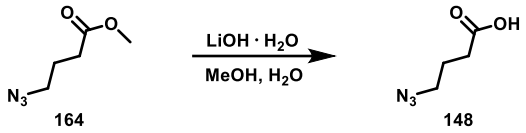

This experiment was carried out by *Alexander Klingert*. According to a modified procedure by *Albat*[193]: In a 100 mL round bottom flask, 1.44 g (10.1 mmol; 1.00 eq.) of ester **164** were dissolved in 24 mL of MeOH and 12 mL of H_2O. Next, 1.18 g (28.2 mmol; 2.8 eq.) of LiOH hydrate were added, the mixture was stirred at room temperature until full conversion of ester **164** was observed by TLC after 21 h, and the solution was concentrated under reduced pressure. 20 mL of HCl (1M) and 20 mL of CH_2Cl_2 were added and the layers were separated. The aqueous phase was extracted five times with 20 mL of CH_2Cl_2 and the combined organic layers were dried over $MgSO_4$, filtered, and the solvent was removed under reduced pressure to obtain 1.12 g (8.64 mmol; 86%) of the desired product **148** as a pale-yellow oil.

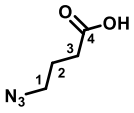

M ($C_4H_7N_3O_2$):	129.12 g/mol.
Yield:	1.12 g (8.64 mmol; 86%).
R_f:	(SiO_2, *c*Hex/EtOAc 1:2) = 0.25.
^{1}H NMR:	(500 MHz, $CDCl_3$) δ [ppm] = 3.38 (t, ^3J = 6.7 Hz, 2H, H1), 2.48 (t, ^3J = 7.3 Hz, 2H, H3), 1.92 (quin, ^3J = 7.0 Hz, 2H, H2).
^{13}C NMR:	(125 MHz, $CDCl_3$) δ [ppm] = 179.0 (C4); 50.6 (C1); 31.0 (C3); 24.1 (C2).

6.2.6.4 Synthesis of 152

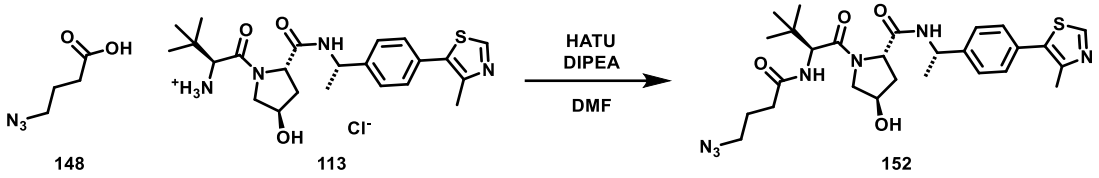

In a 50 mL *Schlenk* tube, 68 mg (0.53 mmol; 1.0 eq.) of linker **148**, 209 mg (550 μmol; 1.10 eq.) of HATU, and 305 μL (1.75 mmol; 3.50 eq.) of DIPEA were added in 15 mL of DMF. After 30 min, 240 mg (500 μmol; 1.00 eq.) of recruiter **113** were added and the mixture was stirred at room temperature until full conversion of recruiter **113** was observed by TLC after 16 h and the solvent was removed under reduced pressure. The residue was purified by column chromatography (SiO_2, EtOAc/MeOH 1:0 to 10:1). The residue was dissolved in CH_2Cl_2, filtered through a syringe filter, and the solvent was removed under reduced pressure. The residue was dissolved in *t*BuOH/MeCN/H_2O and lyophilized to obtain 191 mg (343 μmol; 69%; 88 wt%) of the desired product **152** as a colorless lyophilizate.

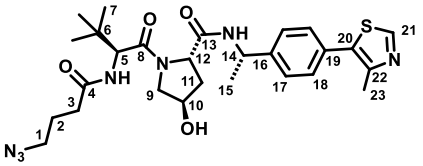

M ($C_{27}H_{37}N_7O_4S$): 555.70 g/mol.

Yield: 191 mg (343 μmol; 69%; 88 wt%).

R_f: (SiO_2, EtOAc/MeOH 10:1) = 0.24.

^{1}H NMR: (400 MHz, $CDCl_3$) δ [ppm] = 8.70 (s, 1H, H21), 7.51 (d, ^3J = 8.0 Hz, 1H, N*H*), 7.40 (d, ^3J = 8.4 Hz, 2H, H18), 7.37 (d, ^3J = 8.0 Hz, 2H, H17), 6.70 (d, ^3J = 9.2 Hz, 1H, N*H*), 5.10 (quin, ^3J = 7.7 Hz, 1H, H14), 4.69 (t, ^3J = 8.0 Hz, 1H, H12); 4.64 (d, ^3J = 9.0 Hz, 1H, H5), 4.51 (s, 1H, H10), 4.01 (d, ^3J = 11.2 Hz, 1H, H9a), 3.65 (dd, ^3J = 11.2 Hz, ^3J = 3.6 Hz, 1H, H9b), 3.32 (td, ^3J = 6.5 Hz, ^3J = 1.8 Hz, 2H, H1), 2.51 (s, 3H, H23), 2.42-2.36 (m, 1H, H11a), 2.35-2.21 (m, 2H, H2), 2.10-2.01 (m, 1H, H11b), 1.96-1.80 (m, 2H, H3), 1.48 (d, ^3J = 7.0 Hz, 3H, H15), 1.05 (s, 9H, H7).

^{13}C NMR:	(100 MHz, $CDCl_3$) δ [ppm] = 172.3 (C4); 171.6 (C8); 170.0 (C13); 150.5 (C21); 148.3 (C22); 143.2 (C16); 131.6 (C20); 130.7 (C19); 129.5 (C18); 126.4 (C17); 69.7 (C10); 58.8 (C12); 57.5 (C5); 56.8 (C9); 50.6 (C1); 48.7 (C14); 35.9 (C11); 35.4 (C6); 32.8 (C2); 26.5 (C7); 24.7 (C3); 22.0 (C15); 16.0 (C23).			
HR-MS (ESI):	Ion	Calc. mass [u]	Exp. mass [u]	Δ [ppm]
	$[M+H]^+$	556.27005	556.27000	-0.09
	$[M+Na]^+$	578.25200	578.25257	-0.74
LC-MS (ESI):	t_r [min]		11.15-13.92	
	Ion	Calc. mass [u]	Exp. mass [u]	Purity [%]
	$[M+H]^+$	556.27	556.27	>99

6.2.6.5 Synthesis of 168

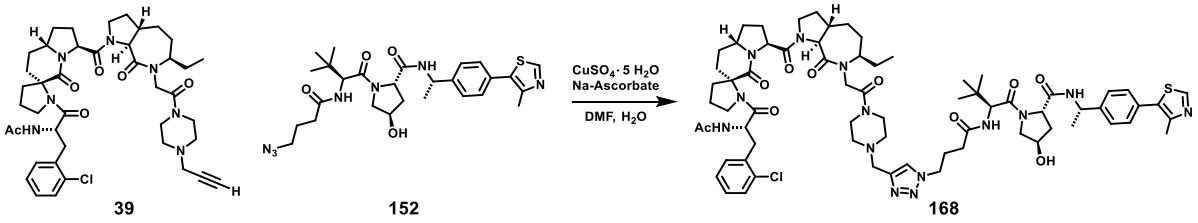

According to a modified procedure by *Banerjee et al*.[196]: In a headspace vial, 23 mg (29 μmol; 1.0 eq.) of warhead-linker conjugate **39** and 24 mg (44 μmol; 1.5 eq.) of linker-recruiter conjugate **152** were dissolved in 2 mL of DMF. Next, 1 mL of an aqueous solution (3mM; 3 μmol; 10 mol%) of $CuSO_4$ and 1 mL of an aqueous solution (6mM; 6 μmol; 20 mol%) of sodium ascorbate were added, and the mixture was stirred at room temperature for 42 h. Full conversion of warhead-linker conjugate **39** was observed by TLC and the solvent was removed under reduced pressure. The crude product was purified by column chromatography (dryload, 5 g ultra-pure silica, EtOAc/MeOH/NEt_3 1:0:0 to 20:4:1). The product was dissolved in CH_2Cl_2, filtered through a syringe filter, and the solvent was removed under reduced pressure. The residue was purified by reverse phase column chromatography (MeCN/H_2O 3:7 to 7:3) and lyophilized to obtain 15 mg (11 μmol; 38%) of the desired product **168** as a colorless lyophilizate.

M ($C_{69}H_{93}N_{14}O_{10}SCl$):	1346.10 g/mol.			
Yield:	15 mg (11 μmol; 38%).			
R_f:	(SiO_2, EtOAc/MeOH/NEt_3 20:4:1) = 0.03.			
HR-MS (ESI):	Ion	Calc. mass [u]	Exp. mass [u]	Δ [ppm]
	$[M+H]^+$	1345.66811	1345.67187	+2.80
	$[M+Na]^+$	1367.65005	1367.65276	+1.98
LC-MS (ESI):	t_r [min]		8.67-11.41	
	Ion	Calc. mass [u]	Exp. mass [u]	Purity [%]
	$[M+H]^+$	1345.67	1345.96	99

6.2.6.6 Synthesis of 161

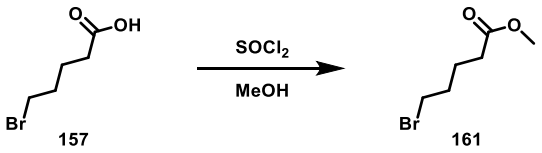

This experiment was carried out by *Alexander Klingert*. According to a modified procedure by *Albat*[193]: 5.00 g (27.6 mmol; 1.00 eq.) of linker **157** were dissolved in 92 mL of MeOH and 3.01 mL of $SOCl_2$ (41.4 mmol; 1.50 eq.) were added. The mixture was stirred at room temperature until full conversion of linker **157** was observed by TLC after 2 h. The solvent was removed under reduced pressure and the residue was purified by column chromatography (SiO_2, *c*Hex/EtOAc 10:1) to obtain 4.98 g (25.4 mmol; 92%) of the desired product **161** as a pale-yellow oil.

M ($C_6H_{11}O_2$):	195.056 g/mol.
Yield:	4.98 g (25.4 mmol; 92%).
R_f:	(SiO_2, *c*Hex/EtOAc 2:1) = 0.73.
^{1}H NMR:	(500 MHz, $CDCl_3$) δ [ppm] = 3.68 (s, 3H, H6), 3.42 (t, ^3J = 8.2 Hz, 2H, H1), 2.36 (t, ^3J = 8.2 Hz, 2H, H4), 1.93-1.88 (m, 2H, H2), 1.82-1.76 (m, 2H, H3).
^{13}C NMR:	(125 MHz, $CDCl_3$) δ [ppm] = 173.7 (C5); 51.8 (C6); 33.2, 33.1 (C1, C4); 32.1 (C2); 23.6 (C3).

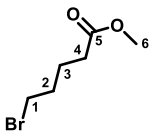

6.2.6.7 Synthesis of 165

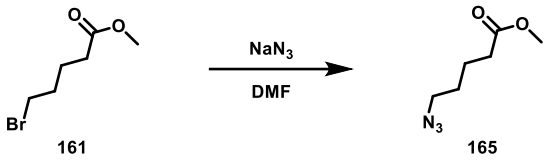

This experiment was carried out by *Alexander Klingert*. According to a modified procedure by *Simonin et al*.[215]: In a 50 mL round bottom flask, 4.98 g (25.5 mmol; 1.00 eq.) of ester **161** were dissolved in 15 mL of DMF, 6.64 g (102 mmol; 4.00 eq.) of NaN_3 were added, and the mixture was stirred at 60 °C until full conversion of ester **161** was observed by TLC after 17 h. At room temperature, 10 mL of H_2O were added, and the mixture was extracted with 20 mL of Et_2O three times. The combined organic layers were washed with 20 mL of H_2O three times, followed by 20 mL of NaCl solution. The mixture was dried over $MgSO_4$, filtered, and the solvent was removed under reduced pressure to obtain 3.26 g (20.5 mmol; 80%) of the desired product **165** as a pale-yellow oil.

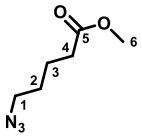

M ($C_6H_{11}N_3O_2$):	157.17 g/mol.
Yield:	3.26 g (20.5 mmol; 80%).
R_f:	(SiO_2, *c*Hex/EtOAc 2:1) = 0.58.
^{1}H NMR:	(500 MHz, $CDCl_3$) δ [ppm] = 3.68 (s, 3H, H6), 3.30 (t, ^3J = 6.6 Hz, 2H, H1), 2.36 (t, ^3J = 7.4 Hz, 2H, H4), 1.75-1.69 (m, 2H, H2), 1.67-1.61 (m, 2H, H3).

6.2.6.8 Synthesis of 149

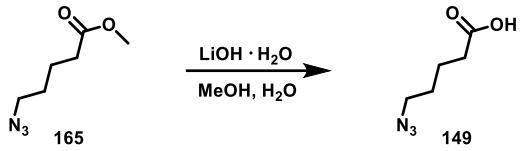

This experiment was carried out by *Alexander Klingert*. According to a modified procedure by *Albat*[193]: In a 100 mL round bottom flask, 1.85 g (10.7 mmol; 1.00 eq.) of ester **165** were dissolved in 30 mL of MeOH and 15 mL of H_2O. Next, 1.26 g (30.1 mmol; 2.80 eq.) of LiOH hydrate were added, the mixture was stirred at room temperature for 23 h, and the solution was concentrated under reduced pressure. 20 mL of HCl (1M) and 20 mL of CH_2Cl_2 were added and the layers were separated. The aqueous phase was extracted five times with 20 mL of CH_2Cl_2 and the combined organic layers were dried over $MgSO_4$, filtered, and the solvent was removed under reduced pressure to obtain 1.60 g (10.1 mmol; 94%) of the desired product **149** as a pale-yellow oil.

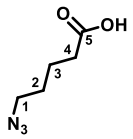

M ($C_5H_9N_3O_2$):	143.07 g/mol.
Yield:	1.60 g (10.1 mmol; 94%).
R_f:	(SiO_2, *c*Hex/EtOAc 10:1) = 0.00.
^{1}H NMR:	(500 MHz, $CDCl_3$) δ [ppm] = 3.31 (t, ^3J = 6.7 Hz, 2H, H1), 2.41 (t, ^3J = 7.0 Hz, 2H, H4), 1.76-1.71 (m, 2H, H2), 1.69-1.63 (m, 2H, H3).

6.2.6.9 Synthesis of 153

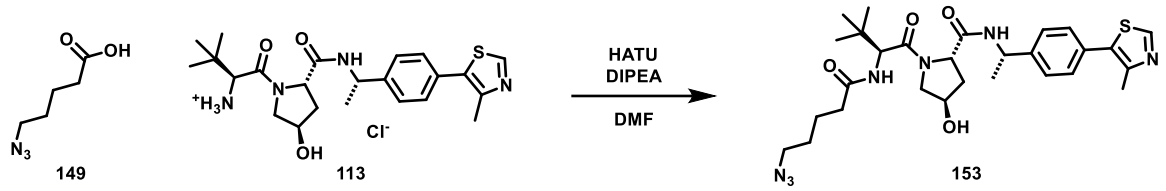

149 113 153

In a 50 mL *Schlenk* tube, 75 mg (0.52 mmol; 1.0 eq.) of linker **149**, 209 mg (550 μmol; 1.10 eq.) of HATU, and 305 μL (1.75 mmol; 3.50 eq.) of DIPEA were added in 15 mL of DMF. After 30 min, 240 mg (500 μmol; 1.00 eq.) of recruiter **113** were added and the mixture was stirred at room temperature until full conversion of recruiter **113** was observed by TLC after 16 h and the solvent was removed under reduced pressure. The residue was purified by column chromatography (SiO_2, EtOAc/MeOH 1:0 to 10:1). The residue was dissolved in CH_2Cl_2, filtered through a syringe filter, and the solvent was removed under reduced pressure. The residue was dissolved in MeCN/H_2O and lyophilized to obtain 206 mg (361 μmol; 72%) of the desired product **153** as a colorless lyophilizate.

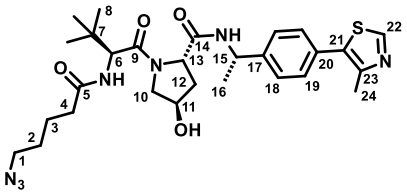

M ($C_{28}H_{39}N_7O_4S$): 569.72 g/mol.

Yield: 206 mg (361 μmol; 72%).

R_f: (SiO_2, EtOAc/MeOH 10:1) = 0.25.

^{1}H NMR: (400 MHz, $CDCl_3$) δ [ppm] = 8.69 (s, 1H, H22), 7.51 (d, ^3J = 8.0 Hz, 1H, N*H*), 7.41 (d, ^3J = 8.4 Hz, 2H, H19), 7.37 (d, ^3J = 8.4 Hz, 2H, H18), 6.37-6.31 (m, 1H, N*H*), 5.09 (quin, ^3J = 7.3 Hz, 1H, H15), 4.69 (t, ^3J = 7.8 Hz, 1H, H13); 4.59 (d, ^3J = 9.0 Hz, 1H, H6), 4.51 (s, 1H, H11), 4.03 (d, ^3J = 11.1 Hz, 1H, H10a), 3.64 (dd, ^3J = 11.1 Hz, ^3J = 3.9 Hz, 1H, H10b), 3.28 (t, ^3J = 6.7 Hz, 2H, H1), 2.51 (s, 3H, H24), 2.49-2.41 (m, 1H, H12a), 2.27-2.15 (m, 2H, H4), 2.08-2.00 (m, 1H, H12b), 1.73-1.65 (m, 2H, H3), 1.62-1.55 (m, 2H, H2), 1.48 (d, ^3J = 6.6 Hz, 3H, H16), 1.05 (s, 9H, H8).

^{13}C NMR:	(100 MHz, $CDCl_3$) δ [ppm] = 173.0 (C5); 172.0 (C9); 169.9 (C14); 150.5 (C22); 148.5 (C23); 143.2 (C17); 131.6 (C21); 131.0 (C20); 129.6 (C19); 126.5 (C18); 70.0 (C11); 58.8 (C13); 57.6 (C6); 56.8 (C10); 51.1 (C1); 48.9 (C15); 35.8, 35.7 (C12, C4); 35.3 (C7); 28.4 (C2); 26.6 (C8); 22.8 (C3); 22.3 (C16); 16.2 (C24).			
HR-MS (ESI):	Ion	Calc. mass [u]	Exp. mass [u]	Δ [ppm]
	$[M+H]^+$	570.28570	570.28499	-1.24
	$[M+Na]^+$	592.26764	592.26691	-1.24
LC-MS (ESI):	t_r [min]		11.50-14.27	
	Ion	Calc. mass [u]	Exp. mass [u]	Purity [%]
	$[M+H]^+$	570.29	570.28	98

6.2.6.10 Synthesis of 169

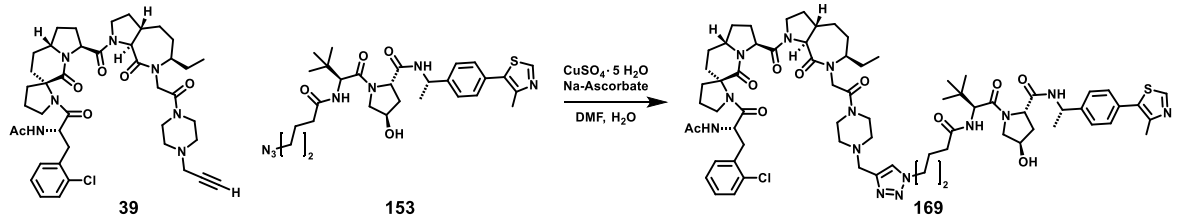

39 153 169

According to a modified procedure by *Banerjee et al*.[196]: In a headspace vial, 23 mg (29 μmol; 1.0 eq.) of warhead-linker conjugate **39** and 25 mg (44 μmol; 1.5 eq.) of linker-recruiter conjugate **153** were dissolved in 2 mL of DMF. Next, 1 mL of an aqueous solution (3mM; 3 μmol; 10 mol%) of $CuSO_4$ and 1 mL of an aqueous solution (6mM; 6 μmol; 20 mol%) of sodium ascorbate were added, and the mixture was stirred at room temperature for 18 h. Full conversion of warhead-linker conjugate **39** was observed by TLC and the solvent was removed under reduced pressure. The crude product was purified by column chromatography (dryload, 5 g ultra-pure silica, EtOAc/MeOH/NEt_3 1:0:0 to 20:4:1). The product was dissolved in CH_2Cl_2, filtered through a syringe filter, and the solvent was removed under reduced pressure. The residue was purified by reverse phase column chromatography (MeCN/H_2O 3:7 to 7:3) and lyophilized to obtain 20 mg (15 μmol; 50%) of the desired product **169** as a colorless lyophilizate.

M ($C_{70}H_{95}N_{14}O_{10}SCl$):	1360.13 g/mol.			
Yield:	20 mg (15 μmol; 50%).			
R_f:	(SiO_2, EtOAc/MeOH/NEt_3 20:4:1) = 0.03.			
HR-MS (ESI):	Ion	Calc. mass [u]	Exp. mass [u]	Δ [ppm]
	$[M+H]^+$	1359.68376	1359.68281	-0.70
	$[M+Na]^+$	1381.66570	1381.66283	-2.08
LC-MS (ESI):	t_r [min]		8.57-11.34	
	Ion	Calc. mass [u]	Exp. mass [u]	Purity [%]
	$[M+H]^+$	1359.68	1359.96	>99

6.2.6.11 Synthesis of 159

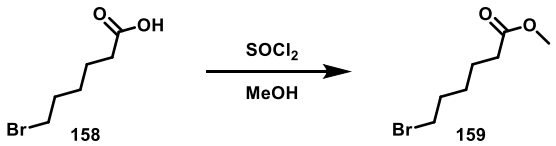

This experiment was carried out by *Alexander Klingert*. According to a modified procedure by *Albat*[193]: 2.97 g (15.3 mmol; 1.00 eq.) of acid **158** were dissolved in 51 mL of MeOH and 1.66 mL (22.9 mmol; 1.50 eq.) of $SOCl_2$ were added. The mixture was stirred at room temperature until full conversion of acid **158** was observed by TLC after 2.5 h. The solvent was removed under reduced pressure and the residue was purified by column chromatography (SiO_2, *c*Hex/EtOAc 10:1) to obtain 2.99 g (14.3 mmol; 84%) of the desired product **159** as a pale-yellow oil.

M ($C_7H_{13}O_2Br$):	209.08 g/mol.
Yield:	2.99 g (14.3 mmol; 84%).
R_f:	(SiO_2, *c*Hex/EtOAc 2:1) = 0.62.
^{1}H NMR:	(300 MHz, $CDCl_3$) δ [ppm] = 3.68 (s, 3H, H7), 3.41 (t, ^3J = 6.8 Hz, 2H, H1), 2.33 (t, ^3J = 7.5 Hz, 2H, H5), 1.93-1.83 (m, 2H, H4), 1.71-1.59 (m, 2H, H2), 1.52-1.42 (m, 2H, H3).

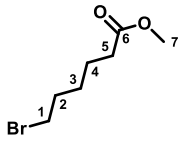

6.2.6.12 Synthesis of 166

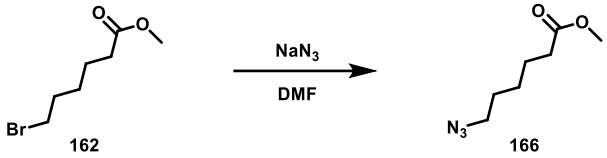

This experiment was carried out by *Alexander Klingert*. According to a modified procedure by *Simonin et al*.[215]: In a 50 mL round bottom flask, 3.00 g (14.35 mmol; 1.0 eq.) of ester **159** were dissolved in 9 mL of DMF, 3.73 g (57.40 mmol; 4.0 eq.) of NaN_3 were added, and the mixture was stirred at 60 °C until full conversion of ester **159** was observed by TLC after 17 h. At room temperature, 10 mL of H_2O were added, and the mixture was extracted with 20 mL of Et_2O three times. The combined organic layers were washed with 20 mL of H_2O three times, followed by 20 mL of NaCl solution. The mixture was dried over $MgSO_4$, filtered, and the solvent was removed under reduced pressure to obtain 1.92 g (11.1 mmol; 77%) of the desired product **166** as a pale-yellow oil.

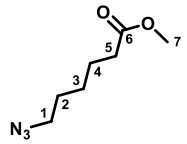

M ($C_7H_{13}N_3O_2$):	171.20 g/mol.
Yield:	1.92 g (11.1 mmol; 77%).
R_f:	(SiO_2, *c*Hex/EtOAc 2:1) = 0.57.
^{1}H NMR:	(500 MHz, $CDCl_3$) δ [ppm] = 3.68 (s, 3H, H7), 3.28 (t, ^3J = 6.8 Hz, 2H, H1), 2.33 (t, ^3J = 7.4 Hz, 2H, H5), 1.69-1.59 (m, 4H, H2, H4), 1.47-1.38 (m, 2H, H3).
^{13}C NMR:	(125 MHz, $CDCl_3$) δ [ppm] = 174.1 (C6); 51.7 (C7); 51.4 (C1); 34.0 (C5); 28.7 (C2); 26.4 (C3); 24.6 (C4).

6.2.6.13 Synthesis of 150

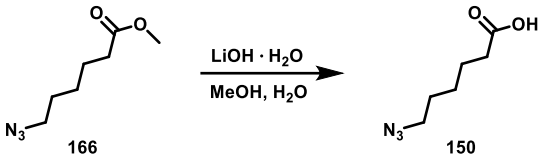

This experiment was carried out by *Alexander Klingert*. According to a modified procedure by *Albat*[193]: In a 250 mL round bottom flask, 3.20 g (20.1 mmol; 1.00 eq.) of ester **166** were dissolved in 52 mL of MeOH and 26 mL of H_2O. Next, 2.36 g (56.3 mmol; 2.80 eq.) of LiOH hydrate were added, the mixture was stirred at room temperature for 19 h and the solution was concentrated under reduced pressure. 20 mL of HCl (1M) and 20 mL of CH_2Cl_2 were added, and the layers were separated. The aqueous phase was extracted five times with 20 mL of CH_2Cl_2 and the combined organic layers were dried over $MgSO_4$, filtered, and the solvent was removed under reduced pressure to obtain 2.71 g (18.7 mmol; 93%) of the desired product **150** as a pale-yellow oil.

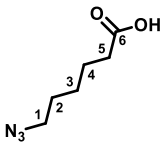

M ($C_6H_{11}N_3O_2$): 157.17 g/mol.

Yield: 2.71 g (18.7 mmol; 93%).

R_f: (SiO_2, *c*Hex/EtOAc 10:1) = 0.0.

^{1}H NMR: (400 MHz, $CDCl_3$) δ [ppm] = 3.39 (t, ^3J = 6.9 Hz, 2H, H1), 2.38 (t, ^3J = 7.1 Hz, 2H, H5), 1.71-1.60 (m, 4H, H2, H4), 1.48-1.40 (m, 2H, H3).

^{13}C NMR: (100 MHz, $CDCl_3$) δ [ppm] = 179.8 (C6); 51.3 (C1); 33.9 (C5); 28.7 (C2); 26.3 (C3); 24.3 (C4).

6.2.6.14 Synthesis of 154

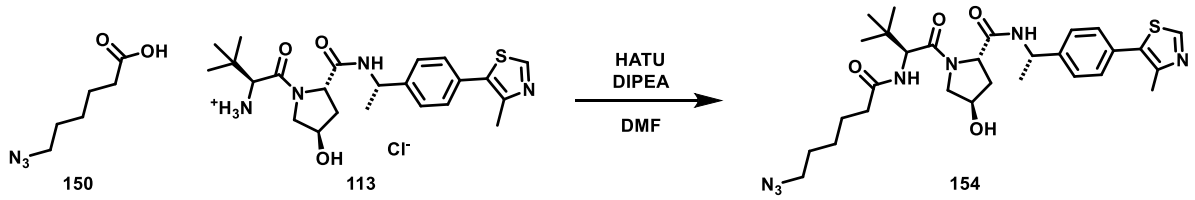

In a 50 mL *Schlenk* tube, 90 mg (0.57 mmol; 1.1 eq.) of linker **150**, 209 mg (550 μmol; 1.10 eq.) of HATU, and 305 μL (1.75 mmol; 3.50 eq.) of DIPEA were added in 15 mL of DMF and the mixture as stirred for 30 min. Next, 240 mg (500 μmol; 1.00 eq.) of recruiter **113** were added and the mixture was stirred at room temperature until full conversion of recruiter **113** was observed by TLC after 16 h and the solvent was removed under reduced pressure. The residue was purified by column chromatography (SiO_2, EtOAc/MeOH 1:0 to 10:1). The residue was dissolved in CH_2Cl_2, filtered through a syringe filter, and the solvent was removed under reduced pressure. The residue was dissolved in MeCN/H_2O and lyophilized to obtain 249 mg (427 μmol; 85%; 95 wt%) of the desired product **154** as a colorless lyophilizate.

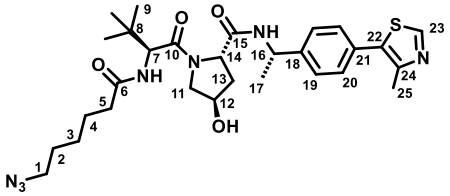

M ($C_{29}H_{41}N_7O_4S$): 583.75 g/mol.

Yield: 249 mg (427 μmol; 85%; 95 wt%).

R_f: (SiO_2, EtOAc/MeOH 10:1) = 0.46.

^{1}H NMR: (400 MHz, $CDCl_3$) δ [ppm] = 8.69 (s, 1H, H23), 7.50 (d, ^3J = 7.8 Hz, 1H, N*H*), 7.40 (d, ^3J = 8.4 Hz, 2H, H20), 7.37 (d, ^3J = 8.4 Hz, 2H, H19), 6.31 (d, ^3J = 8.7 Hz, 1H, N*H*), 5.10 (quin, ^3J = 7.3 Hz, 1H, H16), 4.66 (t, ^3J = 8.0 Hz, 1H, H14); 4.55 (d, ^3J = 8.7 Hz, 1H, H7), 4.50 (s, 1H, H12), 4.03 (d, ^3J = 11.4 Hz, 1H, H11a), 3.63 (dd, ^3J = 11.3 Hz, ^3J = 3.6 Hz, 1H, H11b), 3.24 (t, ^3J = 6.8 Hz, 2H, H1), 2.52 (s, 3H, H25), 2.39 (ddd, ^3J = 13.1 Hz, ^3J = 8.0 Hz, ^3J = 4.6 Hz, 1H, H13a), 2.15 (t, ^3J = 7.5 Hz, 2H, H5), 2.07-2.02 (m, 1H, H13b), 1.66-1.53 (m, 4H, H2, H4), 1.49 (d, ^3J = 7.0 Hz, 3H, H17), 1.39-1.31 (m, 2H, H3), 1.05 (s, 9H, H9).

^{13}C NMR:	(100 MHz, $CDCl_3$) δ [ppm] = 173.5 (C6); 171.8 (C10); 170.0 (C15); 150.5 (C23); 148.5 (C24); 143.3 (C18); 131.6 (C22); 130.9 (C21); 130.0 (C20); 126.6 (C19); 70.0 (C12); 58.8 (C14); 57.7 (C7); 56.8 (C11); 51.2 (C1); 48.8 (C16); 36.2 (C5); 36.0 (C13); 35.2 (C8); 28.6 (C2); 27.0 (C9); 26.3 (C3); 25.1 (C4); 22.2 (C17); 16.1 (C25).			
HR-MS (ESI):	Ion	Calc. mass [u]	Exp. mass [u]	Δ [ppm]
	$[M+H]^+$	584.30135	584.30185	+0.86
	$[M+Na]^+$	606.28329	606.28363	+0.55
LC-MS (ESI):	t_r [min]		12.04-12.30	
	Ion	Calc. mass [u]	Exp. mass [u]	Purity [%]
	$[M+H]^+$	584.30	584.28	>99

6.2.6.15 Synthesis of 170

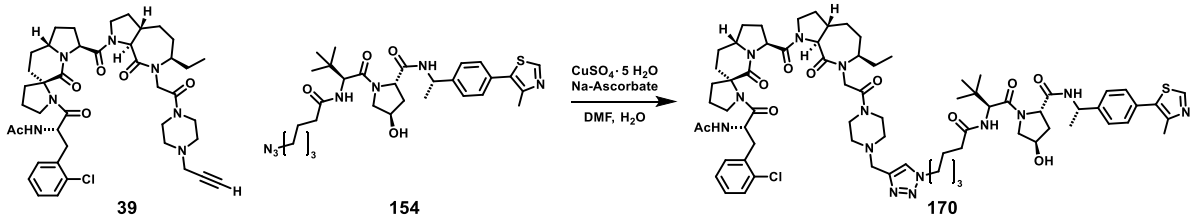

According to a modified procedure by *Banerjee et al*.[196]: In a headspace vial, 23 mg (29 μmol; 1.0 eq.) of warhead-linker conjugate **39** and 25 mg (44 μmol; 1.5 eq.) of linker-recruiter conjugate **154** were dissolved in 2 mL of DMF. Next, 1 mL of an aqueous solution (3mM; 3 μmol; 10 mol%) of $CuSO_4$ and 1 mL of an aqueous solution (6mM; 6 μmol; 20 mol%) of sodium ascorbate were added, and the mixture was stirred at room temperature for 18 h. Full conversion of warhead-linker conjugate **39** was observed by TLC and the solvent was removed under reduced pressure. The crude product was purified by column chromatography (dryload, 5 g ultra-pure silica, EtOAc/MeOH/NEt_3 1:0:0 to 20:4:1). The product was dissolved in CH_2Cl_2, filtered through a syringe filter, and the solvent was removed under reduced pressure. The residue was purified by reverse phase column chromatography (MeCN/H_2O 3:7 to 7:3) and lyophilized to obtain 14 mg (10 μmol; 35%) of the desired product **170** as a colorless lyophilizate.

M ($C_{71}H_{97}N_{14}O_{10}SCl$):	1374.15 g/mol.			
Yield:	14 mg (10 μmol; 35%).			
R_f:	(SiO_2, EtOAc/MeOH/NEt_3 20:4:1) = 0.03.			
HR-MS (ESI):	Ion	Calc. mass [u]	Exp. mass [u]	Δ [ppm]
	$[M+H]^+$	1373.69941	1373.69901	-0.29
	$[M+Na]^+$	1395.68135	1395.67986	-1.07
LC-MS (ESI):	t_r [min]		8.67-11.79	
	Ion	Calc. mass [u]	Exp. mass [u]	Purity [%]
	$[M+H]^+$	1373.70	1374.00	>99

6.2.6.16 Synthesis of 163

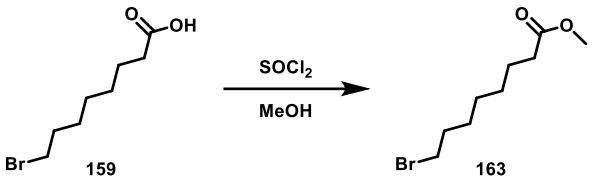

This experiment was carried out by *Alexander Klingert*. According to a modified procedure by *Albat*[193]: 4.69 g (21.0 mmol; 1.00 eq.) of acid **159** were dissolved in 75 mL of MeOH and 2.44 mL (33.6 mmol; 1.50 eq.) of $SOCl_2$ were added. The mixture was stirred at room temperature until full conversion of acid **159** was observed by TLC after 2 h. The solvent was removed under reduced pressure and the residue was purified by column chromatography (SiO_2, *c*Hex/EtOAc 10:1) to obtain 4.82 g (20.3 mmol; 97%) of the desired product **163** as a pale-yellow oil.

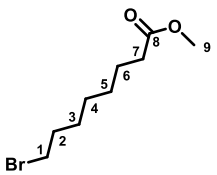

M ($C_9H_{17}O_2Br$):	237.14 g/mol.
Yield:	4.82 g (20.3 mmol; 97%).
R_f:	(SiO_2, *c*Hex/EtOAc 10:1) = 0.39.
^{1}H NMR:	(500 MHz, $CDCl_3$) δ [ppm] = 3.67 (s, 3H, H9), 3.40 (t, ^3J = 6.9 Hz, 2H, H1), 2.31 (t, ^3J = 7.4 Hz, 2H, H7), 1.85 (quin, ^3J = 7.5 Hz, 2H, H6), 1.65-1.59 (m, 2H, H2), 1.46-1.42 (m, 2H, H3), 1.36-1.30 (m, 4H, H4, H5).

6.2.6.17 Synthesis of 167

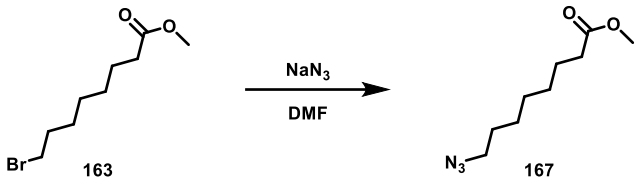

This experiment was carried out by *Alexander Klingert*. According to a modified procedure by *Simonin et al*.[215]: In a 50 mL round bottom flask, 4.69 g (19.8 mmol; 1.00 eq.) of ester **163** were dissolved in 14 mL of DMF, 5.12 g (79.1 mmol; 4.00 eq.) of NaN_3 were added, and the mixture was stirred at 60 °C until full conversion of ester **163** was observed by TLC after 20 h. After cooling to room temperature, 10 mL of H_2O were added, and the mixture was extracted with 20 mL of Et_2O three times. The combined organic layers were washed with 20 mL of H_2O three times, followed by 20 mL of NaCl solution. The mixture was dried over $MgSO_4$, filtered, and the solvent was removed under reduced pressure to obtain 3.73 g (18.6 mmol; 94%) of the desired product **167** as a pale-yellow oil.

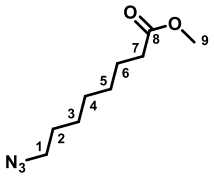

M ($C_9H_{17}N_3O_2$):	199.25 g/mol.
Yield:	3.73 g (18.6 mmol; 94%).
R_f:	(SiO_2, *c*Hex/EtOAc 2:1) = 0.62.
^{1}H NMR:	(500 MHz, $CDCl_3$) δ [ppm] = 3.67 (s, 3H, H9), 3.26 (t, ^3J = 7.0 Hz, 2H, H1), 2.31 (t, ^3J = 7.5 Hz, 2H, H5), 1.64-1.57 (m, 4H, H2, H6), 1.39-1.32 (m, 6H, H3, H4, H5).

6.2.6.18 Synthesis of 151

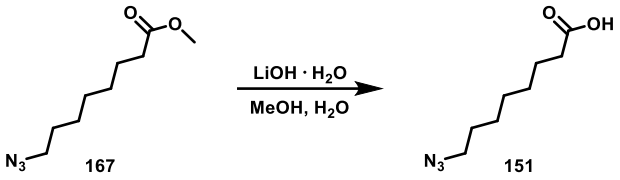

This experiment was carried out by *Alexander Klingert*. According to a modified procedure by *Albat*[193]: In a 250 mL round bottom flask, 3.44 g (17.2 mmol; 1.00 eq.) of ester **167** were dissolved in 56 mL of MeOH and 28 mL of H_2O. Next, 2.02 g (48.1 mmol; 2.80 eq.) of LiOH hydrate were added, the mixture was stirred at room temperature for 21 h and the solution was concentrated under reduced pressure. To the residue, 20 mL of HCl (1M) and 20 mL of CH_2Cl_2 were added, and the layers were separated. The aqueous phase was extracted five times with 20 mL of CH_2Cl_2 and the combined organic layers were dried over $MgSO_4$, filtered, and the solvent was removed under reduced pressure to obtain 3.10 g (16.6 mmol; 97%) of the desired product **151** as a pale-yellow oil.

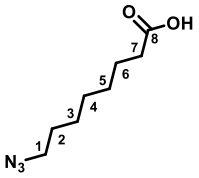

M ($C_8H_{15}N_3O_2$):	185.23 g/mol.
Yield:	3.10 g (16.6 mmol; 97%).
R_f:	(SiO_2, *c*Hex/EtOAc 10:1) = 0.0.
^{1}H NMR:	(400 MHz, $CDCl_3$) δ [ppm] = 3.26 (t, ^3J = 6.9 Hz, 2H, H1), 2.36 (t, ^3J = 7.5 Hz, 2H, H7), 1.68-1.57 (m, 4H, H2, H6), 1.42-1.32 (m, 6H, H3, H4, H5).
^{13}C NMR:	(100 MHz, $CDCl_3$) δ [ppm] = 180.1 (C8); 51.5 (C1); 34.1 (C7); 29.0, 28.9, 28.9 (C4, C5, C6); 26.6 (C3); 24.7 (C2).

6.2.6.19 Synthesis of 155

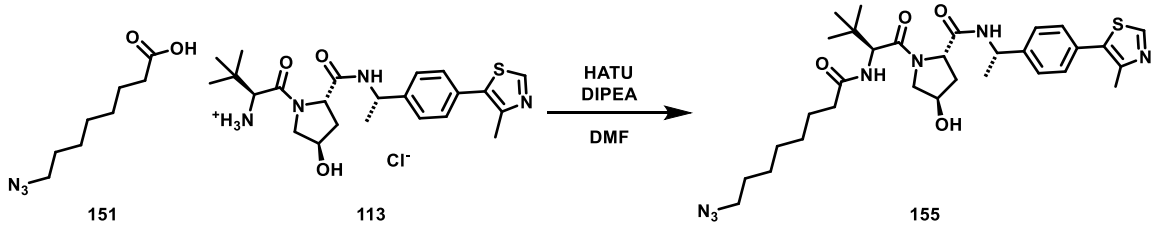

151 113 155

In a 50 mL *Schlenk* tube, 97 mg (0.52 mmol; 1.0 eq.) of linker **151**, 209 mg (550 μmol; 1.10 eq.) of HATU, and 305 μL (1.75 mmol; 3.50 eq.) of DIPEA were added in 15 mL of DMF. After 30 min, 240 mg (500 μmol; 1.00 eq.) of recruiter **113** were added and the mixture was stirred at room temperature until full conversion of recruiter **113** was observed by TLC after 16 h and the solvent was removed under reduced pressure. The residue was purified by column chromatography (SiO_2, EtOAc/MeOH 1:0 to 10:1). The residue was dissolved in CH_2Cl_2, filtered through a syringe filter, and the solvent was removed under reduced pressure. The residue was dissolved in MeCN/*t*BuOH/H_2O and lyophilized to obtain 272 mg (444 μmol; 88%; 95 wt%) of the desired product **155** as a colorless lyophilizate.

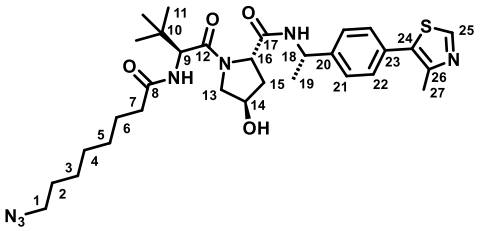

M ($C_{31}H_{45}N_7O_4S$): 611.81 g/mol.

Yield: 272 mg (444 μmol; 88%; 95 wt%).

R_f: (SiO_2, EtOAc/MeOH/NEt_3 20:4:1) = 0.59.

^{1}H NMR: (400 MHz, $CDCl_3$) δ [ppm] = 8.71 (s, 1H, H25), 7.51 (d, ^3J = 8.0 Hz, 1H, N*H*), 7.42-7.36 (m, 4H, H21, H22), 6.25 (d, ^3J = 8.6 Hz, 1H, N*H*), 5.10 (quin, ^3J = 7.0 Hz, 1H, H18), 4.66 (t, ^3J = 8.0 Hz, 1H, H16); 4.55 (d, ^3J = 8.6 Hz, 1H, H9), 4.51 (s, 1H, H14), 4.05 (d, ^3J = 11.2 Hz, 1H, H13a), 3.63 (dd, ^3J = 11.3 Hz, ^3J = 3.7 Hz, 1H, H13b), 3.24 (t, ^3J = 6.9 Hz, 2H, H1), 2.52 (s, 3H, H27), 2.44-2.36 (m, 1H, H15a), 2.14 (t, ^3J = 7.7 Hz, 2H, H7), 2.09-2.02 (m, 1H, H15b), 1.62-1.53 (m, 4H, H2, H6), 1.49 (d, ^3J = 6.9 Hz, 3H, H19), 1.37-1.28 (m, 6H, H3-5), 1.05 (s, 9H, H11).

^{13}C NMR:	(100 MHz, $CDCl_3$) δ [ppm] = 173.9 (C8); 171.9 (C11); 170.0 (C17); 150.6 (C25); 148.4 (C26); 143.4 (C20); 131.7 (C24); 130.9 (C23); 129.6 (C22); 126.6 (C21); 70.0 (C14); 58.8 (C16); 57.7 (C9); 56.8 (C13); 51.5 (C1); 48.9 (C18); 36.4 (C7); 35.2 (C10, C15); 29.1 (C3/C4/C5) 28.8 (C2); 28.8 (C3/C4/C5); 26.6 (C11, C3/C4/C5); 25.5 (C6); 22.2 (C19); 16.1 (C27).			
HR-MS (ESI):	Ion	Calc. mass [u]	Exp. mass [u]	Δ [ppm]
	$[M+H]^+$	612.33265	612.33311	+0.75
	$[M+Na]^+$	634.31459	634.31461	+0.03
LC-MS (ESI):	t_r [min]		13.41-13.70	
	Ion	Calc. mass [u]	Exp. mass [u]	Purity [%]
	$[M+H]^+$	612.33	612.34	>99

6.2.6.20 Synthesis of 171

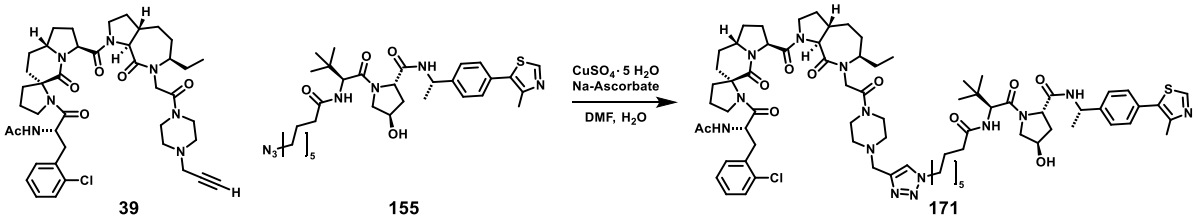

According to a modified procedure by *Banerjee et al*.[196]: In a headspace vial, 23 mg (29 μmol; 1.0 eq.) of warhead-linker conjugate **39** and 27 mg (44 μmol; 1.5 eq.) of linker-recruiter conjugate **155** were dissolved in 2 mL of DMF. Next, 1 mL of an aqueous solution (3mM; 3 μmol; 10 mol%) of $CuSO_4$ and 1 mL of an aqueous solution (6mM; 6 μmol; 20 mol%) of sodium ascorbate were added, and the mixture was stirred at room temperature for 18 h. Full conversion of warhead-linker conjugate **39** was observed by TLC and the solvent was removed under reduced pressure. The crude product was purified by column chromatography (dryload, 6 g ultra-pure silica, EtOAc/MeOH/NEt_3 1:0:0 to 20:4:1). The product was dissolved in CH_2Cl_2, filtered through a syringe filter, and the solvent was removed under reduced pressure. The residue was purified by reverse phase column chromatography (MeCN/H_2O 3:7 to 7:3) and lyophilized to obtain 17 mg (12 μmol; 41%) of the desired product **171** as a colorless lyophilizate.

M ($C_{73}H_{101}N_{14}O_{10}SCl$):	1402.21 g/mol.			
Yield:	17 mg (12 μmol; 41%).			
R_f:	(SiO_2, EtOAc/MeOH/NEt_3 20:4:1) = 0.04.			
HR-MS (ESI):	Ion	Calc. mass [u]	Exp. mass [u]	Δ [ppm]
	$[M+H]^+$	1401.73071	1401.73128	+0.41
	$[M+Na]^+$	1423.71265	1423.71120	-1.02
LC-MS (ESI):	t_r [min]		9.05-11.18	
	Ion	Calc. mass [u]	Exp. mass [u]	Purity [%]
	$[M+H]^+$	1401.73	1402.02	>99

6.2.7 Synthesis towards PROTACs 172-174

6.2.7.1 Synthesis of 178

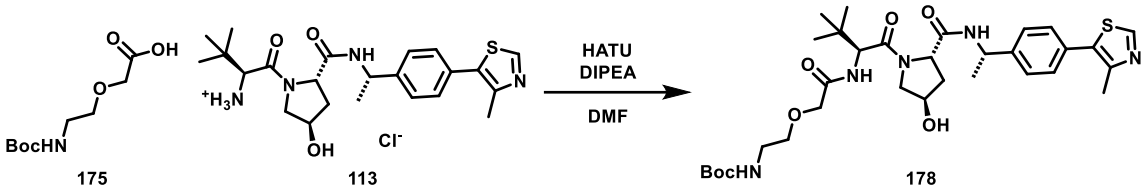

In a 50 mL *Schlenk* flask, 121 mg (550 μmol; 1.10 eq.) of acid **175**, 209 mg (550 μmol; 1.10 eq.) of HATU, and 305 μL (1.75 mmol; 3.50 eq.) of DIPEA were added in 15 mL of DMF. The mixture was stirred at room temperature for 1 h and 240 mg (500 μmol; 1.00 eq.) of recruiter **113** were added. After 16 h, full conversion of recruiter **113** was observed by TLC and the solvent was removed under reduced pressure. The residue was purified by column chromatography (SiO_2, EtOAc/MeOH 10:1 to 5:1). The residue was dissolved in CH_2Cl_2, filtered through a syringe filter, and the solvent was removed under reduced pressure to obtain 242 mg (374 μmol; 75%) of the desired product **178** as a colorless foam.

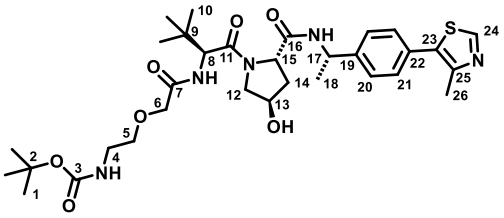

M ($C_{32}H_{47}N_5O_7S$): 645.82 g/mol.

Yield: 242 mg (374 μmol; 75%).

R_f: (SiO_2, EtOAc/MeOH/NEt_3 20:4:1) = 0.11.

^{1}H NMR: (500 MHz, $CDCl_3$) δ [ppm] = 8.71 (s, 1H, H24), 7.41-7.36 (m, 5H, H20, H21, N*H*), 7.22 (d, ^3J = 8.4 Hz, 1H, N*H*), 5.16 (s, 1H, O*H*), 5.09 (quin, ^3J = 7.4 Hz, 1H, H17), 4.74 (t, ^3J = 7.7 Hz, 1H, H15), 4.56-4.52 (m, 2H, H8, H13), 4.12-4.04 (m, 2H, H12a, H6a), 3.94-3.91 (m, 1H, H6b), 3.70-3.64 (m, 1H, H5a), 3.61 (dd, ^3J = 11.4 Hz, ^3J = 3.5 Hz, 1H, H12b), 3.58-3.52 (m, 1H, H5b), 3.42-3.29 (m, 2H, H4), 2.58-2.51 (m, 1H, H14a), 2.53 (s, 3H, H26), 2.10-2.04 (m, 1H, H14b), 1.48 (d, ^3J = 7.1 Hz, 3H, H18), 1.44 (s, 9H, H1), 1.07 (s, 9H, H10).

^{13}C NMR: (125 MHz, $CDCl_3$) δ [ppm] = 171.9 (C7); 170.6 (C11); 169.6 (C16); 155.3 (C3); 150.1 (C24); 148.4 (C25); 143.3 (C19); 131.9 (C23); 130.9 (C22); 129.7 (C21); 126.6 (C20); 79.4 (C2); 71.3 (C5), 70.3 (C6), 70.2 (C13); 58.6 (C15); 57.4 (C8); 56.8 (C12); 49.1 (C17); 40.2 (C4); 35.4 (C9); 35.0 (C14); 28.6 (C1); 26.7 (C10); 22.4 (C18); 16.1 (C26). Note: C2, C4, C5, C6, C14, and C19 were assigned by HMBC and HSQC.

6.2.7.2 Synthesis of 181

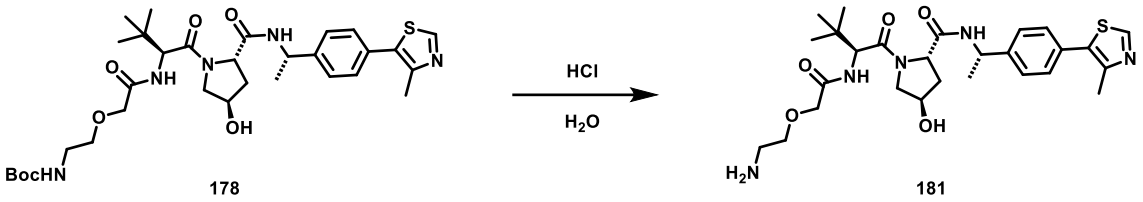

In a 25 mL round bottom flask, 240 mg (372 μmol; 1.00 eq.) of linker-recruiter conjugate **178** were dissolved in 5 mL of HCl (1M). After 1 h, major conversion of linker-recruiter conjugate **178** was observed by TLC and 10 mL of CH_2Cl_2 were added. The solution was adjusted to pH 8 by the addition of $NaHCO_3$, the layers were separated, and the aqueous phase was extracted four times with 20 mL of CH_2Cl_2. The combined organic layers were dried over $MgSO_4$, filtered, and the solvent was removed under reduced pressure. The residue was purified by column chromatography (SiO_2, dryload, EtOAc/MeOH/NEt_3 1:0:0 to 20:4:1). The residue was dissolved in CH_2Cl_2, filtered through a syringe filter, and the solvent was removed under reduced pressure. The residue was dissolved in H_2O/*t*BuOH/MeCN and lyophilized to obtain 53 mg (97 μmol; 26%) of the desired product **181** as a colorless lyophilizate.

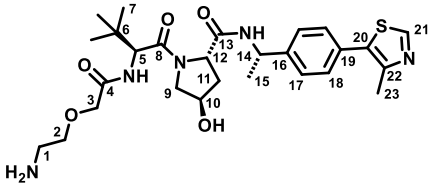

M ($C_{27}H_{39}N_5O_5S$): 545.70 g/mol.

Yield: 53 mg (97 μmol; 26%).

R_f: (SiO_2, EtOAc/MeOH/NEt_3 20:4:1) = 0.08.

^{1}H NMR: (400 MHz, $CDCl_3$) δ [ppm] = 8.66 (s, 1H, H21), 7.89 (d, ^3J = 7.1 Hz, 1H, N*H*), 7.76 (d, ^3J = 8.4 Hz, 1H, N*H*), 7.41-7.34 (m, 5H, H17, H18, N*H*), 5.10 (quin, ^3J = 7.1 Hz, 1H, H14), 4.70 (t, ^3J = 8.1 Hz, 1H, H12), 4.60 (d, ^3J = 8.9 Hz, 1H, H5), 4.46 (s, 1H, H10), 4.06-3.94 (m, 3H, H9a, H3), 3.69-3.52 (m, 3H, H2, H19b), 3.07-3.04 (m, 2H, H1), 2.52-2.49 (m, 1H, H11a), 2.50 (s, 3H, H23), 2.23-2.19 (m, 1H, H11b), 1.47 (d, ^3J = 7.2 Hz, 3H, H15), 1.06 (s, 9H, H7).

^{13}C NMR: (100 MHz, $CDCl_3$) δ [ppm] = 171.5 (C4); 170.4 (C8); 170.3 (C13); 150.4 (C21); 148.5 (C22); 143.6 (C16); 131.8 (C20); 130.8 (C19); 129.6 (C18); 126.6 (C17); 70.0 (C2); 69.9 (C3); 69.8 (C10); 57.9 (C12); 57.5 (C5); 56.8 (C9); 48.8 (C14); 39.9 (C1); 35.6 (C6); 34.6 (C11); 26.7 (C7); 22.4 (C15); 16.2 (C23).

Note: C9 was assigned by HMBC and HSQC.

HR-MS (ESI):

Ion	Calc. mass [u]	Exp. mass [u]	Δ [ppm]
$[M+H]^+$	546.27445	546.27452	+0.09
$[M+Na]^+$	568.25641	568.25642	+0.02

6.2.7.3 Synthesis of 172

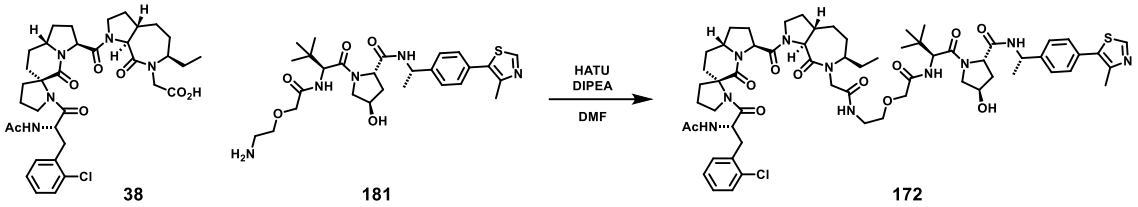

38 181 172

In a 10 mL *Schlenk* tube, 27 mg (40 μmol; 1.1 eq.) of warhead **38**, 18 mg (48 μmol; 1.3 eq.) of HATU and 22.4 μL (128 μmol; 3.50 eq.) of DIPEA were added in 1.5 mL of DMF. After 1 h at room temperature, 20 mg (37 μmol; 1.0 eq.) of linker-recruiter conjugate **181** were added and the mixture was stirred until full conversion of linker-recruiter conjugate **181** was observed by TLC after 19 h and the solvent was removed under reduced pressure. The residue was purified by column chromatography (SiO_2, dryload, EtOAc/MeOH/NEt_3 1:0:0 to 20:4:1). The residue was dissolved in CH_2Cl_2, filtered through a syringe filter, and the solvent was removed under reduced pressure. The residue was then purified by reverse phase column chromatography (MeCN/H_2O 2:8 to 8:2) and lyophilized to obtain 26 mg (21 μmol; 58%) of the desired product **172** as a colorless lyophilizate.

M ($C_{62}H_{83}N_{10}O_{11}SCl$):	1211.91 g/mol.			
Yield:	26 mg (21 μmol; 58%).			
R_f:	(SiO_2, EtOAc/MeOH/NEt_3 20:4:1) = 0.20.			
HR-MS (ESI):	Ion	Calc. mass [u]	Exp. mass [u]	Δ [ppm]
	$[M+H]^+$	1211.57248	1211.57431	+1.51
	$[M+Na]^+$	1233.55442	1233.55422	-0.16
HPLC:	t_r [min]		10.45-11.39	
	Purity [%]		86	

6.2.7.4 Synthesis of 179

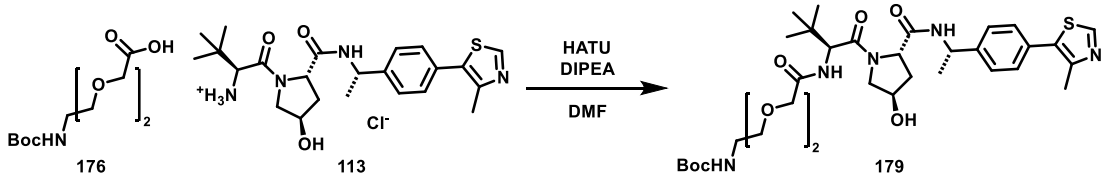

In a 50 mL *Schlenk* flask, 138 mg (525 μmol; 1.05 eq.) of acid **176**, 209 mg (550 μmol; 1.10 eq.) of HATU, and 305 μL (1.75 mmol; 3.50 eq.) of DIPEA were added in 15 mL of DMF. The mixture was stirred at room temperature for 1 h and 240 mg (500 μmol; 1.00 eq.) of recruiter **113** were added. After 16 h, full conversion of recruiter **113** was observed by TLC and the solvent was removed under reduced pressure. The residue was purified by column chromatography (SiO_2, EtOAc/MeOH 10:1 to 5:1). The residue was dissolved in CH_2Cl_2, filtered through a syringe filter, and the solvent was removed under reduced pressure to obtain 262 mg (380 μmol; 76%) of the desired product **179** as a colorless foam.

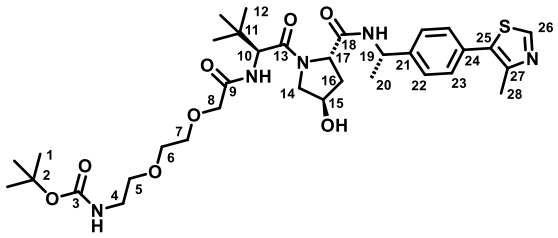

M ($C_{34}H_{51}N_5O_8S$): 689.87 g/mol.

Yield: 262 mg (380 μmol; 76%).

R_f: (SiO_2, EtOAc/MeOH 5:1) = 0.23.

^{1}H NMR: (500 MHz, $CDCl_3$) δ [ppm] = 8.75 (s, 1H, H26), 7.43-7.34 (m, 5H, H22, H23, N*H*), 5.18-5.04 (m, 1H, H19), 4.80-4.54 (m, 3H, H10, H15, H17), 4.14-3.87 (m, 3H, H14a, H8), 3.73-3.62 (m, 9H, H4, H5, H6, H7, H14b), 2.58-2.50 (m, 1H, H16a), 2.54 (s, 3H, H28), 2.09-2.03 (m, 1H, H16b), 1.49-1.39 (m, 12H, H1, H20), 1.05 (s, 9H, H12).

^{13}C NMR: (125 MHz, $CDCl_3$) δ [ppm] = 171.6 (C9); 170.8 (C13); 169.5 (C18); 147.8 (C27); 143.1 (C21); 132.2 (C25); 130.4 (C24); 129.8 (C23); 126.8 (C22); 79.6 (C2); 71.7, 70.9, 70.7, 70.5 (C5, C6, C7, C8, C15); 58.7 (C17); 57.2 (C10); 56.9 (C14); 49.0 (C19); 40.7 (C4); 35.8 (C11); 28.6 (C1); 26.7 (C12); 22.0 (C20); 16.0 (C28).
Note: C9, C11, C13, C18, C21, C24, C25, and C27 were detected in HSQC, C3, C16, and C26 were not detected.

6.2.7.5 Synthesis of 182

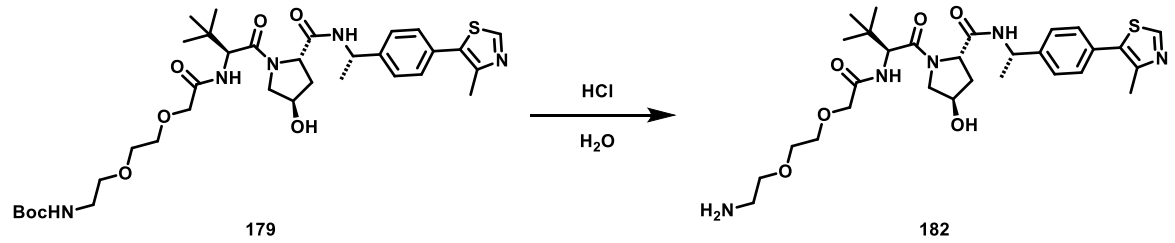

In a 25 mL round bottom flask, 250 mg (424 μmol; 1.00 eq.) of linker-recruiter conjugate **179** were dissolved in 5 mL of HCl (1M). After 2.5 h, major conversion of linker-recruiter conjugate **179** was observed by TLC and 10 mL of CH_2Cl_2 were added. The solution was adjusted to pH 8 by the addition of $NaHCO_3$, the layers were separated, and the aqueous phase was extracted four times with 20 mL of CH_2Cl_2. The combined organic layers were dried over $MgSO_4$, filtered, and the solvent was removed under reduced pressure. The residue was purified by column chromatography (SiO_2, dryload, EtOAc/MeOH/NEt_3 1:0:0 to 20:4:1). The residue was dissolved in CH_2Cl_2, filtered through a syringe filter, and the solvent was removed under reduced pressure. The residue was dissolved in H_2O/*t*BuOH/MeCN and lyophilized to obtain 177 mg (300 μmol; 71%) of the desired product **182** as a colorless lyophilizate.

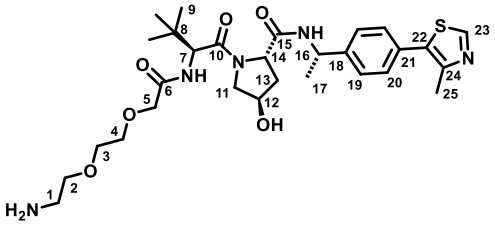

M ($C_{29}H_{43}N_5O_6S$): 589.75 g/mol.

Yield: 177 mg (300 μmol; 71%).

R_f: (SiO_2, EtOAc/MeOH/NEt_3 20:4:1) = 0.06.

^{1}H NMR: (400 MHz, $CDCl_3$) δ [ppm] = 8.67 (s, 1H, H23), 7.97 (d, ^3J = 7.9 Hz, 1H, N*H*), 7.49 (d, ^3J = 9.5 Hz, 1H, N*H*), 7.38 (s, 4H, H19, H20), 5.11 (quin, ^3J = 7.3 Hz, 1H, H16), 4.73-4.66 (m, 2H, H7, H14), 4.45 (s, 1H, H12), 4.11-4.08 (m, 1H, H5a), 4.00-3.96 (m, 2H, H5b, H11a), 3.79-3.56 (m, 7H, H2, H3, H4, H21b), 2.97 (t, ^3J = 4.9 Hz, 2H, H1), 2.52 (s, 3H, H25), 2.28-2.22 (m, 1H, H13a), 2.17-2.10 (m, 1H, H13b), 1.50 (d, ^3J = 7.2 Hz, 3H, H17), 1.04 (s, 9H, H9).

^{13}C NMR: (100 MHz, $CDCl_3$) δ [ppm] = 171.2 (C6); 170.4 (C10, C15); 150.4 (C23); 148.5 (C24); 143.7 (C18); 131.8 (C22); 130.8 (C21); 129.6 (C20); 126.6 (C19); 71.4, 71.1, 70.7, 70.6 (C2, C3, C4, C5); 70.0 (C12); 59.0 (C14); 57.2 (C11); 56.9 (C7); 48.9 (C16); 40.7 (C1); 36.9 (C8); 36.4 (C13); 26.6 (C9); 22.4 (C17); 16.2 (C25).

HR-MS (ESI):

Ion	Calc. mass [u]	Exp. mass [u]	Δ [ppm]
$[M+H]^+$	590.30068	590.30040	-0.48
$[M+Na]^+$	612.28263	612.28261	-0.03

6.2.7.6 Synthesis of 173

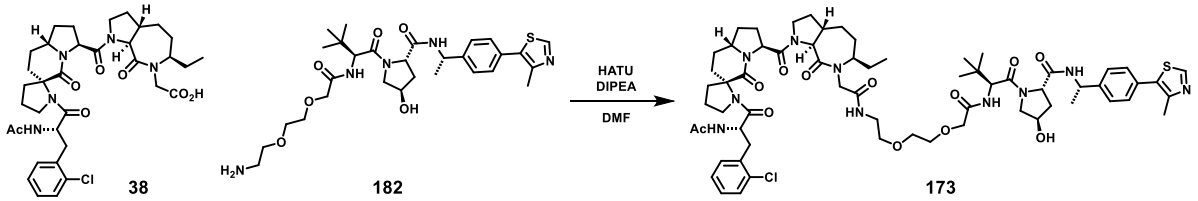

In a 10 mL *Schlenk* tube, 25 mg (37 μmol; 1.1 eq.) of warhead **38**, 17 mg (44 μmol; 1.3 eq.) of HATU, and 20.7 μL (119 μmol; 3.50 eq.) of DIPEA were added in 1.5 mL of DMF. After 30 min at room temperature, 20 mg (34 μmol; 1.0 eq.) of linker-recruiter conjugate **182** were added and the mixture was stirred until full conversion of linker-recruiter conjugate **182** was observed by TLC after 16 h and the solvent was removed under reduced pressure. The residue was purified by column chromatography (SiO_2, dryload, EtOAc/MeOH/NEt_3 1:0:0 to 20:4:1). The residue was dissolved in CH_2Cl_2, filtered through a syringe filter, and the solvent was removed under reduced pressure. The residue was then purified by reverse phase column chromatography (MeCN/H_2O 2:8 to 8:2) and lyophilized to obtain 31 mg (25 μmol; 73%) of the desired product **173** as a colorless lyophilizate.

M ($C_{64}H_{87}N_{10}O_{12}SCl$):	1255.97 g/mol.			
Yield:	31 mg (25 μmol; 73%).			
R_f:	(SiO_2, EtOAc/MeOH/NEt_3 20:4:1) = 0.23.			
HR-MS (ESI):	Ion	Calc. mass [u]	Exp. mass [u]	Δ [ppm]
	$[M+H]^+$	1255.59869	1255.60068	+1.58
	$[M+Na]^+$	1277.58064	1277.58044	-0.16
HPLC:	t_r [min]		10.46-11.10	
	Purity [%]		95	

6.2.7.7 Synthesis of 180

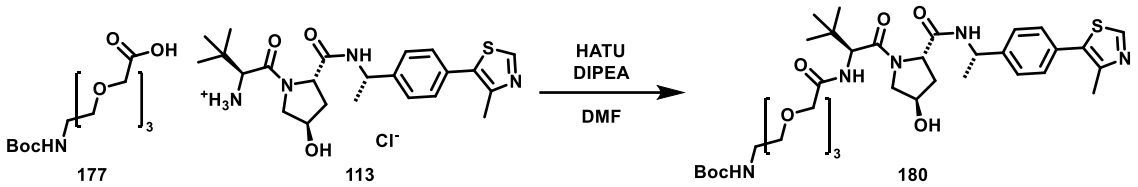

In a 50 mL *Schlenk* flask, 161 mg (525 μmol; 1.05 eq.) of linker **177**, 209 mg (550 μmol; 1.10 eq.) of HATU, and 305 μL (1.75 mmol; 3.50 eq.) of DIPEA were added in 15 mL of DMF. The mixture was stirred at room temperature for 1h, and 240 mg (500 μmol; 1.00 eq.) of recruiter **113** were added. After 18 h, full conversion of recruiter **113** was observed by TLC and the solvent was removed under reduced pressure. The residue was purified by column chromatography (SiO_2, EtOAc/MeOH 10:1 to 5:1). The residue was dissolved in CH_2Cl_2, filtered through a syringe filter, and the solvent was removed under reduced pressure to obtain 237 mg (323 μmol; 65%) of the desired product **180** as a colorless foam.

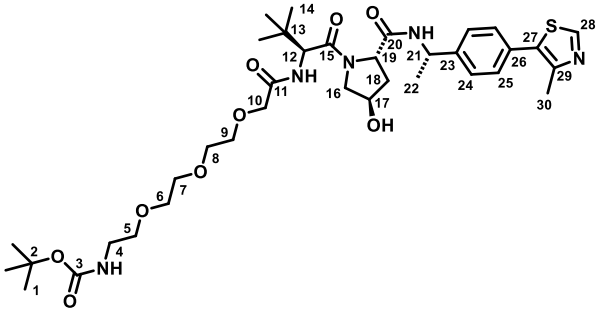

M ($C_{36}H_{55}N_5O_9S$): 733.92 g/mol.

Yield: 237 mg (323 μmol; 65%).

R_f: (SiO_2, EtOAc/MeOH 5:1) = 0.34.

^{1}H NMR: (500 MHz, $CDCl_3$) δ [ppm] = 8.71 (s, 1H, H28), 7.40-7.36 (m, 5H, H24, H25, N*H*), 5.13-5.09 (m, 2H, H21, O*H*), 4.73 (t, ^3J = 8.0 Hz, 1H, H19), 4.58 (d, ^3J = 8.1 Hz, 1H, H12), 4.52 (s, 1H, H17), 4.12-4.01 (m, 3H, H16a, H10), 3.72-3.62 (m, 9H, H6, H7, H8, H9, H16b), 3.56-3.52 (m, 2H, H5), 3.32 (s, 2H, H4), 2.58-2.51 (m, 1H, H18a), 2.53 (s, 3H, H30), 2.10-2.04 (m, 1H, H18b), 1.48 (d, ^3J = 7.1 Hz, 3H, H22), 1.44 (s, 9H, H1), 1.07 (s, 9H, H14).

^{13}C NMR: (125 MHz, $CDCl_3$) δ [ppm] = 171.6 (C11); 170.8 (C15); 170.0 (C20); 156.6 (C3); 150.5 (C28); 148.4 (C29); 143.5 (C23); 131.9 (C27); 130.8 (C26); 129.7 (C25); 126.6 (C24); 79.6 (C2); 71.0, 70.7, 70.5, 70.3, 70.2, 70.1 (C5, C6, C7, C8, C9, C10, C17); 58.6 (C19); 57.4 (C12); 56.9 (C16); 49.0 (C21); 40.5 (C4); 35.8 (C13); 35.2 (C18); 28.5 (C1); 26.6 (C14); 22.3 (C22); 16.1 (C30).

6.2.7.8 Synthesis of 183

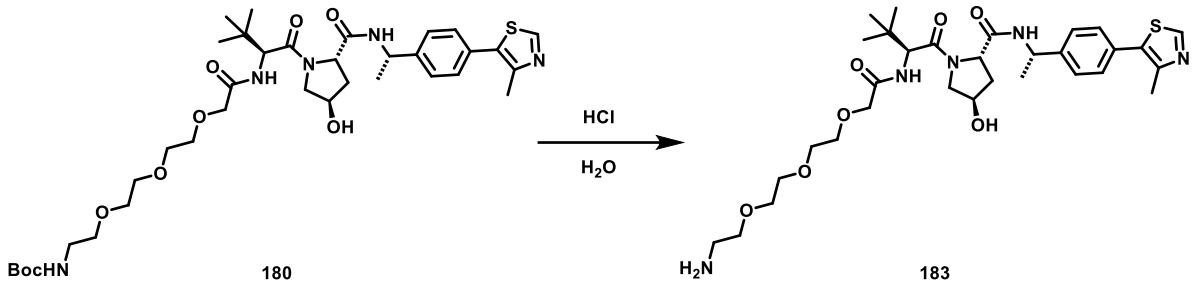

In a 25 mL round bottom flask, 225 mg (307 μmol; 1.00 eq.) of linker-recruiter conjugate **180** were dissolved in 5 mL of HCl (1M). After 2.5 h, major conversion of linker-recruiter conjugate **180** was observed by TLC and 10 mL of CH_2Cl_2 were added. The solution was adjusted to pH 8 by the addition of $NaHCO_3$, the layers were separated, and the aqueous phase was extracted four times with 20 mL of CH_2Cl_2. The combined organic layers were dried over $MgSO_4$, filtered, and the solvent was removed under reduced pressure. The residue was purified by column chromatography (SiO_2, dryload, EtOAc/MeOH/NEt_3 1:0:0 to 20:4:1). The residue was dissolved in CH_2Cl_2, filtered through a syringe filter, and the solvent was removed under reduced pressure. The residue was dissolved in H_2O/*t*BuOH/MeCN and lyophilized to obtain 117 mg (185 μmol; 60%) of the desired product **183** as a colorless lyophilizate.

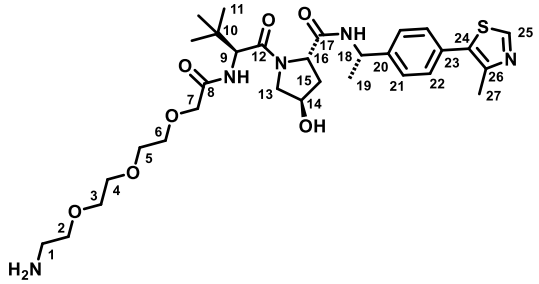

M ($C_{31}H_{47}N_5O_7S$): 633.80 g/mol.

Yield: 117 mg (185 μmol; 60%).

R_f: (SiO_2, EtOAc/MeOH/NEt_3 20:4:1) = 0.04.

^{1}H NMR: (400 MHz, $CDCl_3$) δ [ppm] = 8.67 (s, 1H, H25), 8.22 (d, ^3J = 7.9 Hz, 1H, N*H*), 7.43-7.35 (m, 5H, H21, H22, N*H*), 5.10 (quin, ^3J = 7.2 Hz, 1H, H18), 4.73-4.66 (m, 2H, H9, H16), 4.44 (s, 1H, H14), 4.17-4.12 (m, 1H, H7a), 4.02-3.96 (m, 2H, H7b, H13a), 3.72-3.62 (m, 11H, H2, H3, H4, H5, H6, H23b), 3.08-3.01 (m, 2H, H1), 2.52 (s, 3H, H27), 2.18-2.14 (m, 2H, H15), 1.49 (d, ^3J = 7.0 Hz, 3H, H19), 1.06 (s, 9H, H11).

^{13}C NMR: (100 MHz, $CDCl_3$) δ [ppm] = 171.2 (C8); 170.7 (C12); 170.2 (C17); 150.4 (C25); 148.5 (C26); 143.9 (C20); 131.8 (C24); 130.7 (C23); 129.5 (C22); 126.5 (C21); 70.9, 70.6, 70.4, 70.3, 70.1, 69.4 (C2, C3, C4, C5, C6, C7); 70.0 (C14); 59.1 (C16); 57.5 (C13); 57.0 (C9); 48.8 (C18); 40.3 (C1); 37.3 (C10); 35.9 (C15); 26.6 (C11); 22.5 (C19); 16.2 (C27).

HR-MS (ESI):

Ion	Calc. mass [u]	Exp. mass [u]	Δ [ppm]
$[M+H]^+$	634.32690	634.32664	-0.40
$[M+Na]^+$	656.30884	656.30855	-0.44

6.2.7.9 Synthesis of 174

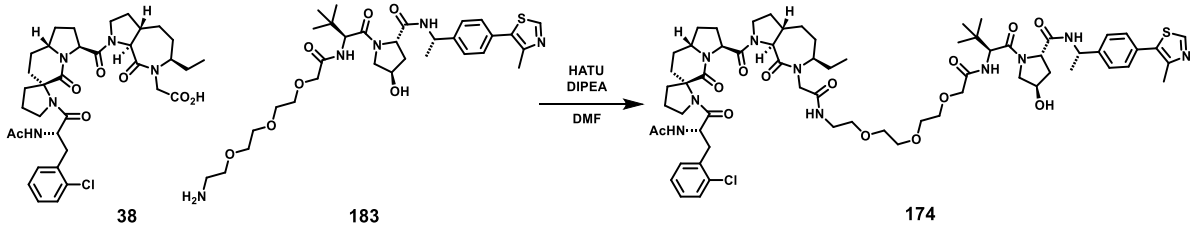

38 183 174

In a 10 mL *Schlenk* tube, 25 mg (37 μmol; 1.1 eq.) of warhead **38**, 17 mg (44 μmol; 1.3 eq.) of HATU, and 20.7 μL (119 μmol; 3.50 eq.) of DIPEA were added in 1.5 mL of DMF. After 30 min at room temperature, 21 mg (34 μmol; 1.0 eq.) of linker-recruiter conjugate **183** were added and the mixture was stirred until full conversion of linker-recruiter conjugate **183** was observed by TLC after 16 h and the solvent was removed under reduced pressure. The residue was purified by column chromatography (SiO_2, dryload, EtOAc/MeOH/NEt_3 1:0:0 to 20:4:1). The residue was dissolved in CH_2Cl_2, filtered through a syringe filter, and the solvent was removed under reduced pressure. The residue was then purified by reverse phase column chromatography (MeCN/H_2O 2:8 to 8:2) and lyophilized to obtain 15 mg (11 μmol; 34%) of the desired product **174** as a colorless lyophilizate.

M ($C_{66}H_{91}N_{10}O_{13}SCl$):	1300.02 g/mol.			
Yield:	15 mg (11 μmol; 34%).			
R_f:	(SiO_2, EtOAc/MeOH/NEt_3 20:4:1) = 0.24.			
HR-MS (ESI):	Ion	Calc. mass [u]	Exp. mass [u]	Δ [ppm]
	$[M+H]^+$	1299.62491	1299.62722	+1.78
	$[M+Na]^+$	1321.60685	1321.60720	+0.27
HPLC:	t_r [min]		10.64-11.04	
	Purity [%]		96	

6.2.8 Synthesis towards PROTACs 184-187

6.2.8.1 Synthesis of 192

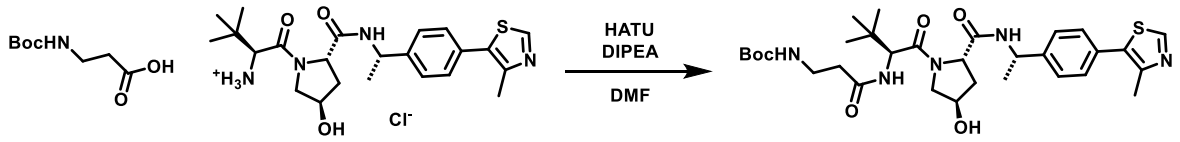

In a 25 mL *Schlenk* flask, 113 mg (600 μmol; 1.20 eq.) of linker **188**, 285 mg (750 μmol; 1.50 eq.) of HATU, and 118 μL (675 μmol; 1.35 eq.) of DIPEA were added in 9 mL of DMF. In a 50 mL *Schlenk* flask, 240 mg (500 μmol; 1.00 eq.) of recruiter **113** and 236 μL (1.35 mmol; 2.70 eq.) of DIPEA were added in 9 mL of DMF. After 30 min, the mixture was added to the solution of linker **188**. The mixture was stirred until full conversion of recruiter **113** was observed by TLC after 15 h and the solvent was removed under reduced pressure. The residue was purified by column chromatography (SiO_2, EtOAc/MeOH 1:0 to 10:1). The residue was dissolved in CH_2Cl_2, filtered through a syringe filter, and the solvent was removed under reduced pressure. The residue was dissolved in MeCN/H_2O and lyophilized to obtain 185 mg (300 μmol; 60%) of the desired product **192** as a colorless lyophilizate.

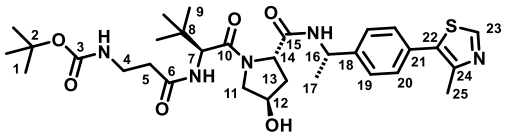

M ($C_{31}H_{45}N_5O_6S$): 615.79 g/mol.

Yield: 185 mg (300 μmol; 60%).

R_f: (SiO_2, EtOAc/MeOH 20:1) = 0.14.

^{1}H NMR: (500 MHz, $CDCl_3$) δ [ppm] = 8.68 (s, 1H, H23), 7.48 (d, ^3J = 7.8 Hz, 1H, N*H*), 7.41 (d, ^3J = 8.2 Hz, 2H, H20), 7.37 (d, ^3J = 8.2 Hz, 2H, H19), 6.45 (d, ^3J = 8.7 Hz, 1H, N*H*), 5.19 (s, 1H, O*H*), 5.08 (quin, ^3J = 7.2 Hz, 1H, H16), 4.77 (t, ^3J = 7.9 Hz, 1H, H14), 4.55-4.52 (m, 2H, H7, H12), 4.11 (d, ^3J = 11.5 Hz, 1H, H11a), 3.60 (dd, ^3J = 11.4 Hz, ^4J = 3.5 Hz, 1H, H11b), 3.47-3.30 (m, 2H, H4), 2.61-2.52 (m, 1H, H13a), 2.51 (s, 3H, H25), 2.50-2.43 (m, 1H, H5a), 2.40-2.33 (m, 1H, H5b), 2.12-2.05 (m, 1H, H13b), 1.47 (d, ^3J = 6.9 Hz, 3H, H17), 1.43 (s, 9H, H1), 1.05 (s, 9H, H9).

^{13}C NMR: (125 MHz, $CDCl_3$) δ [ppm] = 172.5 (C6); 171.1 (C10); 169.6 (C15); 156.2 (C3); 150.1 (C23); 148.6 (C24); 143.3 (C18); 131.7 (C22); 131.1 (C21); 129.7 (C20); 126.6 (C19); 79.5 (C2); 70.3 (C12); 58.5 (C14); 57.8 (C7); 56.6 (C11); 49.0 (C16); 36.6 (C4); 36.3 (C5); 36.2 (C13); 35.3 (C8); 28.5 (C1); 26.6 (C9); 22.5 (C17); 16.2 (C25).
Note: C2, C4, C5, C6, C7, C8, C10, C11, C13, C15, and C23 were assigned by HMBC and HSQC.

6.2.8.2 Synthesis of 196

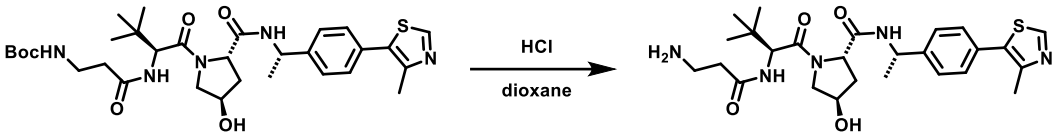

In a 25 mL round bottom flask, 132 mg (214 μmol; 1.00 eq.) of linker-recruiter conjugate **192** were dissolved in 1.5 mL dioxane. To the solution, 1.5 mL of a solution of HCl (4M in dioxane) were added. After 1 h, full conversion of linker-recruiter conjugate **192** was observed by TLC. Next, 10 mL of MeOH were added and the solvent was removed under reduced pressure. The residue was dissolved in 5 mL of HCl (0.05M), washed with 10 mL of M*t*BE, and the solution was adjusted to pH 8 by addition of $NaHCO_3$. The aqueous phase was extracted five times with 50 mL of CH_2Cl_2 and the combined organic layers were dried over $MgSO_4$, filtered, and the solvent was removed under reduced pressure. The residue was purified by column chromatography (SiO_2, EtOAc/MeOH/NEt_3 1:0:0 to 20:4:1). The residue was dissolved in CH_2Cl_2, filtered through a syringe filter and the solvent was removed under reduced pressure. The residue was dissolved in MeCN/H_2O and lyophilized to obtain 73 mg (142 μmol; 66%) of the desired product **196** as a colorless lyophilizate.

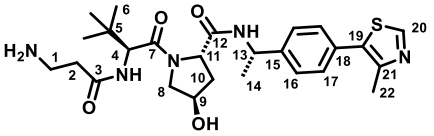

M ($C_{26}H_{37}N_5O_4S$): 515.67 g/mol.

Yield: 73 mg (142 μmol; 66%).

R_f: (SiO_2, EtOAc/MeOH/NEt_3 20:4:1) = 0.06.

^{1}H NMR: (500 MHz, $CDCl_3$) δ [ppm] = 8.67 (s, 1H, H20), 8.39 (d, ^3J = 7.9 Hz, 1H, N*H*), 7.69 (d, ^3J = 7.8 Hz, 1H, N*H*), 7.39 (d, ^3J = 8.3 Hz, 2H, H17), 7.36 (d, ^3J = 8.3 Hz, 2H, H16), 5.09 (quin, ^3J = 7.3 Hz, 1H, H13), 4.75 (t, ^3J = 8.5 Hz, 1H, H11), 4.49-4.43 (m, 2H, H4, H9), 4.15 (d, ^3J = 11.5 Hz, 1H, H8a), 3.57 (dd, ^3J = 11.4 Hz, ^3J = 3.4 Hz, 1H, H8b), 3.31-2.96 (m, 5H, H1, H10a, NH_2) 2.53 (s, 3H, H22), 2.53-2.45 (m, 1H, H2a), 2.37 (t, ^3J = 6.0 Hz, 1H, H2b), 2.11-2.06 (m, 1H, H10b), 1.47 (d, ^3J = 7.0 Hz, 3H, H14), 1.07 (s, 9H, H6).

^{13}C NMR:	(125 MHz, $CDCl_3$) δ [ppm] = 173.2 (C3); 172.5 (C7); 169.9 (C12); 150.4 (C20); 148.6 (C21); 143.4 (C15); 131.7 (C19); 131.0 (C18); 129.7 (C17); 126.6 (C16); 70.1 (C9); 58.4, 58.4 (C4, C11); 57.8 (C8); 48.9 (C13); 36.6 (C1); 36.3 (C2); 36.2 (C10); 35.3 (C5); 26.8 (C6); 22.4 (C14); 16.2 (C22).			
HR-MS (ESI):	Ion	Calc. mass [u]	Exp. mass [u]	Δ [ppm]
	$[M+H]^+$	516.26390	516.26453	+1.22
	$[M+Na]^+$	538.24585	538.24559	-0.48
LC-MS (ESI):	t_r [min]		9.05-9.57	
	Ion	Calc. mass [u]	Exp. mass [u]	
	$[M+H]^+$	516.26	516.32	

6.2.8.3 Synthesis of 184

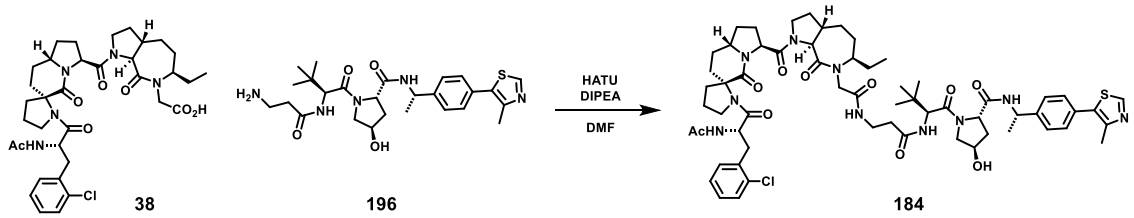

In a 10 mL *Schlenk* tube, 25 mg (36 μmol; 1.0 eq.) of warhead **38**, 15 mg (40 μmol; 1.1 eq.) of HATU, and 16 μL of DIPEA (91 μmol; 2.5 eq.) were added in 1.6 mL of DMF. After 30 min, 20 mg (38 μmol; 1.0 eq.) of linker-recruiter conjugate **196** were added. The mixture was stirred at room temperature until full conversion of warhead **38** was observed by TLC after 17 h and the solvent was removed under reduced pressure. The residue was purified by column chromatography (dryload, SiO_2, EtOAc/MeOH/NEt_3 1:0:0 to 20:4:1). The residue was dissolved in CH_2Cl_2, filtered through a syringe filter, and the solvent was removed under reduced pressure. The residue was purified by reverse phase column chromatography (MeCN/H_2O 2:8 to 7:3) and lyophilized to obtain 22 mg (19 μmol; 51%) of the desired product **184** as a colorless lyophilizate.

M ($C_{61}H_{81}N_{10}O_{10}SCl$):	1181.89 g/mol.			
Yield:	22 mg (19 μmol; 51%).			
R_f:	(SiO_2, EtOAc/MeOH/NEt_3 20:4:1) = 0.17.			
HR-MS (ESI):	Ion	Calc. mass [u]	Exp. mass [u]	Δ [ppm]
	$[M+H]^+$	1181.56191	1181.56592	+3.39
	$[M+Na]^+$	1203.54386	1203.54524	+1.15
LC-MS (ESI):	t_r [min]		12.97-14.29, 14.67-16.52	
	Ion	Calc. mass [u]	Exp. mass [u]	Purity [%]
	$[M+H]^+$	1181.56	1181.77	>99

6.2.8.4 Synthesis of 193

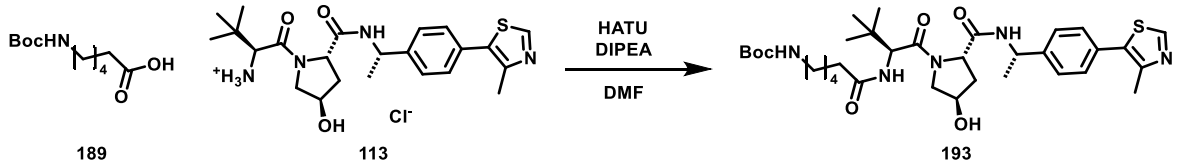

In a 25 mL *Schlenk* flask, 139 mg (600 μmol; 1.20 eq.) of linker **189**, 285 mg (750 μmol; 1.50 eq.) of HATU, and 118 μL (675 μmol; 1.35 eq.) of DIPEA were added in 9 mL of DMF. In a 50 mL *Schlenk* flask, 240 mg (500 μmol; 1.00 eq.) of recruiter **113** and 236 μL (1.35 mmol; 2.70 eq.) of DIPEA were added in 9 mL of DMF. After 30 min, the mixture was added to the solution of linker **189**. The mixture was stirred until full conversion of recruiter **113** was observed by TLC after 16 h and the solvent was removed under reduced pressure. The residue was purified by column chromatography (SiO_2, EtOAc/MeOH 1:0 to 10:1). The residue was dissolved in MeCN/H_2O and lyophilized to obtain 239 mg (364 μmol; 73%) of the desired product **193** as a colorless lyophilizate.

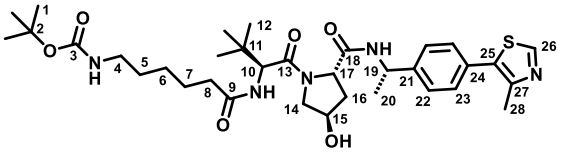

M ($C_{34}H_{51}N_5O_6S$): 657.87 g/mol.

Yield: 239 mg (364 μmol; 73%).

R_f: (SiO_2, EtOAc/MeOH 20:1) = 0.19.

^{1}H NMR: (500 MHz, $CDCl_3$) δ [ppm] = 8.68 (s, 1H, H26), 7.47 (d, ^3J = 6.7 Hz, 1H, N*H*), 7.41-7.37 (m, 4H, H22, H23), 6.17 (d, ^3J = 8.6 Hz, 1H, N*H*), 5.09 (quin, ^3J = 7.2 Hz, 1H, H19), 4.75 (t, ^3J = 7.9 Hz, 1H, H17), 4.68 (s, 1H, N*H*), 4.55 (d, 1H, ^3J = 8.7 Hz, H10), 4.51 (s, 1H, H15), 4.14 (d, ^3J = 11.2 Hz, 1H, H14a), 3.68-3.56 (m, 1H, H14b), 3.09 (s, 2H, H4), 2.57-2.51 (m, 1H, H16a), 2.53 (s, 3H, H28), 2.34-2.08 (m, 3H, H7, H16b), 1.69-1.54 (m, 2H, H5), 1.48-1.42 (m, 14H, H1, H8, H20), 1.33-1.26 (m, 2H, H6), 1.05 (s, 9H, H12).

^{13}C NMR: (125 MHz, $CDCl_3$) δ [ppm] = 174.0 (C9); 172.5 (C13); 169.8 (C18); 154.9 (C3); 150.3 (C26); 148.4 (C27); 143.2 (C21); 131.7 (C25); 130.9 (C24); 129.7 (C23); 126.6 (C22); 79.3 (C2); 70.1 (C15); 58.4 (C17); 57.8 (C10); 56.8 (C14); 49.0 (C19); 40.4 (C4), 36.4 (C7); 36.0 (C16); 35.4 (C11); 29.3 (C8); 28.6 (C1); 26.7 (C12); 26.3 (C6); 25.3 (C5); 22.3 (C20); 16.2 (C28).

Note: C2, C7, C18, C21, C24, C25, C26, C27, were assigned by HMBC and HSQC.

6.2.8.5 Synthesis of 197

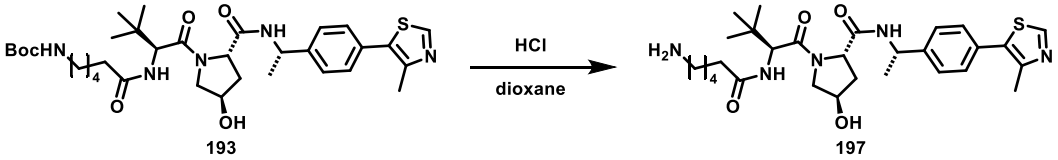

In a 50 mL round bottom flask, 195 mg (296 μmol; 1.00 eq.) of linker-recruiter conjugate **193** were dissolved in 3 mL dioxane. To the solution, 3 mL of a solution of HCl (4M) in dioxane were added. After 1 h, full conversion of linker-recruiter conjugate **193** was observed by TLC. Next, 10 mL of MeOH were added and the solvent was removed under reduced pressure. The residue was dissolved in 10 mL of HCl (0.05M), washed with 10 mL of M*t*BE, and the solution was adjusted to pH 8 by addition of $NaHCO_3$. The aqueous phase was extracted five times with 60 mL of CH_2Cl_2 and the combined organic layers were dried over $MgSO_4$, filtered, and the solvent was removed under reduced pressure. The residue was purified by column chromatography (SiO_2, EtOAc/MeOH/NEt_3 1:0:0 to 20:4:1). The residue was dissolved in CH_2Cl_2, filtered through a syringe filter and the solvent was removed under reduced pressure. The residue was dissolved in MeCN/H_2O and lyophilized to obtain 117 mg (210 μmol; 71%) of the desired product **197** as a colorless lyophilizate.

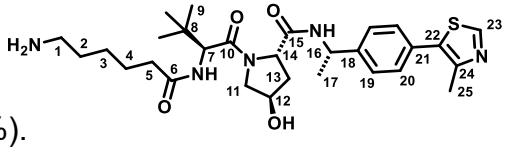

M ($C_{29}H_{43}N_5O_4S$): 557.75 g/mol.

Yield: 117 mg (210 μmol; 71%).

R_f: (SiO_2, EtOAc/MeOH/NEt_3 20:4:1) = 0.05.

^{1}H NMR: (500 MHz, $CDCl_3$) δ [ppm] = 8.68 (s, 1H, H23), 7.82 (d, ^3J = 7.8 Hz, 1H, N*H*), 7.40 (d, ^3J = 8.3 Hz, 2H, H20), 7.37 (d, ^3J = 8.3 Hz, 2H, H19), 6.79 (d, ^3J = 8.9 Hz, 1H, N*H*), 5.54 (s, 2H, NH_2), 5.11 (quin, ^3J = 7.3 Hz, 1H, H16), 4.68 (t, ^3J = 8.4 Hz, 1H, H14), 4.62 (d, ^3J = 9.0 Hz, 1H, H7), 4.47 (s, 1H, H12), 4.02 (d, ^3J = 11.1 Hz, 1H, H11a), 3.63 (dd, ^3J = 10.9 Hz, ^3J = 3.0 Hz, 1H, H11b), 2.81 (t, ^3J = 7.0 Hz, 2H, H1), 2.53 (s, 3H, H25), 2.33-2.26 (m, 2H, H2a, H13a), 2.22-2.13 (m, 2H, H2b, H13b), 1.72-1.52 (m, 4H, H4, H5), 1.50 (d, ^3J = 6.8 Hz, 3H, H17), 1.39-1.31 (m, 2H, H3), 1.06 (s, 9H, H9).

^{13}C NMR:	(125 MHz, $CDCl_3$) δ [ppm] = 173.8 (C6); 172.0 (C10); 170.3 (C15); 150.4 (C23); 148.6 (C24); 143.6 (C18); 131.7 (C22); 130.9 (C21); 129.6 (C20); 126.6 (C19); 69.8 (C12); 59.0 (C14); 57.9 (C7); 57.4 (C11); 48.8 (C16); 39.9 (C1); 36.8 (C2); 35.7 (C13); 35.4 (C8); 28.7 (C4/C5); 26.7 (C9); 25.5 (C3); 24.6 (C4/C5); 22.3 (C17); 16.2 (C25).			
HR-MS (ESI):	Ion	Calc. mass [u]	Exp. mass [u]	Δ [ppm]
	$[M+H]^+$	558.31085	558.31192	+1.92
	$[M+Na]^+$	580.29280	580.29369	+1.54
LC-MS (ESI):	t_r [min]		9.11-10.15	
	Ion	Calc. mass [u]	Exp. mass [u]	
	$[M+H]^+$	558.31	558.43	

6.2.8.6 Synthesis of 185

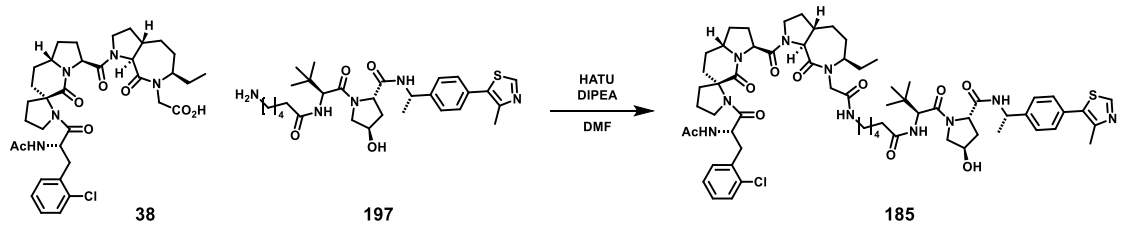

38 197 185

In a 10 mL *Schlenk* tube, 25 mg (36 μmol; 1.0 eq.) of warhead **38**, 15 mg (40 μmol; 1.1 eq.) of HATU, and 16 μL (91 μmol; 2.5 eq.) of DIPEA were added in 1.6 mL of DMF. After 45 min, 21 mg (38 μmol; 1.0 eq.) of linker-recruiter conjugate **197** were added. The mixture was stirred at room temperature until full conversion of warhead **38** was observed by TLC after 17 h and the solvent was removed under reduced pressure. The residue was purified by column chromatography (dryload, SiO_2, EtOAc/MeOH/NEt_3 1:0:0 to 20:4:1). The residue was dissolved in CH_2Cl_2, filtered through a syringe filter, and the solvent was removed under reduced pressure. The residue was purified by reverse phase column chromatography (MeCN/H_2O 2:8 to 7:3) and lyophilized to obtain 25 mg (20 μmol; 56%) of the desired product **185** as a colorless lyophilizate.

M ($C_{64}H_{87}N_{10}O_{10}SCl$):	1223.97 g/mol.			
Yield:	25 mg (20 μmol; 56%).			
R_f:	(SiO_2, EtOAc/MeOH/NEt_3 20:4:1) = 0.24.			
HR-MS (ESI):	Ion	Calc. mass [u]	Exp. mass [u]	Δ [ppm]
	$[M+H]^+$	1223.60886	1223.61251	+2.98
	$[M+Na]^+$	1245.59081	1245.59217	+1.09
LC-MS (ESI):	t_r [min]		12.97-14.29, 14.67-16.52	
	Ion	Calc. mass [u]	Exp. mass [u]	Purity [%]
	$[M+H]^+$	1223.61	1223.85	>99

6.2.8.7 Synthesis of 194

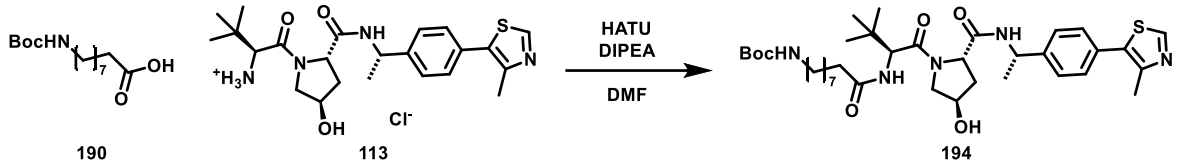

190 113 194

In a 25 mL *Schlenk* flask, 142 mg (600 μmol; 1.20 eq.) of linker **190**, 285 mg (750 μmol; 1.50 eq.) of HATU, and 118 μL (675 μmol; 1.35 eq.) of DIPEA were added in 9 mL of DMF. In a 50 mL *Schlenk* flask, 240 mg (500 μmol; 1.00 eq.) of recruiter **113** and 236 μL of DIPEA (1.35 mmol; 2.70 eq.) were added in 9 mL of DMF. After 30 min, the mixture was added to the solution of linker **190**. The mixture was stirred until full conversion of recruiter **113** was observed by TLC after 16 h and the solvent was removed under reduced pressure. The residue was purified by column chromatography (SiO_2, EtOAc/MeOH 1:0 to 20:1). The residue was dissolved in CH_2Cl_2, filtered through a syringe filter, and the solvent was removed under reduced pressure. The residue was dissolved in MeCN/H_2O and lyophilized to obtain 260 mg (371 μmol; 74%) of the desired product **194** as a colorless lyophilizate.

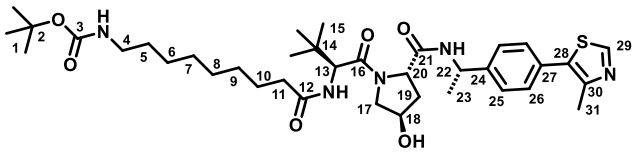

M ($C_{37}H_{57}N_5O_6S$): 699.95 g/mol.

Yield: 260 mg (371 μmol; 74%).

R_f: (SiO_2, EtOAc/MeOH 40:1) = 0.17.

^{1}H NMR: (500 MHz, $CDCl_3$) δ [ppm] = 8.68 (s, 1H, H29), 7.47 (d, ^3J = 7.7 Hz, 1H, N*H*), 7.41 (d, ^3J = 8.2 Hz, 2H, H26), 7.37 (d, ^3J = 8.2 Hz, 2H, H25), 6.11 (d, ^3J = 7.9 Hz, 1H, N*H*), 5.09 (quin, ^3J = 7.2 Hz, 1H, H22), 4.73 (t, ^3J = 7.9 Hz, 1H, H20), 4.56-4.51 (m, 2H, H13, H18), 4.13 (d, ^3J = 11.5 Hz, 1H, H17a), 3.60 (dd, ^3J = 11.4 Hz, ^4J = 3.6 Hz, 1H, H17b), 3.11-3.06 (m, 2H, H4), 2.58-2.50 (m, 1H, H19a), 2.53 (s, 3H, H31), 2.19 (t, ^3J = 7.3 Hz, 2H, H5), 2.10-2.05 (m, 1H, H19b), 1.75 (s, 1H, O*H*), 1.62-1.56 (m, 2H, H10), 1.48-1.42 (m, 14H, H1, H11, H23), 1.33-1.26 (m, 8H, H6-9), 1.05 (s, 9H, H15).

^{13}C NMR: (125 MHz, $CDCl_3$) δ [ppm] = 174.0 (C12); 172.4 (C16); 169.7 (C21); 155.9 (C3); 150.4 (C29); 148.6 (C30); 143.6 (C24); 131.7 (C28); 131.1 (C27); 129.7 (C26); 126.6 (C25); 79.0 (C2); 70.2 (C18); 58.5 (C20); 57.7 (C13); 56.8 (C17); 49.0 (C22); 40.7 (C4), 36.5 (C5); 35.5 (C19); 35.0 (C14); 30.1 (C10); 29.2 (C6/7/8/9); 29.1 (C6/7/8/9); 29.1 (C6/7/8/9); 28.6 (C1); 26.6 (C15); 26.3 (C6/7/8/9); 25.6 (C11); 22.4 (C23); 16.2 (C31).

Note: C2 and C3 were assigned by HMBC and HSQC.

6.2.8.8 Synthesis of 198

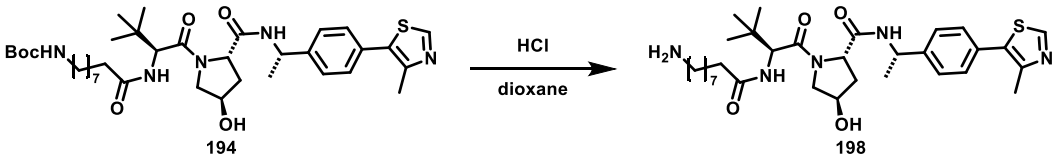

In a 50 mL round bottom flask, 195 mg (296 μmol; 1.00 eq.) of linker-recruiter conjugate **194** were dissolved in 3 mL of dioxane. To the solution, 3 mL of a solution of HCl (4M) in dioxane were added. After 1 h, full conversion of linker-recruiter conjugate **194** was observed by TLC. Next, 10 mL of MeOH were added and the solvent was removed under reduced pressure. The residue was dissolved in 10 mL of HCl (0.05M), washed with 10 mL of M*t*BE, and the solution was adjusted to pH 8 by addition of $NaHCO_3$. The aqueous phase was extracted five times with 60 mL of CH_2Cl_2 and the combined organic layers were dried over $MgSO_4$, filtered, and the solvent was removed under reduced pressure. The residue was purified by column chromatography (SiO_2, EtOAc/MeOH/NEt_3 1:0:0 to 20:4:1). The residue was dissolved in CH_2Cl_2, filtered through a syringe filter and the solvent was removed under reduced pressure. The residue was dissolved in MeCN/H_2O and lyophilized to obtain 76 mg (0.13 mmol; 43%) of the desired product **198** as a colorless lyophilizate.

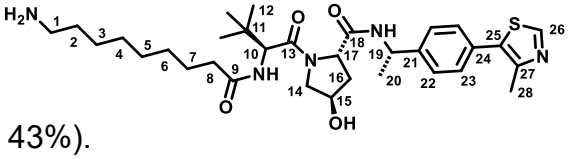

M ($C_{32}H_{49}N_5O_4S$): 599.83 g/mol.

Yield: 76 mg (0.13 mmol; 43%).

R_f: (SiO_2, EtOAc/MeOH/NEt_3 20:4:1) = 0.06.

^{1}H NMR: (500 MHz, $CDCl_3$) δ [ppm] = 8.69 (s, 1H, H26), 7.56 (d, ^3J = 7.7 Hz, 1H, N*H*), 7.42 (d, ^3J = 8.3 Hz, 2H, H23), 7.38 (d, ^3J = 8.3 Hz, 2H, H22), 6.24 (d, ^3J = 8.7 Hz, 1H, N*H*), 5.11 (quin, ^3J = 7.1 Hz, 1H, H19), 4.72 (t, ^3J = 7.7 Hz, 1H, H17), 4.60 (d, ^3J = 8.8 Hz, 1H, H10), 4.51 (s, 1H, H15), 4.06 (d, ^3J = 11.0 Hz, 1H, H14a), 3.63 (dd, ^3J = 11.1 Hz, ^3J = 3.6 Hz, 1H, H14b), 3.36 (s, 2H, NH_2), 2.72 (t, ^3J = 7.0 Hz, 2H, H1), 2.54 (s, 3H, H28), 2.48 (ddd, ^3J = 13.0 Hz, ^3J = 7.7 Hz, ^3J = 4.6 Hz, 1H, H2a), 2.26-2.16 (m, 2H, H2b, H16a), 2.11-2.07 (m, 1H, H16b), 1.66-1.56 (m, 2H, H3), 1.52-1.45 (m, 5H, H4, H20), 1.39-1.31 (m, 8H, H5, H6, H7, H8), 1.06 (s, 9H, H12).

^{13}C NMR: (125 MHz, $CDCl_3$) δ [ppm] = 173.8 (C9); 172.1 (C13); 170.0 (C18); 150.4 (C26); 148.6 (C27); 143.4 (C21); 131.7 (C25); 131.0 (C24); 129.7 (C23); 126.6 (C22); 69.9 (C15); 58.7 (C17); 57.6 (C10); 57.0 (C14); 48.9 (C19); 41.6 (C1); 36.4 (C2); 35.9 (C16); 35.3 (C11); 32.2, 28.9, 28.8, 28.8 (C4, C5, C6, C7/C8); 26.7 (C12); 26.3 (C7/8); 25.4 (C3); 22.4 (C20); 16.2 (C28).

HR-MS (ESI):

Ion	Calc. mass [u]	Exp. mass [u]	Δ [ppm]
$[M+H]^+$	600.35780	600.35827	+0.77
$[M+Na]^+$	622.33975	622.33991	+0.26

6.2.8.9 Synthesis of 186

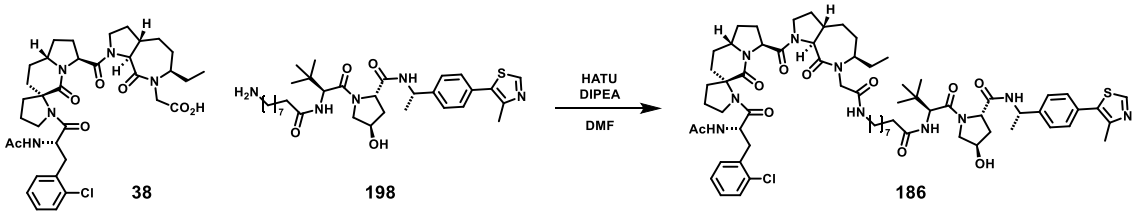

38 198 186

In a 10 mL *Schlenk* tube, 25 mg (36 μmol; 1.0 eq.) of warhead **38**, 15 mg (40 μmol; 1.1 eq.) of HATU, and 16 μL (91 μmol; 2.5 eq.) of DIPEA were added in 1.6 mL of DMF. After 15 min, 23 mg (38 μmol; 1.0 eq.) of linker-recruiter conjugate **198** were added. The mixture was stirred at room temperature until full conversion of warhead **38** was observed by TLC after 17 h and the solvent was removed under reduced pressure. The residue was purified by column chromatography (dryload, SiO_2, EtOAc/MeOH/NEt_3 1:0:0 to 20:4:1). The residue was dissolved in CH_2Cl_2, filtered through a syringe filter, and the solvent was removed under reduced pressure. The residue was purified by reverse phase column chromatography (MeCN/H_2O 3:7 to 7:3) and lyophilized to obtain 29 mg (23 μmol; 63%) of the desired product **186** as a colorless lyophilizate.

M ($C_{67}H_{93}N_{10}O_{10}SCl$):	1266.05 g/mol.			
Yield:	29 mg (23 μmol; 63%).			
R_f:	(SiO_2, EtOAc/MeOH/NEt_3 20:4:1) = 0.23.			
HR-MS (ESI):	Ion	Calc. mass [u]	Exp. mass [u]	Δ [ppm]
	$[M+H]^+$	1265.65581	1265.66031	+3.55
	$[M+Na]^+$	1287.63776	1287.64028	+1.96
LC-MS (ESI):	t_r [min]		14.65-15.31	
	Ion	Calc. mass [u]	Exp. mass [u]	Purity [%]
	$[M+H]^+$	1265.65	1265.87	88

6.2.8.10 Synthesis of 195

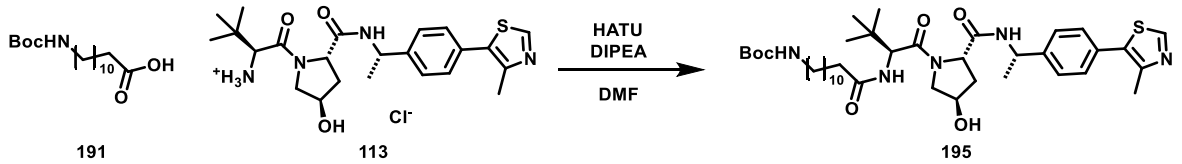

191 113 195

In a 25 mL *Schlenk* flask, 189 mg (600 μmol; 1.20 eq.) of linker **191**, 285 mg (750 μmol; 1.50 eq.) of HATU, and 118 μL (675 μmol; 1.35 eq.) of DIPEA were added in 9 mL of DMF. In a 50 mL *Schlenk* flask, 240 mg (500 μmol; 1.00 eq.) of recruiter **113** and 236 μL (1.35 mmol; 2.70 eq.) of DIPEA were added in 9 mL of DMF. After 30 min, the mixture was added to the solution of linker **191**. The mixture was stirred until full conversion of recruiter **113** was observed by TLC after 19 h the solvent was removed under reduced pressure. The residue was purified by column chromatography (SiO_2, EtOAc/MeOH 1:0 to 20:1). The residue was dissolved in CH_2Cl_2, filtered through a syringe filter, and the solvent was removed under reduced pressure. The residue was dissolved in MeCN/H_2O and lyophilized to obtain 267 mg (360 μmol; 72%) of the desired product **195** as a colorless lyophilizate.

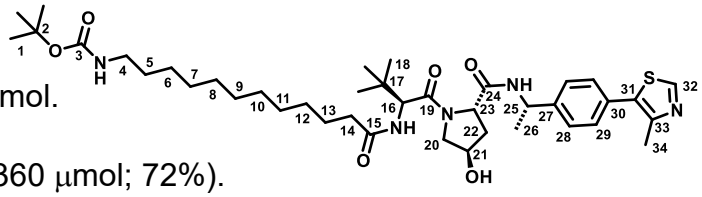

M ($C_{40}H_{63}N_5O_6S$): 742.03 g/mol.

Yield: 267 mg (360 μmol; 72%).

R_f: (SiO_2, EtOAc/MeOH 40:1) = 0.16.

^{1}H NMR: (500 MHz, $CDCl_3$) δ [ppm] = 8.68 (s, 1H, H32), 7.47 (d, ^3J = 7.6 Hz, 1H, N*H*), 7.41 (d, ^3J = 8.2 Hz, 2H, H29), 7.37 (d, ^3J = 8.2 Hz, 2H, H28), 6.09 (d, ^3J = 7.5 Hz, 1H, N*H*), 5.08 (quin, ^3J = 7.2 Hz, 1H, H25), 4.73 (t, ^3J = 7.8 Hz, 1H, H23), 4.54-4.51 (m, 2H, H16, H21), 4.14 (d, ^3J = 11.5 Hz, 1H, H20a), 3.60 (dd, ^3J = 11.3 Hz, ^3J = 3.6 Hz, 1H, H20b), 3.12-3.08 (m, 2H, H4), 2.59-2.52 (m, 1H, H22a), 2.53 (s, 3H, H34), 2.19 (t, ^3J = 7.6 Hz, 2H, H5), 2.08-2.04 (m, 1H, H22b), 1.63-1.57 (m, 2H, H14), 1.48-1.43 (m, 14H, H1, H13, H26), 1.30-1.24 (m, 14H, H6-12), 1.05 (s, 9H, H18).

^{13}C NMR: (125 MHz, $CDCl_3$) δ [ppm] = 174.1 (C15); 172.5 (C19); 169.6 (C24); 155.4 (C3); 150.0 (C32); 148.5 (C33); 143.2 (C27); 131.7 (C31); 131.1 (C30); 129.8 (C29); 126.5 (C28); 79.1 (C2); 70.2 (C21); 58.4 (C23); 57.7 (C16); 56.7 (C20); 49.0 (C25); 40.8 (C4), 36.6 (C5); 35.4 (C22); 34.9 (C17); 30.2 (C13); 29.6, 29.6, 29.6, 29.5, 29.4, 29.3 (C6-12), 28.6 (C1); 26.7 (C18); 25.7 (C14); 22.4 (C26); 16.2 (C34).
Note: C2 was assigned by HMBC and HSQC.

6.2.8.11 Synthesis of 199

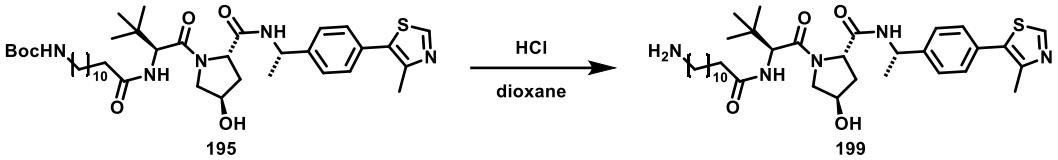

In a 50 mL round bottom flask, 270 mg (296 μmol; 1.00 eq.) of linker-recruiter conjugate **195** were dissolved in 3 mL dioxane. To the solution, 3 mL of a solution of HCl (4M) in dioxane were added. After 1 h, full conversion of linker-recruiter conjugate **195** was observed by TLC. Next, 10 mL of MeOH were added and the solvent was removed under reduced pressure. The residue was dissolved in 5 mL of HCl (0.05M), washed with 10 mL of M*t*BE, and the solution was adjusted to pH 8 by addition of $NaHCO_3$. The aqueous phase was extracted five times with 80 mL of CH_2Cl_2 and the combined organic layers were dried over $MgSO_4$, filtered, and the solvent was removed under reduced pressure. The residue was purified by column chromatography (SiO_2, EtOAc/MeOH/NEt_3 1:0:0 to 20:4:1). The residue was dissolved in CH_2Cl_2, filtered through a syringe filter and the solvent was removed under reduced pressure. The residue was dissolved in MeCN/H_2O and lyophilized to obtain 46 mg (72 μmol; 20%) of the desired product **199** as a colorless lyophilizate.

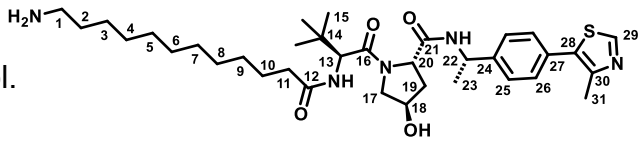

M ($C_{35}H_{55}N_5O_4S$): 641.916 g/mol.

Yield: 46 mg (72 μmol; 20%).

R_f: (SiO_2, EtOAc/MeOH/NEt_3 20:4:1) = 0.06.

^{1}H NMR: (400 MHz, $CDCl_3$) δ [ppm] = 8.67 (s, 1H, H29), 7.60 (d, ^3J = 8.0 Hz, 1H, N*H*), 7.42-7.35 (m, 4H, H25, H26), 6.26 (d, ^3J = 8.5 Hz, 1H, N*H*), 5.13-5.04 (m, 1H, H22), 4.70 (t, ^3J = 8.1 Hz, 1H, H20), 4.55-4.50 (m, 2H, H13, H18), 4.05 (d, ^3J = 11.1 Hz, 1H, H17a), 3.64-3.60 (m, 1H, H17b), 2.84 (t, ^3J = 7.5 Hz, 2H, H1), 2.52 (s, 3H, H31), 2.44-2.37 (m, 1H, H2a), 2.22-2.17 (m, 2H, H2b, H19a), 2.12-2.07 (m, 1H, H19b), 1.63-1.56 (m, 4H, H3, H4), 1.49 (d, ^3J = 6.8 Hz, 3H, H23), 1.34-1.23 (m, 14H, H5-H11), 1.04 (s, 9H, H15).

^{13}C NMR: (125 MHz, $CDCl_3$) δ [ppm] = 174.0 (C12); 172.0 (C16); 170.0 (C21); 150.5 (C29); 148.6 (C30); 143.4 (C24); 131.7 (C28); 131.0 (C27); 129.1 (C26); 126.6 (C25); 70.0 (C18); 58.8 (C20); 57.6 (C13); 57.0 (C17); 49.0 (C22); 41.6 (C1); 36.6 (C2); 35.9 (C19); 35.3 (C14); 32.1, 29.7, 29.6, 29.5, 29.4, 29.4, 29.2, 29.2, 29.1 (C4, C5, C6, C7, C8, C9, C10, C11); 26.6 (C15); 25.6 (C3); 22.4 (C23); 16.2 (C31).

HR-MS (ESI):

Ion	Calc. mass [u]	Exp. mass [u]	Δ [ppm]
$[M+H]^+$	642.40475	642.40469	-0.10
$[M+Na]^+$	664.38670	664.38627	-0.65

6.2.8.12 Synthesis of 187

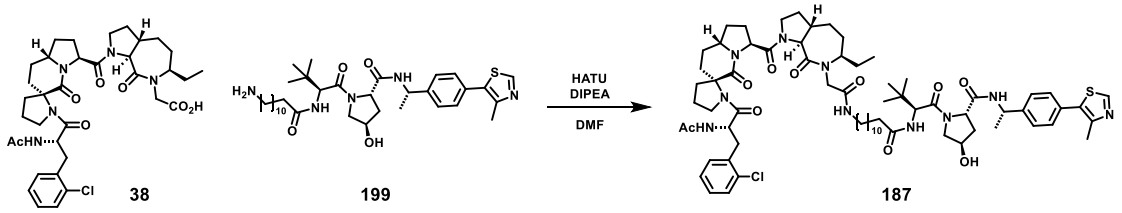

In a 10 mL *Schlenk* tube, 25 mg (36 μmol; 1.0 eq.) of warhead **38**, 15 mg (40 μmol; 1.1 eq.) of HATU, and 16 μL (91 μmol; 2.5 eq.) of DIPEA were added in 1.6 mL of DMF. After 20 min, 24 mg (38 μmol; 1.0 eq.) of linker-recruiter conjugate **199** were added. The mixture was stirred at room temperature until full conversion of warhead **38** was observed by TLC after 46 h and the solvent was removed under reduced pressure. The residue was purified by column chromatography (dryload, SiO_2, EtOAc/MeOH/NEt_3 1:0:0 to 20:4:1). The residue was dissolved in CH_2Cl_2, filtered through a syringe filter, and the solvent was removed under reduced pressure. The residue was purified by reverse phase column chromatography (MeCN/H_2O 3:7 to 7:3) and lyophilized to obtain 22 mg (17 μmol; 46%) of the desired product **187** as a colorless lyophilizate.

M ($C_{70}H_{99}N_{10}O_{10}SCl$):	1308.13 g/mol.			
Yield:	22 mg (17 μmol; 46%).			
R_f:	(SiO_2, EtOAc/MeOH/NEt_3 20:4:1) = 0.29.			
HR-MS (ESI):	Ion	Calc. mass [u]	Exp. mass [u]	Δ [ppm]
	$[M+H]^+$	1307.70276	1307.70721	+3.40
	$[M+Na]^+$	1329.68471	1329.69666	+1.47
LC-MS (ESI):	t_r [min]		16.28-16.82	
	Ion	Calc. mass [u]	Exp. mass [u]	Purity [%]
	$[M+2H]^{2+}$	654.35	654.74	>99

6.3 Solid Phase Peptide Synthesis (SPPS)

6.3.1 Standard operating procedures for SPPS

All peptides were synthesized on solid support. When *C*-terminal acids were aimed for, *Wang* resin preloaded with the first amino acid was used. When *C*-terminal amidation was envisioned, *Rink* amide resin was used. All peptides were either produced with an automated peptide synthesizer, or manually. For each peptide, resin with a total capacity of 15 μmol was used.

For automated peptide synthesis, the desired resins were preswollen in 800 μL of DMF. For Fmoc deprotection, 1 mL of a piperidine solution (40% in DMF) was added and the mixture was incubated for 5 min. The resin was washed with DMF and 1 mL of a 20% solution of piperidine in DMF was added and the mixture was incubated for 14 min. The resin was washed with 600 μL of DMF four times. For peptide coupling, 300 μL (0.4M in DMF, NMP for Fmoc[F]OH; 8 eq.) of a solution of the Fmoc protected amino acid, 50 μL (2.4M in DMF; 8 eq.) of a solution of DIC, and 50 μL of a solution of oxyma (2.4M; 8 eq.) were added to the resin and the mixture was shaken for 40 min. The resin was washed two times with 800 μL of DMF and the reaction was repeated. After the final Fmoc deprotection, resins were washed four times with 600 μL of DMF and then manually washed five times with 1 mL of CH_2Cl_2, MeOH, and Et_2O before drying.

For manual coupling, resins were swollen in 1 mL of DMF for 20 min. A mixture of 2 eq. of the respective acid, 2 eq. of HATU and 3 eq. of DIPEA in 300 μL of DMF were added onto the resin and the mixture was shaken for 2 h at room temperature. The resin was washed five times with 1 mL of DMF, CH_2Cl_2, MeOH, and Et_2O, respectively before the resin was allowed to dry. The procedure was repeated until full conversion was indicated by *Kaiser* test.

To test for successful coupling, a *Kaiser* test was performed. A sample of the resin was transferred and incubated with one drop of solution 1, 2, and 3, respectively for 5 min at 95 °C. Solution 1: 1 g of ninhydrin in EtOH. Solution 2: 80 g of phenol in 20 mL of EtOH. Solution 3: 0.4 mL (1mM in H_2O) KCN solution in 20 mL of pyridine. In the presence of free amines, the resin beads turn blue indicating incomplete conversion.

To deprotect the Fmoc protection group, the resin was swollen in 1 mL of DMF. The resin was then incubated with a 30% piperidine solution in DMF for 30 min two times.

The resin was washed five times with 1 mL of DMF, CH_2Cl_2, MeOH, and Et_2O respectively and allowed to dry.

To deprotect Dde groups, the resin was swollen in 1 mL of DMF for 20 min. The resin was incubated with 1 mL of a 2% hydrazine solution for 10 min. The procedure was repeated 10 times. The resin was washed five times with 1 mL of DMF, CH_2Cl_2, MeOH, and Et_2O respectively and allowed to dry.

For acetylation, the resin was swollen in 1 mL of CH_2Cl_2 for 20 min. The resin was incubated with 50 µL of Ac_2O and 50 µL of DIPEA in 300 µL of CH_2Cl_2 for 15 min. The resin was washed five times with 1 mL of CH_2Cl_2, MeOH, and Et_2O respectively and allowed to dry. The reaction was repeated until full acetylation was observed by *Kaiser* test.

To cleave the peptide from the resin while simultaneously deprotecting all side chains, either 25 µL H_2O and 25 µL tri*iso*propylsilane, or, in the case of cysteine, methionine, or tryptophane containing peptides 70 µL of thioanisole and 30 µL of ethanedithiol were added onto the dry resin. The volume was filled up to 1 mL with TFA and the mixture was incubated for 3 h. The solution was filtered into 10 mL of Et_2O which was pre-cooled to -20 °C. The mixture was stored at -20 °C for at least 1 h. If no precipitation was observed, the solvent was removed under reduced pressure. If precipitate was observed, the mixture was centrifuged (5.000 g, 4 °C) for 4 min and the liquid was decanted off. The pellet was then resuspended in Et_2O and centrifuged four times. The resulting pellet was allowed to dry, dissolved in a mixture of H_2O and *t*BuOH, frozen at -80 °C, and lyophilized to freeze the crude peptide.

For purification, samples were dissolved in 1 mL of H_2O and MeCN. The solution was centrifuged and the pellet was discarded. The peptide solution was then subjected to preparative HPLC. The UV spectrum (220 nm) was monitored for fraction collection. Each fraction was submitted to LC-MS. Product fractions were combined, depleted in MeCN, frozen at -80 °C, and lyophilized to obtain the pure product.

To exchange the anions of the peptide salts, samples were suspended in 3 mL of HCl (0.08M) and incubated for 30 min. The mixture was then frozen in liquid nitrogen and lyophilized. The procedure was repeated for a total of three times to obtain the final peptides.

6.3.2 Amino acids and Building blocks for SPPS

For all SPPS reactions, the following protection group strategy was used:

Glycine

Fmoc[G]OH

Alanine

Fmoc[A]OH

Valine

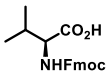

Fmoc[V]OH

Leucine

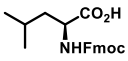

Fmoc[L]OH

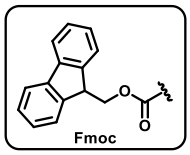

Isoleucine

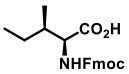

Fmoc[I]OH

Phenylalanine

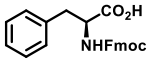

Fmoc[F]OH

Proline

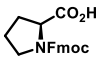

Fmoc[P]OH

Methionine

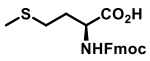

Fmoc[M]OH

Aspertatic Acid

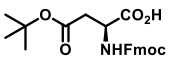

Fmoc[D(tBu)]OH

Glutamic Acid

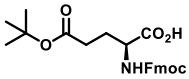

Fmoc[E(tBu)]OH

Serine

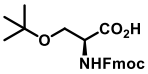

Fmoc[S(tBu)]OH

Threonine

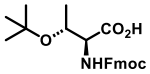

Fmoc[T(tBu)]OH

Tyrosine

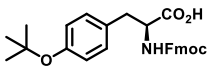

Fmoc[Y(tBu)]OH

Cysteine

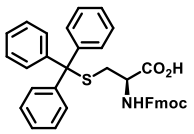

Fmoc[C(Trt)]OH

Asparagine

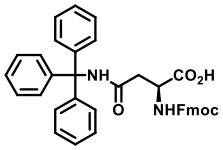

Fmoc[N(Trt)]OH

Glutamine

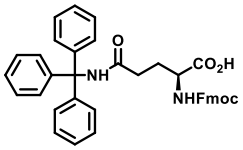

Fmoc[Q(Trt)]OH

Histidine

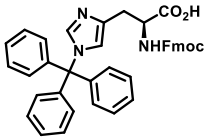

Fmoc[H(Trt)]OH

Tryptophan

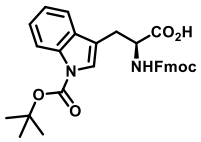

Fmoc[W(Boc)]OH

Arginine

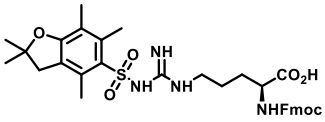

Fmoc[R(Pbf)]OH

Lysine

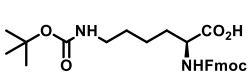

Fmoc[K(Boc)]OH

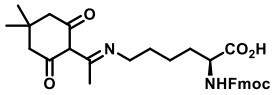

Fmoc[K(Dde)]OH

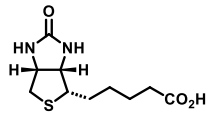

Biotin

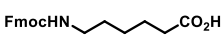

Fmoc[Ahx]OH

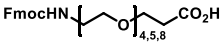

Fmoc[PEG4/5/8]OH

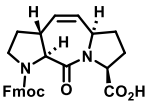

Fmoc[ProM-1]OH
239

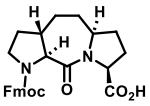

Fmoc[dH-1]OH
222

7 Appendix

7.1 Abbreviations

2-Cl-F	2-Chloro-phenylalanine
ActA	Actin-assembly inducing protein
Ax	6-amino-hexanoic acid
ADP	Adenosine diphosphate
AMP	Adenosine monophosphate
ATG	Autophagy-related protein
ATP	Adenosine triphosphate
BET	Bromo- and estray-terminal domain
BLI	Biolayer interferometry
Boc	*tert*-Butyloxycarbonyl
BRD4	Bromodomain-containing protein 4
CBz	Benzyloxy carbonyl
Cdc34	Cell division cycle 34
cIAP1	Cellular inhibitor of apoptosis protein 1
cLogP	calculated distribution coefficient between water and octanol
CODD	*C*-terminal oxygen-dependent degradation domain
Conc.	Concentrated
CP	Core particle
CRBN	Cereblon
Cul2	Cullin-2
Da	Dalton
DC50	Half-maximal degradation constant

DIC	Di*iso*propylcarbodiimid
Dioxane	1,4-Dioxane
DIPEA	Di*iso*propylethylamine
DMF	N,N-Dimethylformamide
DMSO	Dimethyl sulfoxide
DUB	Deubiquitinase
E. coli	Escherichia coli
EAR	Enoyl-ACP reductase
EloBC	Elongin B, Elongin C
EM	Electron microscope
EnaH	Enabled human Protein
EPSA	Experimental polar surface area
eq.	Equivalents
ER	Estrogen receptor
Erk	Extracellular-signal regulated kinase
ESI	Electrospray ionization
EVH1	Ena/VASP Homology 1
EVH2	Ena/VASP Homology 2
FAB	F-Actin-binding segment
F-Actin	Filamentous actin
FDA	Food and drug administration
Fmoc	Fluorenyl methoxycarbonyl
FT-IR	Fourier transform infrared spectroscopy
GAB	G-Actin-binding segment
G-Actin	Globular actin

GDP	Guanosine diphosphate
GmbH	Gesellschaft mit beschränkter Haftung
GRB2	Growth factor receptor-bound protein 2
GTP	Guanosine triphosphate
GYF	Glycine-tyrosine-phenylalanine domain
HATU	*O*-(7-Azabenzotriazol-1-yl)-*N*,*N*,*N*′,*N*′-tetramethyluronium hexafluorophosphate
HECT	Homologous to the E6-AP carboxy terminus
Her2	Human epidermal growth factor receptor 2
HIF1α	Hypoxia-inducible factor 1α
HIF1β	Hypoxia-inducible factor 1β
HPLC	High performance liquid chromatography
HR-MS	High resolution mass spectroscopy
HyPro	Hydroxyproline
IAP	Inhibitor of Apoptosis proteins
IC50	half-maximal inhibitory concentration
ISG15	Interferon-stimulated gene 15
K_d	Dissociation constant
LATS1/2	Large tumor suppressor kinases 1/2
LRRK2	Leucine-rich repeat kinase 2
M	Molar (mol/L)
MAP4Ks	Mitogen-activated protein kinase kinase kinase kinase
MDa	mega Dalton
MDM2	Mouse double minute 2 homolog
Mek	Mitogen-activated protein kinase kinase

Mena	Mammalian-enabled protein
MOB1	Mps one binder
MSR1	Macrophage scavenger receptor 1
MST1/2	Mammalian sterile 20-like kinases 1/2
M*t*BE	Methyl-*tert*-butyl ether
N	Normality
NEDD8	neural-precursor-cell-expressed developmentally down-regulated 8
NMP	N-Methyl-2-pyrrolidone
NMR	*Nuclear magnetic resonance*
NOE	Nuclear Overhauser effect
Nu	Nucleophile
PBS	Phosphate buffered saline
PD	Phenyl dihydrouracil
PDB	Protein Data Bank
PDZ	PSD-95, Discs large, and Zonula occludens-1
PEG	Polyethylene glycol
PG	Phenyl glutarimide
POI	Protein of interest
PPI	Protein-protein interaction
PPII-Helix	Polyproline helix type II
Ppm	Parts per million
PRM	Proline-rich motif
ProM	Proline mimetic
PROTAC	Proteolysis targeting chimera
Raf	Rapidly accelerated fibrosarcoma

Ras	Rat-sarcoma
RBR	Retinoblastoma-related protein
Rbx1	RING-box protein 1
Rf	Retention factor
RING	Really interesting new gene
RNA	Ribonucleic acid
RP	Regulatory Particle
Rpn	Regulatory particle non-ATPase
Rpt	Regulatory particle Triple-ATPase
SALL4	Sal-like protein 4
SAV1	Salvador homolog 1
SAR	Structure activity relationship
SH2	Src-homology 2 domain
SH3	Src-homology 3 domain
SOS	Son of sevenless
SPPS	Solid phase peptide synthesis
SRF	Serum-response-factor protein
STRIPAK	Striatin-interacting phosphatase and kinase
SUMO	Small ubiquitin-related Modifier
TCEP	Tris(2-carboxyethyl)phosphine
TEAD	Transcriptional enhancer factor domain family
TFA	Trifluoroacetic acid
THF	Tetrahydrofuran
TLC	Thin layer chromatography
TMSOTf	Trimethylsilyl trifluoromethanesulfonate

TPSA	Topological polar surface area
TRIM9	Tripartite motif containing protein 9
TsCl	Tosylchloride
Ub	Ubiquitin
UBA	Ubiquitin-activating enzyme
UEV	Ubiquitin-conjugating enzyme E2 variant
UFM1	Ubiquitin-fold modifier 1
UPS	Ubiquitin proteasome system
URM1	Ubiquitin-related modifier-1
UV	Ultraviolet
VASP	Vasodilator-stimulated phosphoprotein
VHL	*Von Hippel-Lindau* tumor suppressor protein
WW	Tryptophan-tryptophan domain
YAP1	Yes-associated protein 1

7.2 NMR Spectra

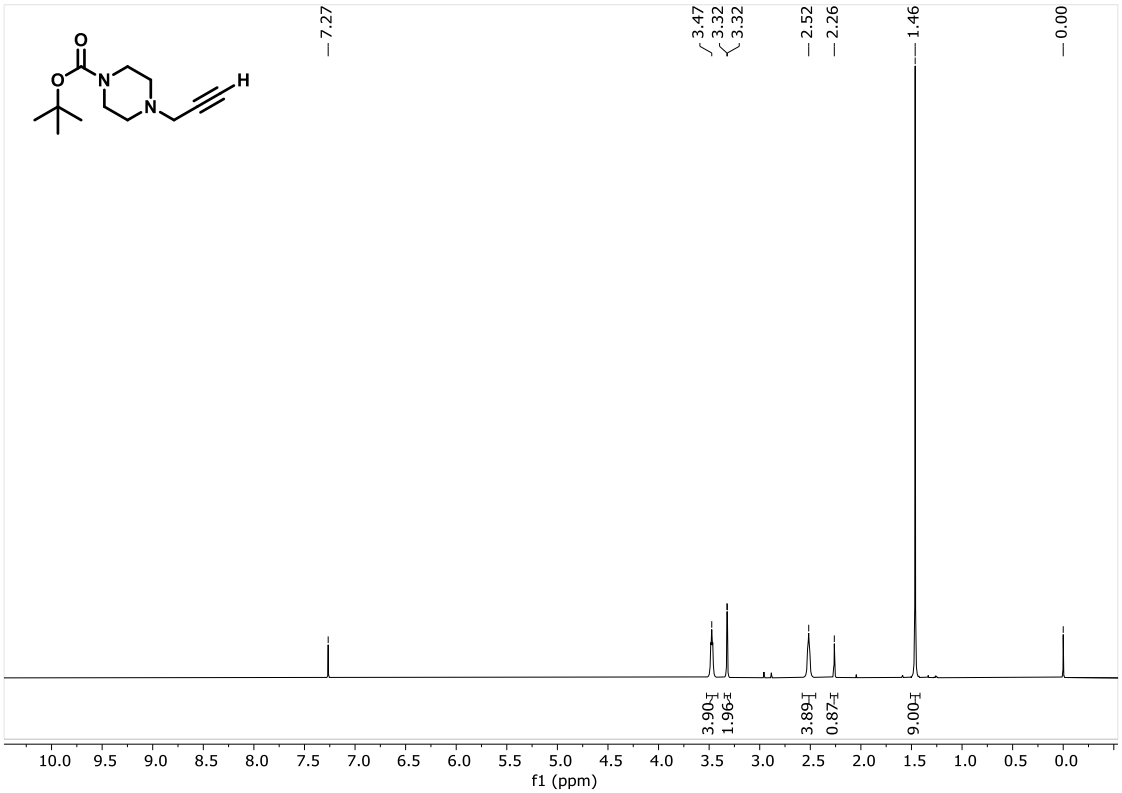

Figure 36: ^{1}H NMR (500 MHz, $CDCl_3$) of **42**.

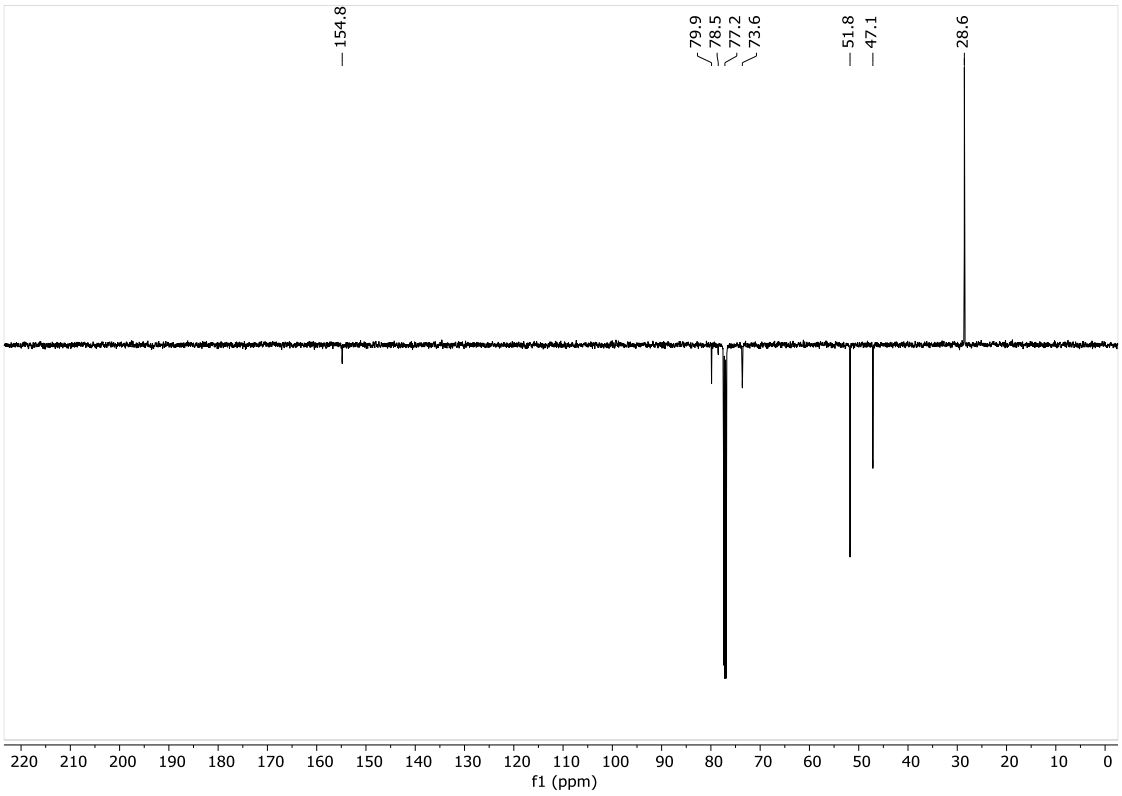

Figure 37: ^{13}C NMR (125 MHz, $CDCl_3$) of **42**.

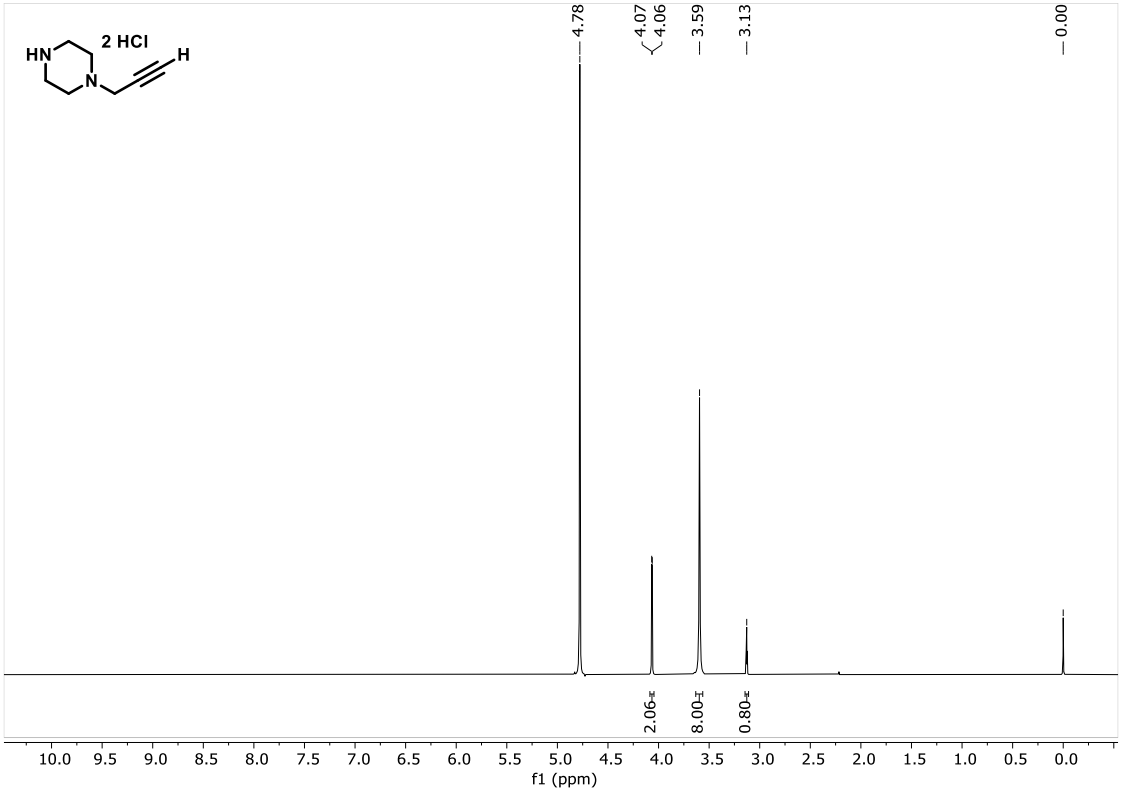

Figure 38: ^{1}H NMR (500 MHz, D_2O) of **37**.

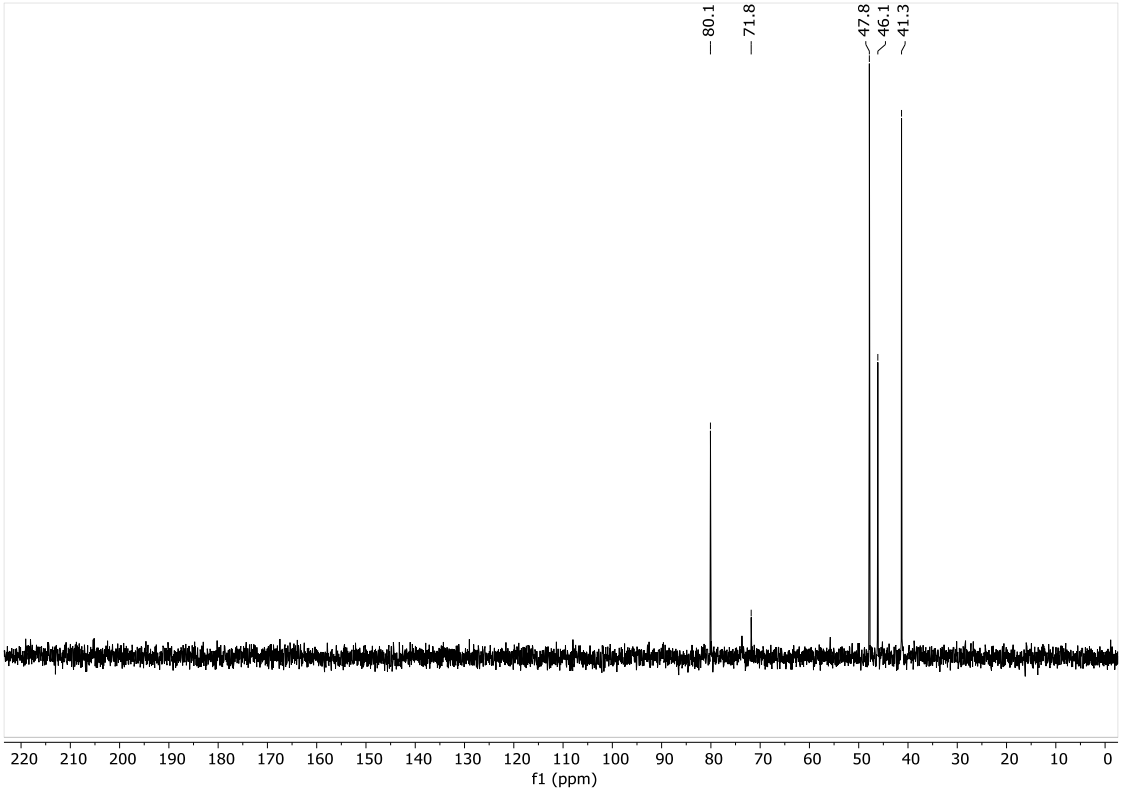

Figure 39: ^{13}C NMR (125 MHz, D_2O) of **37**.

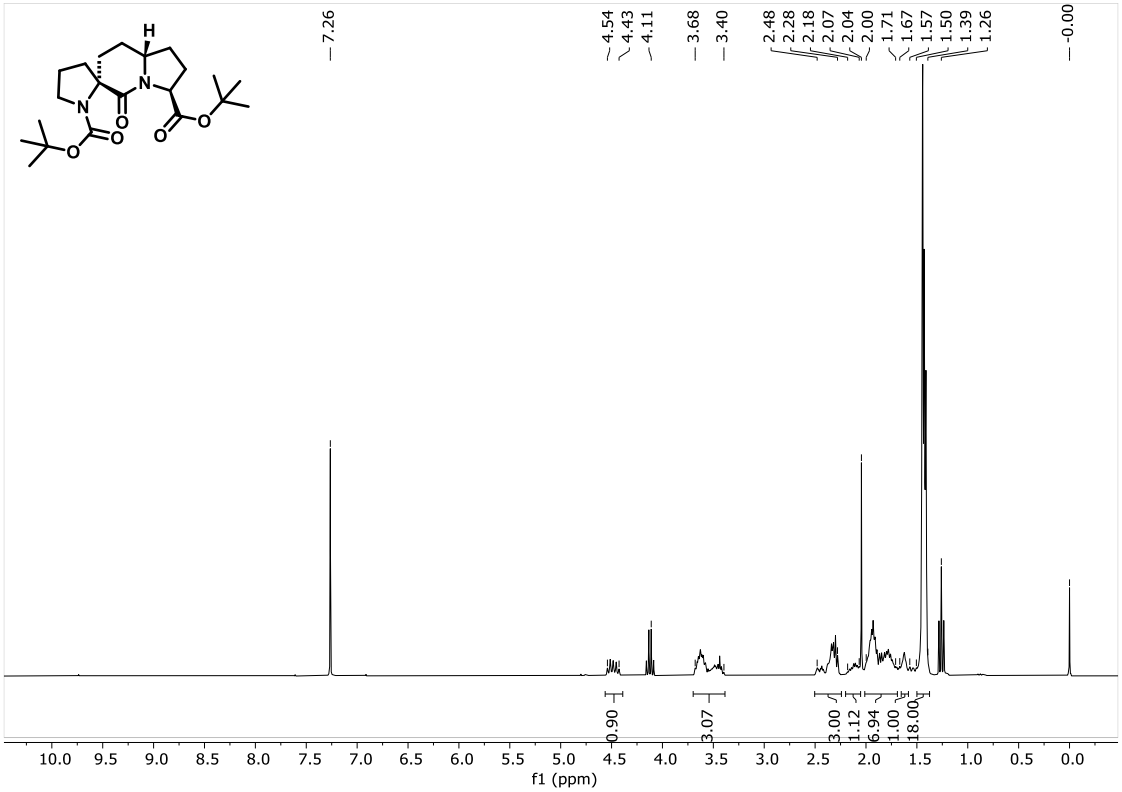

Figure 40: ^{1}H NMR (300 MHz, $CDCl_3$) of **46**.

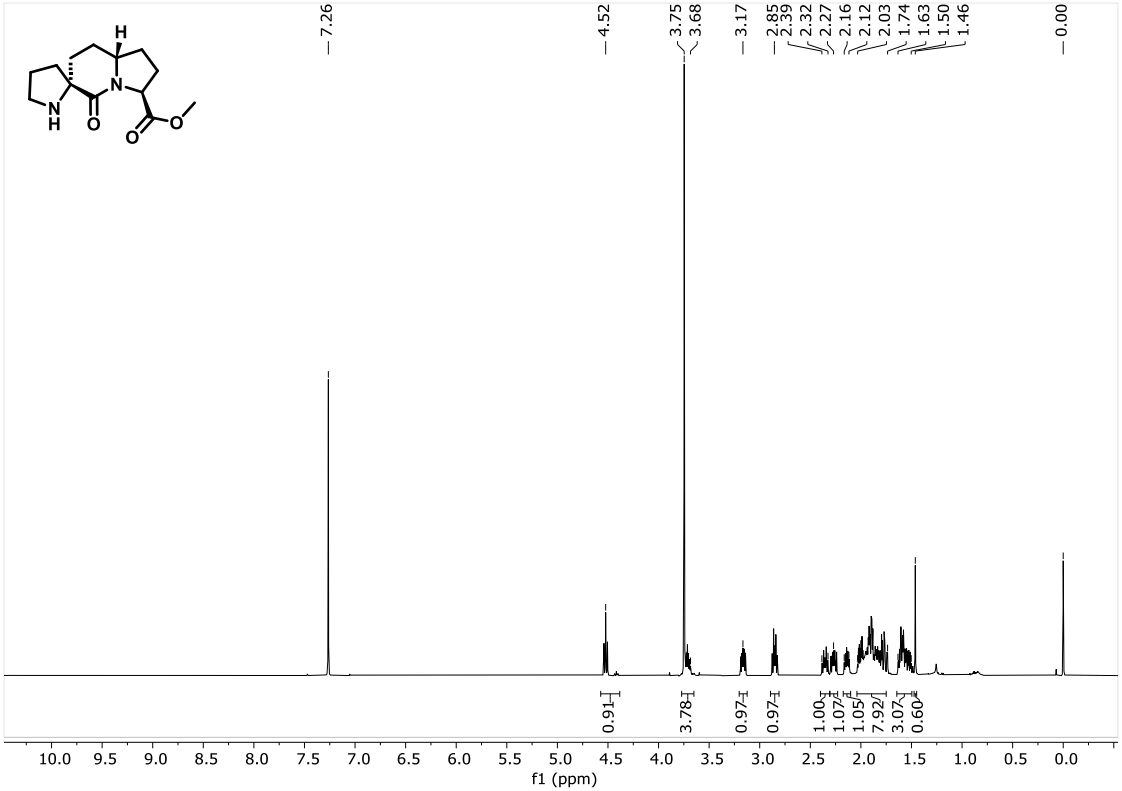

Figure 41: ^{1}H NMR (300 MHz, $CDCl_3$) of **47**.

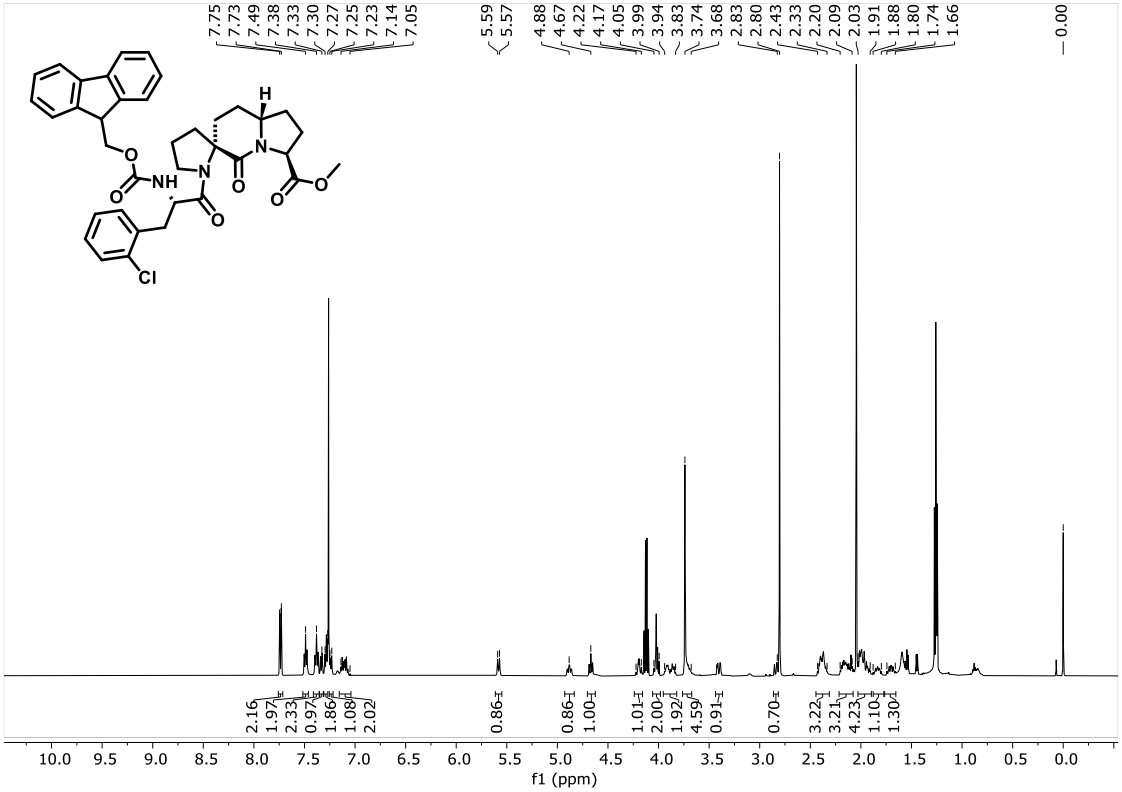

Figure 42: ^{1}H NMR (500 MHz, $CDCl_3$) of **49**.

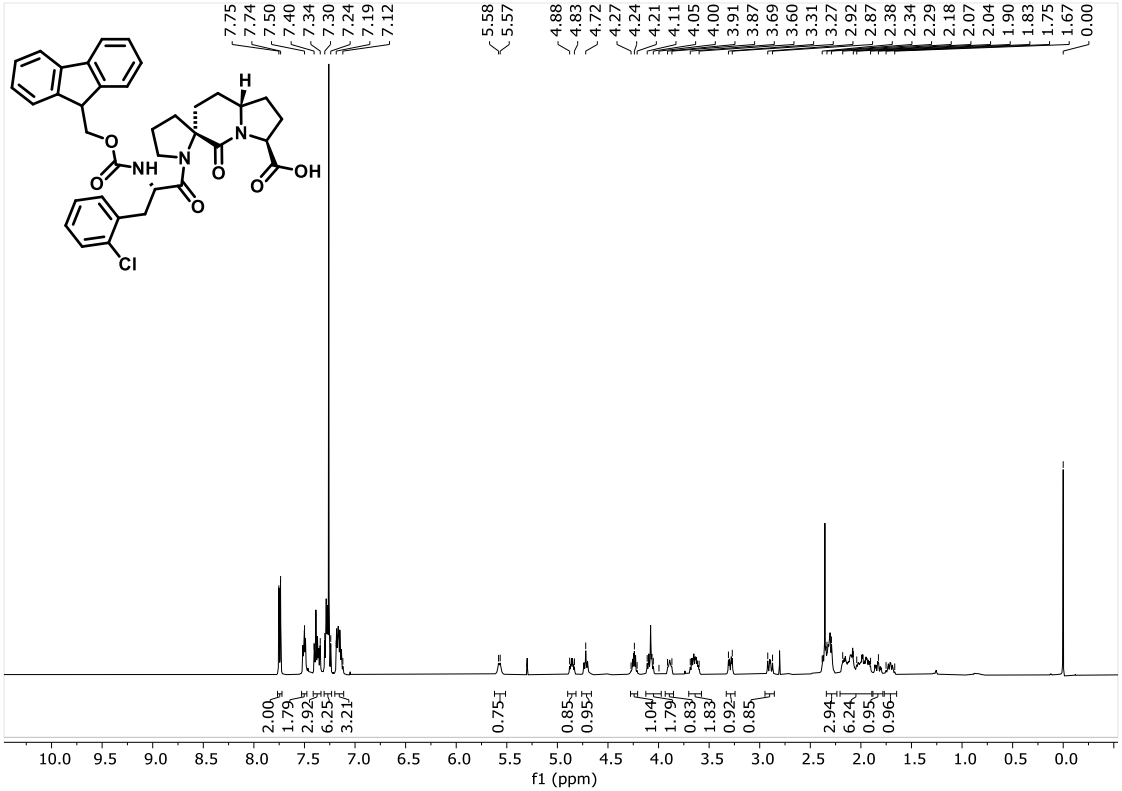

Figure 43: ^{1}H NMR (500 MHz, $CDCl_3$) of **50**.

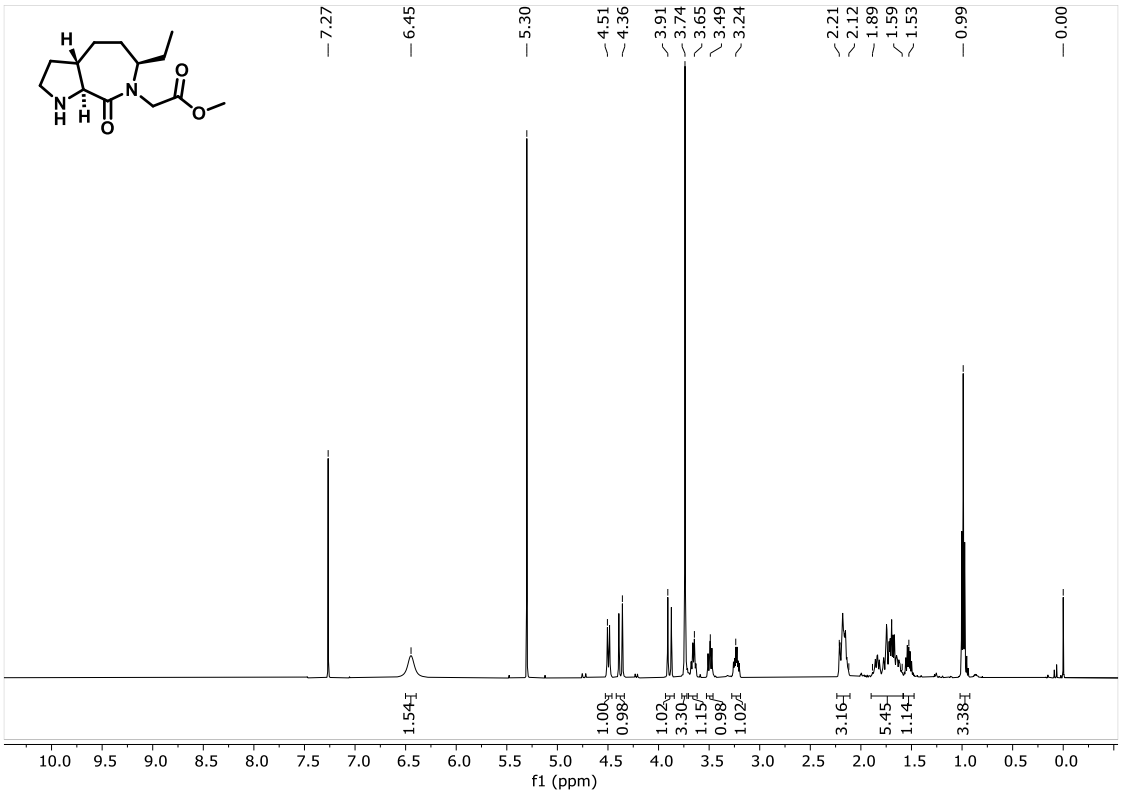

Figure 44: ^{1}H NMR (500 MHz, $CDCl_3$) of **44**.

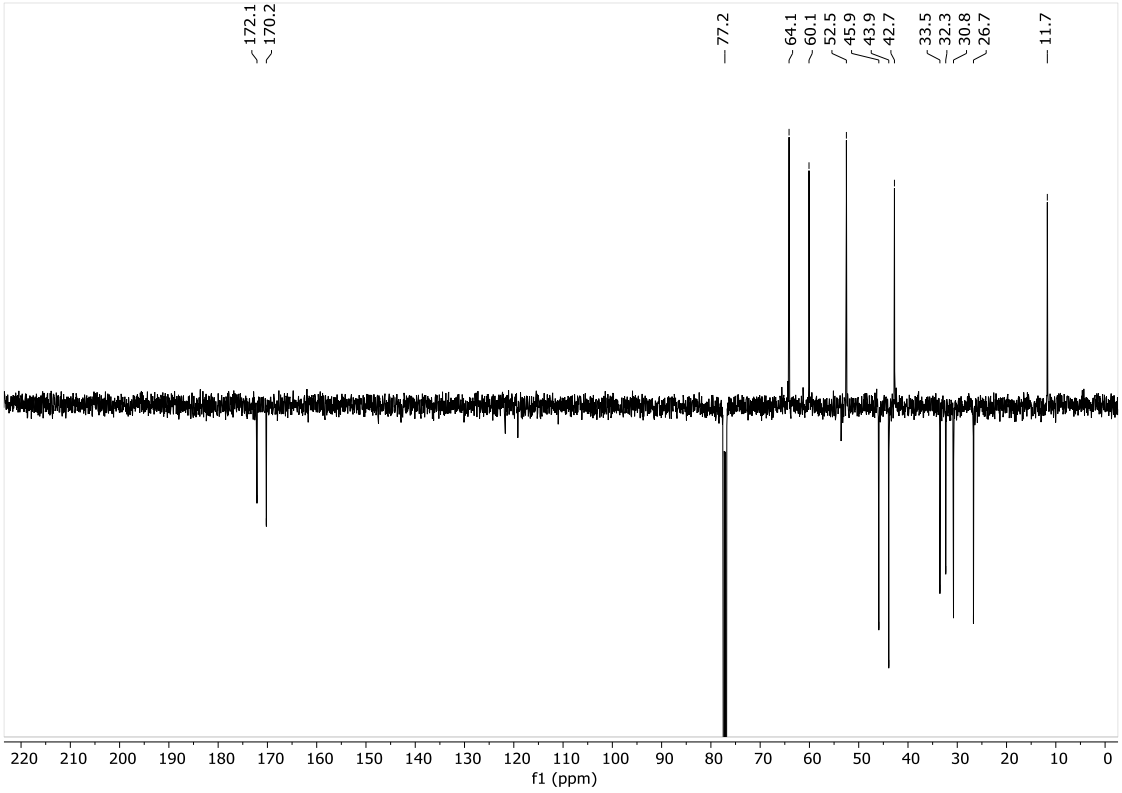

Figure 45: ^{13}C NMR (125 MHz, $CDCl_3$) of **44**.

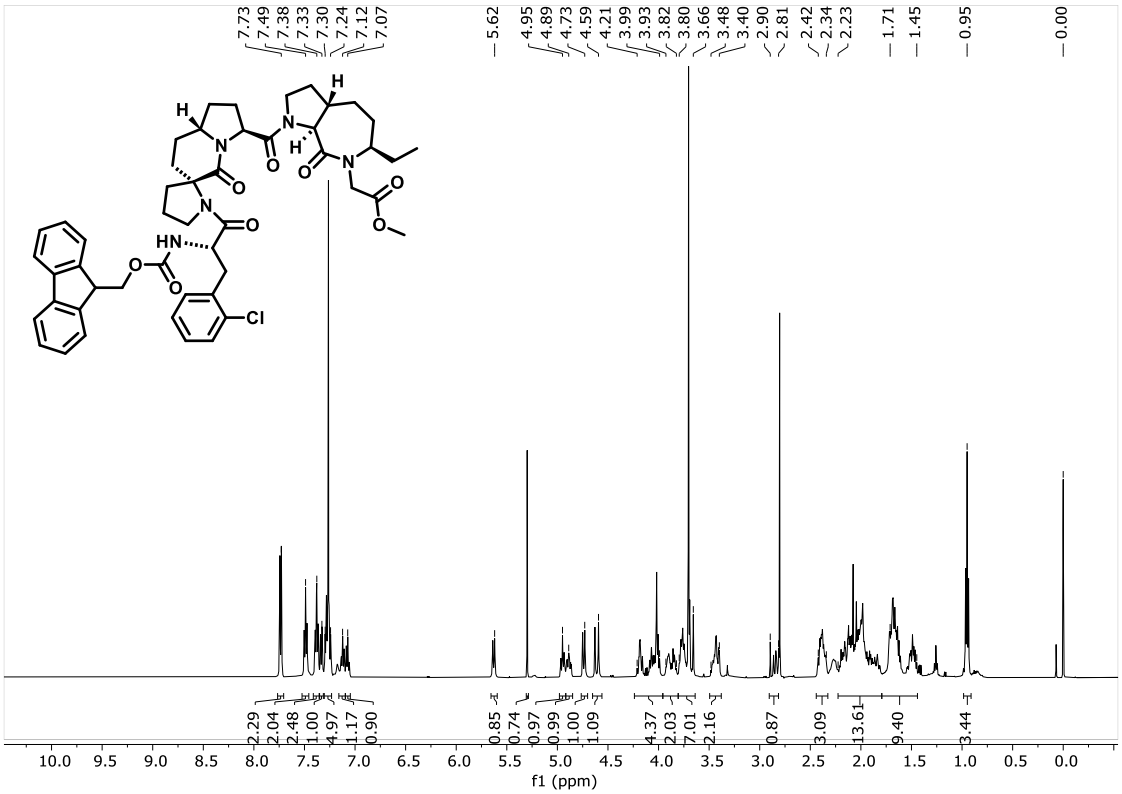

Figure 46: ^{1}H NMR (500 MHz, $CDCl_3$) of **51**.

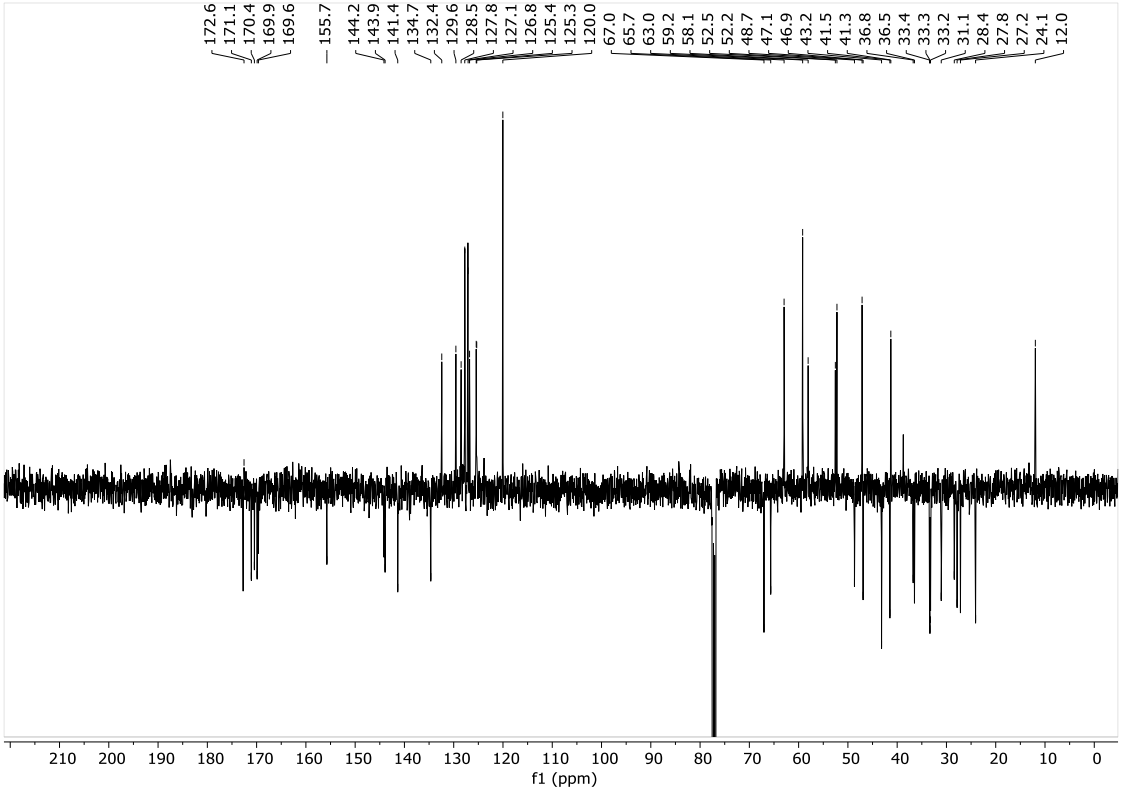

Figure 47: ^{13}C NMR (125 MHz, $CDCl_3$) of **51**.

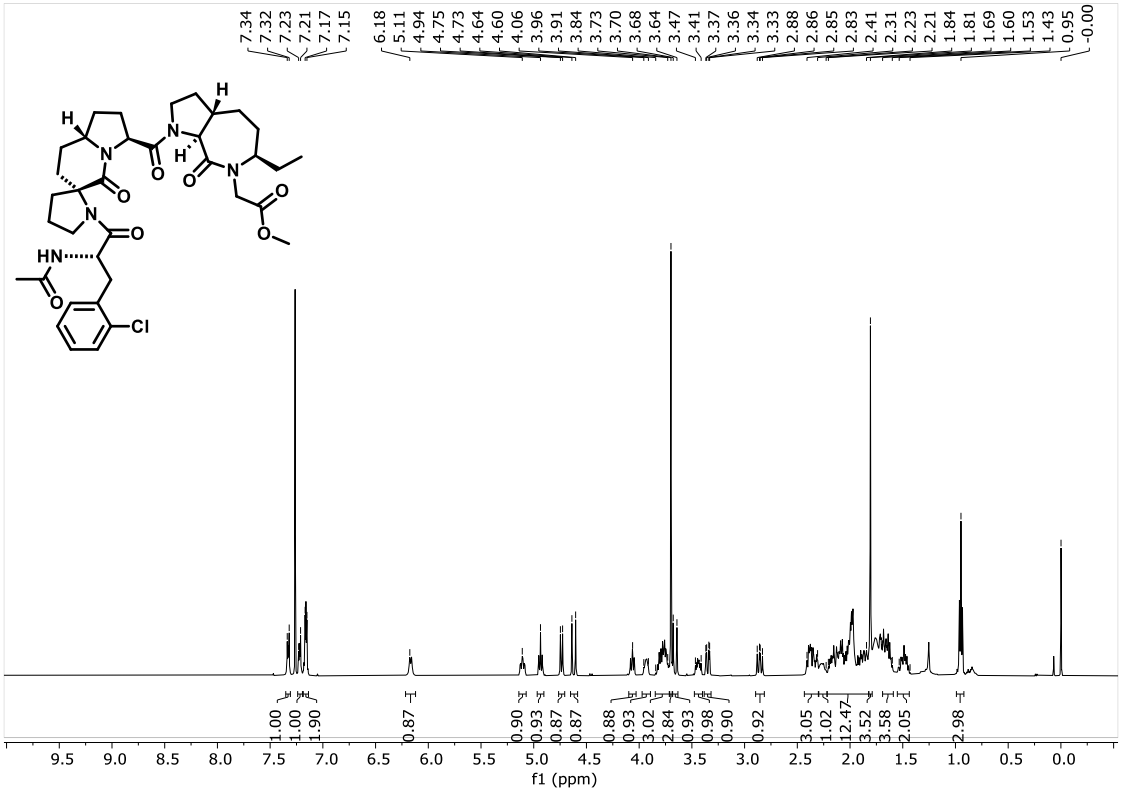

Figure 48: ^{1}H NMR (500 MHz, $CDCl_3$) of **22**.

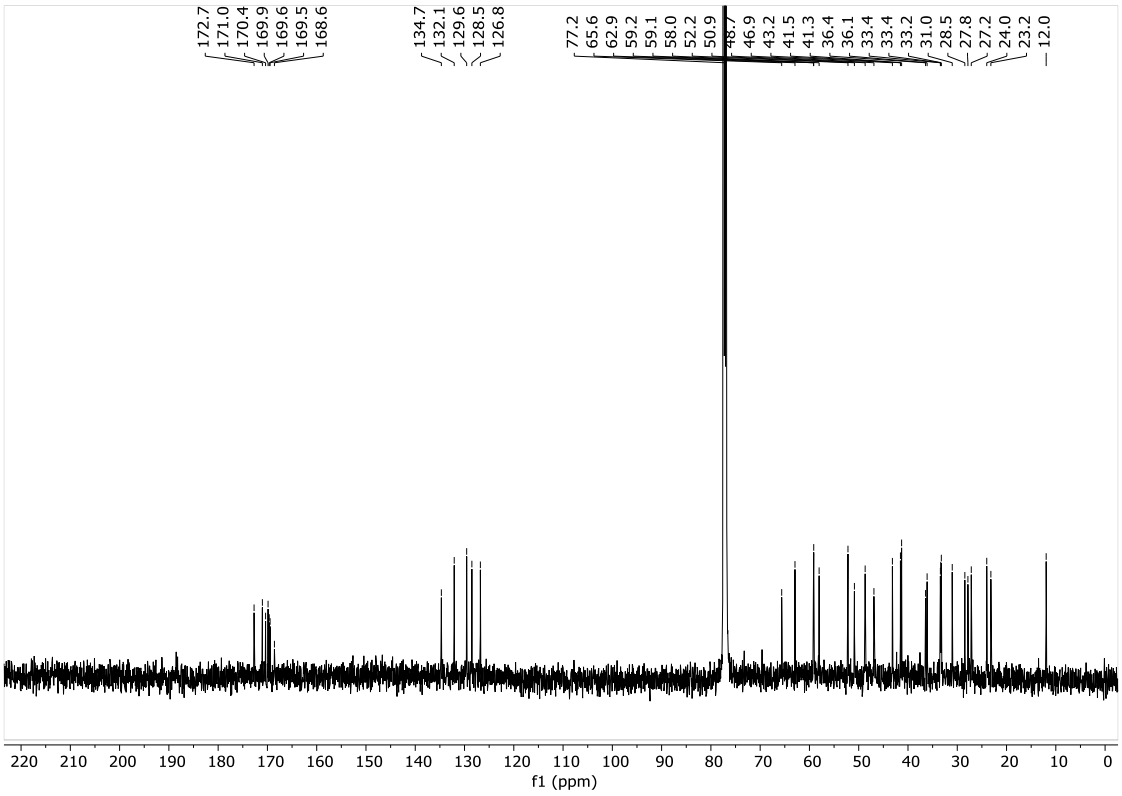

Figure 49: ^{13}C NMR (125 MHz, $CDCl_3$) of **22**.

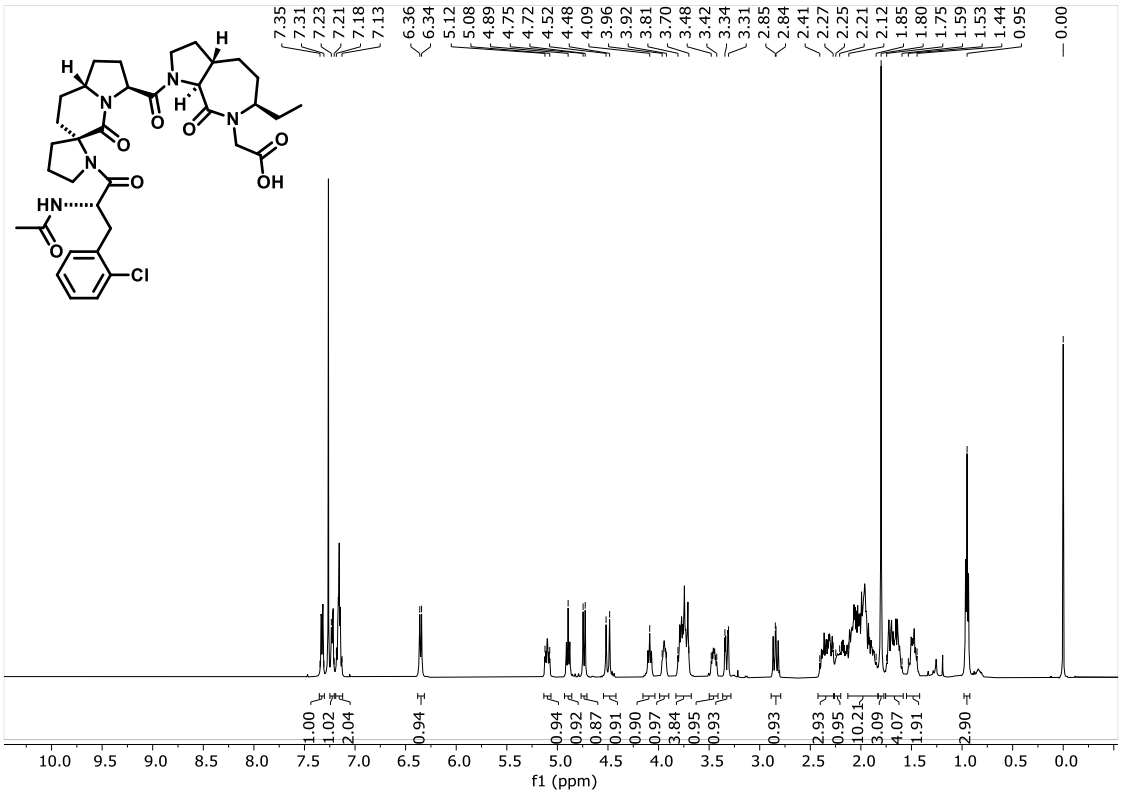

Figure 50: ^{1}H NMR (500 MHz, $CDCl_3$) of **38**.

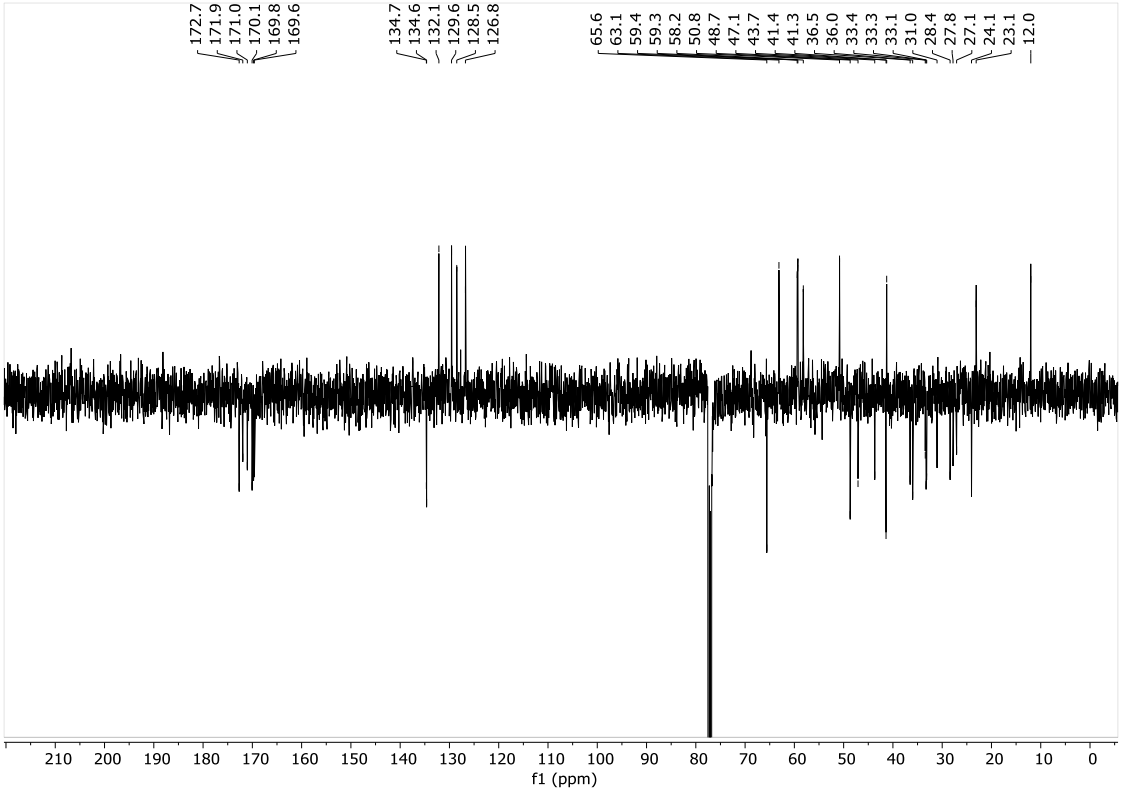

Figure 51: ^{13}C NMR (125 MHz, $CDCl_3$) of **38**.

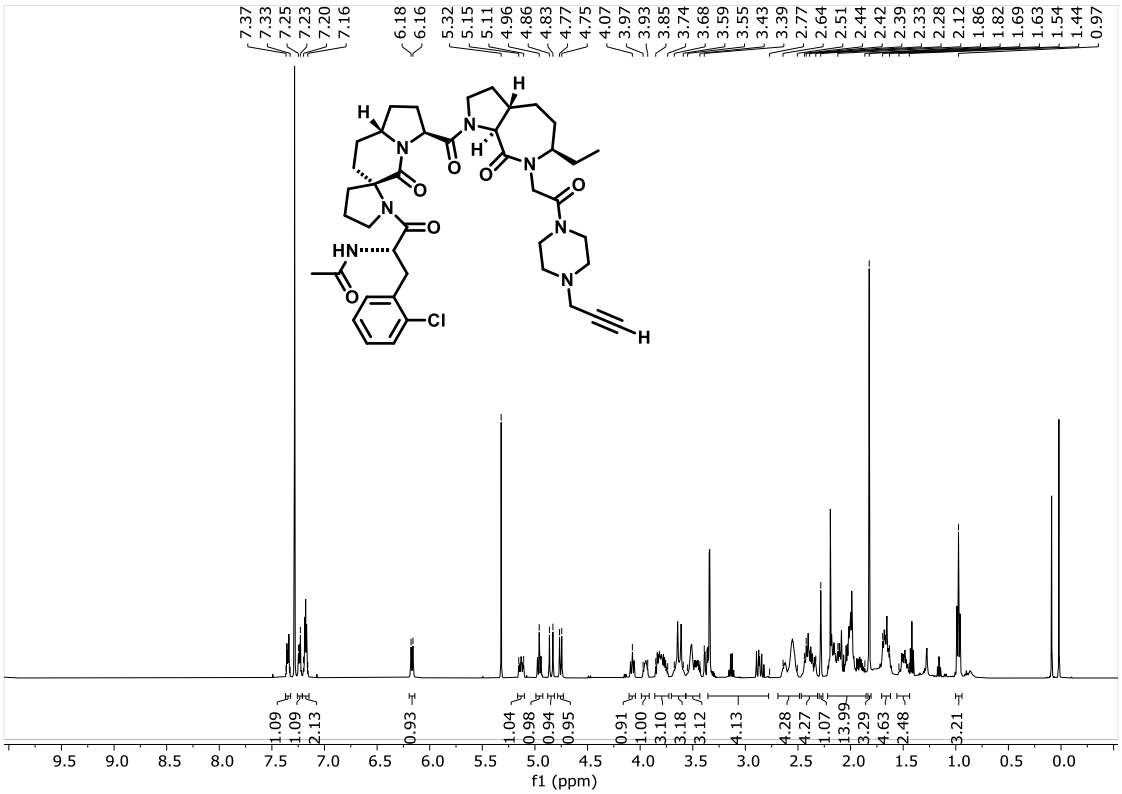

Figure 52: ^{1}H NMR (500 MHz, $CDCl_3$) of **39**.

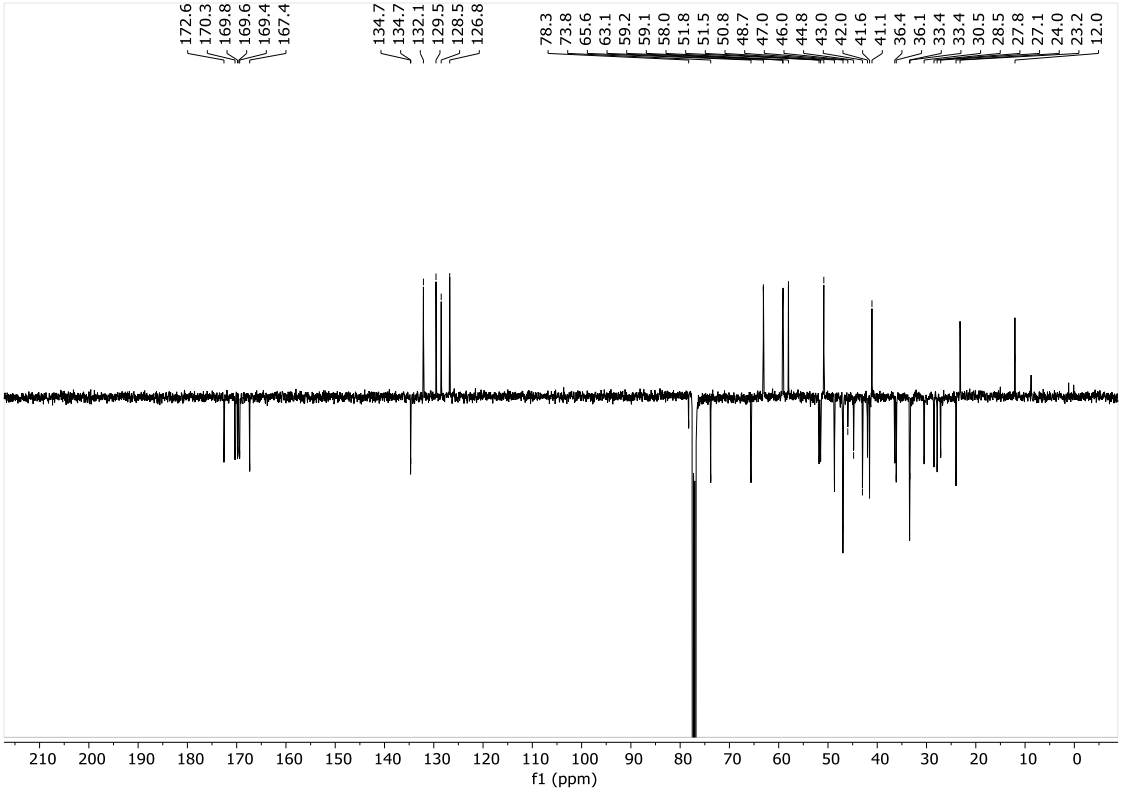

Figure 53: ^{13}C NMR (125 MHz, $CDCl_3$) of **39**.

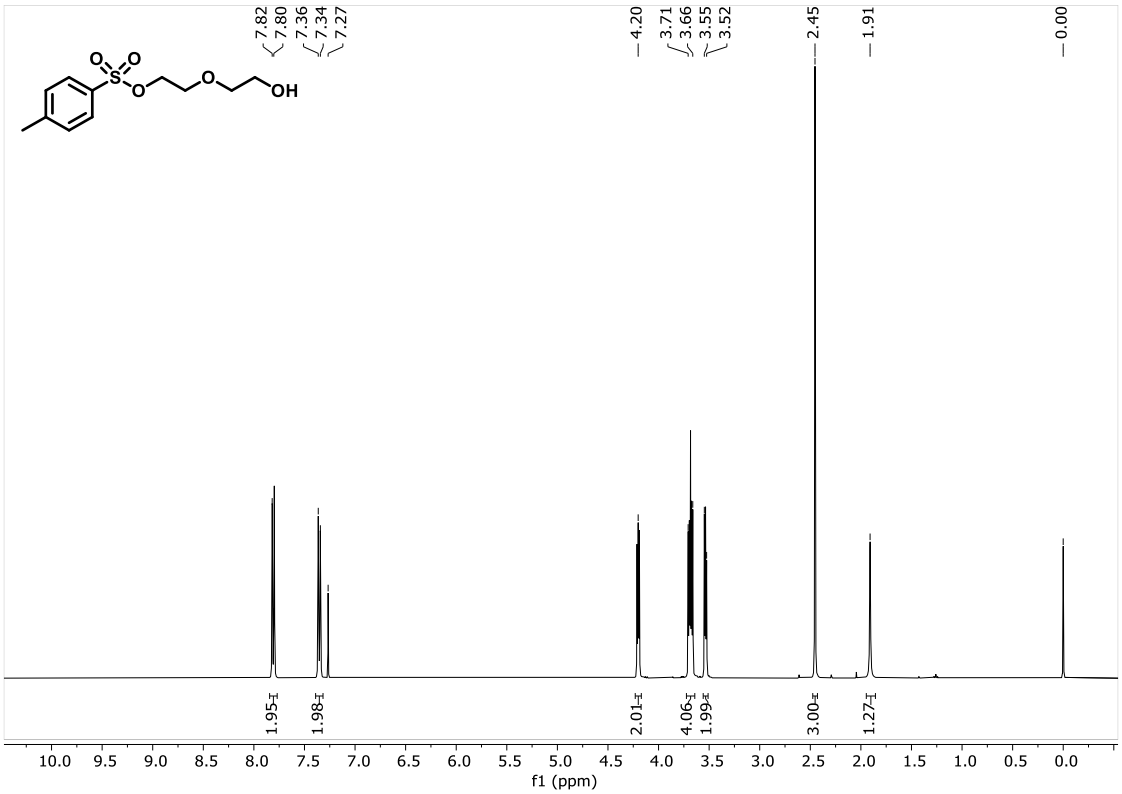

Figure 54: ^{1}H NMR (400 MHz, $CDCl_3$) of **55**.

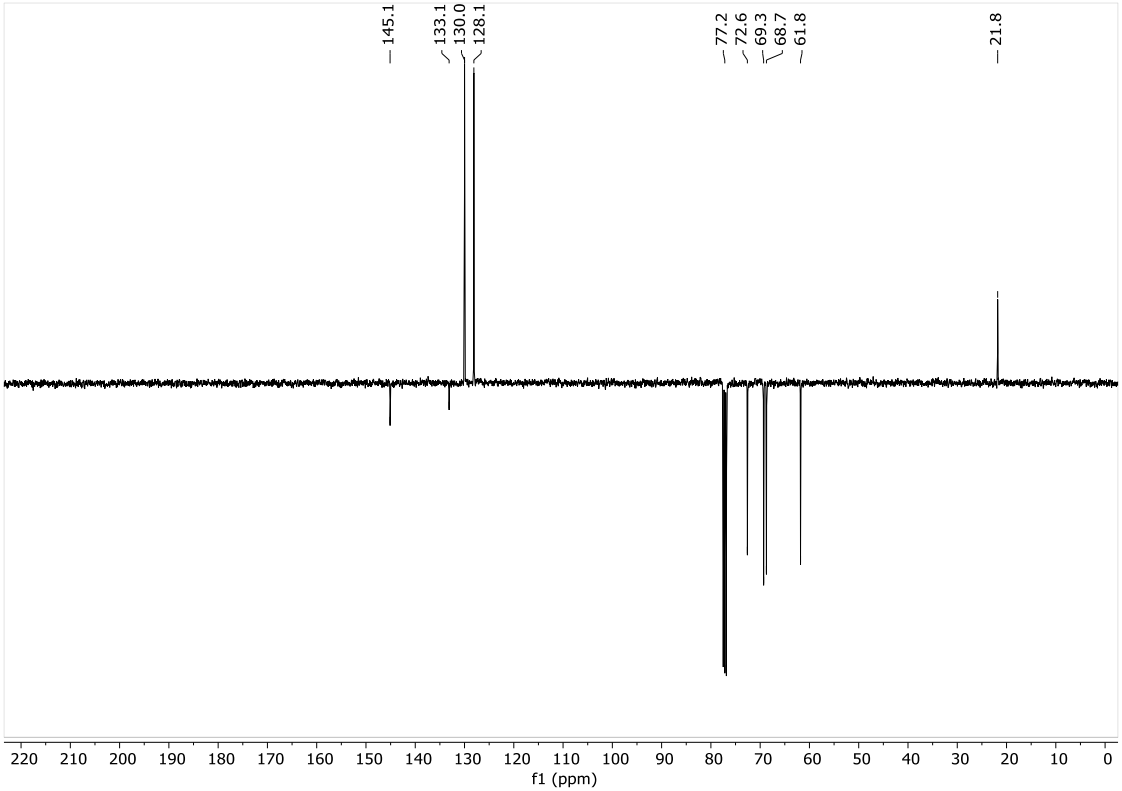

Figure 55: ^{13}C NMR (100 MHz, $CDCl_3$) of **55**.

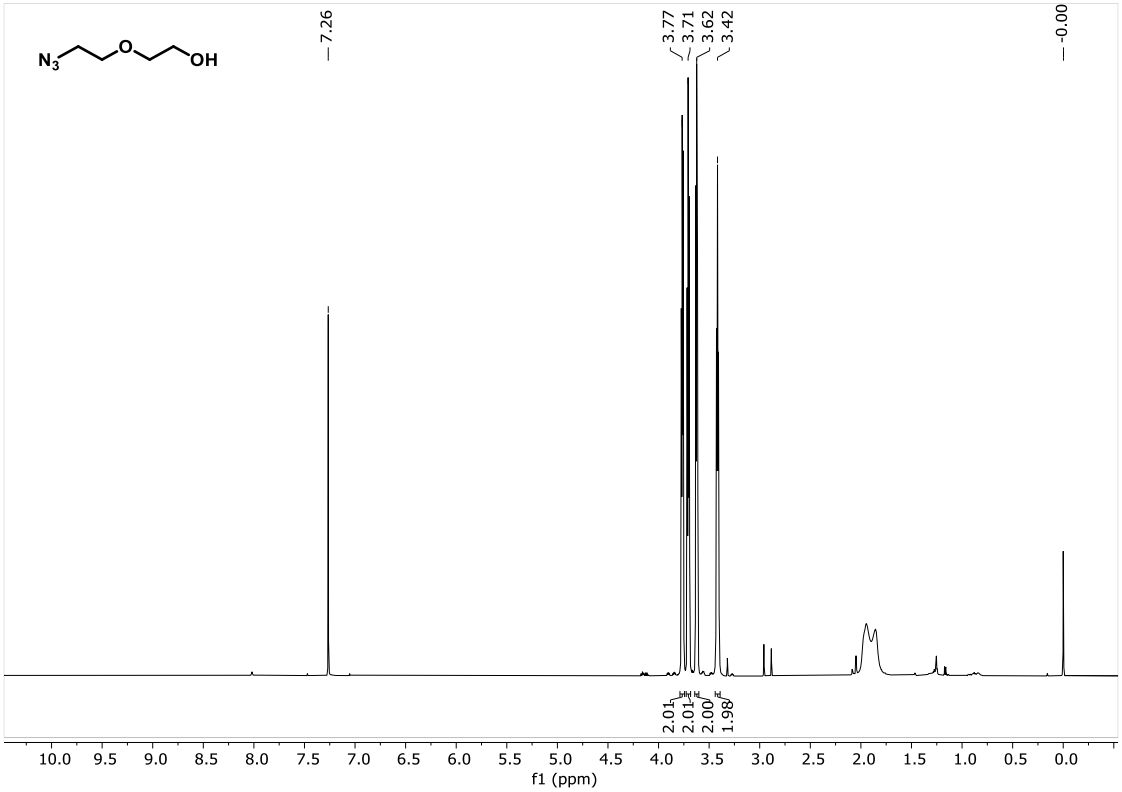

Figure 56: ^{1}H NMR (500 MHz, $CDCl_3$) of **56**.

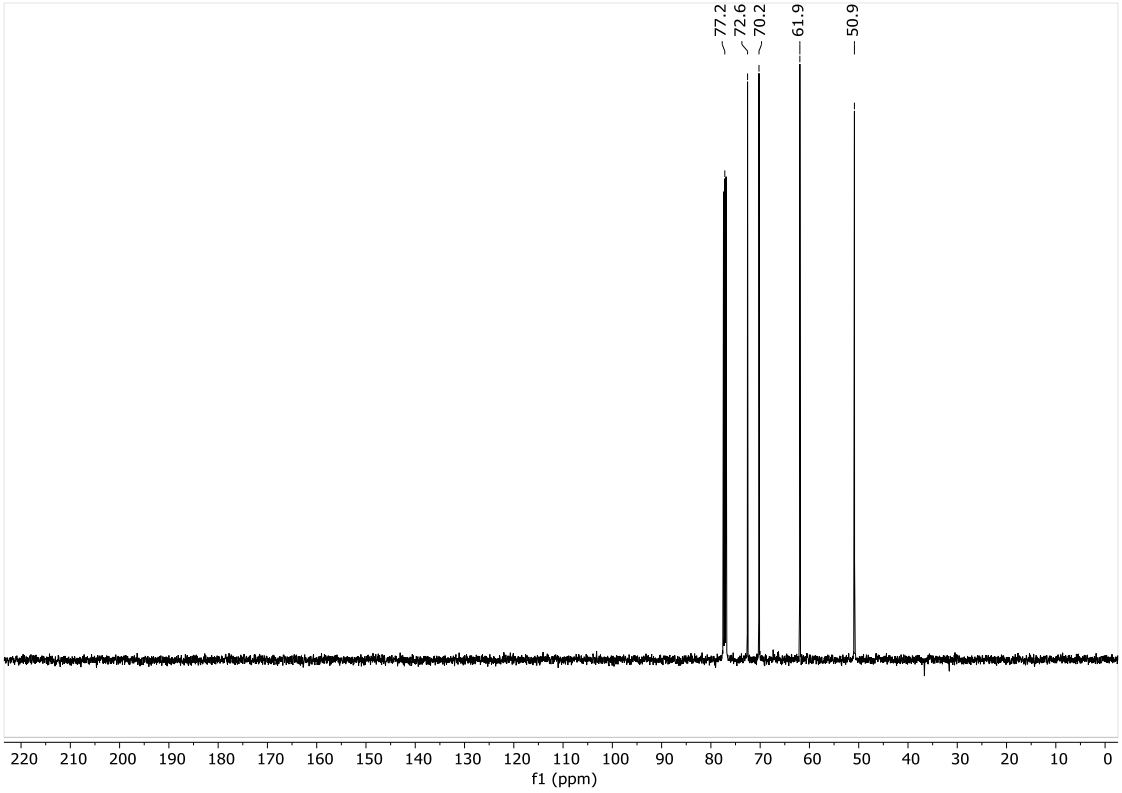

Figure 57: ^{13}C NMR (125 MHz, $CDCl_3$) of **56**.

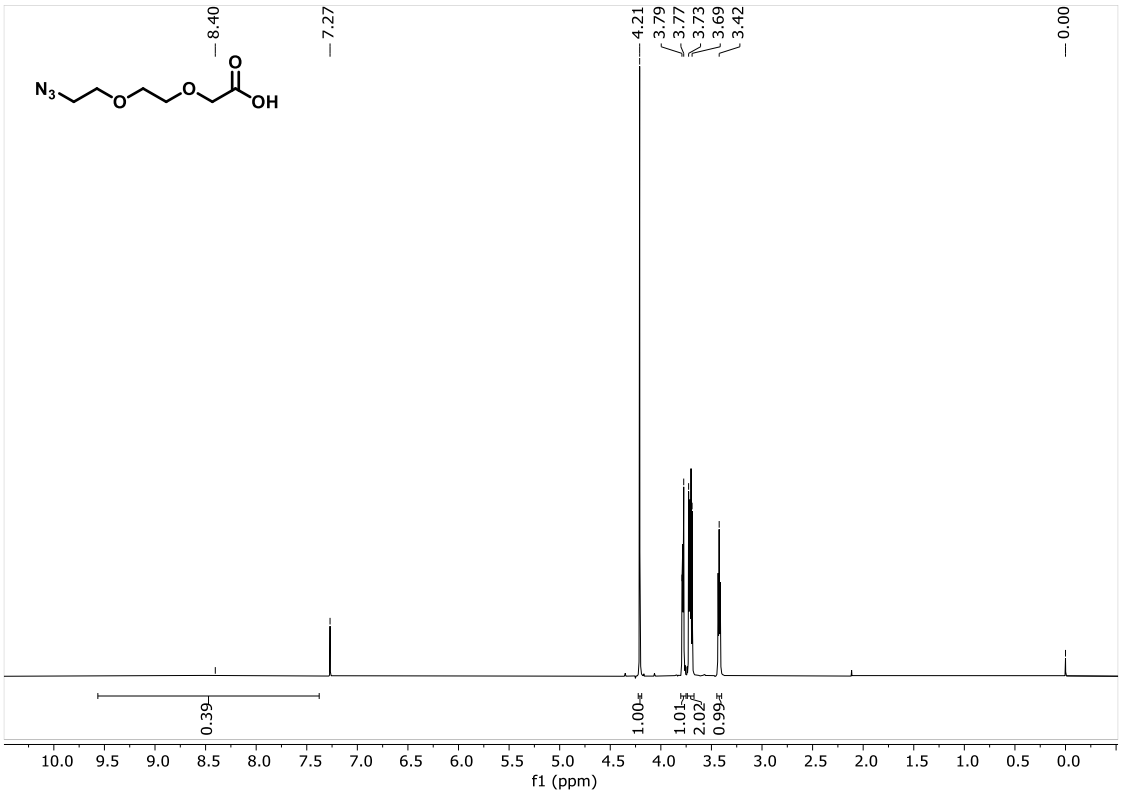

Figure 58: ^{1}H NMR (500 MHz, $CDCl_3$) of **52**.

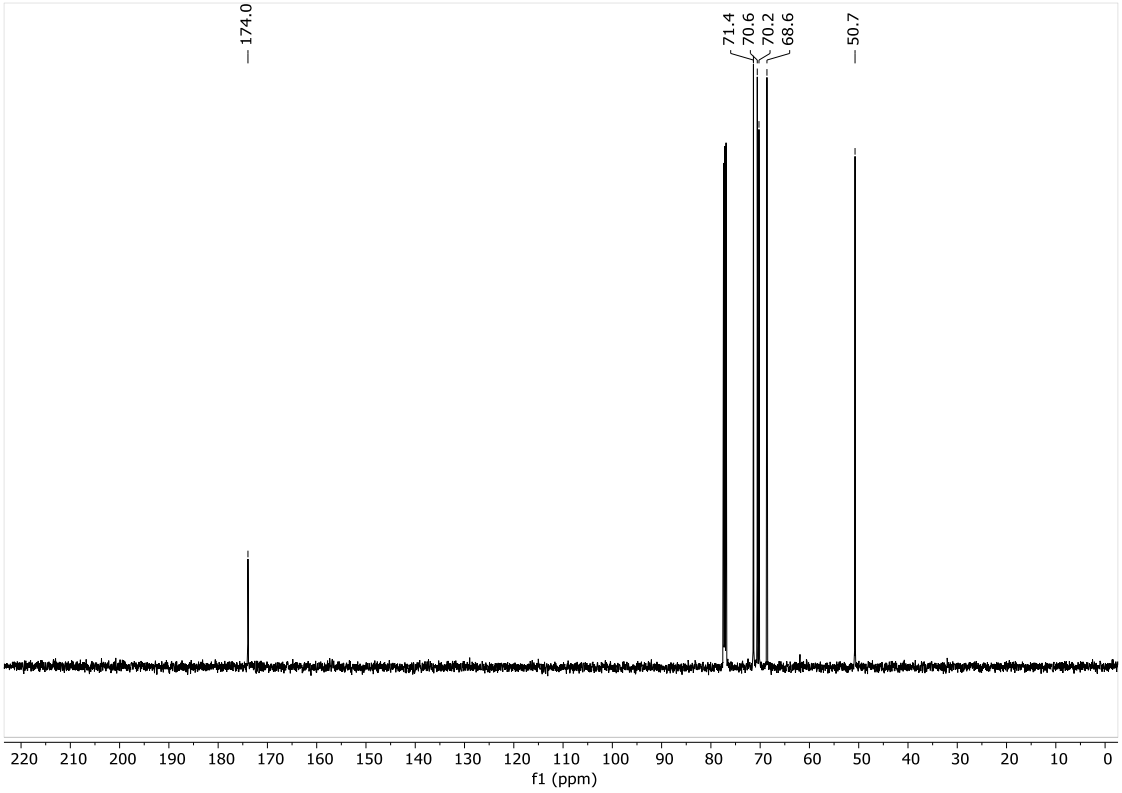

Figure 59: ^{13}C NMR (125 MHz, $CDCl_3$) of **52**.

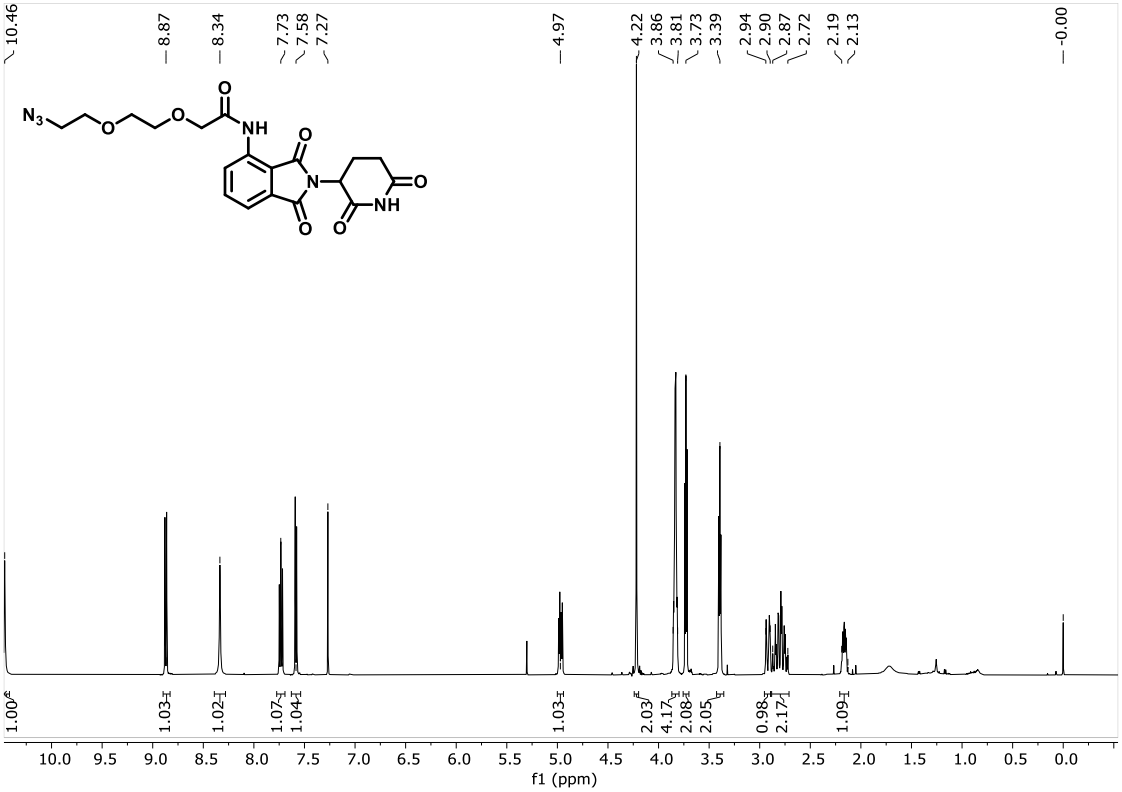

Figure 60: ^{1}H NMR (500 MHz, $CDCl_3$) of **58**.

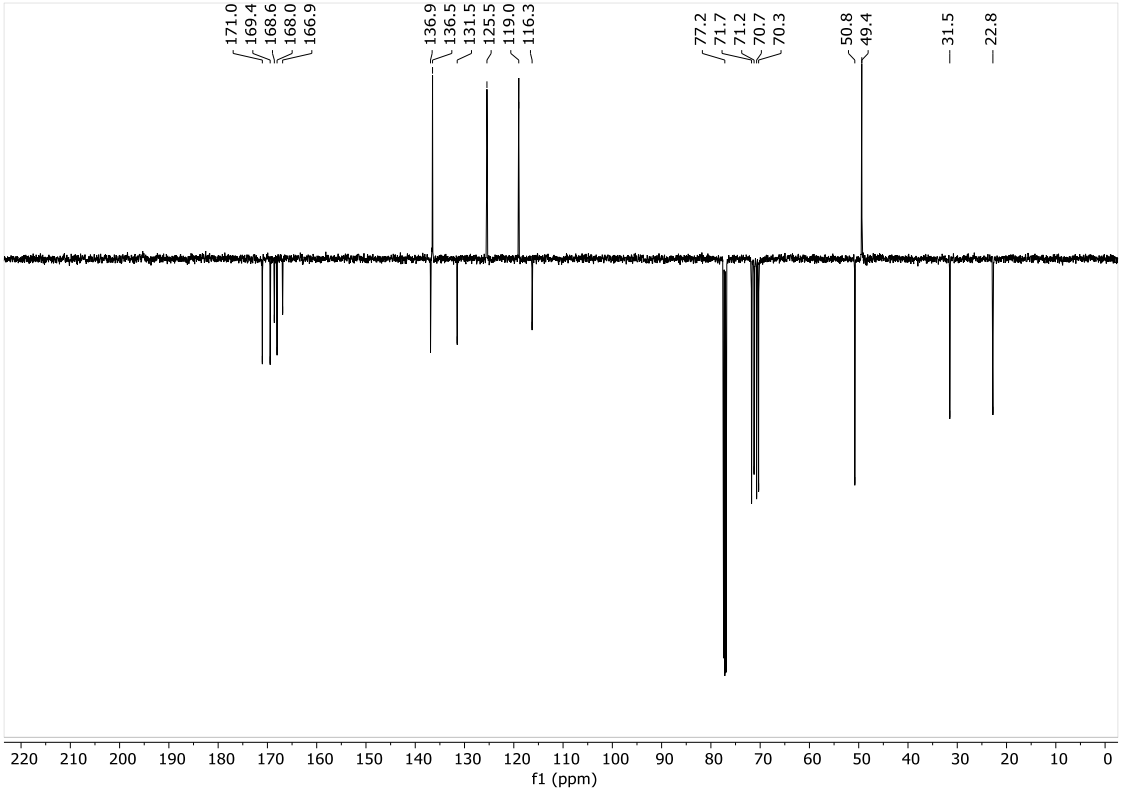

Figure 61: ^{13}C NMR (125 MHz, $CDCl_3$) of **58**.

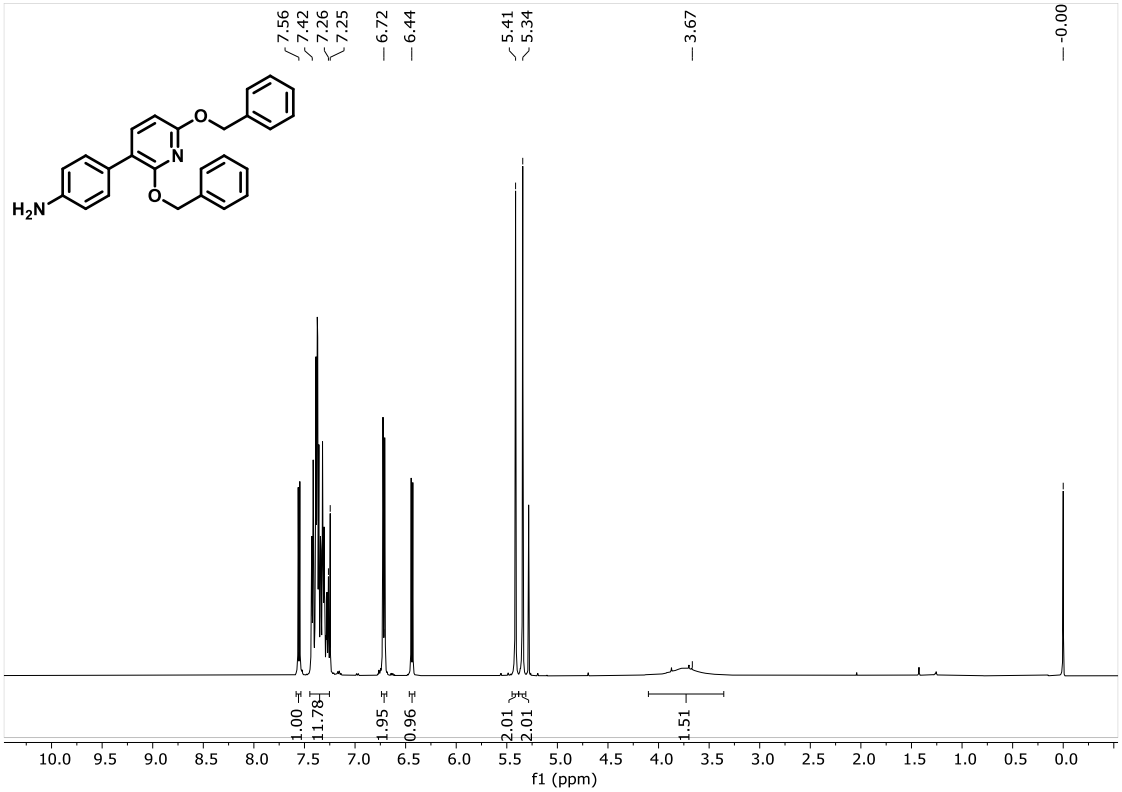

Figure 62: ^{1}H NMR (500 MHz, $CDCl_3$) of **63**.

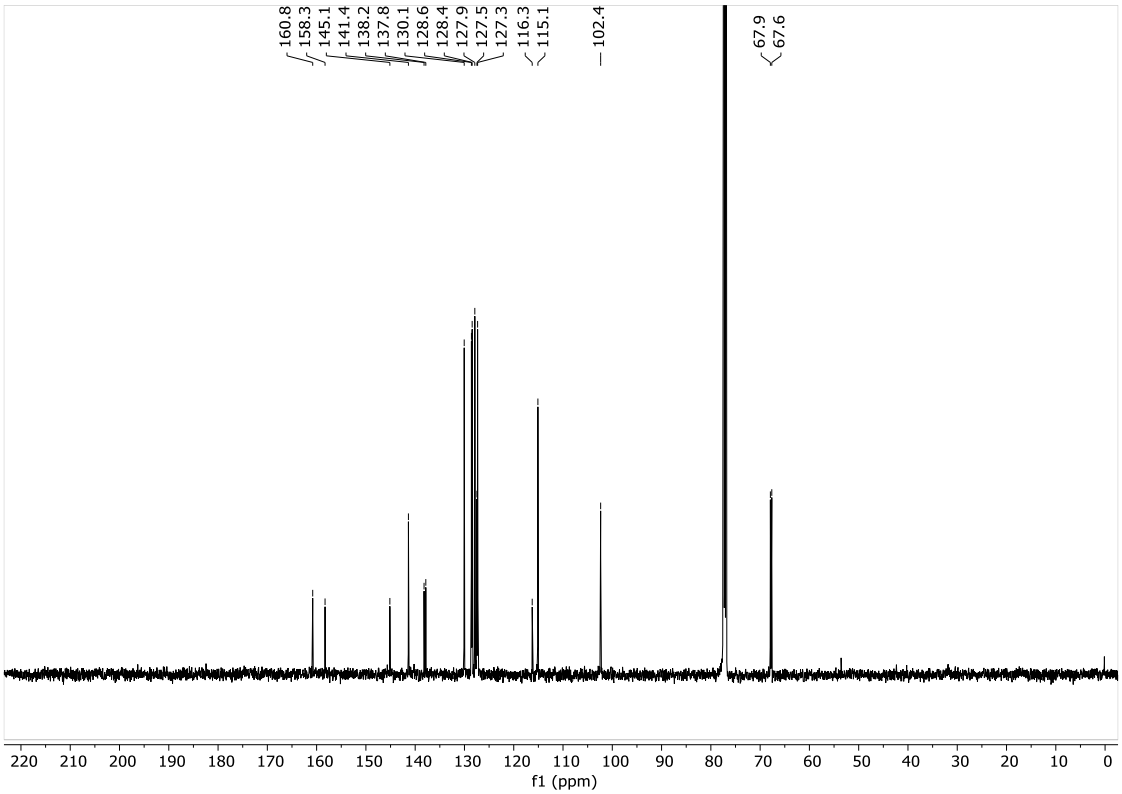

Figure 63: ^{13}C NMR (125 MHz, $CDCl_3$) of **63**.

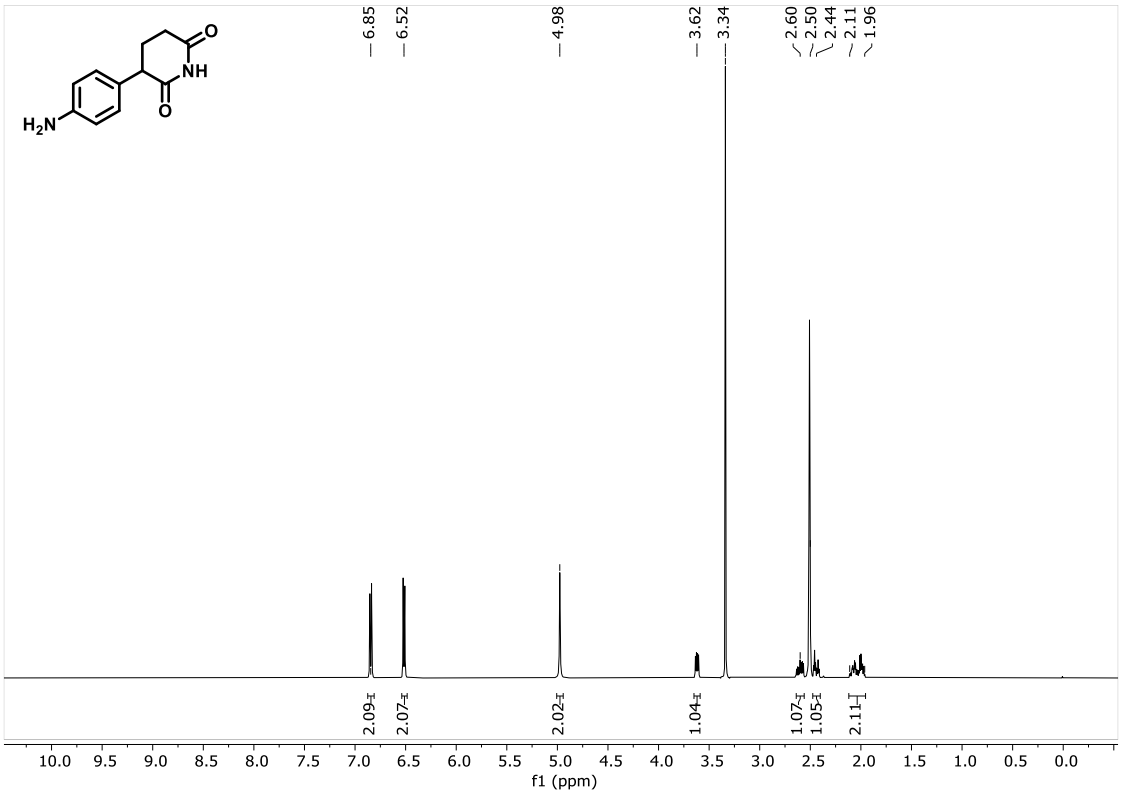

Figure 64: ^{1}H NMR (500 MHz, DMSO-d_6) of **59**.

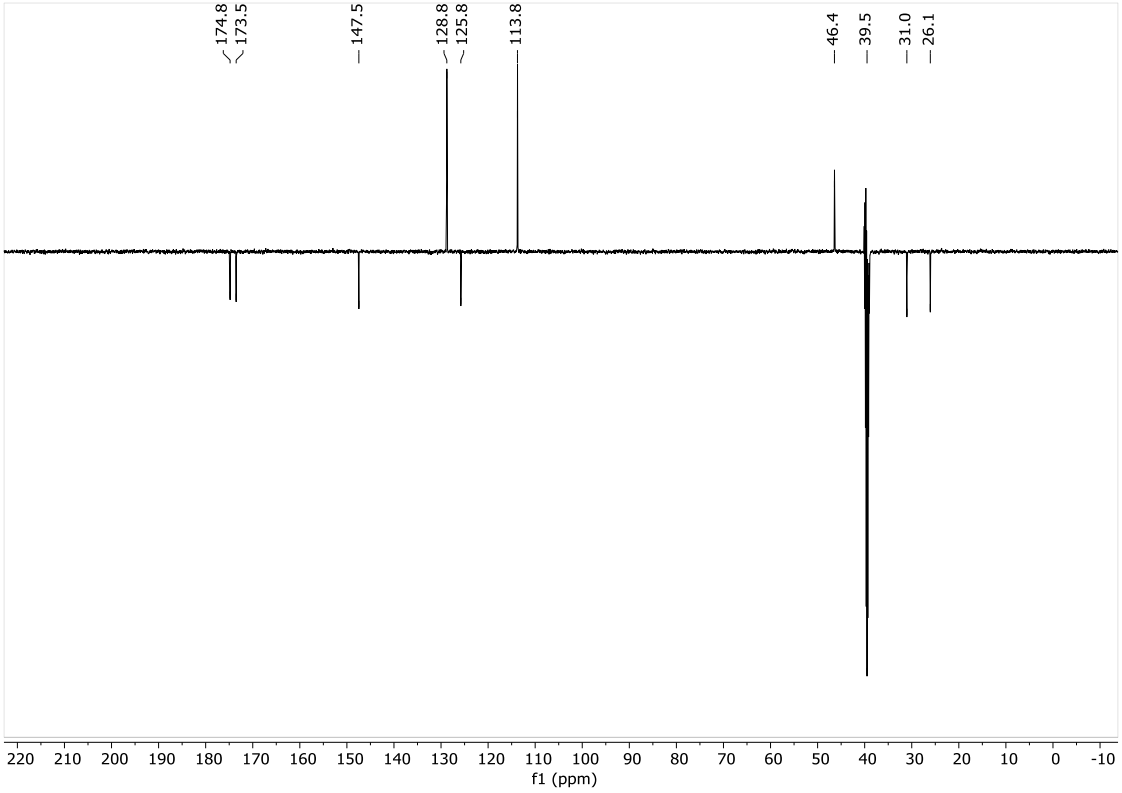

Figure 65: ^{13}C NMR (125 MHz, DMSO-d_6) of **59**.

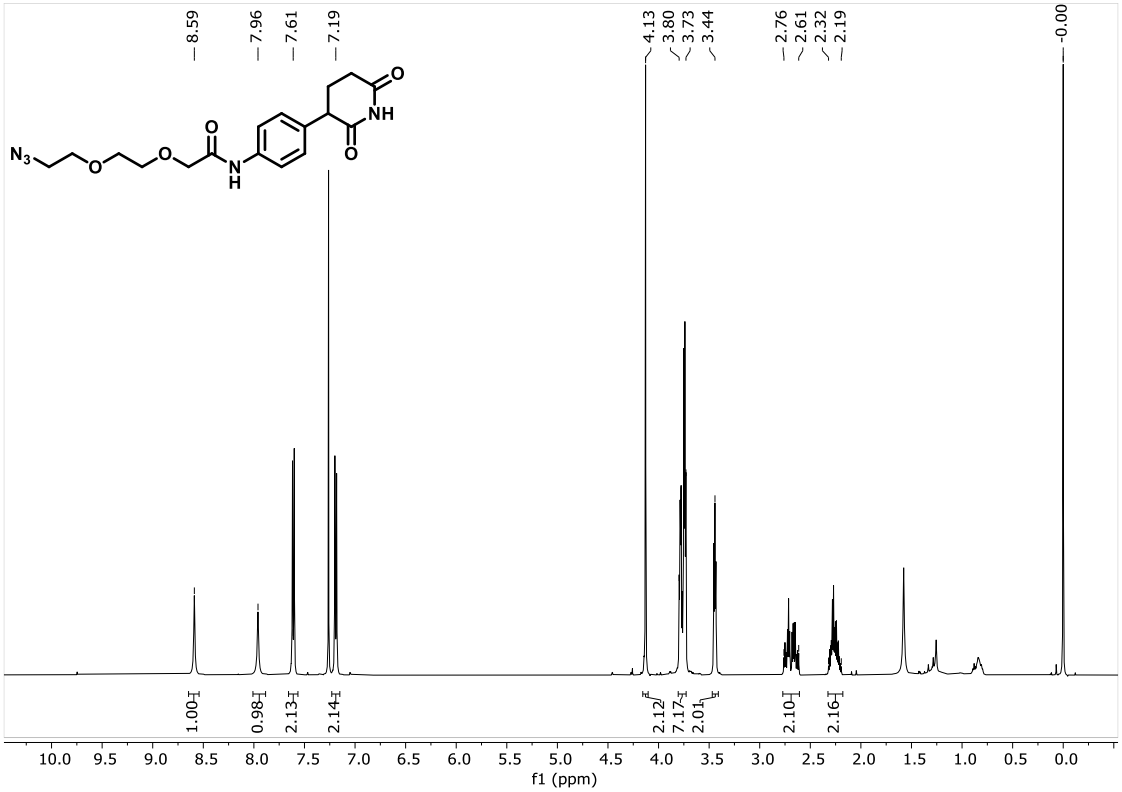

Figure 66: ^{1}H NMR (500 MHz, $CDCl_3$) of **64**.

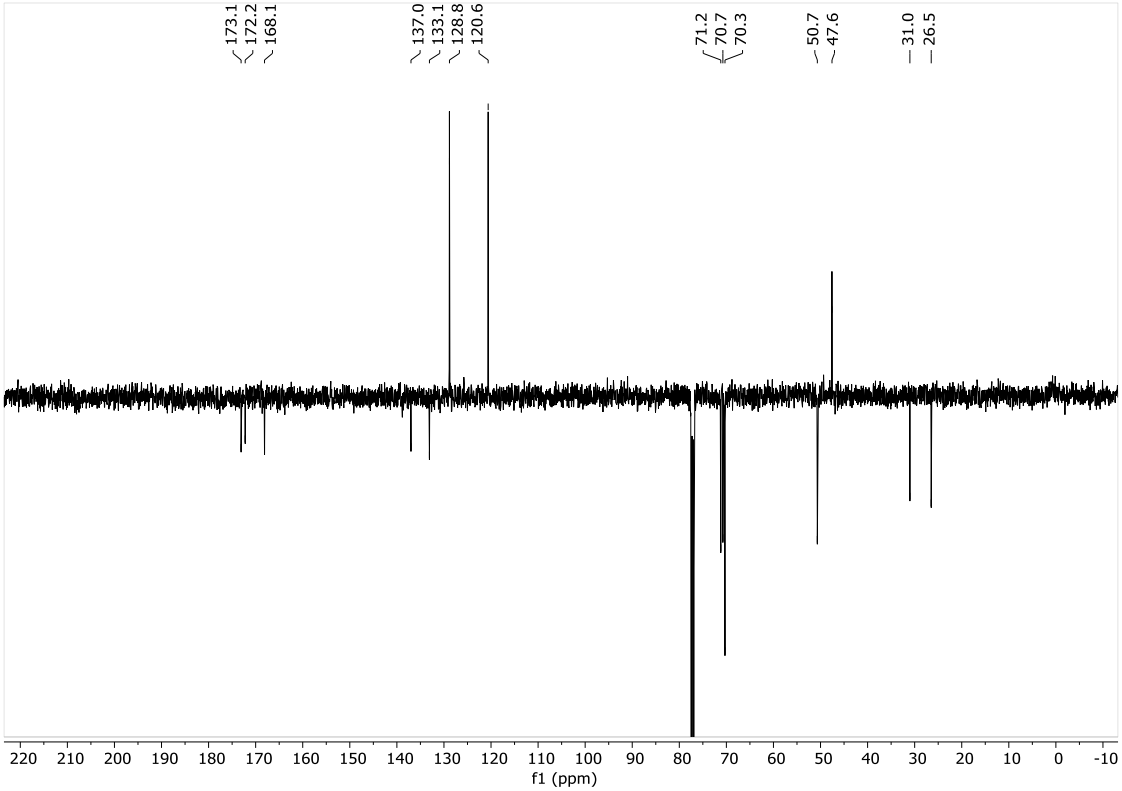

Figure 67: ^{13}C NMR (125 MHz, $CDCl_3$) of **64**.

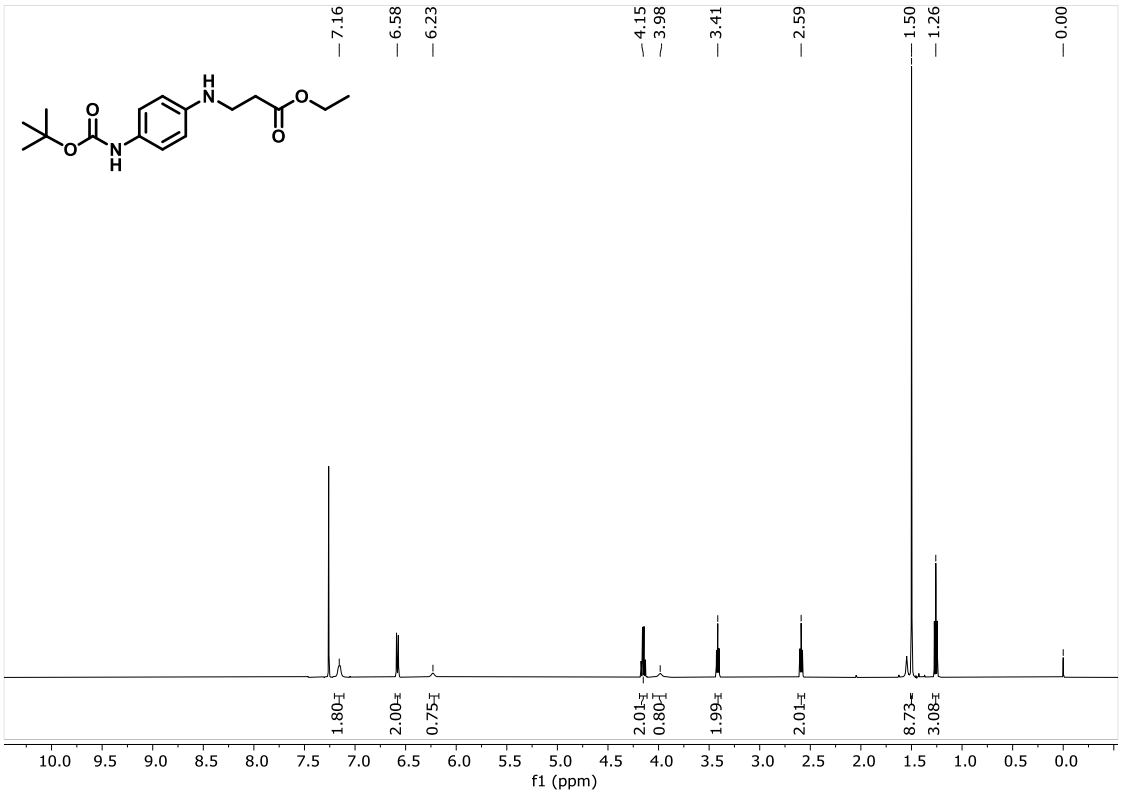

Figure 68: ^{1}H NMR (500 MHz, $CDCl_3$) of **69**.

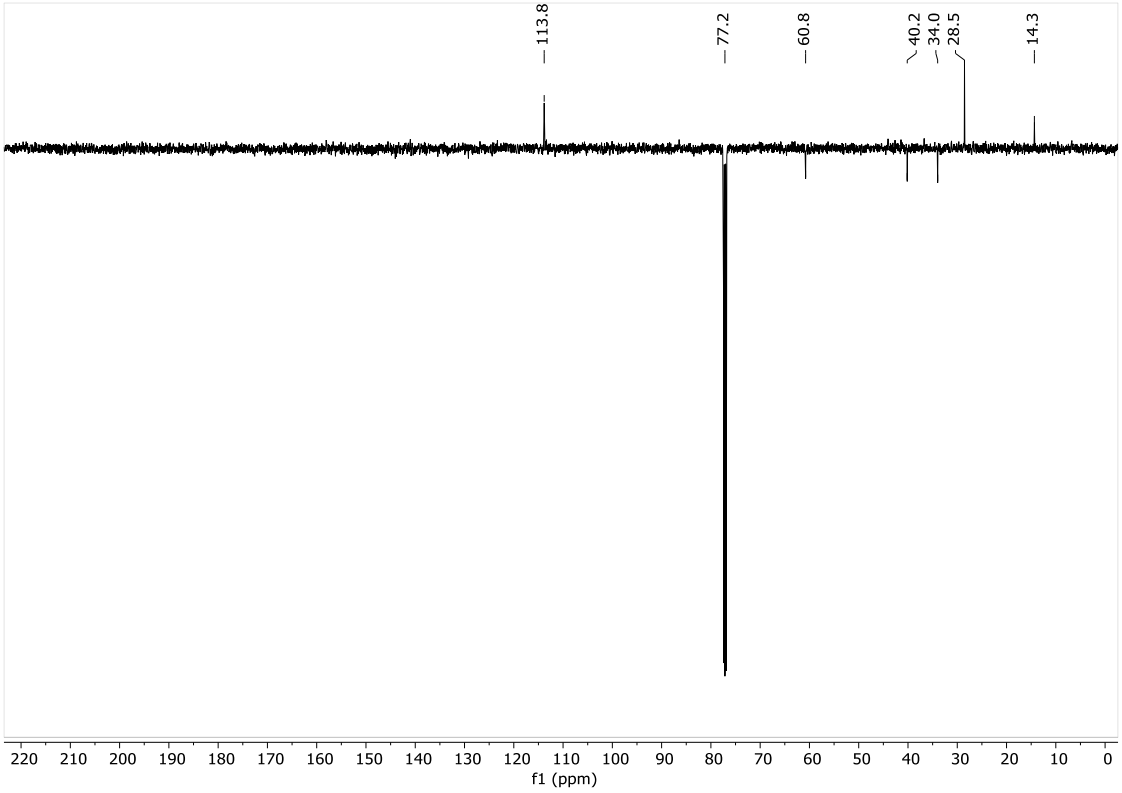

Figure 69: ^{13}C NMR (125 MHz, $CDCl_3$) of **69**.

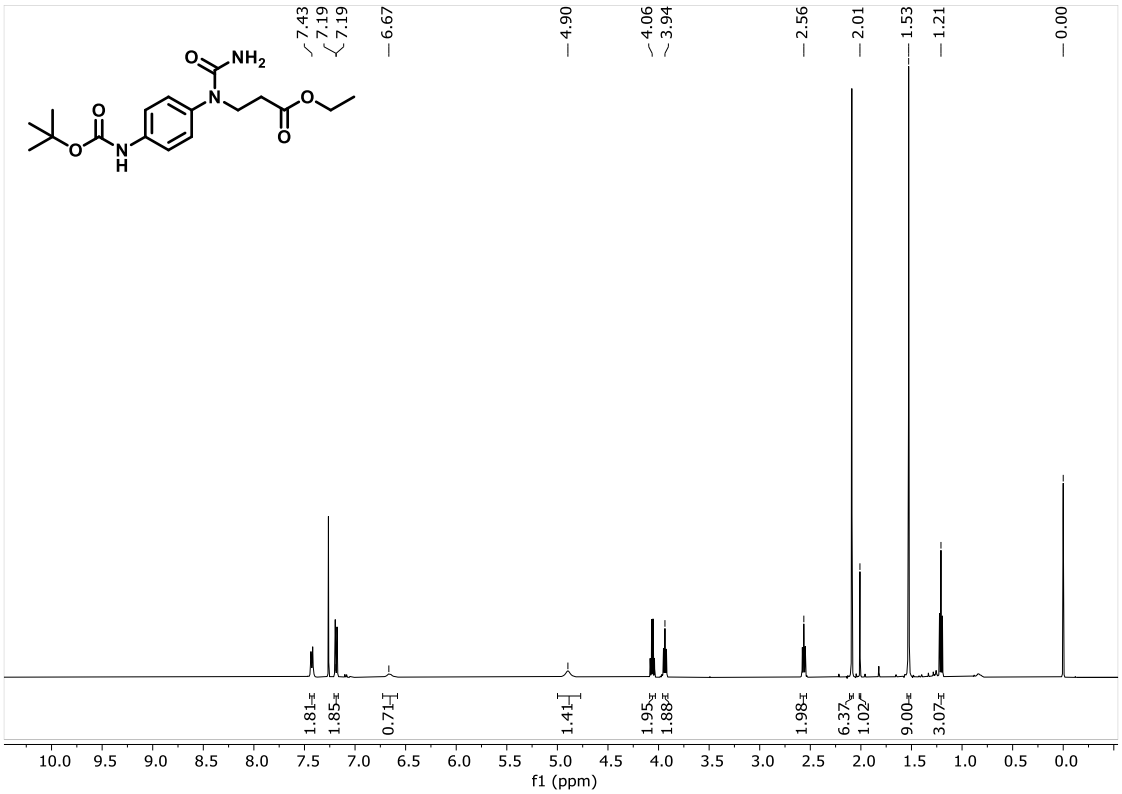

Figure 70: ^{1}H NMR (500 MHz, $CDCl_3$) of **70**.

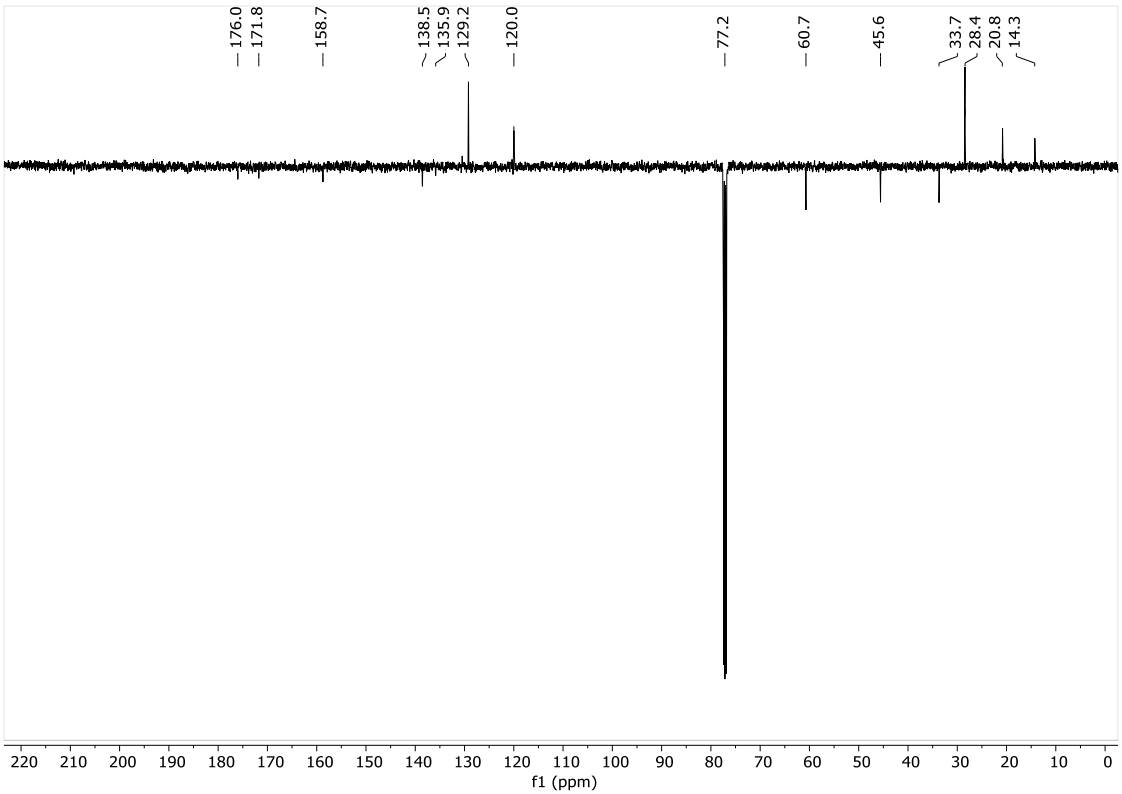

Figure 71: ^{13}C NMR (125 MHz, $CDCl_3$) of **70**.

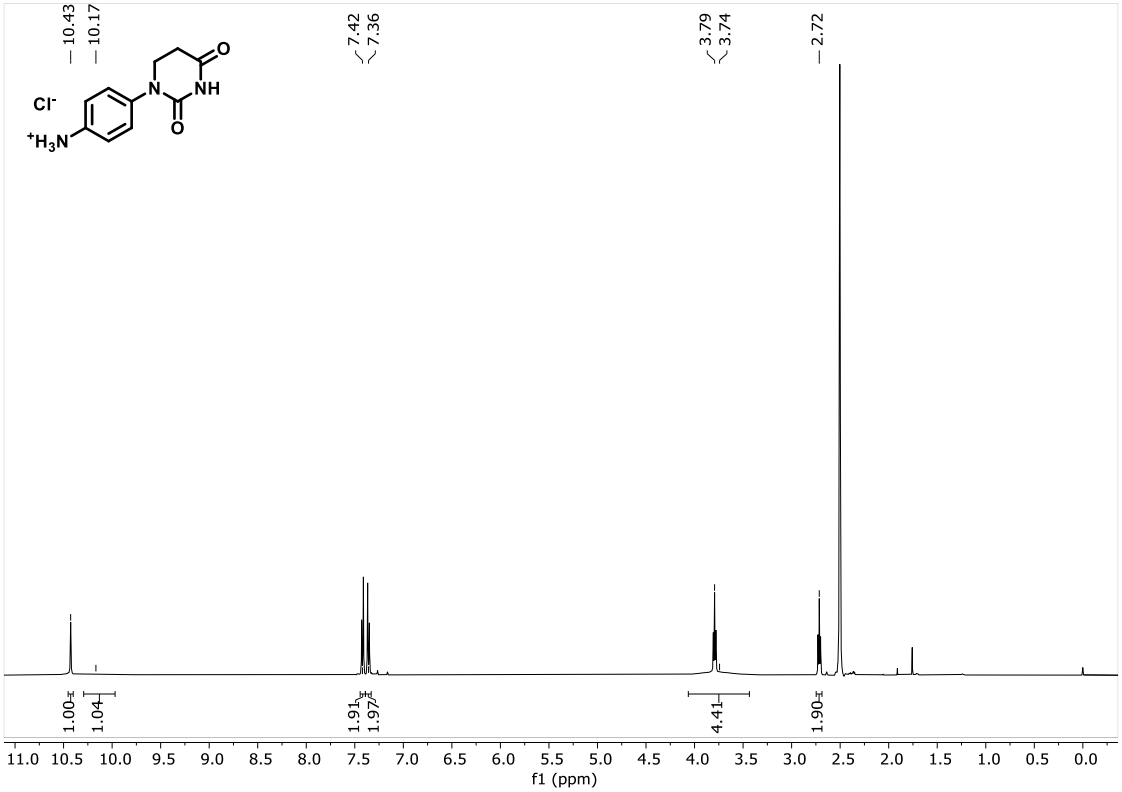

Figure 72: ^{1}H NMR (500 MHz, DMSO-d_6) of **65**.

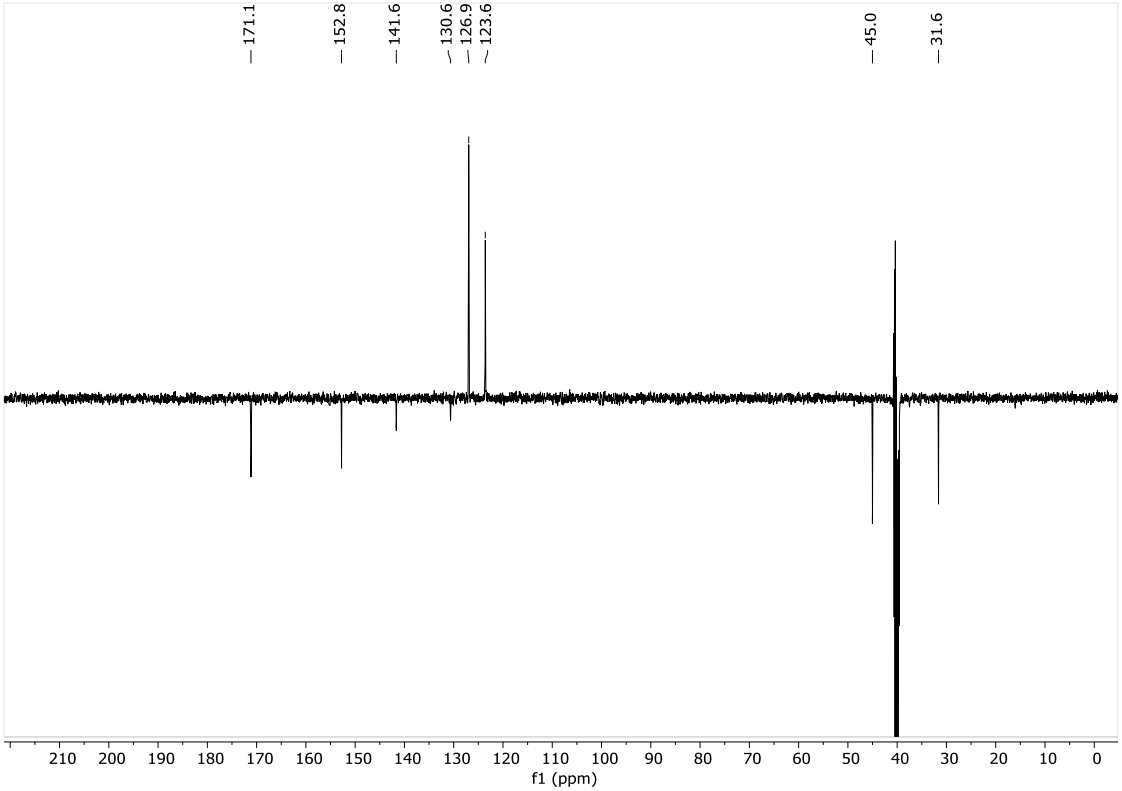

Figure 73: ^{13}C NMR (125 MHz, DMSO-d_6) of **65**.

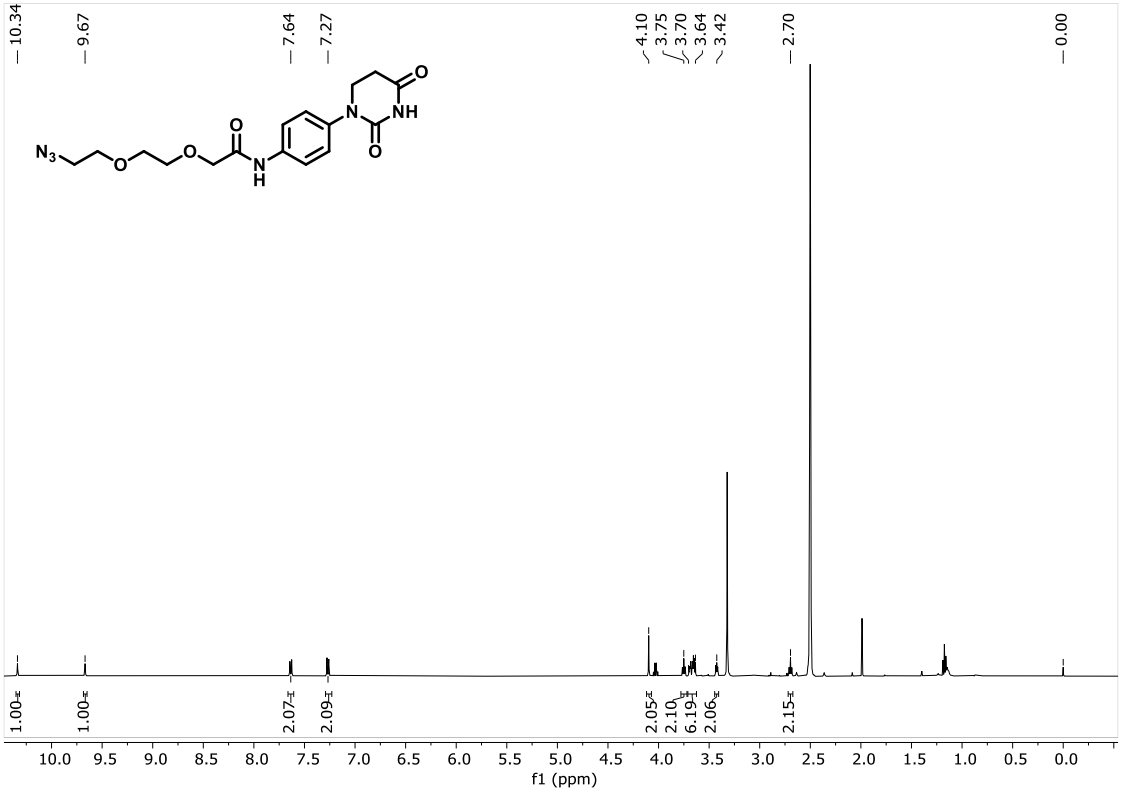

Figure 74: ^{1}H NMR (500 MHz, $CDCl_3$) of **71**.

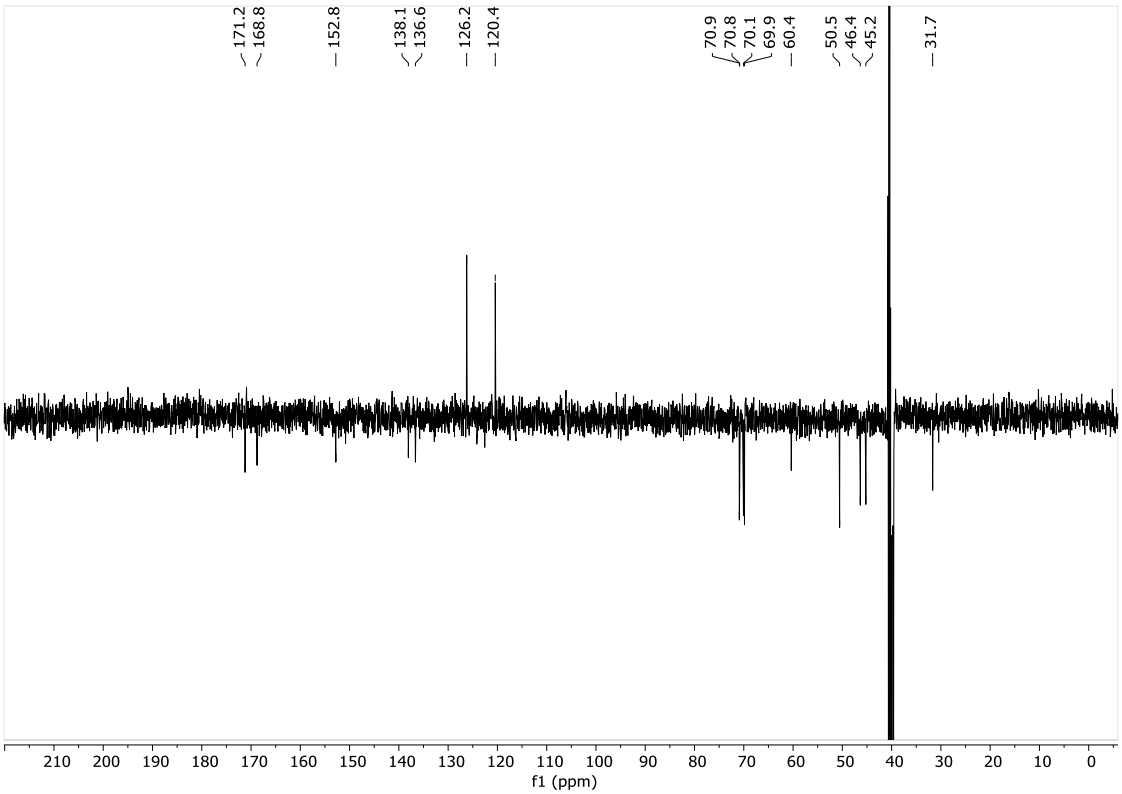

Figure 75: ^{13}C NMR (125 MHz, $CDCl_3$) of **71**.

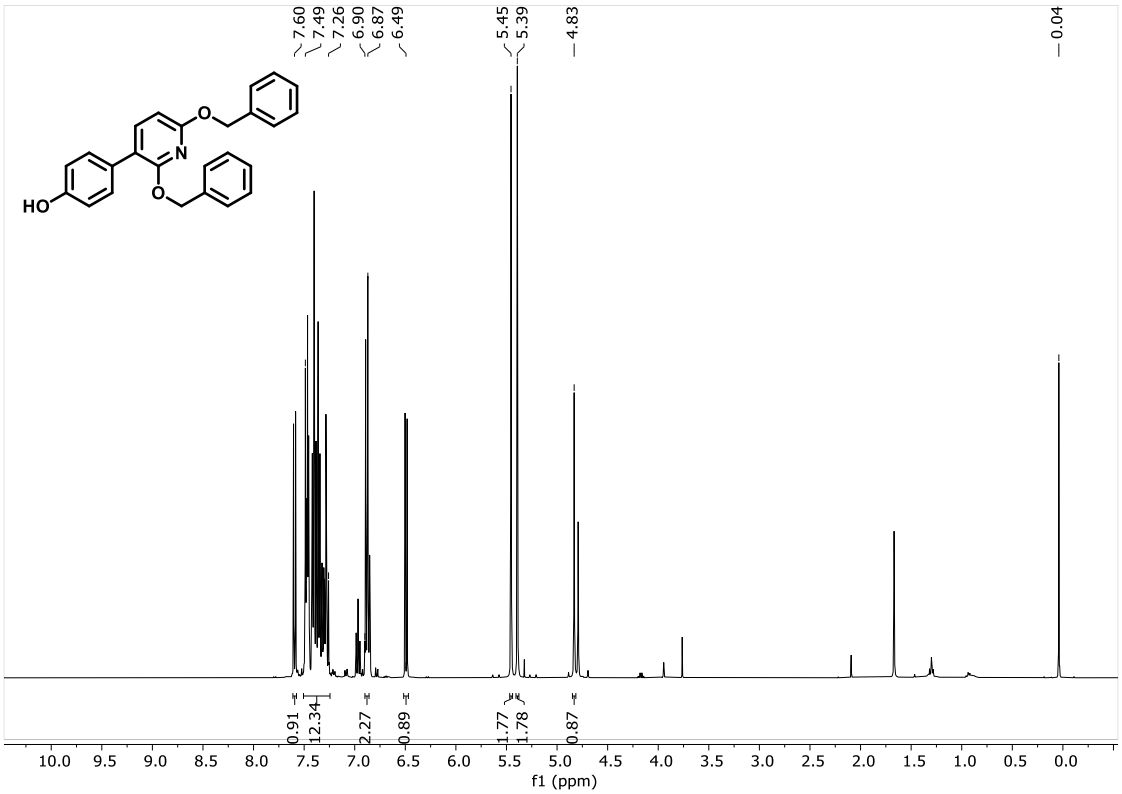

Figure 76: ^{1}H NMR (400 MHz, $CDCl_3$) of **72**.

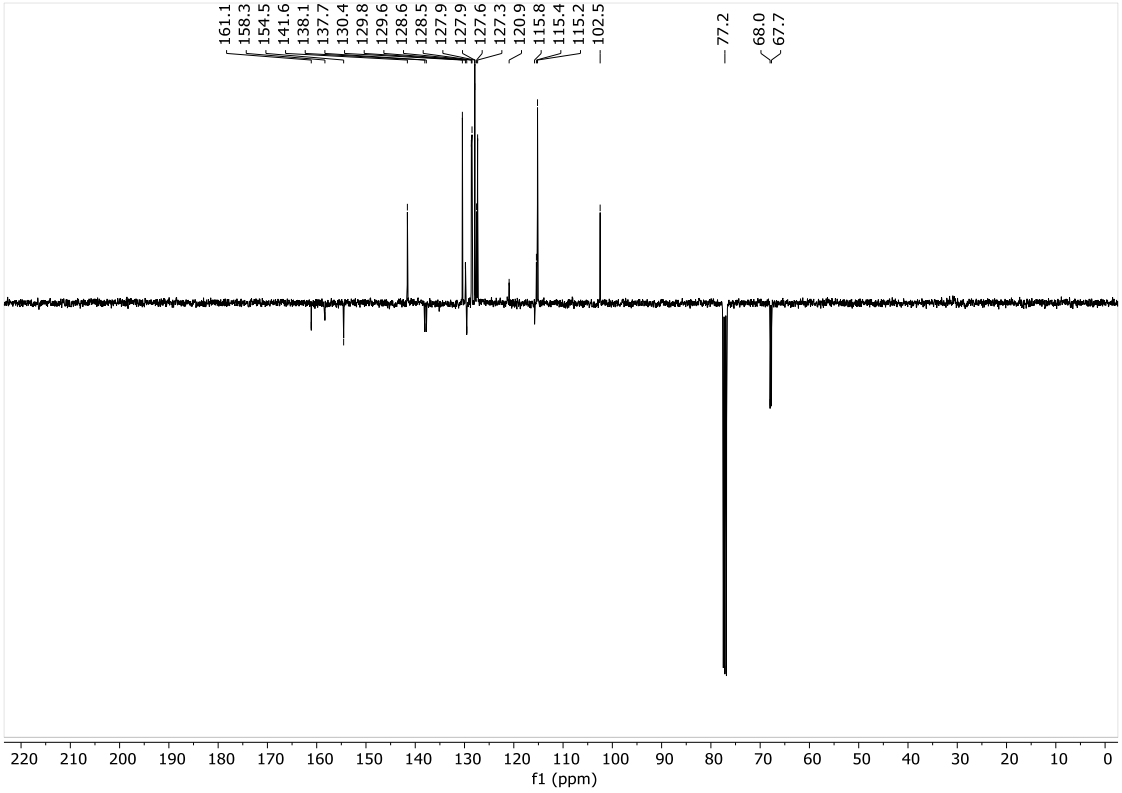

Figure 77: ^{13}C NMR (100 MHz, $CDCl_3$) of **72**.

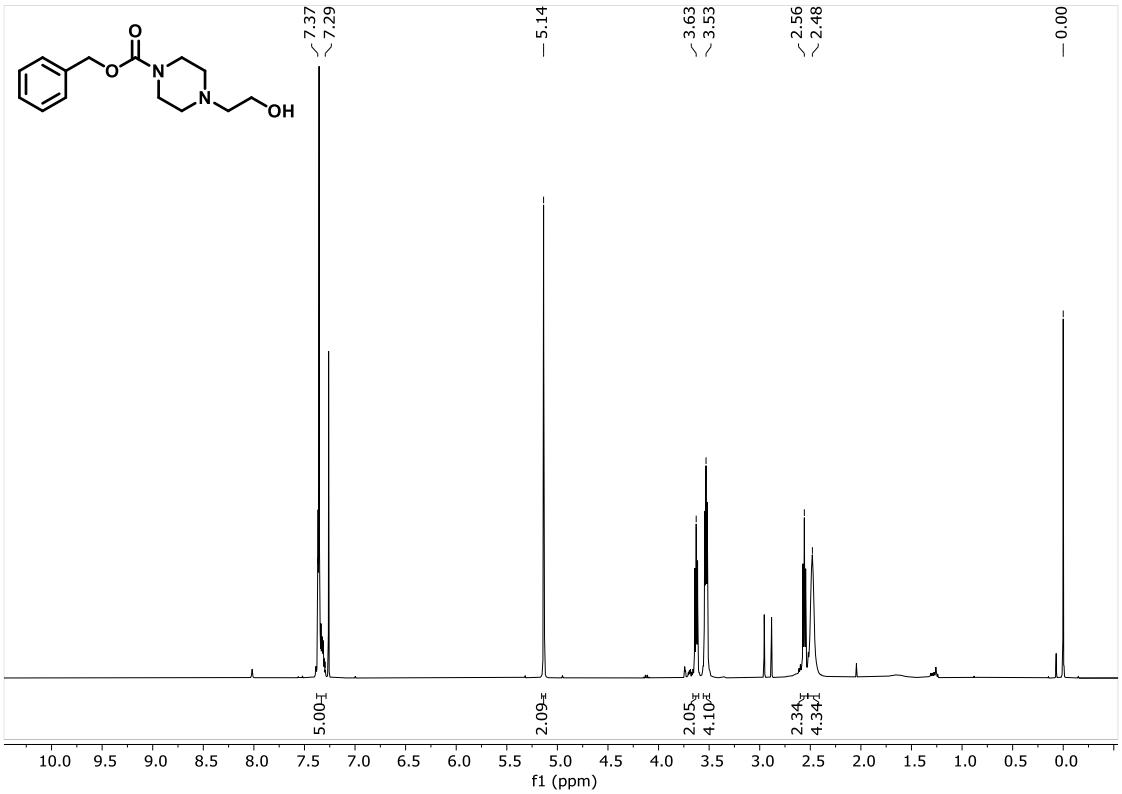

Figure 78: ^{1}H NMR (400 MHz, $CDCl_3$) of **98**.

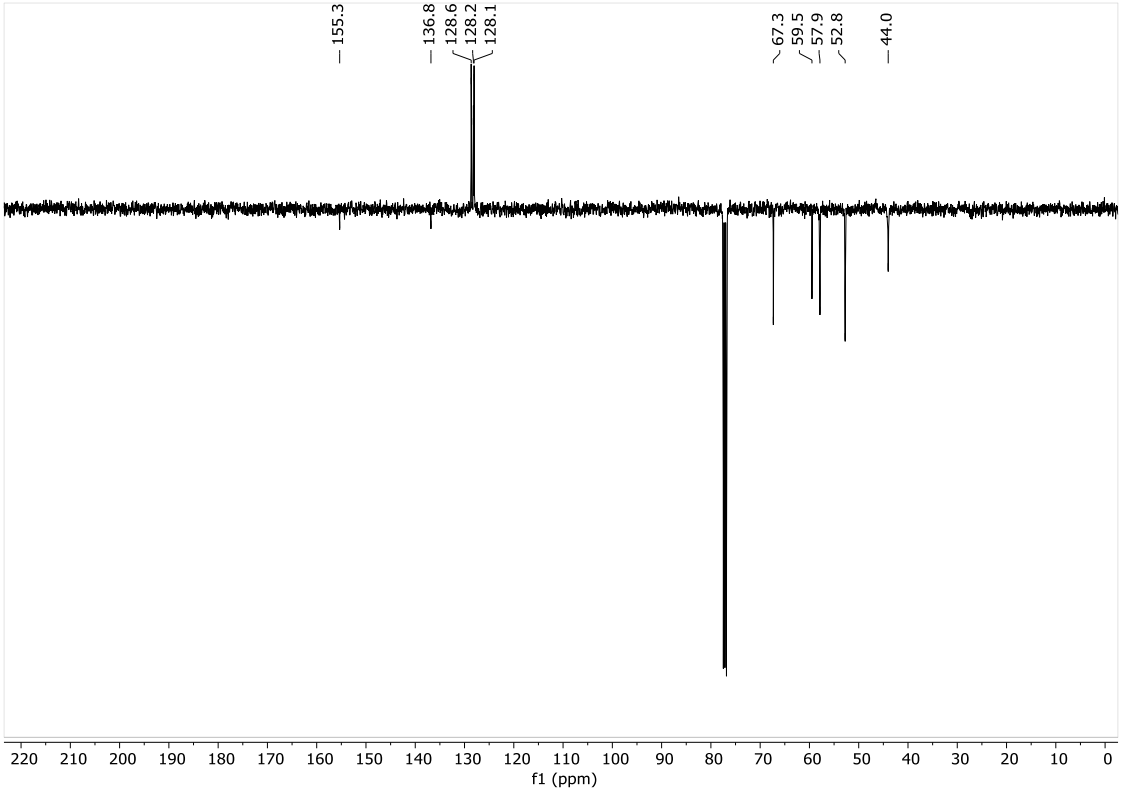

Figure 79: ^{13}C NMR (100 MHz, $CDCl_3$) of **98**.

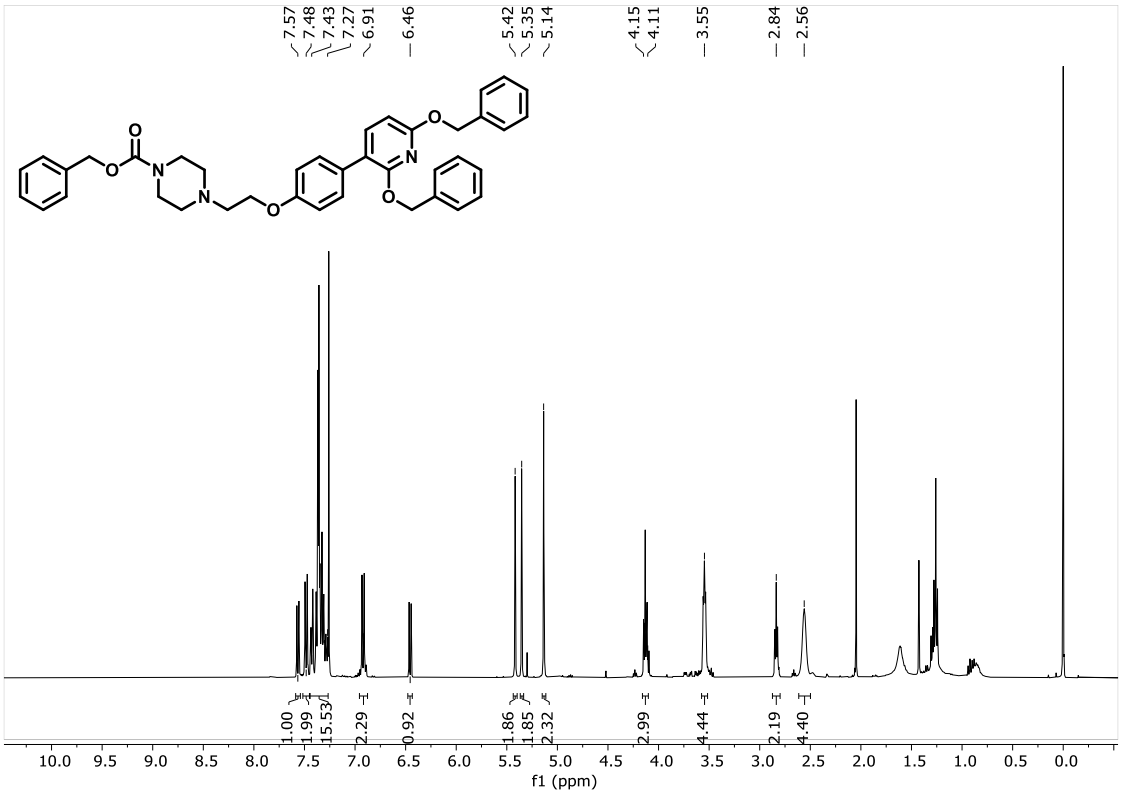

Figure 80: ^{1}H NMR (400 MHz, $CDCl_3$) of **93**.

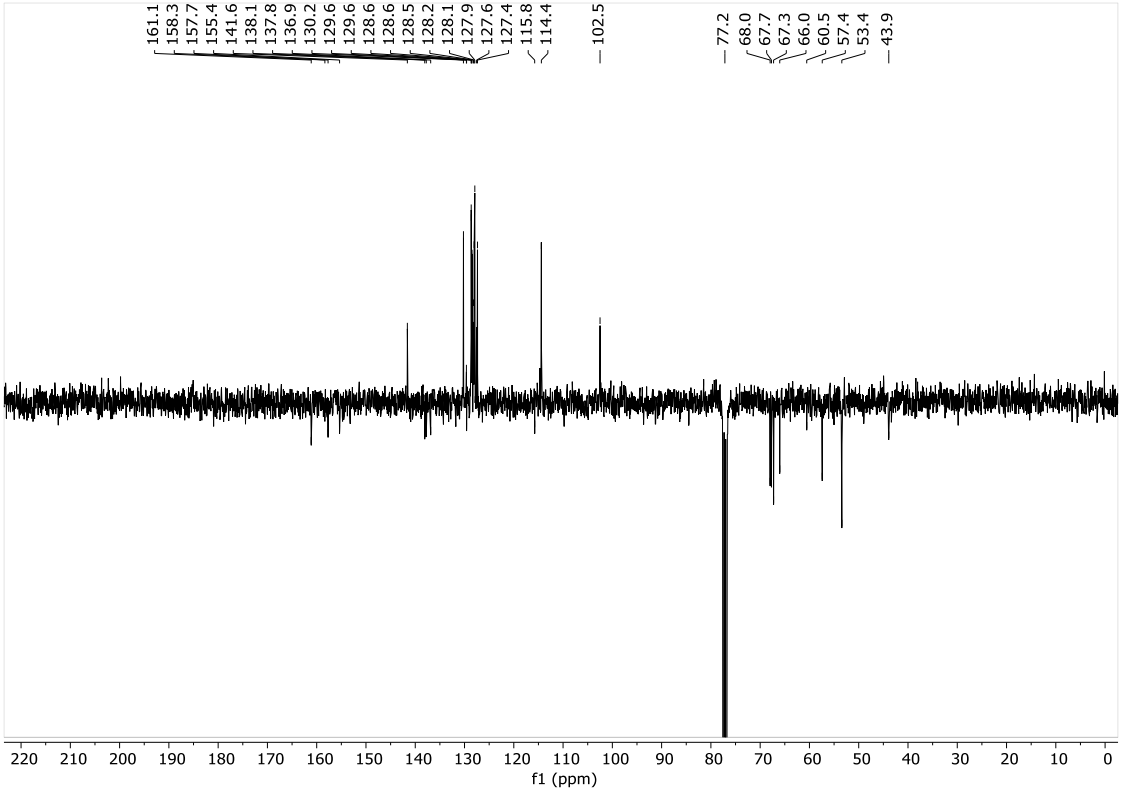

Figure 81: ^{13}C NMR (100 MHz, $CDCl_3$) of **93**.

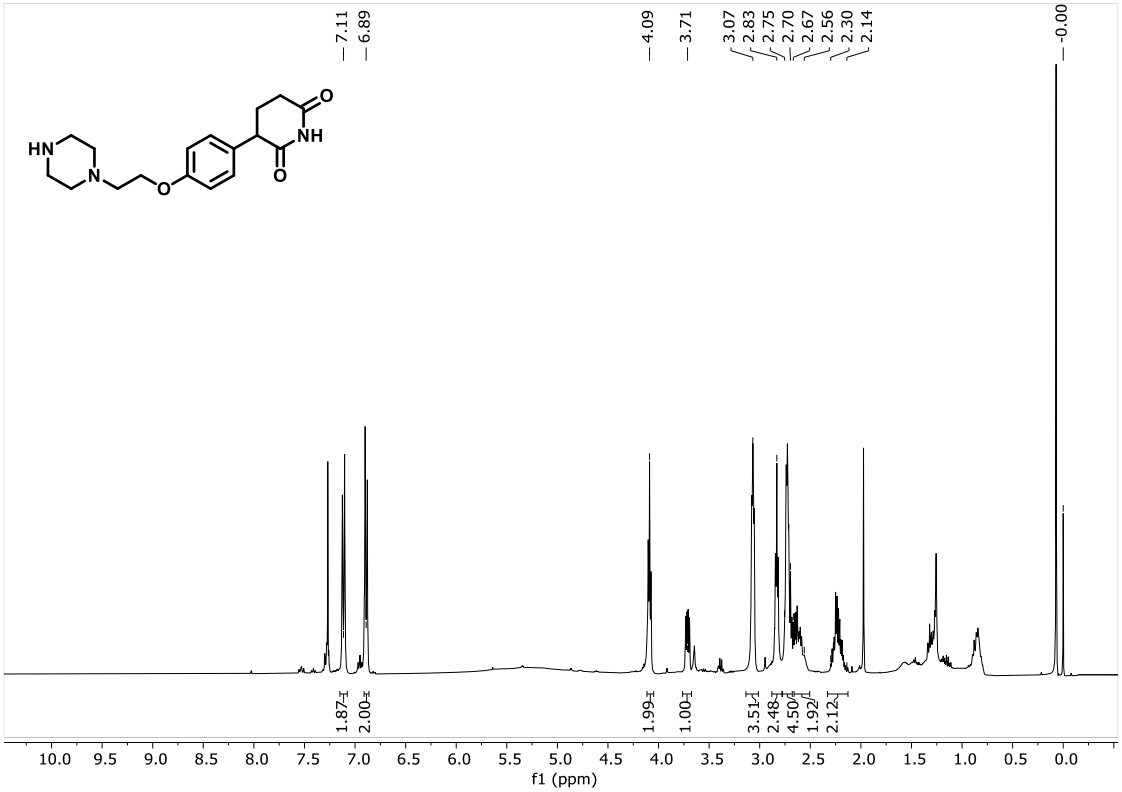

Figure 82: ^{1}H NMR (400 MHz, $CDCl_3$) of **105**.

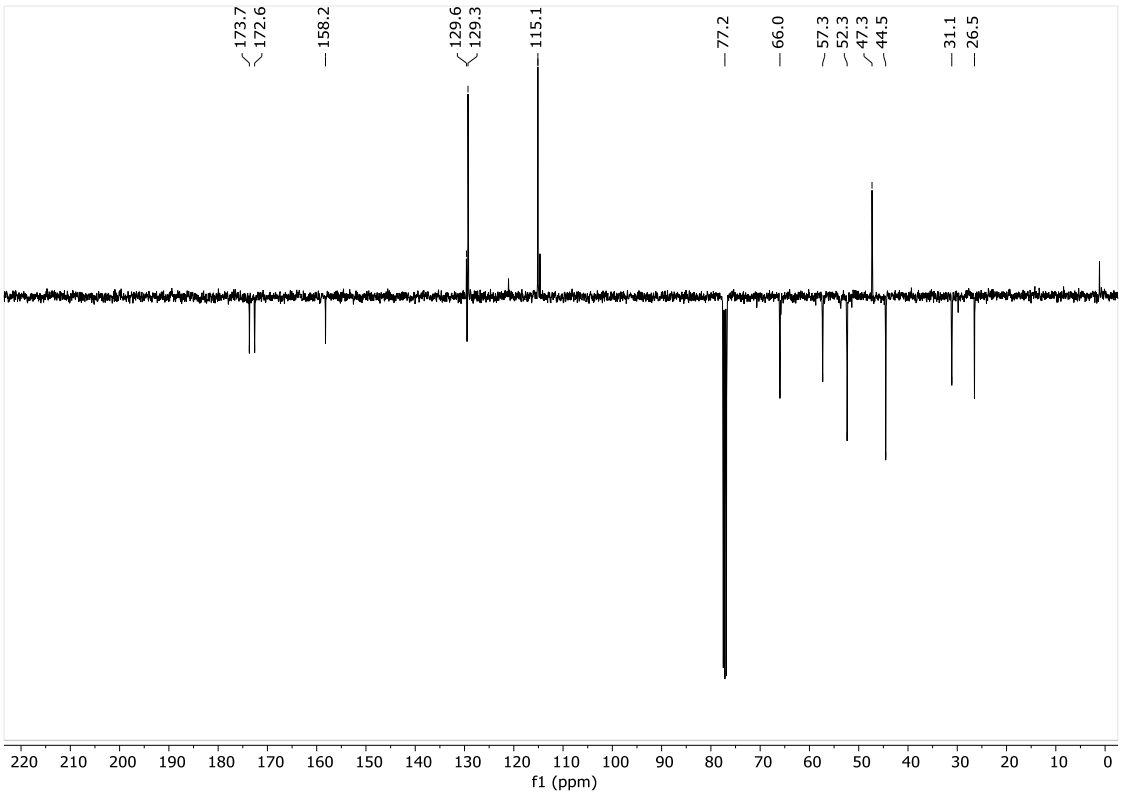

Figure 83: ^{13}C NMR (100 MHz, $CDCl_3$) of **105**.

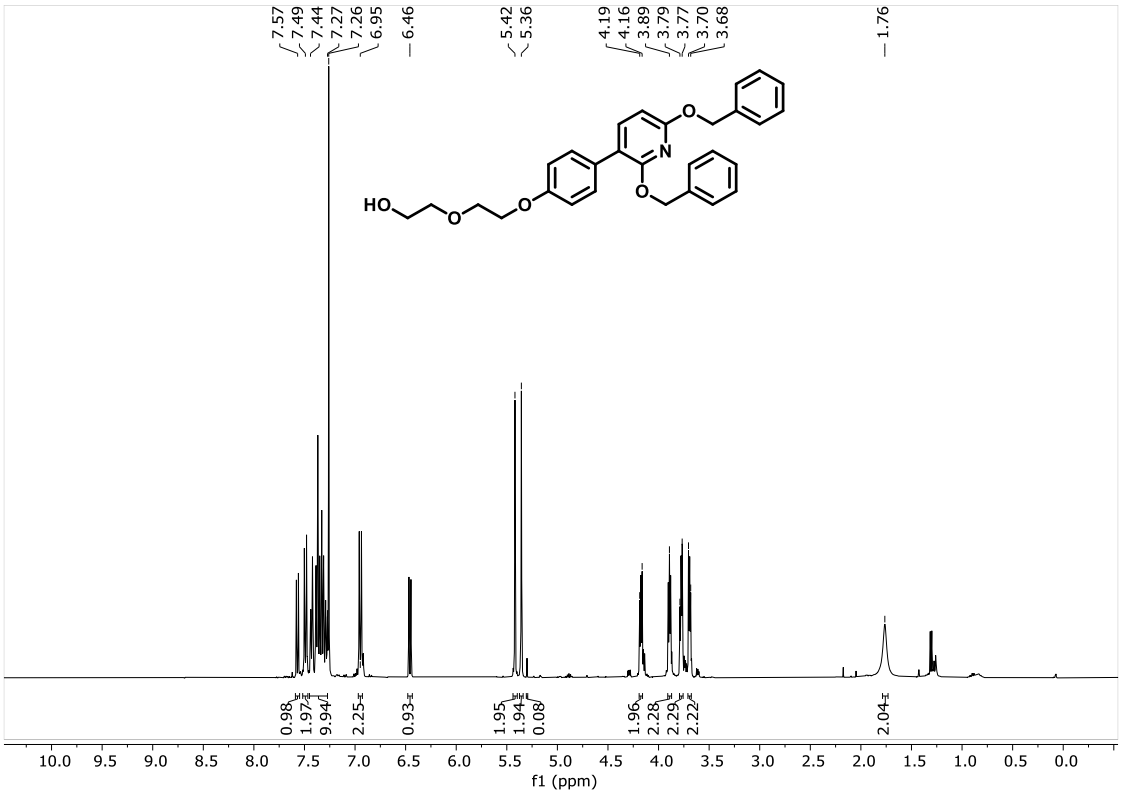

Figure 84: ^{1}H NMR (400 MHz, $CDCl_3$) of **99**.

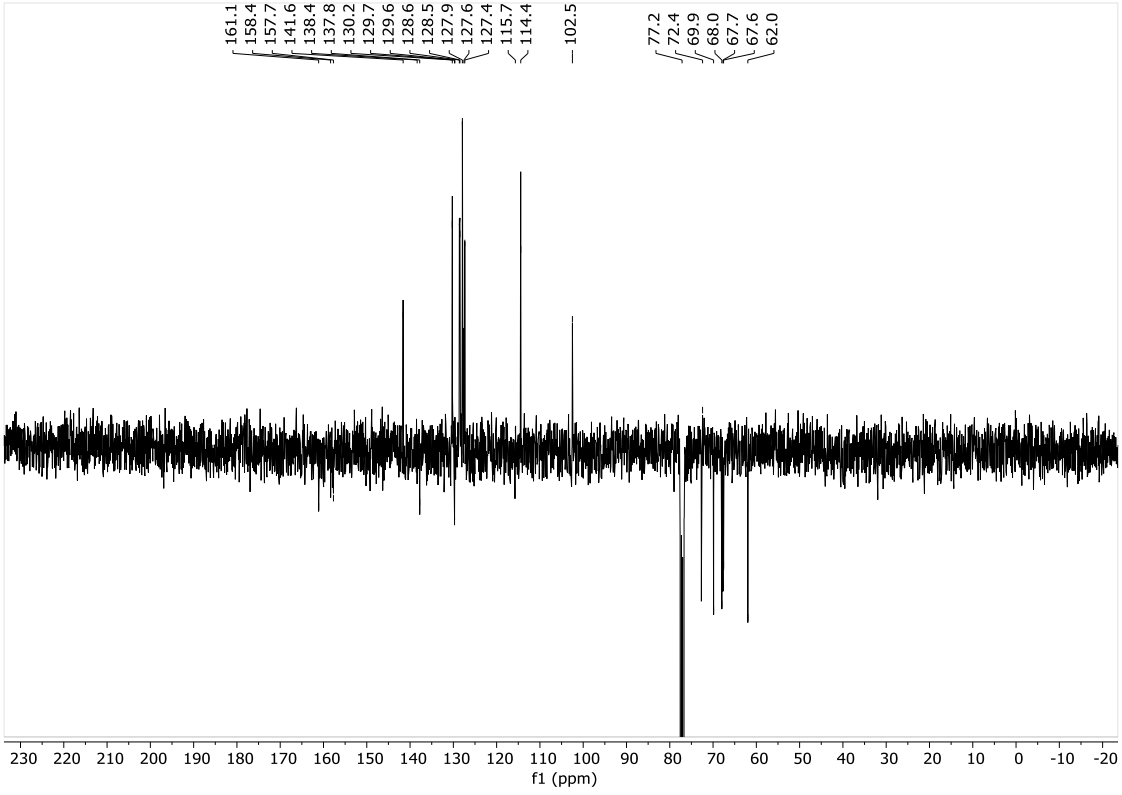

Figure 85: ^{13}C NMR (100 MHz, $CDCl_3$) of **99**.

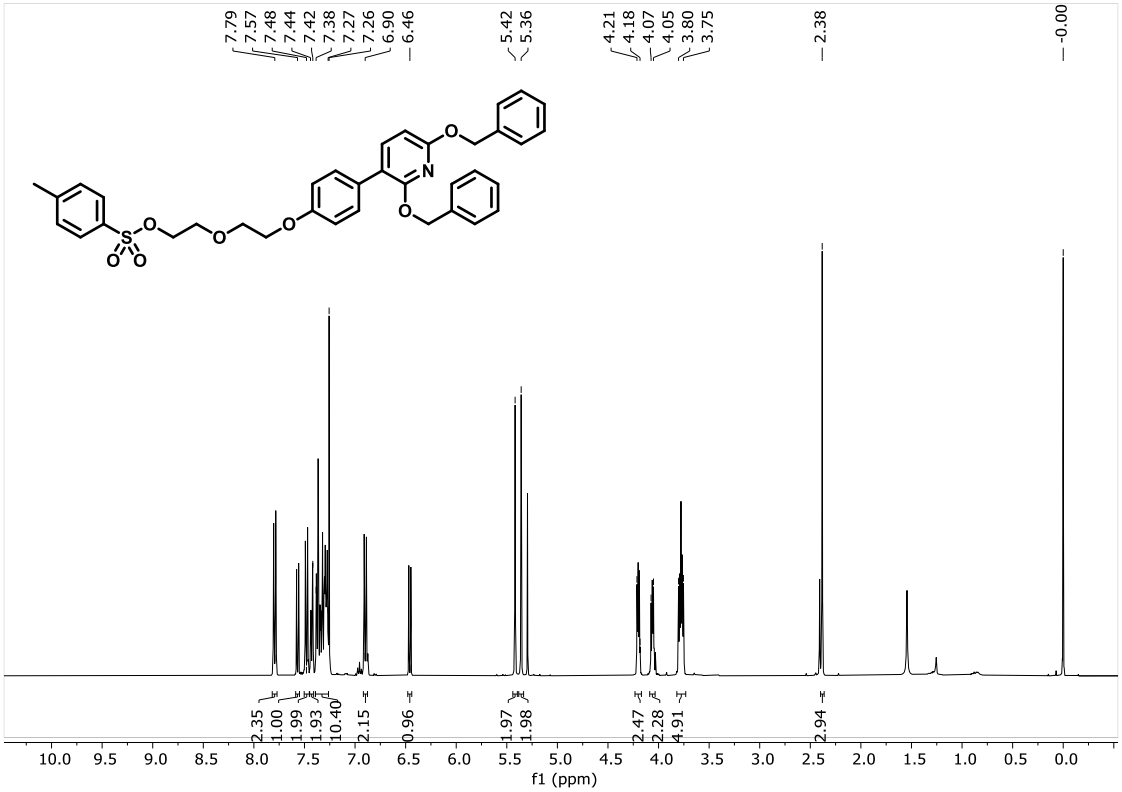

Figure 86: ^{1}H NMR (400 MHz, $CDCl_3$) of **102**.

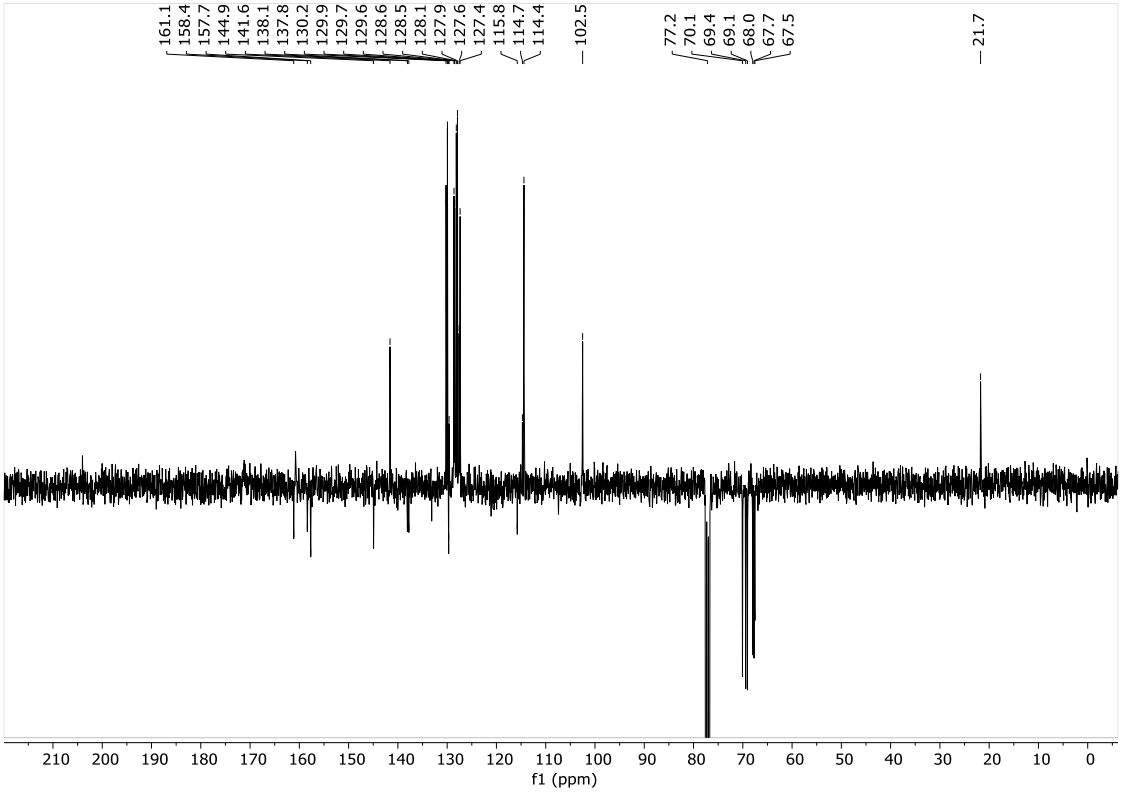

Figure 87: ^{13}C NMR (100 MHz, $CDCl_3$) of **102**.

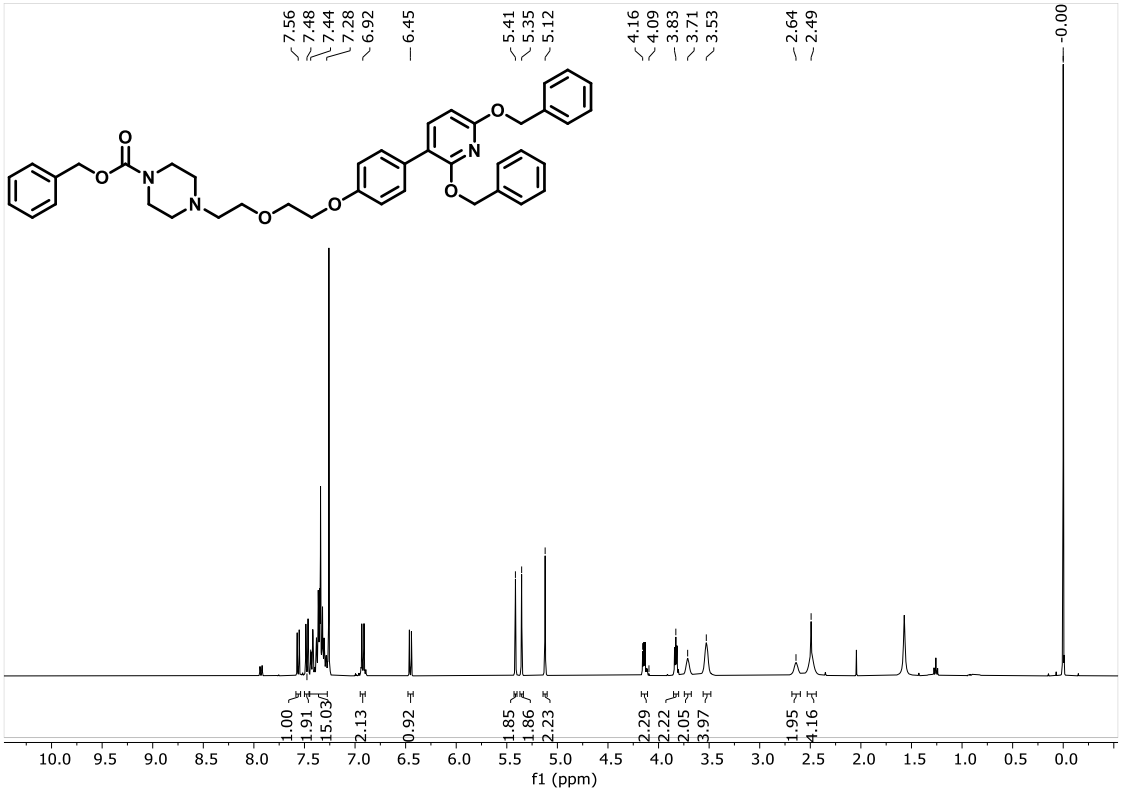

Figure 88: ^{1}H NMR (400 MHz, $CDCl_3$) of **94**.

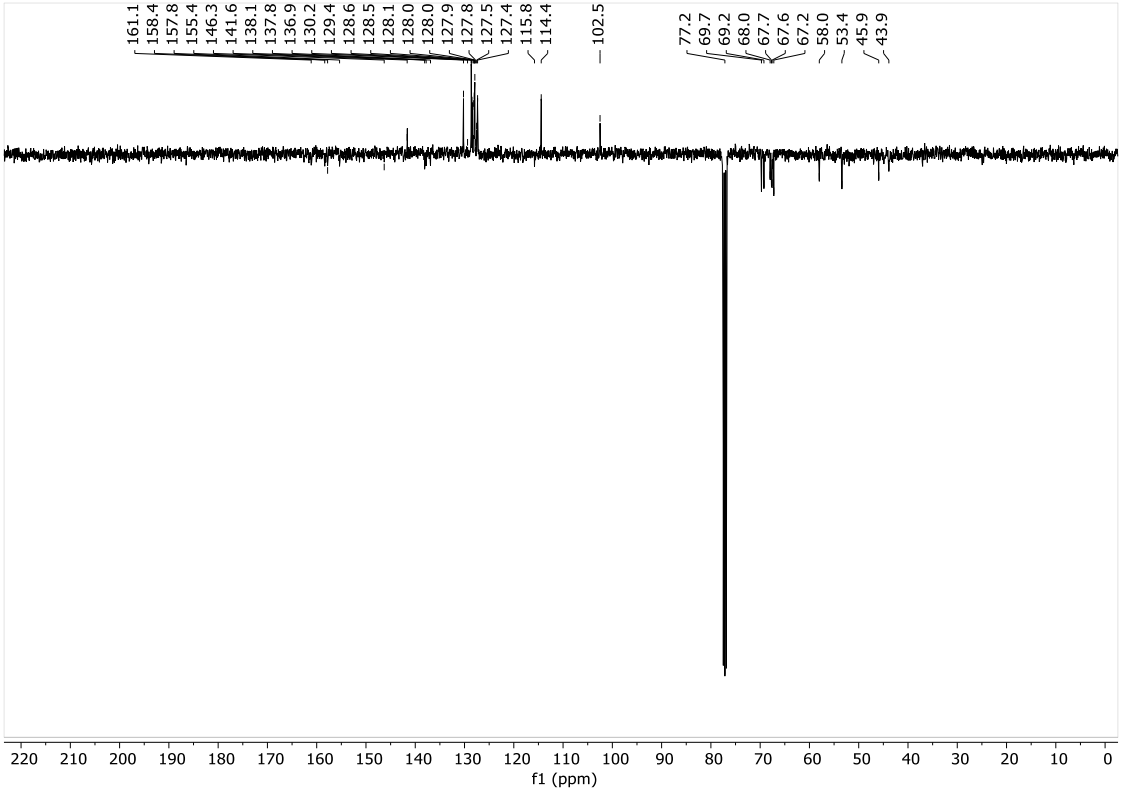

Figure 89: ^{13}C NMR (100 MHz, $CDCl_3$) of **94**.

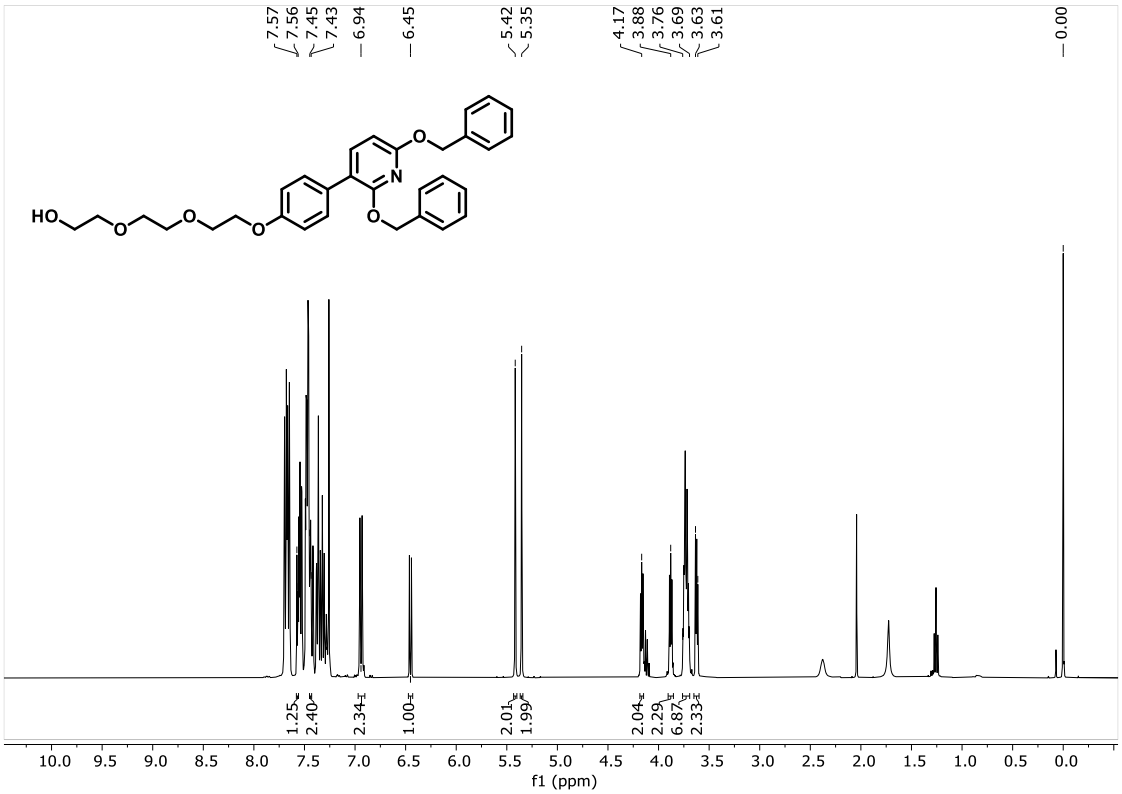

Figure 90: ^{1}H NMR (400 MHz, $CDCl_3$) of **100**.

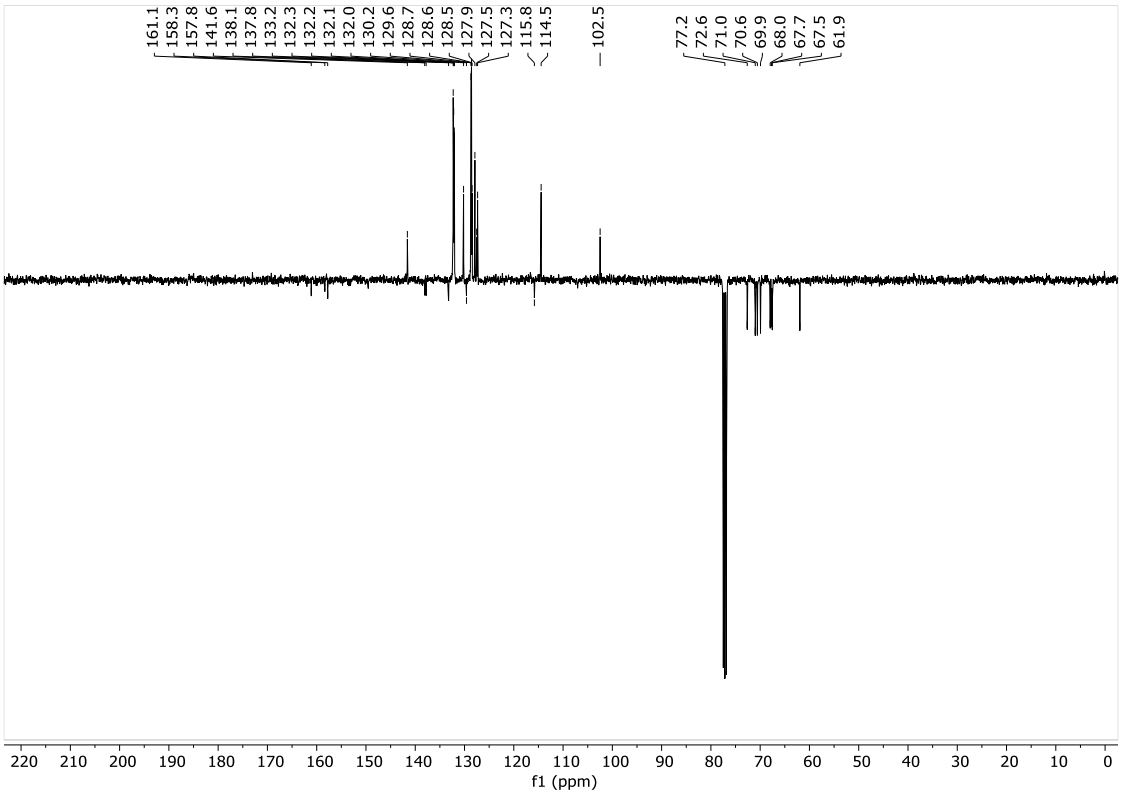

Figure 91: ^{13}C NMR (100 MHz, $CDCl_3$) of **100**.

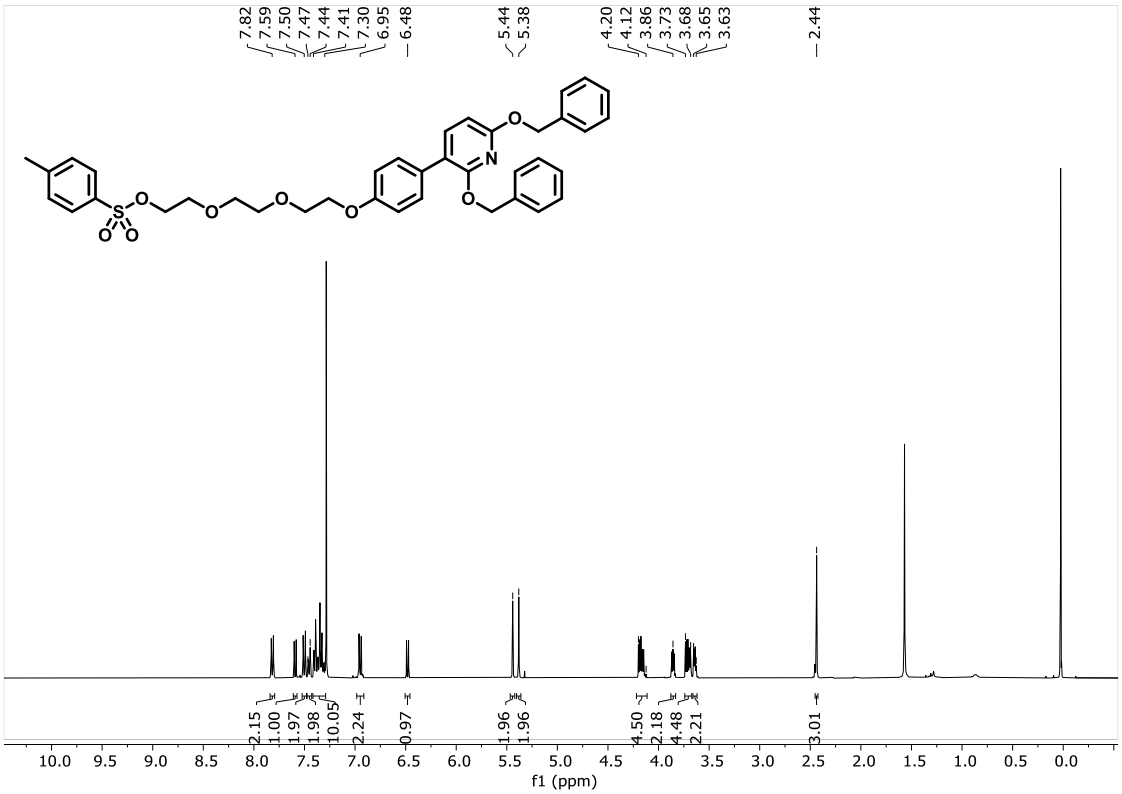

Figure 92: ^{1}H NMR (400 MHz, $CDCl_3$) of **103**.

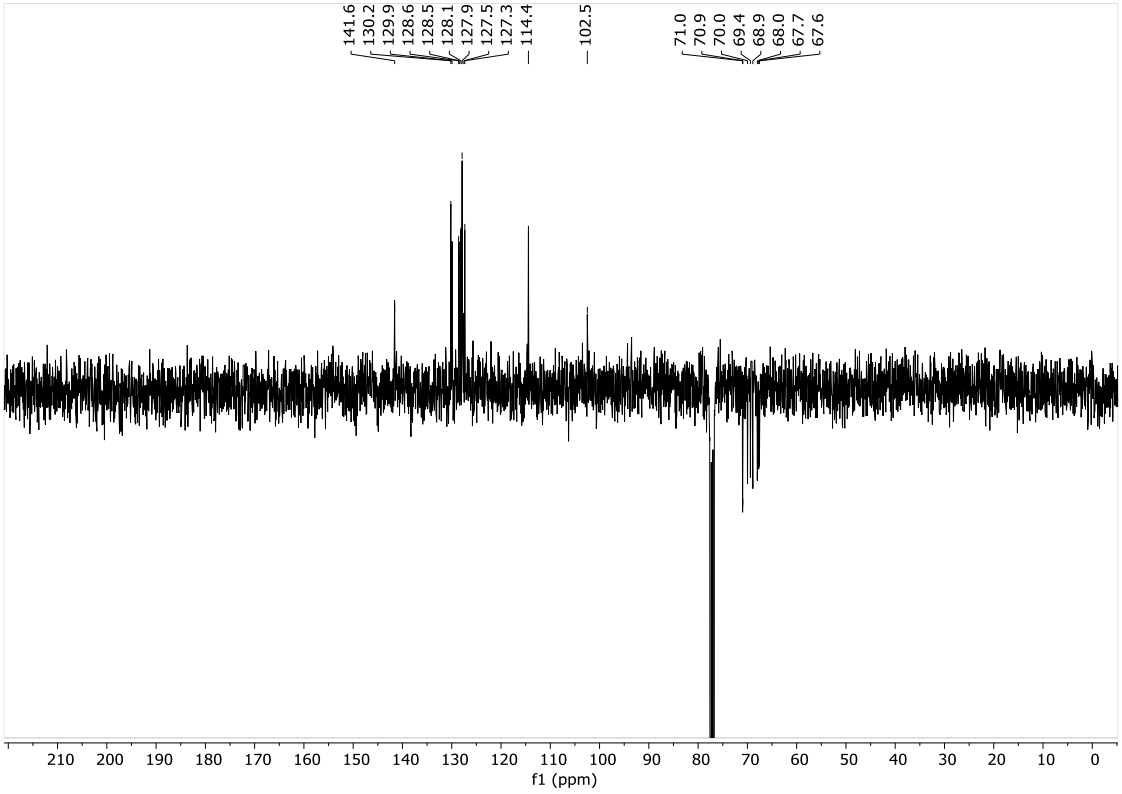

Figure 93: ^{13}C NMR (100 MHz, $CDCl_3$) of **103**.

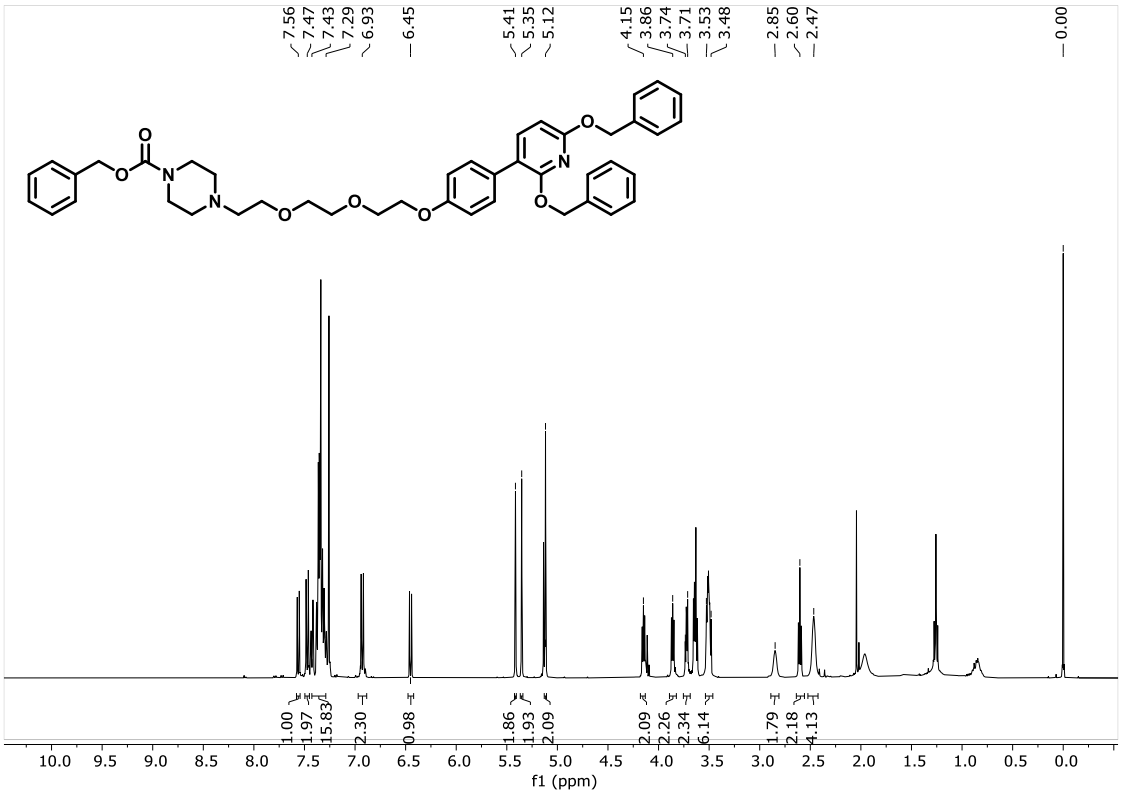

Figure 94: ^{1}H NMR (400 MHz, $CDCl_3$) of **95**.

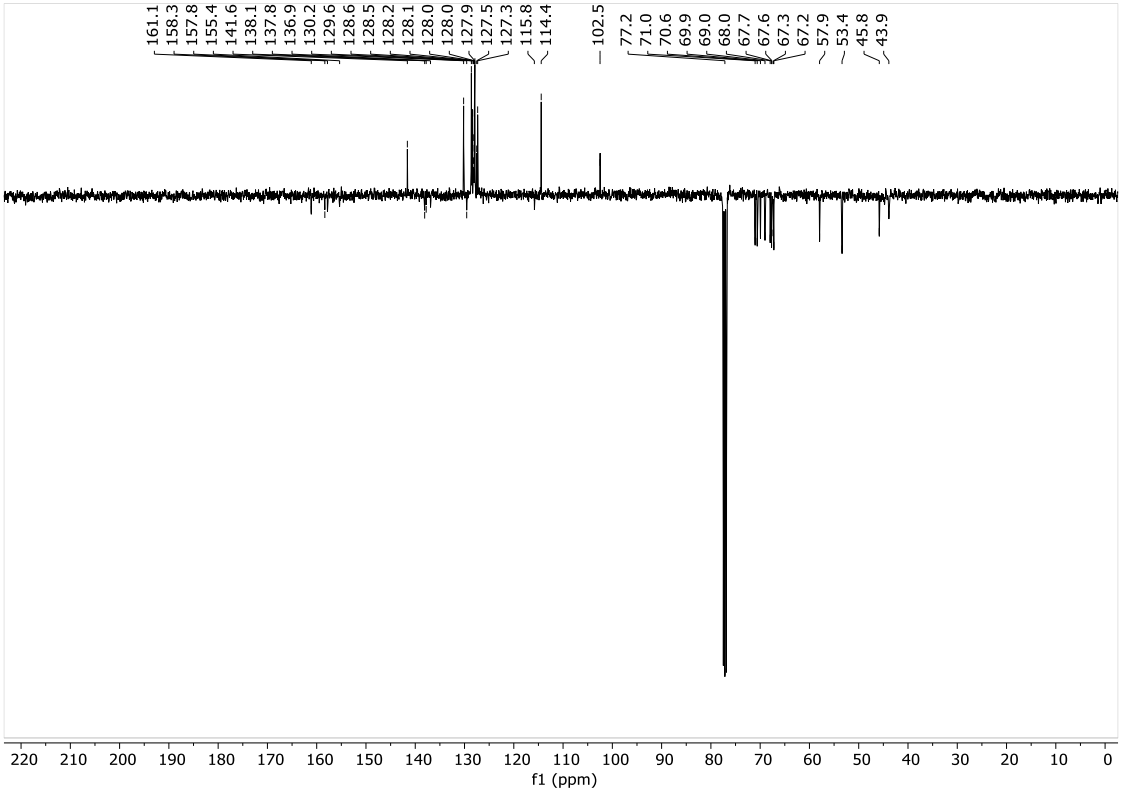

Figure 95: ^{13}C NMR (100 MHz, $CDCl_3$) of **95**.

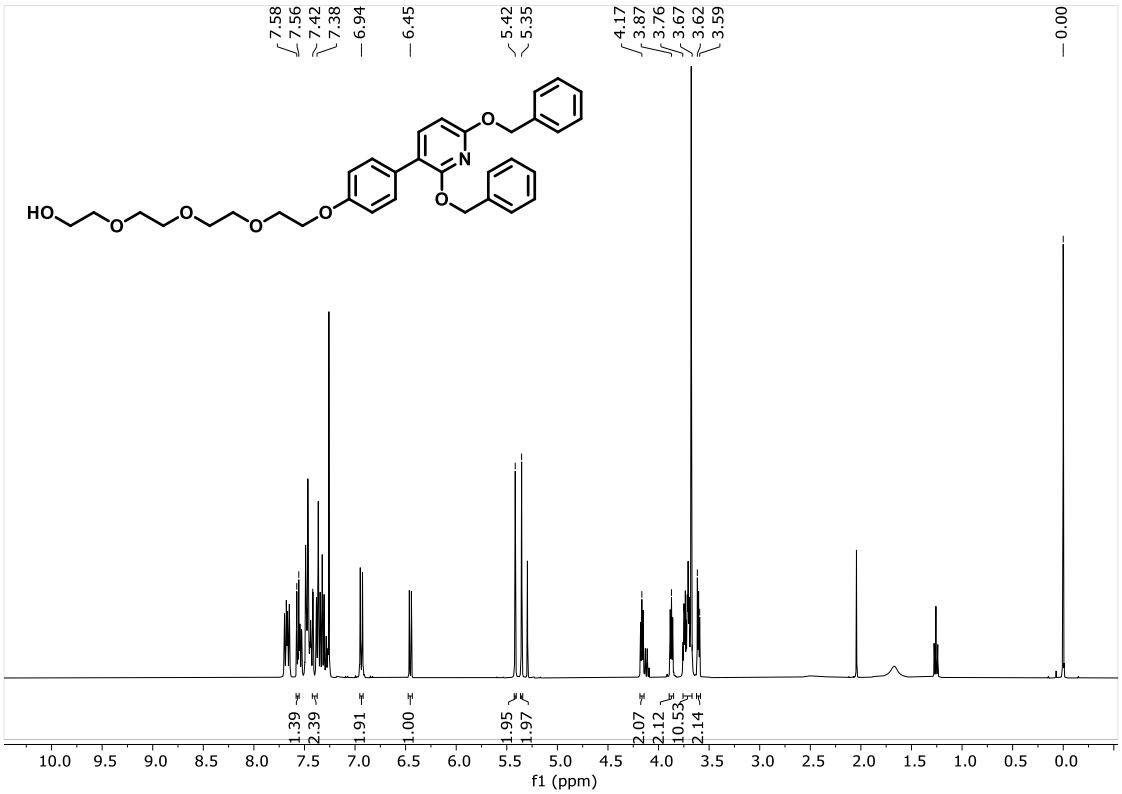

Figure 96: ^{1}H NMR (400 MHz, $CDCl_3$) of **101**.

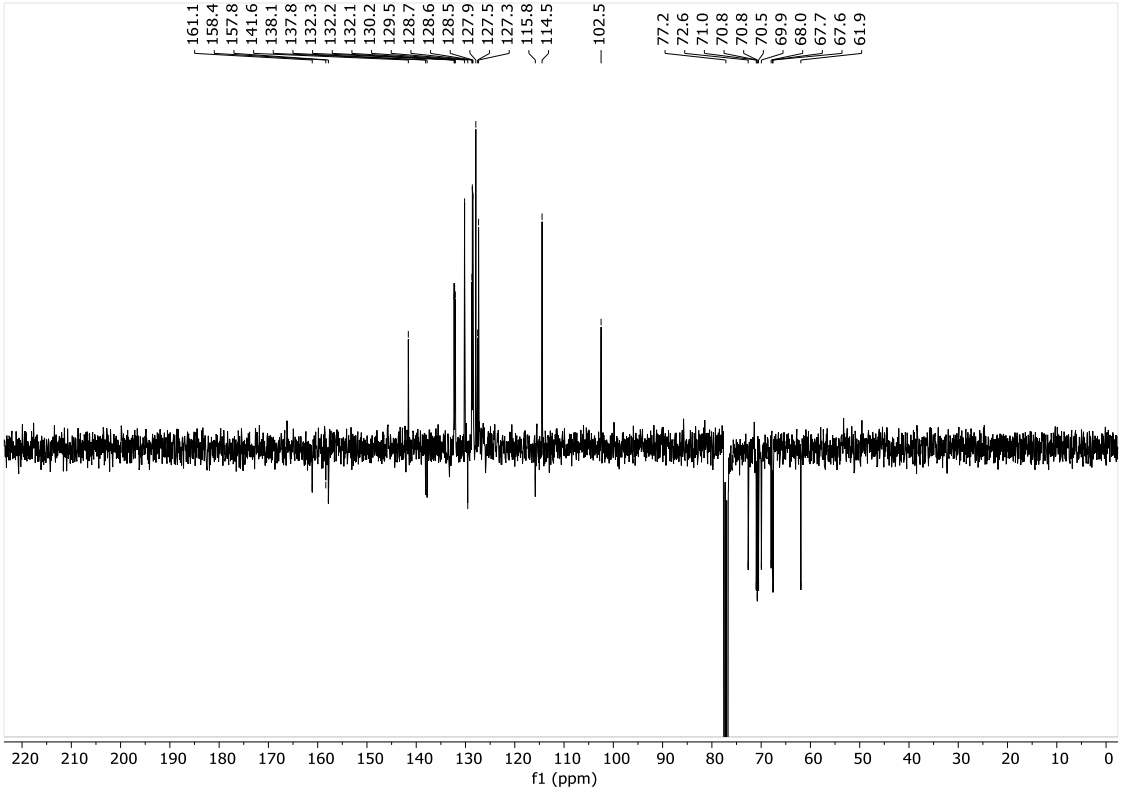

Figure 97: ^{13}C NMR (100 MHz, $CDCl_3$) of **101**.

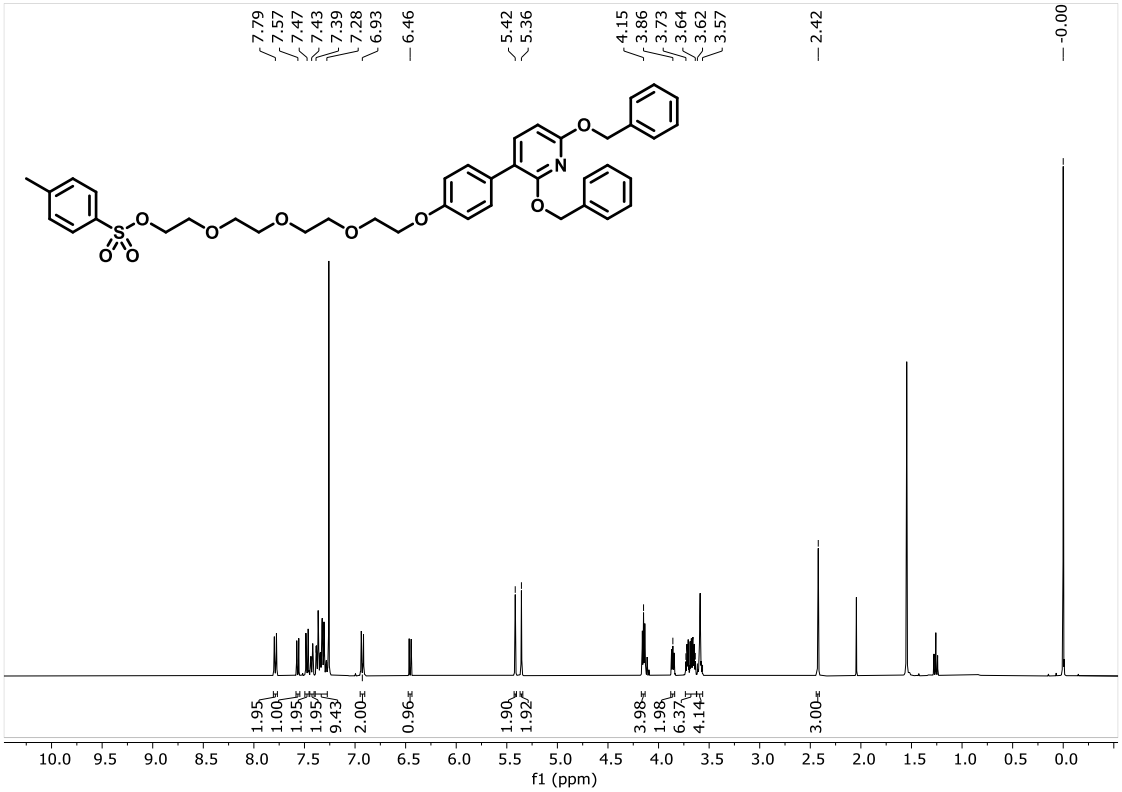

Figure 98: ^{1}H NMR (400 MHz, $CDCl_3$) of **104**.

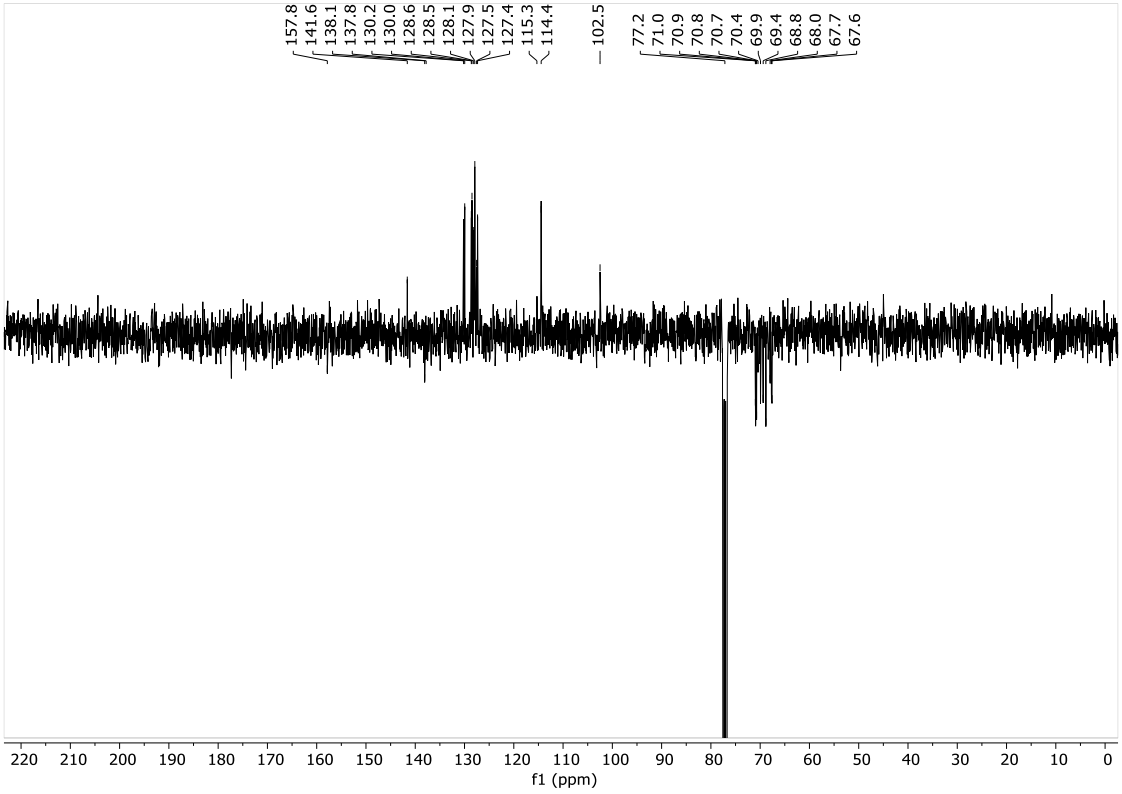

Figure 99: ^{13}C NMR (100 MHz, $CDCl_3$) of **104**.

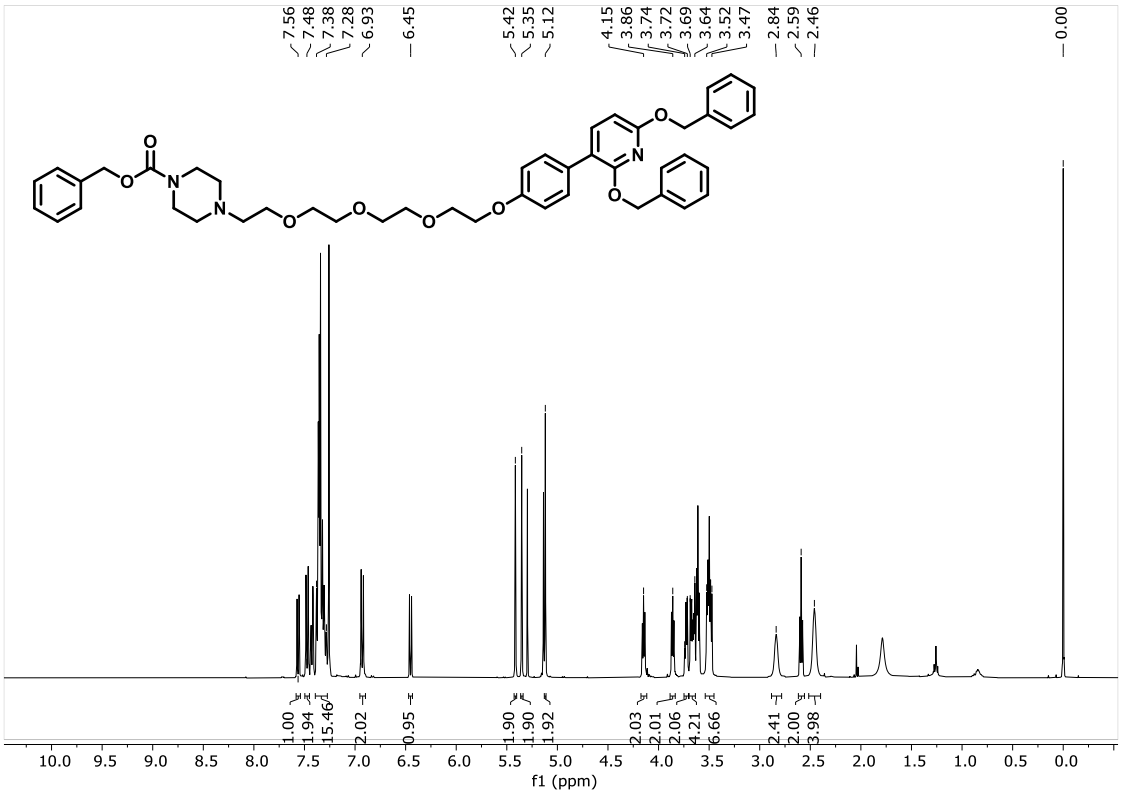

Figure 100: ^{1}H NMR (400 MHz, $CDCl_3$) of **96**.

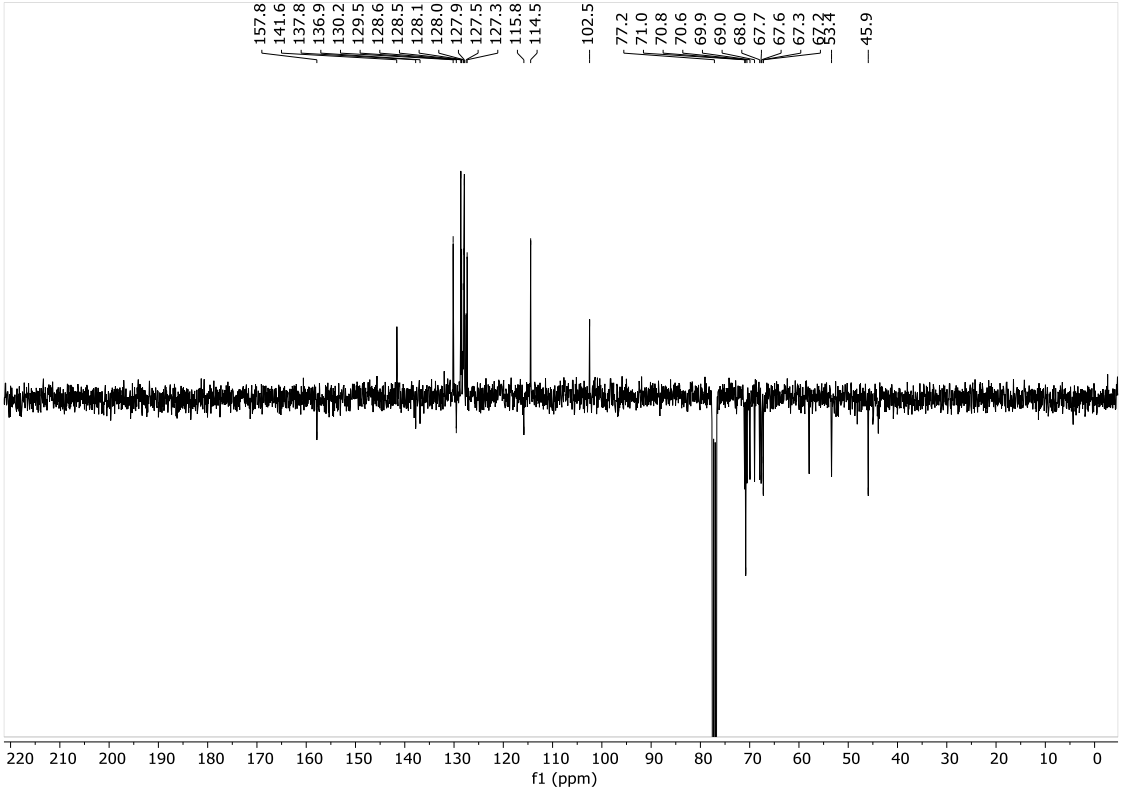

Figure 101: ^{13}C NMR (100 MHz, $CDCl_3$) of **96**.

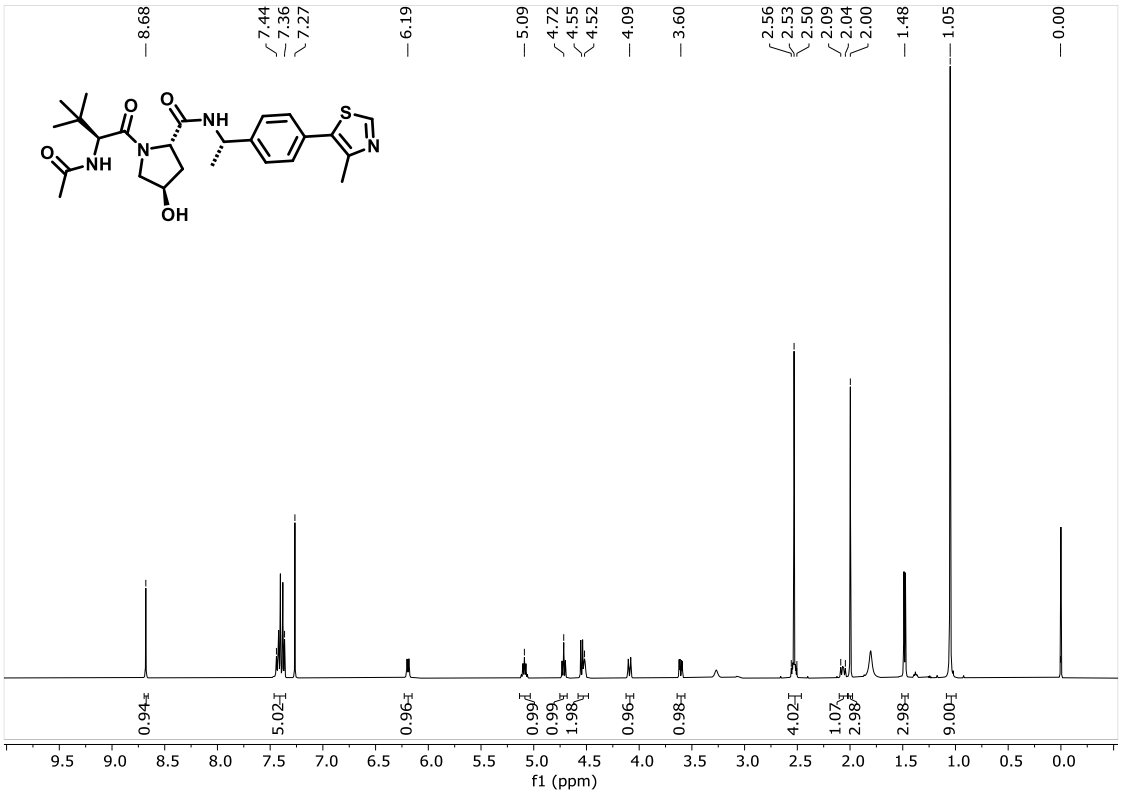

Figure 102: ^{1}H NMR (500 MHz, $CDCl_3$) of **114**.

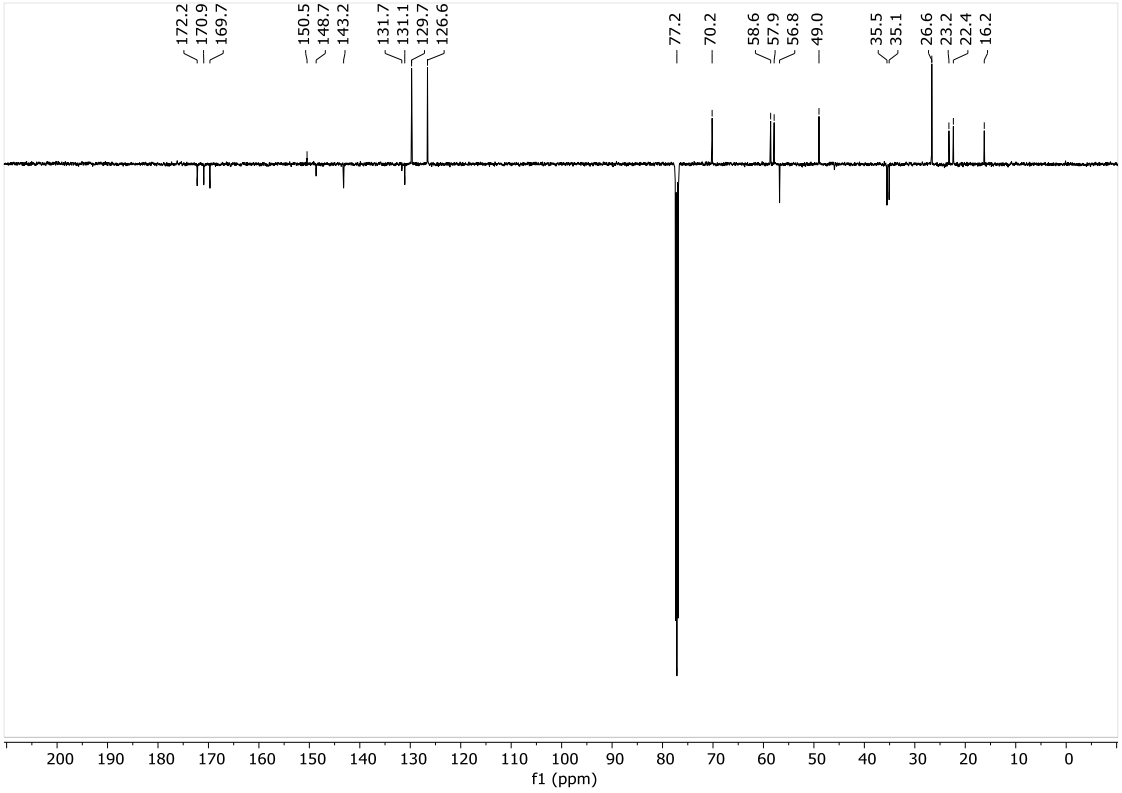

Figure 103: ^{13}C NMR (125 MHz, $CDCl_3$) of **114**.

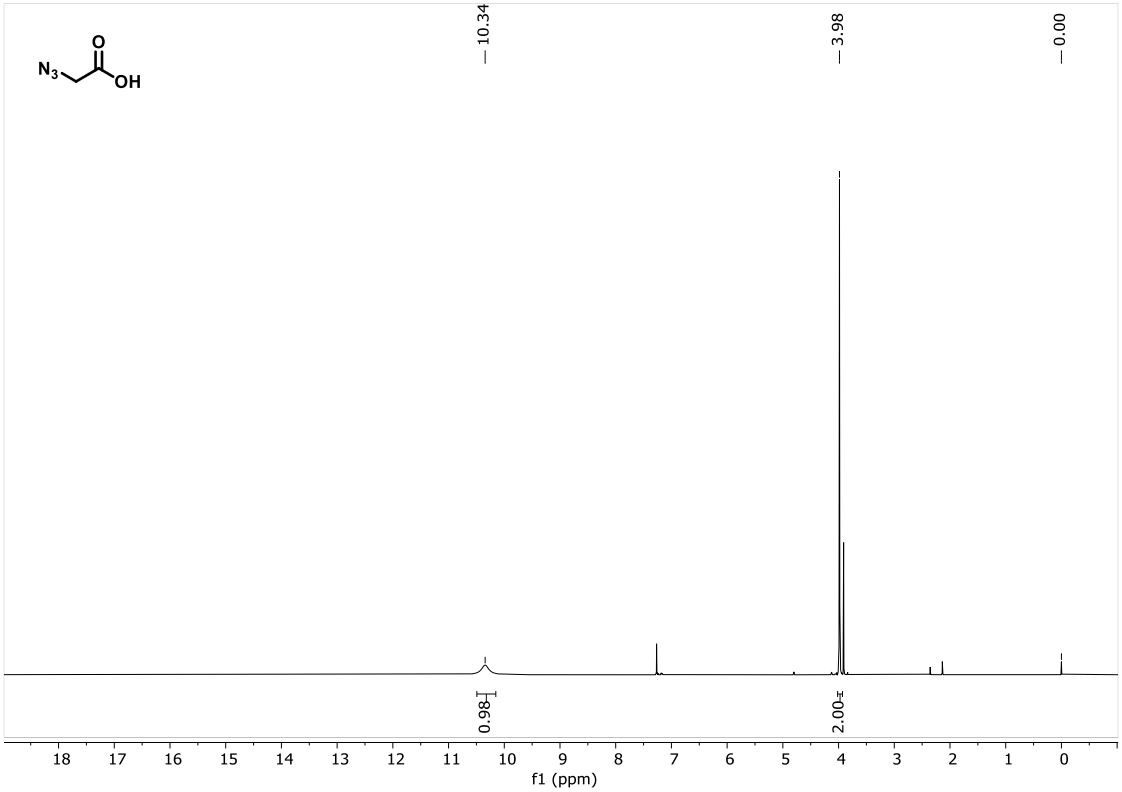

Figure 104: ^{1}H NMR (500 MHz, $CDCl_3$) of **121**.

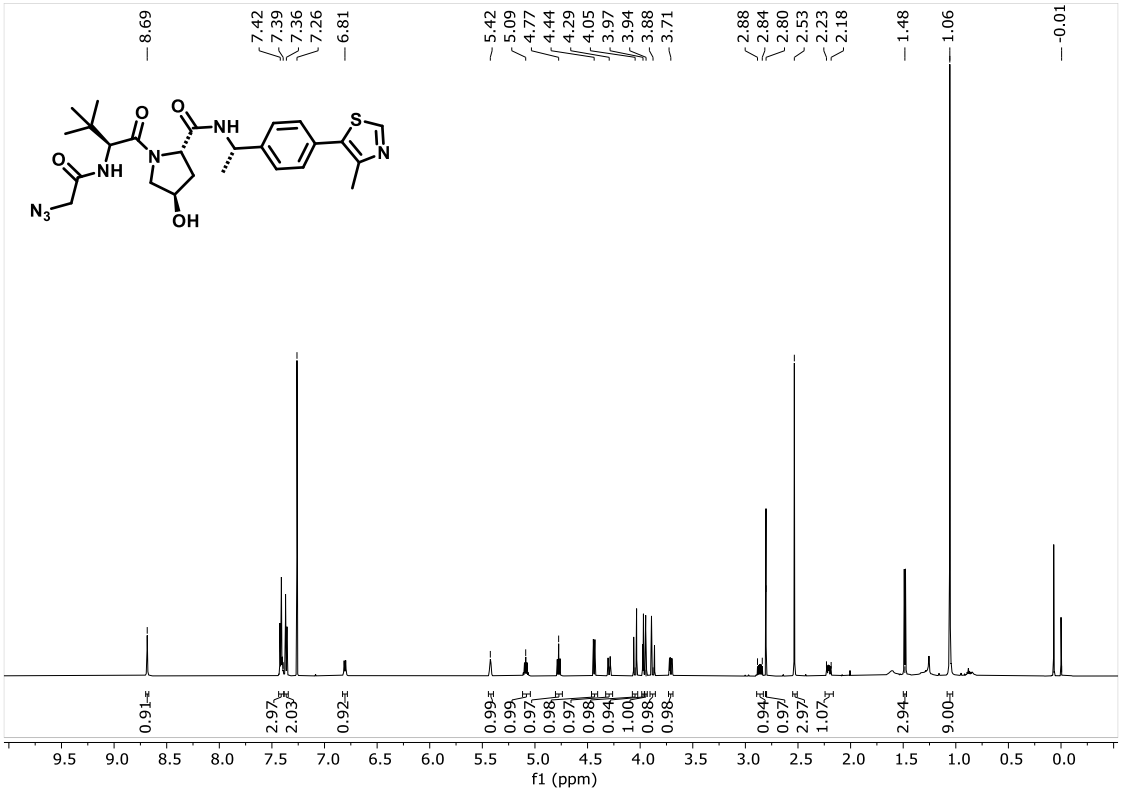

Figure 105: ^{1}H NMR (600 MHz, $CDCl_3$) of **125**.

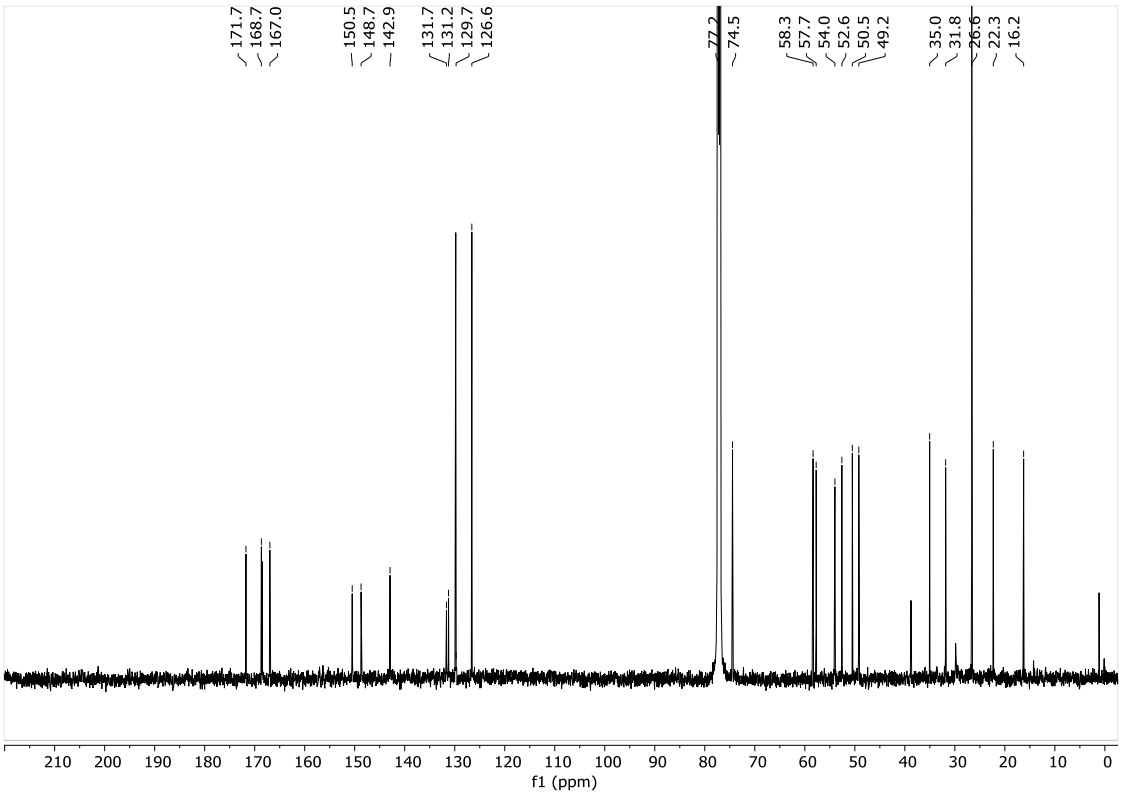

Figure 106: ^{13}C NMR (150 MHz, $CDCl_3$) of **125**.

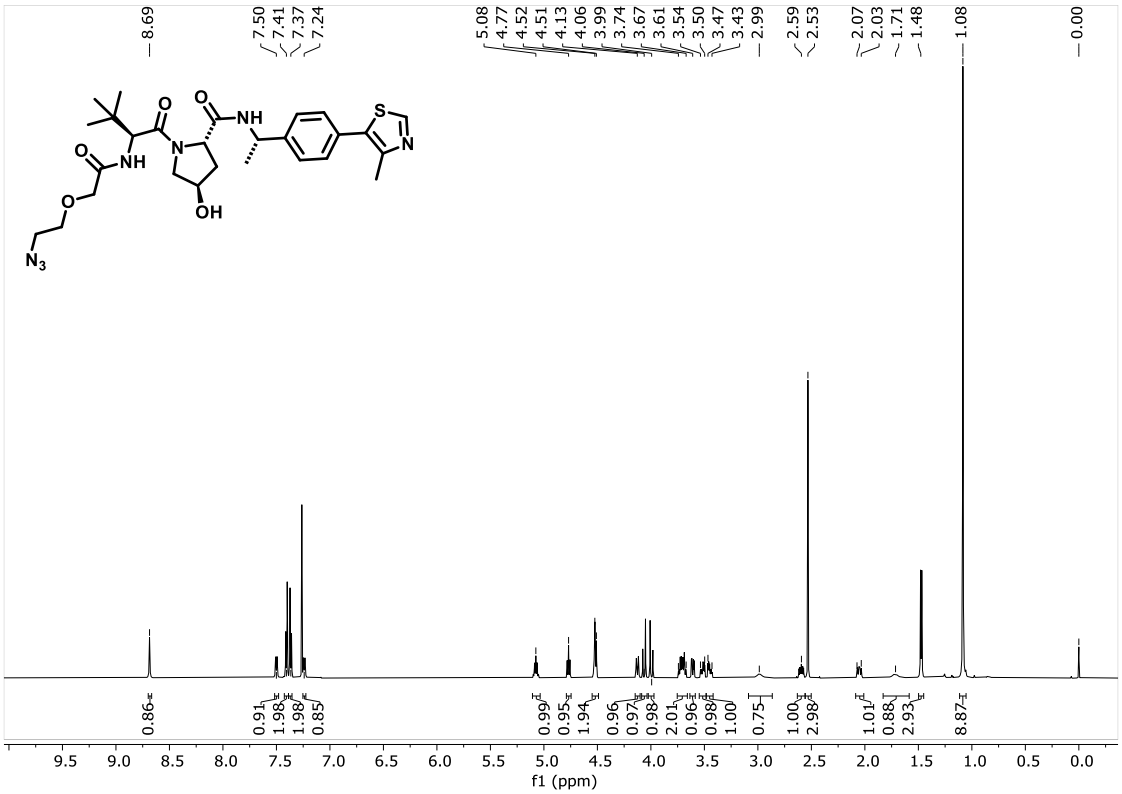

Figure 107: ^{1}H NMR (500 MHz, $CDCl_3$) of **126**.

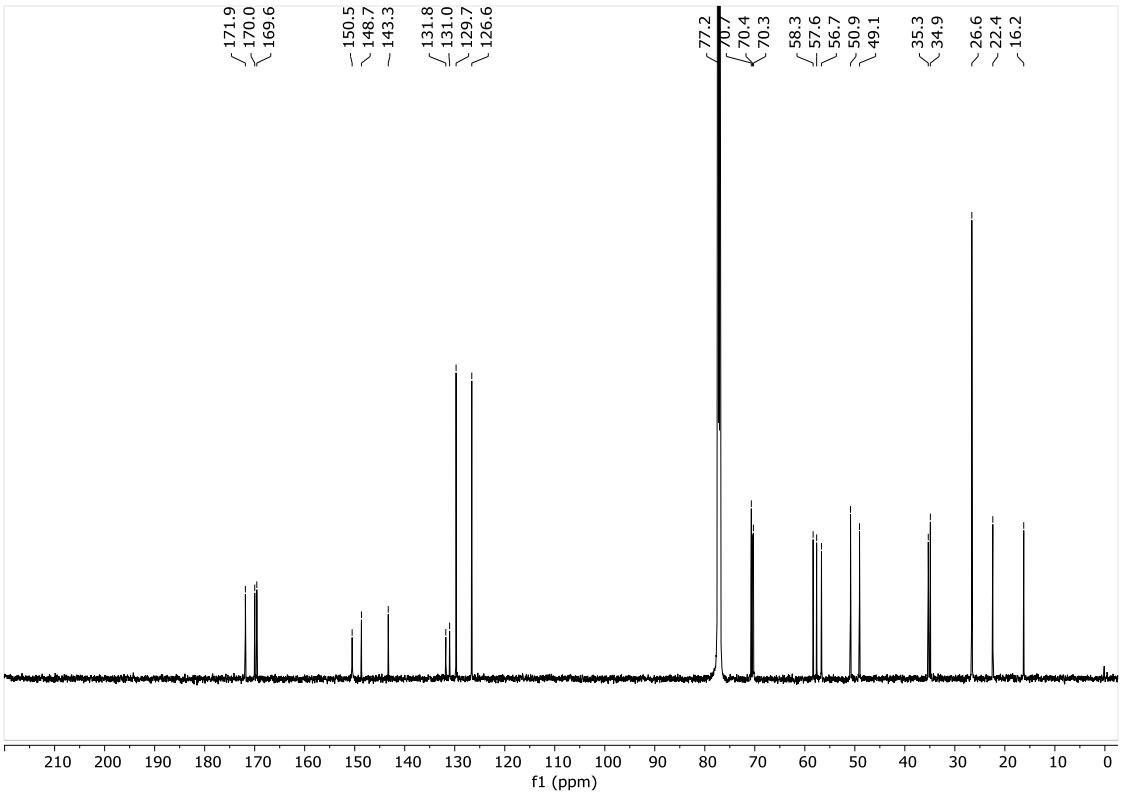

Figure 108: ^{13}C NMR (125 MHz, $CDCl_3$) of **126**.

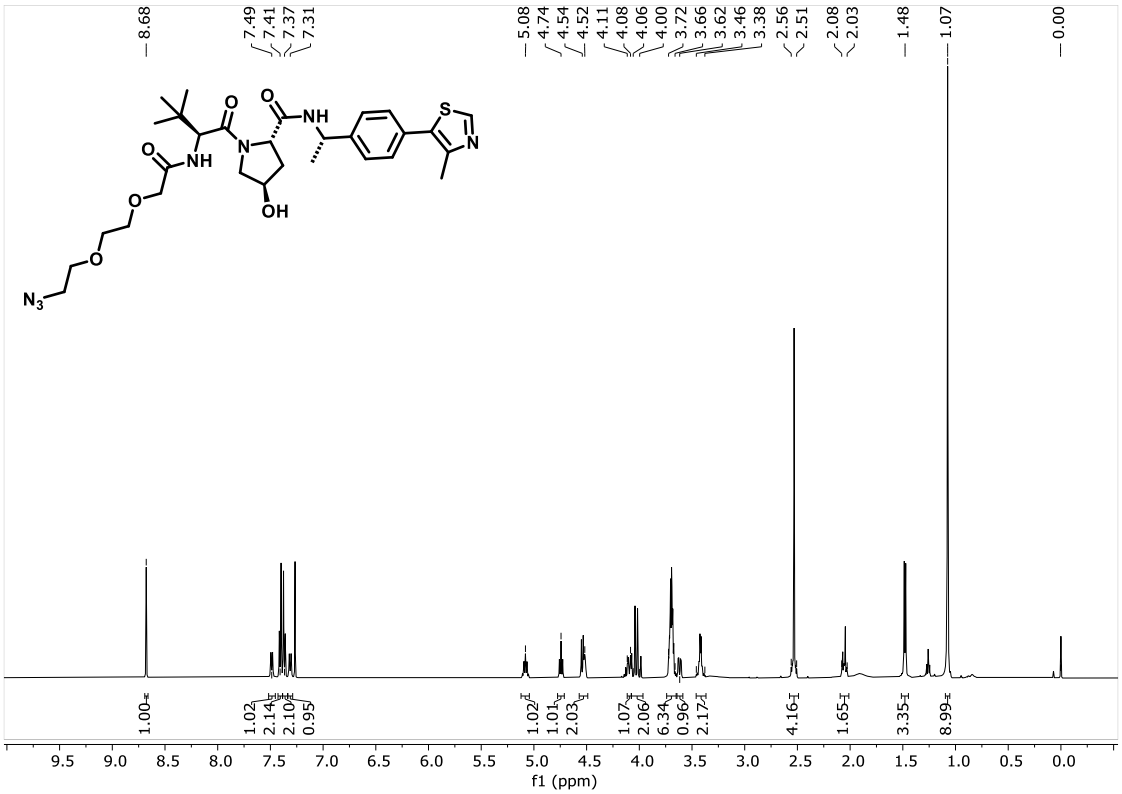

Figure 109: ^{1}H NMR (500 MHz, $CDCl_3$) of **127**.

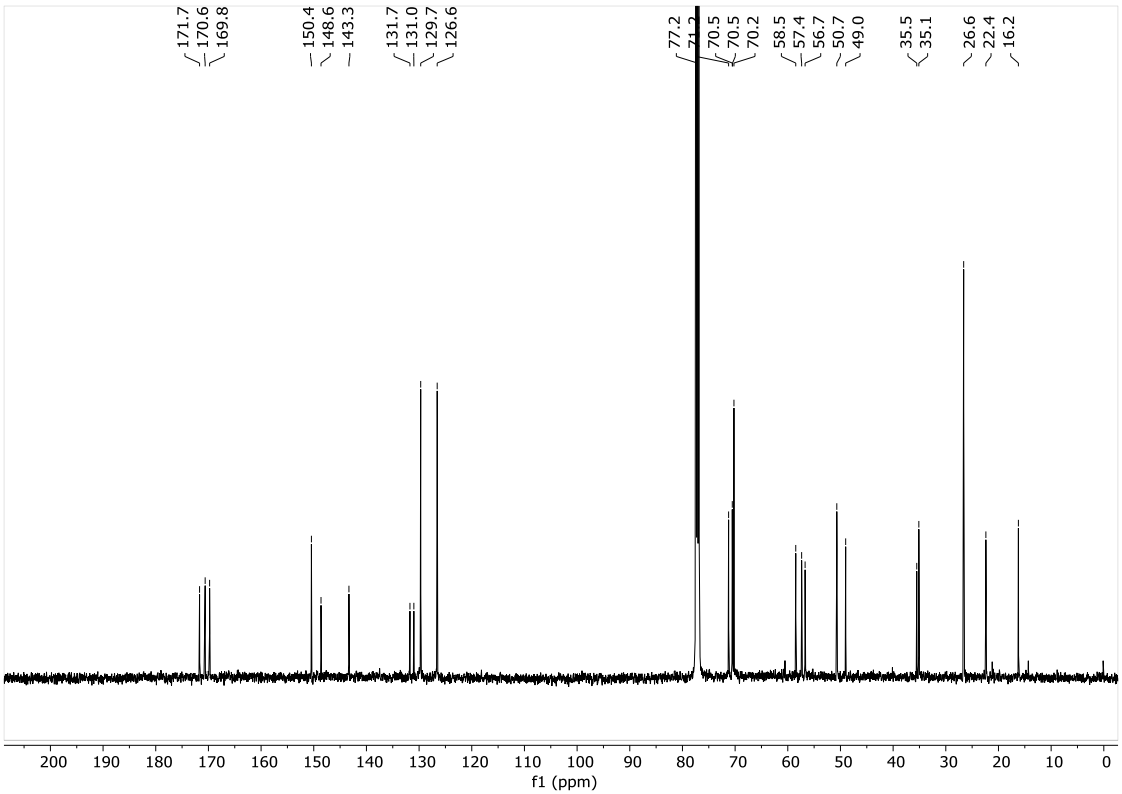

Figure 110: ^{13}C NMR (125 MHz, $CDCl_3$) of **127**.

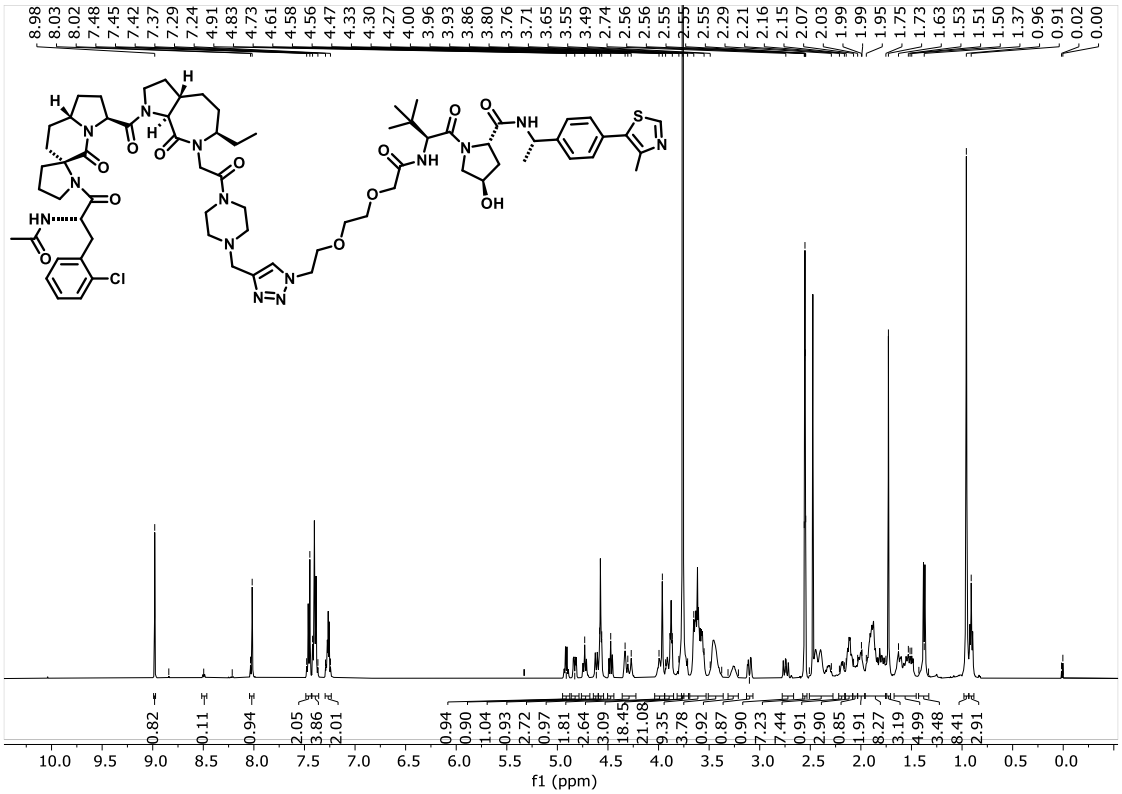

Figure 111: ^{1}H NMR (500 MHz, DMSO-d_6/D_2O 9:1) of **118**.

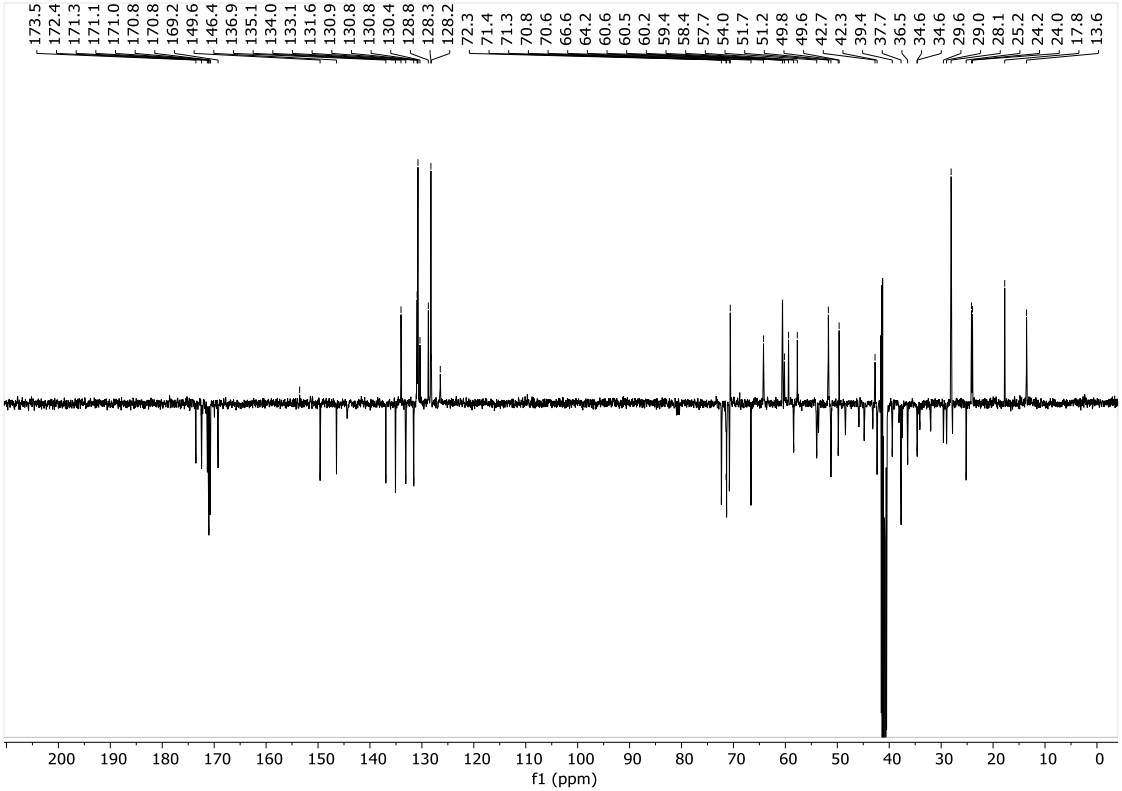

Figure 112: ^{13}C NMR (125 MHz, DMSO-d_6/D_2O 9:1) of **118**.

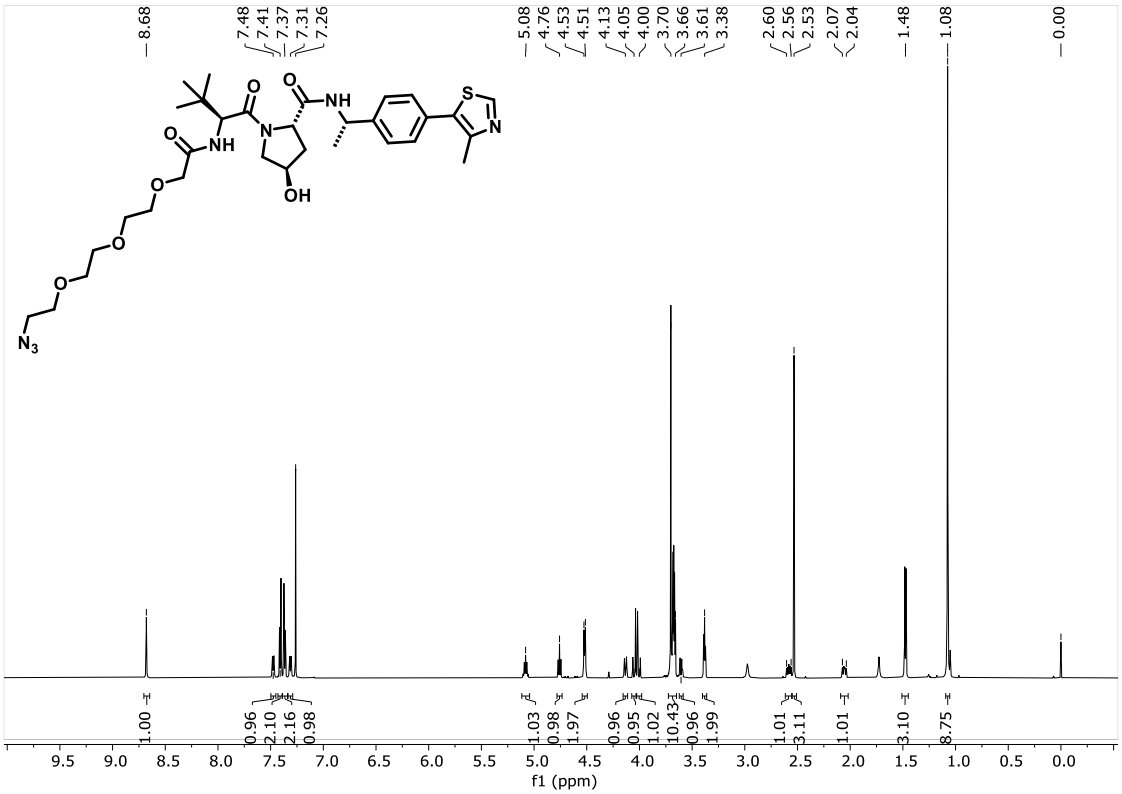

Figure 113: ^{1}H NMR (600 MHz, $CDCl_3$) of **128**.

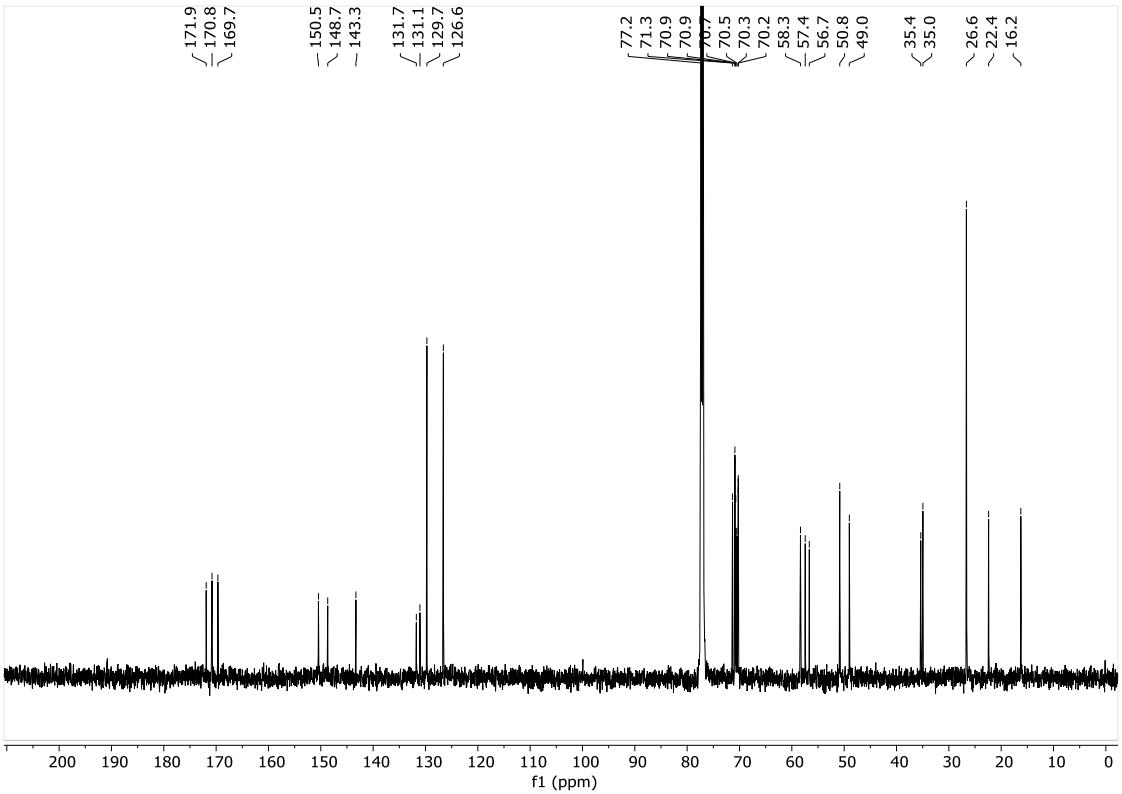

Figure 114: ^{13}C NMR (150 MHz, $CDCl_3$) of **128**.

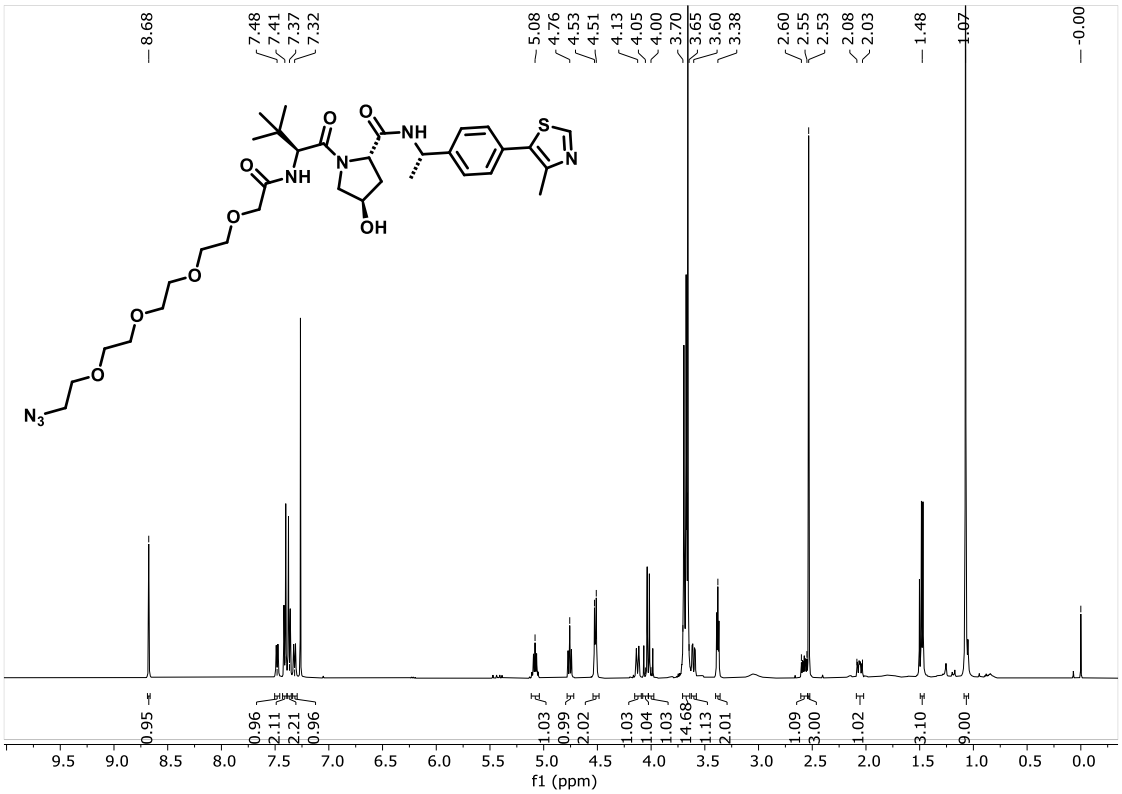

Figure 115: ^{1}H NMR (500 MHz, $CDCl_3$) of **129**.

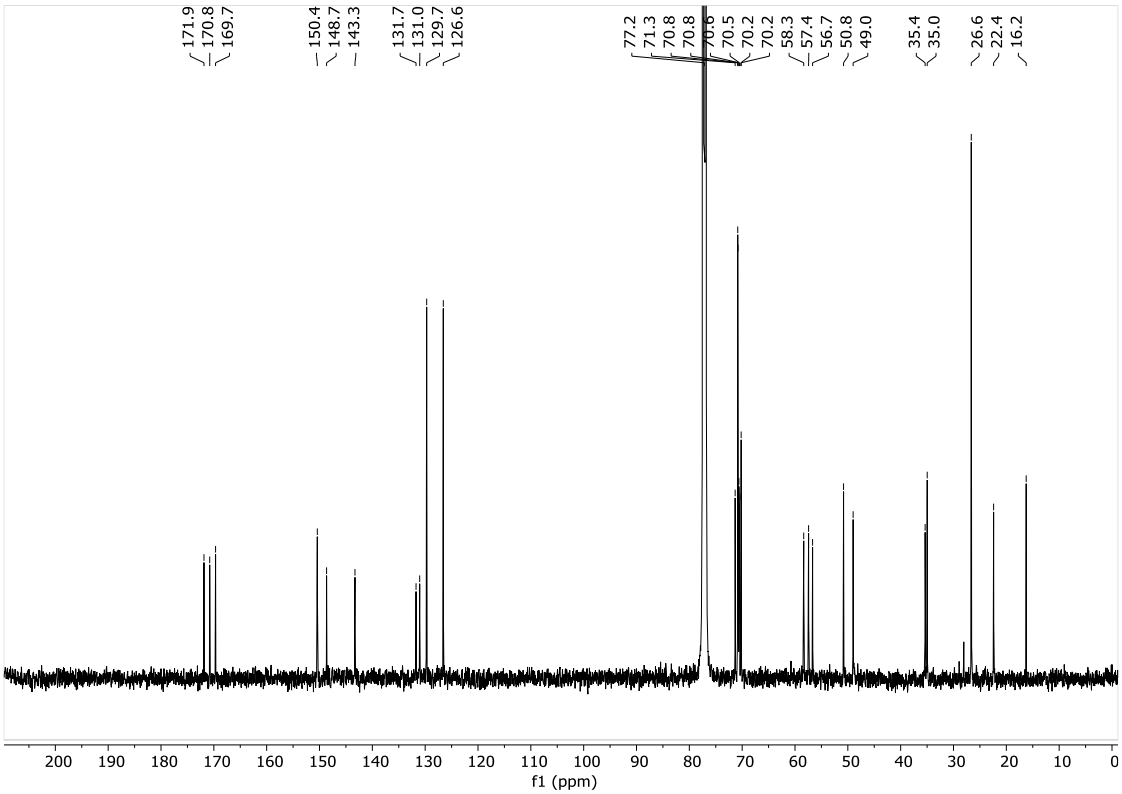

Figure 116: ^{13}C NMR (125 MHz, $CDCl_3$) of **129**.

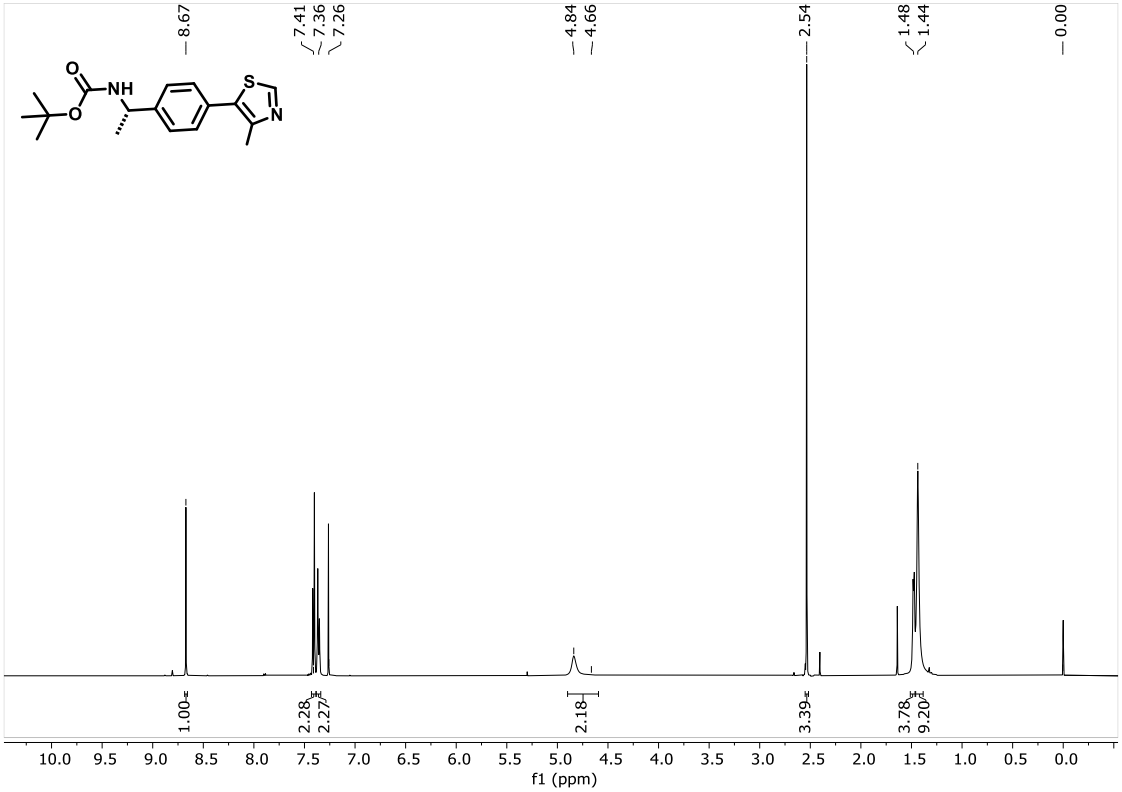

Figure 117: ^{1}H NMR (500 MHz, $CDCl_3$) of **139**.

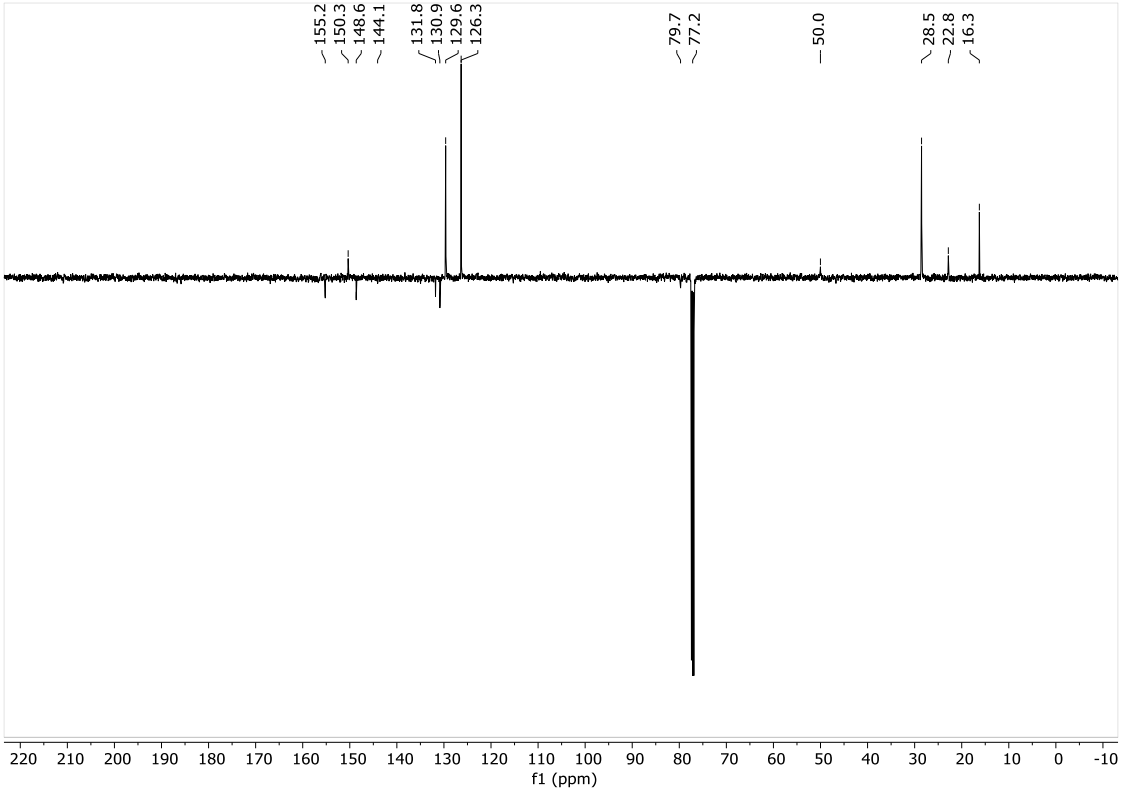

Figure 118: ^{13}C NMR (125 MHz, $CDCl_3$) of **139**.

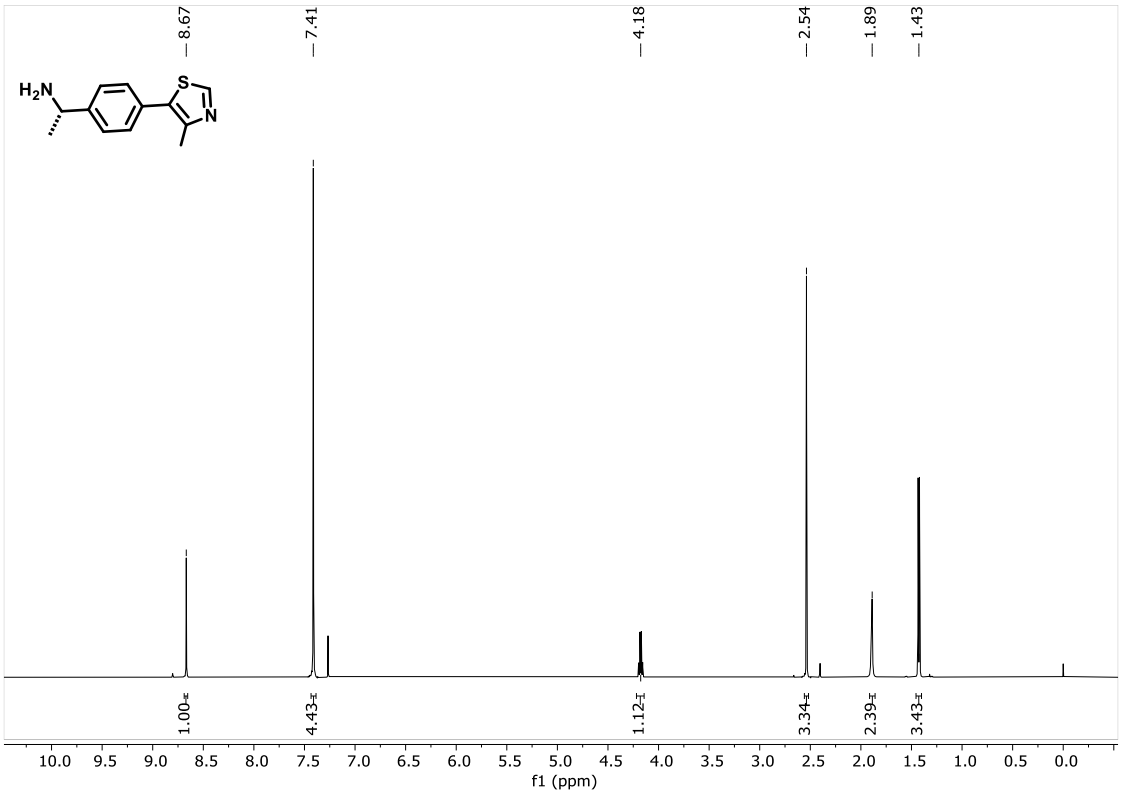

Figure 119: ^{1}H NMR (500 MHz, $CDCl_3$) of **136**.

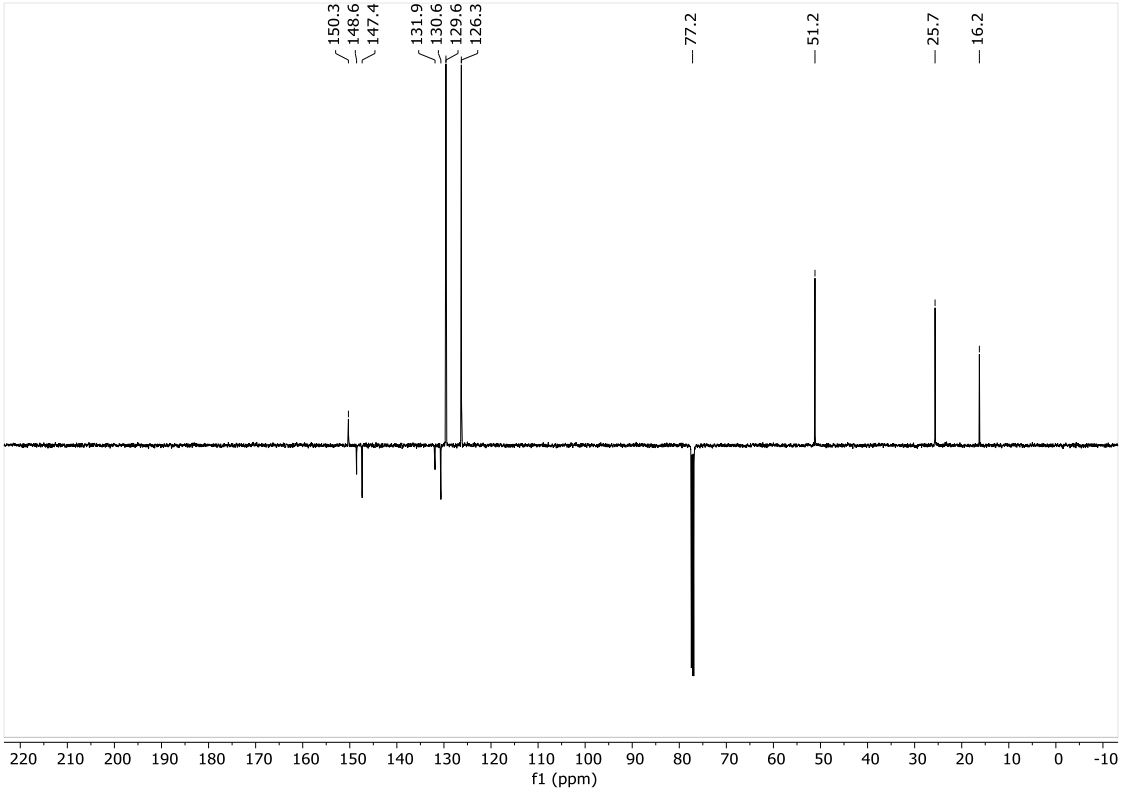

Figure 120: ^{13}C NMR (125 MHz, $CDCl_3$) of **136**.

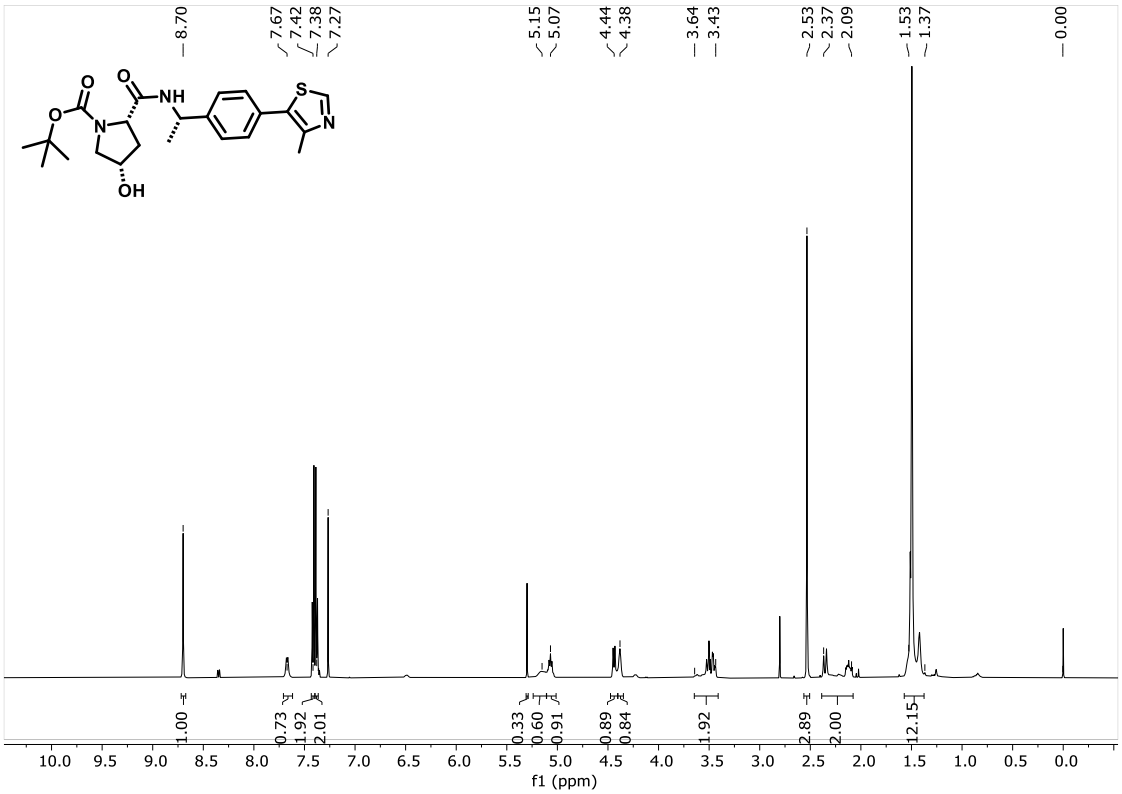

Figure 121: ^{1}H NMR (500 MHz, $CDCl_3$) of **146**.

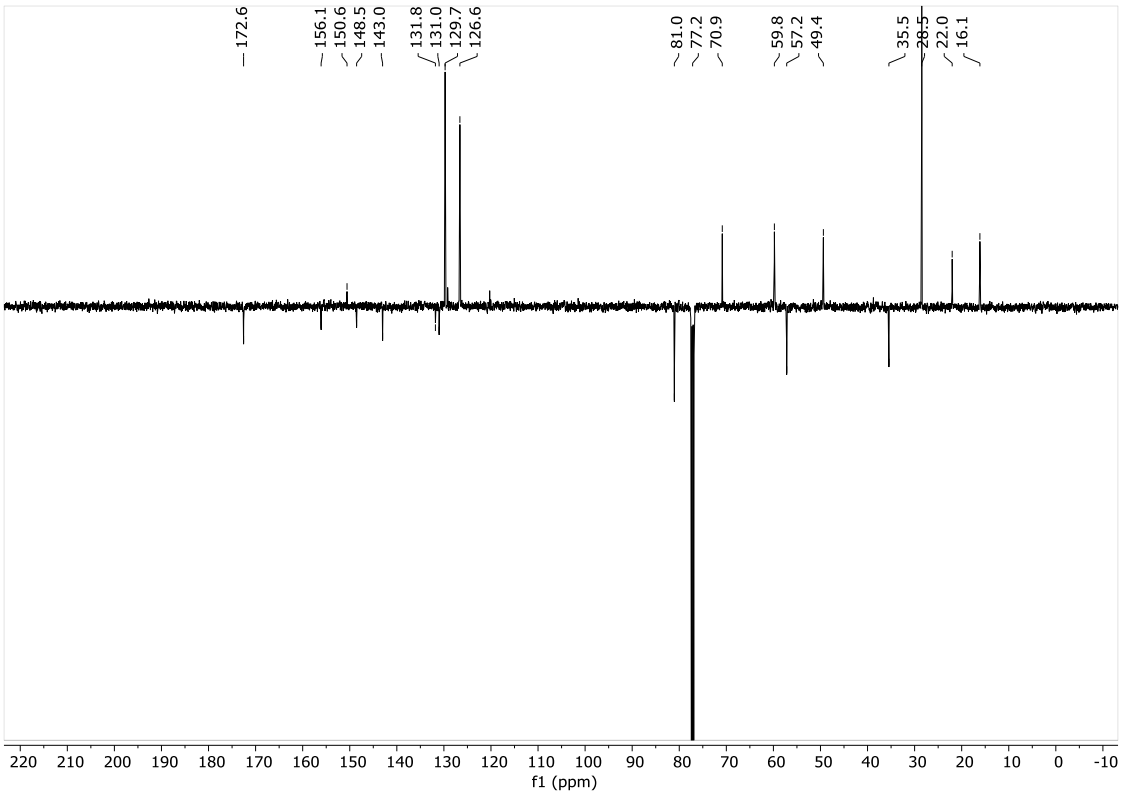

Figure 122: ^{13}C NMR (125 MHz, $CDCl_3$) of **146**.

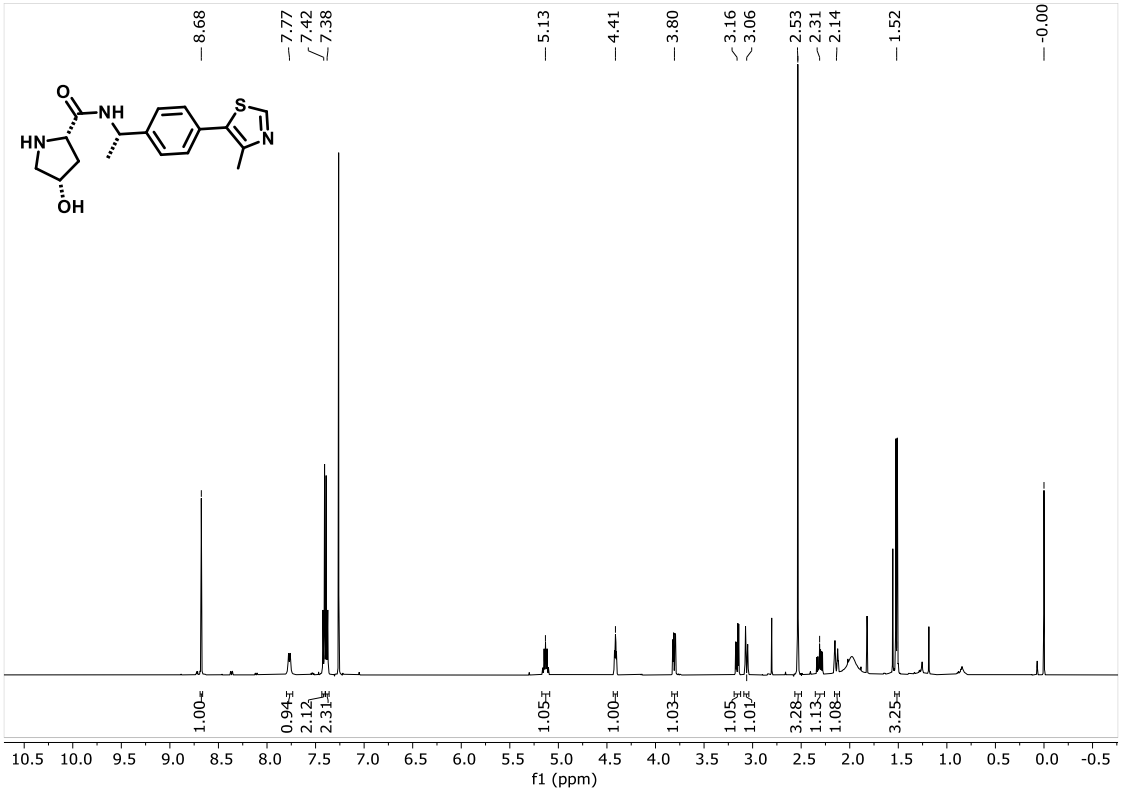

Figure 123: ^{1}H NMR (500 MHz, $CDCl_3$) of **147**.

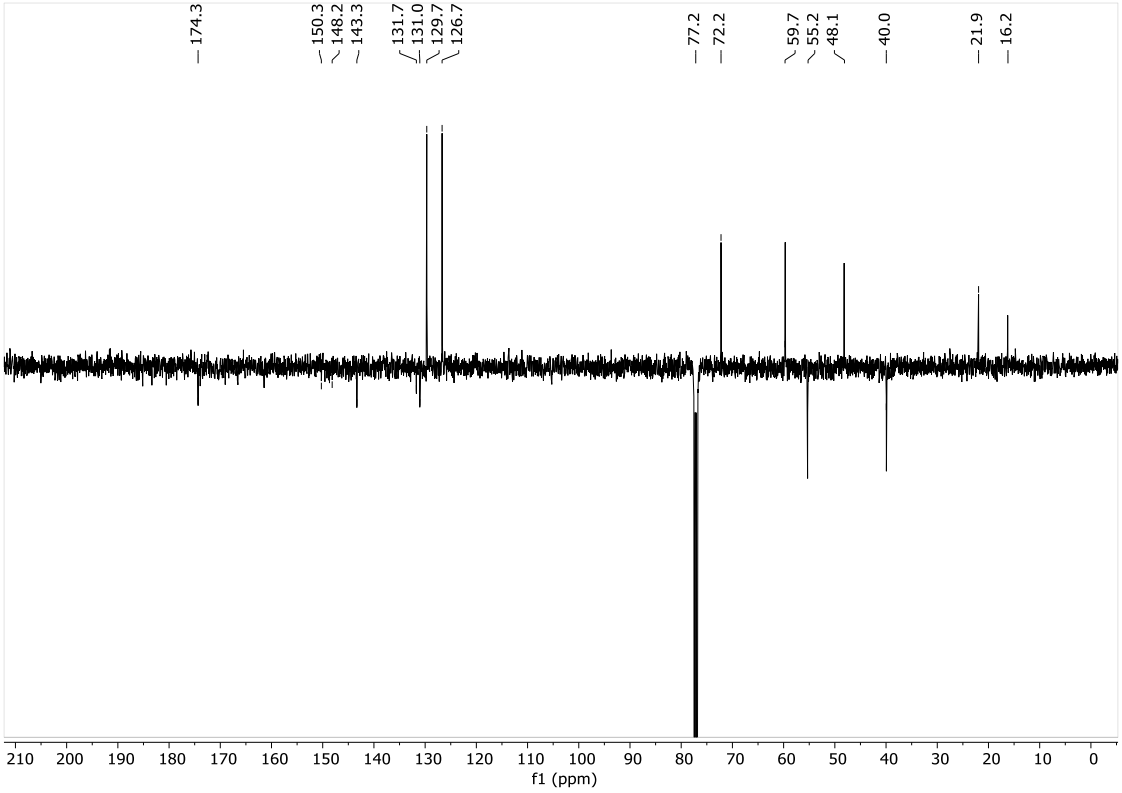

Figure 124: ^{13}C NMR (125 MHz, $CDCl_3$) of **147**.

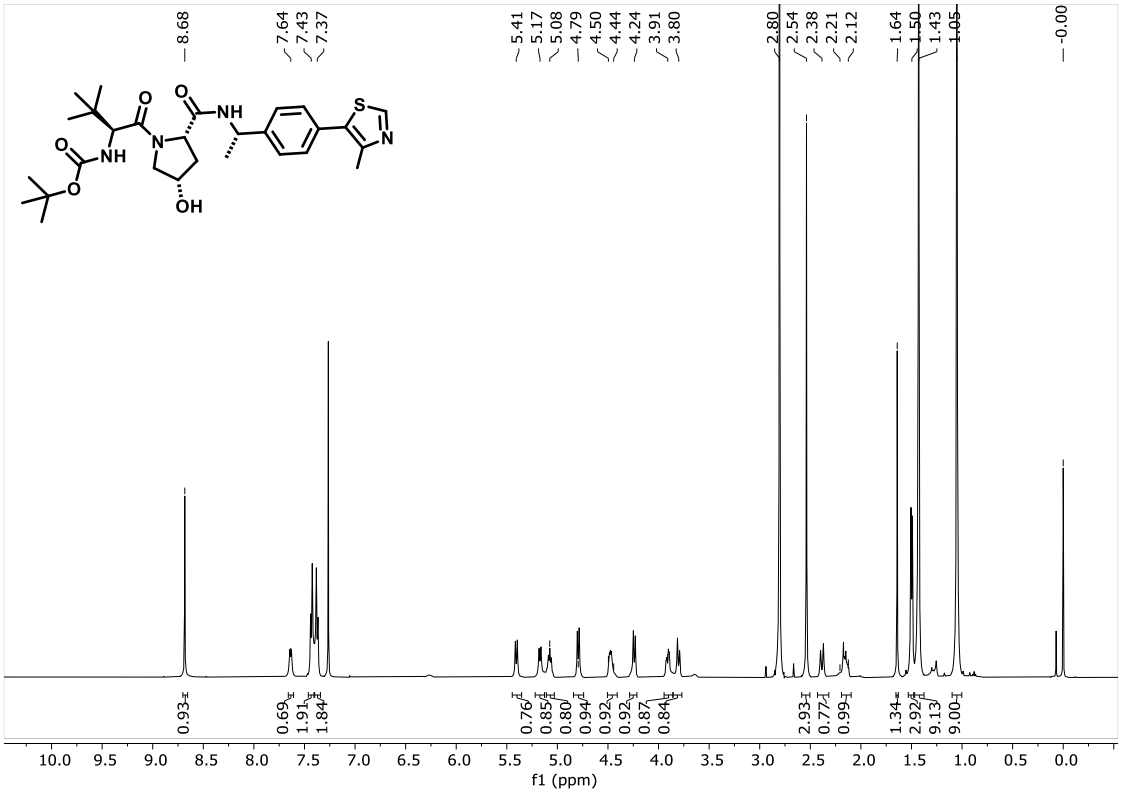

Figure 125: ^{1}H NMR (500 MHz, $CDCl_3$) of **135**.

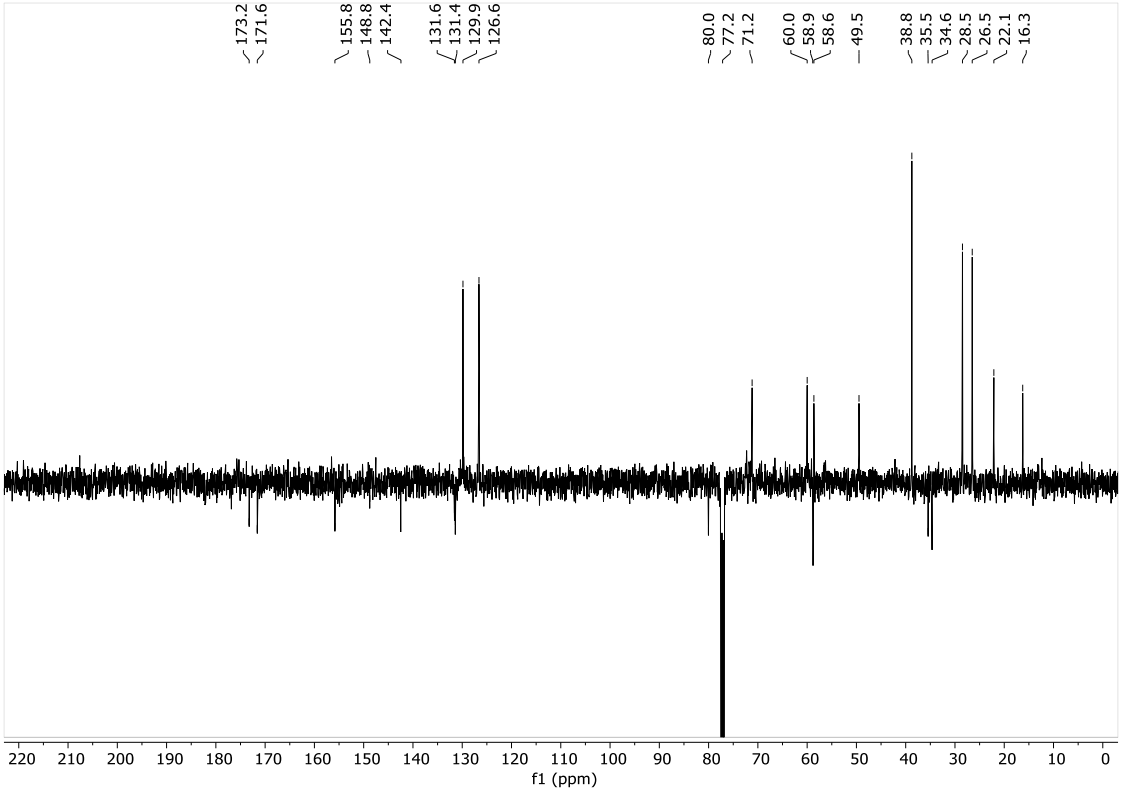

Figure 126: ^{13}C NMR (125 MHz, $CDCl_3$) of **135**.

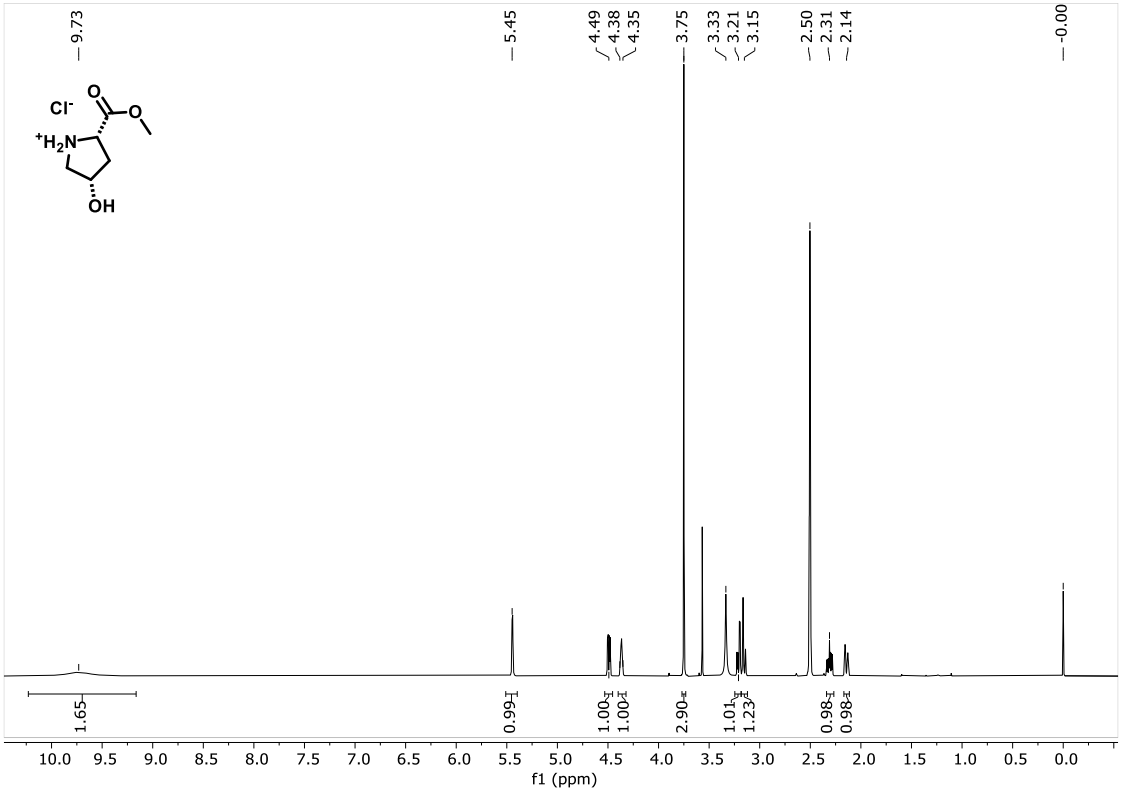

Figure 127: ^{1}H NMR (500 MHz, DMSO-d_6) of **141**.

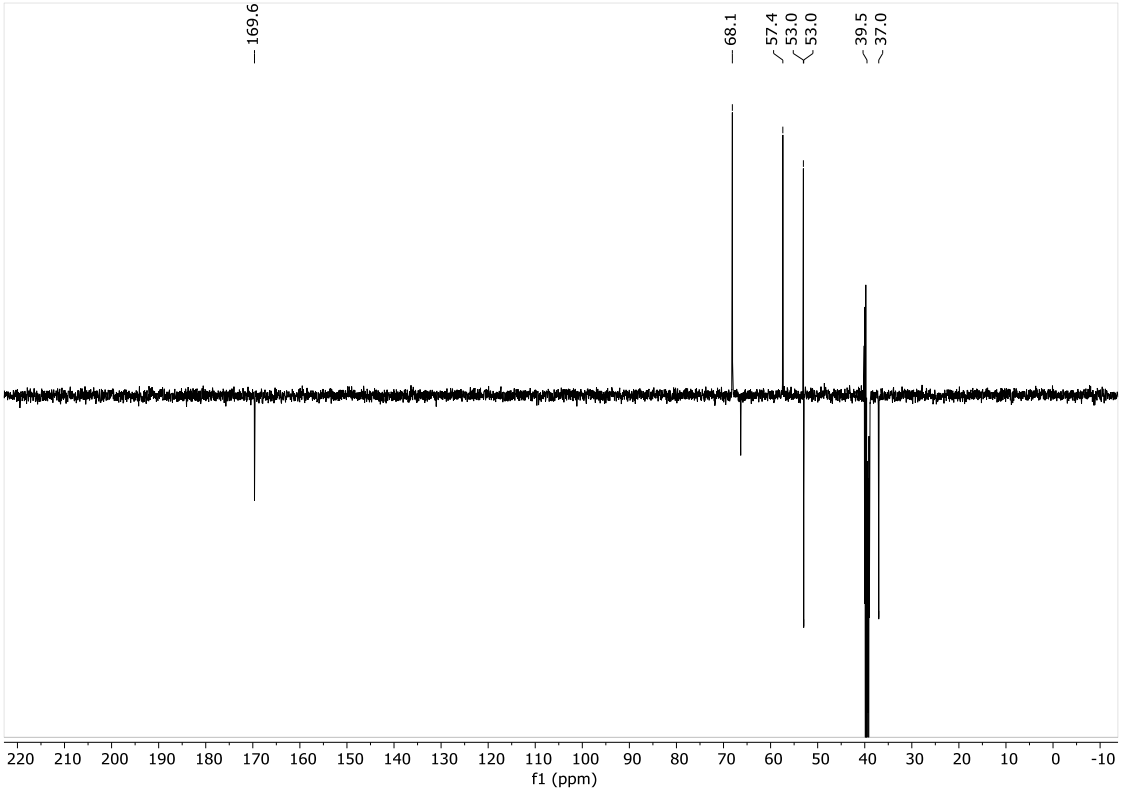

Figure 128: ^{13}C NMR (125 MHz, DMSO-d_6) of **141**.

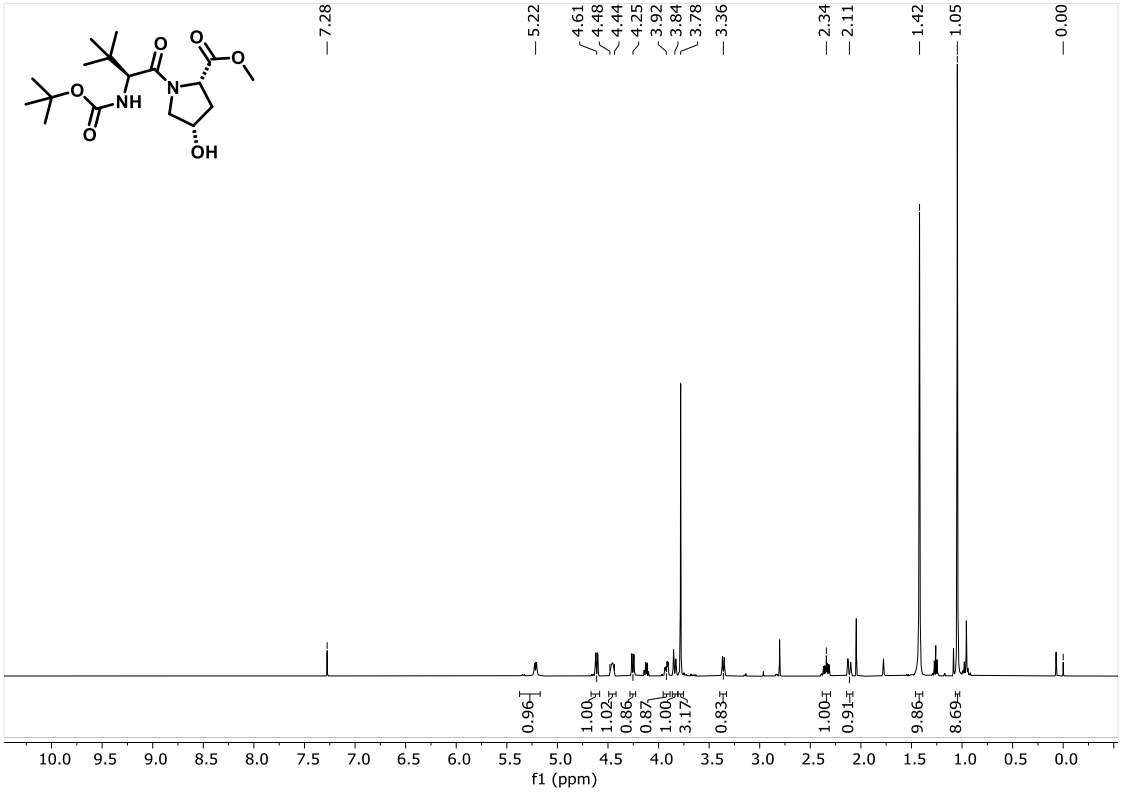

Figure 129: ^{1}H NMR (500 MHz, $CDCl_3$) of **143**.

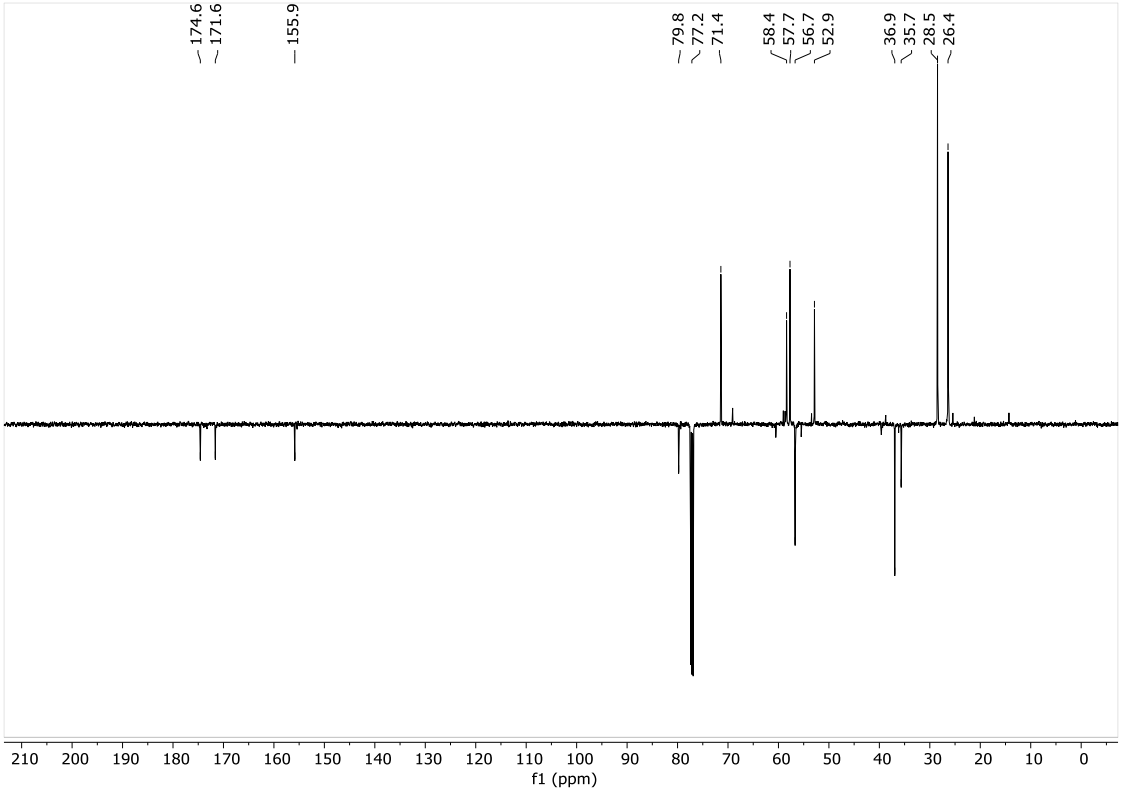

Figure 130: ^{13}C NMR (125 MHz, $CDCl_3$) of **143**.

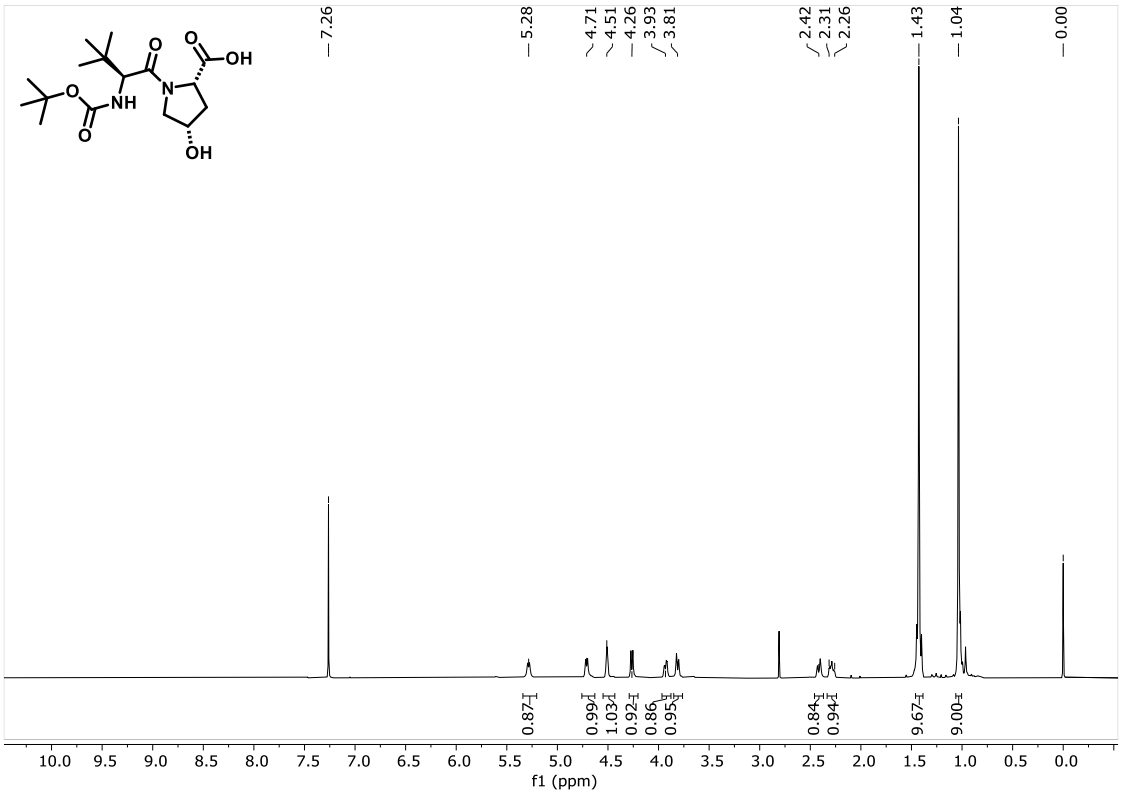

Figure 131: ^{1}H NMR (500 MHz, $CDCl_3$) of **144**.

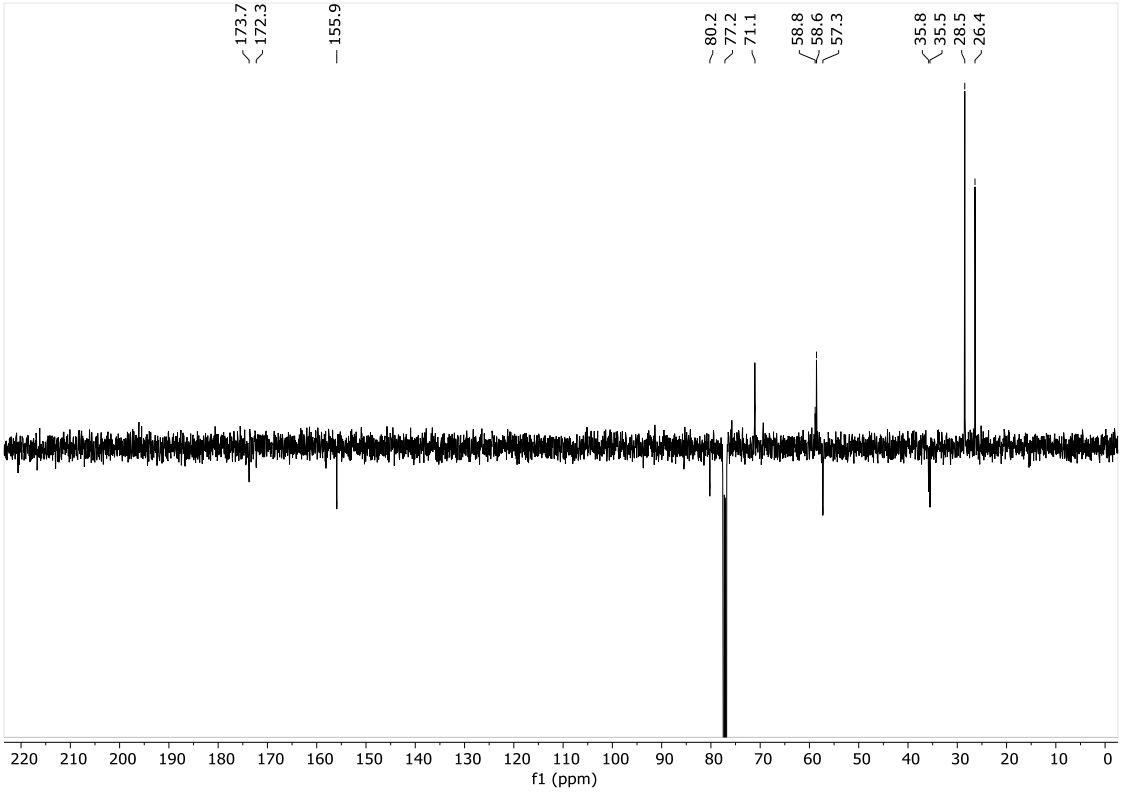

Figure 132: ^{13}C NMR (125 MHz, $CDCl_3$) of **144**.

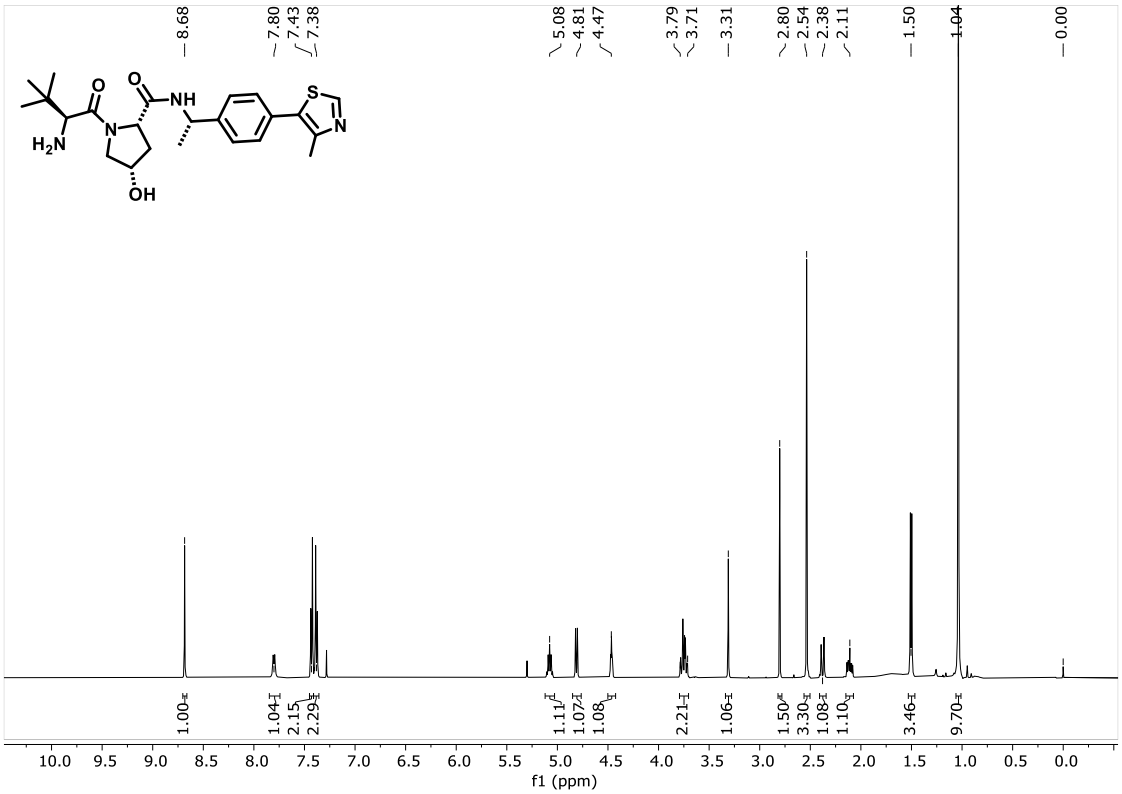

Figure 133: ^{1}H NMR (500 MHz, $CDCl_3$) of ***epi*-113**.

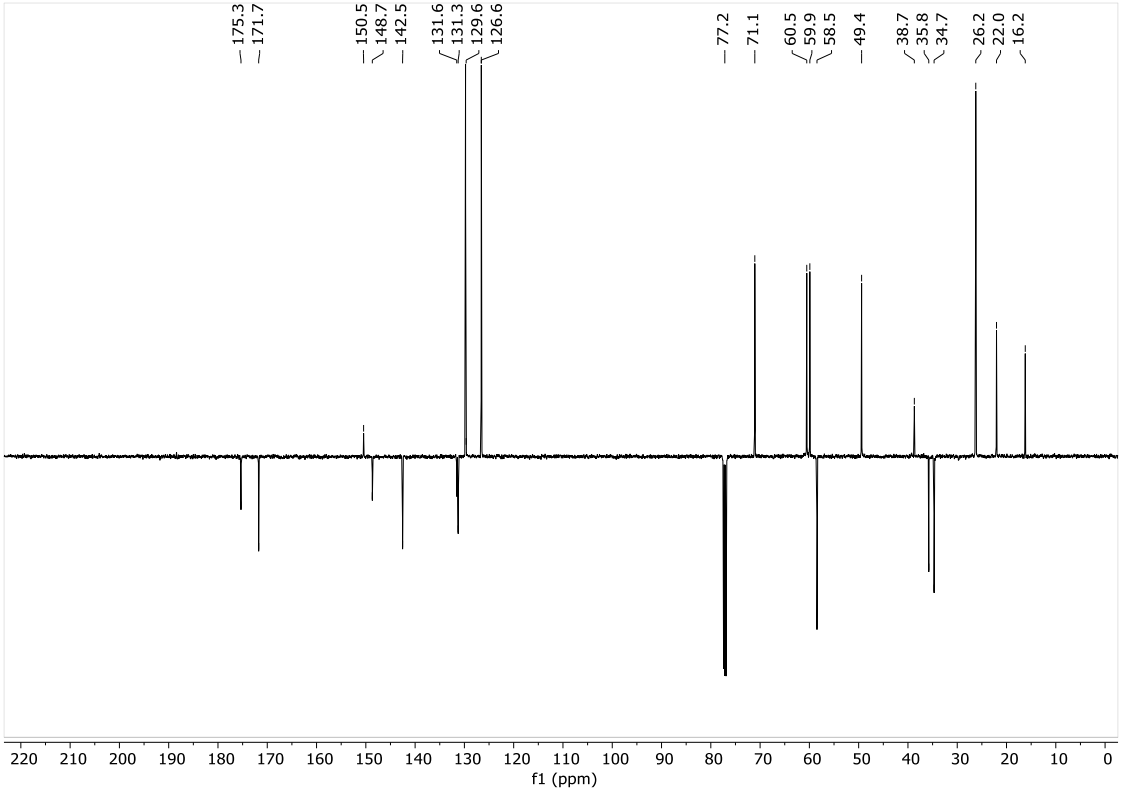

Figure 134: ^{13}C NMR (125 MHz, $CDCl_3$) of ***epi*-113**.

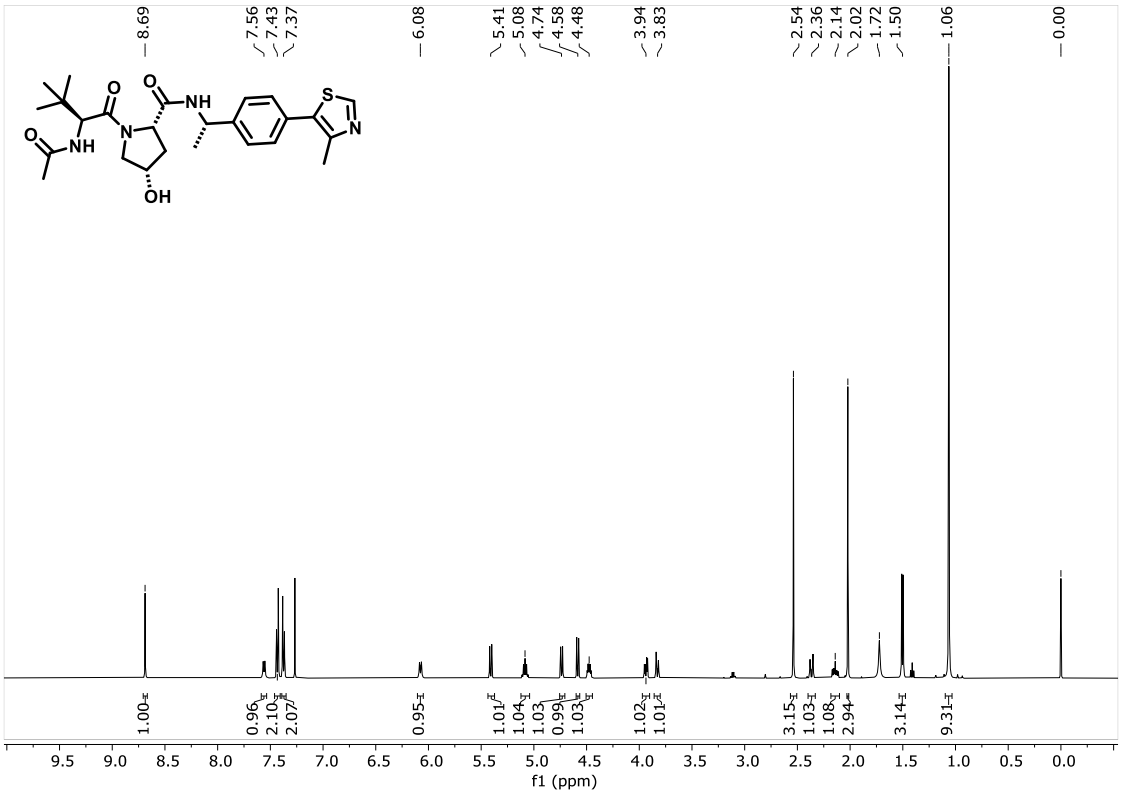

Figure 135: ^{1}H NMR (500 MHz, $CDCl_3$) of ***epi*-114**.

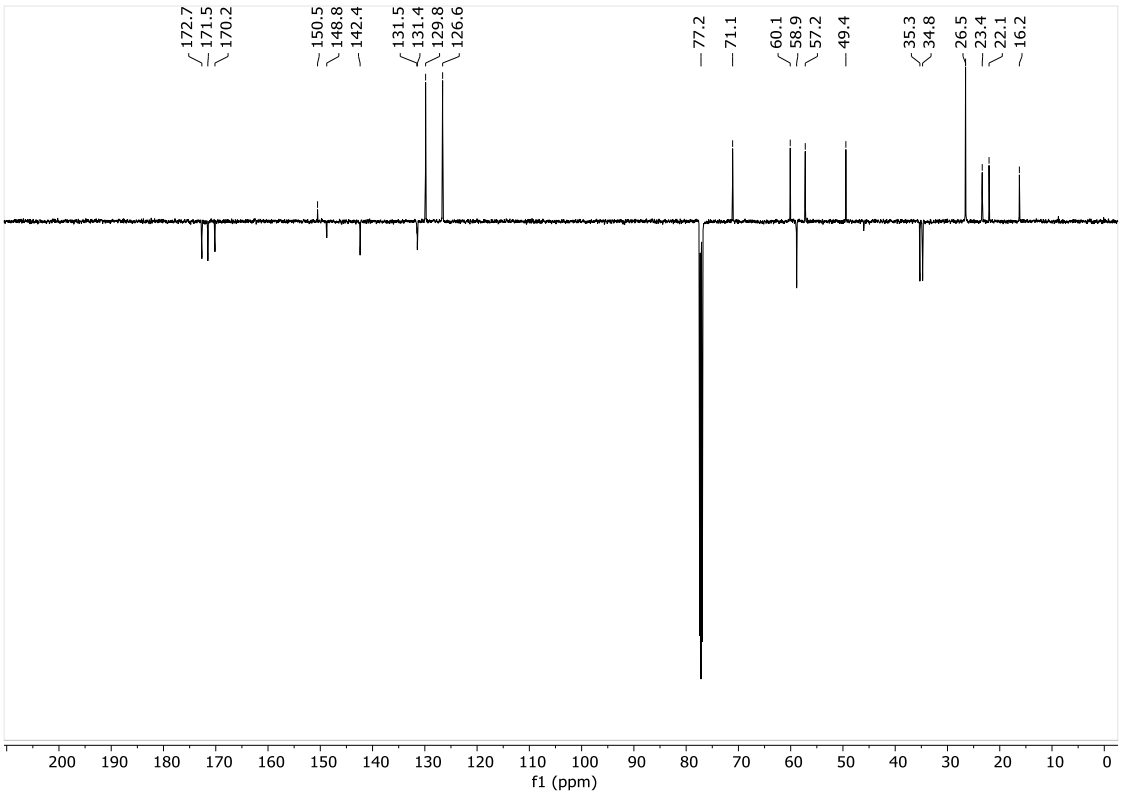

Figure 136: ^{13}C NMR (125 MHz, $CDCl_3$) of ***epi*-114**.

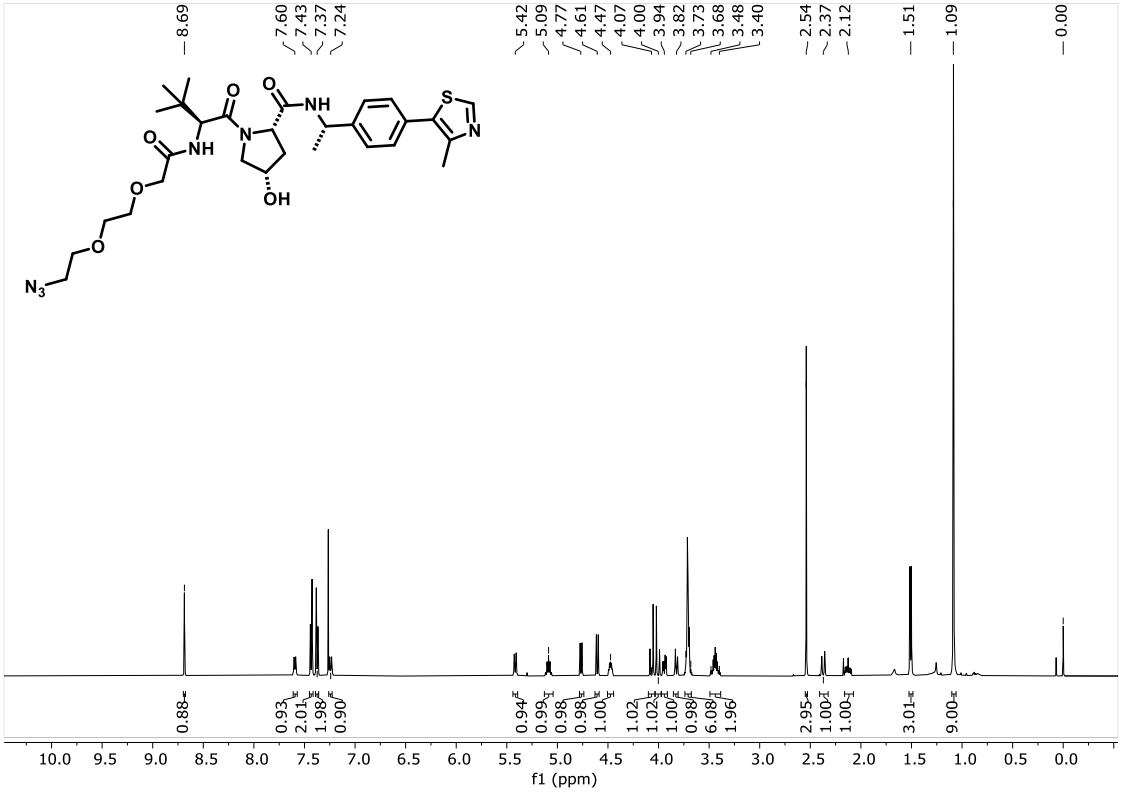

Figure 137: ^{1}H NMR (500 MHz, $CDCl_3$) of ***epi*-127**.

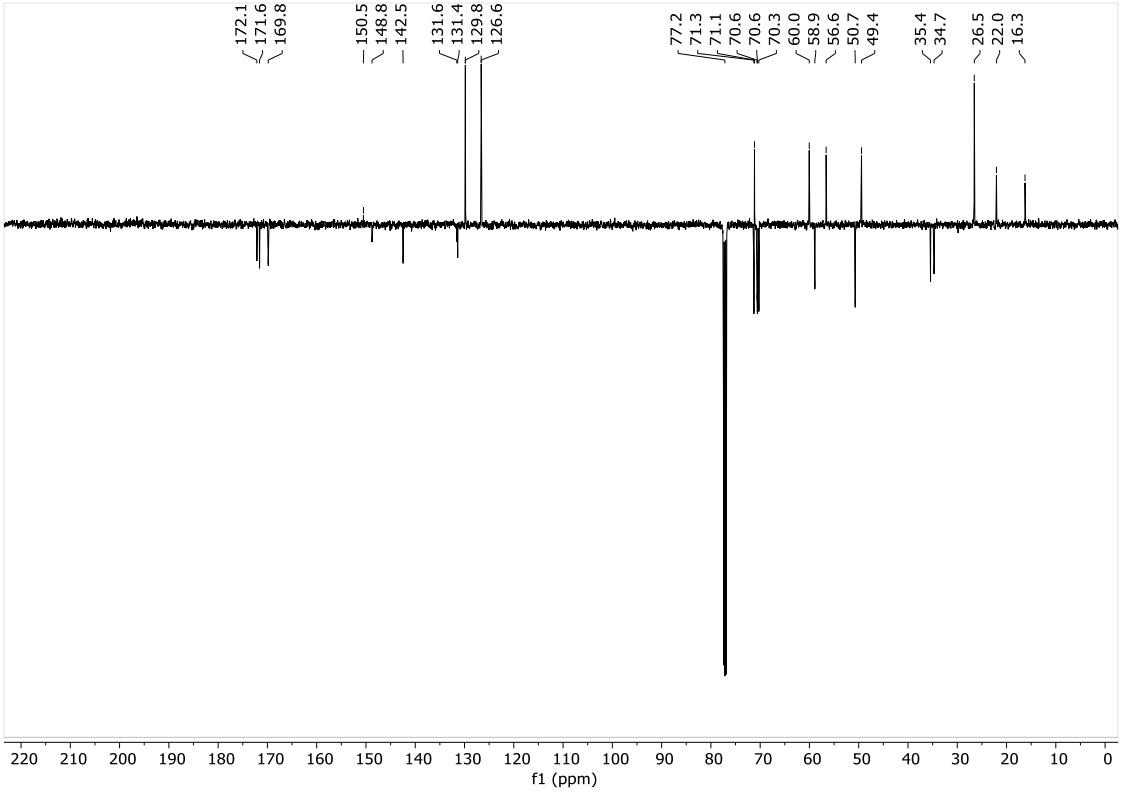

Figure 138: ^{13}C NMR (125 MHz, $CDCl_3$) of ***epi*-127**.

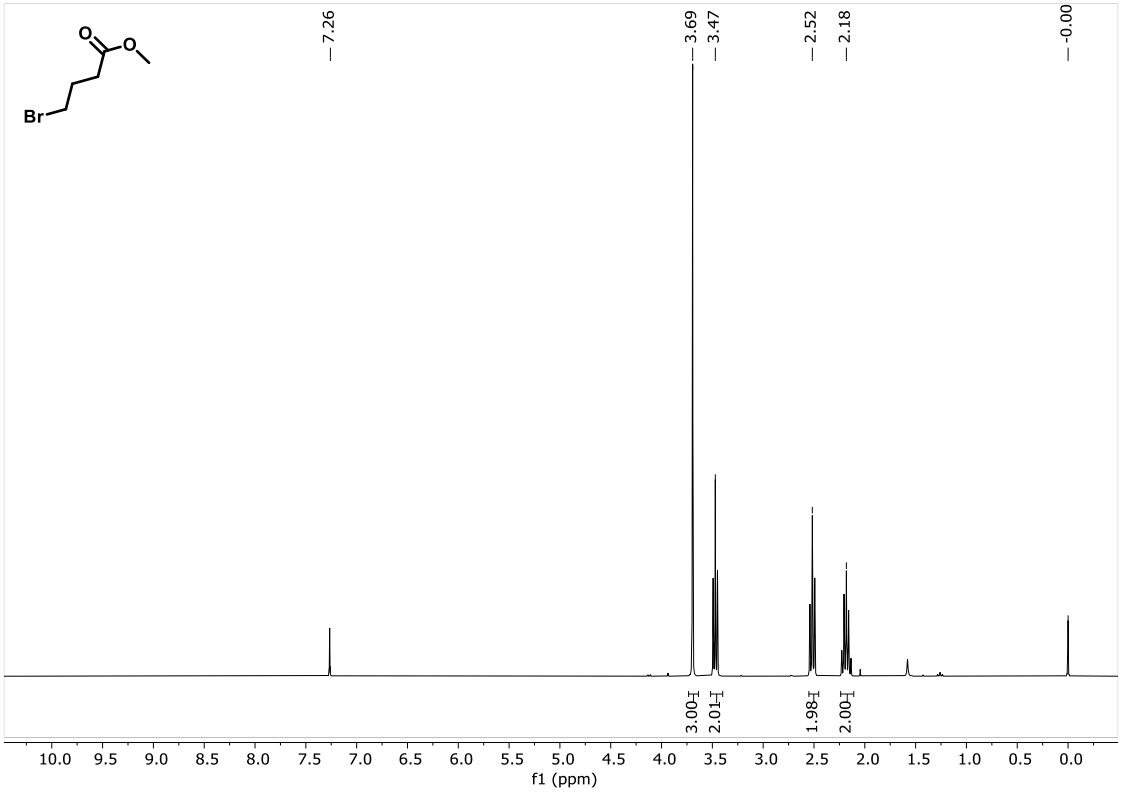

Figure 139: ^{1}H NMR (300 MHz, $CDCl_3$) of **160**.

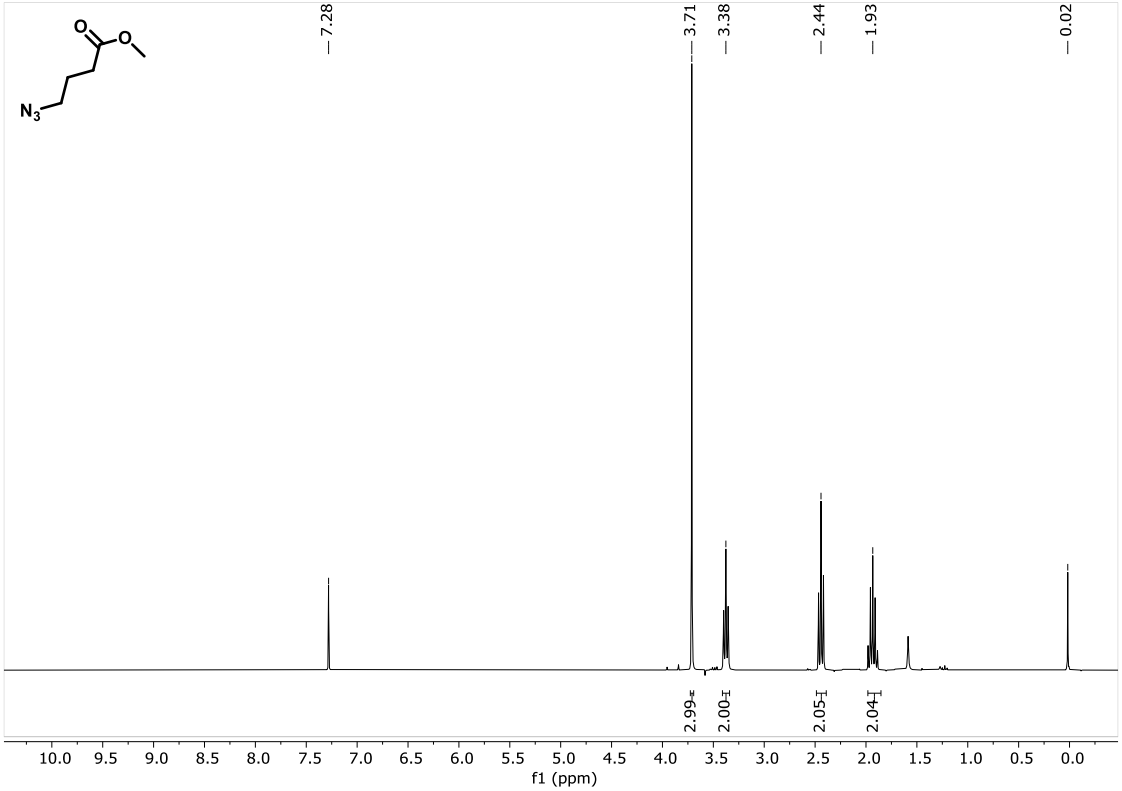

Figure 140: ^{1}H NMR (300 MHz, $CDCl_3$) of **164**.

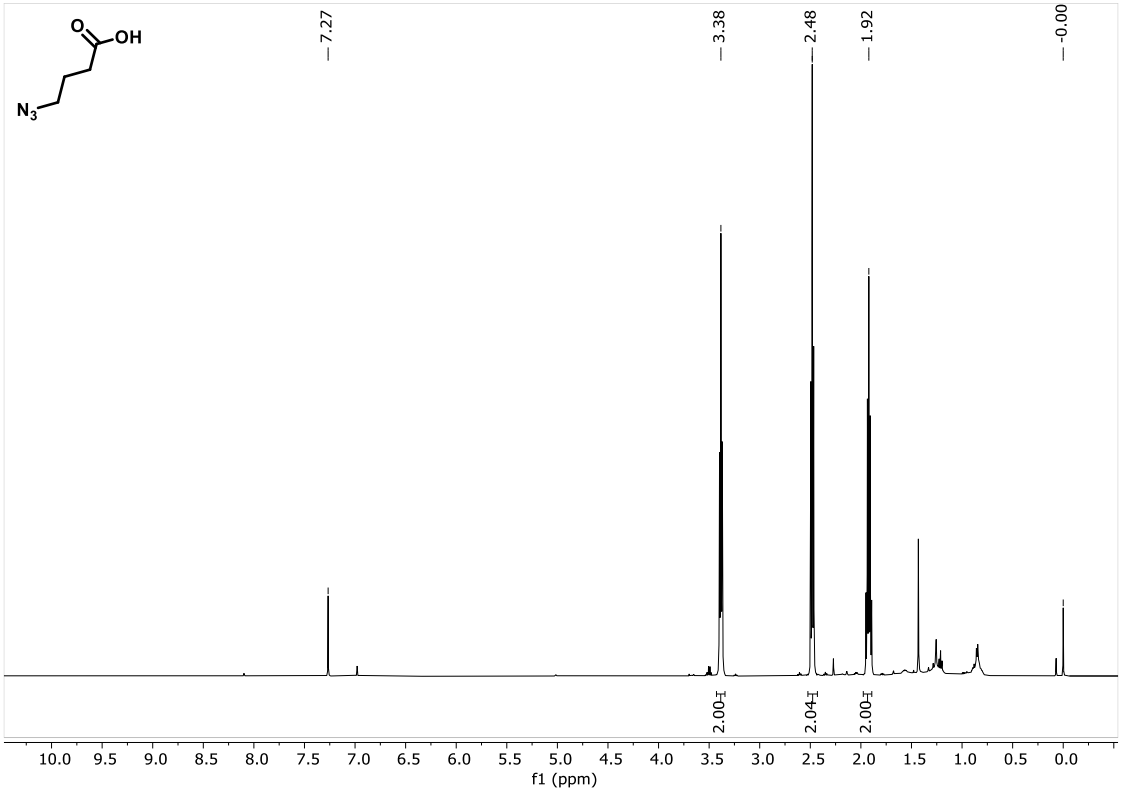

Figure 141: ^{1}H NMR (500 MHz, $CDCl_3$) of **148**.

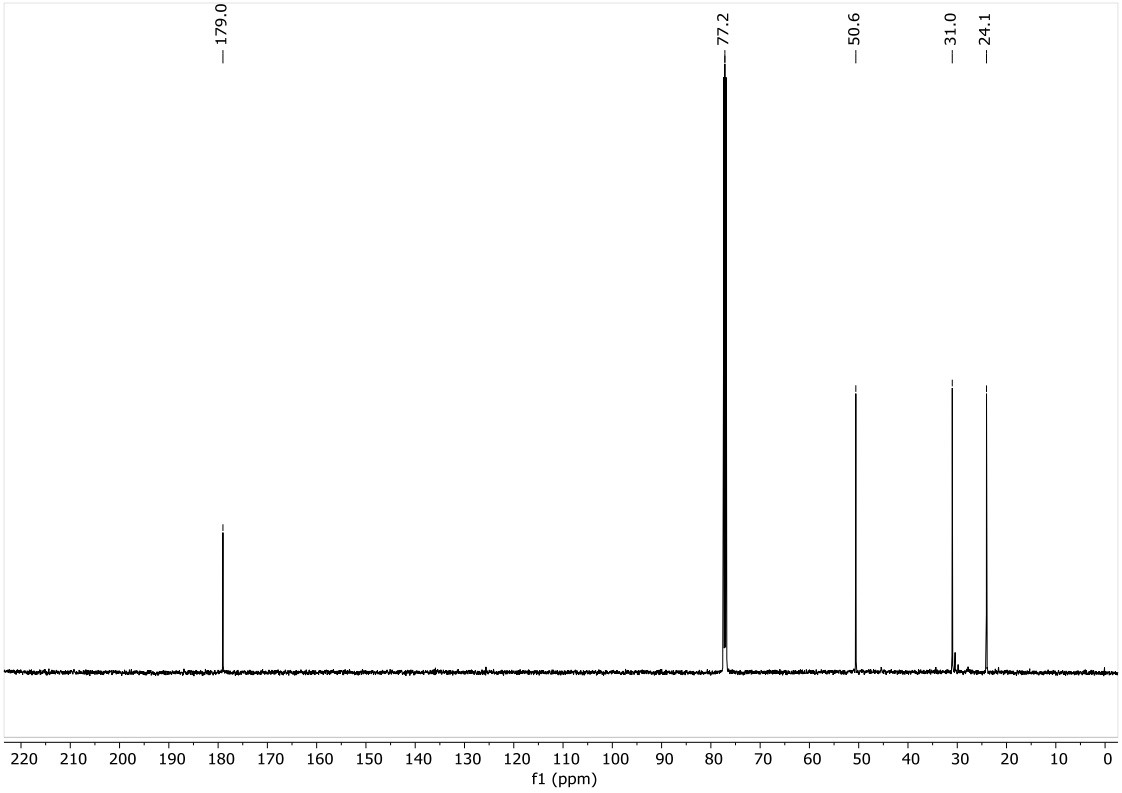

Figure 142: ^{13}C NMR (125 MHz, $CDCl_3$) of **148**.

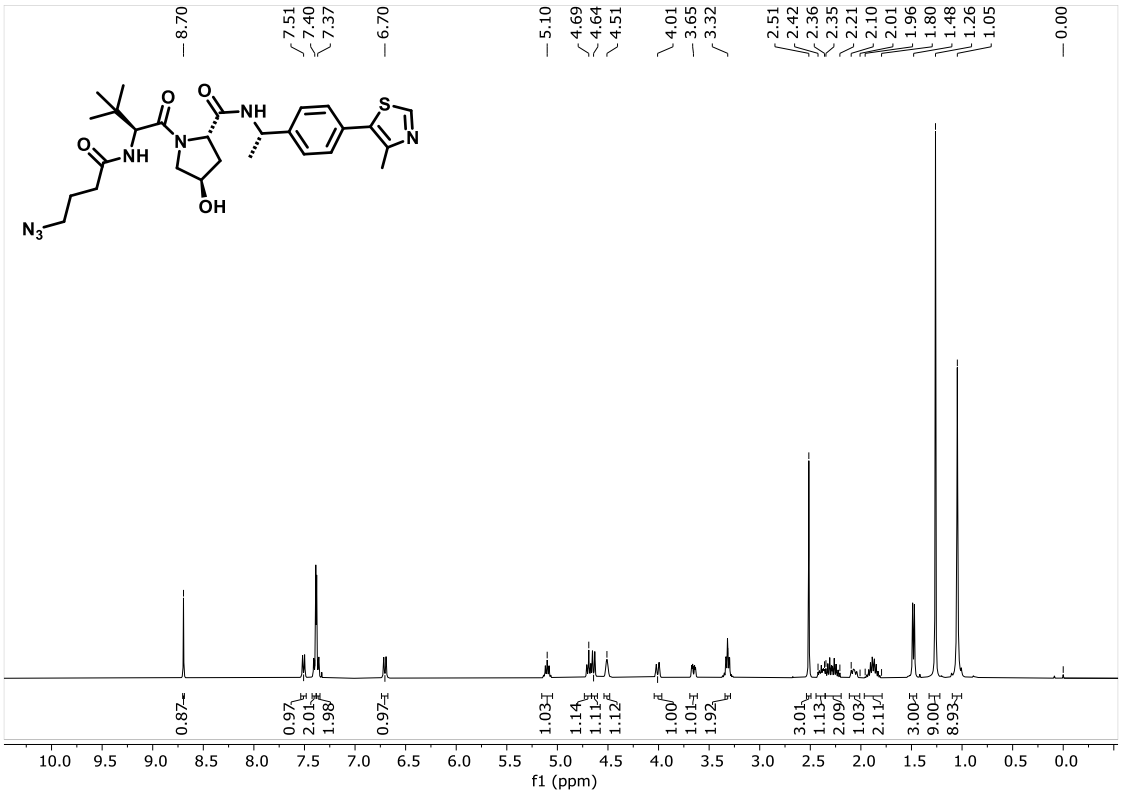

Figure 143: ^{1}H NMR (400 MHz, $CDCl_3$) of **152**.

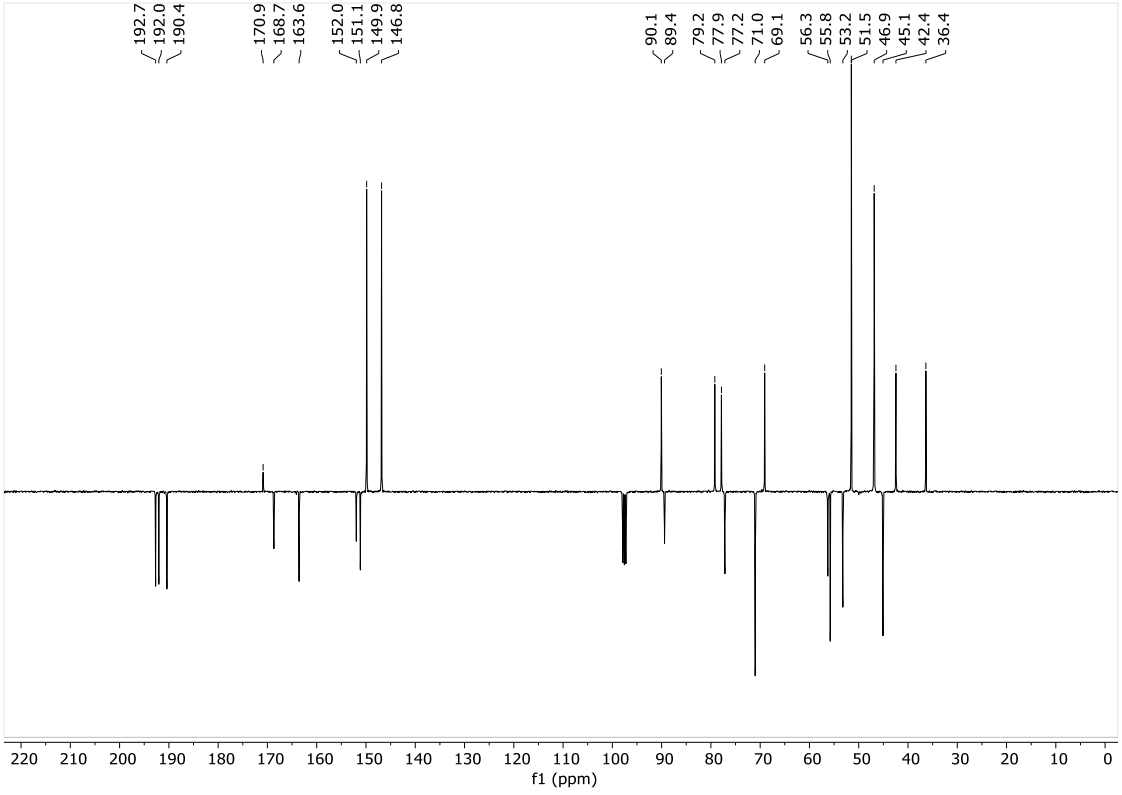

Figure 144: ^{13}C NMR (100 MHz, $CDCl_3$) of **152**.

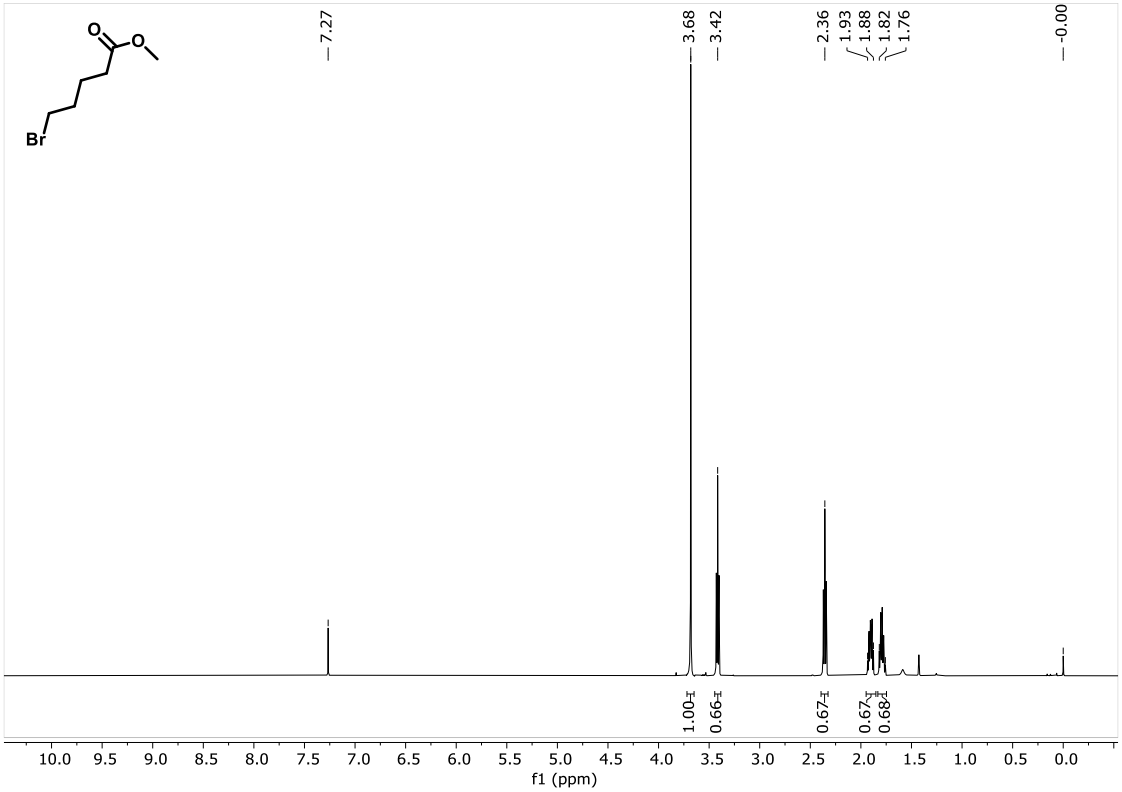

Figure 145: ^{1}H NMR (500 MHz, $CDCl_3$) of **161**.

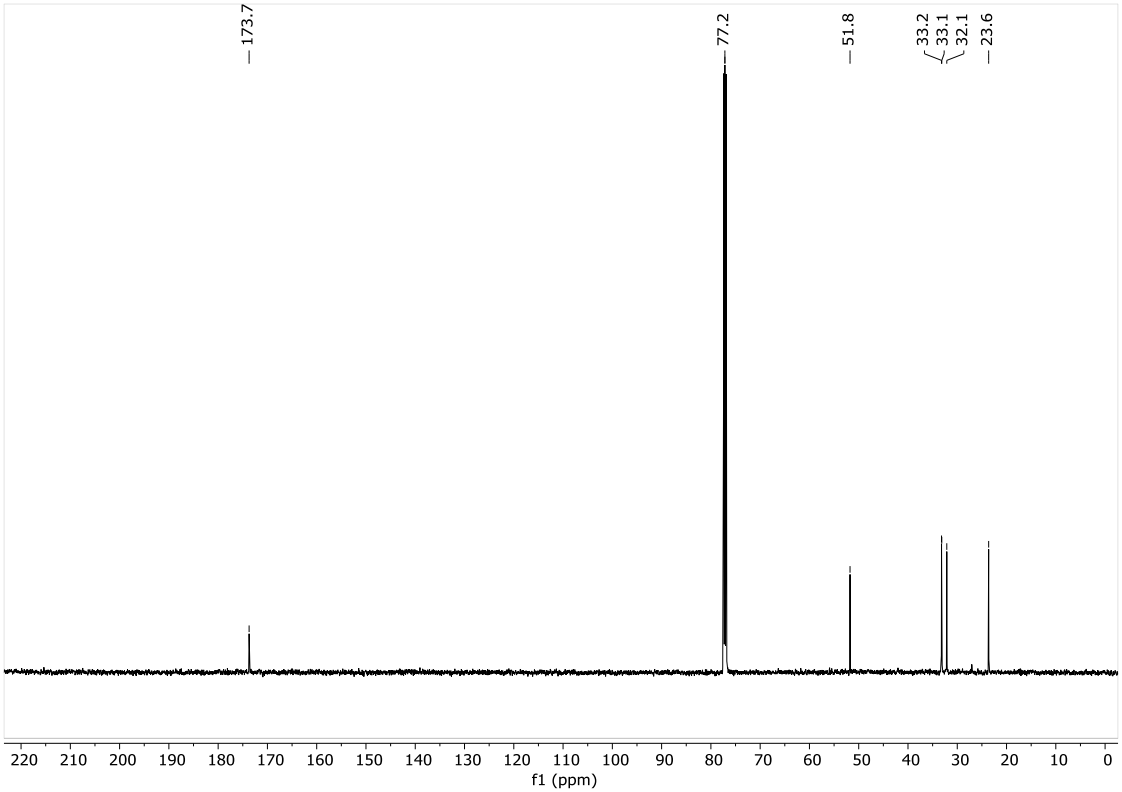

Figure 146: ^{13}C NMR (125 MHz, $CDCl_3$) of **161**.

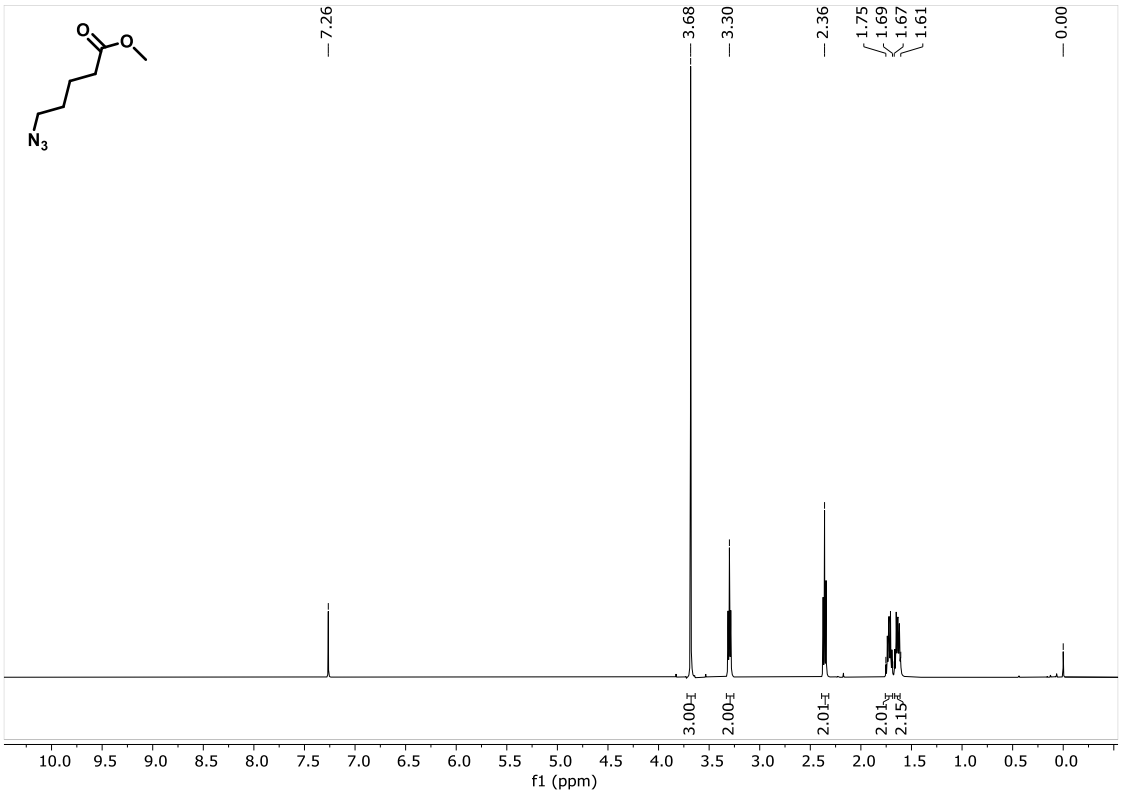

Figure 147: ^{1}H NMR (500 MHz, $CDCl_3$) of **165**.

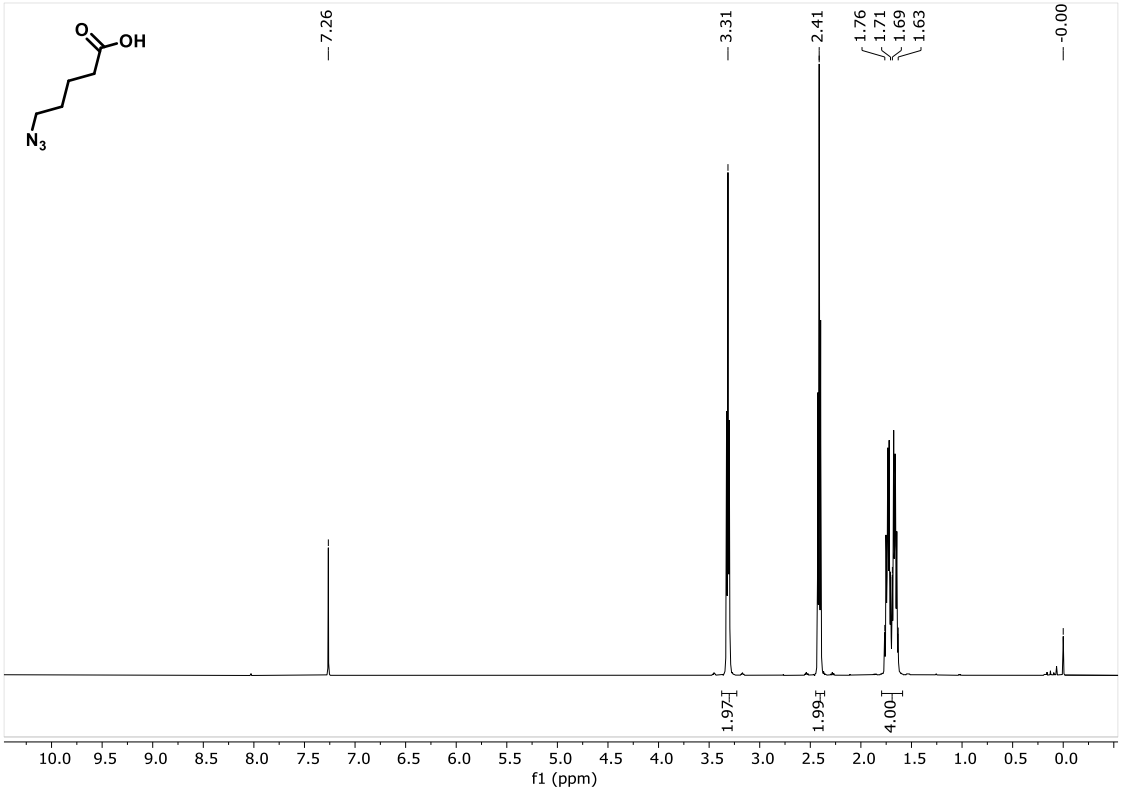

Figure 148: ^{1}H NMR (500 MHz, $CDCl_3$) of **149**.

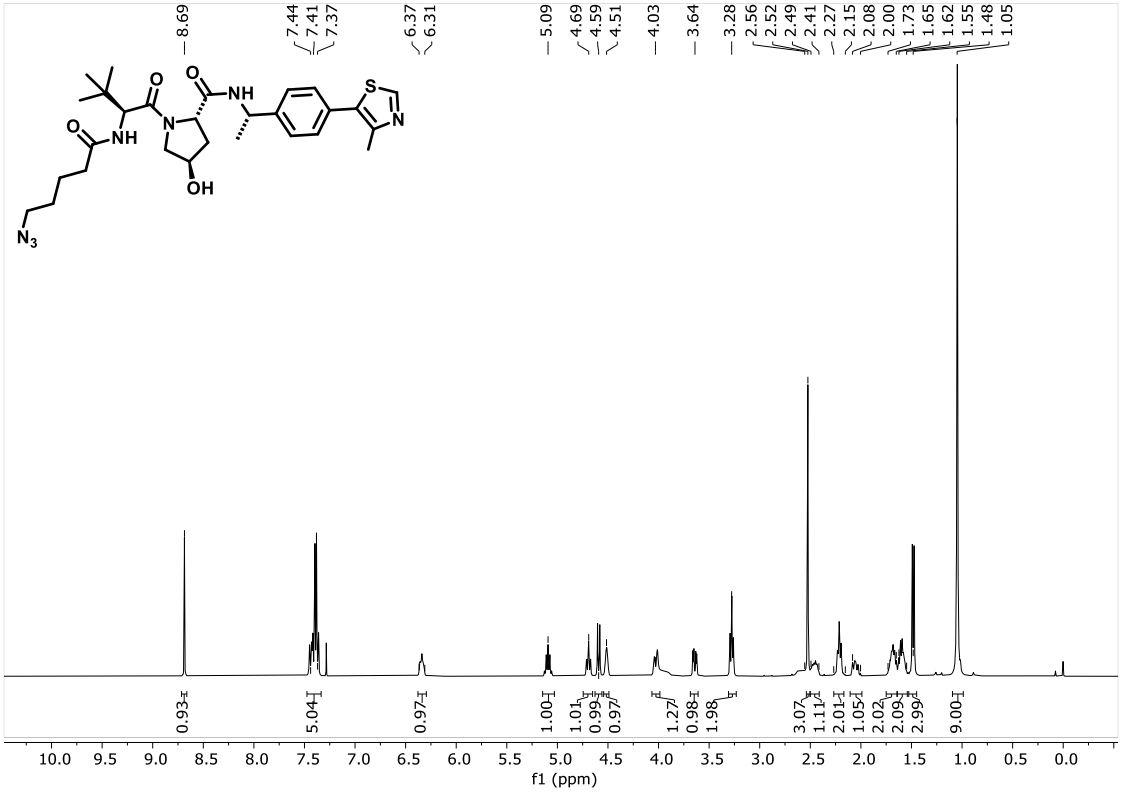

Figure 149: ^{1}H NMR (400 MHz, $CDCl_3$) of **153**.

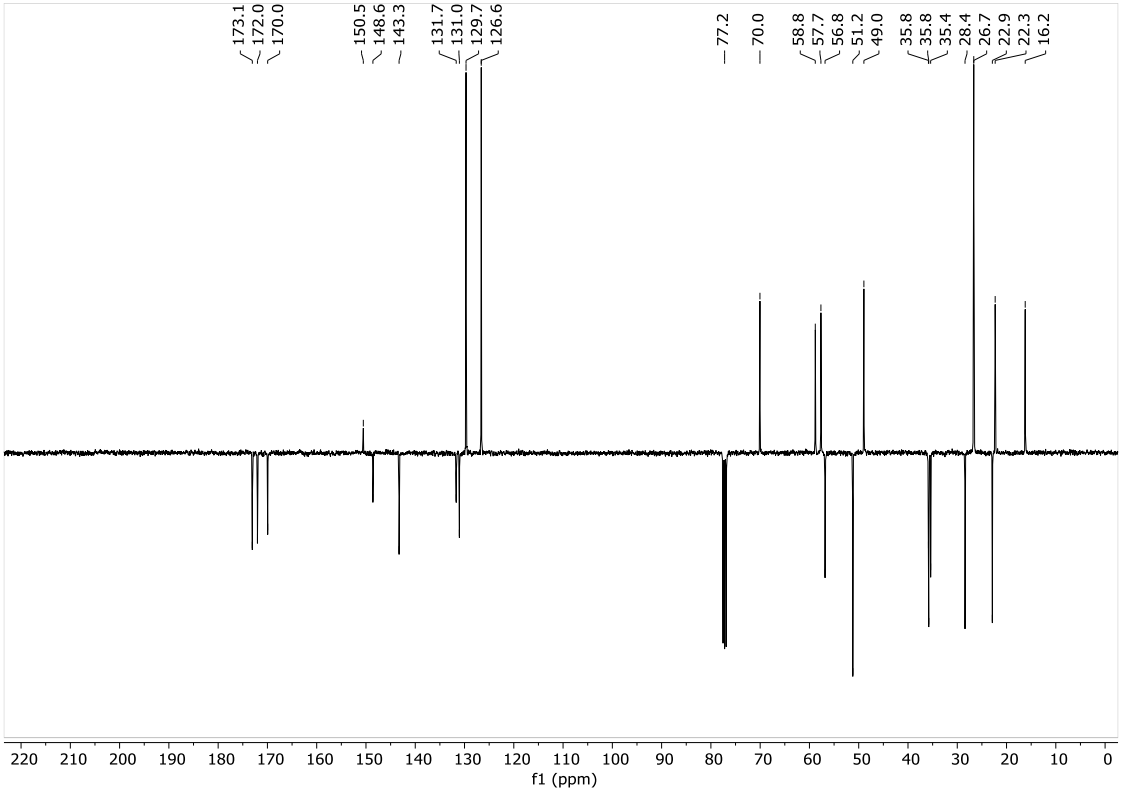

Figure 150: ^{13}C NMR (100 MHz, $CDCl_3$) of **153**.

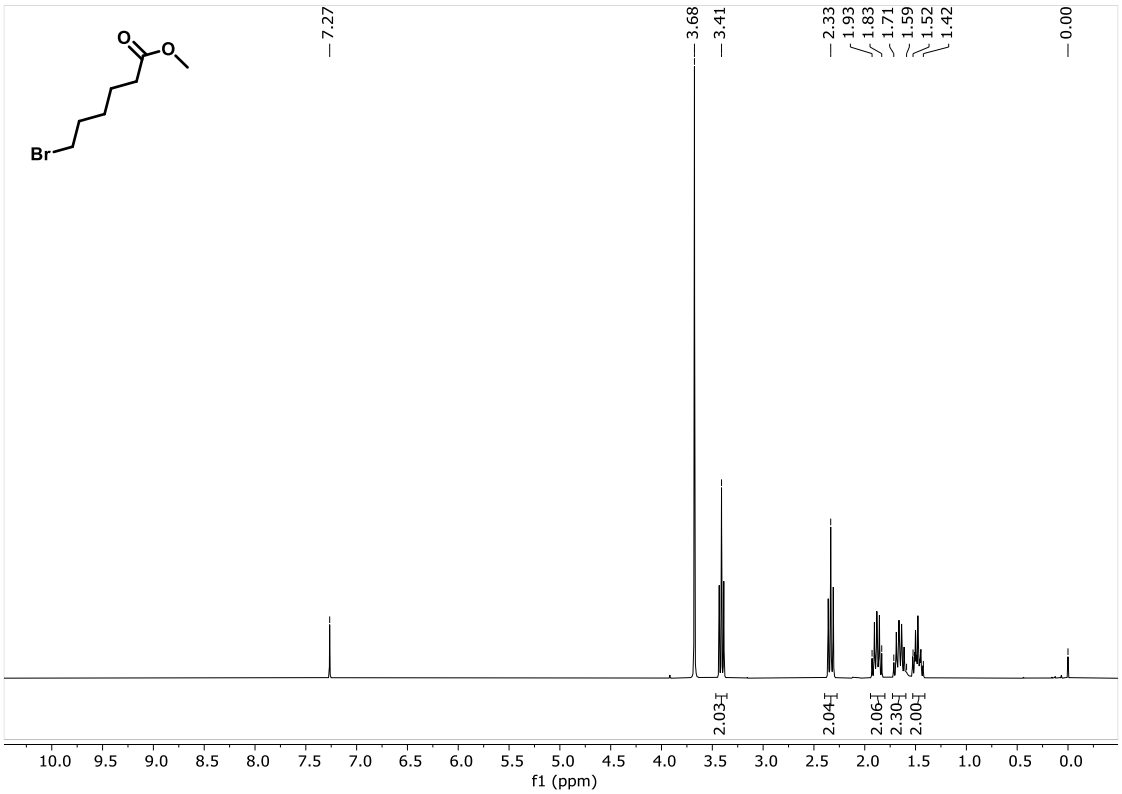

Figure 151: ^{1}H NMR (500 MHz, $CDCl_3$) of **159**.

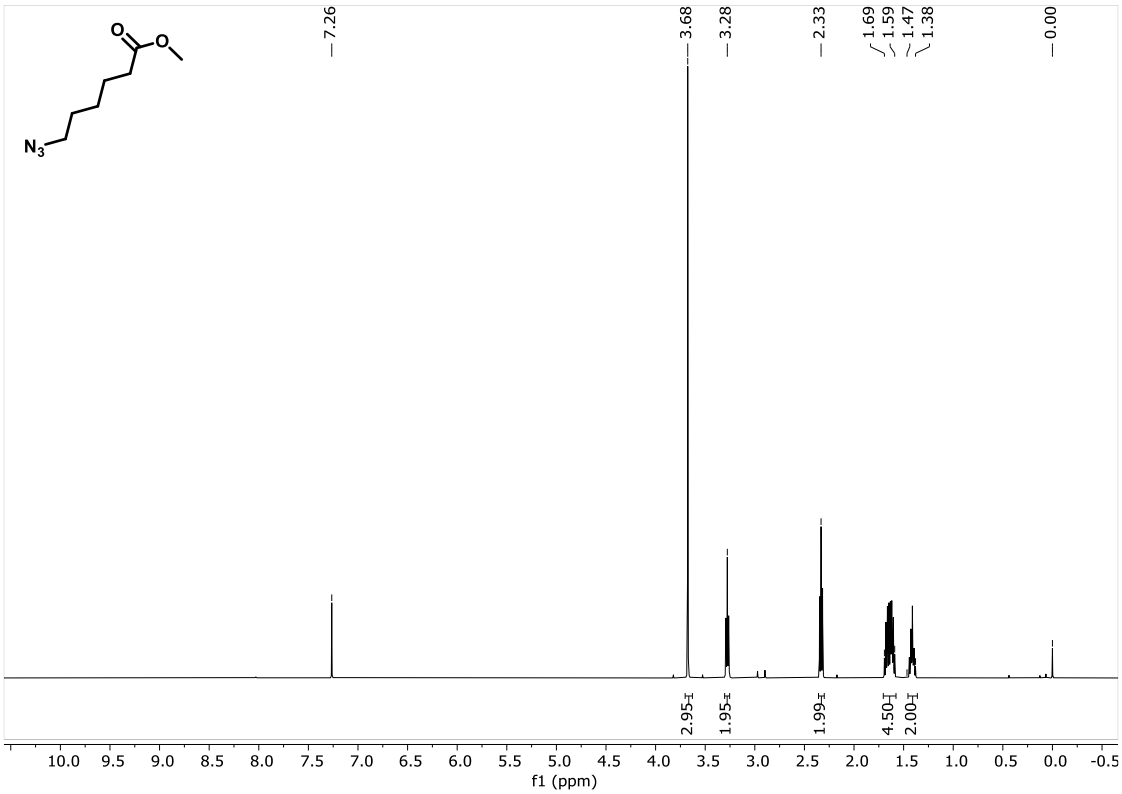

Figure 152: ^{1}H NMR (500 MHz, $CDCl_3$) of **166**.

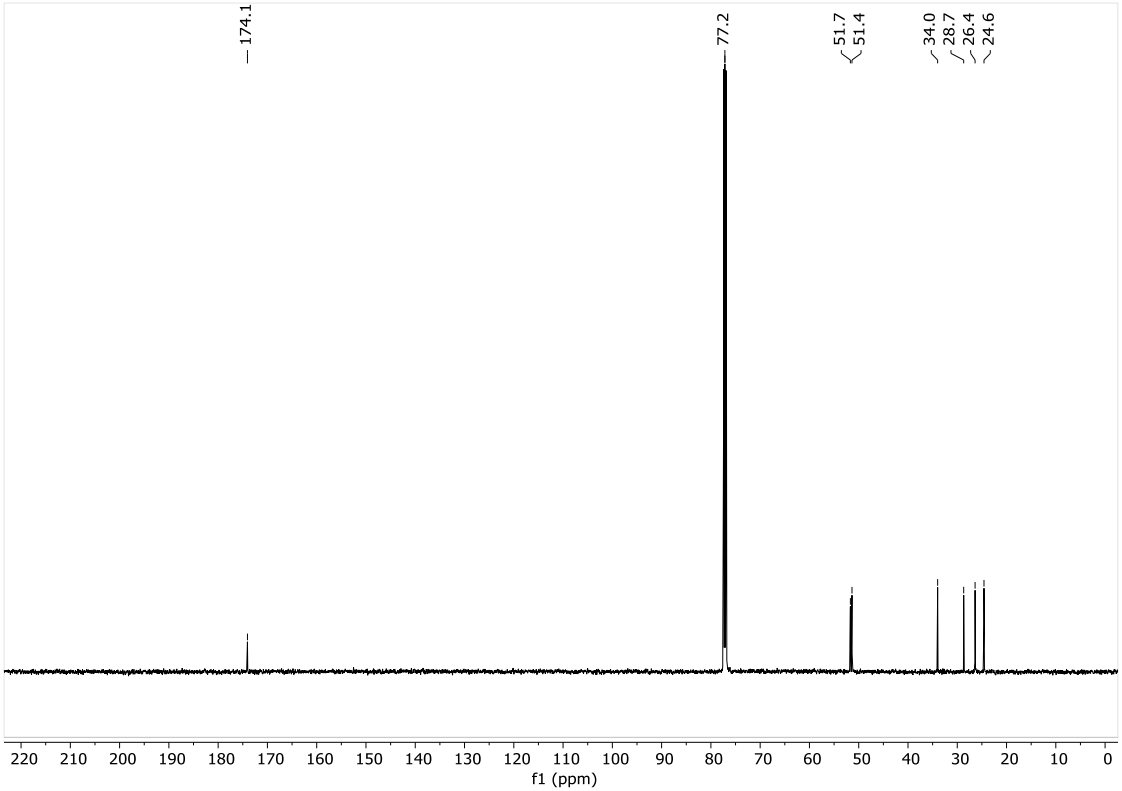

Figure 153: ^{13}C NMR (125 MHz, $CDCl_3$) of **166**.

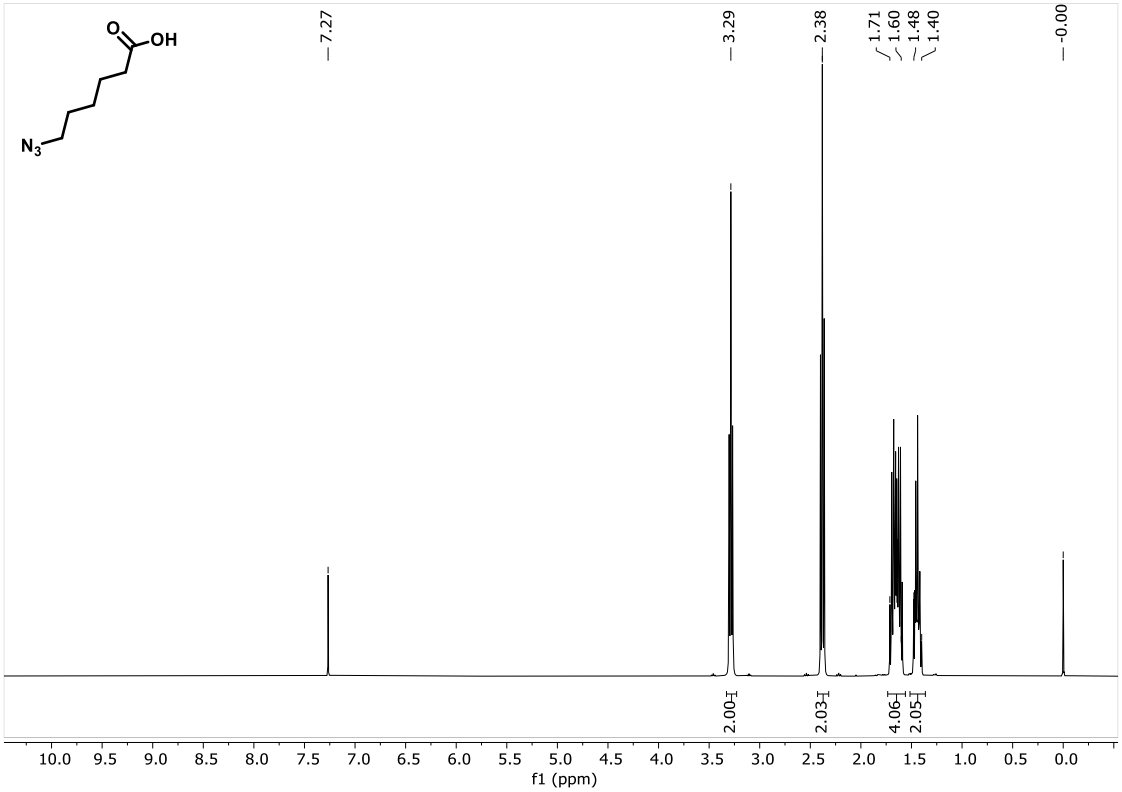

Figure 154: ^{1}H NMR (400 MHz, $CDCl_3$) of **150**.

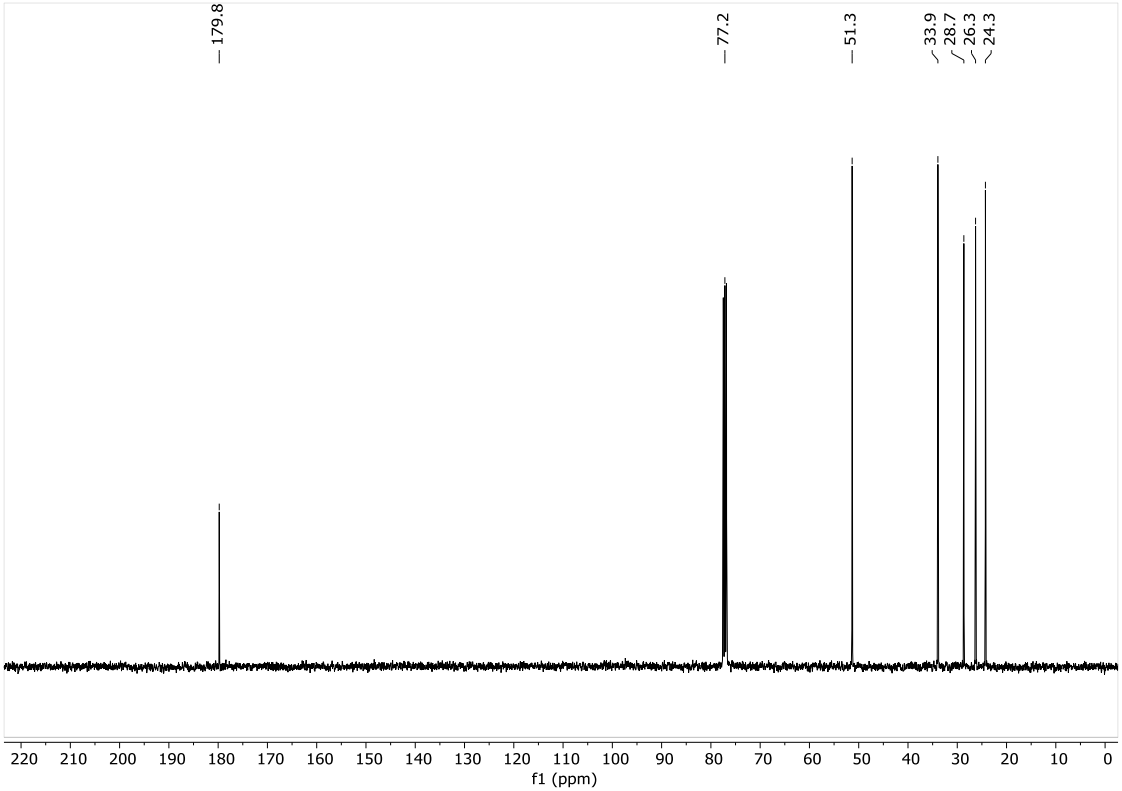

Figure 155: ^{13}C NMR (100 MHz, $CDCl_3$) of **150**.

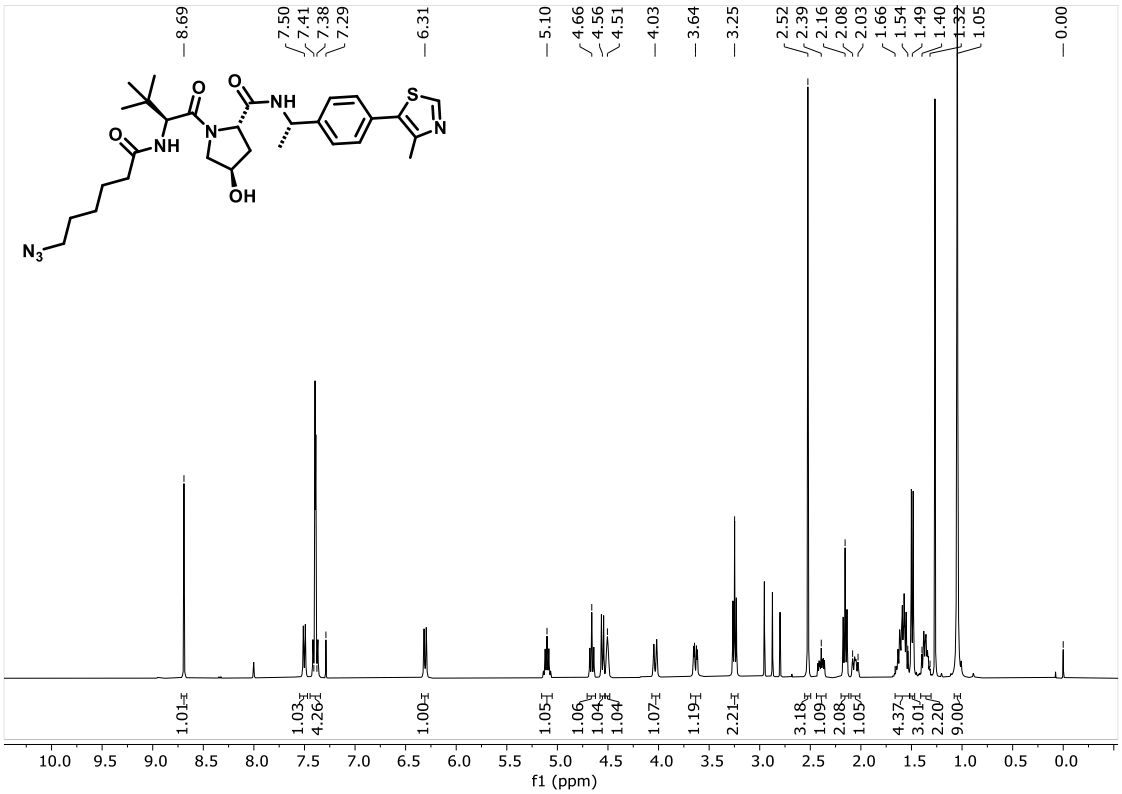

Figure 156: ^{1}H NMR (400 MHz, $CDCl_3$) of **154**.

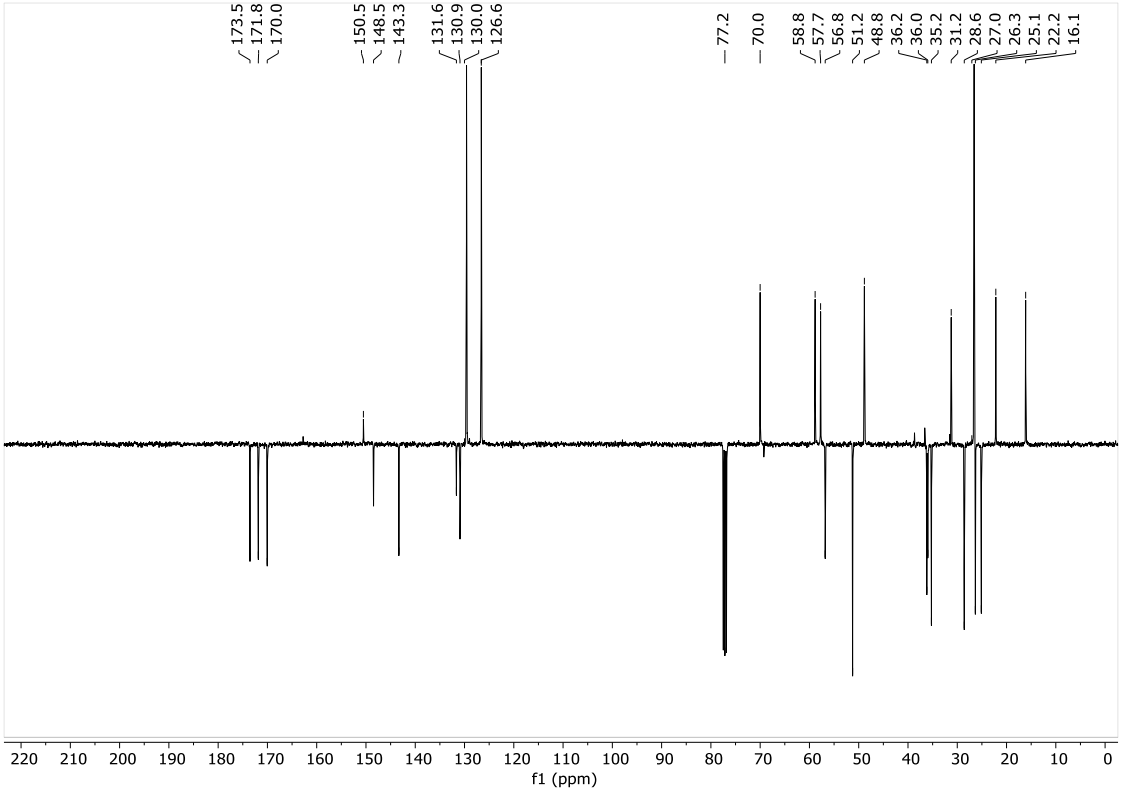

Figure 157: ^{13}C NMR (100 MHz, $CDCl_3$) of **154**.

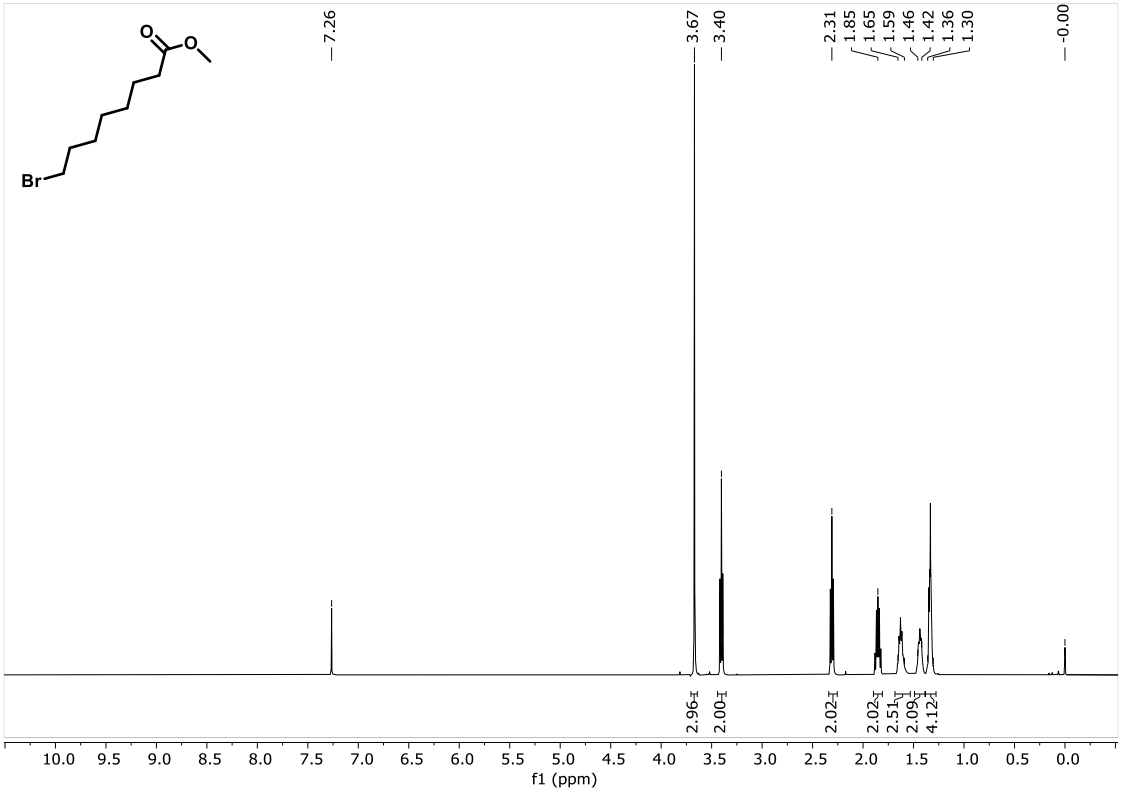

Figure 158: ^{1}H NMR (500 MHz, $CDCl_3$) of **163**.

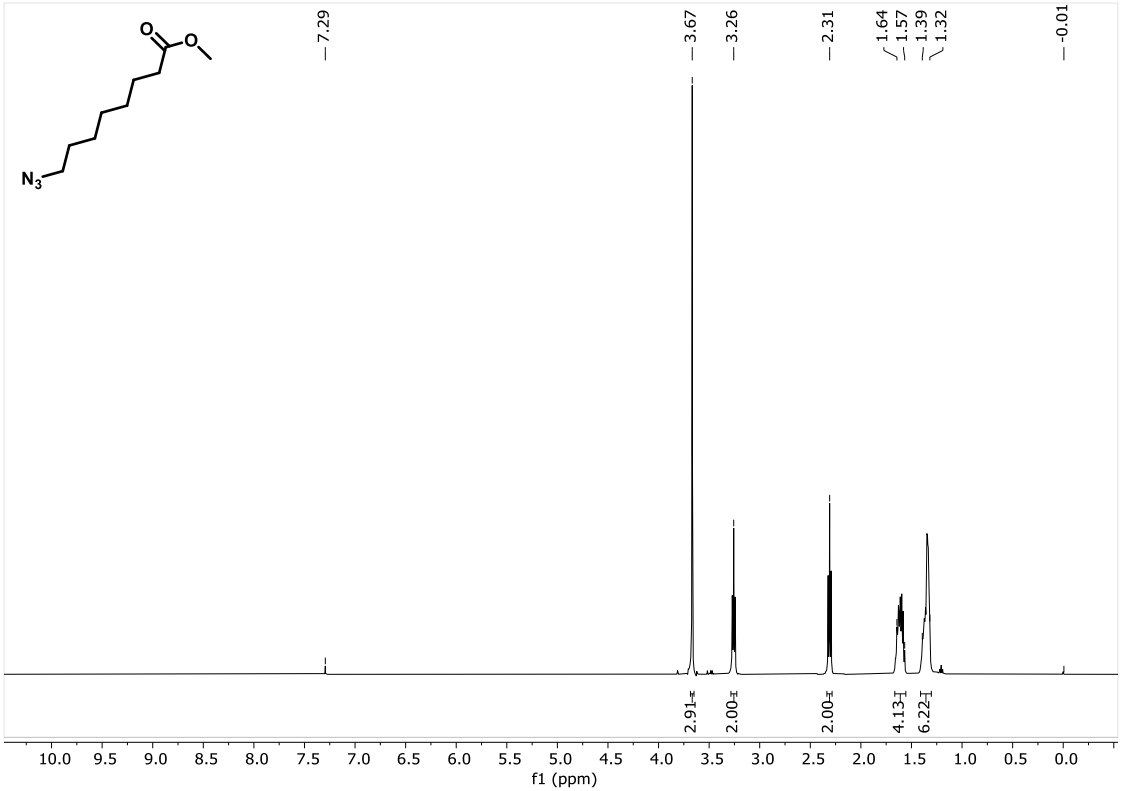

Figure 159: ^{1}H NMR (500 MHz, $CDCl_3$) of **167**.

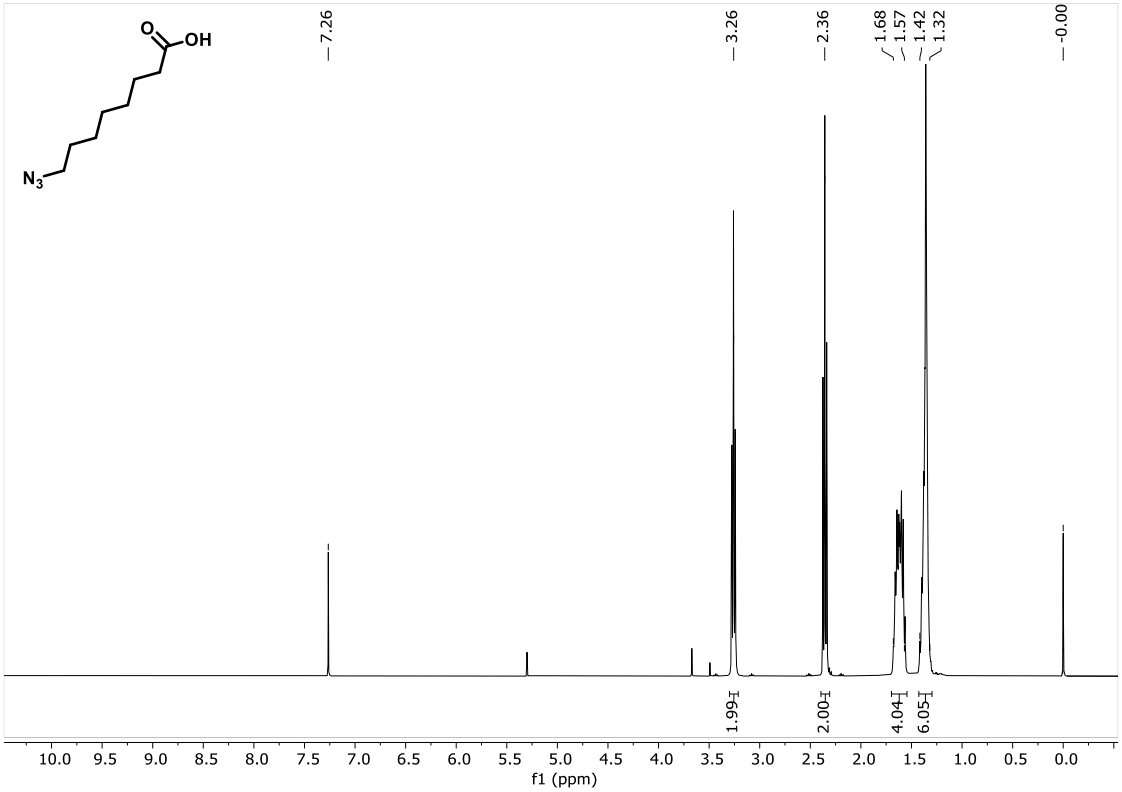

Figure 160: ^{1}H NMR (400 MHz, $CDCl_3$) of **151**.

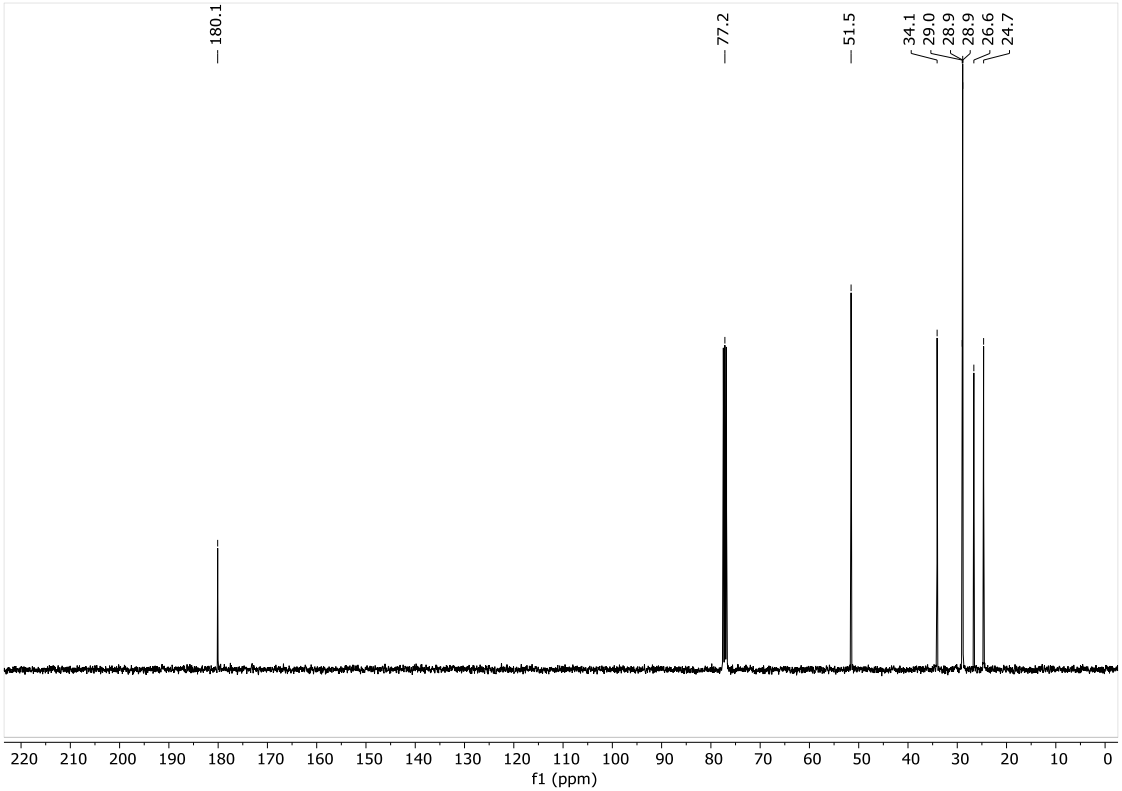

Figure 161: ^{13}C NMR (100 MHz, $CDCl_3$) of **151**.

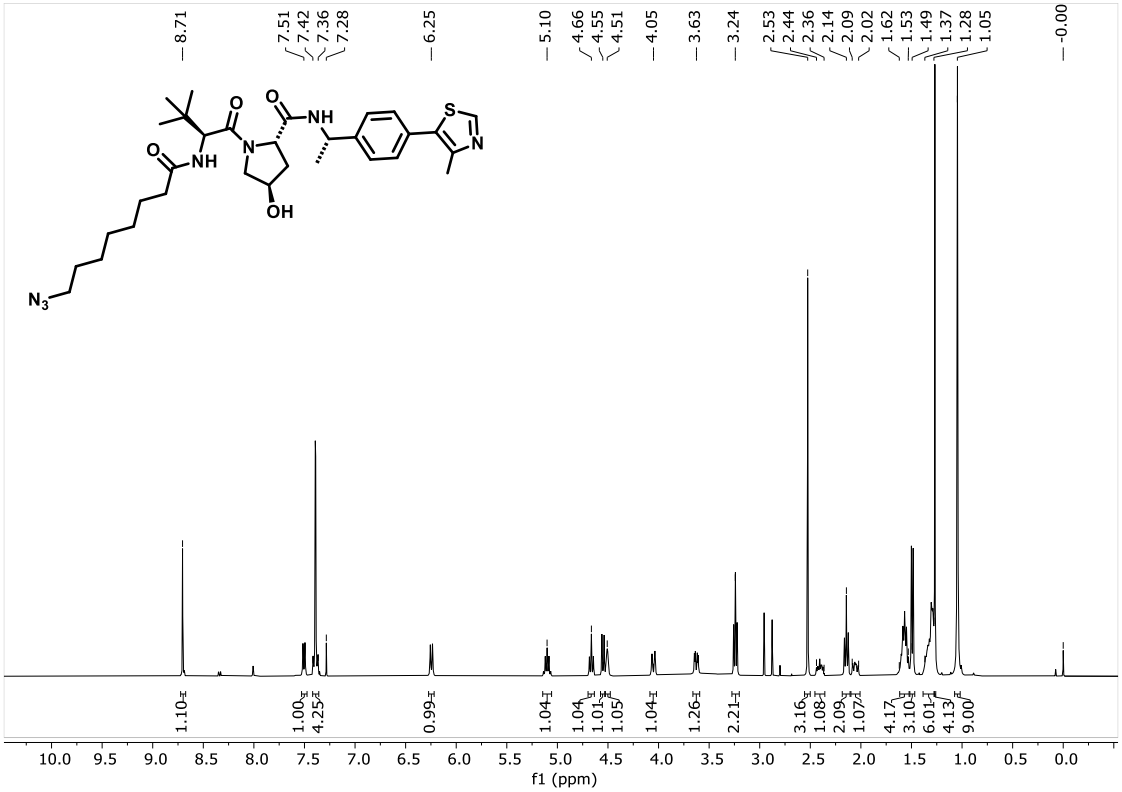

Figure 162: ^{1}H NMR (400 MHz, $CDCl_3$) of **155**.

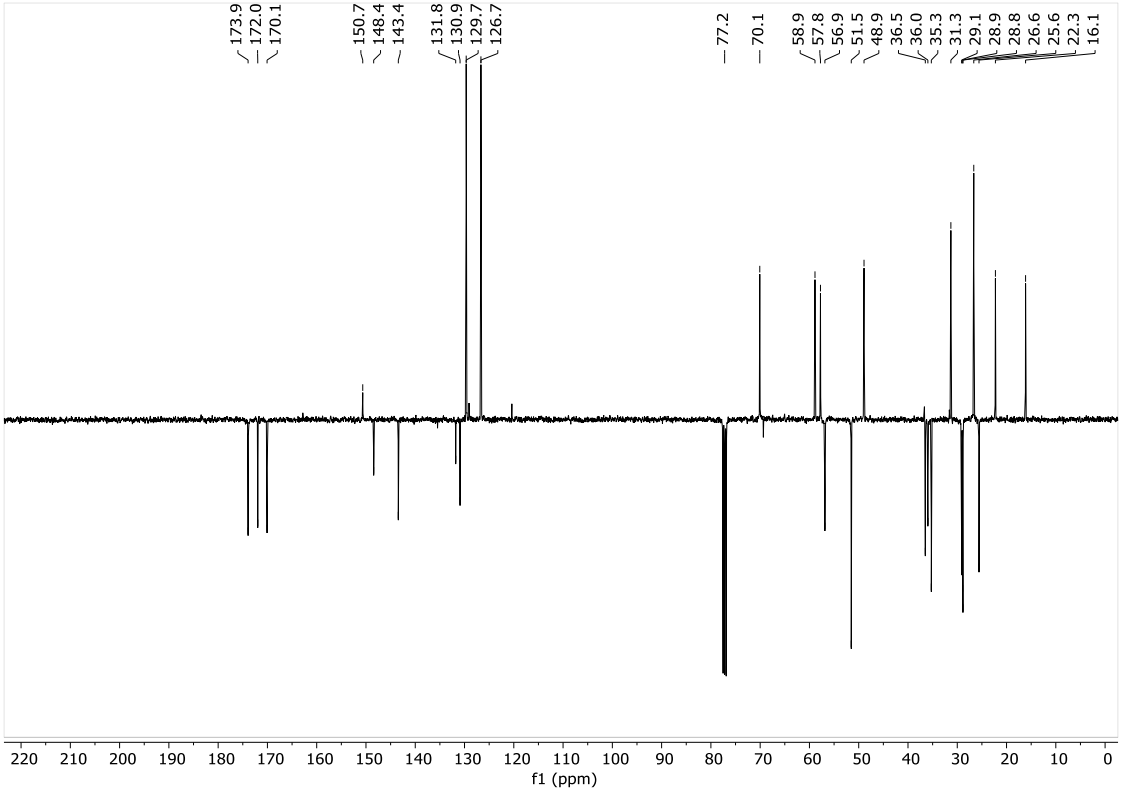

Figure 163: ^{13}C NMR (100 MHz, $CDCl_3$) of **155**.

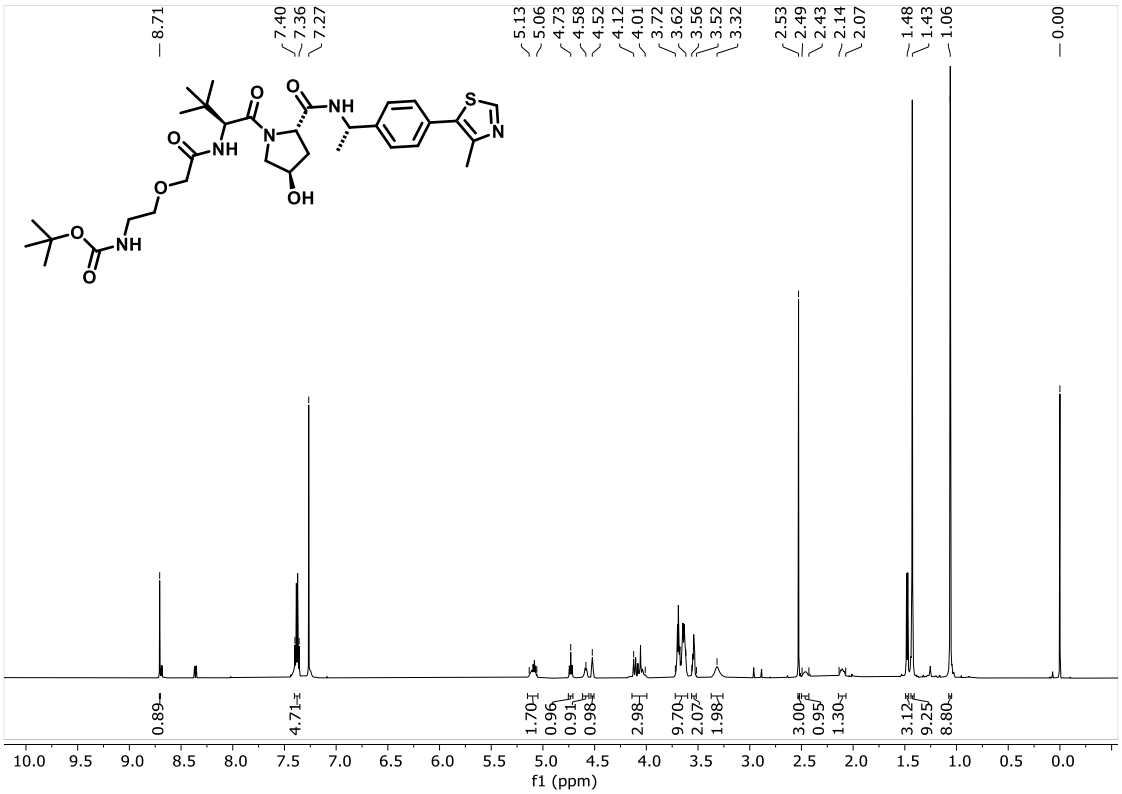

Figure 164: ^{1}H NMR (500 MHz, $CDCl_3$) of **178**.

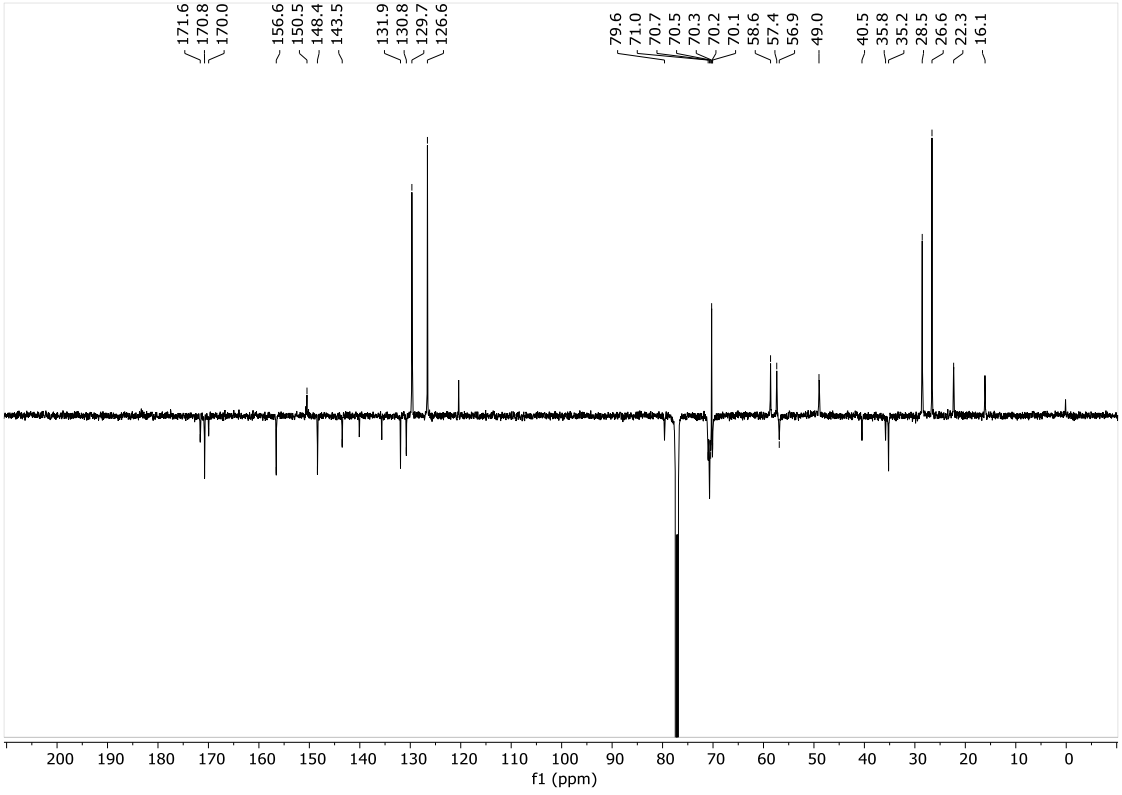

Figure 165: ^{13}C NMR (125 MHz, $CDCl_3$) of **178**.

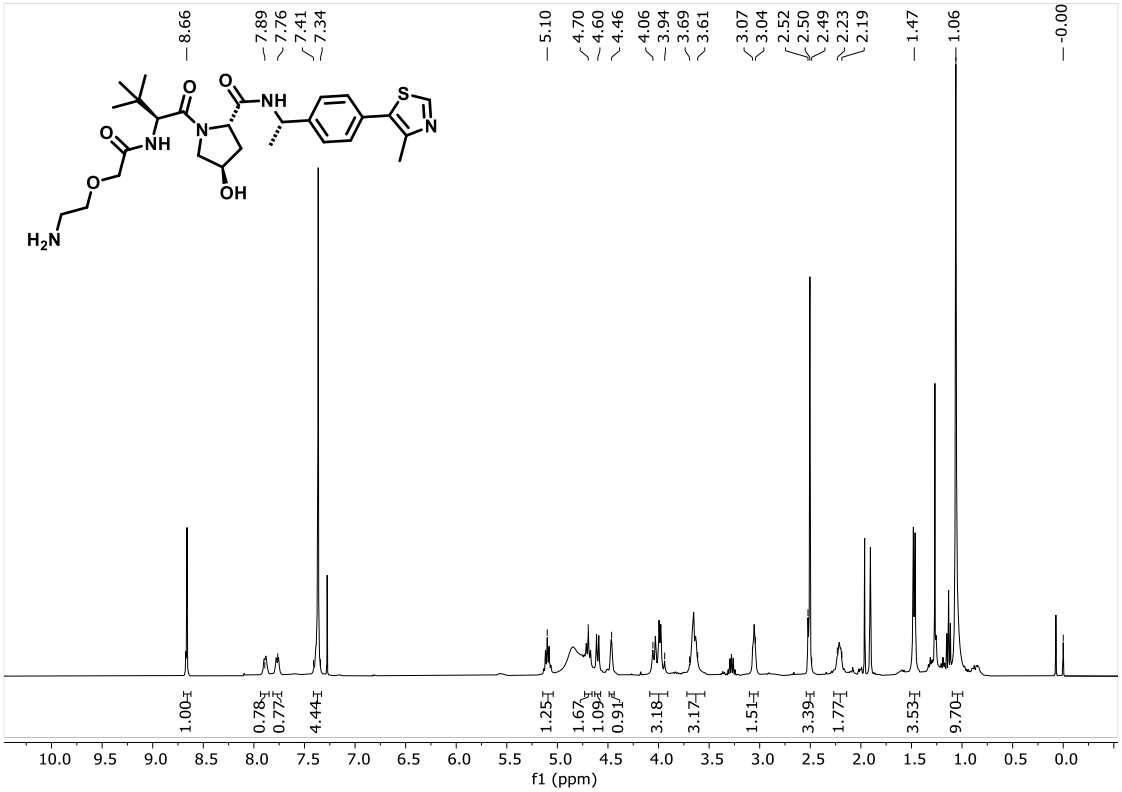

Figure 166: ^{1}H NMR (400 MHz, $CDCl_3$) of **181**.

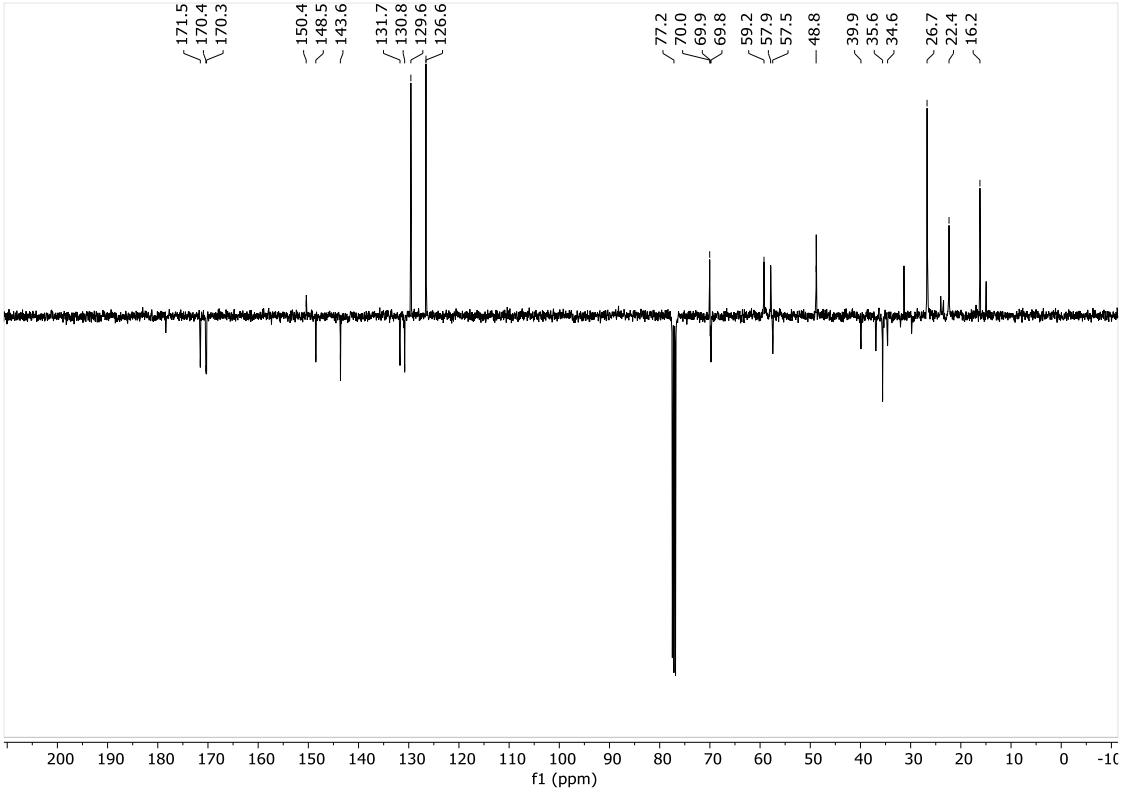

Figure 167: ^{13}C NMR (100 MHz, $CDCl_3$) of **181**.

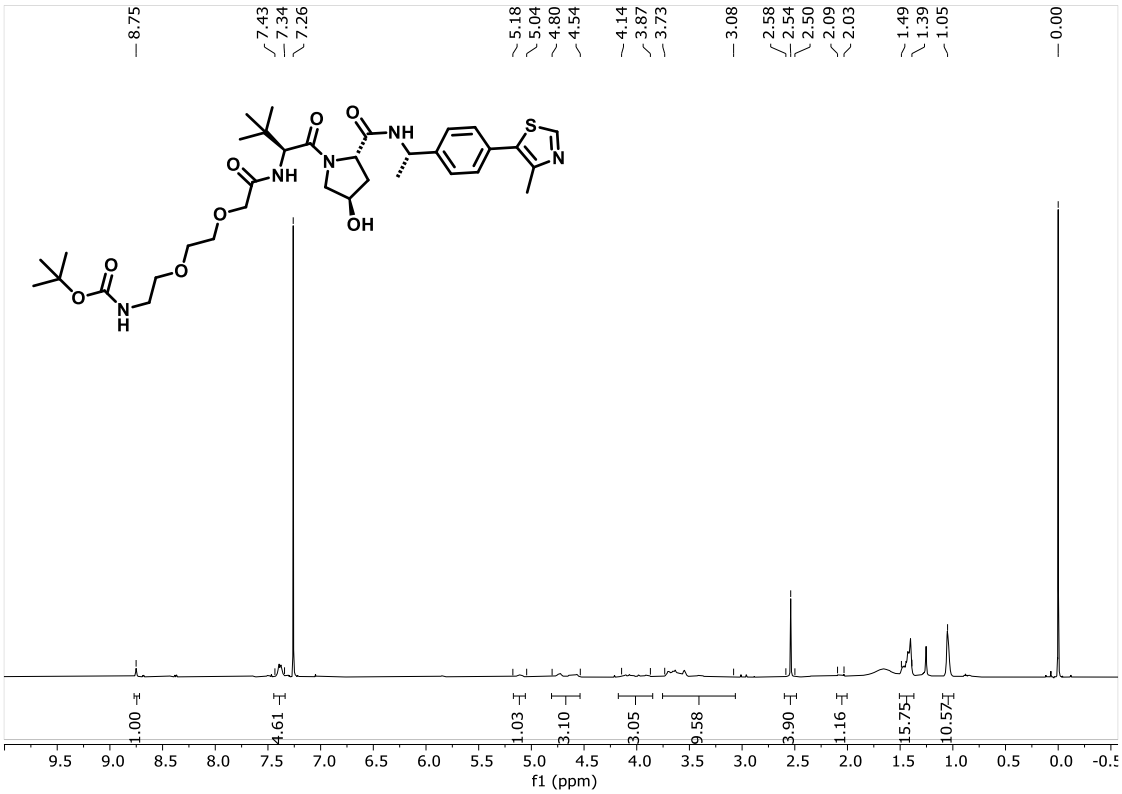

Figure 168: ^{1}H NMR (500 MHz, $CDCl_3$) of **179**.

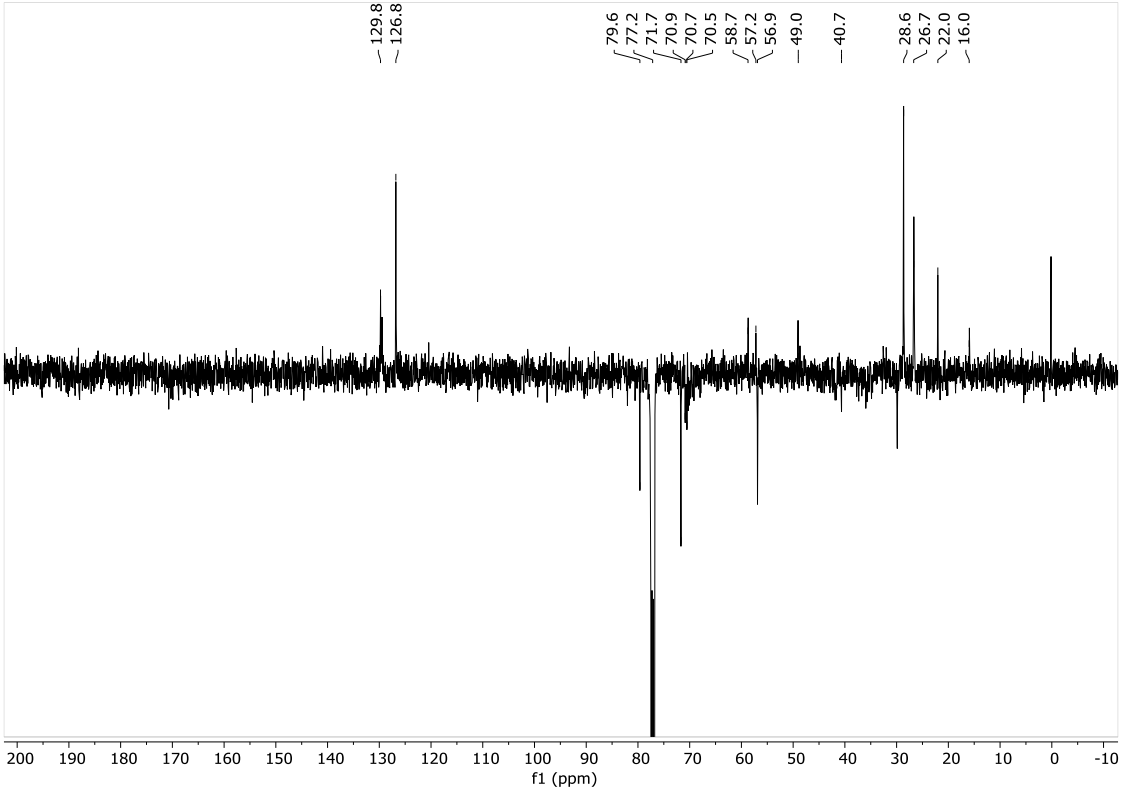

Figure 169: ^{13}C NMR (125 MHz, $CDCl_3$) of **179**.

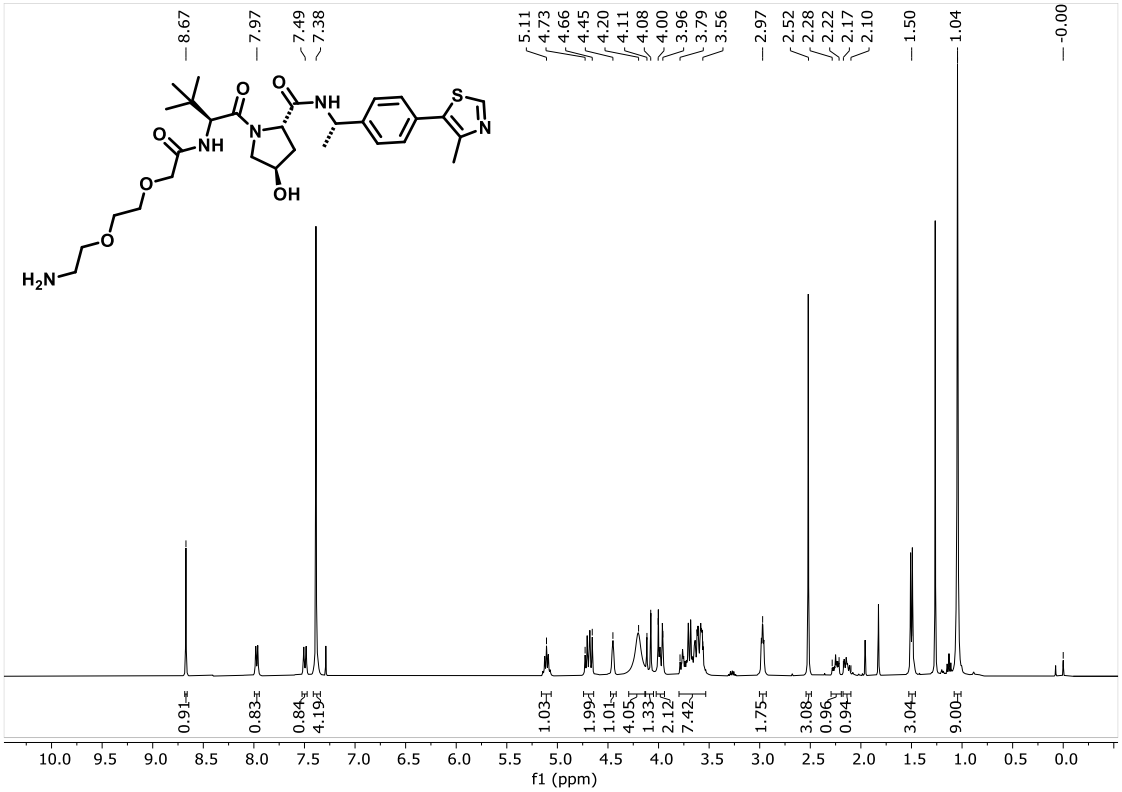

Figure 170: ^{1}H NMR (400 MHz, $CDCl_3$) of **182**.

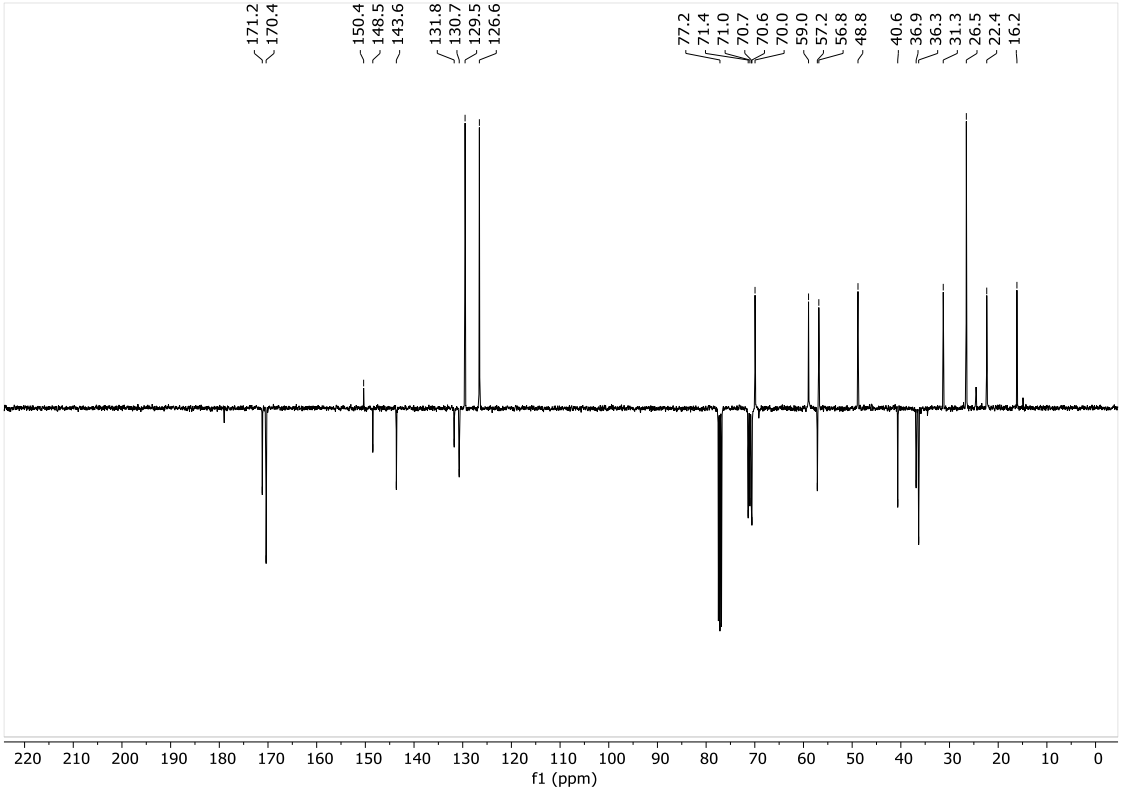

Figure 171: ^{13}C NMR (100 MHz, $CDCl_3$) of **182**.

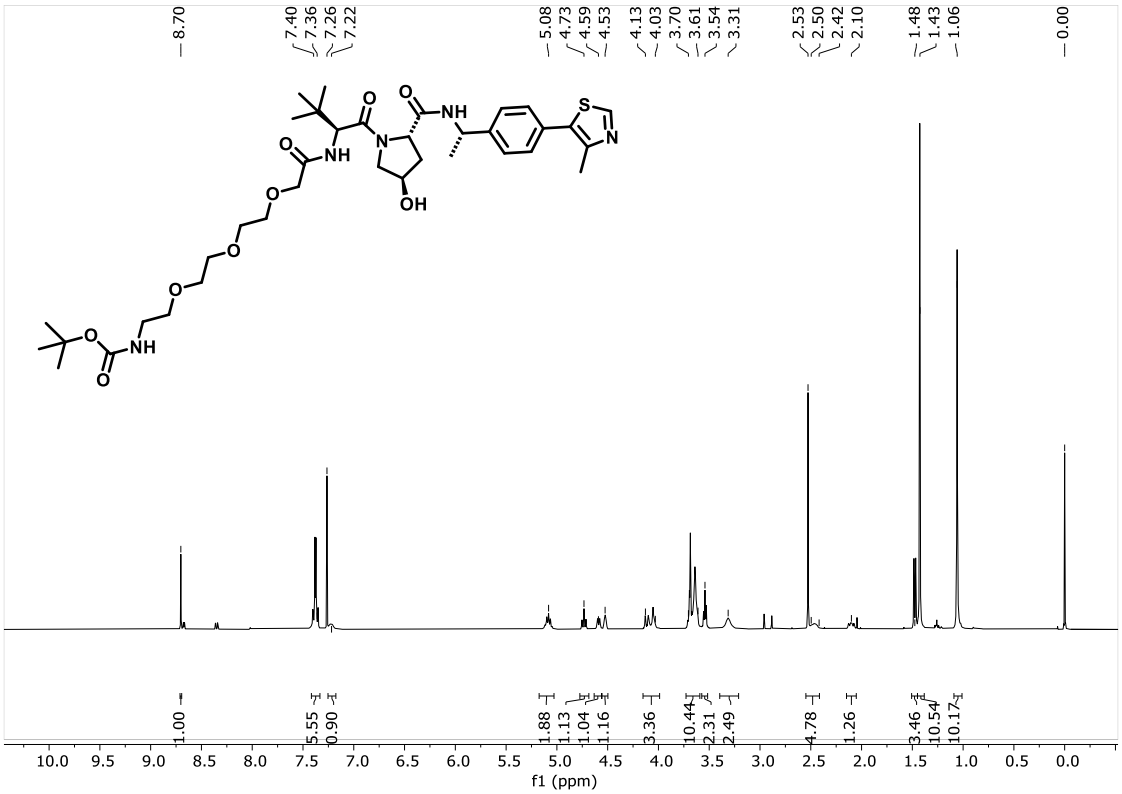

Figure 172: ^{1}H NMR (500 MHz, $CDCl_3$) of **180**.

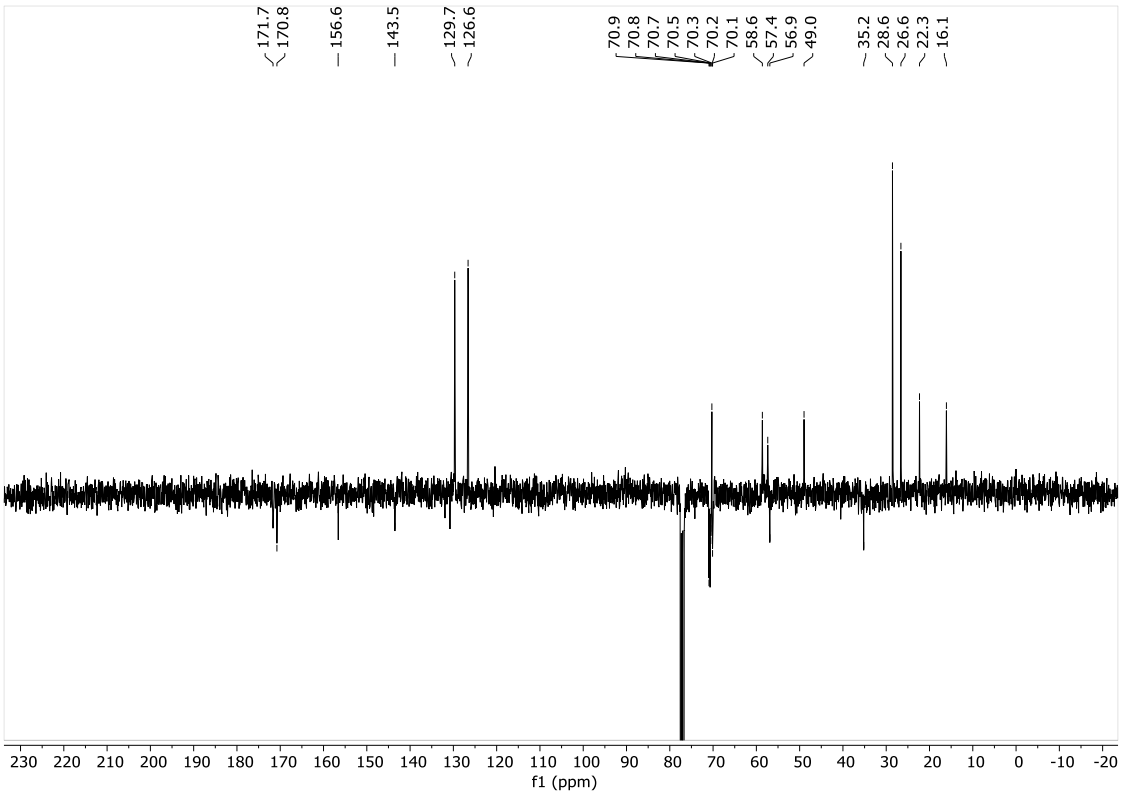

Figure 173: ^{13}C NMR (125 MHz, $CDCl_3$) of **180**.

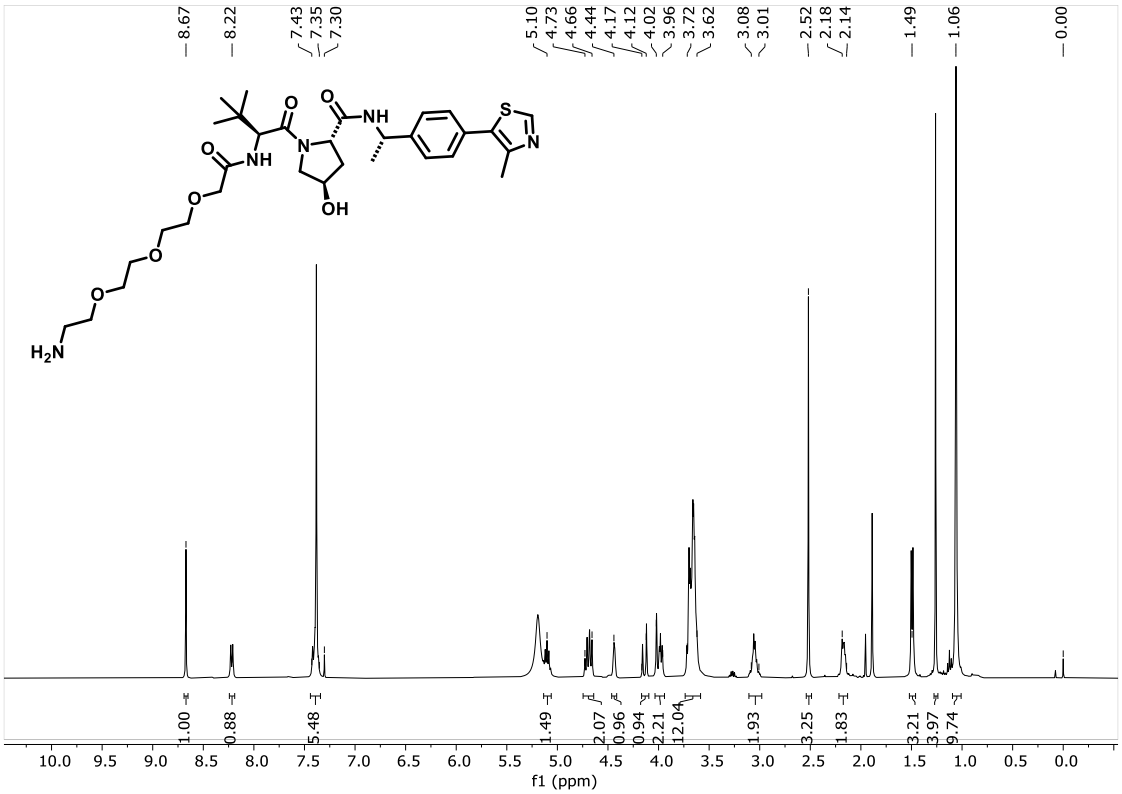

Figure 174: ^{1}H NMR (400 MHz, $CDCl_3$) of **183**.

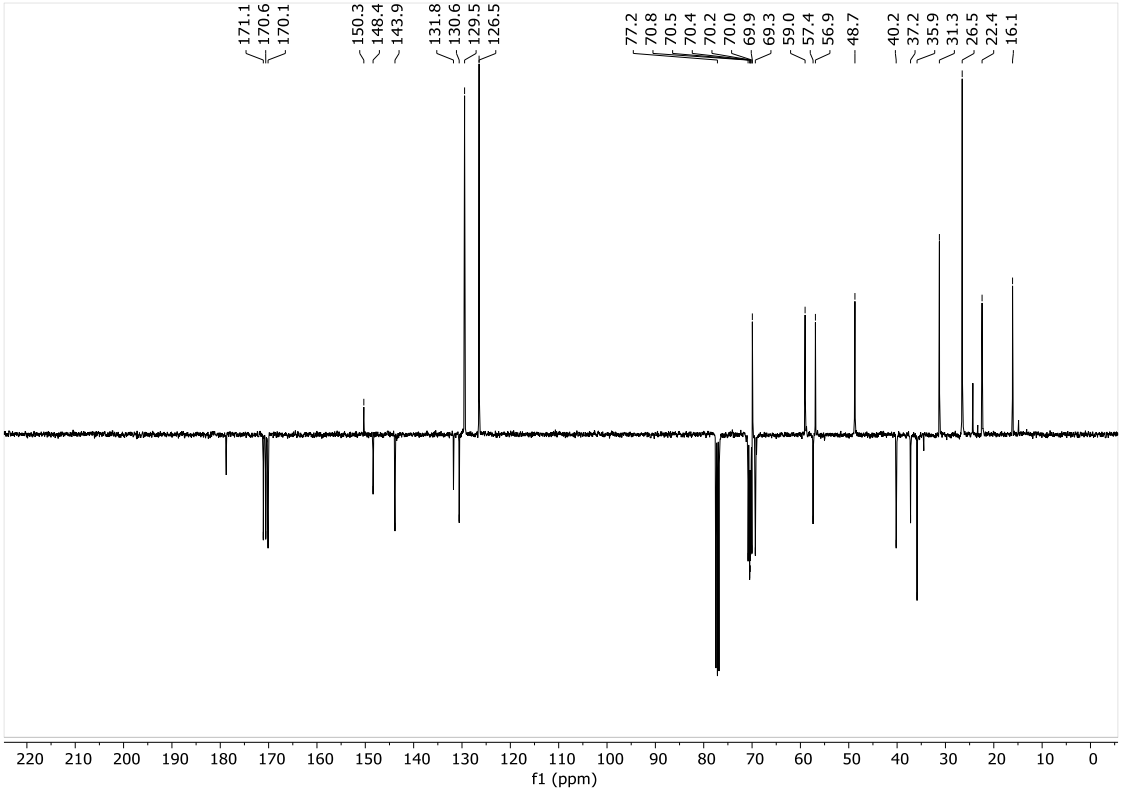

Figure 175: ^{13}C NMR (100 MHz, $CDCl_3$) of **183**.

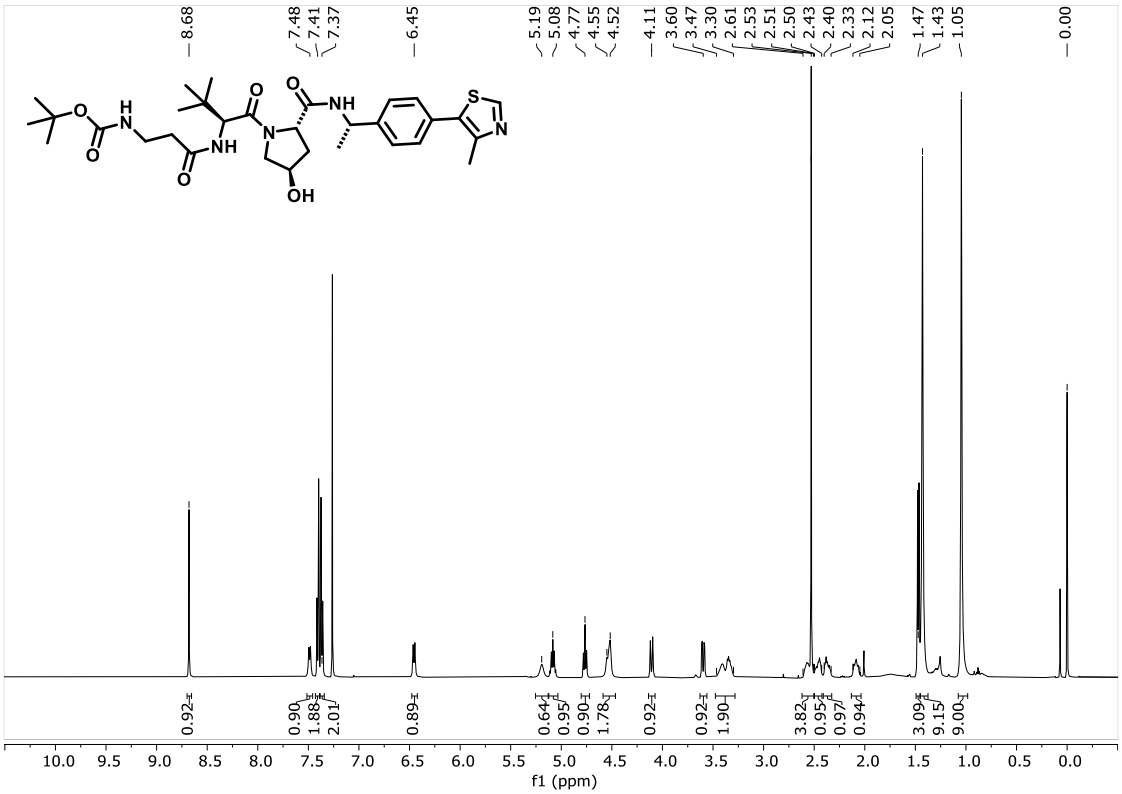

Figure 176: ^{1}H NMR (500 MHz, $CDCl_3$) of **192**.

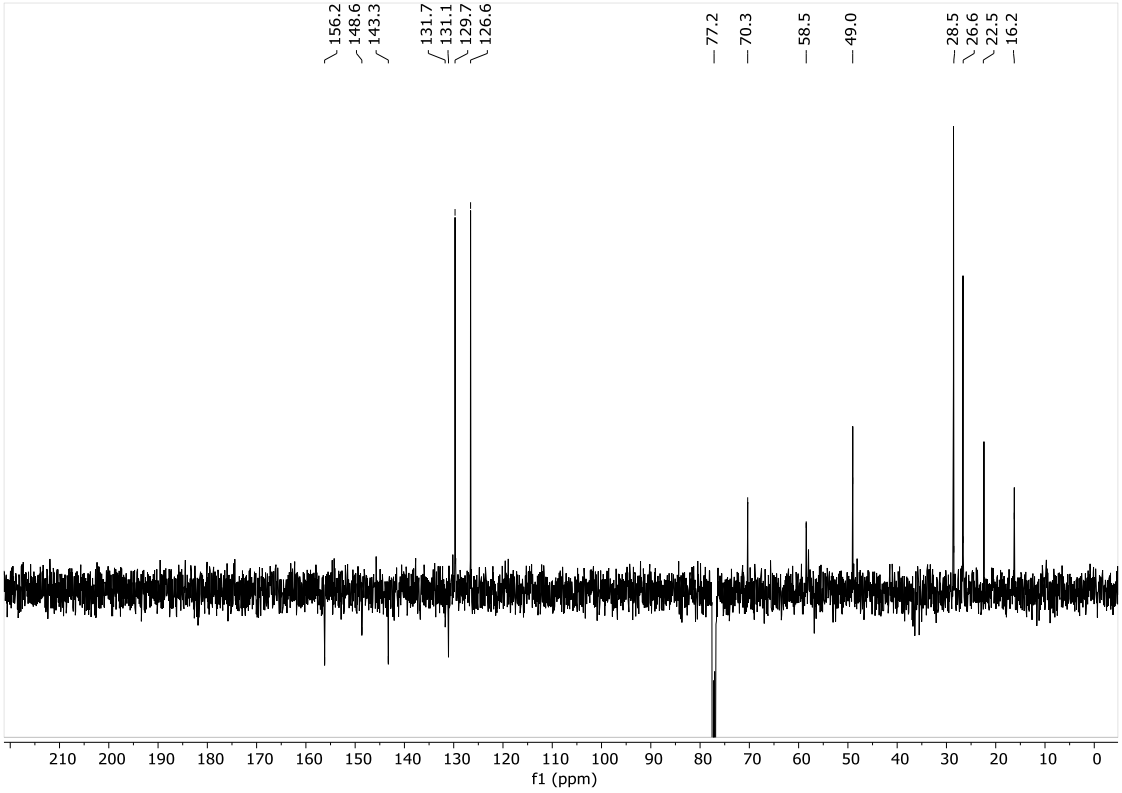

Figure 177: ^{13}C NMR (125 MHz, $CDCl_3$) of **192**.

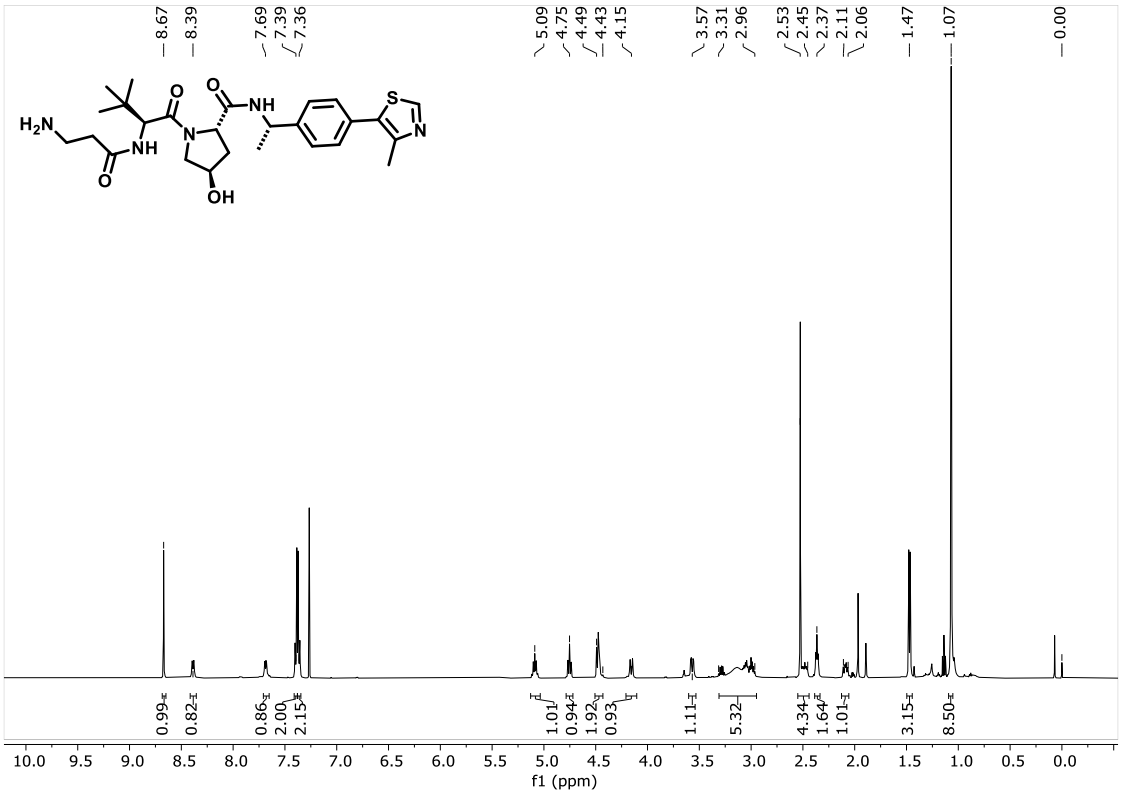

Figure 178: ^{1}H NMR (500 MHz, $CDCl_3$) of **196**.

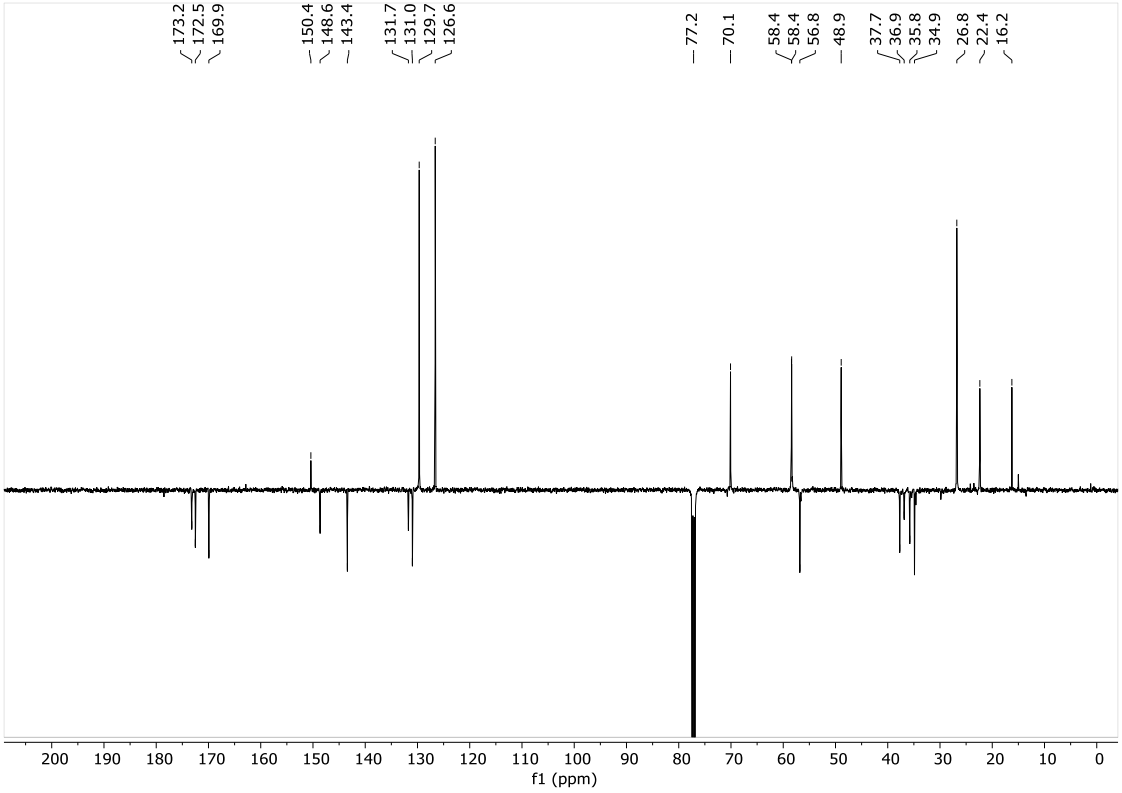

Figure 179: ^{13}C NMR (125 MHz, $CDCl_3$) of **196**.

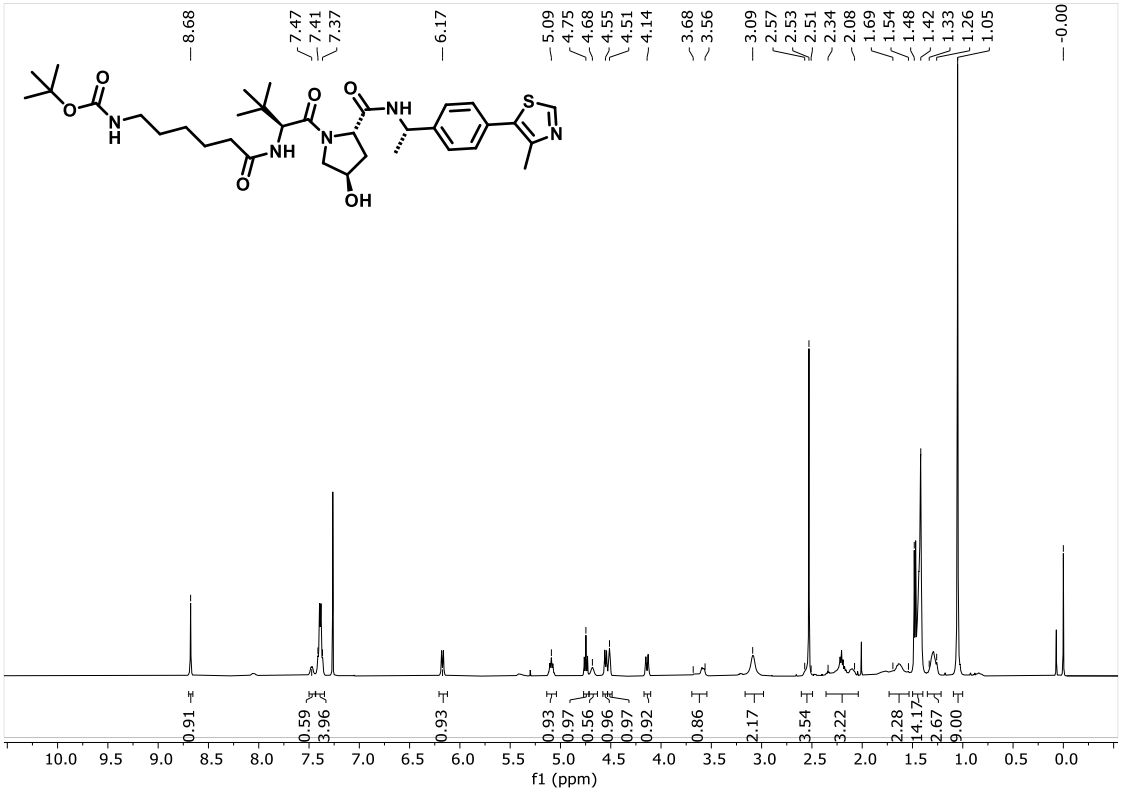

Figure 180: ^{1}H NMR (500 MHz, $CDCl_3$) of **193**.

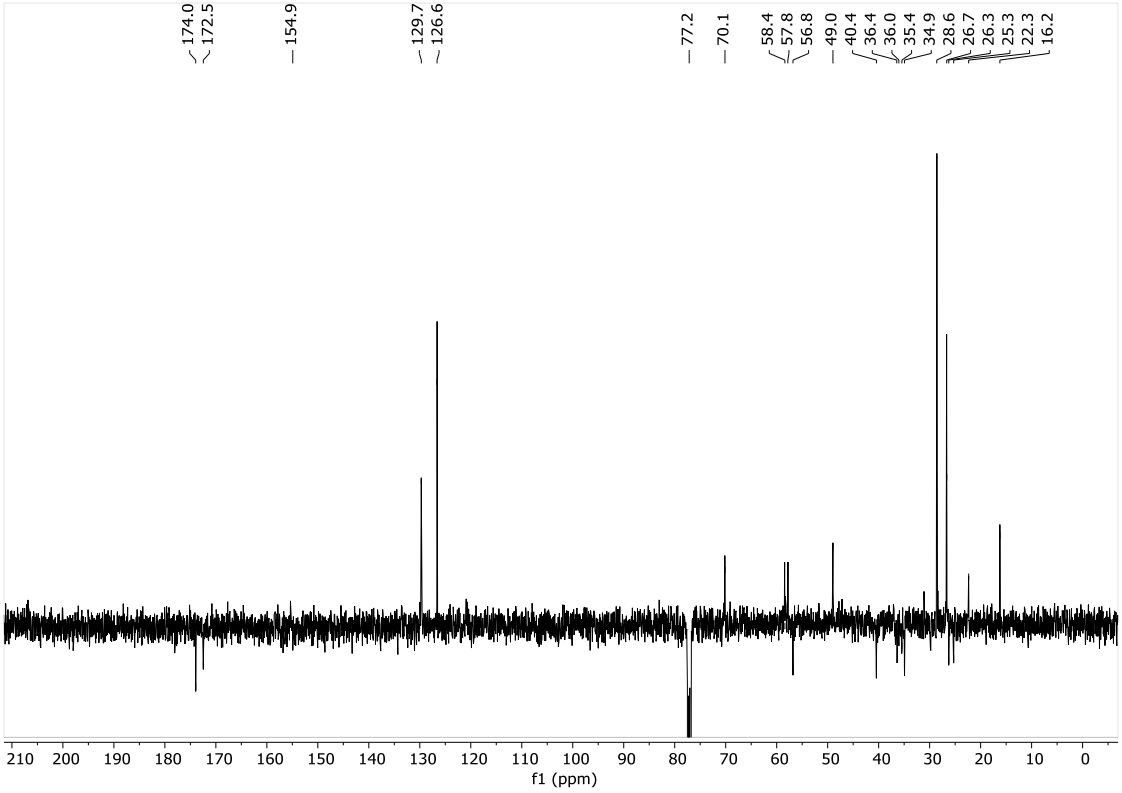

Figure 181: ^{13}C NMR (125 MHz, $CDCl_3$) of **193**.

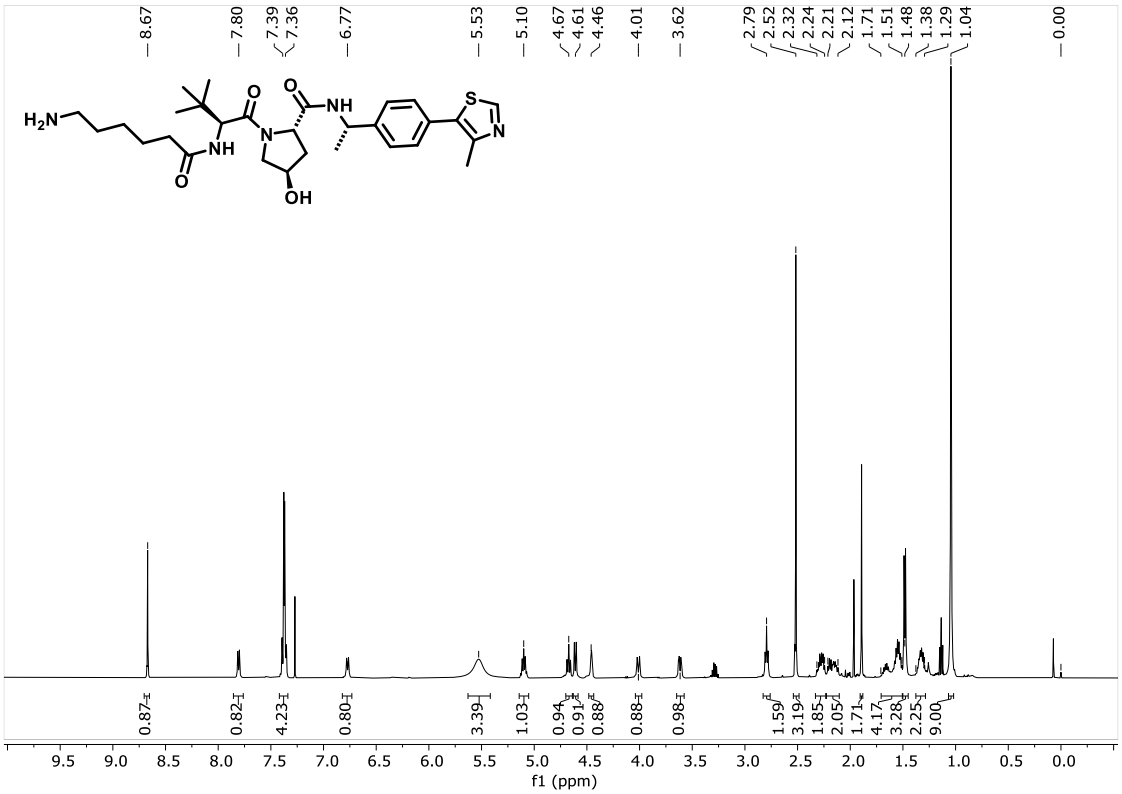

Figure 182: ^{1}H NMR (500 MHz, $CDCl_3$) of **197**.

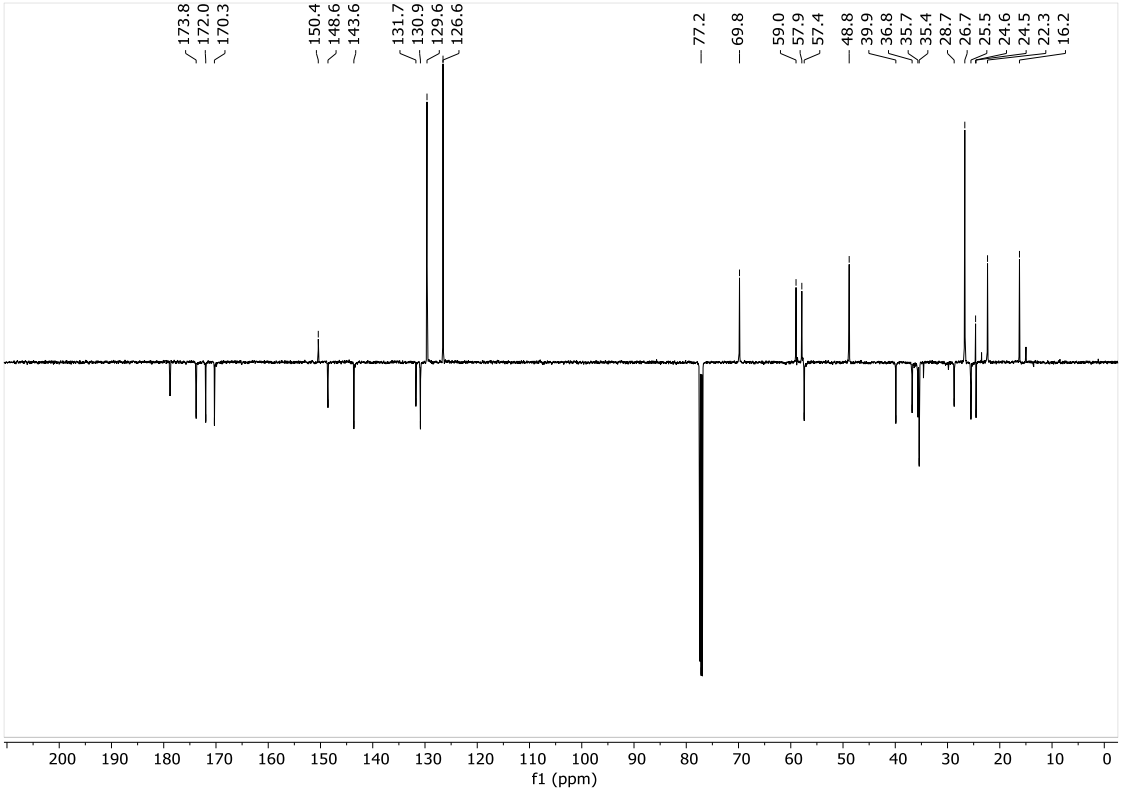

Figure 183: ^{13}C NMR (125 MHz, $CDCl_3$) of **197**.

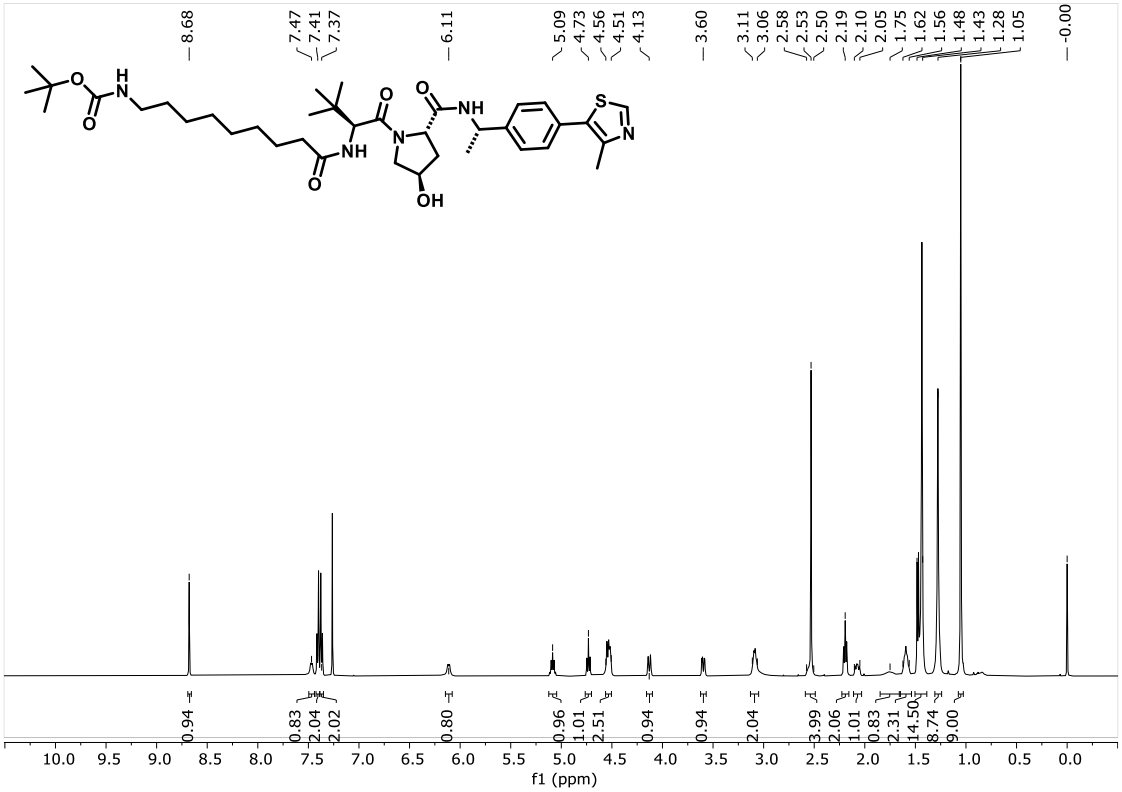

Figure 184: ^{1}H NMR (500 MHz, $CDCl_3$) of **194**.

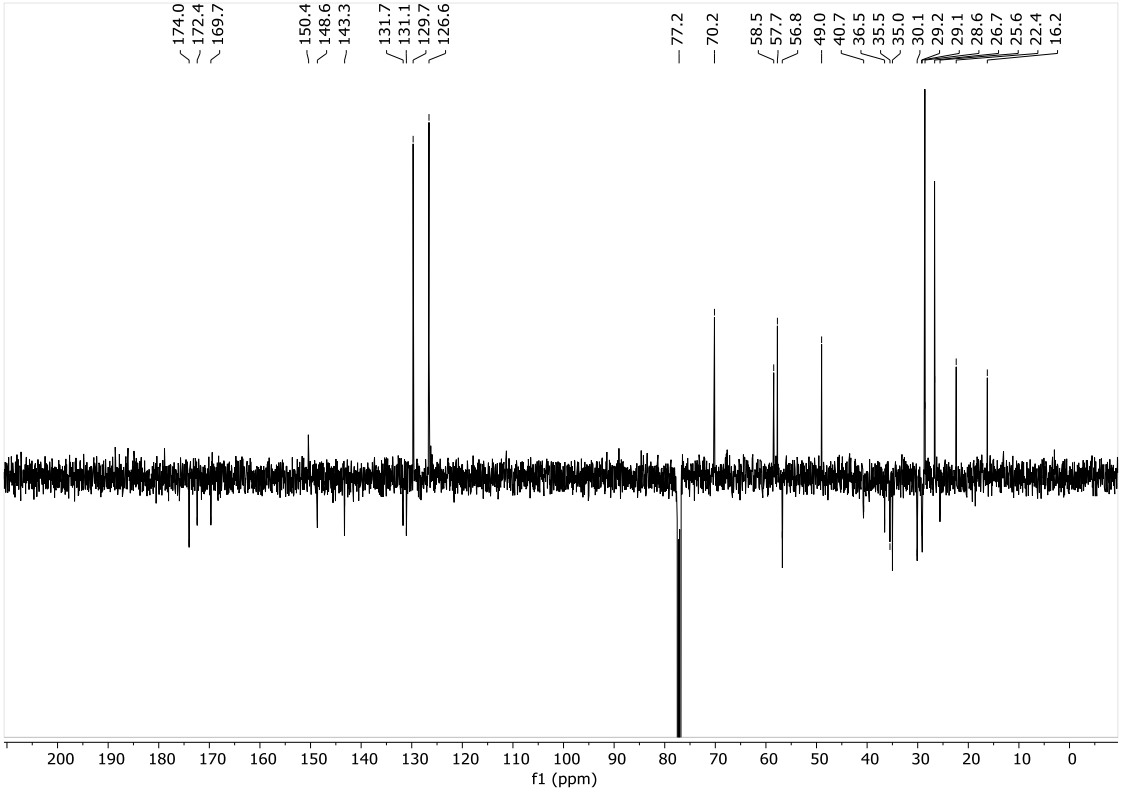

Figure 185: ^{13}C NMR (125 MHz, $CDCl_3$) of **194**.

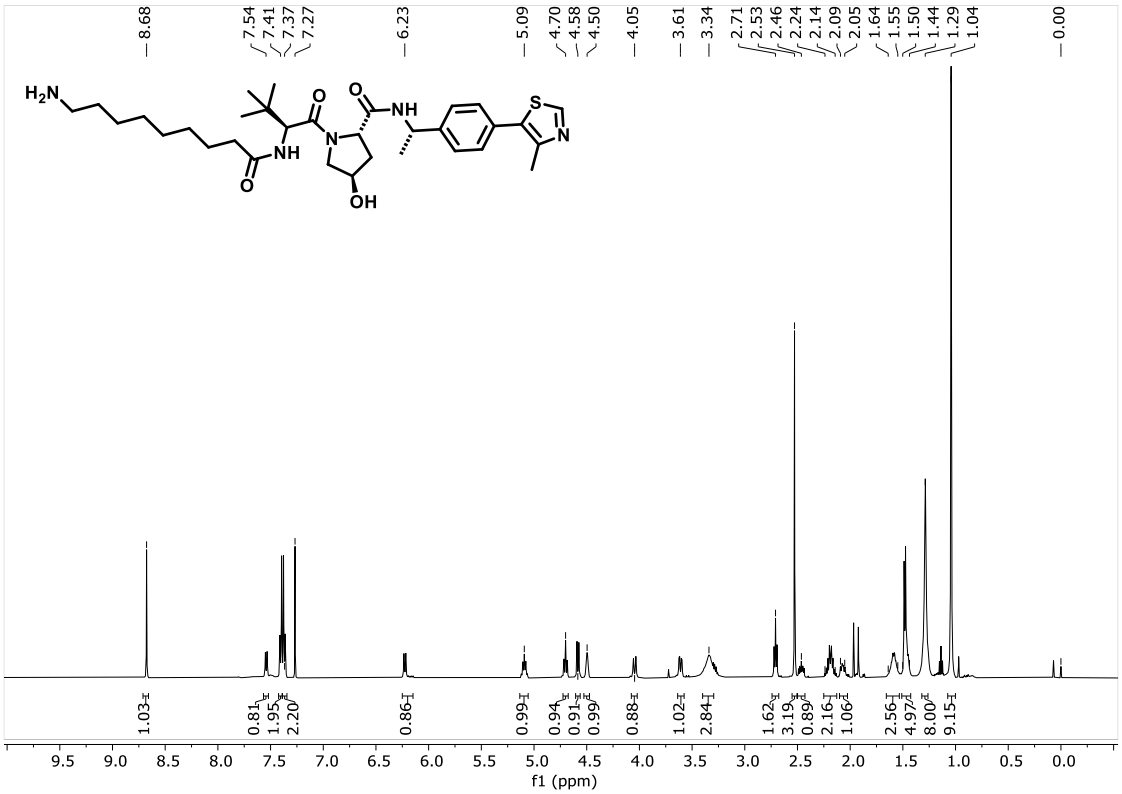

Figure 186: ^{1}H NMR (500 MHz, $CDCl_3$) of **198**.

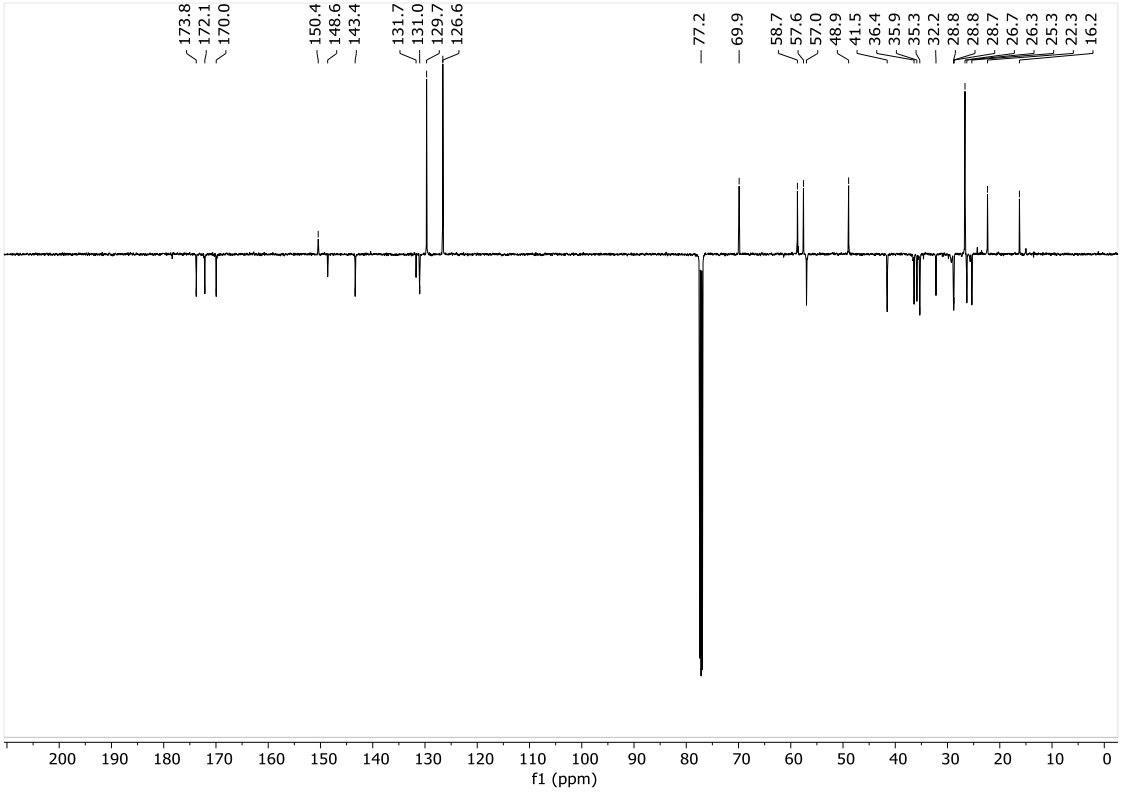

Figure 187: ^{13}C NMR (125 MHz, $CDCl_3$) of **198**.

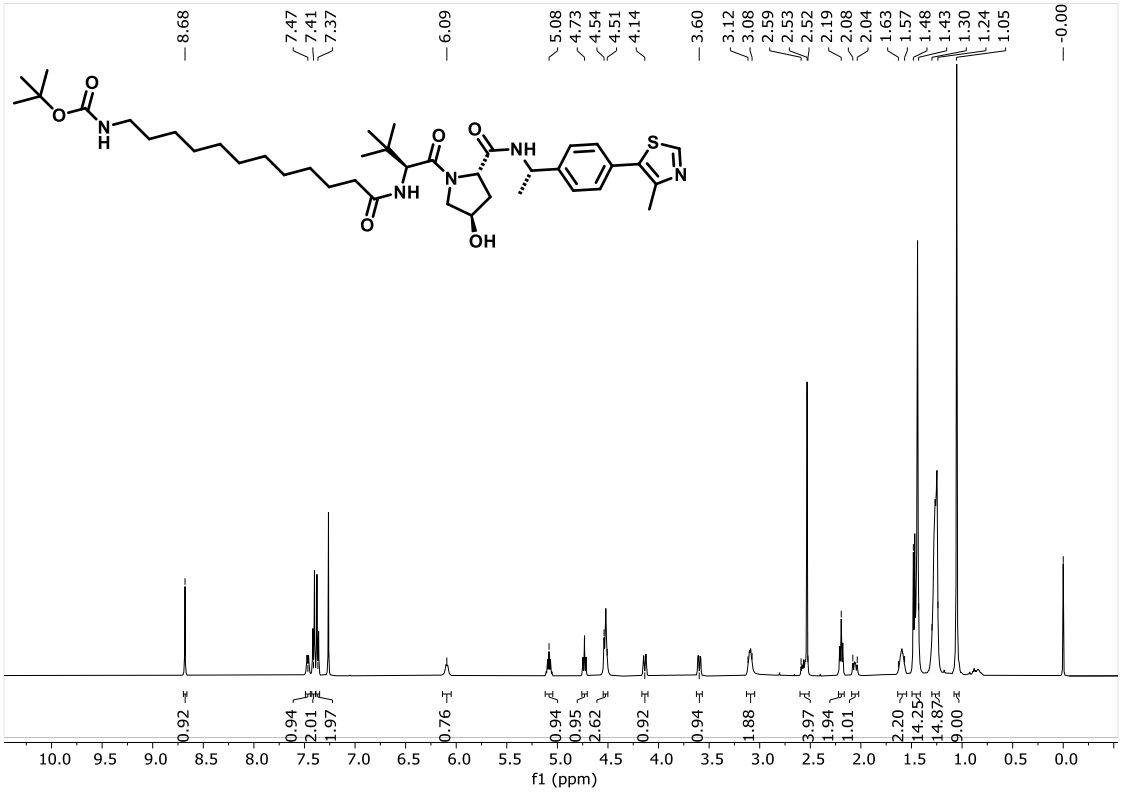

Figure 188: ^{1}H NMR (500 MHz, $CDCl_3$) of **195**.

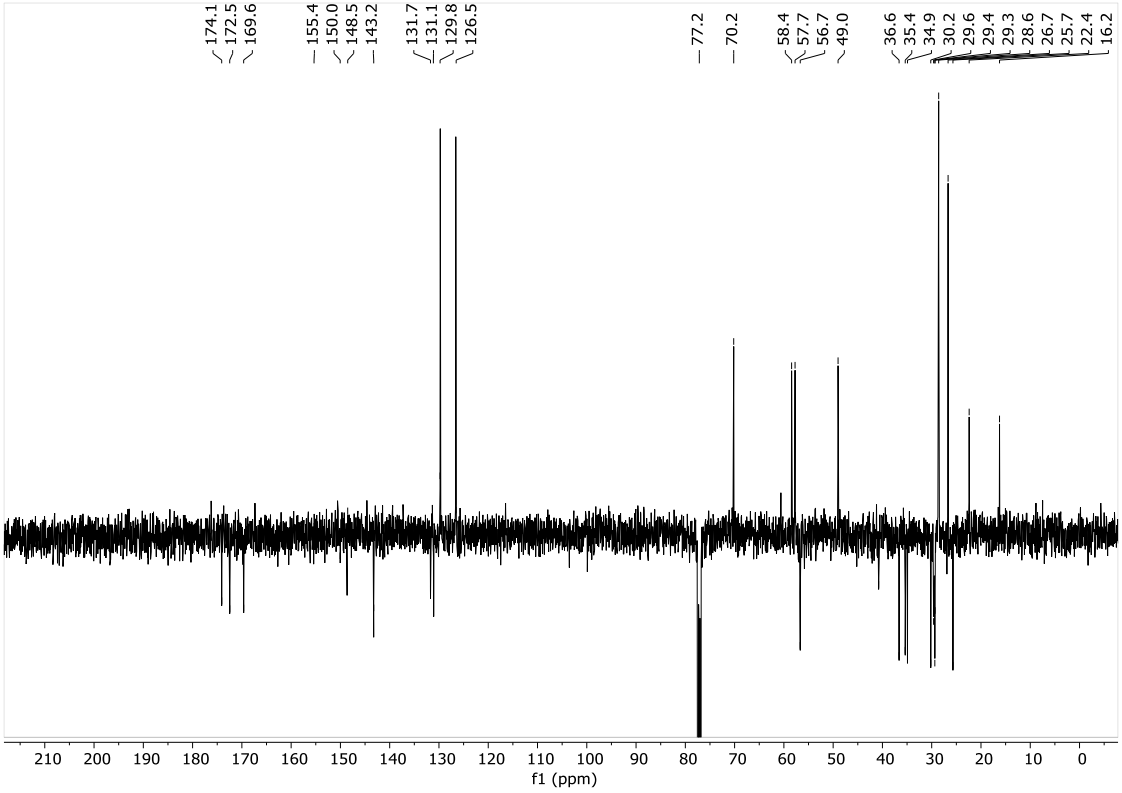

Figure 189: ^{13}C NMR (125 MHz, $CDCl_3$) of **195**.

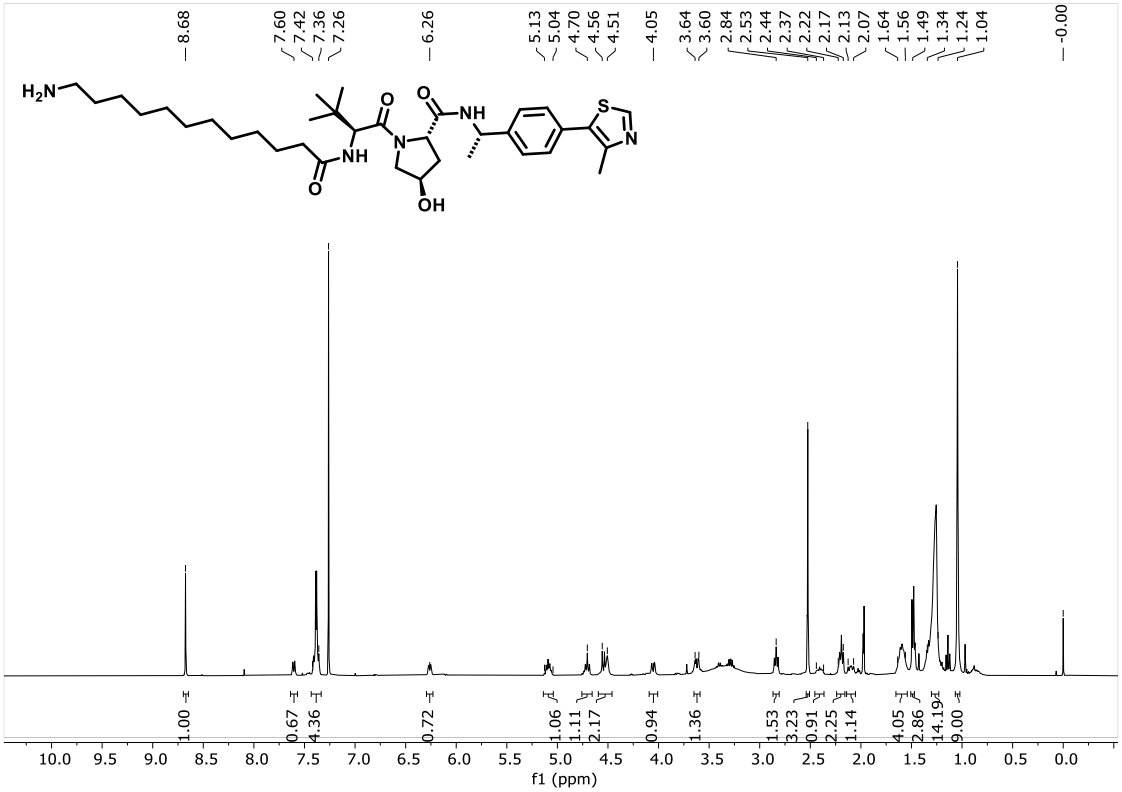

Figure 190: ^{1}H NMR (400 MHz, $CDCl_3$) of **199**.

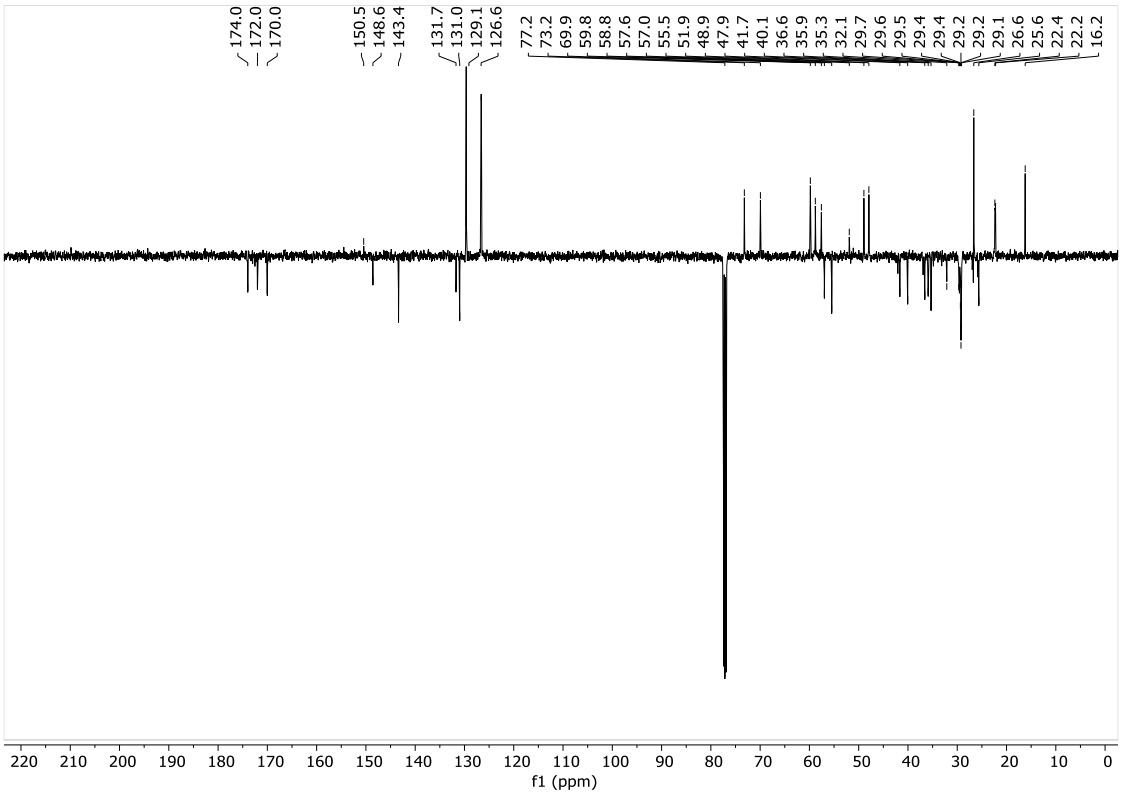

Figure 191: ^{13}C NMR (125 MHz, $CDCl_3$) of **199**.

7.3 HPLC Chromatograms of Small Molecules

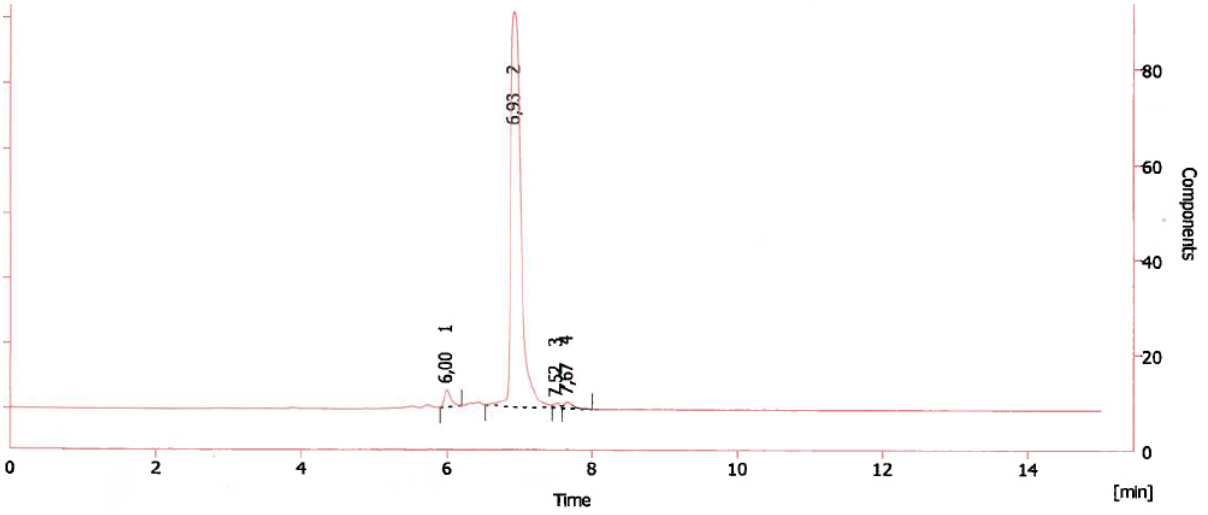

Figure 192: HPLC UV chromatogram of **53**.

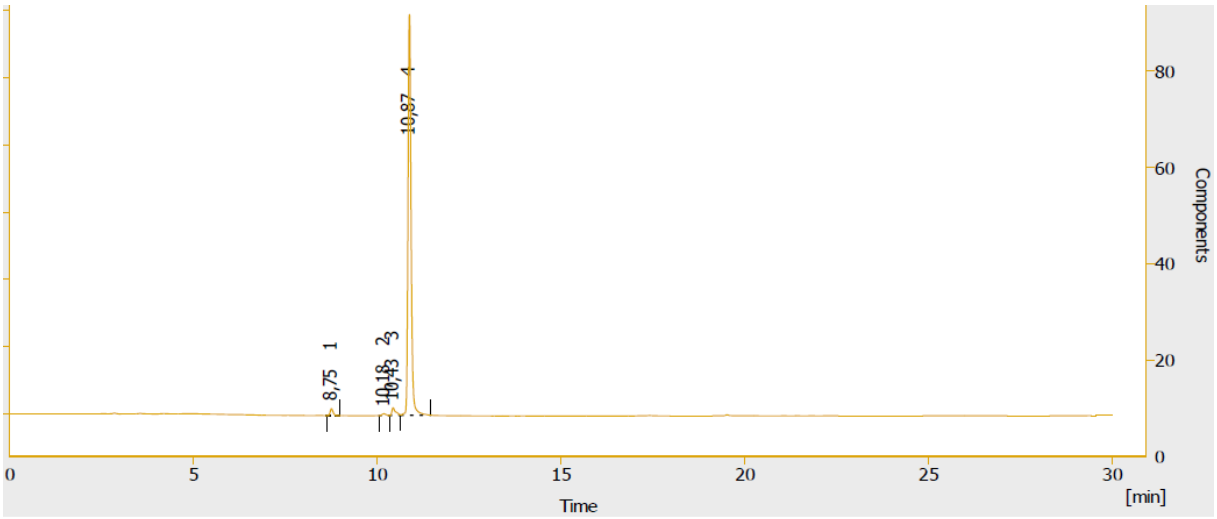

Figure 193: HPLC UV chromatogram of **60**.

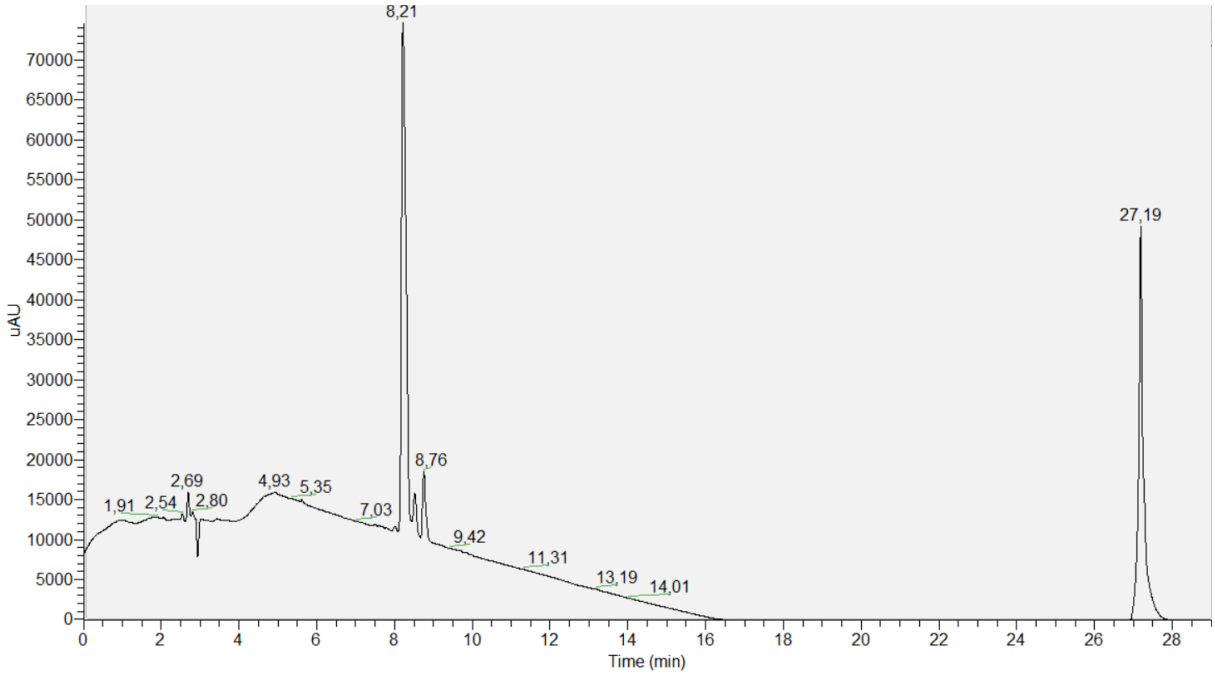

Figure 194: HPLC UV chromatogram of **109**.

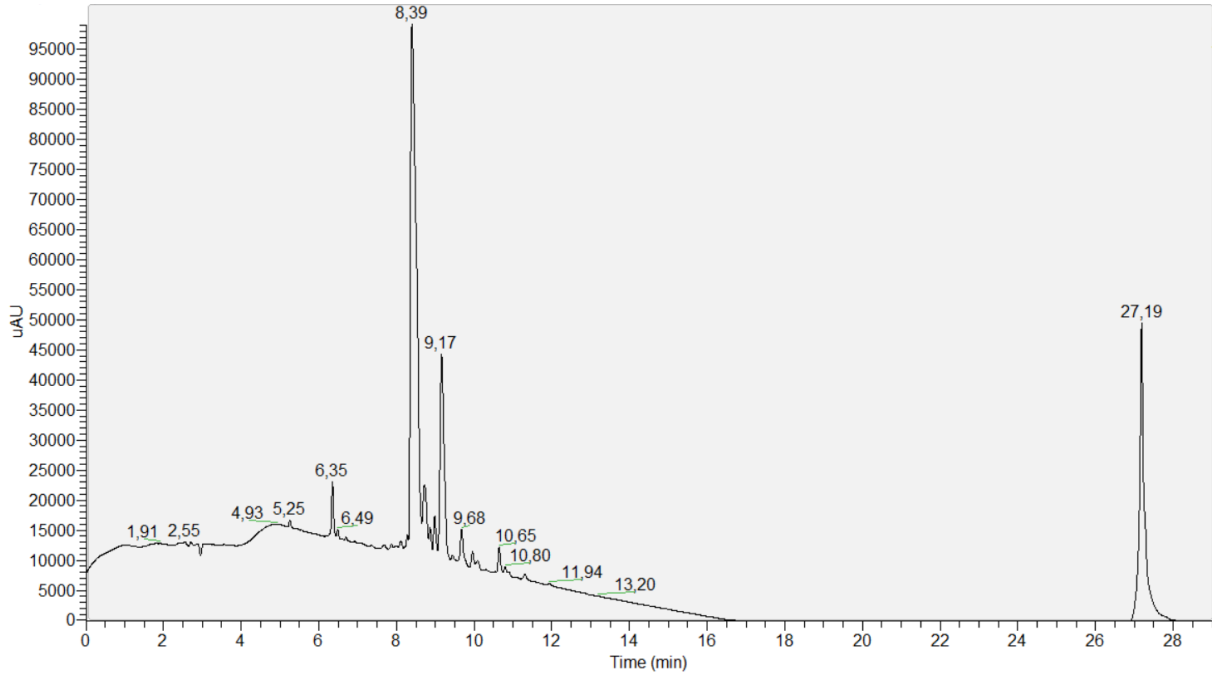

Figure 195: HPLC UV chromatogram of **111**.

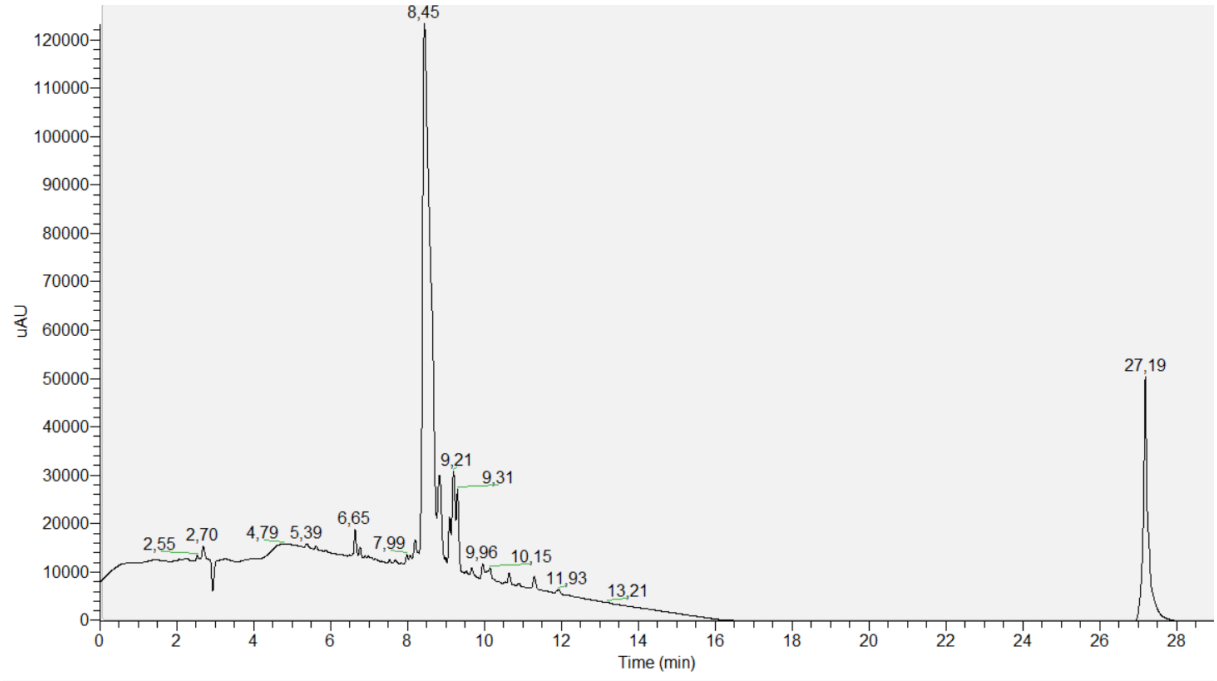

Figure 196: HPLC UV chromatogram of **112**.

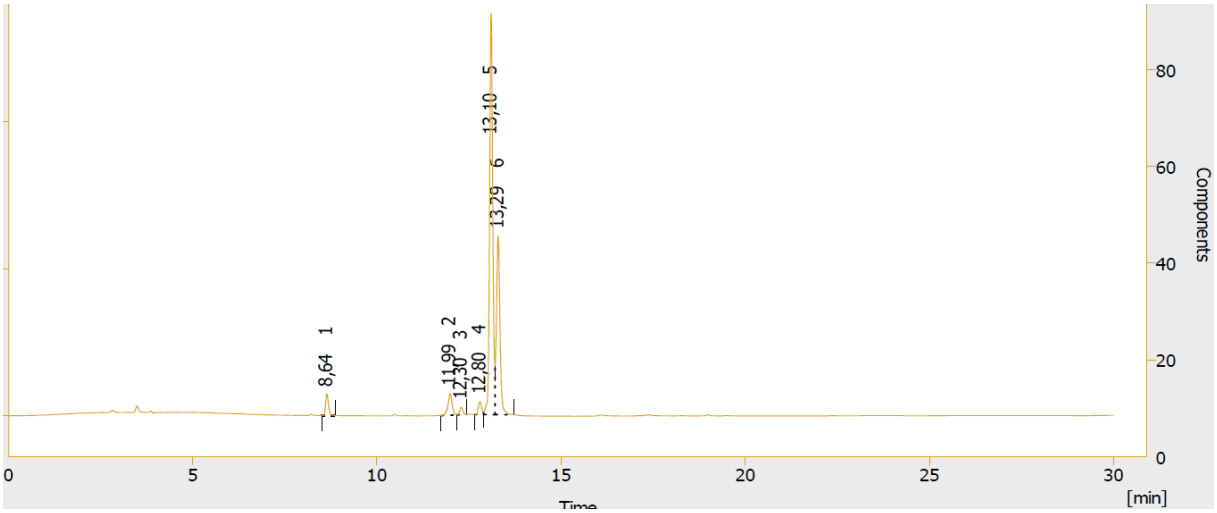

Figure 197: HPLC UV chromatogram of **116**.

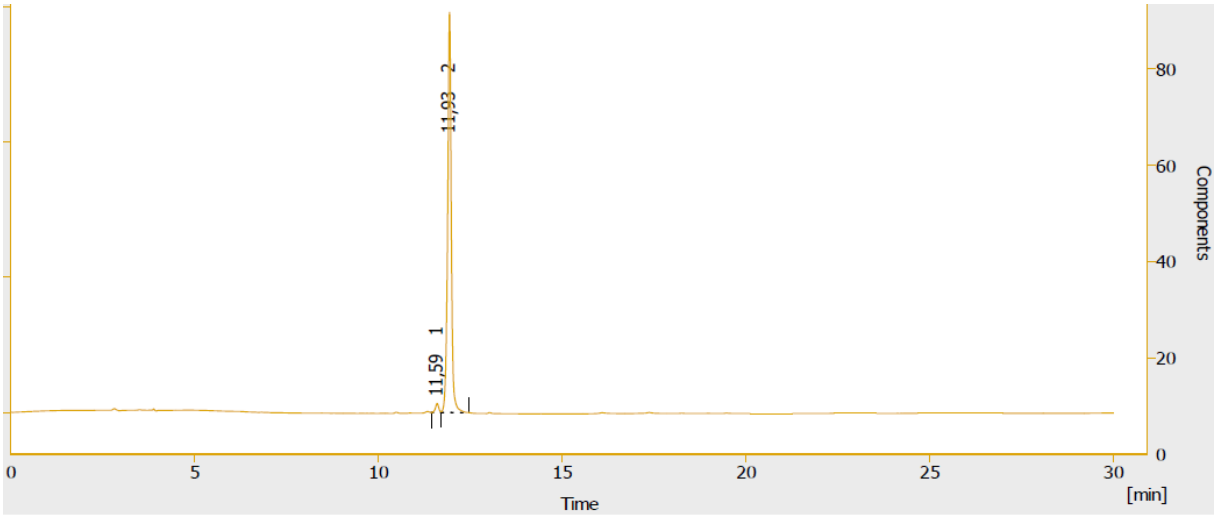

Figure 198: HPLC UV chromatogram of **117**.

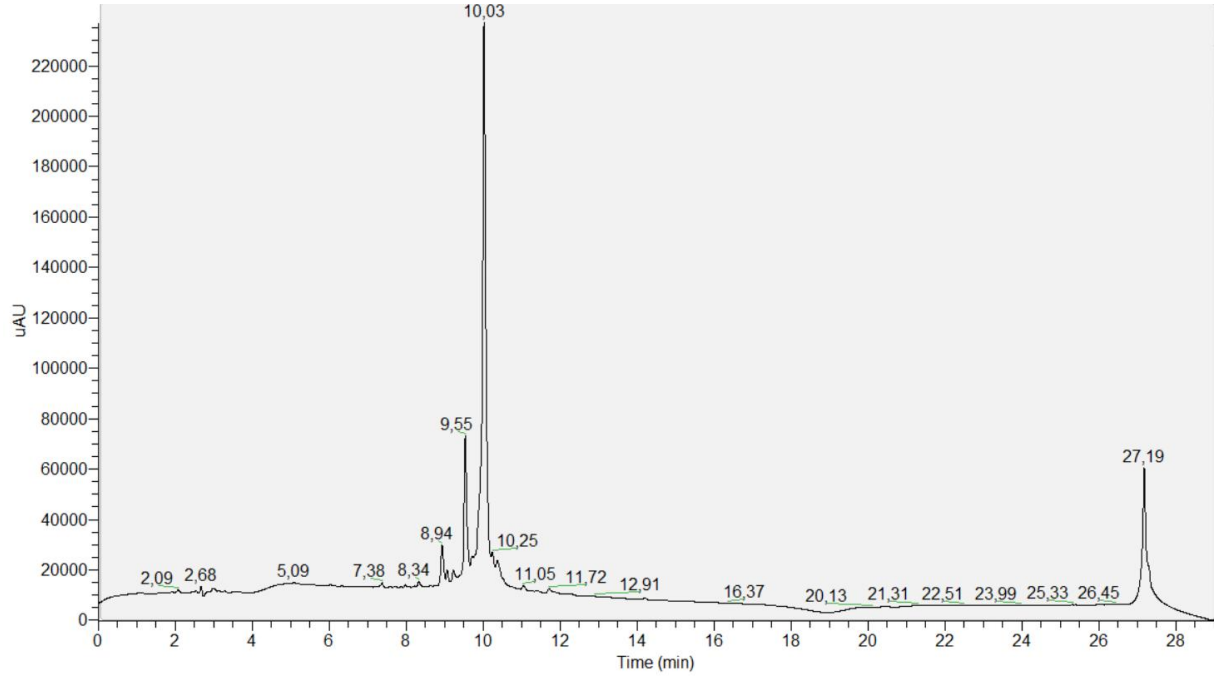

Figure 199: HPLC UV chromatogram of **133**.

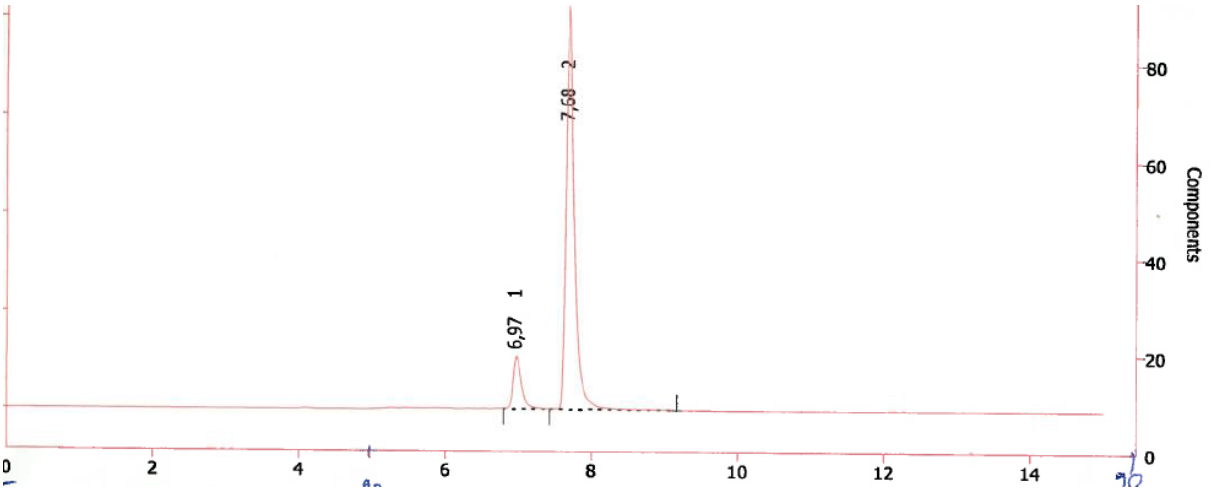

Figure 200: HPLC UV chromatogram of **118**.

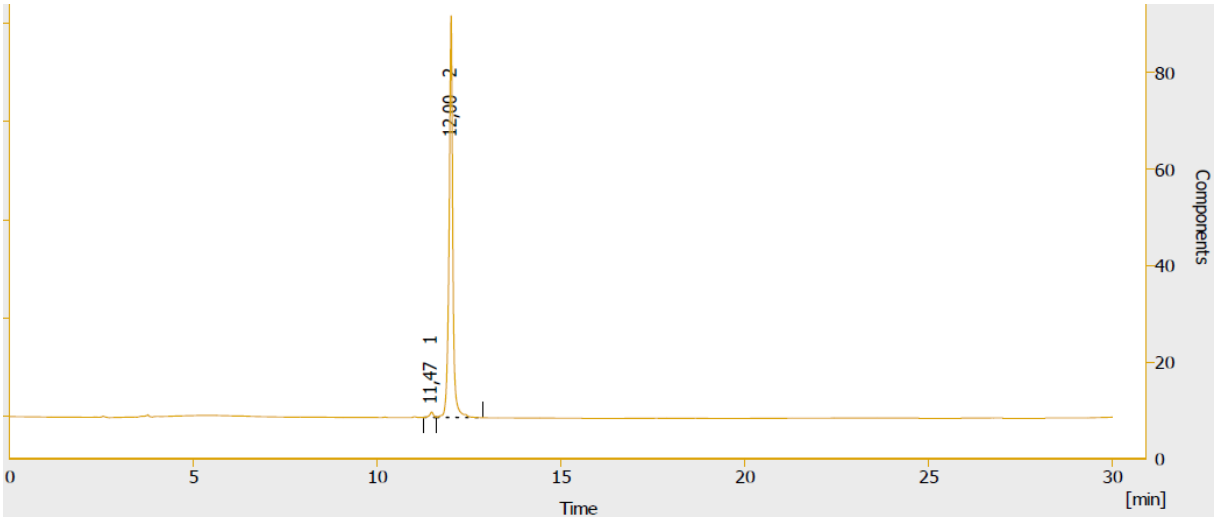

Figure 201: HPLC UV chromatogram of **132**.

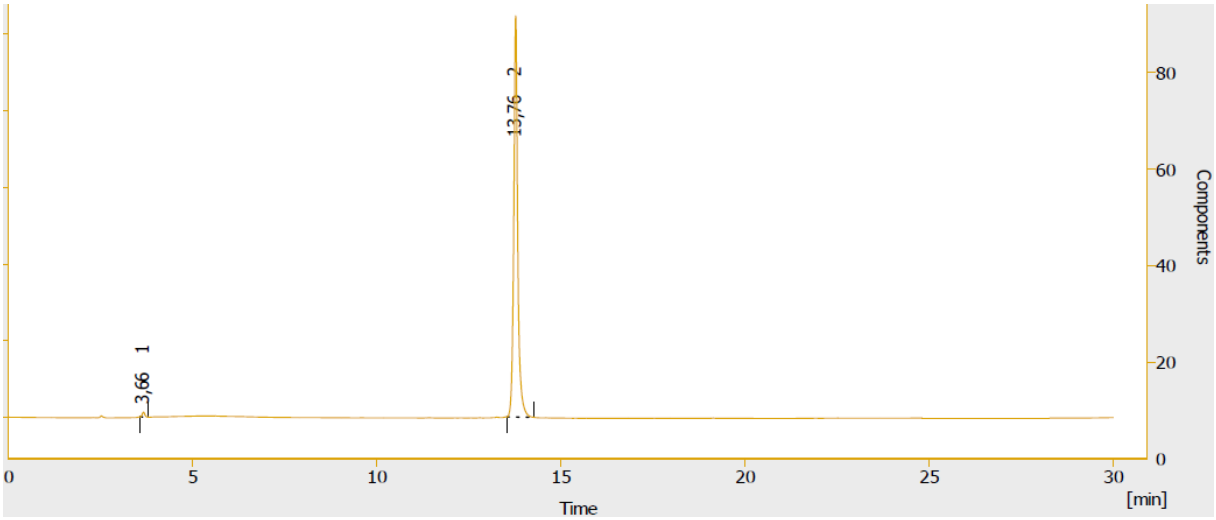

Figure 202: HPLC UV chromatogram of **134**.

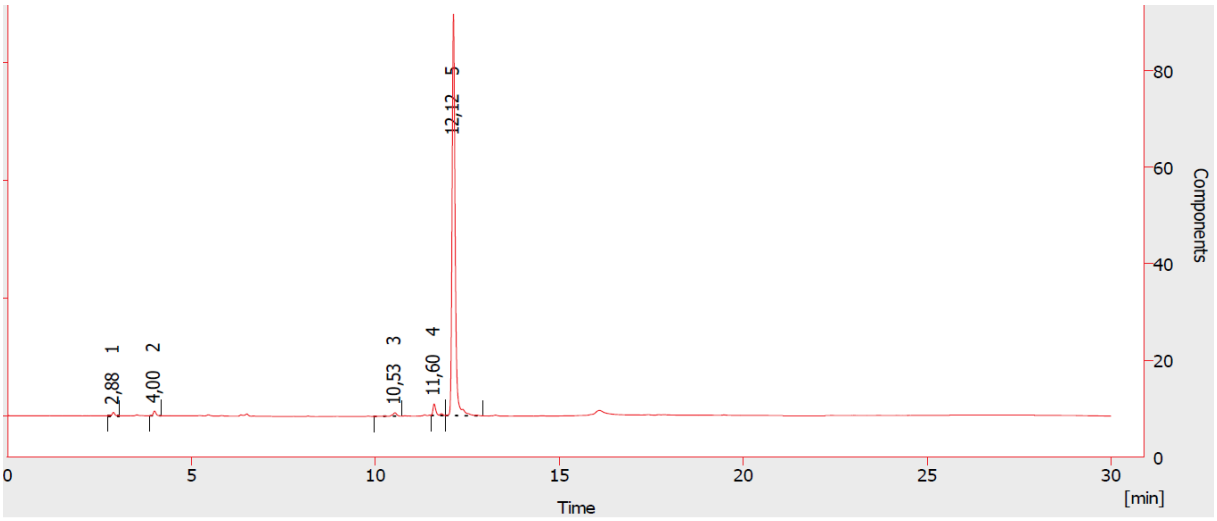

Figure 203: HPLC UV chromatogram of ***epi*-118**.

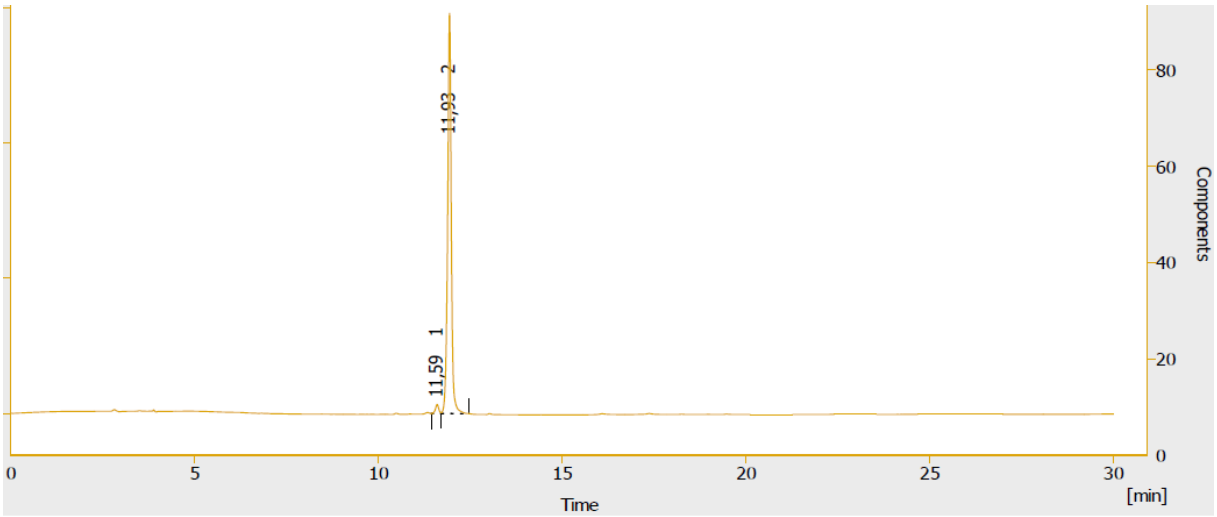

Figure 204: HPLC UV chromatogram of **119**.

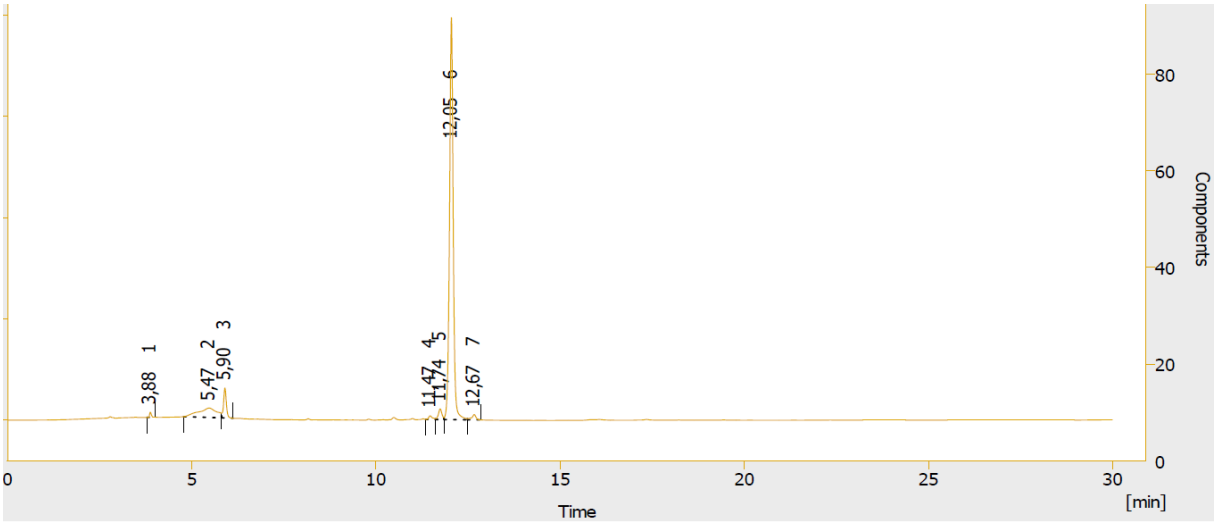

Figure 205: HPLC UV chromatogram of **120**.

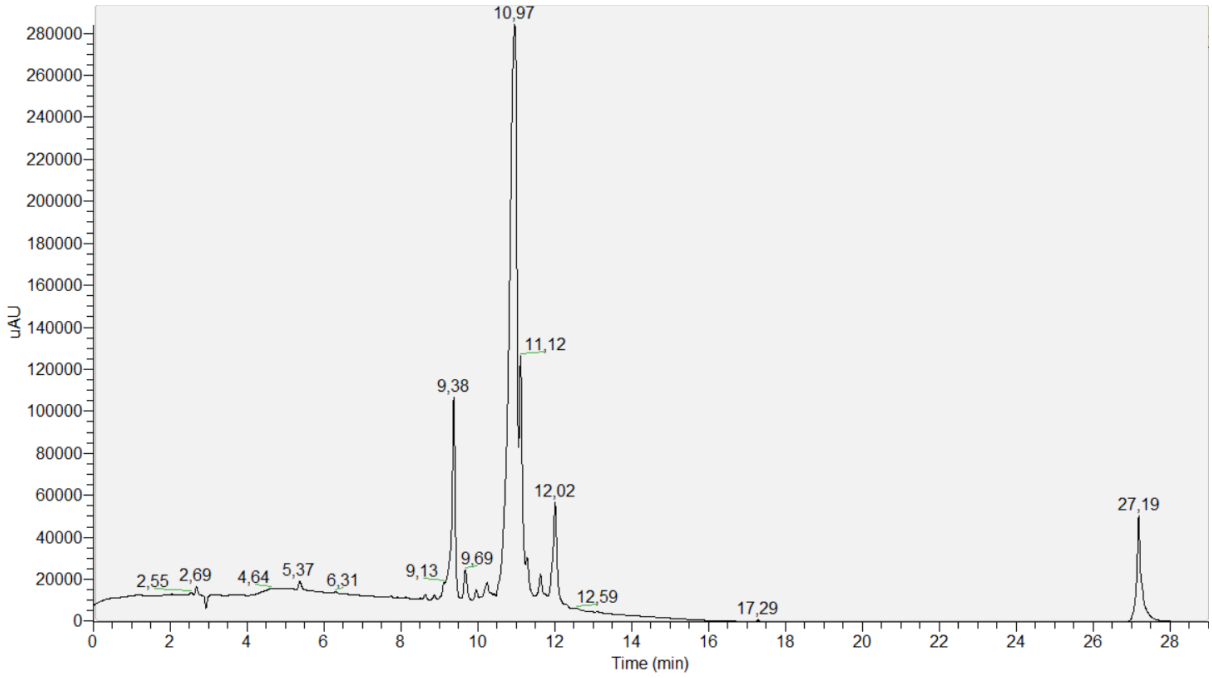

Figure 206: HPLC UV chromatogram of **172**.

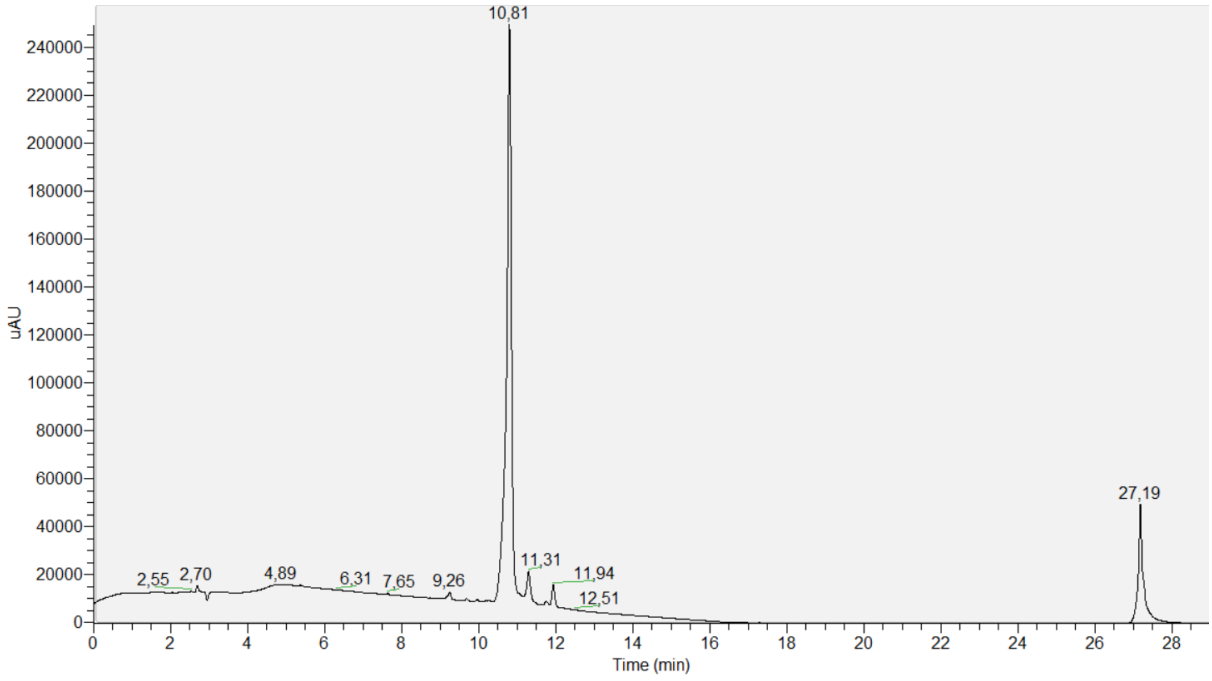

Figure 207: HPLC UV chromatogram of **173**.

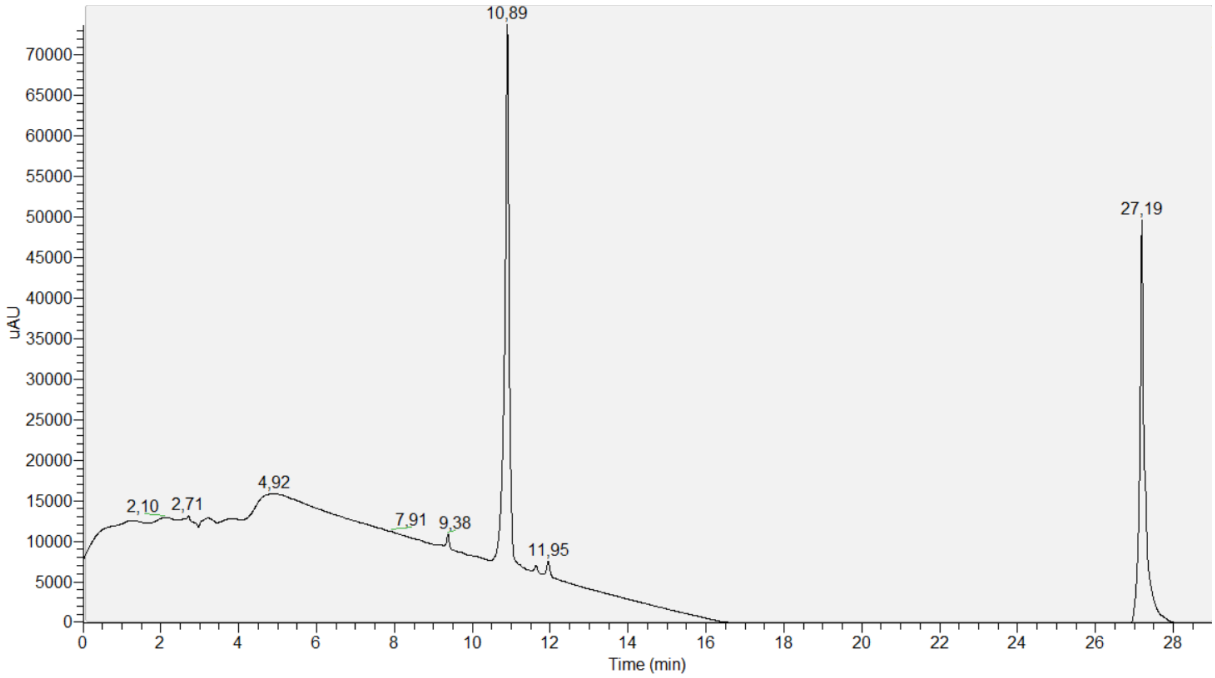

Figure 208: HPLC UV chromatogram of **174**.

7.4 LC-MS Chromatograms of Small Molecules

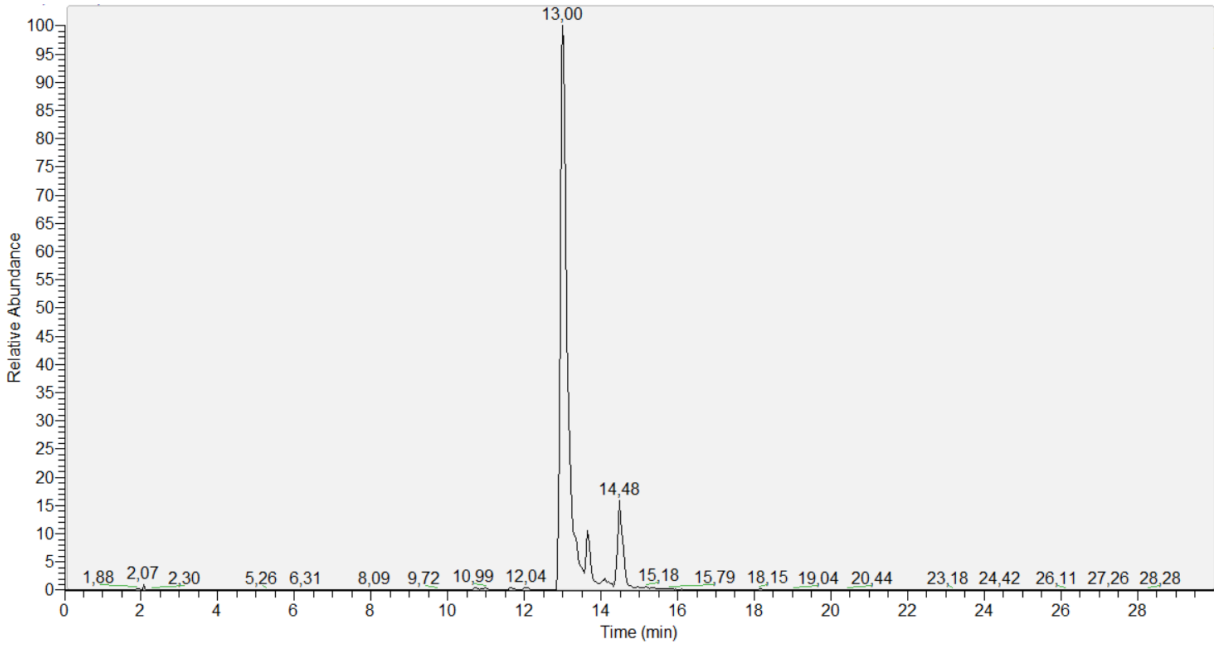

Figure 209: LC-MS total ion count chromatogram of **38**.

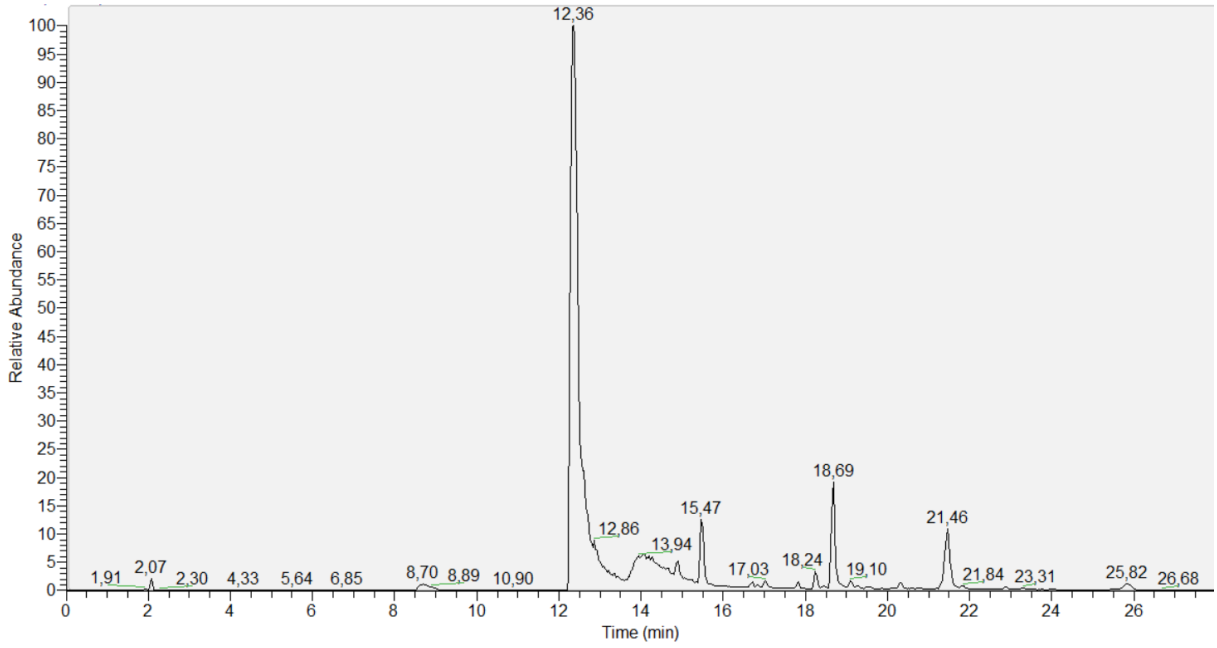

Figure 210: LC-MS total ion count chromatogram of **55**.

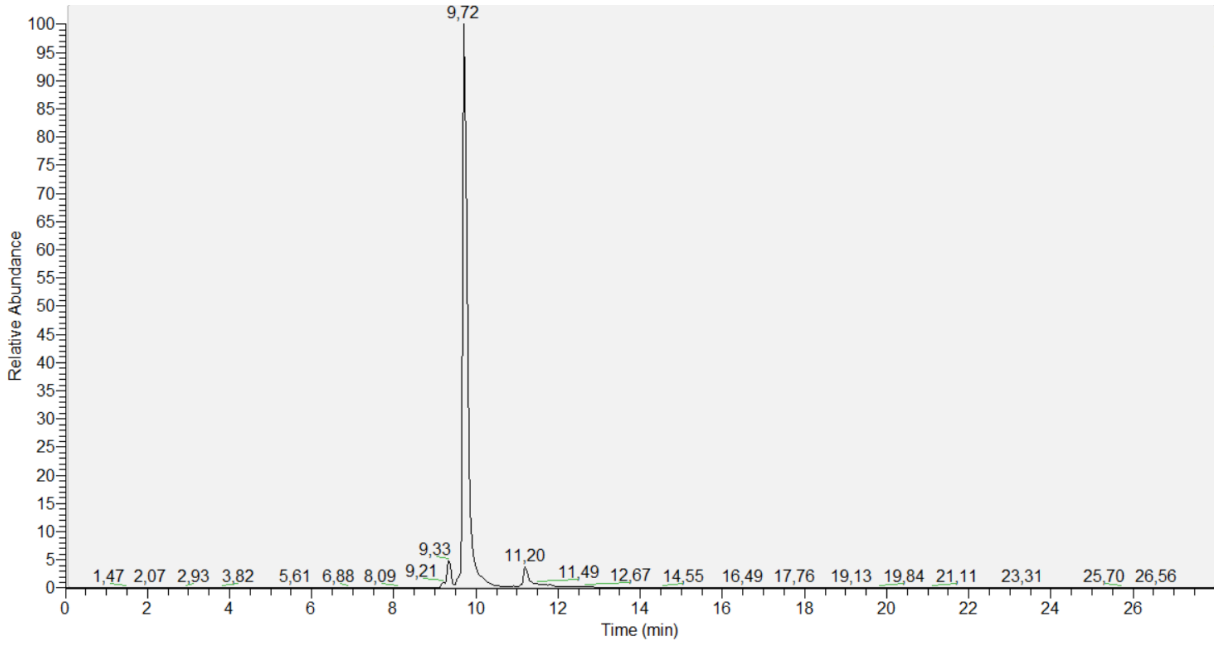

Figure 211: LC-MS total ion count chromatogram of **66**.

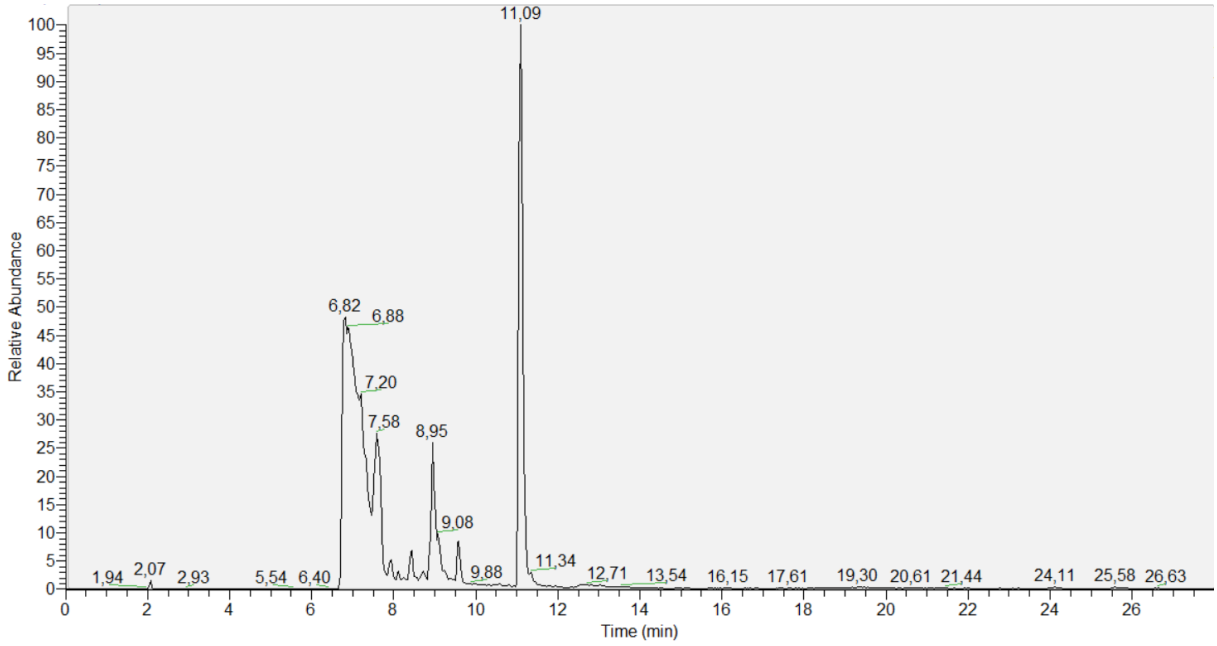

Figure 212: LC-MS total ion count chromatogram of **98**.

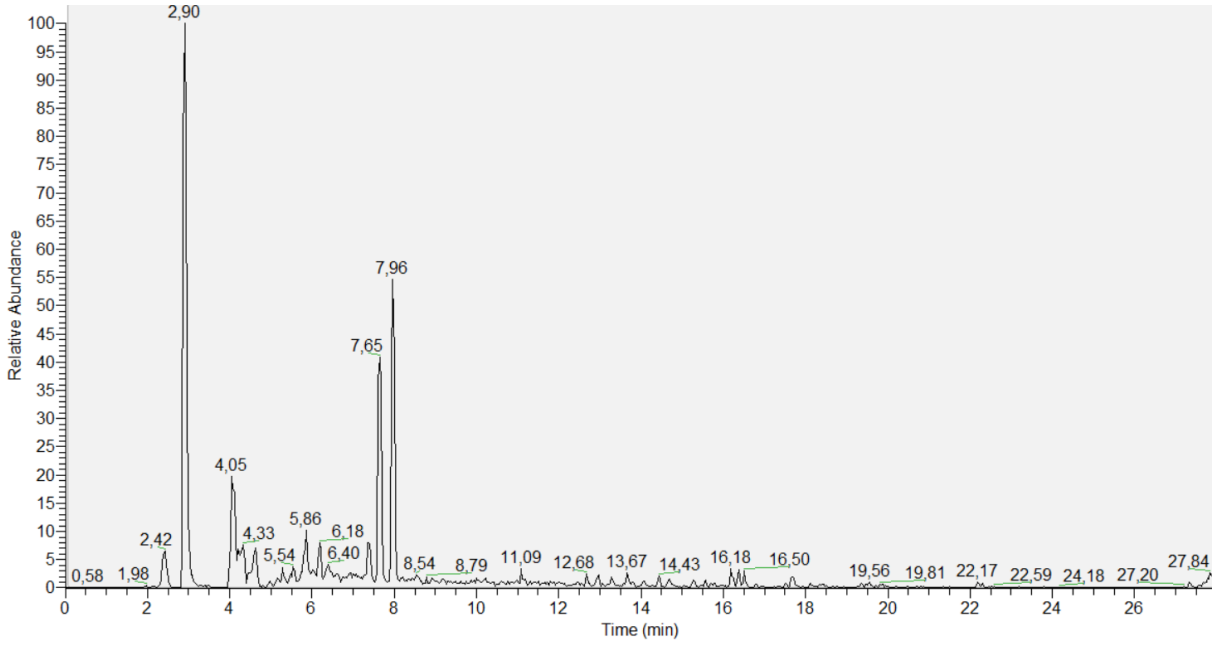

Figure 213: LC-MS total ion count chromatogram of **106**.

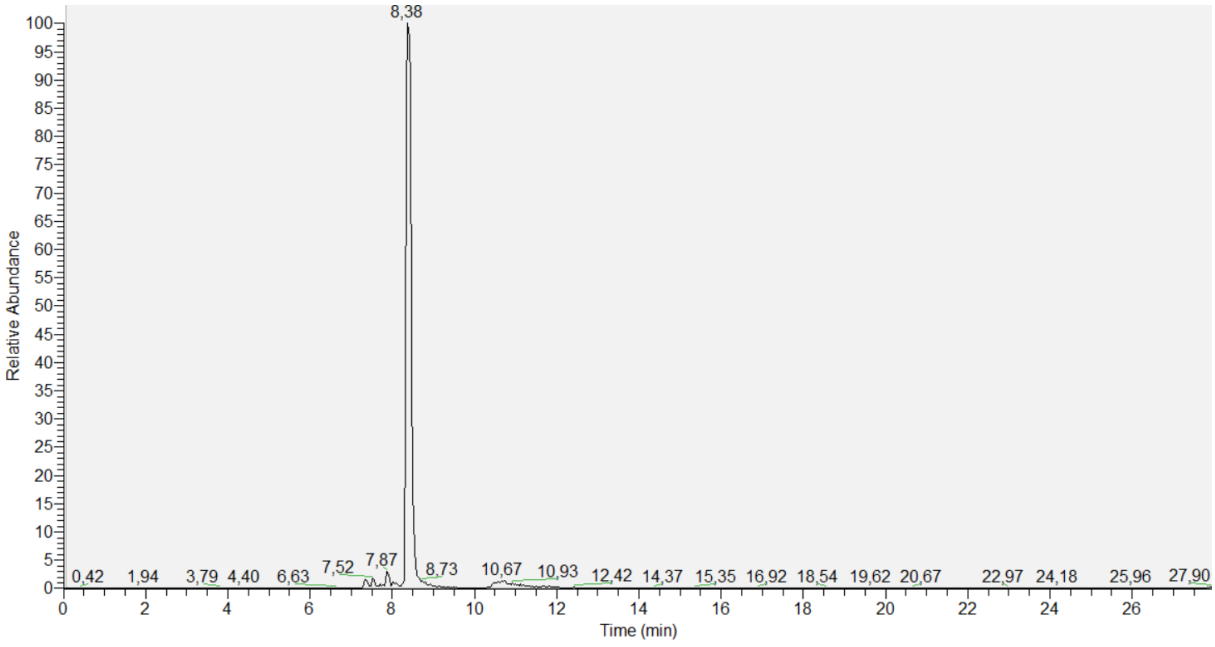

Figure 214: LC-MS total ion count chromatogram of **110**.

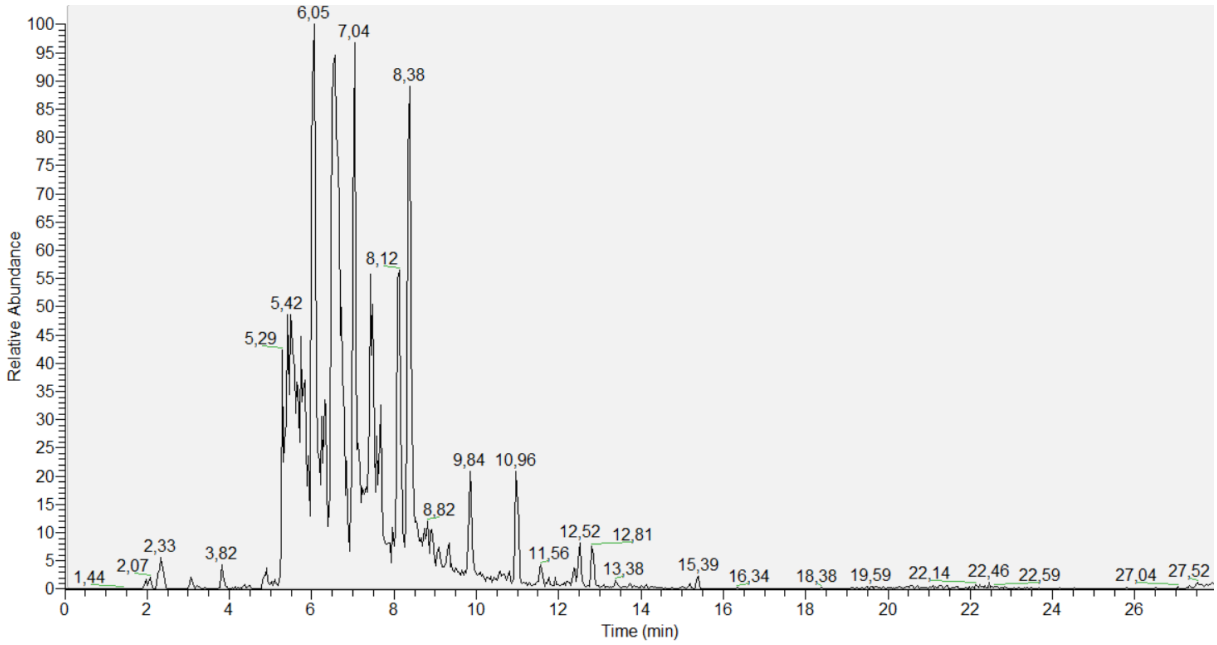

Figure 215: LC-MS total ion count chromatogram of **108**.

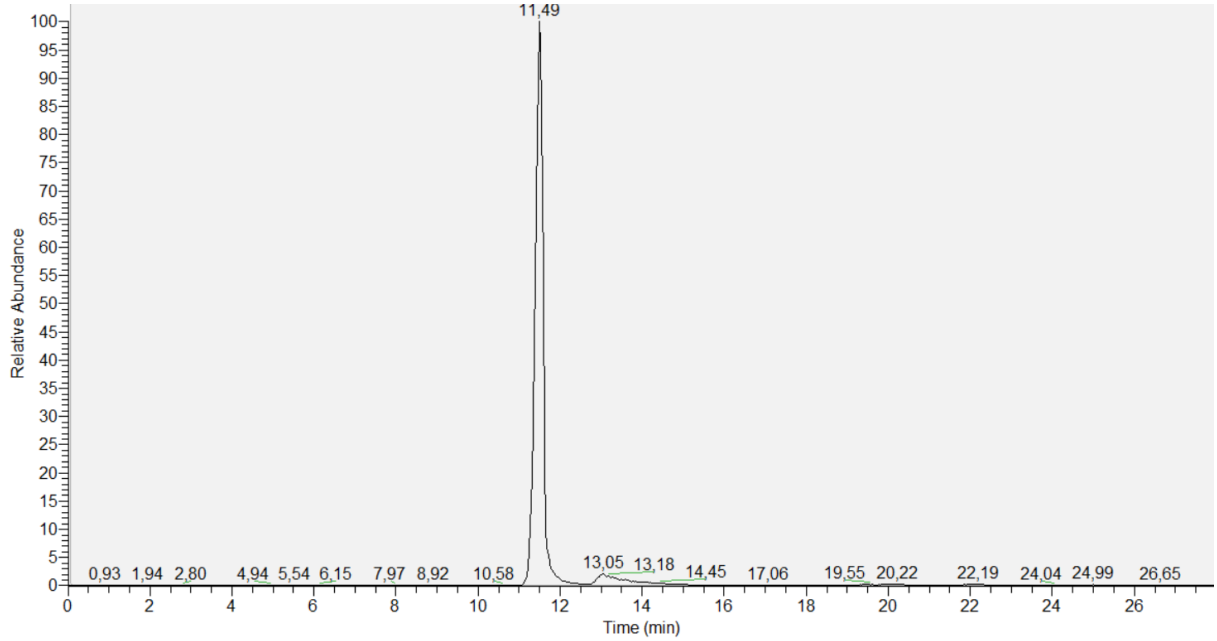

Figure 216: LC-MS total ion count chromatogram of **114**.

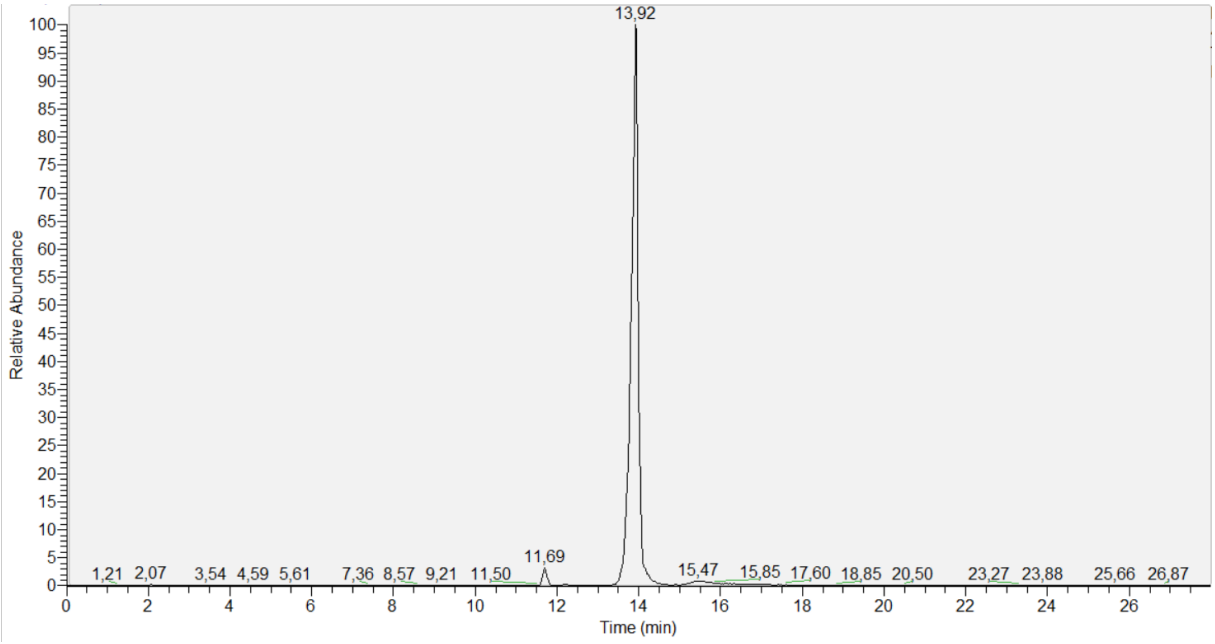

Figure 217: LC-MS total ion count chromatogram of **115**.

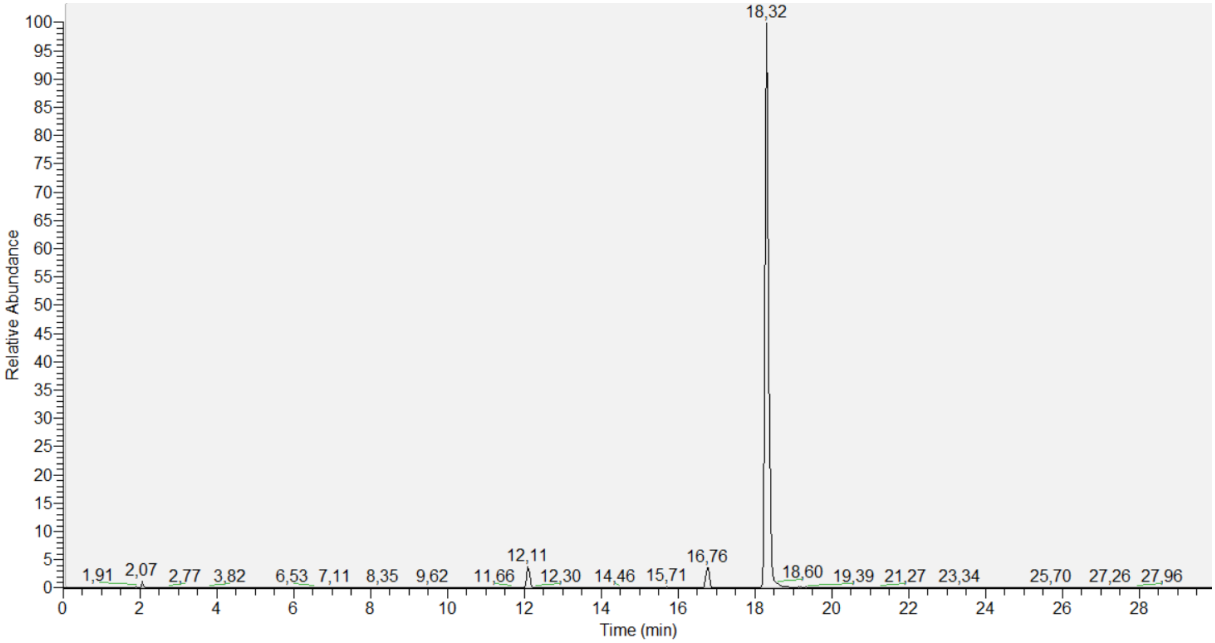

Figure 218: LC-MS total ion count chromatogram of **135**.

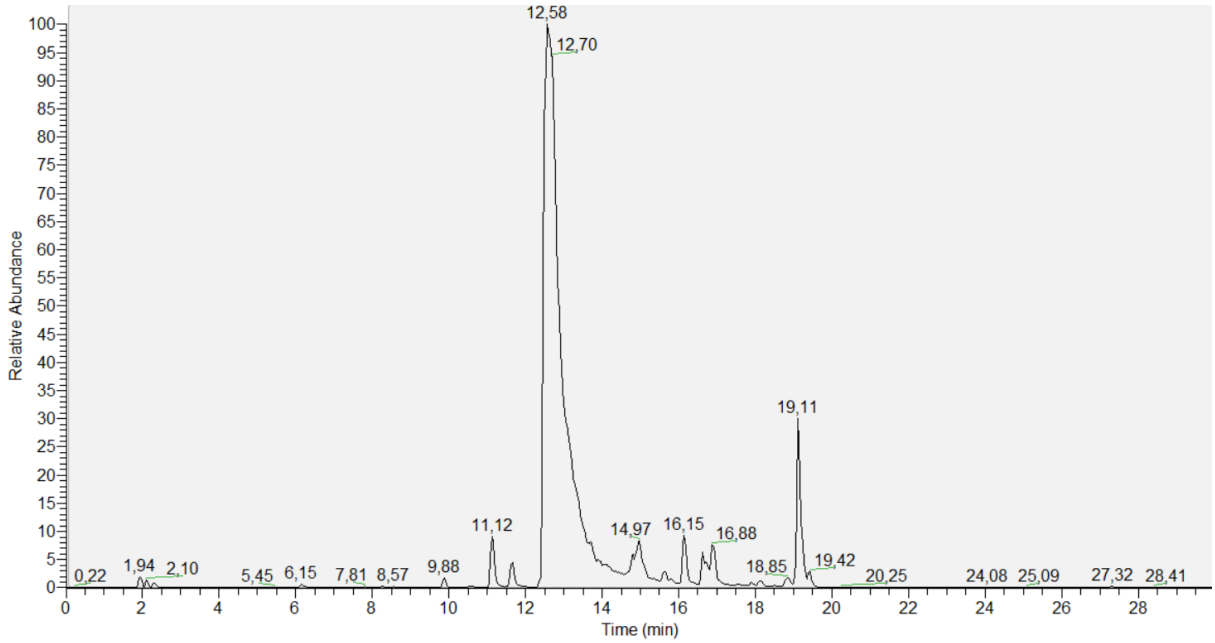

Figure 219: LC-MS total ion count chromatogram of **144**.

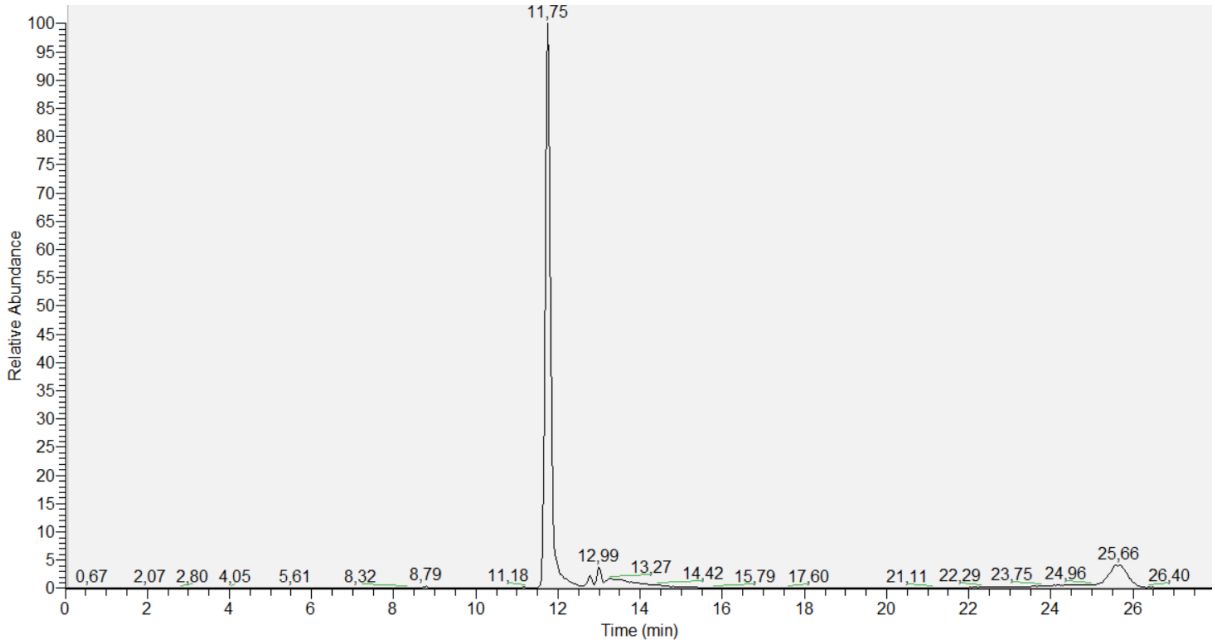

Figure 220: LC-MS total ion count chromatogram of ***epi*-114**.

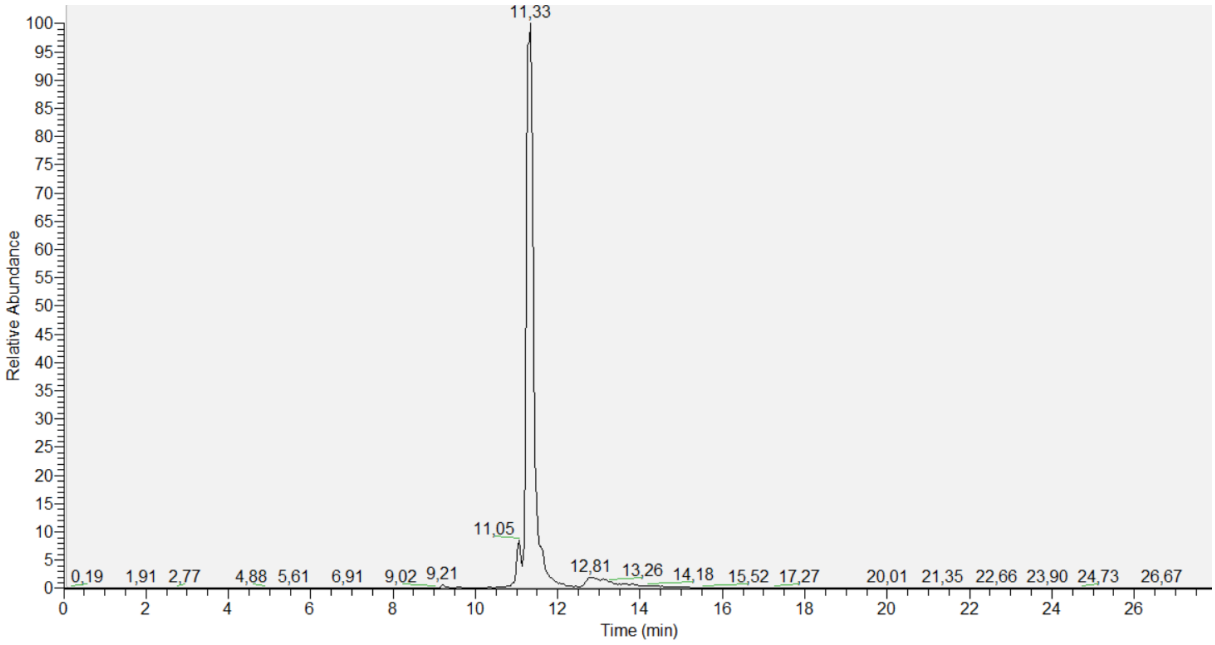

Figure 221: LC-MS total ion count chromatogram of ***epi*-118**.

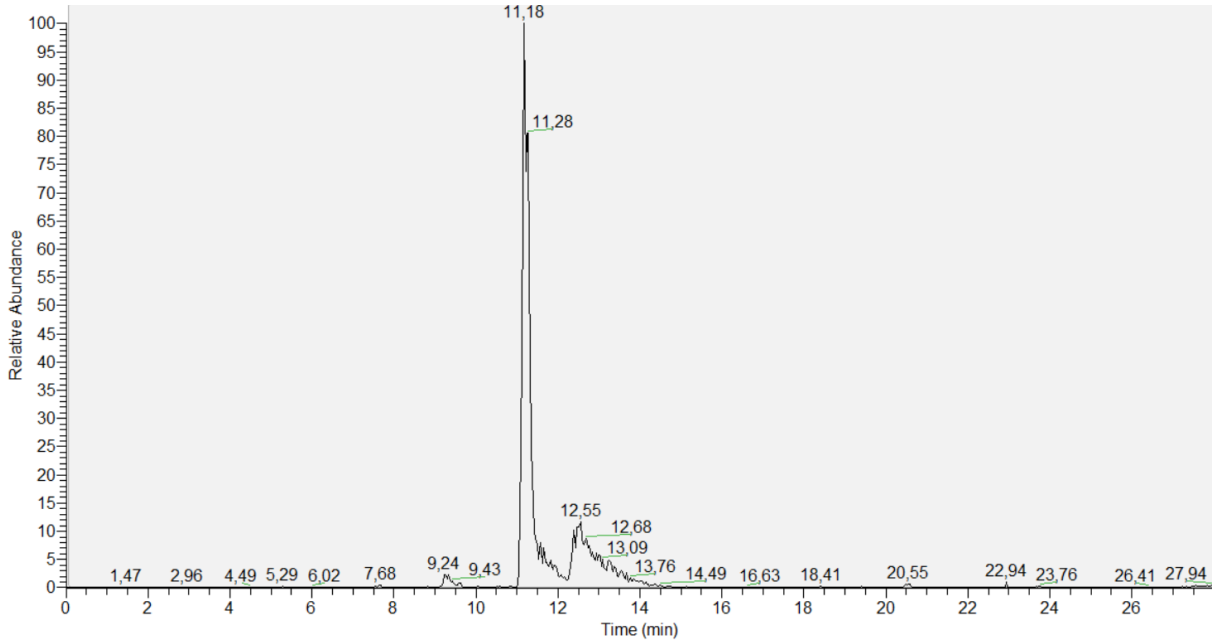

Figure 222: LC-MS total ion count chromatogram of **152**.

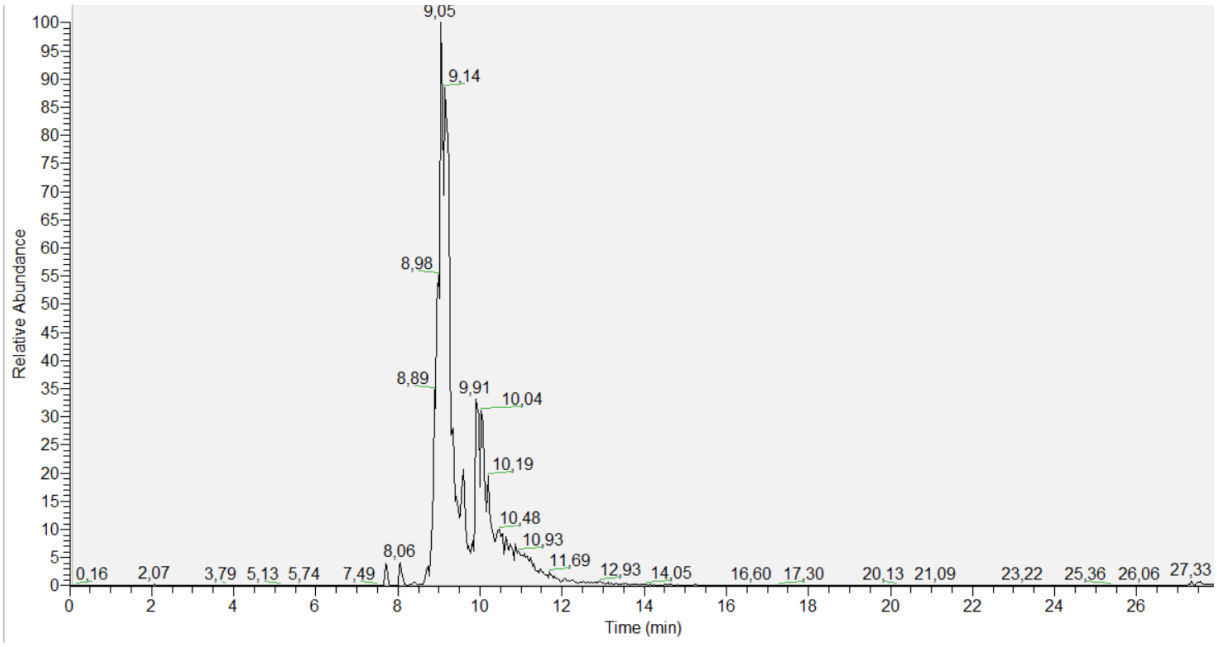

Figure 223: LC-MS total ion count chromatogram of **168**.

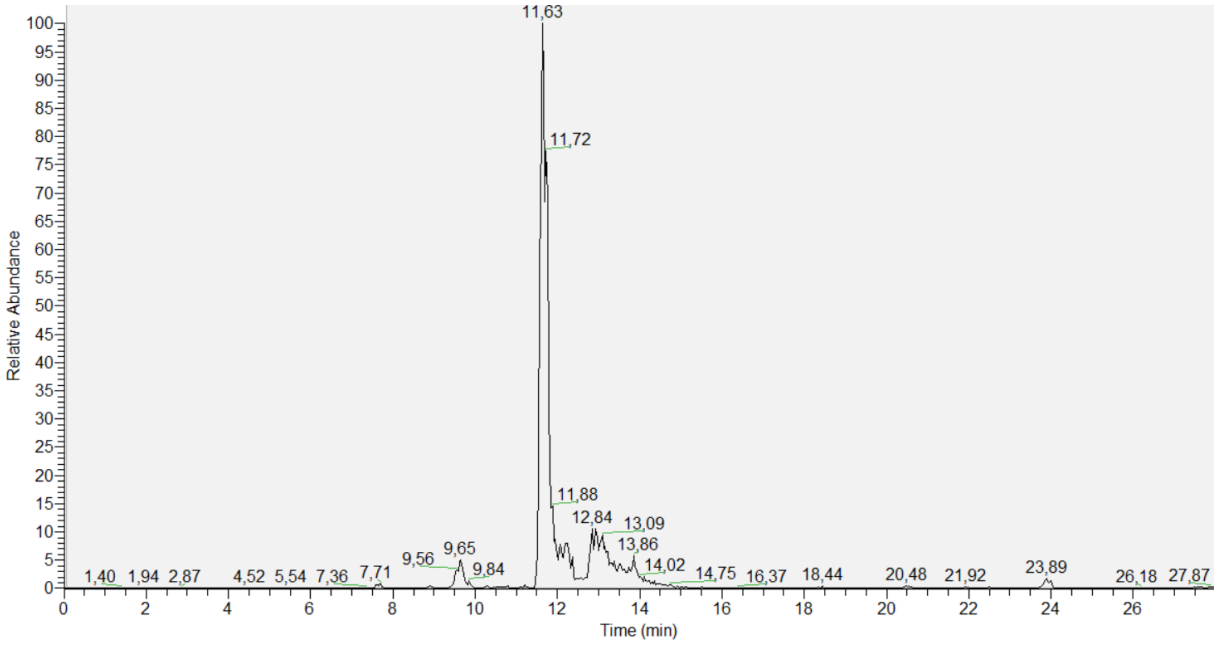

Figure 224: LC-MS total ion count chromatogram of **153**.

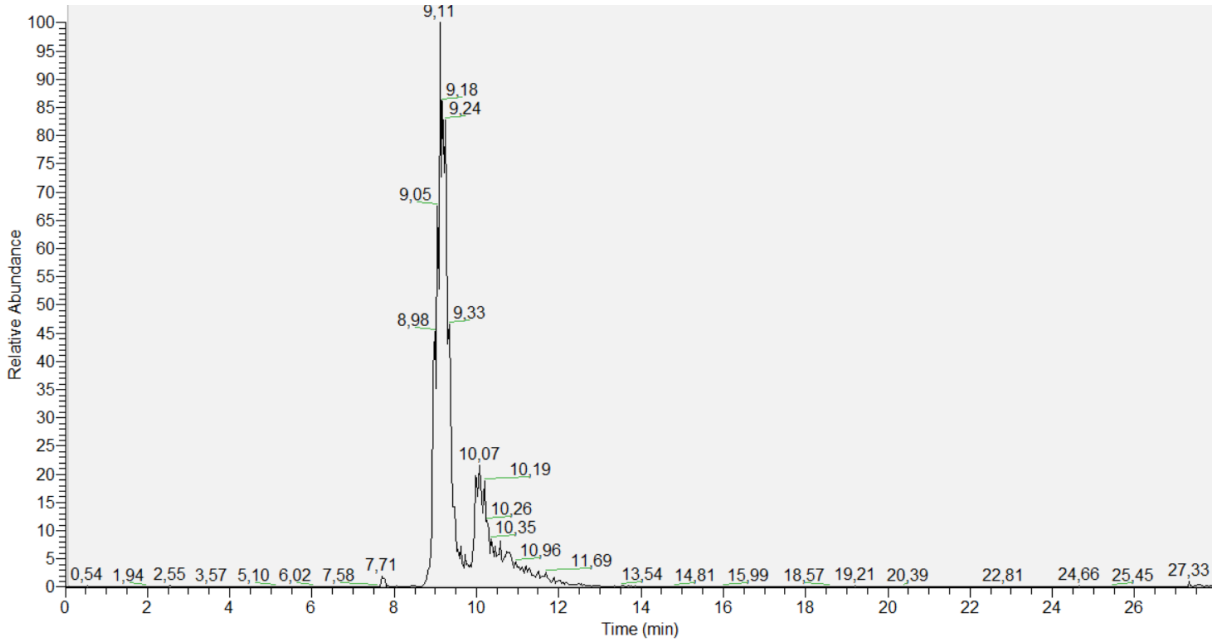

Figure 225: LC-MS total ion count chromatogram of **169**.

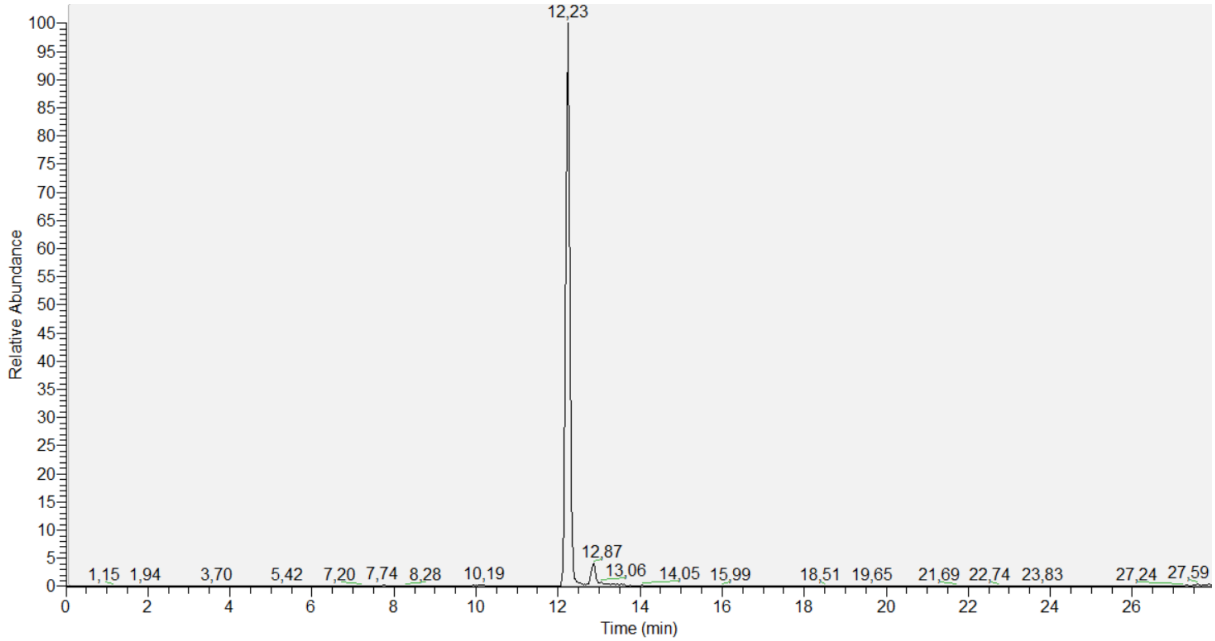

Figure 226: LC-MS total ion count chromatogram of **154**.

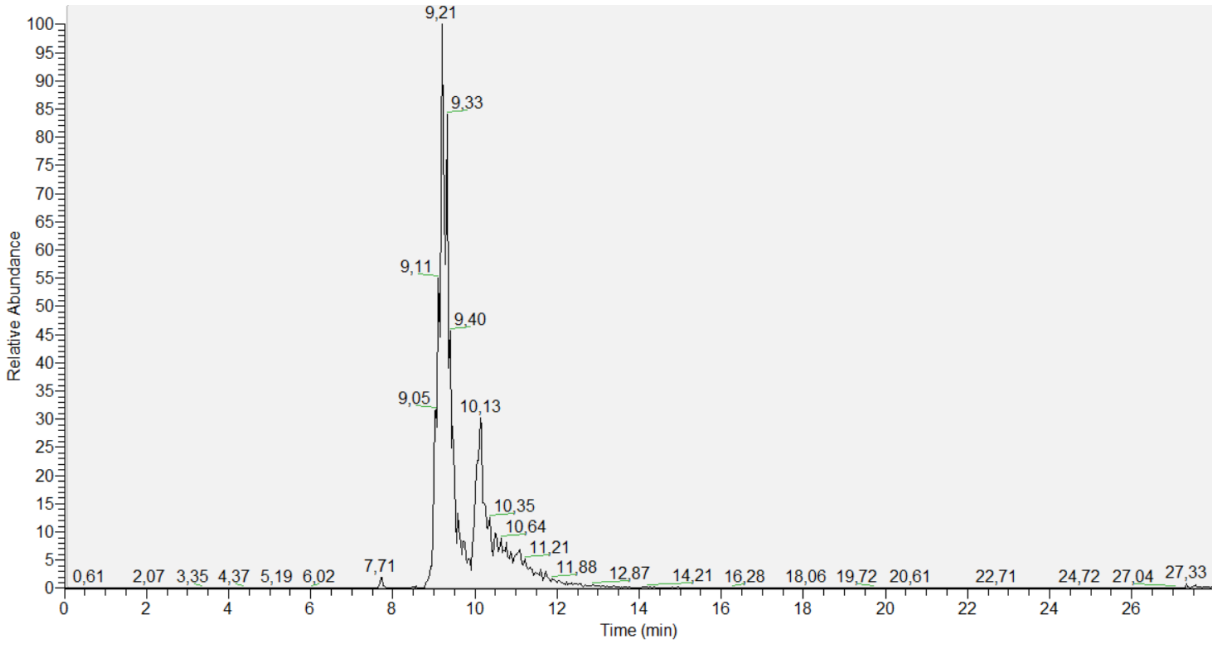

Figure 227: LC-MS total ion count chromatogram of **170**.

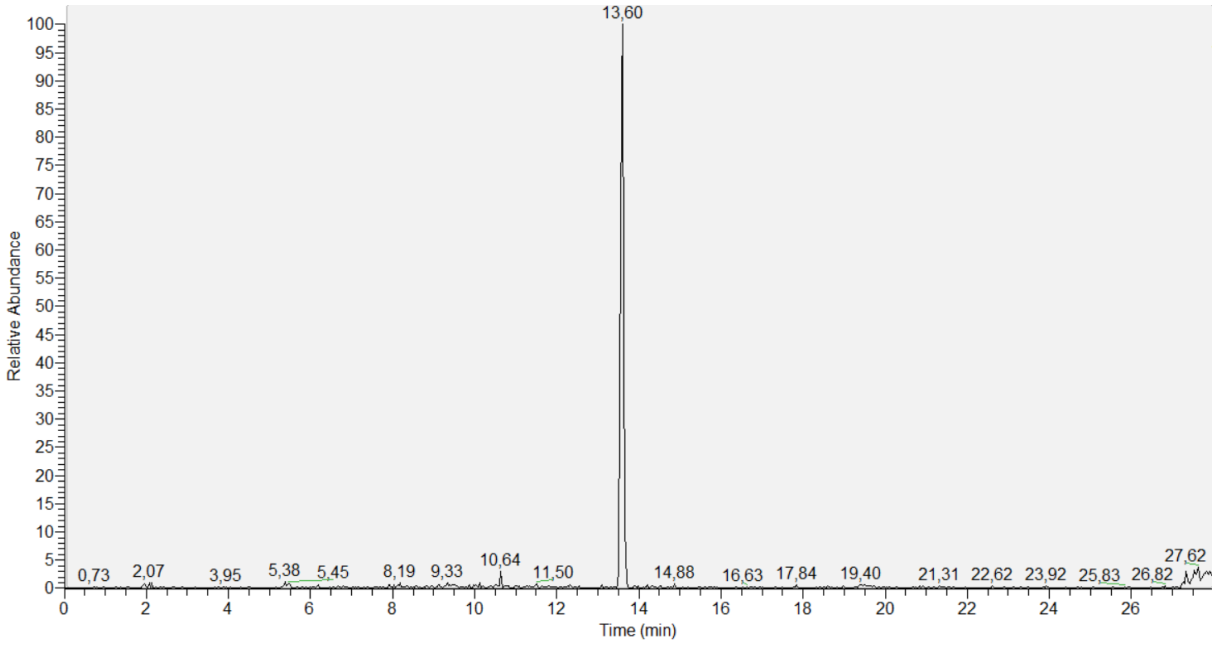

Figure 228: LC-MS total ion count chromatogram of **155**.

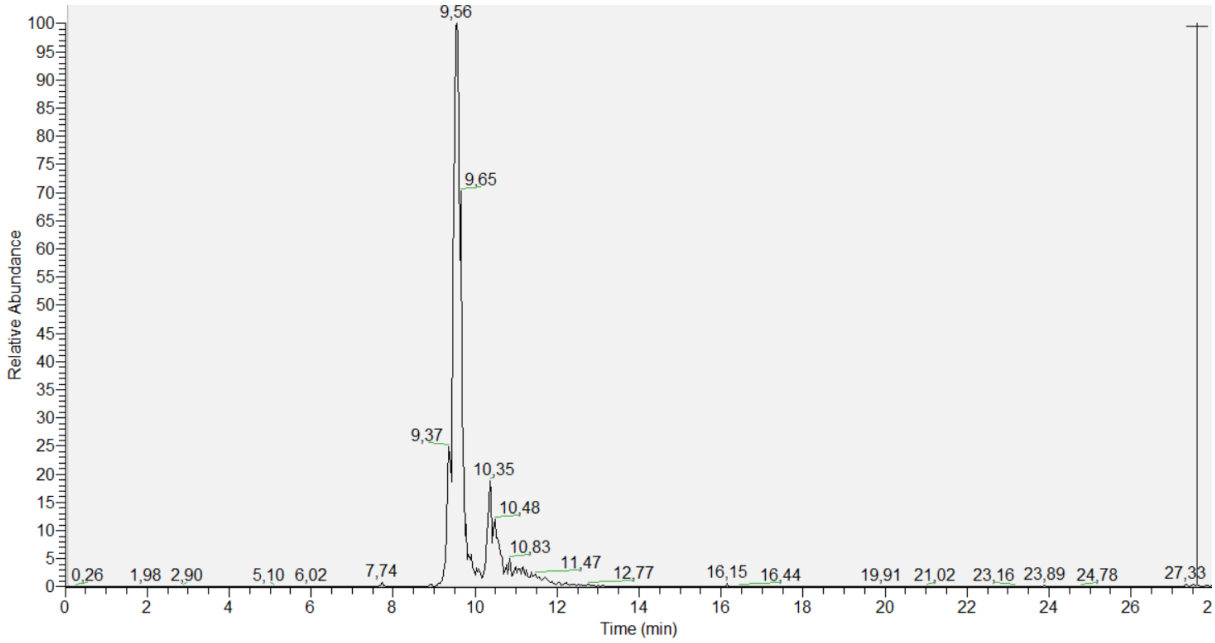

Figure 229: LC-MS total ion count chromatogram of **171**.

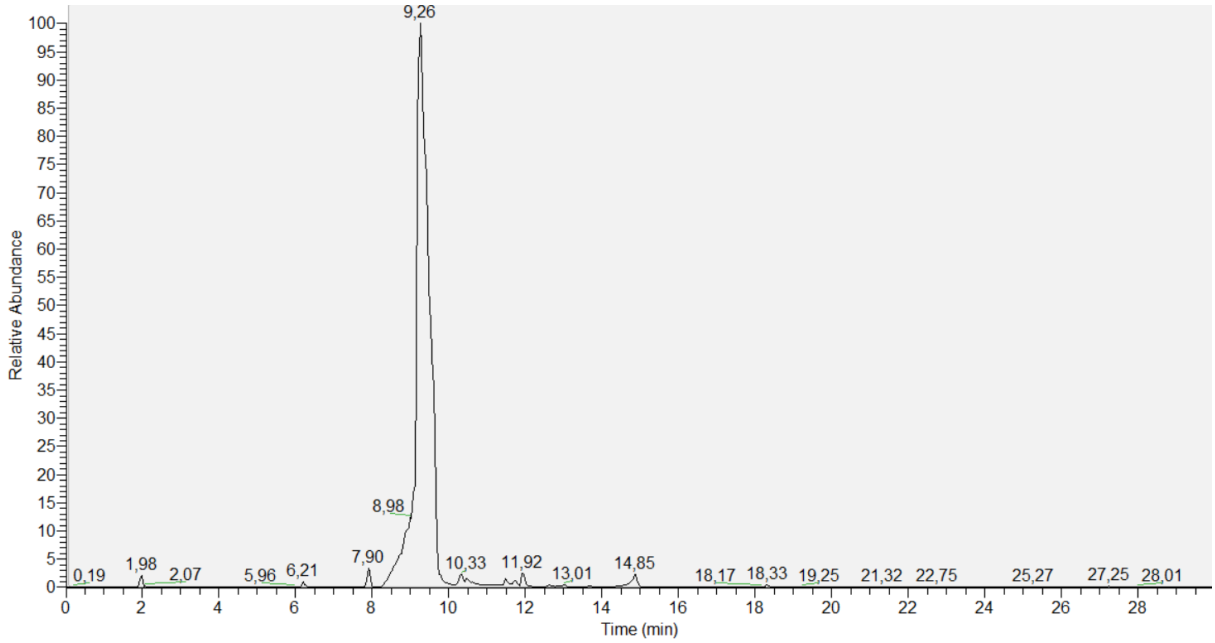

Figure 230: LC-MS total ion count chromatogram of **196**.

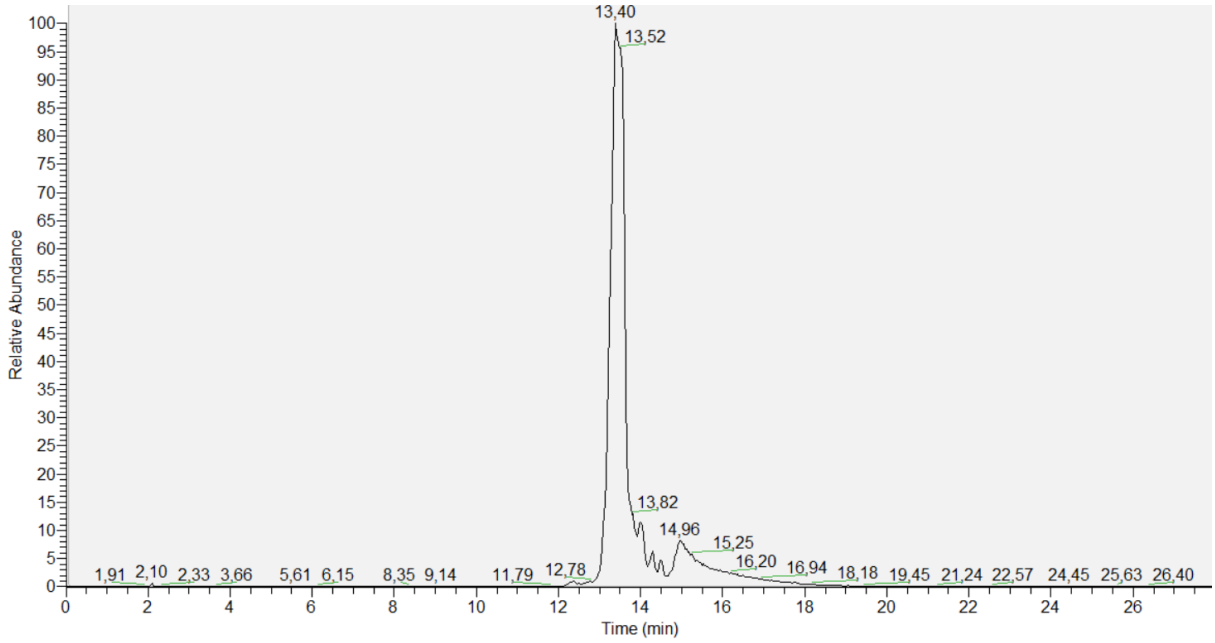

Figure 231: LC-MS total ion count chromatogram of **184**.

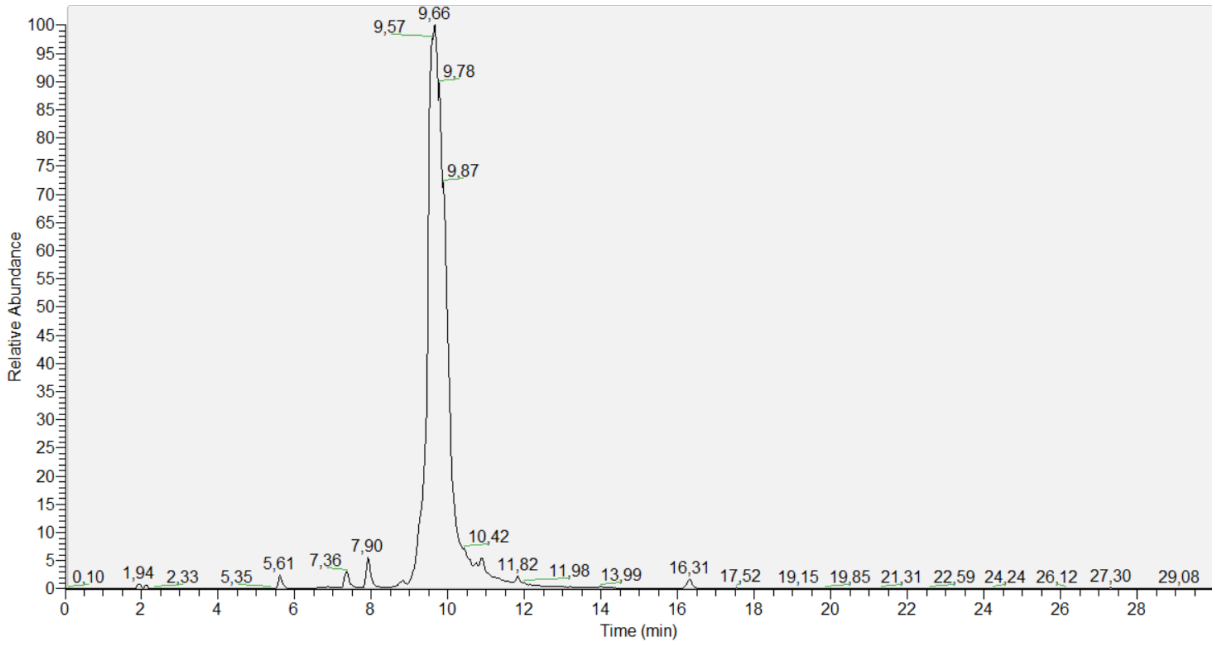

Figure 232: LC-MS total ion count chromatogram of **197**.

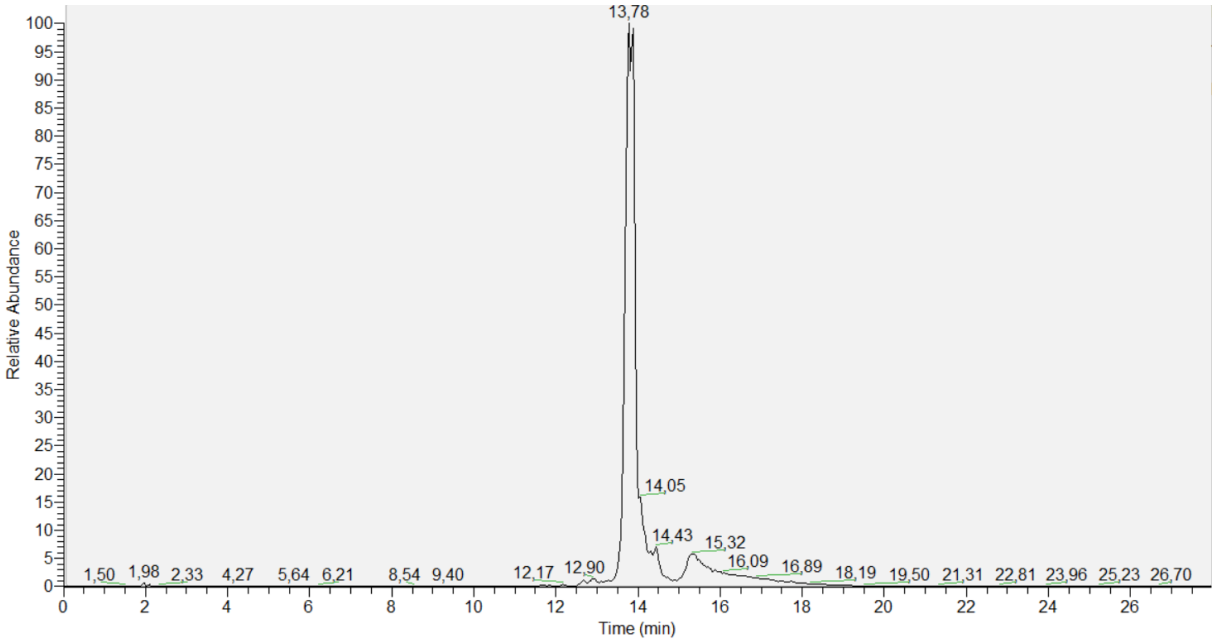

Figure 233: LC-MS total ion count chromatogram of **185**.

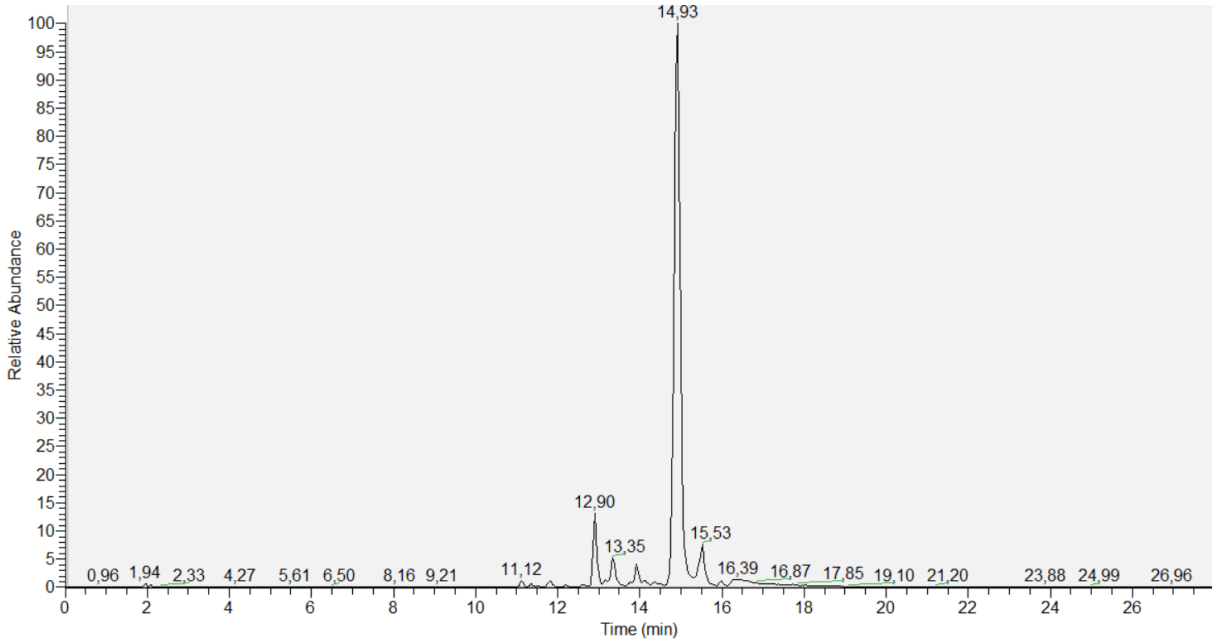

Figure 234: LC-MS total ion count chromatogram of **186**.

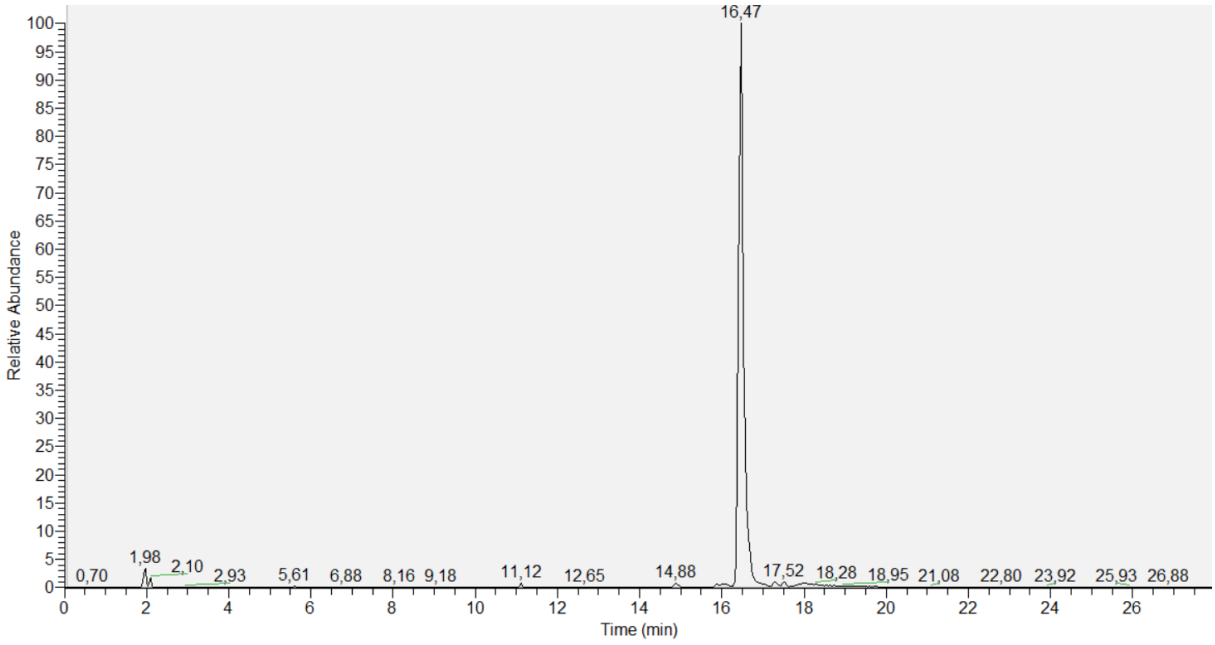

Figure 235: LC-MS total ion count chromatogram of **187**.

7.5 LC-MS Chromatograms of Peptides

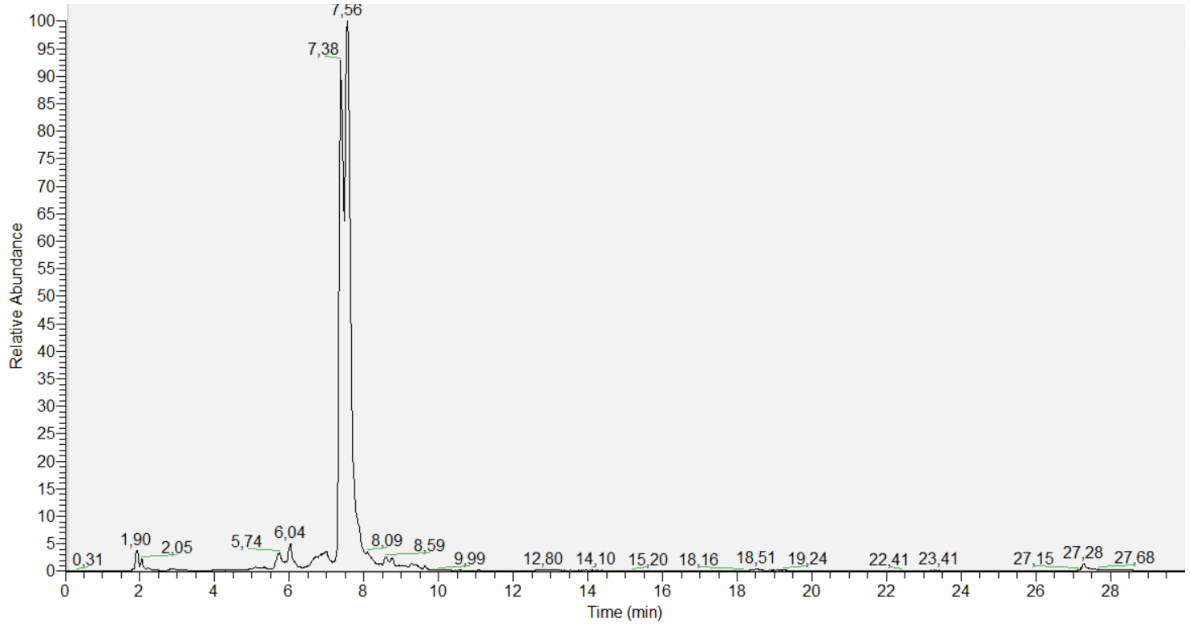

LC-MS (ESI)	$[M+2H]^{2+}$
m/z (calculated)	760.36
m/z (found)	760.03

Figure 236: LC-MS total ion count chromatogram (top) and m/z (bottom) of **223**.

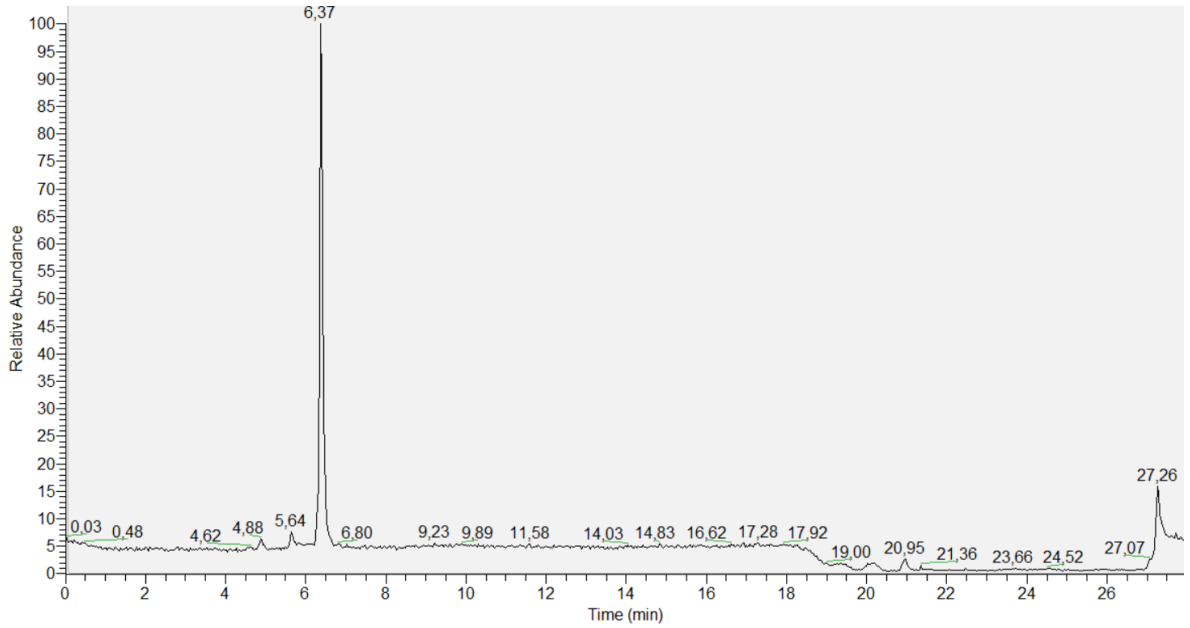

LC-MS (ESI)	$[M+2H]^{2+}$
m/z (calculated)	932.04
m/z (found)	932.01

Figure 237: LC-MS total ion count chromatogram (top) and m/z (bottom) of **224**.

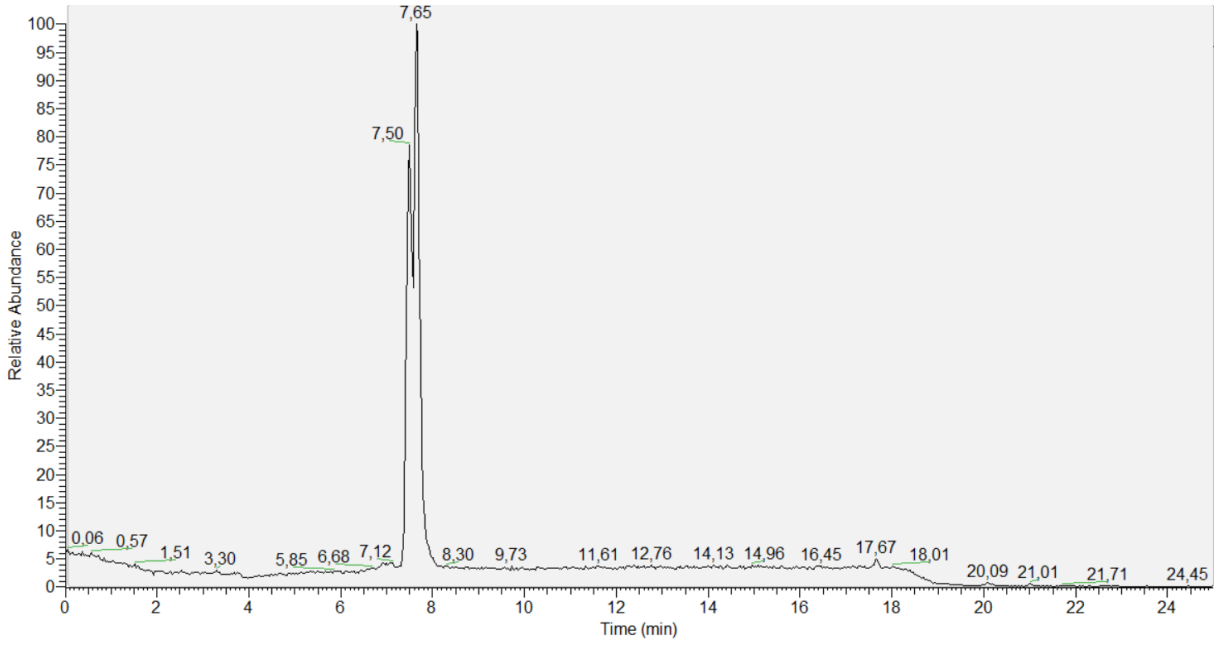

LC-MS (ESI)	$[M+2H]^{2+}$
m/z (calculated)	960.57
m/z (found)	960.54

Figure 238: LC-MS total ion count chromatogram (top) and m/z (bottom) of **225**.

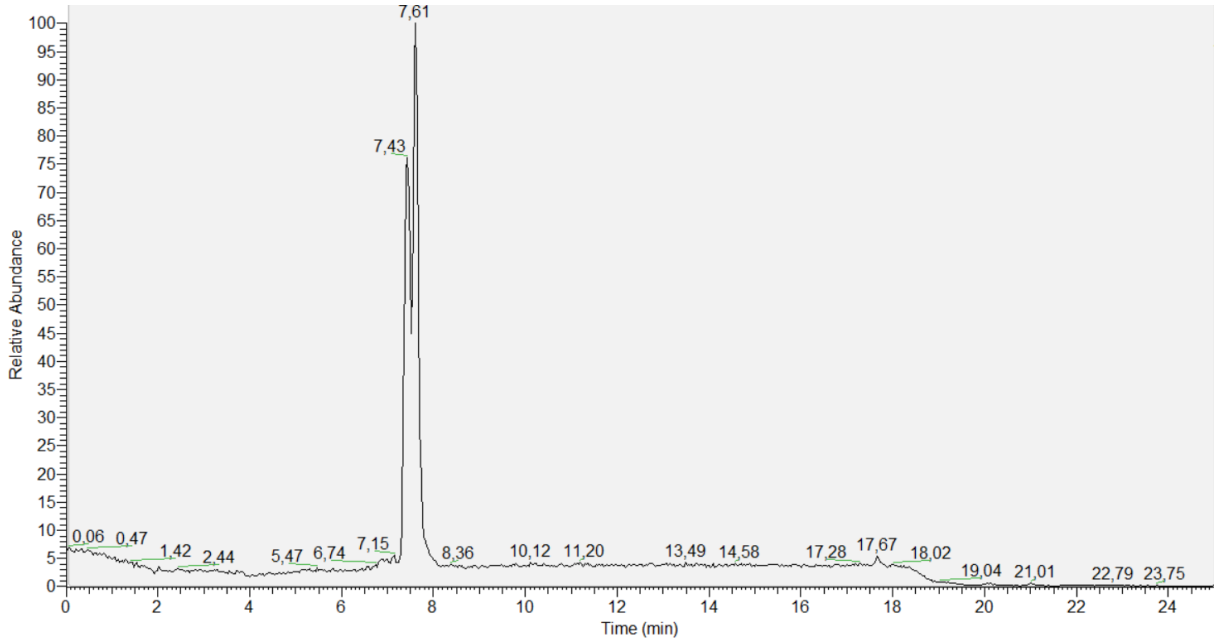

LC-MS (ESI)	$[M+2H]^{2+}$
m/z (calculated)	1004.11
m/z (found)	1004.05

Figure 239: LC-MS total ion count chromatogram (top) and m/z (bottom) of **226**.

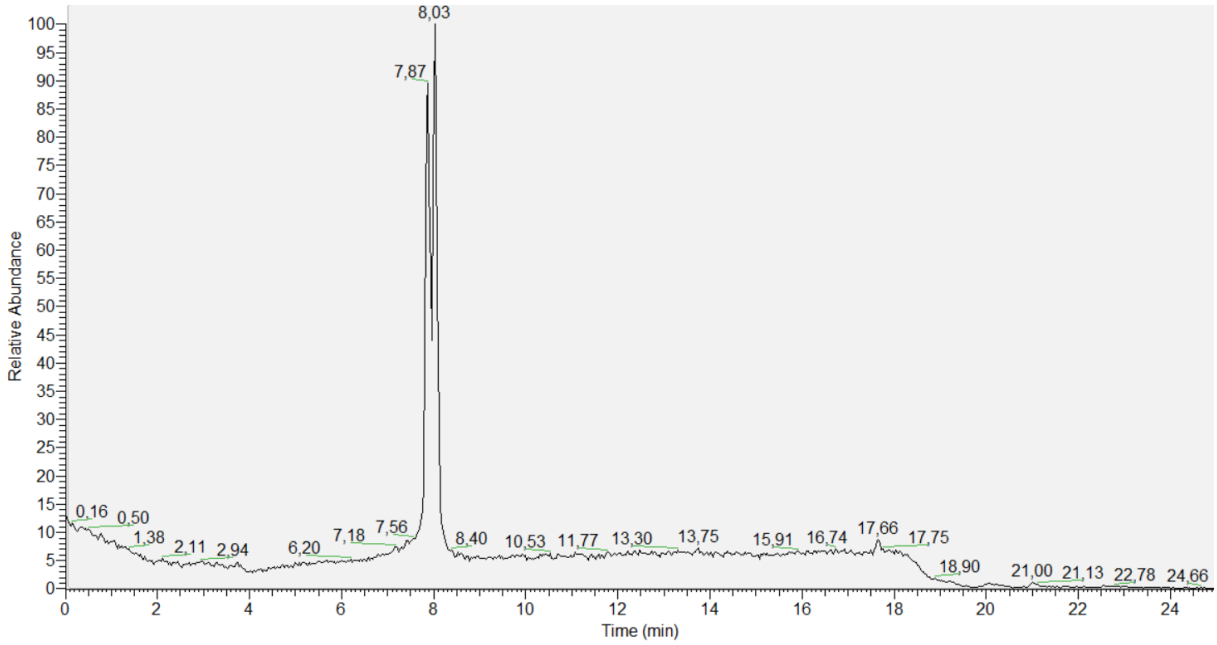

LC-MS (ESI)	$[M+2H]^{2+}$
m/z (calculated)	883.51
m/z (found)	883.50

Figure 240: LC-MS total ion count chromatogram (top) and m/z (bottom) of **227**.

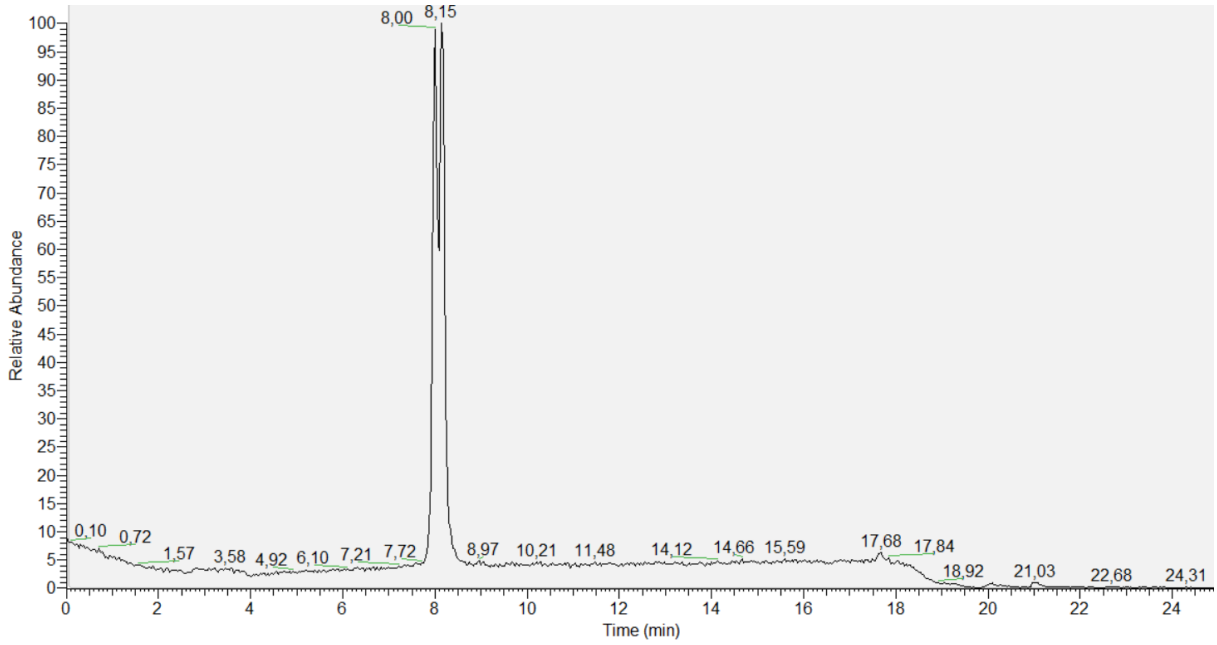

LC-MS (ESI)	$[M+2H]^{2+}$
m/z (calculated)	905.51
m/z (found)	905.48

Figure 241: LC-MS total ion count chromatogram (top) and m/z (bottom) of **228**.

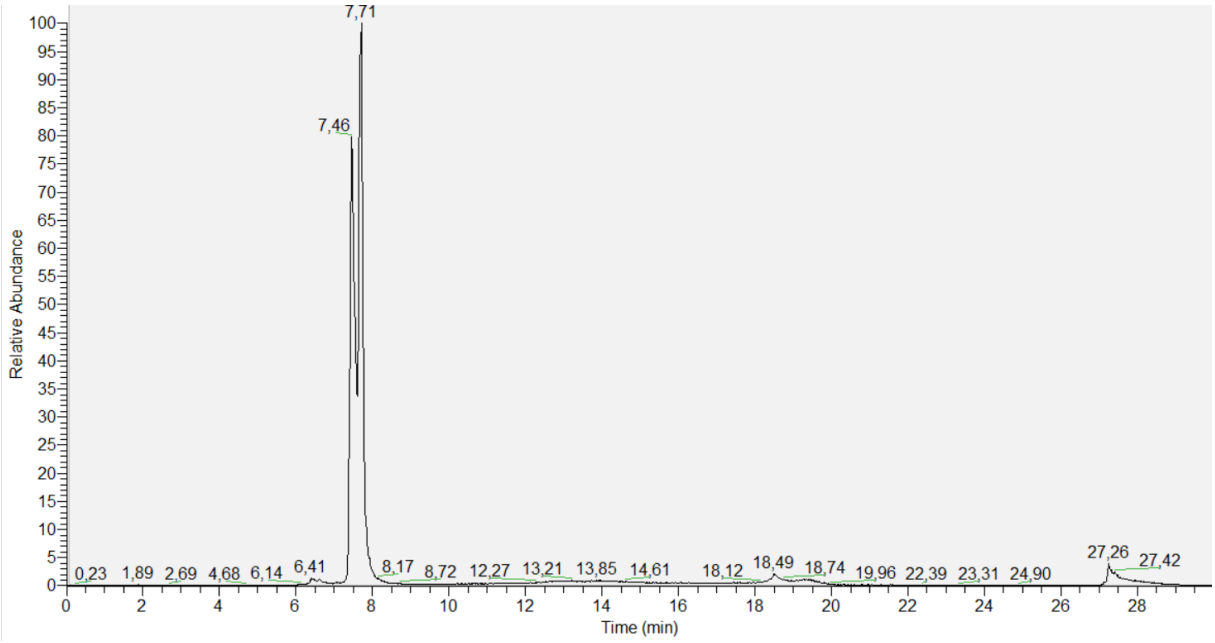

LC-MS (ESI)	$[M+2H]^{2+}$
m/z (calculated)	844.96
m/z (found)	844.82

Figure 242: LC-MS total ion count chromatogram (top) and m/z (bottom) of **229**.

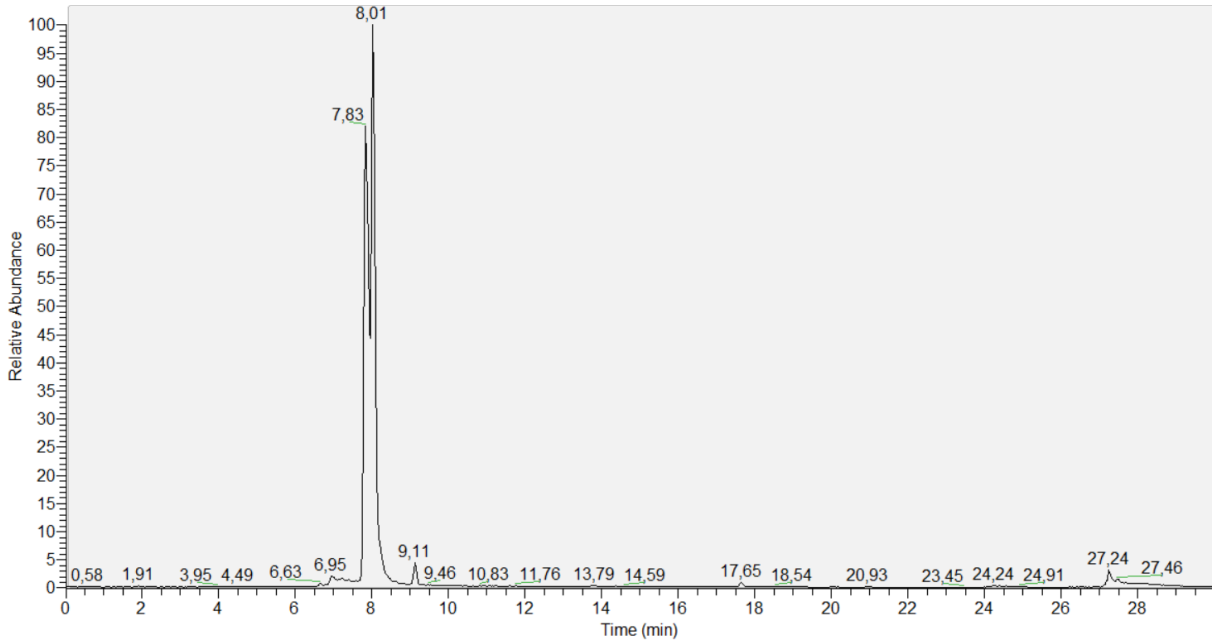

LC-MS (ESI)	$[M+2H]^{2+}$
m/z (calculated)	968.61
m/z (found)	968.48

Figure 243: LC-MS total ion count chromatogram (top) and m/z (bottom) of **230**.

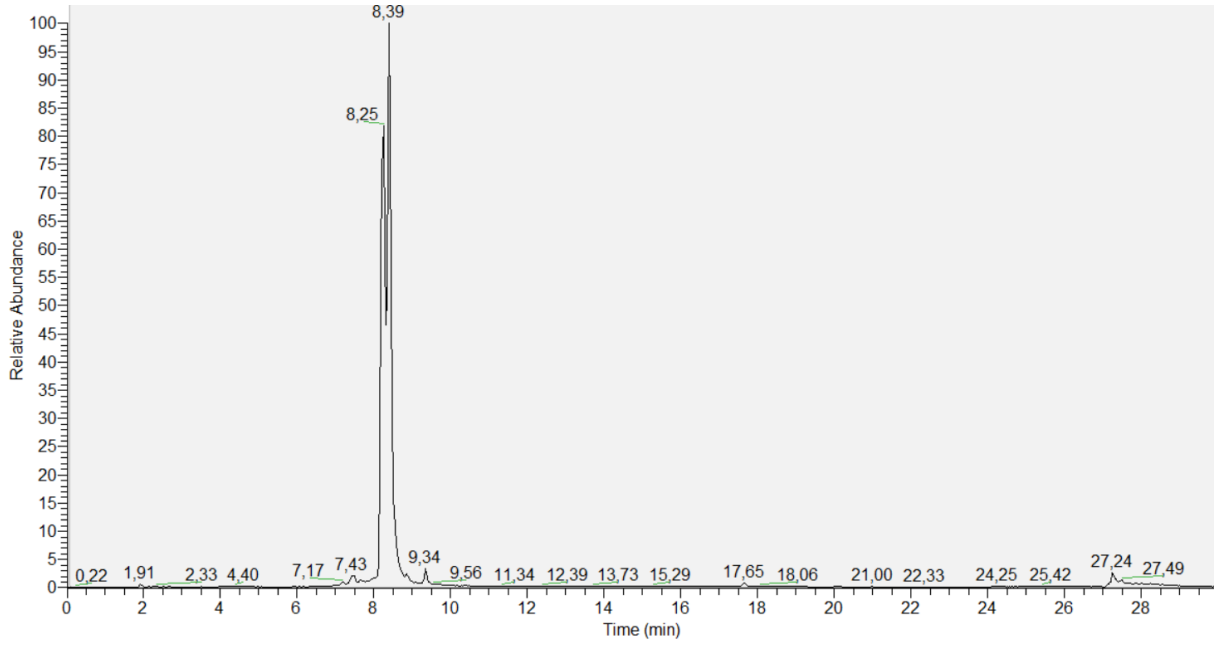

LC-MS (ESI)	$[M+2H]^{2+}$
m/z (calculated)	1056.72
m/z (found)	1056.52

Figure 244: LC-MS total ion count chromatogram (top) and m/z (bottom) of **231**.

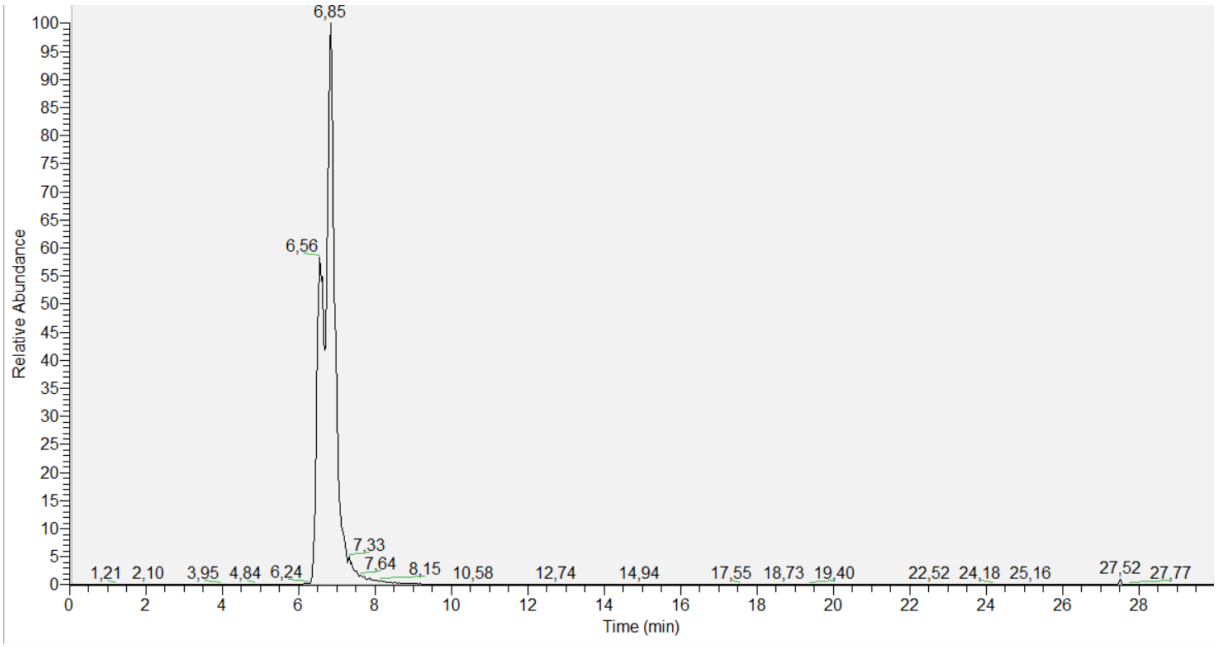

LC-MS (ESI)	$[M+2H]^{2+}$
m/z (calculated)	667.73
m/z (found)	667.66

Figure 245: LC-MS total ion count chromatogram (top) and m/z (bottom) of **232**.

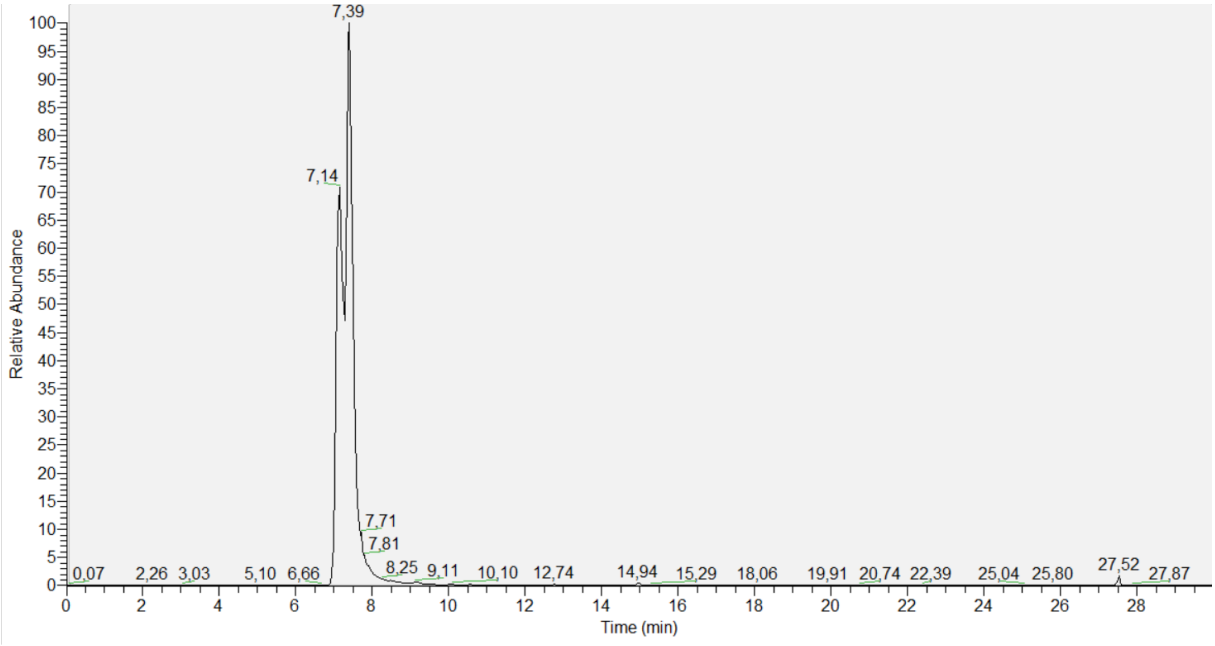

LC-MS (ESI)	$[M+2H]^{2+}$
m/z (calculated)	647.21
m/z (found)	647.13

Figure 246: LC-MS total ion count chromatogram (top) and m/z (bottom) of **233**.

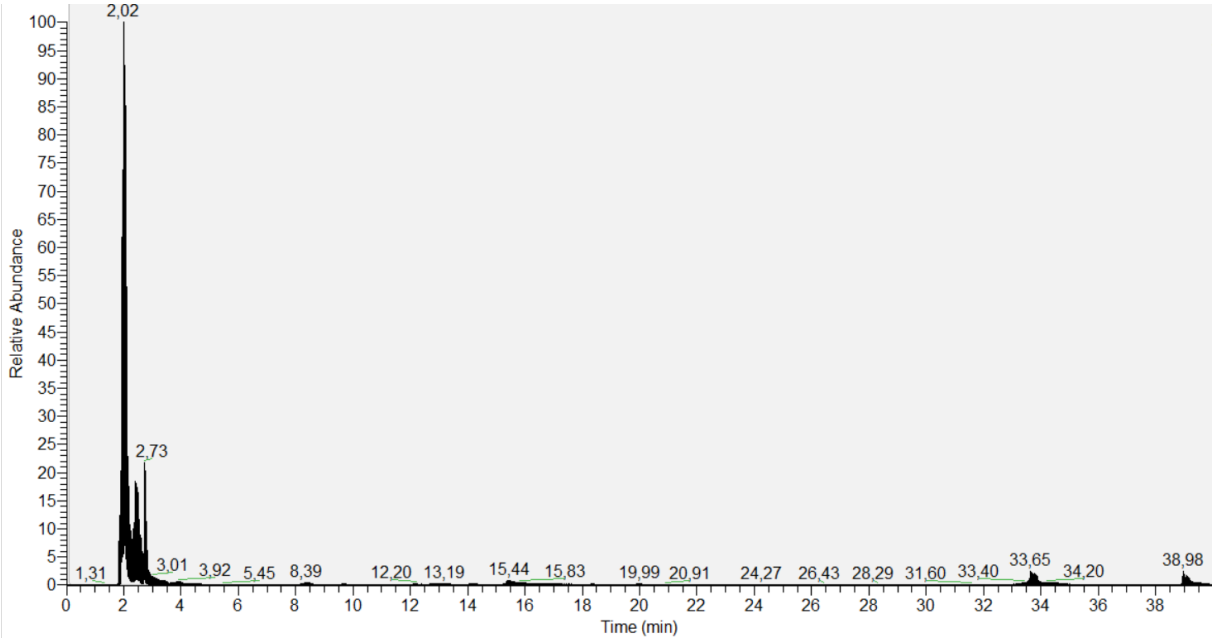

LC-MS (ESI)	$[M+2H]^{2+}$
m/z (calculated)	587.69
m/z (found)	587.68

Figure 247: LC-MS total ion count chromatogram (top) and m/z (bottom) of **234**.

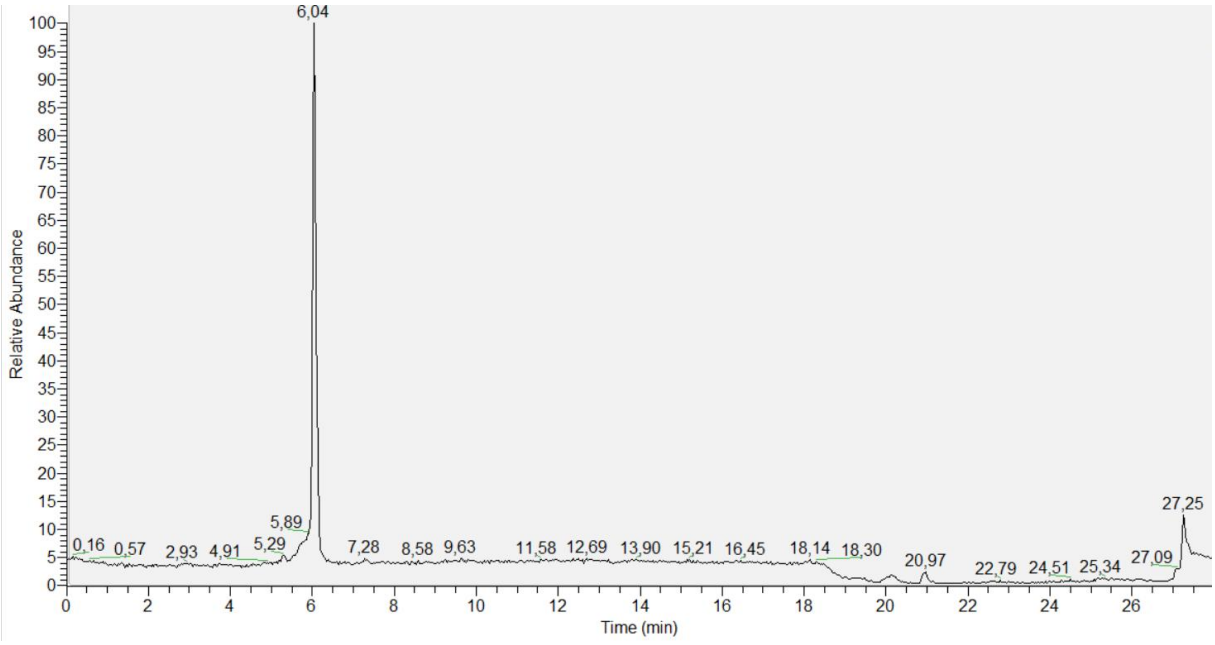

LC-MS (ESI)	$[M+2H]^{2+}$
m/z (calculated)	599.71
m/z (found)	599.70

Figure 248: LC-MS total ion count chromatogram (top) and m/z (bottom) of **237**.

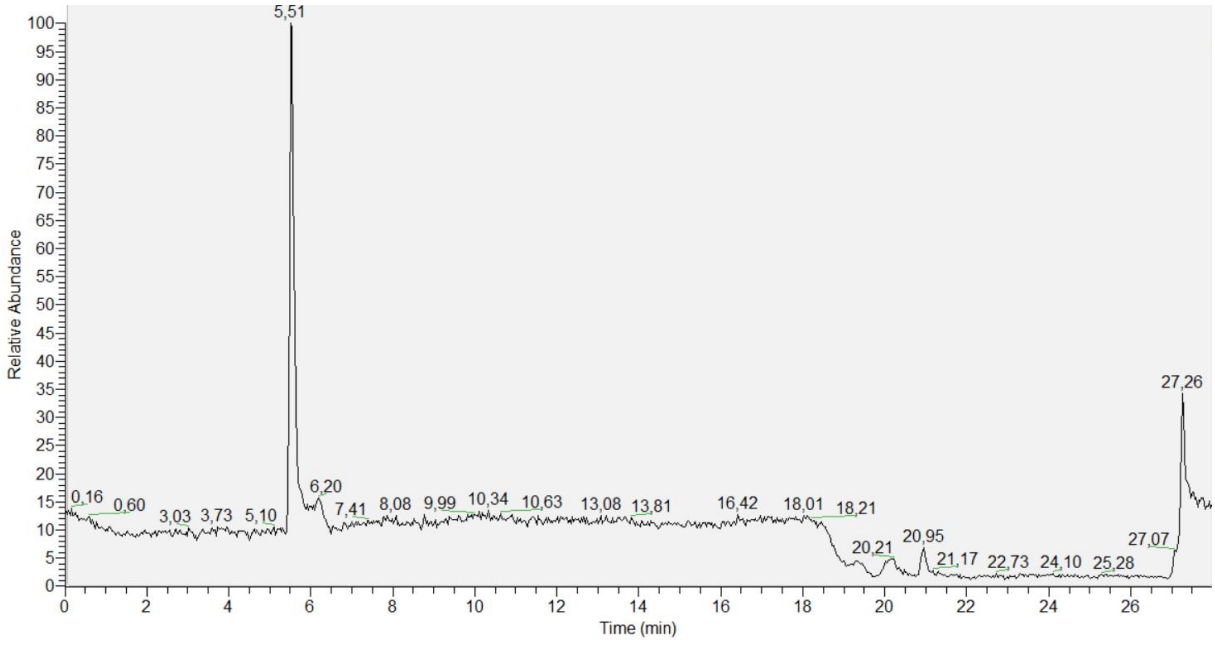

LC-MS (ESI)	$[M+2H]^{2+}$
m/z (calculated)	599.71
m/z (found)	599.70

Figure 249: LC-MS total ion count chromatogram (top) and m/z (bottom) of **236**.

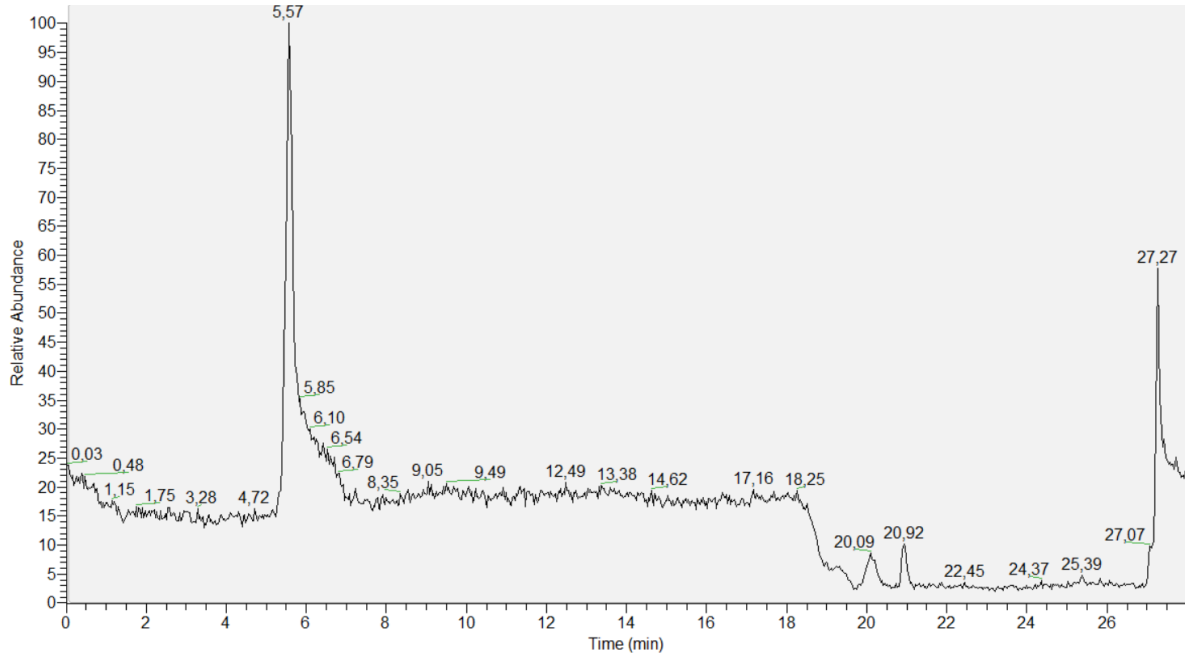

LC-MS (ESI)	$[M+2H]^{2+}$
m/z (calculated)	599.71
m/z (found)	599.68

Figure 250: LC-MS total ion count chromatogram (top) and m/z (bottom) of **235**.

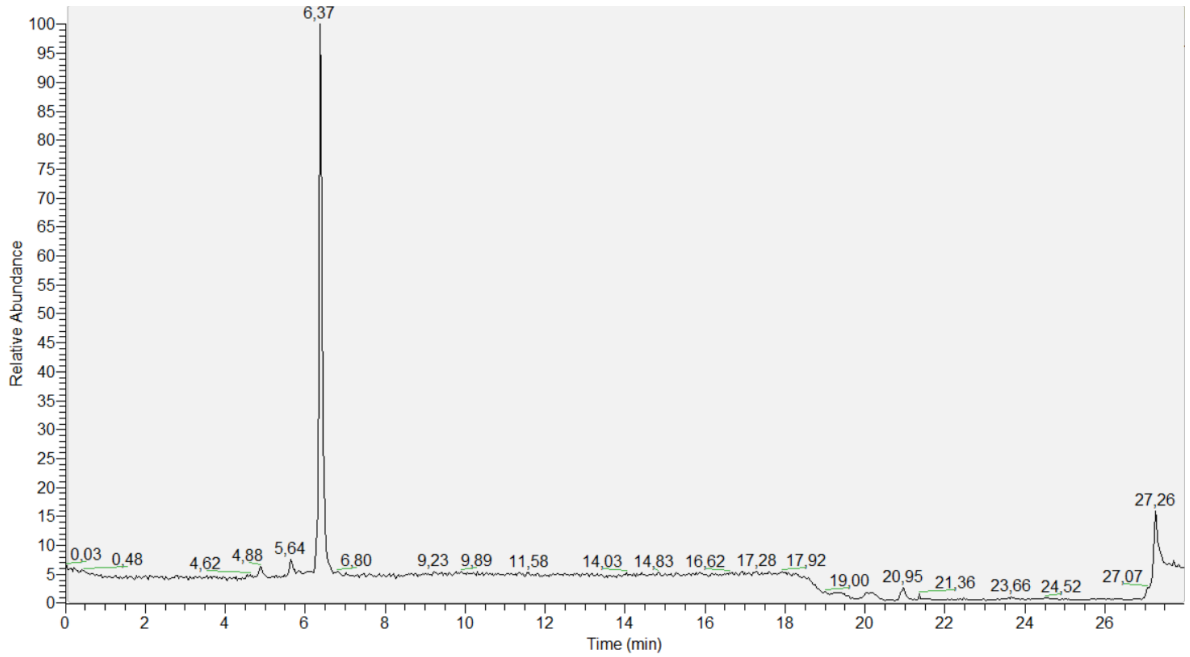

LC-MS (ESI)	$[M+2H]^{2+}$
m/z (calculated)	613.73
m/z (found)	613.71

Figure 251: LC-MS total ion count chromatogram (top) and m/z (bottom) of **238**.

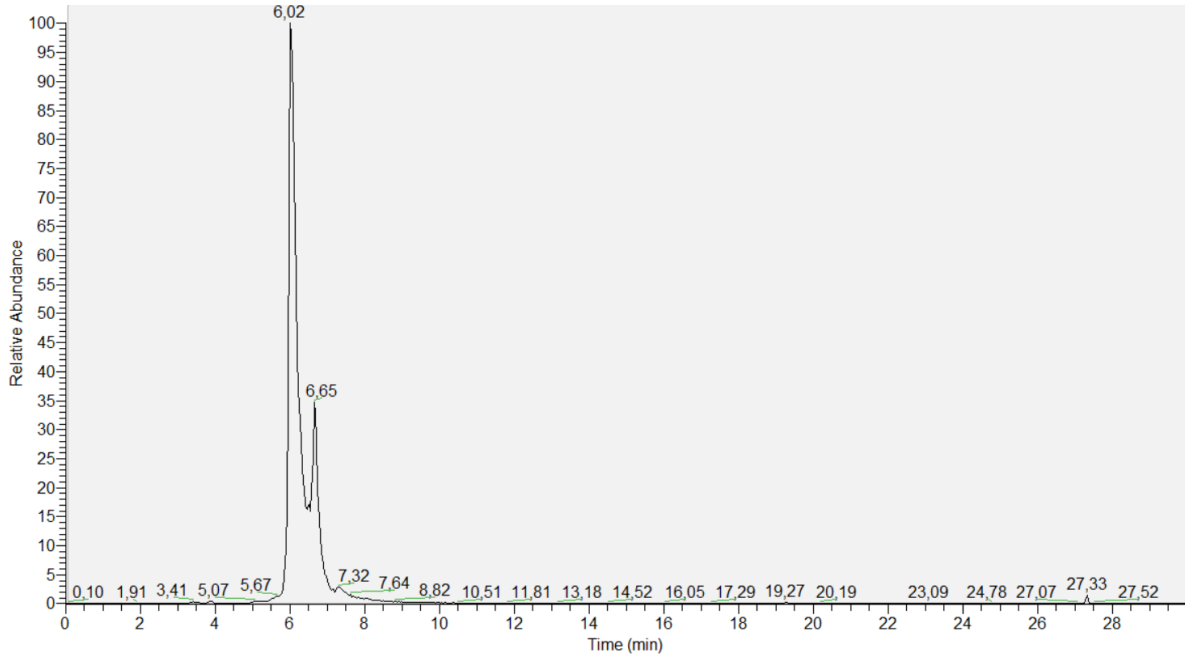

LC-MS (ESI)	$[M+2H]^{2+}$
m/z (calculated)	839.54
m/z (found)	839.40

Figure 252: LC-MS total ion count chromatogram (top) and m/z (bottom) of **203**.

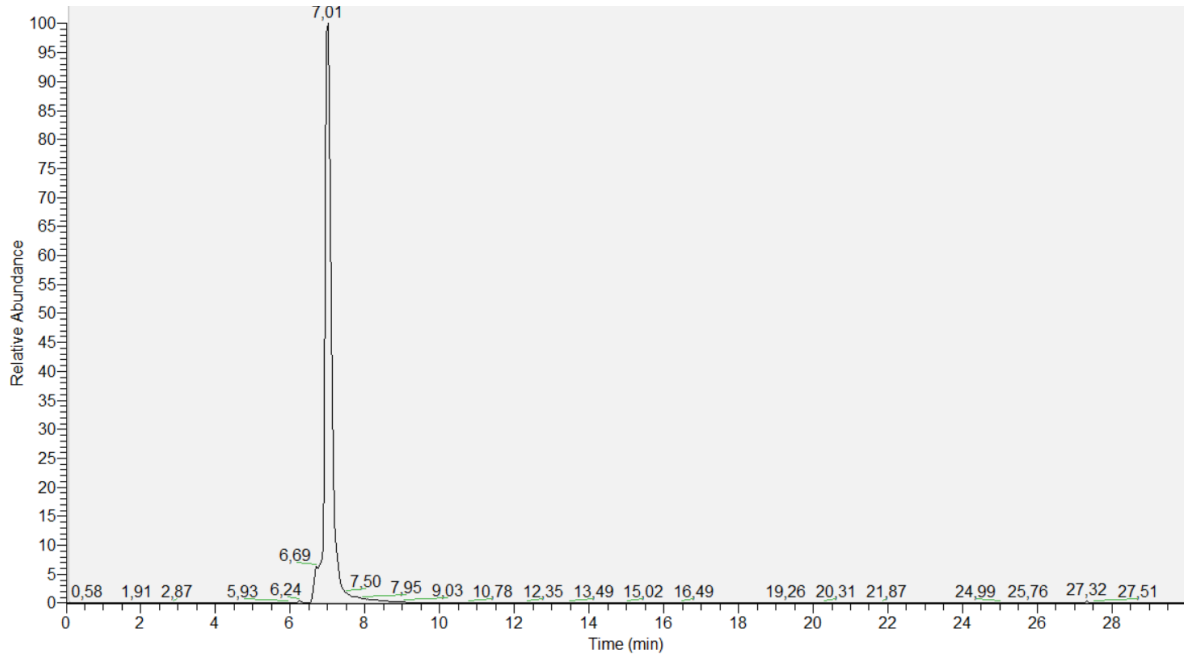

LC-MS (ESI)	$[M+2H]^{2+}$
m/z (calculated)	1056.27
m/z (found)	1056.57

Figure 253: LC-MS total ion count chromatogram (top) and m/z (bottom) of **202**.

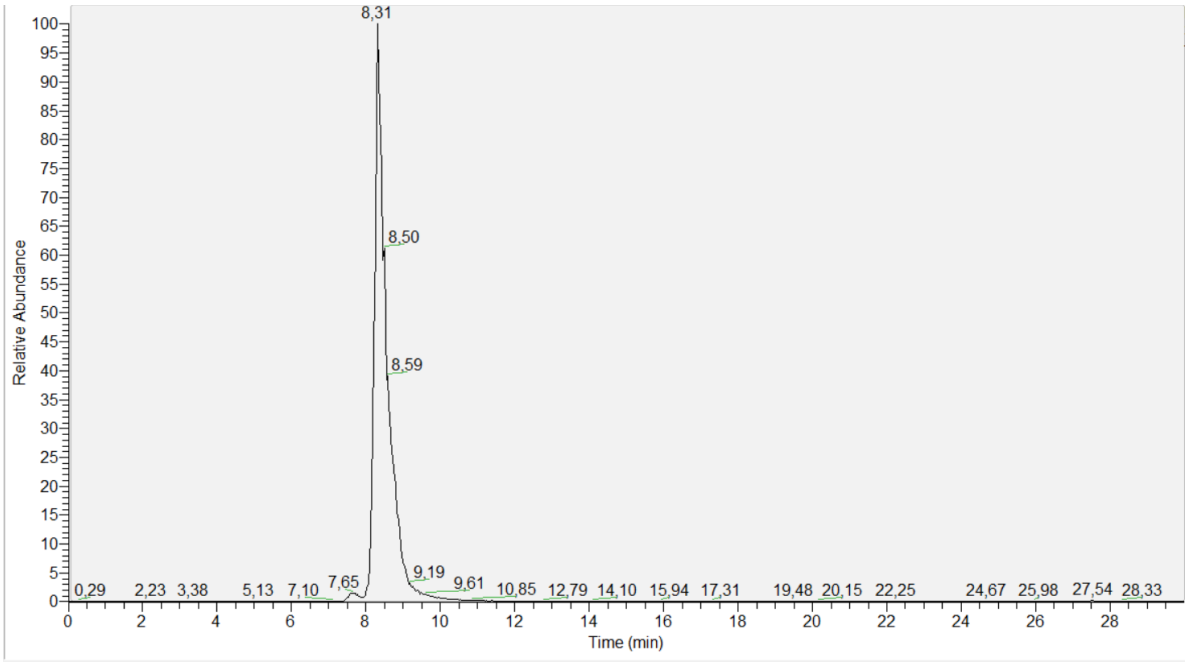

LC-MS (ESI)	$[M+2H]^{2+}$
m/z (calculated)	1090.81
m/z (found)	1090.54

Figure 254: LC-MS total ion count chromatogram (top) and m/z (bottom) of **204**.

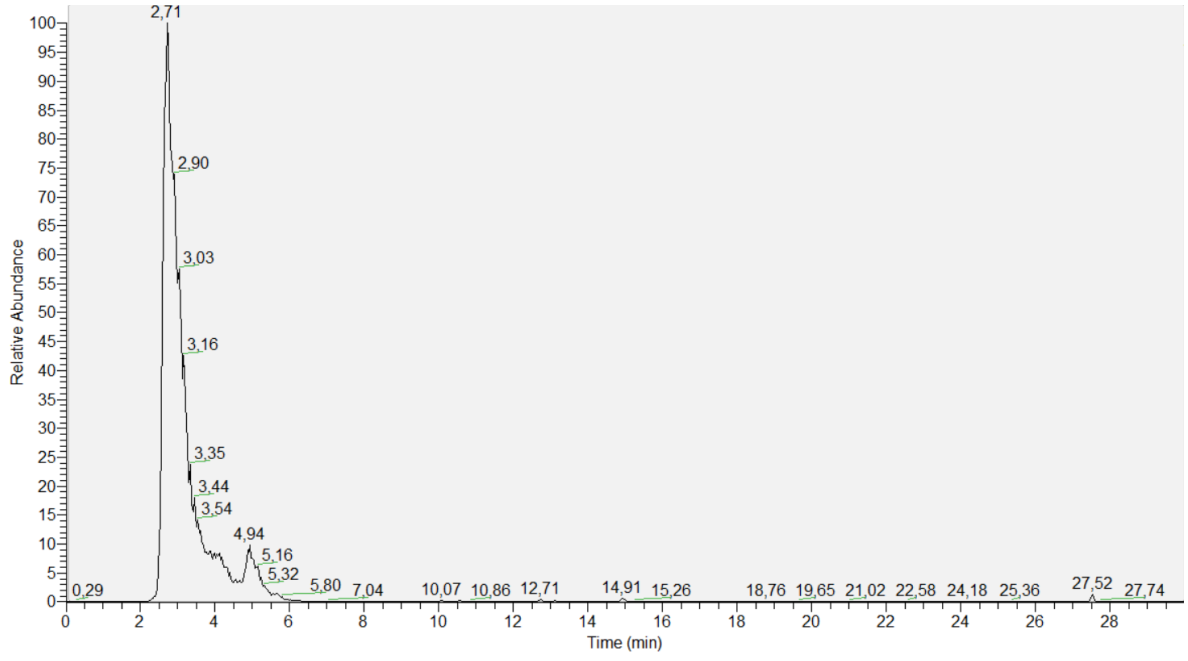

LC-MS (ESI)	$[M+2H]^{2+}$
m/z (calculated)	690.83
m/z (found)	690.74

Figure 255: LC-MS total ion count chromatogram (top) and m/z (bottom) of **205**.

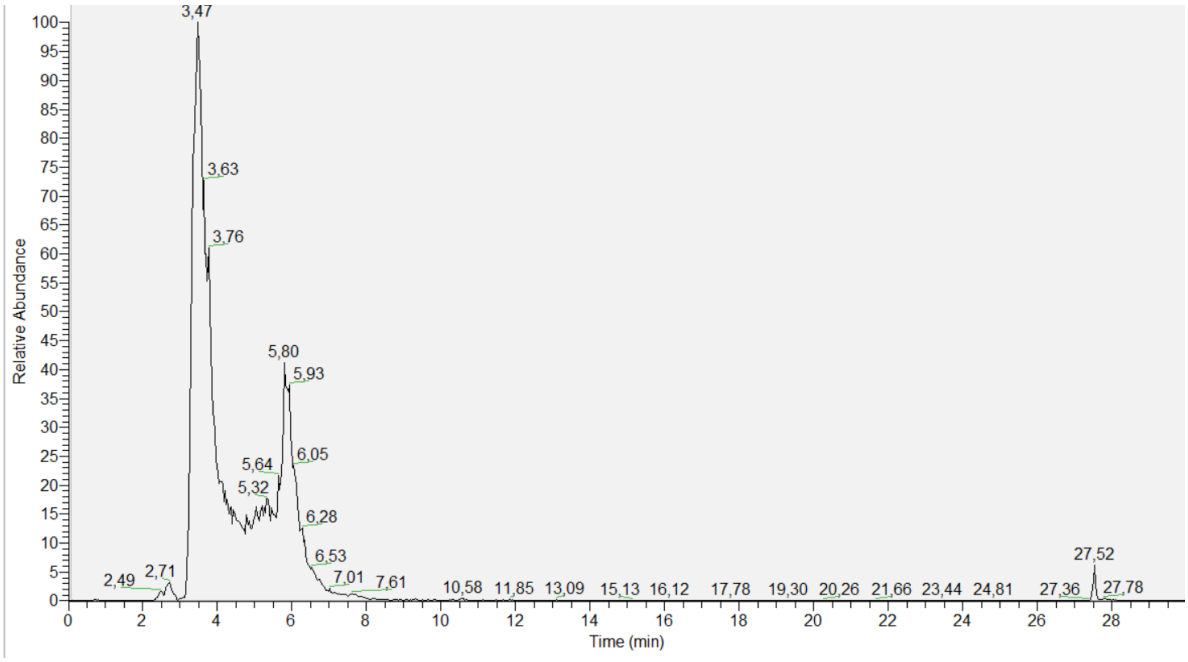

LC-MS (ESI)	$[M+2H]^{2+}$
m/z (calculated)	703.85
m/z (found)	703.74

Figure 256: LC-MS total ion count chromatogram (top) and m/z (bottom) of **206**.

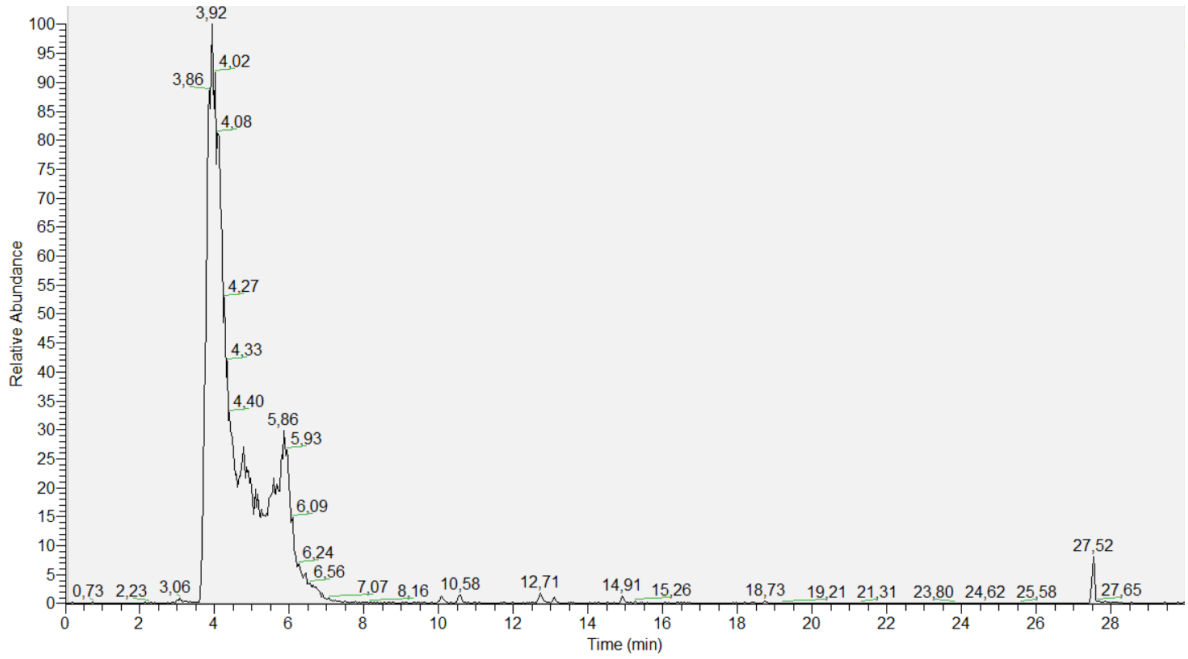

LC-MS (ESI)	$[M+2H]^{2+}$
m/z (calculated)	703.85
m/z (found)	703.74

Figure 257: LC-MS total ion count chromatogram (top) and m/z (bottom) of **207**.

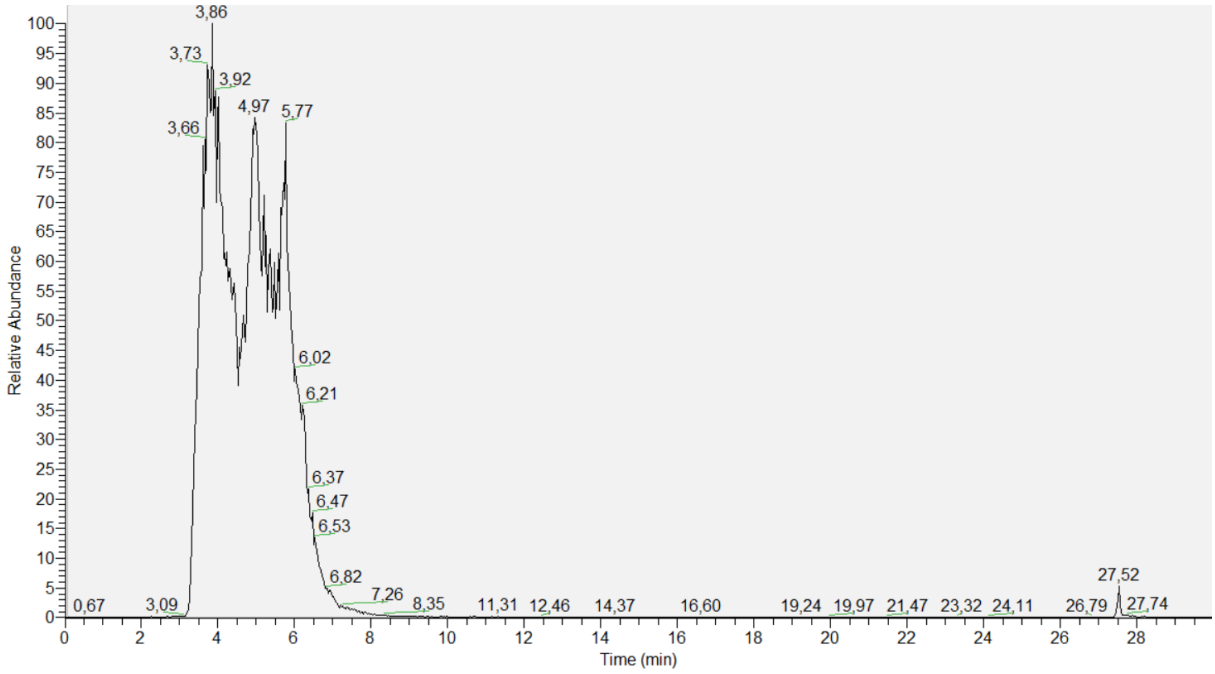

LC-MS (ESI)	$[M+2H]^{2+}$
m/z (calculated)	703.85
m/z (found)	703.73

Figure 258: LC-MS total ion count chromatogram (top) and m/z (bottom) of **208**.

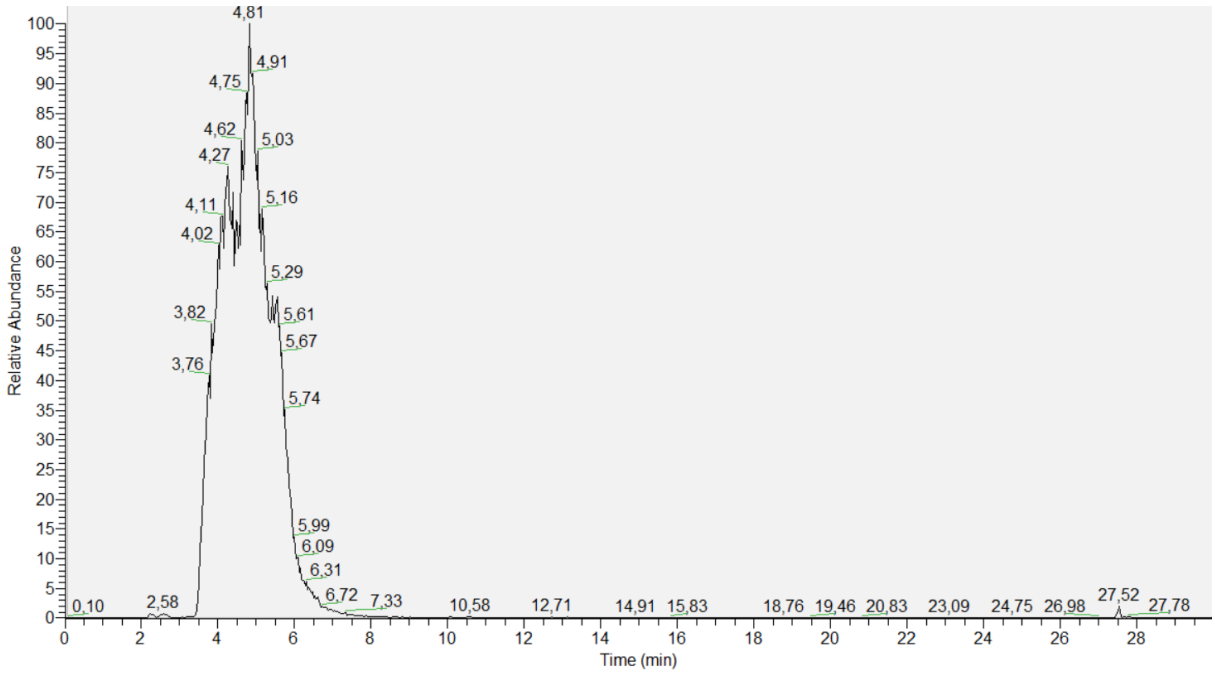

LC-MS (ESI)	$[M+2H]^{2+}$
m/z (calculated)	703.85
m/z (found)	703.75

Figure 259: LC-MS total ion count chromatogram (top) and m/z (bottom) of **209**.

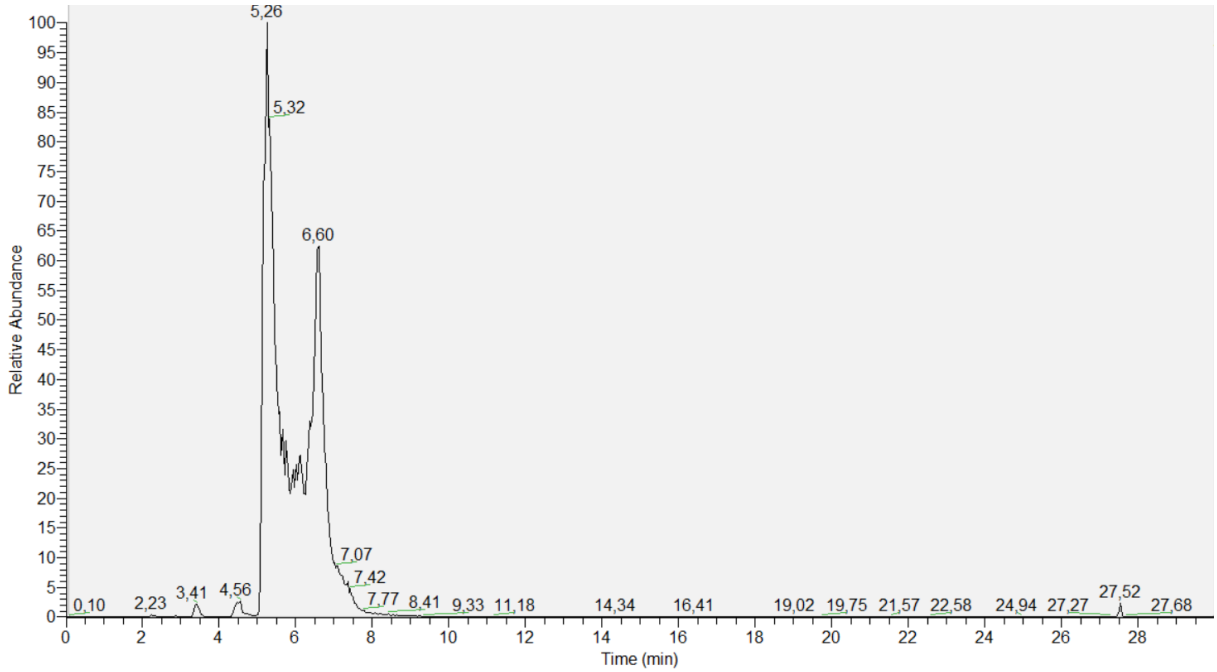

LC-MS (ESI)	$[M+2H]^{2+}$
m/z (calculated)	716.87
m/z (found)	716.75

Figure 260: LC-MS total ion count chromatogram (top) and m/z (bottom) of **210**.

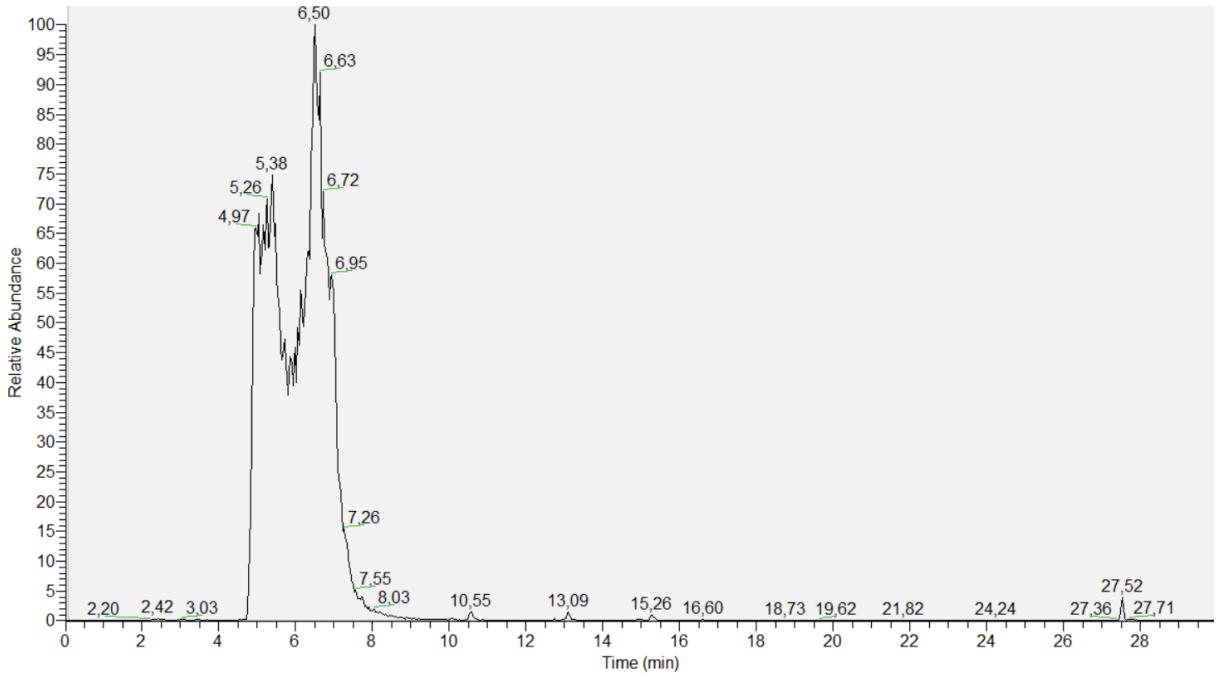

LC-MS (ESI)	$[M+2H]^{2+}$
m/z (calculated)	716.87
m/z (found)	716.74

Figure 261: LC-MS total ion count chromatogram (top) and m/z (bottom) of **211**.

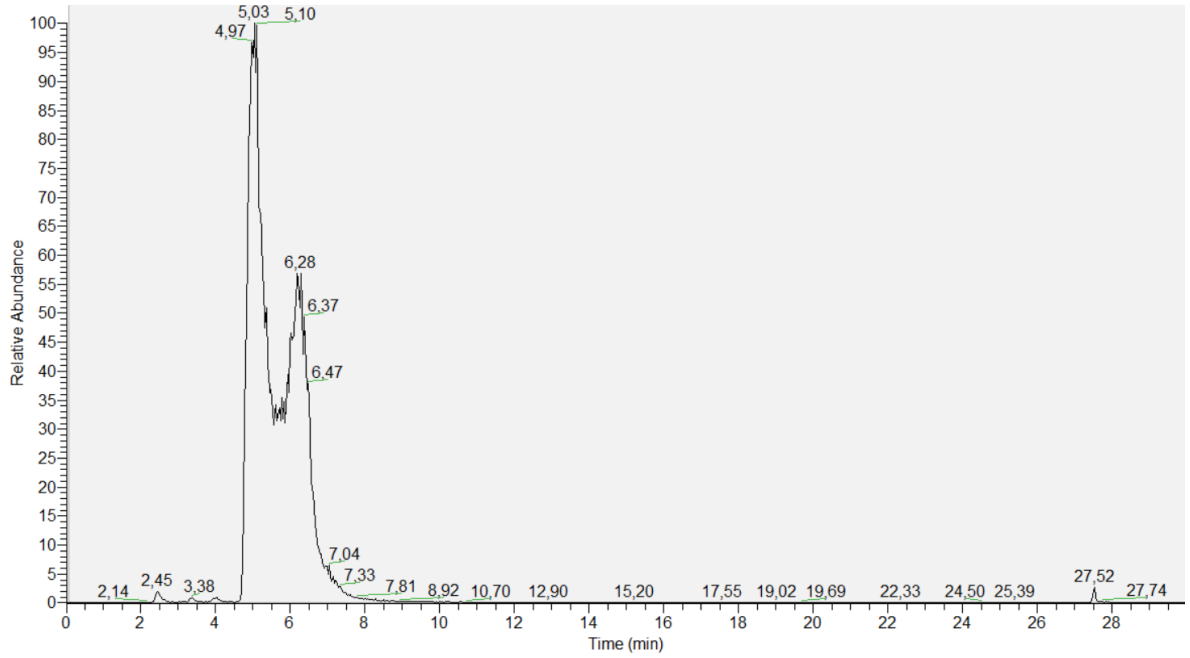

LC-MS (ESI)	$[M+2H]^{2+}$
m/z (calculated)	716.87
m/z (found)	716.73

Figure 262: LC-MS total ion count chromatogram (top) and m/z (bottom) of **212**.

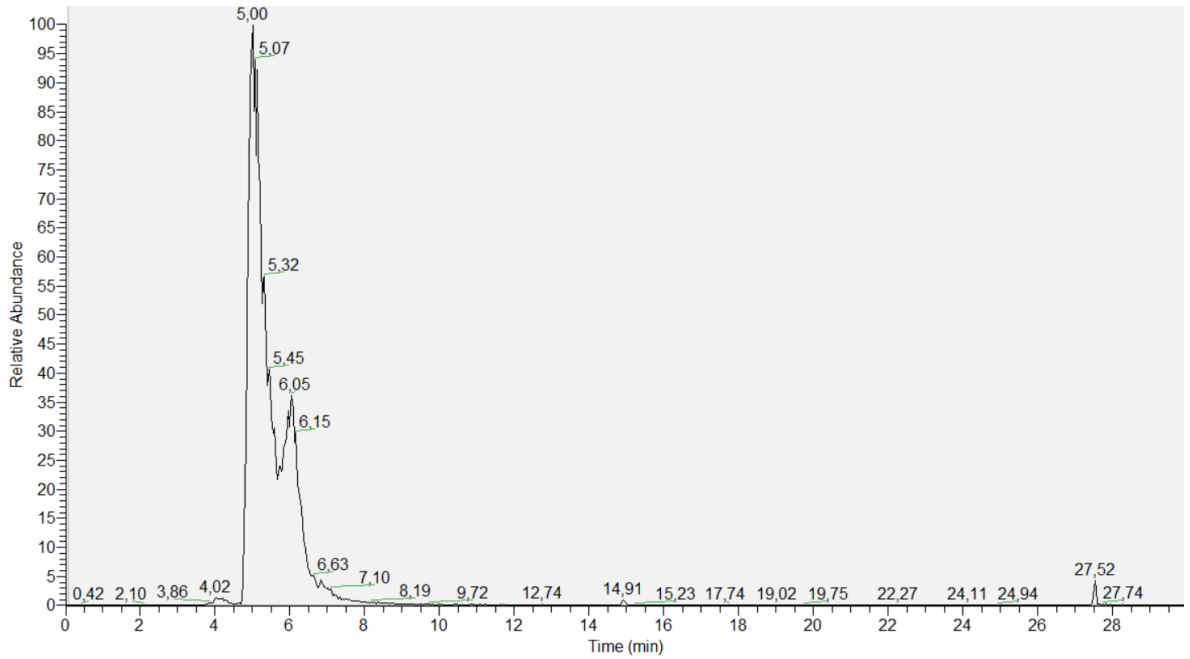

LC-MS (ESI)	$[M+2H]^{2+}$
m/z (calculated)	716.87
m/z (found)	716.73

Figure 263: LC-MS total ion count chromatogram (top) and m/z (bottom) of **213**.

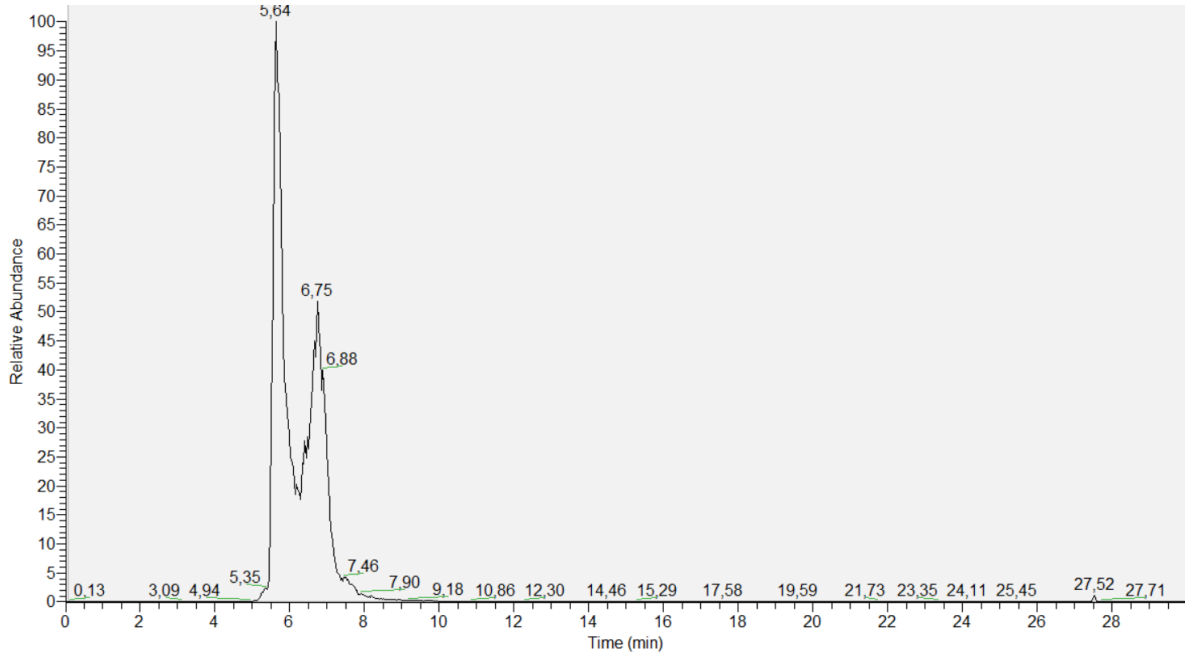

LC-MS (ESI)	$[M+2H]^{2+}$
m/z (calculated)	729.89
m/z (found)	729.75

Figure 264: LC-MS total ion count chromatogram (top) and m/z (bottom) of **214**.

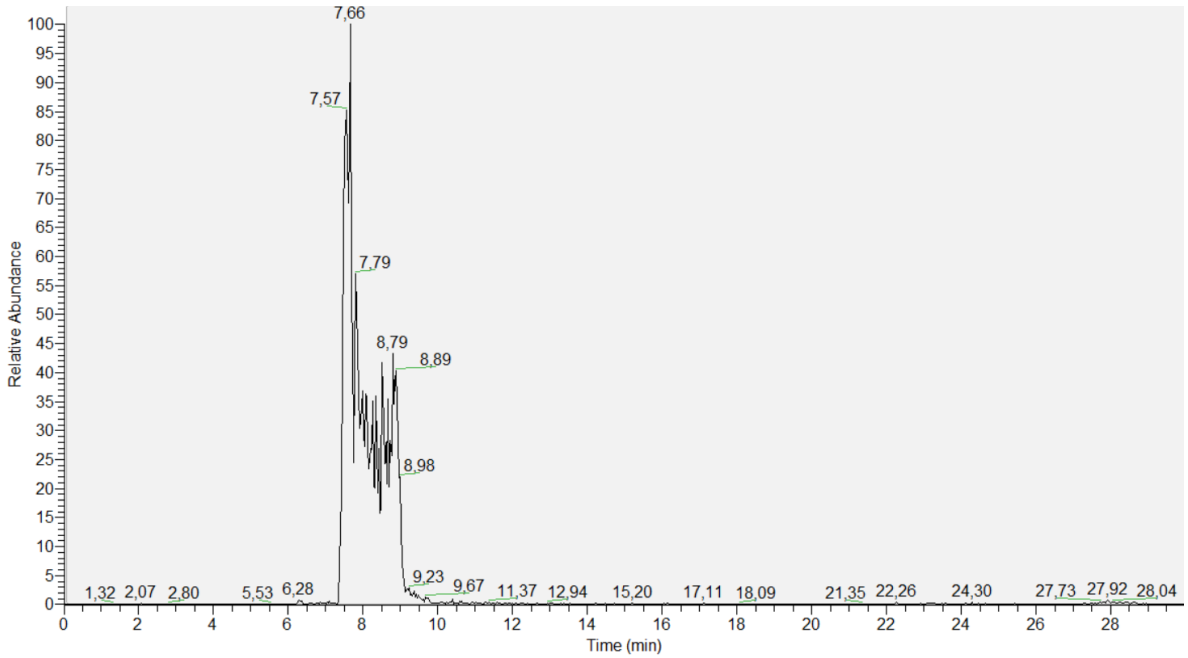

LC-MS (ESI)	$[M+2H]^{2+}$
m/z (calculated)	469.57
m/z (found)	469.57

Figure 265: LC-MS total ion count chromatogram (top) and m/z (bottom) of **216**.

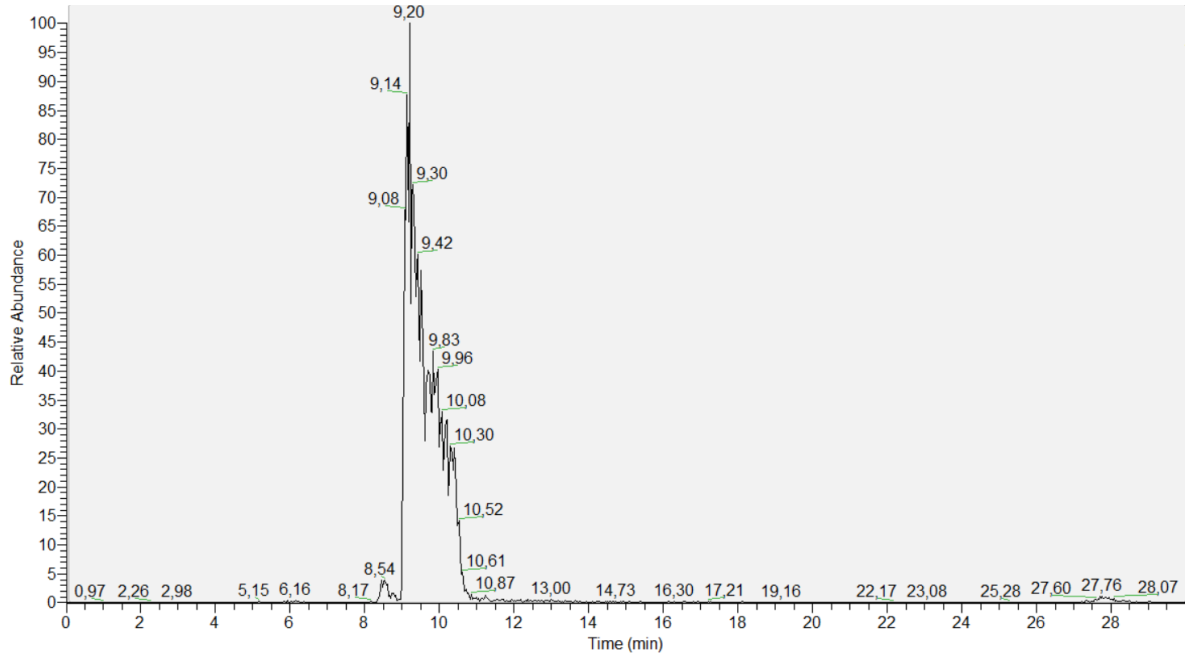

LC-MS (ESI)	$[M+2H]^{2+}$
m/z (calculated)	391.48
m/z (found)	391.45

Figure 266: LC-MS total ion count chromatogram (top) and m/z (bottom) of **217**.

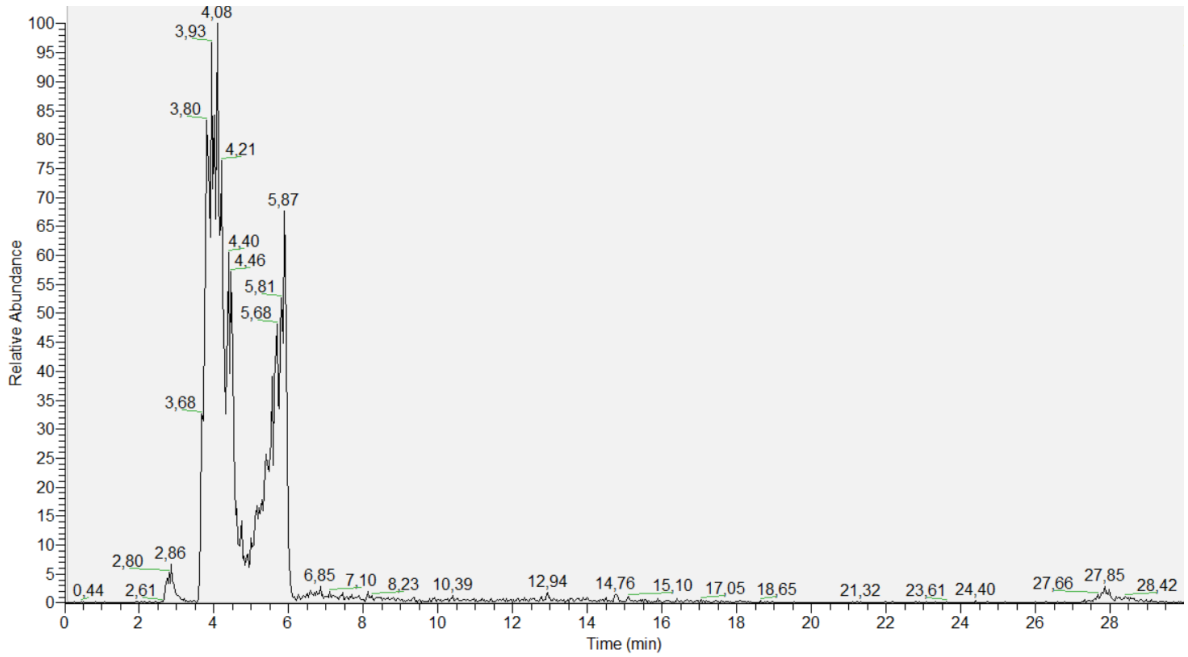

LC-MS (ESI)	$[M+2H]^{2+}$
m/z (calculated)	606.74
m/z (found)	606.72

Figure 267: LC-MS total ion count chromatogram (top) and m/z (bottom) of **218**.

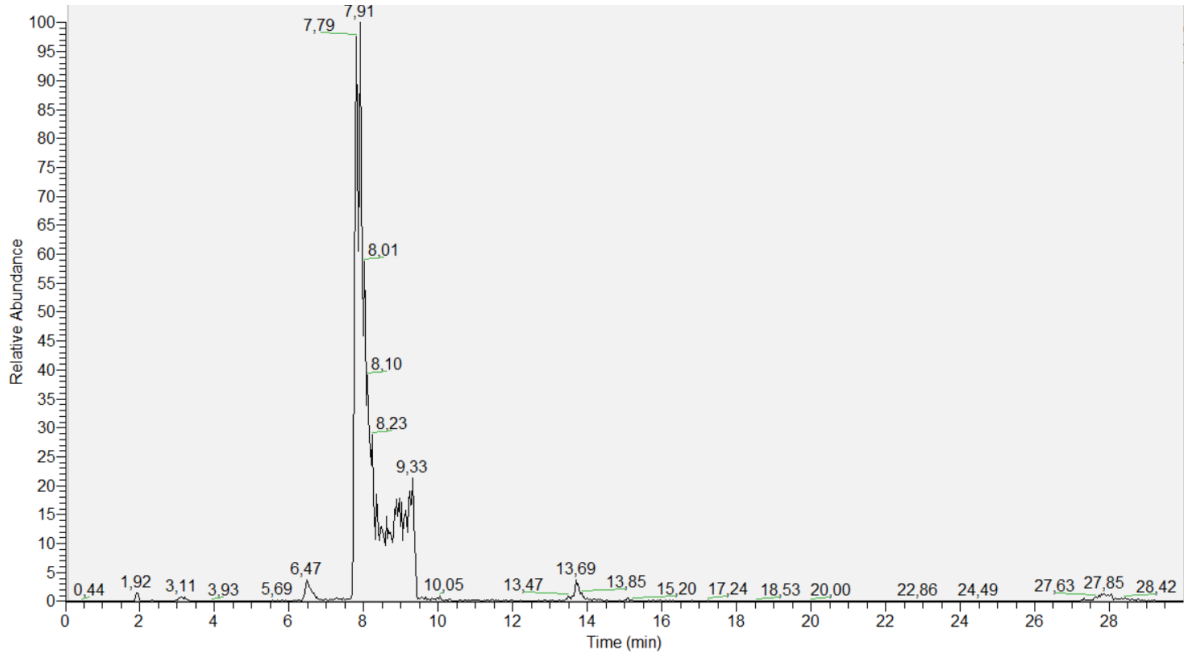

LC-MS (ESI)	$[M+2H]^{2+}$
m/z (calculated)	372.45
m/z (found)	372.45

Figure 268: LC-MS total ion count chromatogram (top) and m/z (bottom) of **219**.

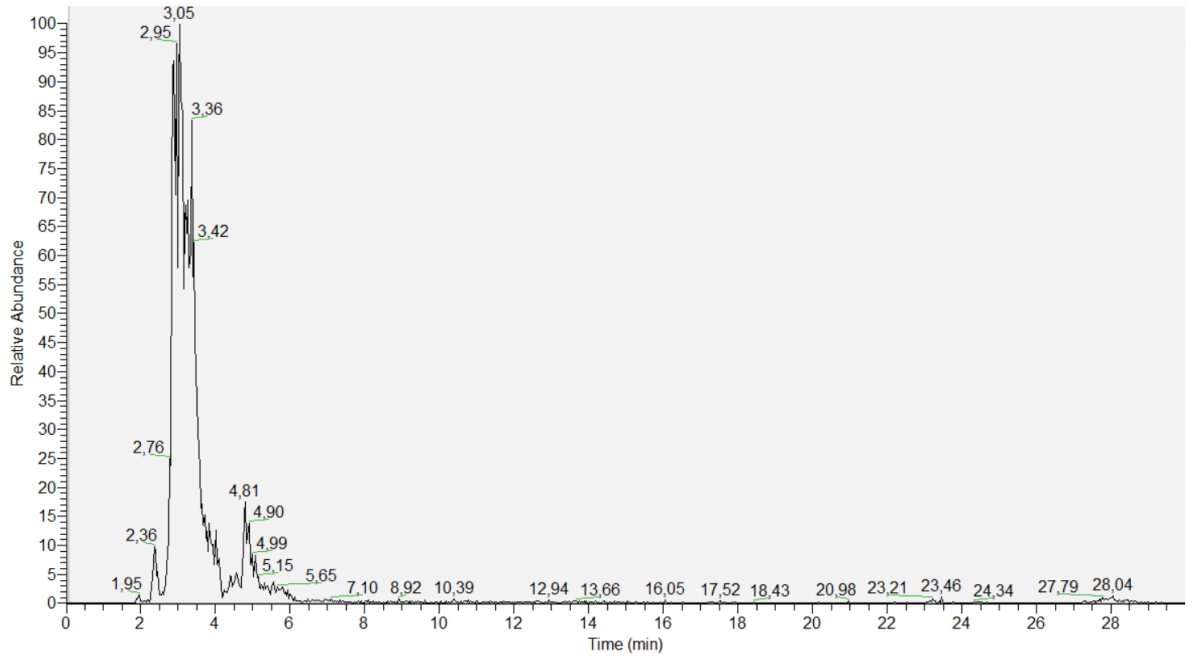

LC-MS (ESI)	$[M+2H]^{2+}$
m/z (calculated)	696.84
m/z (found)	696.83

Figure 269: LC-MS total ion count chromatogram (top) and m/z (bottom) of **215**.

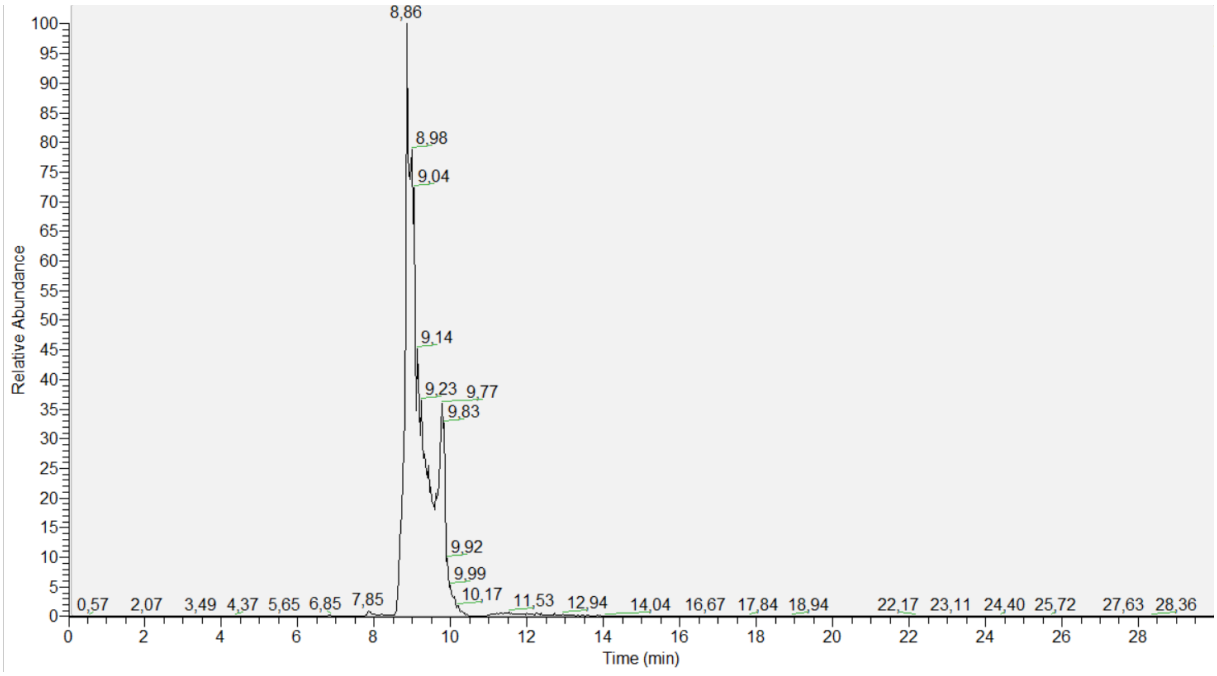

LC-MS (ESI)	$[M+2H]^{2+}$
m/z (calculated)	385.48
m/z (found)	385.53

Figure 270: LC-MS total ion count chromatogram (top) and m/z (bottom) of **220**.

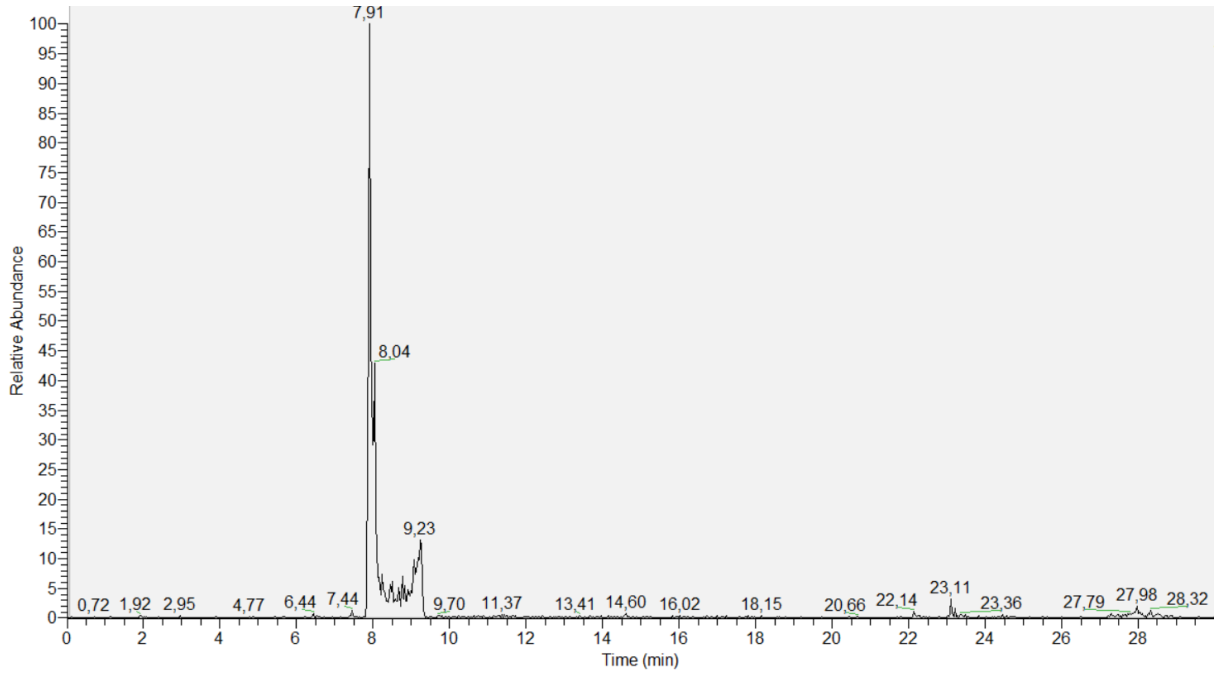

LC-MS (ESI)	$[M+2H]^{2+}$
m/z (calculated)	378.46
m/z (found)	378.49

Figure 271: LC-MS total ion count chromatogram (top) and m/z (bottom) of **221**.

8 Literature

[1] R. Morris, K. A. Black, E. J. Stollar, *Essays Biochem.* **2022**, *66*, 255-285.

[2] M. R. Arkin, Y. Tang, J. A. Wells, *Chem. Biol.* **2014**, *21*, 1102-1114.

[3] X. Xie, T. Yu, X. Li, N. Zhang, L. J. Foster, C. Peng, W. Huang, G. He, *Signal Transduct. Target. Ther.* **2023**, *8*, 1-71.

[4] L. Thelander, *Advanced information on the Nobel Prize in Chemistry* **2004**, Royal Swedish Academy of Sciences, Stockholm.

[5] K. T. G. Samarasinghe, C. M. Crews, *Cell Chem. Biol.* **2021**, *28*, 934-951.

[6] C. M. Pickart, M. J. Eddins, *Biochim. Biophys. Acta* **2004**, *1695*, 55-72.

[7] C. Arkinson, K. C. Dong, C. L. Gee, A. Martin, *Nat. Rev. Mol. Cell Biol.* **2025**, *26*, 104-122.

[8] E. H. Koo, P. T. Lansbury, J. W. Kelly, *Proc. Natl. Acad. Sci. U.S.A.* **1999**, *96*, 9989-9990.

[9] T. E. Golde, D. R. Borchelt, B. I. Giasson, J. Lewis, *J. Clin. Invest.* **2013**, *123*, 1847-1855.

[10] S. Martín-Villanueva, G. Gutiérrez, D. Kressler, J. de la Cruz, *Int. J. Mol. Sci.* **2021**, *22*, 4359.

[11] J. A. Maupin-Furlow, *Trends Microbiol.* **2013**, *21*, 31-38.

[12] P. Coulombe, G. Rodier, E. Bonneil, P. Thibault, S. Meloche, *Mol. Cell. Biol.* **2004**, *24*, 6140-6150.

[13] S. Vijay-Kumar, C. E. Bugg, W. J. Cook, *J. Mol. Biol.* **1987**, *194*, 531-544.

[14] K. N. Swatek, D. Komander, *Cell Res.* **2016**, *26*, 399-422.

[15] Y. Akizuki, S. Kaypee, F. Ohtake, F. Ikeda, *J. Cell Biol.* **2024**, *223*, 1-14.

[16] R. Agrata, D. Komander, *Mol. Cell* **2025**, *85*, 323-346.

[17] D. Gödderz, C. Heinen, F. P. Marchese, T. Kurz, K. Acs, N. P. Dantuma, *Sci. Rep.* **2015**, *5*, 7615.

[18] J. S. Thrower, L. Hoffman, M. Rechsteiner, C. M. Pickart, *EMBO J.* **2000**, *19*, 94-102.

[19] Y. Lu, B.-H. Lee, R. W. King, D. Finley, M. W. Kirschner, *Science* **2015**, *348*, 1250834.

[20] S. Prakash, L. Tian, K. S. Ratliff, R. E. Lehotzky, A. Matouschek, *Nat. Struct. Mol. Biol.* **2004**, *11*, 830-837.

[21] Y. Saeki, *J. Biochem.* **2017**, *161*, 113-124.

[22] G. A. Collins, A. L. Goldberg, *Cell* **2017**, *169*, 792-806.

[23] L. Spyracopoulos, *Structure* **2016**, *24*, 1221-1223.

[24] W. Heinemeyer, M. Fischer, T. Krimmer, U. Stachon, D. H. Wolf, *J. Biol. Chem.* **1997**, *272*, 25200-25209.

[25] J. Rabl, D. M. Smith, Y. Yu, S.-C. Chang, A. L. Goldberg, Y. Cheng, *Mol. Cell* **2008**, *30*, 360-368.

[26] Z. Yu, Y. Yu, F. Wang, A. G. Myasnikov, P. Coffino, Y. Cheng, *Nat. Commun.* **2020**, *11*, 4580.

[27] B. Luan, X. Huang, J. Wu, Z. Mei, Y. Wang, X. Xue, C. Yan, J. Wang, D. J. Finley, Y. Shi, F. Wang, *Proc. Natl. Acad. Sci. U.S.A.* **2016**, *113*, 2642-2647.

[28] D. Park, J. Izaguirre, R. Coffey, H. Xu, *ACS Bio. Med. Chem. Au* **2023**, *3*, 74-86.
[29] A. H. De la Peña, E. A. Goodall, S. N. Gates, G. C. Lander, A. Martin, *Science* **2018**, *362*, eaav0725.
[30] E. Isono, K. Nishihara, Y. Saeki, H. Yashiroda, N. Kamata, L. Ge, T. Ueda, Y. Kikuchi, K. Tanaka, A. Nakano, A. Toh-E, *Mol. Biol. Cell* **2007**, *18*, 569-580.
[31] Z. M. Htet, K. C. Dong, A. Martin, *Cell Rep.* **2025**, *44*, 115736.
[32] M. R. Eisele, R. G. Reed, T. Rudack, A. Schweitzer, F. Beck, I. Nagy, G. Pfeifer, J. M. Plitzko, W. Baumeister, R. J. Tomko, E. Sakata, *Cell Rep.* **2018**, *24*, 1301-1315.
[33] I. Sahu, M. H. Glickman, *Biochem. Soc. Trans.* **2021**, *49*, 629-644.
[34] M. E. Matyskiela, G. C. Lander, A. Martin, *Nat. Struct. Mol. Biol.* **2013**, *20*, 781-788.
[35] D. A. Kraut, E. Israeli, E. K. Schrader, A. Patil, K. Nakai, D. Nanavati, T. Inobe, A. Matouschek, *ACS Chem. Biol.* **2012**, *7*, 1444-1453.
[36] D. Berko, S. Tabachnick-Cherny, D. Shental-Bechor, P. Cascio, S. Mioletti, Y. Levy, A. Admon, T. Ziv, B. Tirosh, A. L. Goldberg, A. Navon, *Mol. Cell* **2012**, *48*, 601-611.
[37] A. F. Kisselev, T. N. Akopian, K. M. Woo, A. L. Goldberg, *J. Biol. Chem.* **1999**, *274*, 3363-3371.
[38] K. Tanaka, *Proc. Jpn. Acad. Ser. B* **2009**, *85*, 12-36.
[39] S. Hutschenreiter, A. Tinazli, K. Model, R. Tampé, *EMBO J.* **2004**, *23*, 2488-2497.
[40] M. Scheffner, U. Nuber, J. M. Hulbregtse, *Nature* **1995**, *373*, 81-83.
[41] B. A. Schulman, J. Wade Harper, *Nat. Rev. Mol. Cell Biol.* **2009**, *10*, 319-331.
[42] L. Yuan, F. Gao, Z. Lv, D. Nayak, A. Nayak, P. dos Santos Bury, K. E. Cano, L. Jia, N. Oleinik, F. C. Atilgan, B. Ogretmen, K. M. Williams, C. Davies, F. El Oualid, E. V. Wasmuth, S. K. Olsen, *Nat. Commun.* **2022**, *13*, 4880.
[43] H. Chen, H. Li, M. He, Z. Lai, L. Huang, D. Wen, M. Shi, A. Kan, *Cancer Sci.* **2024**, *115*, 2998-3012.
[44] M. Sokołowski, D. Kwasna, K. E. Ravichandran, C. Eggers, R. Krutyhołowa, M. Kaczmarczyk, B. Skupien-Rabian, M. Jaciuk, M. Walczak, P. Dahate, M. Pabis, M. Jemioła-Rzemińska, U. Jankowska, S. A. Leidel, S. Glatt, *Nucleic Acids Res.* **2024**, *52*, 13980-13995.
[45] M. Afsar, G. Q. Liu, L. Jia, E. A. Ruben, D. Nayak, Z. Sayyad, P. dos Santos Bury, K. E. Cano, A. Nayak, X. R. Zhao, A. Shukla, P. Sung, E. V. Wasmuth, M. U. Gack, S. K. Olsen, *Nat. Commun.* **2023**, *14*, 4786.
[46] N. N. Noda, K. Satoo, Y. Fujioka, H. Kumeta, K. Ogura, H. Nakatogawa, Y. Ohsumi, F. Inagaki, *Mol. Cell* **2011**, *44*, 462-475.
[47] G. W. Xu, J. I. Toth, S. R. Da Silva, S. L. Paiva, J. L. Lukkarila, R. Hurren, N. Maclean, M. A. Sukhai, R. N. Bhattacharjee, C. A. Goard, P. T. Gunning, S. Dhe-Paganon, M. D. Petroski, A. D. Schimmer, *PLoS One* **2014**, *9*, e93530.
[48] J. M. Gavin, K. Hoar, Q. Xu, J. Ma, Y. Lin, J. Chen, W. Chen, F. J. Bruzzese, S. Harrison, W. D. Mallender, N. J. Bump, M. D. Sintchak, N. F. Bence, P. Li, L. R. Dick, A. E. Gould, J. J. Chen, *J. Biol. Chem.* **2014**, *289*, 22648-22658.

[49] I. Lee, H. Schindelin, *Cell* **2008**, *134*, 268-278.
[50] A. Schäfer, M. Kuhn, H. Schindelin, *Acta Crystallogr. D Biol. Crystallogr.* **2014**, *70*, 1311-1320.
[51] S. K. Olsen, C. D. Lima, *Mol. Cell* **2013**, *49*, 884-896.
[52] Z. S. Hann, C. Ji, S. K. Olsen, X. Lu, M. C. Lux, D. S. Tan, C. D. Lima, *Proc. Natl. Acad. Sci. U.S.A.* **2019**, *116*, 15475-15484.
[53] Y. Sheng, J. H. Hong, R. Doherty, T. Srikumar, J. Shloush, G. V. Avvakumov, J. R. Walker, S. Xue, D. Neculai, J. W. Wan, S. K. Kim, C. H. Arrowsmith, B. Raught, S. Dhe-Paganon, *Mol. Cell. Proteomics* **2012**, *11*, 329-341.
[54] L. Yuan, Z. Lv, M. J. Adams, S. K. Olsen, *Nat. Commun.* **2021**, *12*, 2370.
[55] E. Sakata, T. Satoh, S. Yamamoto, Y. Yamaguchi, M. Yagi-Utsumi, E. Kurimoto, K. Tanaka, S. Wakatsuki, K. Kato, *Structure* **2010**, *18*, 138-147.
[56] D. T. Huang, H. W. Hunt, M. Zhuang, M. D. Ohi, J. M. Holton, B. A. Schulman, *Nature* **2007**, *445*, 394-398.
[57] Y. Ye, M. Rape, *Nat. Rev. Mol. Cell Biol.* **2009**, *10*, 755-764.
[58] M. D. Stewart, T. Ritterhoff, R. E. Klevit, P. S. Brzovic, *Cell Res.* **2016**, *26*, 423-440.
[59] B. S. Tolbert, S. G. Tajc, H. Webb, J. Snyder, J. E. Nielsen, B. L. Miller, R. Basavappa, *Biochemistry* **2005**, *44*, 16385-16391.
[60] Y. Liu, J. Yang, T. Wang, M. Luo, Y. Chen, C. Chen, Z. e. Ronai, Y. Zhou, E. Ruppin, L. Han, *Nat. Commun.* **2023**, *14*, 6509.
[61] A. Dutta, A. Cristiani, S. V. Nikte, J. Eisert, R. M. Bhaskara, *Nat. Commun.* **2025**, *16*, 11382.
[62] Q. Yang, J. Zhao, D. Chen, Y. Wang, *Mol. Biomed.* **2021**, *2*, 23.
[63] T. A. F. Cardote, M. S. Gadd, A. Ciulli, *Structure* **2017**, *25*, 901-911.
[64] R. J. Deshaies, C. A. P. Joazeiro, *Annu. Rev. Biochem.* **2009**, *78*, 399-434.
[65] A. J. Wathan, N. M. Deschene, J. M. Litz, I. Sumner, *J. Phys. Chem. B* **2025**, *129*, 4962-4968.
[66] Y. David, T. Ziv, A. Admon, A. Navon, *J. Biol. Chem.* **2010**, *285*, 8595-8604.
[67] H. B. Kamadurai, Y. Qiu, A. Deng, J. S. Harrison, C. Macdonald, M. Actis, P. Rodrigues, D. J. Miller, J. Souphron, S. M. Lewis, I. Kurinov, N. Fujii, M. Hammel, R. Piper, B. Kuhlman, B. A. Schulman, *eLife* **2013**, *2*, e00828.
[68] K. K. Dove, R. E. Klevit, *J. Mol. Biol.* **2017**, *429*, 3363-3375.
[69] K. A. Rutherford, K. J. McManus, *Mol. Cancer Ther.* **2024**, *23*, 454-463.
[70] K. M. Sakamoto, K. B. Kim, A. Kumagai, F. Mercurio, C. M. Crews, R. J. Deshaies, *Proc. Natl. Acad. Sci. U.S.A.* **2001**, *98*, 8554-8559.
[71] D. Antermite, S. D. Friis, J. R. Johansson, O. D. Putra, L. Ackermann, M. J. Johansson, *Nat. Commun.* **2023**, *14*, 8222.
[72] L. Zhao, J. Zhao, K. Zhong, A. Tong, D. Jia, *Signal Transduct. Target. Ther.* **2022**, *7*, 113.
[73] M. J. Bond, C. M. Crews, *RSC Chem. Biol.* **2021**, *2*, 725-742.
[74] N. Ma, S. Bhattacharya, S. Muk, Z. Jandova, P. S. Schmalhorst, S. Ghosh, K. M. Le, E. Diers, N. Trainor, W. Farnaby, M. J. Roy, C. Kofink, P. Greb, H.

Weinstabl, A. Ciulli, G. Bader, K. Sanker, A. Bergner, N. Vaidehi, *Nat. Commun.* **2024**, *16*, 8595.
[75] R. I. Troup, C. Fallan, M. G. J. Baud, *Explor. Target. Antitumor Ther.* **2020**, *1*, 273-312.
[76] B. Lu, J. Ye, *Acta Pharm. Sin. B* **2021**, *11*, 3335-3336.
[77] R. T. U. Haid, A. Reichel, *Pharmaceutics* **2023**, *15*, 195.
[78] K. M. Riching, E. A. Caine, M. Urh, D. L. Daniels, *Chem. Soc. Rev.* **2022**, *51*, 6210-6221.
[79] D. P. Bondeson, B. E. Smith, G. M. Burslem, A. D. Buhimschi, J. Hines, S. Jaime-Figueroa, J. Wang, B. D. Hamman, A. Ishchenko, C. M. Crews, *Cell Chem. Biol.* **2018**, *25*, 78-87.
[80] M. S. Gadd, A. Testa, X. Lucas, K.-H. Chan, W. Chen, D. J. Lamont, M. Zengerle, A. Ciulli, *Nat. Chem. Biol.* **2017**, *13*, 514-521.
[81] B. P. Belcher, C. C. Ward, D. K. Nomura, *Biochemistry* **2023**, *62*, 588-600.
[82] S. Ribes, E. Nittinger, C. Tyrchan, R. Mercado, *Artif. Intell. Life Sci.* **2024**, *6*, 100104.
[83] Z. Liu, M. Hu, Y. Yang, C. Du, H. Zhou, C. Liu, Y. Chen, L. Fan, H. Ma, Y. Gong, Y. Xie, *Mol. Biomed.* **2022**, *3*, 46.
[84] N. Vargesson, *Birth Defects Res.* **2015**, *105*, 140-156.
[85] A. N. Lupas, H. Zhu, M. Korycinski, *PLoS Comput. Biol.* **2015**, *11*, e1004023.
[86] K. A. Donovan, J. An, R. P. Nowak, J. C. Yuan, E. C. Fink, B. C. Berry, B. L. Ebert, E. S. Fischer, *eLife* **2018**, *7*, 38430.
[87] J. M. Sasso, R. Tenchov, D. S. Wang, L. S. Johnson, X. Wang, Q. A. Zhou, *Biochemistry* **2023**, *62*, 601-623.
[88] S. Rana, J. R. Mallareddy, S. Singh, L. Boghean, A. Natarajan, *Cancers* **2021**, *13*, 5506.
[89] T. Mori, T. Ito, S. Liu, H. Ando, S. Sakamoto, Y. Yamaguchi, E. Tokunaga, N. Shibata, H. Handa, T. Hakoshima, *Sci. Rep.* **2018**, *8*, 1294.
[90] E. S. Fischer, K. Böhm, J. R. Lydeard, H. Yang, M. B. Stadler, S. Cavadini, J. Nagel, F. Serluca, V. Acker, G. M. Lingaraju, R. B. Tichkule, M. Schebesta, W. C. Forrester, M. Schirle, U. Hassiepen, J. Ottl, M. Hild, R. E. J. Beckwith, J. W. Harper, J. L. Jenkins, N. H. Thomä, *Nature* **2014**, *512*, 49-53.
[91] T. Ito, H. Ando, H. Handa, *Cell. Mol. Life Sci.* **2011**, *68*, 1569-1579.
[92] C. Patel, B. De Barros, S. L. Walker, *Skin Health Dis.* **2024**, *4*, 339.
[93] H. Furihata, S. Yamanaka, T. Honda, Y. Miyauchi, A. Asano, N. Shibata, M. Tanokura, T. Sawasaki, T. Miyakawa, *Nat. Commun.* **2020**, *11*, 4578.
[94] S. A. Holstein, P. L. McCarthy, *Drugs* **2017**, *77*, 505-520.
[95] M. D. Hartmann, I. Boichenko, M. Coles, F. Zanini, A. N. Lupas, B. Hernandez Alvarez, *J. Struct. Biol.* **2014**, *188*, 225-232.
[96] Y. X. Zhu, K. M. Kortuem, A. K. Stewart, *Leuk. Lymphoma* **2013**, *54*, 683-687.
[97] C. M. Almodóvar-Rivera, Z. Zhang, J. Li, H. Xie, Y. Zhao, L. Guo, M. G. Mannhardt, W. Tang, *ChemBioChem* **2023**, *24*, e202300482.
[98] J. Min, A. Mayasundari, F. Keramatnia, B. Jonchere, S. Wook Yang, J. Jarusiewicz, M. Actis, S. Das, B. Young, J. Slavish, L. Yang, Y. Li, X. Fu, S. H.

Garrett, M.-K. Yun, Z. Li, S. Nithianantham, S. Chai, T. Chen, A. Shelat, R. E. Lee, G. Nishiguchi, S. W. White, M. F. Roussel, P. Ryan Potts, M. Fischer, Z. Rankovic, *Angew. Chem. Int. Ed.* **2022**, *60*, 26663-26670.

[99] J. A. Jarusiewicz, S. Yoshimura, A. Mayasundari, M. Actis, A. Aggarwal, K. McGowan, L. Yang, Y. Li, X. Fu, V. Mishra, R. Heath, S. Narina, S. M. Pruett-Miller, G. Nishiguchi, J. J. Yang, Z. Rankovic, *ACS Med. Chem. Lett.* **2023**, *14*, 141-145.

[100] A. Kroupova, V. A. Spiteri, Z. J. Rutter, H. Furihata, D. Darren, S. Ramachandran, S. Chakraborti, K. Haubrich, J. Pethe, D. Gonzales, A. J. Wijaya, M. Rodriguez-Rios, M. Sturbaut, D. M. Lynch, W. Farnaby, M. A. Nakasone, D. Zollman, A. Ciulli, *Nat. Commun.* **2024**, *15*, 8885.

[101] P. J. Ratcliffe, *J. Clin. Invest.* **2007**, *117*, 862-865.

[102] F. Yu, S. B. White, Q. Zhao, F. S. Lee, *Proc. Natl. Acad. Sci. U.S.A.* **2001**, *98*, 9630-9635.

[103] W. G. Kaelin, *J. Clin. Invest.* **2022**, *132*, e162480.

[104] J. S. Schneekloth, F. N. Fonseca, M. Koldobskiy, A. Mandal, R. Deshaies, K. Sakamoto, C. M. Crews, *J. Am. Chem. Soc.* **2004**, *126*, 3748-3754.

[105] I. Van Molle, A. Thomann, D. L. Buckley, E. C. So, S. Lang, C. M. Crews, A. Ciulli, *Chem. Biol.* **2012**, *19*, 1300-1312.

[106] C. Galdeano, M. S. Gadd, P. Soares, S. Scaffidi, I. Van Molle, I. Birced, S. Hewitt, D. M. Dias, A. Ciulli, *J. Med. Chem.* **2014**, *57*, 8657-8663.

[107] C. J. Diehl, A. Ciulli, *Chem. Soc. Rev.* **2022**, *51*, 8216-8257.

[108] T. P. Padera, A. Kadambi, E. Di Tomaso, C. Mouta Carreira, E. B. Brown, Y. Boucher, N. C. Choi, D. Mathisen, J. Wain, E. J. Mark, L. L. Munn, R. K. Jain, *Science* **2002**, *296*, 1883-1886.

[109] T. Ishida, A. Ciulli, *SLAS Discov.* **2021**, *26*, 484-502.

[110] A. Zagidullin, V. Milyukov, A. Rizvanov, E. Bulatov, *Explor. Target. Antitumor Ther.* **2020**, *1*, 381-390.

[111] M. Békés, D. R. Langley, C. M. Crews, *Nat. Rev. Drug Discov.* **2022**, *21*, 181-200.

[112] H. J. Maple, N. Clayden, A. Baron, C. Stacey, R. Felix, *Med. Chem. Commun.* **2019**, *10*, 1755-1764.

[113] C. Cecchini, S. Tardy, L. Scapozza, *Chimia* **2022**, *76*, 341-345.

[114] G. Weng, X. Cai, D. Cao, H. Du, C. Shen, Y. Deng, Q. He, B. Yang, D. Li, T. Hou, *Nucleic Acids Res.* **2023**, *51*, 1367-1372.

[115] P. Filippakopoulos, J. Qi, S. Picaud, Y. Shen, W. B. Smith, O. Fedorov, E. M. Morse, T. Keates, T. T. Hickman, I. Felletar, M. Philpott, S. Munro, M. R. McKeown, Y. Wang, A. L. Christie, N. West, M. J. Cameron, B. Schwartz, T. D. Heightman, N. La Thangue, C. A. French, O. Wiest, A. L. Kung, S. Knapp, J. E. Bradner, *Nature* **2010**, *468*, 1067-1073.

[116] C.-Y. Yang, C. Qin, L. Bai, S. Wang, *Drug Discov. Today Technol.* **2019**, *31*, 43-51.

[117] G. E. Winter, A. Mayer, D. L. Buckley, M. A. Erb, J. E. Roderick, S. Vittori, J. M. Reyes, J. di Iulio, A. Souza, C. J. Ott, J. M. Roberts, R. Zeid, T. G. Scott, J.

Paulk, K. Lachance, C. M. Olson, S. Dastjerdi, S. Bauer, C. Y. Lin, N. S. Gray, M. A. Kelliher, L. S. Churchman, J. E. Bradner, *Mol. Cell* **2017**, *67*, 5-18.
[118] M. Zengerle, K.-H. Chan, A. Ciulli, *ACS Chem. Biol.* **2015**, *10*, 1770-1777.
[119] N. Ohoka, O. Ujikawa, K. Shimokawa, T. Sameshima, N. Shibata, T. Hattori, H. Nara, N. Cho, M. Naito, *Chem. Pharm. Bull.* **2019**, *67*, 203-209.
[120] J. Hines, S. Lartigue, H. Dong, Y. Qian, C. M. Crews, *Cancer Res.* **2019**, *79*, 251-262.
[121] Z. Ma, J. Zhou, *J. Med. Chem.* **2025**, *68*, 14129-14136.
[122] L. B. Snyder, T. K. Neklesa, R. R. Willard, D. A. Gordon, J. Pizzano, N. Vitale, K. Robling, M. A. Dorso, W. Moghrabi, S. Landrette, R. Gedrich, S. H. Lee, I. C. A. Taylor, J. G. Houston, *Mol. Cancer Ther.* **2025**, *24*, 511-522.
[123] R. Guieze, A. Frustaci, C. Cheah, J. Seymour, D. H. Yoon, I. Mocanu, E. Mou, P. L. Zinzani, A. Mehta, C. Tam, J. Trotman, Y. Zhang, L. Xu, K. By, A. Lussier, S. Fabre, D. Persky, R. Advani, *Blood* **2025**, *146*, 3584-3584.
[124] X. Liu, A. F. Kalogeropulou, S. Domingos, N. Makukhin, R. S. Nirujogi, F. Singh, N. Shpiro, A. Saalfrank, E. Sammler, I. G. Ganley, R. Moreira, D. R. Alessi, A. Ciulli, *J. Am. Chem. Soc.* **2022**, *144*, 16930-16952.
[125] G. Zhong, X. Chang, W. Xie, X. Zhou, *Signal Transduct. Target. Ther.* **2024**, *9*, 308.
[126] A. Zarrinpar, R. P. Bhattacharyya, W. A. Lim, *Sci. STKE* **2003**, *179*, re8.
[127] S. S.-C. Li, *Biochem. J.* **2005**, *390*, 641-653.
[128] L. Ball, R. Kühne, B. Hoffmann, A. Häfner, P. Schmieder, *EMBO J.* **2000**, *19*, 4903-4914.
[129] K. Prehoda, D. J. Lee, W. A. Lim, *Cell* **1999**, *97*, 471-480.
[130] C. B. McDonald, K. L. Seldeen, B. J. Deegan, A. Farooq, *Biochemistry* **2009**, *48*, 4074-4085.
[131] S. Feng, C. Kasahara, R. J. Ricklest, S. L. Schreiber, *Proc. Natl. Acad. Sci. U.S.A.* **1995**, *92*, 12408-12415.
[132] C. B. McDonald, S. K. N. McIntosh, D. C. Mikles, V. Bhat, B. J. Deegan, K. L. Seldeen, A. M. Saeed, L. Buffa, M. Sudol, Z. Nawaz, A. Farooq, *Biochemistry* **2011**, *50*, 9616-9627.
[133] J. Â Ricardo Pires, F. Taha-Nejad, F. Toepert, T. Ast, U. Hoffmüller, J. Schneider-Mergener, R. Kühne, M. J. Macias, H. Oschkinat, *J. Mol. Biol.* **2001**, *314*, 1147-1156.
[134] N. M. Mahoney, D. A. Rozwarski, E. Fedorov, A. A. Fedorov, S. C. Almo, *Nat. Struct. Biol.* **1999**, *6*, 666-671.
[135] A. Georgiev, M. Sjöström, Å. Wieslander, *Protein Eng. Des. Sel.* **2007**, *20*, 443-452.
[136] C. Freund, R. Kühne, H. Vang, S. Park, E. L. Reinherz, G. Wagner, *EMBO J.* **2002**, *21*, 5985-5995.
[137] O. Pornillos, S. L. Alam, D. R. Davis, W. I. Sundquist, *Nat. Struct. Biol.* **2002**, *9*, 812-817.
[138] O. Pornillos, S. L. Alam, R. Rich, D. Myszke, D. Davis, W. I. Sundquist, *EMBO J.* **2002**, *21*, 2397-2406.

[139] M. Srinivasan, A. K. Dunker, *Int. J. Pept. Res. Ther.* **2012**, *18*, 634769.
[140] S. P. Visweshwaran, H. Nayab, L. Hoffmann, M. Gil, F. Liu, R. Kühne, T. Maritzen, *Front. Cell Dev. Biol.* **2022**, *10*, 3389.
[141] H. Döppler, L. Bastea, S. Borges, X. Geiger, P. Storz, *Oncotarget* **2015**, *6*, 29740-29752.
[142] J. E. Bear, T. M. Svitkina, M. Krause, D. A. Schafer, J. J. Loureiro, G. A. Strasser, I. V. Maly, O. Y. Chaga, J. A. Cooper, G. G. Borisy, F. B. Gertler, *Cell* **2002**, *109*, 509-521.
[143] S. D. Hansen, R. D. Mullins, *eLife* **2015**, *4*, e06585.
[144] T. Hwang, R. A. Grant, M. W. Ilunga, V. Sivaraman, A. E. Keating, *eLife* **2022**, *11*, e70680.
[145] X. J. Chen, A. J. Squarr, R. Stephan, B. Chen, T. E. Higgins, D. J. Barry, M. C. Martin, M. K. Rosen, S. Bogdan, M. Way, *Dev. Cell* **2014**, *30*, 569-584.
[146] J. E. Bear, F. B. Gertler, *J. Cell Sci.* **2009**, *122*, 1947-1953.
[147] S. Menon, N. P. Boyer, C. C. Winkle, L. M. McClain, C. C. Hanlin, D. Pandey, S. Rothenfußer, A. M. Taylor, S. L. Gupton, *Dev. Cell* **2015**, *35*, 698-712.
[148] L. E. McCormick, C. Suarez, L. E. Herring, K. S. Cannon, D. R. Kovar, N. G. Brown, S. L. Gupton, *J. Cell. Sci.* **2024**, *137*, 261527.
[149] N. P. Boyer, L. E. McCormick, S. Menon, F. L. Urbina, S. L. Gupton, *J. Cell Biol.* **2020**, *219*, e201902088.
[150] F. Ferron, G. Rebowski, S. H. Lee, R. Dominguez, *EMBO J.* **2007**, *26*, 4597-4606.
[151] M. Müller, M. Barone, M. van Dinther, K. Motzny, J. Ren, J. Eichhorst, D. Albat, S. Chiha, M. Lehmann, R. Volkmer, H. Oschkinat, H.-G. Schmalz, P. ten Dijke, R. Kühne, *Proc. Natl. Acad. Sci. U.S.A.* **2025**, *122*, e2423512122.
[152] M. Barone, S. Chiha, J. Ren, D. Albat, A. Soicke, S. Dohmen, M. Klein, J. Bruns, M. van Dinther, R. Opitz, P. Lindemann, M. Beerbaum, K. Motzny, Y. Roske, P. Schmieder, R. Volkmer, M. Nazaré, U. Heinemann, H. Oschkinat, P. ten Dijke, H.-G. Schmalz, *Proc. Natl. Acad. Sci. U.S.A.* **2020**, *117*, 29684-29690.
[153] D. Albat, S. Chiha, S. Dohmen, P. M. Engelhardt, H. Sebode, A. Soicke, M. Barone, M. Müller, R. Kühne, H.-G. Schmalz, *Eur. J. Org. Chem.* **2023**, *26*, e202300771.
[154] P. Kumar, M. Bansal, *J. Struct. Biol.* **2016**, *196*, 414-425.
[155] C. Reuter, R. Opitz, A. Soicke, S. Dohmen, M. Barone, S. Chiha, M. T. Klein, J.-M. Neudörfl, R. Kühne, H.-G. Schmalz, *Chem. Eur. J.* **2015**, *21*, 8464-8470.
[156] J. Zaminer, C. Brockmann, P. Huy, R. Opitz, C. Reuter, M. Beyermann, C. Freund, M. Muller, H. Oschkinat, R. Kuhne, H.-G. Schmalz, *Angew. Chem. Int. Ed.* **2010**, *49*, 7111-7115.
[157] P. Huy, J.-M. Neudörfl, H.-G. Schmalz, *Org. Lett.* **2011**, *13*, 216-219.
[158] C. Reuter, P. Huy, J.-M. Neudörfl, R. Kühne, H.-G. Schmalz, *Chem. Eur. J.* **2011**, *17*, 12037-12044.
[159] P. Huy, H.-G. Schmalz, *Synthesis* **2011**, 954-960.

[160] P. M. Engelhardt, S. Florez-Rueda, M. Drexelius, J.-M. Neudörfl, D. Lauster, C. P. R. Hackenberger, R. Kühne, I. Neundorf, H.-G. Schmalz, *ChemBioChem* **2022**, *23*, e202200372.
[161] V. Hack, C. Reuter, R. Opitz, P. Schmieder, M. Beyermann, J.-M. Neudörfl, R. Kühne, H.-G. Schmalz, *Angew. Chem. Int. Ed.* **2013**, *52*, 9539-9543.
[162] C. Reuter, M. Kleczka, S. De Mazancourt, J.-M. Neudörfl, R. Kühne, H.-G. Schmalz, *Eur. J. Org. Chem.* **2014**, *2014*, 2664-2667.
[163] S. Dohmen, M. Reiher, D. Albat, S. Akyol, M. Barone, J.-M. Neudörfl, R. Kühne, H.-G. Schmalz, *Chem. Eur. J.* **2020**, *26*, 3049-3053.
[164] D. Albat, A. Köcher, J. Witt, H.-G. Schmalz, *Eur. J. Org. Chem.* **2022**, e202200188.
[165] A. Soicke, C. Reuter, M. Winter, J.-M. Neudörfl, N. Schlörer, R. Kühne, H.-G. Schmalz, *Eur. J. Org. Chem.* **2014**, *2014*, 6467-6480.
[166] A. Maaßen, J. M. Gebauer, E. Theres Abraham, I. Grimm, J.-M. Neudörfl, R. Kühne, I. Neundorf, U. Baumann, H.-G. Schmalz, *Angew. Chem. Int. Ed.* **2020**, *59*, 5747-5755.
[167] S. Chiha, A. Soicke, M. Barone, M. Müller, J. Bruns, R. Opitz, J.-M. Neudörfl, R. Kühne, H.-G. Schmalz, *Eur. J. Org. Chem.* **2018**, 455-460.
[168] P. M. Engelhardt, J. Strippel, D. Albat, S. Chiha, J. Rojas Pión, L. Plein, R. Kühne, M. Müller, H.-G. Schmalz, *Chem. Eur. J.* **2024**, *30*, e202401678.
[169] R. Opitz, M. Müller, C. Reuter, M. Barone, A. Soicke, Y. Roske, K. Piotukh, P. Huy, M. Beerbaum, B. Wiesner, M. Beyermann, P. Schmieder, C. Freund, R. Volkmer, H. Oschkinat, H.-G. Schmalz, R. Kühne, *Proc. Natl. Acad. Sci. U.S.A.* **2015**, *112*, 5011-5016.
[170] F. Malagrinò, E. Puglisi, L. Pagano, C. Travaglini-Allocatelli, A. Toto, *Biochem. Biophys. Rep.* **2024**, *39*, 101803.
[171] I. K. Jang, D. G. Cronshaw, L.-K. Xie, G. Fang, J. Zhang, H. Oh, Y. X. Fu, H. Gu, Y. Zou, *Proc. Natl. Acad. Sci. U.S.A.* **2011**, *108*, 7926-7931.
[172] E. Y. Skolnik, C. H. Lee, A. Batzer, L. M. Vicentini, M. Zhou, R. Daly, M. J. Myers, J. M. Backer, A. Ullrich, M. F. White, J. Schlessinger, *EMBO J.* **1993**, *12*, 1929-1936.
[173] N. S. Kazemein Jasemi, M. Reza Ahmadian, *Small GTPases* **2022**, *13*, 282-286.
[174] C. Seiler, A. K. Stainthorp, S. Ketchen, C. M. Jones, K. Marks, P. Quirke, J. E. Ladbury, *Commun. Biol.* **2022**, *5*, 1029.
[175] S.-K. Hong, S. Yoon, C. Moelling, D. Arthan, J.-I. Park, *J. Biol. Chem.* **2009**, *284*, 33006-33018.
[176] D. N. Tran, Y. J. Hwang, K. C. Kim, R. Li, R. M. Marquardt, C. Chen, S. L. Young, B. A. Lessey, T. H. Kim, Y.-P. Cheon, J.-W. Jeong, *Nat. Commun.* **2025**, *16*, 2192.
[177] C. G. Hansen, Y. L. D. Ng, W. L. M. Lam, S. W. Plouffe, K.-L. Guan, *Cell Res.* **2015**, *25*, 1299-1313.
[178] M. Iglesias-Bexiga, F. Castillo, E. S. Cobos, T. Oka, M. Sudol, I. Luque, *PLoS One* **2015**, *10*, e113828.

[179] Y.-A. Chen, C.-Y. Lu, T.-Y. Cheng, S.-H. Pan, H.-F. Chen, N.-S. Chang, *Front. Oncol.* **2019**, *9*, 60.
[180] Z. Li, B. Zhao, P. Wang, F. Chen, Z. Dong, H. Yang, K.-L. Guan, Y. Xu, *Genes Dev.* **2010**, *24*, 235-240.
[181] F. Kanai, P. Marignani, D. Sarbassova, R. Yagi, R. Hall, M. Donowitz, A. Hisaminato, T. Fujiwara, Y. Ito, L. Cantley, M. Yaffe, *EMBO J.* **2000**, *19*, 6778-6791.
[182] S. W. Plouffe, K. C. Lin, J. L. Moore, F. E. Tan, S. Ma, Z. Ye, Y. Qiu, B. Ren, K.-L. Guan, *J. Biol. Chem.* **2018**, *293*, 11230-11240.
[183] B. Zhao, L. Li, K. Tumaneng, C.-Y. Wang, K.-L. Guan, *Genes Dev.* **2010**, *24*, 72-85.
[184] H. Liang, Y. Xu, J. Zhao, M. Chen, M. Wang, *Cancer Gene Ther.* **2024**, *31*, 652-666.
[185] B. Zhao, L. Li, Q. Lei, K.-L. Guan, *Genes Dev.* **2010**, *24*, 862-874.
[186] X. Hu, Y. Zhang, H. Yu, Y. Zhao, X. Sun, Q. Li, Y. Wang, *Front. Immunol.* **2022**, *13*, e1012173.
[187] C. Zhou, C. Sun, M. Huang, X. Tang, L. Pi, C. Li, *J. Med. Chem.* **2024**, *67*, 15168-15198.
[188] R. Zhou, H. Wang, G. M. Zhang, Y. Liu, X. L. Liu, Z. Li, G. Shi, J. Yuan, C. Qu, Y. Li, L. Chen, J. Huang, H. Zhou, L. Dai, C. Bai, J. Wang, L. Yu, Z. Li, Y. L. Li, *Nat. Commun.* **2025**, *16*, 9374.
[189] D. Albat, N. Klangwart, F. Blüm, L. La Pietra, M. Müller, K. Puls, M. Payton Jones, C. Hanzlik, U. Rauh, S. Chiha, *Prosion GmbH* **2025**, *unpublished results*.
[190] H. M. R. de Souza, J. S. Guedes, R. H. C. N. Freitas, L. G. V. Gelves, H. H. Fokoue, C. M. R. Sant'Anna, E. J. Barreiro, L. M. Lima, *J. Enzyme Inhib. Med. Chem.* **2022**, *37*, 718-727.
[191] S. Kapić, H. Čipčić Paljetak, I. Palej Jakopović, A. Fajdetić, M. Ilijaš, V. Štimac, K. Brajša, D. J. Holmes, J. Berge, S. Alihodžić, *Bioorg. Med. Chem.* **2011**, *19*, 7281-7298.
[192] R. Kühne, H.-G. Schmalz, S. Dohmen, M. Barone, M. Müller, S. Chiha, D. Albat, *WO 2019/162524 B2* **2019**.
[193] D. Albat, Stereoselektive Palladium- und Iridium-katalysierte N-Allylierung von Aminosäureestern und die Synthese von PPII-Sekundärstrukturmimetika als Metastase-Inhibitoren, *Dissertation*, Universität zu Köln, **2021**.
[194] J. Li, C.-L. Sun, R. Shen, X.-Y. Cao, B. Zhou, D.-C. Bai, H.-L. Zhang, *J. Am. Chem. Soc.* **2014**, *136*, 11050-11056.
[195] J. Yang, Y. Chang, J. C.-Y. Tien, Z. Wang, Y. Zhou, P. Zhang, W. Huang, J. Vo, I. J. Apel, C. Wang, V. Z. Zeng, Y. Cheng, S. Li, G. X. Wang, A. M. Chinnaiyan, K. Ding, *J. Med. Chem.* **2022**, *65*, 11066-11083.
[196] A. Banerjee, S. Maschauer, H. Hübner, P. Gmeiner, O. Prante, *Bioorg. Med. Chem. Lett.* **2013**, *23*, 6079-6082.
[197] B. Lei, H. Liu, Z. Wang, *WO 2022/068849 A1* **2022**.
[198] S. Norris, X. Ba, J. Rhodes, D. Huang, G. Khambatta, J. Buenviaje, S. Nayak, J. Meiring, S. Reiss, S. Xu, L. Shi, B. Whitefield, M. Alexander, E. J. Horn, M.

Correa, L. Tehrani, J. D. Hansen, P. Papa, D. S. Mortensen, *J. Med. Chem.* **2023**, *66*, 16388-16409.

[199] G. Nishiguchi, F. Keramatnia, J. Min, Y. Chang, B. Jonchere, S. Das, M. Actis, J. Price, D. Chepyala, B. Young, K. McGowan, P. J. Slavish, A. Mayasundari, J. A. Jarusiewicz, L. Yang, Y. Li, X. Fu, S. H. Garrett, J. B. Papizan, K. Kodali, J. Peng, S. M. Pruett Miller, M. F. Roussel, C. Mullighan, M. Fischer, Z. Rankovic, *J. Med. Chem.* **2021**, *64*, 7296-7311.

[200] R. Soo Hee, M. Im Suk, L. Han Kyu, K. Seong Hoon, R. Hye Guk, K. Keum Young, K. Sang Youn, C. So Hyun, L. Jun Kyu, L. Gibbeum, *WO 2023/017446 A1* **2023**.

[201] H.-Y. Zhao, X.-Y. Yang, H. Lei, X.-X. Xi, S.-M. Lu, J.-J. Zhang, M. Xin, S.-Q. Zhang, *Eur. J. Med. Chem.* **2020**, *208*, 112781.

[202] S. He, F. Gao, J. Ma, H. Ma, G. Dong, C. Sheng, *Angew. Chem. Int. Ed.* **2021**, *60*, 23299-23305.

[203] R. R. Shah, E. De Vita, P. S. Sathyamurthi, D. Conole, X. Zhang, E. Fellows, E. R. Dickinson, C. M. Fleites, M. A. Queisser, J. D. Harling, E. W. Tate, *J. Med. Chem.* **2024**, *67*, 4641-4654.

[204] J. Desantis, A. Bazzacco, M. Eleuteri, S. Tuci, E. Bianconi, A. Macchiarulo, B. Mercorelli, A. Loregian, L. Goracci, *Eur. J. Med. Chem.* **2024**, *268*, 116202.

[205] J. S. Scott, I. N. Michaelides, M. Schade, *RSC Med. Chem.* **2024**, *16*, 449-456.

[206] A. Whitty, M. Zhong, L. Viarengo, D. Beglov, D. R. Hall, S. Vajda, *Drug Discov. Today* **2016**, *21*, 712-717.

[207] X. Han, Y. Sun, *Cell Rep. Phys. Sci.* **2022**, *3*, 101062.

[208] A. Mullard, *Nat. Rev. Drug Discov.* **2018**, *17*, 777-779.

[209] M. Harkiolaki, T. Tsirka, M. Lewitzky, P. C. Simister, D. Joshi, L. E. Bird, E. Y. Jones, N. O'Reilly, S. M. Feller, *Structure* **2009**, *17*, 809-822.

[210] A. V. Pereboev, N. Ahmed, N. Thi Man, G. E. Morris, *Biochim. Biophys. Acta* **2001**, *1527*, 54-60.

[211] C. Kardinal, B. Konkol, H. Lin, M. Eulitz, E. K. Schmidt, Z. Estrov, M. Talpaz, R. B. Arlinghaus, S. M. Feller, *Blood* **2001**, *98*, 1773-1781.

[212] D. Chen, S. Liu, W. Zhang, L. Sun, *J. Pept. Sci.* **2015**, *21*, 826-832.

[213] A. Komuro, M. Nagai, N. E. Navin, M. Sudol, *J. Biol. Chem.* **2003**, *278*, 33334-33341.

[214] S. K. Tipparaju, S. Joyasawal, S. Forrester, D. C. Mulhearn, S. Pegan, M. E. Johnson, A. D. Mesecar, A. P. Kozikowski, *Bioorg. Med. Chem. Lett.* **2008**, *18*, 3565-3569.

[215] J. Simonin, S. K. V. Vernekar, A. J. Thompson, J. D. Hothersall, C. N. Connolly, S. C. R. Lummis, M. Lochner, *Bioorg. Med. Chem. Lett.* **2012**, *22*, 1151-1155.

[216] K. Heller, P. Ochtrop, M. F. Albers, F. B. Zauner, A. Itzen, C. Hedberg, *Angew. Chem. Int. Ed.* **2015**, *54*, 10327-10330.

[217] Y. Kawamata, K. Hayashi, E. Carlson, S. Shaji, D. Waldmann, B. J. Simmons, J. T. Edwards, C. W. Zapf, M. Saito, P. S. Baran, *J. Am. Chem. Soc.* **2021**, *143*, 16580-16588.

[218] D. A. Brown, M. Mishra, S. Zhang, S. Biswas, I. Parrington, T. Antonio, M. E. A. Reith, A. K. Dutta, *Bioorg. Med. Chem.* **2009**, *17*, 3923-3933.
[219] R. J. Vaz, J. Desantis, M. Eleuteri, *WO 2024/102810 A1* **2024**.
[220] B. Lei, H. Liu, S. Han, Z. Wang, *WO 2022/012622 A1* **2022**.
[221] Z. Xiao, S. Song, D. Chen, R. van Merkerk, P. E. van der Wouden, R. H. Cool, W. J. Quax, G. J. Poelarends, B. N. Melgert, F. J. Dekker, *Angew. Chem. Int. Ed.* **2021**, *60*, 17514-17521.